Kinetic Template-Guided Tethering of Fragments

Rebecca Helen Nonoo

Thesis submitted in partial fulfilment of the
requirements for the degree of Doctor of Philosophy

Chemistry Department
Imperial College London

Supervisors:
Prof. Alan Armstrong
Dr. David Mann

Abstract

This thesis is composed of two separate projects: Kinetic Template-Guided Tethering of Fragments and Design and Synthesis of a Chemical Probe to Dissect the Cellular Signalling Cascade leading to Cyclin D1 Degradation after DNA Damage.

Kinetic Template-Guided Tethering of Fragments

The development of a novel methodology for the site-directed discovery of small molecule, protein-binding ligands is described. The protein of interest, with a cysteine thiol (either native or engineered) adjacent to the desired binding pocket, is incubated with mixtures of low molecular weight compounds (fragments) modified with either an acrylamide or a vinyl sulfonamide capture group. Any ligand within the mixture that binds within the pocket brings the capture group into close proximity with the cysteine thiol, promoting a conjugate addition reaction at an increased rate over the background reaction. The capture reaction is designed to be slow, such that during the time course of an experiment, no adduct formation is observed *unless* the reaction is templated by the protein. By this method, binding ligands are rapidly identified by mass spectrometry analysis of the crude reaction mixtures. The methodology has been termed 'kinetic template-guided tethering'.
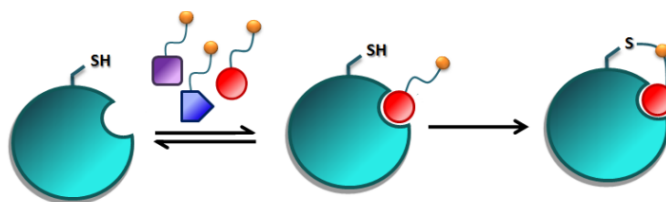
Design and Synthesis of a Chemical Probe to Dissect the Cellular Signalling Cascade leading to Cyclin D1 Degradation after DNA Damage

An inhibitor described within the literature was found to attenuate the reduction of cyclin D1 after DNA damage to cells. In order to implement a two-step chemical proteomics strategy to find the molecular target of this inhibitor, a synthesis of the compound with an alkyne appendage was required. The alkyne acts as a functional handle for attachment of a reporter molecule in cells *via* the Huisgen cycloaddition ('Click') reaction. The design and synthesis of this inhibitor with the alkyne appendage is described.
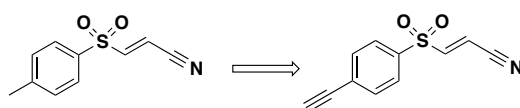
Acknowledgements

I would like to thank my supervisors Prof Alan Armstrong and Dr David Mann for the opportunity to work on this project and for all their guidance and support during my PhD studies.

Additionally, I would like to acknowledge:

- The Mann and Armstrong lab members for help and advice, and for making Imperial College such a nice place to work. A special thanks to Dr Alex Ferguson for your support and friendship and to Drs James Bull and Daniel Emmerson for your synthetic chemistry expertise.
- John Barton for allowing me unlimited use of the mass spectrometry lab, and for guidance in protein mass spectrometry.
- NMR technicans Dr Dick Sheppard and Peter Haycock for helpful discussions and advice.
- Dr Kenji Ocuse for the use of the qPCR, which allowed me to obtain protein melting temperature data.
- The Institute of Chemical Biology for the oppportunity to work on an interdisciplinary project.
- The EPSRC for funding this research.

Declaration of originality
I declare that this thesis is my own work. Where this is not the case appropriate acknowledgement has been given.

TABLE OF CONTENTS

Abbreviations

ABHD6	serine hydrolase
ABPP	activity based protein profiling
Ac	acetyl
AChE	acetyl choline esterase
ADP	adenosine diphosphate
AL	affinity labelling
AMP	adenosine monophosphate
aq.	aqueous
Ar	aryl/argon
ArCP	aryl carrier protein
Arg	arginine
Asp	aspartic acid
ATP	adenosine triphosphate
A.U.	arbitrary units
BACE-1	β-secretase 1 (aspartic acid protease)
bCA	bovine carbonic anhydrase
Bcl-X$_L$	B-cell lymphoma-extra large protein
BH3	protein domain
BINAP	2,2'-bis(diphenylphosphino)-1,1'-binaphthyl
βME	β-mercaptoethanol
Bn	benzyl
Boc	*tert*-butoxycarbonyl
br	broad
B-RAF	serine/threonine kinase
BSA	bovine serum albumin
Bu	butyl
C	cysteine
CA	carbonic anhydrase
cat.	catalyst/catalytic
Caspase	cysteine aspartyl protease
cbz	benzyloxycarbonyl
Cdc	cell division cycle
Cdk	cyclin-dependent kinase
CHA255	anti-(metal chelate) antibody
CI	chemical ionisation MS
clogP	calculated partition coefficient
CoA	co-enzyme A
COS-7	monkey kidney cell line
CSD	charge state distribution
CuAAC	Cu(I)-catalysed azide-alkyne 1,3-dipolar cycloaddition
Cyc	cyclin
Cys	cysteine
d	doublet/day(s)
Da	daltons
DABCO	1,4-diazabicyclo[2.2.2]octane
dA	deoxyadenosine
DCC	dynamic combinatorial chemistry/dicyclohexyl carbodiimide
DCE	dichloroethane
DCL	dynamic combinatorial library
DCX	dynamic combinatorial crystallography
DE-52	diethylaminoethyl functionalised anion exchange cellulose
DHF	dihydrofolate
dH$_2$O	distilled water
DIBAL-H	diisobutylaluminium hydride
DMAP	dimethylaminopyridine

DMF	*N*,*N*-dimethylformamide
DMSO	dimethyl sulfoxide
DNA	deoxyribonucleic acid
dNTP	deoxyribonucleotide triphosphate
DPDS	diphenyl diselenide
dTMP	deoxythymidine monophosphate
DTT	dithiothreitol
dUMP	deoxyuridine monophosphate
$E1_{CB}$	elimination unimolecular conjugate base
E. coli	*Escherichia coli*
EDTA	ethylenediaminetetraacetic acid
EGFR	epidermal growth factor receptor
eq./equiv.	equivalent(s)
ESI	electrospray ionisation
Et	ethyl
FBDD	fragment-based drug discovery
FDA	Food and Drug Administration
FP	fluorophosphonate
g	gram(s)
GAR Tfase	glycinamide ribonucleotide transformylase
GF	gel filtration
GSH	reduced glutathione
h	hour(s)
HCV NS3/4A	hepatitis C virus serine protease
hGH	human growth hormone
hGHbp	extracellular domain of the hGH receptor
His	histidine
HIV	human immunodeficiency virus
HPLC	high-performance liquid chromatography
HRMS	high resolution mass spectrometry
HSP90	heat shock protein 90
HSQC	Heteronuclear Single Quantum Coherence
HTS	high throughput screening
Hz	Hertz
IC_{50}	half maximal inhibitory concentration
IL	interleukin
IPTG	isopropyl β-D-thiogalactopyranoside
IR	infra-red
ITC	isothermal titration calorimetry
J	coupling constant
kbp	kilobase pair(s)
K_d	Dissociation constant
kDa	kilo-Daltons
KOD	*Thermococcus kodakaraensis*
KTGT	kinetic template-guided tethering
kV	kilovolt(s)
LB	Luria Broth
L. casei	*Lactobacillus casei*
LC-MS	liquid chromatography mass spectrometry
LC-MS SIM	liquid chromatography mass spectrometry single ion mode
LHMDS	lithium bis(trimethylsilyl)amide
LE	ligand efficiency
μg	microgram(s)
μL	microlitre(s)
μm	micrometre(s)
μM	micromolar
m	multiplet

M	molar
mA	milliamp(s)
MALDI	matrix-assisted laser desorption ionisation
MbtA	adenylating enzyme from *Mycobacterium tuberculosis*
*m*CPBA	*meta*-chloroperoxybenzoic acid
Me	methyl
mg	milligram(s)
MHz	megaHertz
min	minute(s)
mL	millilitre(s)
mM	Millimolar
MMP	matrix metalloproteinase
mmol	millimole(s)
mp	melting point
MS	mass spectrum/mass spectrometry
mTHF	methylene tetrahydrofolate
MW	molecular weight
m/z	mass/charge ratio
NAD^+	nicotinamide adenine dinucleotide
nm	nanometre
NMR	nuclear magnetic resonance
NOE	Nuclear Overhauser Effect
NROT	number of rotable bonds
OMFP	3-*O*-methylfluorescein phosphate
p	phospho
PCR	polymerase chain reaction
PDB	protein data bank
PDGF	platelet-derived growth factor
Ph	phenyl
PPI	protein protein interaction
ppm	parts per million
PSA	polar surface area
PTP	protein tyrosine phosphatase
R	arginine
RAS	receptor-accelerated synthesis
R_f	retention factor
RNA	ribonucleic acid
Ro5	Rule of five
rpm	rotations per minute
r.t.	room temperature
s	second(s), singlet
SAR	structure-activity relationship(s)
SDS	sodium dodecylsulfate
SDS-PAGE	SDS-polyacrylamide gel electrophoresis
SH	serine hydrolase
SIRT	sirtuin enzyme
S_N2	Bimolecular nucleophilic substitution
SPR	surface plasmon resonance
STD	saturation transfer difference
t	triplet
TAE	TRIS-HCl/acetate/EDTA
Taq	*Thermus aquaticus*
TFA	trifluoroacetic acid
THF	tetrahydrofuran/tetrahydrofolate
thr	threonine
TLC	thin layer chromatography
T_m	protein melting temperature

TMEDA	tetramethylethylenediamine
TMS	trimethylsilyl/tetramethylsilane
ToF	time-of-flight
TRIS	tris(hydroxymethyl)aminomethane
TS	thymidylate synthase
Tween	polysorbate 20
Tyr	tyrosine
UV	ultra-violet
WT	wild type
Y	tyrosine

Kinetic Template-Guided Tethering of Fragments

1. Introduction

1.1. High-throughput screening and chemical space

Central to both drug discovery and chemical biology is the search for new small molecule, protein-binding ligands. In the early 1990s, the number of molecules contained within 'drug discovery chemical space' was estimated to be in excess of 10^{50}.[1] Attempts to search this vast chemical arena led to the advent of high-throughput screening (HTS) and combinatorial chemistry. Large libraries of compounds were generated by the pharmaceutical industry, containing molecular structures of high complexity, with physicochemical properties that were later identified as unsuitable for medicinal chemistry optimisation. Such large libraries were expensive to produce, maintain and screen, and it became evident at the start of the 21st century that this approach was failing in the discovery of new drugs.

A simple model to describe protein-ligand molecular complimentarity was proposed by Hann and colleagues in 2001, where the interaction between a ligand and a protein was modelled as a series of interaction types (+/-).[2] In this model, an interaction occurs only if all features between ligand and protein match exactly. This model predicted a rapid decrease in the probability of successful binding upon increase in ligand molecular complexity, due to the decreasing number of ways to generate a match in comparison to the increasing number of ways to generate a mismatch. This 'complexity model' has been used to explain why hit compounds generated *via* HTS tend to be of low quality, with many suboptimal interactions and mismatches, and low affinity (usually micromolar) considering their high molecular weight and lipophilicity. A set of empirical rules to describe the physicochemical properties of orally bioavailable drugs was suggested by Lipinski in 1997, now referred to as Lipinski's rule of 5 (Ro5).[3] Lipinski's rules state that MW < 500, cLogP < 5, number of H-bond donors < 5, number of H-bond acceptors < 10 and number of rotable bonds (NROT) < 10. Compounds detected as hits in HTS were difficult to optimise in potency without increasing molecular weight and lipophilicity, pushing them outside of the suggested limits set by Lipinski. In support of Lipinksi, compounds of higher lipophilicity and MW have been found to suffer higher attrition rates in the clinic.[4, 5] The compounds generated by HTS were suggested as not 'lead-like', and publications in the late 1990s suggested a revision in the design of libraries, to move towards lower molecular complexity, lower MW and lower lipophilicity to improve the lead-optimisation process.[4-7]

1.2. Fragment-based drug discovery

Fragment-based drug discovery (FBDD), developed as a means to overcome the difficulties encountered during optimisation of HTS lead compounds, involves screening low molecular weight (*ca*. 110-350 Da) compounds ('fragments') against the biological target. As initially proposed by Congreve *et al.*, fragments are generally designed to conform to a rule-of-three; MW ≤ 300, H-bond donors ≤ 3, H-bond acceptors ≤ 3, NROT ≤ 3, cLogP ≤ 3 and PSA ≤ 60.[8] The low MW and lipophilicity of fragment starting points allows significant increases in both physicochemical profiles upon optimisation of potency, without breaching the limits set by Lipinski for orally bioavailable drugs. The hits generated by FBDD also tend to be of higher quality that those identified from HTS. This is measured by ligand efficiency, a concept designed to identify the binding affinity conferred by each heavy atom (non-hydrogen) within the molecule.[9, 10] All small molecules must overcome a binding entropic barrier, which is approximately independent

of molecular weight.[11] Therefore, fragments must form high quality binding interactions in order to have a measurable affinity, and are highly ligand efficient. Fragments are unlikely to be identified as hits if any of the interactions made between protein and ligand are suboptimal. By their nature, fragments bind only very weakly to proteins, usually with low millimolar or high micromolar binding affinities. Specialised biophysical screens are usually adopted to measure these weak interactions, which cannot generally be detected using functional enzyme assays. As discussed by Hann *et al*. the molecular weight and complexity of fragments must not be so low that an unambiguous binding mode cannot be identified.[2] A simplified protein-ligand interaction model predicted that ligands of very low complexity would bind in multiple orientations. In addition, a basal level of complexity was required in order to be able to detect the interaction at all.

Fragment library size

An advantage conferred by FBDD is that only small libraries of compounds need to be screened against the target protein in comparison to HTS approaches. Reymond *et al*. calculated the number of possible chemical structures per number of heavy atoms, and found this number to increase approximately exponentially.[12] For each heavy atom added, the number of possible structures increased approximately 8-fold. A library of 1000 molecules, which contain 12 or fewer heavy atoms, samples *ca*. 0.001 % of the total theoretical number of chemical structures of this size.[13] However, if the number of heavy atoms is increased to ≤ 25, a library of 1000 compounds only samples a meagre 10^{-14} %.[13] Fragment libraries tend to include between 1000-20000 ligands; Astex Therapeutics screened a library of 1600 fragments, with an average molecular weight *ca*. 170 Da against HSP90, whereas Plexxikon screened 20,000 compounds against B-RAF with fragments which had a slightly higher molecular weight range of 150-350 Da.[13] These small libraries of fragments are easier to characterise and maintain than larger HTS libraries. In addition, fragments are often synthetically more accessible than the larger, more complex molecules employed in HTS campaigns.

Fragment optimisation: linking and growing

The pioneering work of Fesik, Hajduk and colleagues, published in the mid-1990s, was key in the development of fragment-based drug discovery.[14, 15] They noted the low probability of generating a hit compound, which contained all the required functional groups in the proper spatial arrangement for tight binding, by screening lead-like molecules against a biological target. This led them to develop a methodology they termed structure-activity relationships by NMR or 'SAR by NMR', where small fragments of lead-like compounds were screened against a protein. These fragments were then linked or grown to form high affinity binders at a later point during optimisation. They detected the binding of fragments to the protein surface by measuring peturbations in amide ^{15}N shifts using NMR and ^{15}N-labelled protein. Such NMR techniques allow the detection of very weak millimolar binding, and are therefore ideal for fragment screening. In this early work, fragment screening against a matrix metalloproteinase (MMP), Stromelysin (MMP3), using SAR by NMR led to the identification of two weak binding fragments, acetohydroxamic acid ($K_d = 17$ μM) and (4'-hydroxybiphenyl-3-yl)-acetonitrile ($K_d = 20$ μM), which were linked by a methylene unit to generate a highly potent inhibitor with $K_d = 15$ nM.[14] The potency of the linked compound was higher than the sum of the two individual fragment affinities (termed 'superadditivity'), originating from the high energy penalty paid by fragments

upon binding due to the loss of both translational and rotational entropy.[11] This early example of fragment linking is highly impressive considering the challenges which have since been encountered by others to optimise fragments in this way. Howard *et al.* reported that during the course of their work to develop an inhibitor of the protease enzyme thrombin, linking two optimally bound fragments together compromised the original fragment orientations.[16] Huth *et al.* failed to observe the desired increase in potency upon linking of two HSP90-binding fragments, potentially due to a suboptimal linker strategy, which introduced an unfavorable energy penalty.[17] Both the length and the chemical nature of the linker influence fragment binding.[18]

'Fragment growing', where structure-guided drug design is used to form additional interactions by growing out from the original fragment, has generally been the most successful strategy for fragment-to-lead optimisation. Hajduk has shown that it is possible to optimise fragments to lead compounds whilst keeping the ligand efficiency constant using a retrospective study of 18 drug leads from 15 different internal projects at Abbott Laboratories.[19] In this study, the drug leads were systematically reduced in size until the smallest compound with reported potency was reached, with the ligand efficiency reported at each stage.

Fragment-based drug discovery (FBDD) is now considered a validated approach for the discovery of new inhibitors, and a large number of reviews have been published[13, 20-22] in addition to a number of books.[23] There are now several compounds in clinical trials that have emerged from fragment-based approaches.[24] In addition, Vemurafenib, developed by Plexxicon using a fragment-based approach,[25] was approved by the FDA in 2011 for the treatment of late stage melanoma.

Challenges for FBDD: fragment screening

A crucial challenge for FBDD is the identification of weak binding fragments, and over the past decade considerable effort has been put into the development of specialised screening technologies.[26] Fragments cannot usually be detected using biochemical assays, but require biophysical screening technologies such as NMR,[27] X-ray crystallography,[28] surface plasmon resonance (SPR),[29] isothermal titration calorimetry (ITC)[30] and Thermofluor®,[31] Figure 1. Despite significant progress in this area, fragments often need to be screened at high concentrations, leading to additional problems. Screening at high concentrations can lead to the generation of false positives, where inhibition is not caused by one-to-one protein-ligand binding.[32]

Usually a combination of biophysical techniques is applied during the search for a hit fragment, where a tradeoff between throughput and structural information is made.[33] For Thermofluor® and SPR, high throughput can be achieved (≥100,000 compounds is routine), but no information on the binding location is gained and fragment solubility is crucial due to the high screening concentrations required. Ligand-based NMR techniques such as saturation transfer difference (STD) experiments involve measurement of the 1D chemical shift of the ligand in the presence of a stoichiometric amount of protein, with and without selective irradiation of the protein resonances.[34] Irradiation of the spectrum is usually carried out between 1-2 ppm, which is highly populated with protein signals and not usually ligand signals. If the relaxation rate of the ligand protons is longer than the protein-ligand dissociation rate (k_{off}), usually true for high micromolar to low millimolar binders, an accumulation of saturated ligand occurs and a

difference between the irradiated and non-irradiated spectrum is observed. Such ligand-based NMR techniques are still amenable to high-throughput, but give no information on the binding site. At best, the part of the ligand in contact with the protein surface (binding epitope) can be identified.

Perhaps the most utilised approach for hit identification and validation by NMR identifies chemical shift changes upon binding of free protein to ligand using 2D ^{15}N/^{1}H and/or ^{13}C/^{1}H heteronuclear single quantum coherence (HSQC) correlation spectroscopy.[35] The initial challenge in the use of such an NMR technique is the expression of milligram quantities of isotopically enriched protein. A significant advantage of this technique is that compounds that bind to the protein can be characterised without knowledge of the protein function. Additionally, ligand binding can be detected over an unlimited binding affinity range. However, in order gain structural information about the binding site, the NMR spectrum must be assigned, a process usually only possible for proteins with a molecular weight of less than 40 kDa. Nuclear Overhauser Effect (NOE) experiments can be used to provide a more precise determination of the ligand binding mode.[36] The chemical shift approach is thought to be one of the most reliable, robust and reproducible methods to monitor ligand binding. One of the major disadvantages of this technique is that the protein must be stable over the long data acquisition process.[37] Wang *et al*. screened a 10,000-member custom made fragment library against ^{15}N-labelled BACE-1, a target currently thought to be important for the treatment of Alzheimers disease, using HSQC NMR.[38] They identified a thiourea fragment with a K_d of 550 μM, which was rapidly optimised using a combination of HSQC NMR and a functional assay to improve affinity by a factor of 36, to give a K_d of 15 μM. An X-ray crystal structure, in addition to NMR structural data, allowed the characterisation of the binding mode and further optimisation studies.

Screening by X-ray crystallography yields the highest degree of structural information, but represents the lowest in terms of throughput.[33] A robust method for obtaining high quality protein crystals is required.
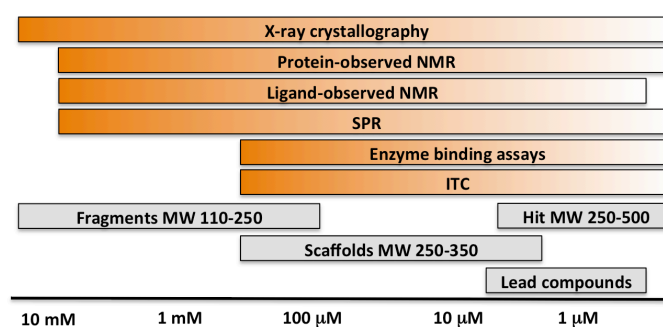
Figure 1 Comparison of screening techniques and the potency ranges they are suitable to identify.

Whilst biophysical methods for FBDD have been highly successful against certain target classes, they do not provide the means to target a specific site on a protein surface. Such site-directed drug discovery becomes important in the field of protein-protein interaction (PPI) inhibition. PPIs are thought to be crucial therapeutic targets in a number of diseases.[39, 40] PPI interfaces tend to be large, flat and featureless, and many were initially labelled as undruggable by small molecules. However, a report by Clackson and Wells in 1995 changed this perception.[41] They discovered that only a few key residues were responsible for a large proportion of the energetics of the hGH-hGHbp PPI by the

generation of a series of alanine scanning mutants. Such 'hotspots' have not only been discovered as a feature of many PPIs, but there are now a number of examples of small molecules able to disrupt a PPI by binding to a hotspot pocket.[42-44] Despite some successes, the search for selective small molecule inhibitors of PPIs remains challenging. The development of methods to target them in a site-directed manner with fragments would be of high importance, allowing access to this class of therapeutics.

1.3. Site-directed drug discovery

1.3.1. Protein-directed dynamic combinatorial chemistry

In accordance with the law of mass action, a dynamic equilibrium of compounds generated by a reversible reaction is shifted upon addition of a protein, which binds certain combinations, towards the best binding components.[45] This protein-directed dynamic combinatorial chemistry (DCC) offers an opportunity to combine synthesis and screening all in one step, in addition to a providing a potential solution to the fragment-linking problem. Furthermore, if one of the components of the mixture is a known binder, the selection of a higher-affinity binding combination is site-directed. Protein-directed DCC was first demonstrated by Huc and Lehn, who incubated a mixure of 3 aromatic aldehydes with a 15-fold excess of 4 aliphatic amines under physiological conditions in the presence and absence of carbonic anhydrase (CA) II.[46] The virtual combinatorial library generated by the freely reversible amine-aldehyde condensation was affected by the presence of CAII, which directly assembles binding combinations. The position of equilibrium was fixed by reduction of the resulting imines with sodium cyanoborohydride, and the resulting mixtures analysed by HPLC. Amplification of one aldehyde-amine pair at the expense of others suggested a binding combination, which was consistent with previous inhibitors of CAII.

Eliseev *et al*. identified that deconvolution of DCLs becomes very difficult, and sometimes impossible, as the number of molecular components increases.[47] They used the reversible reaction between aldehydes and a core amine scaffold **1**, to probe a hydrophobic pocket on influenza virus A neuraminidase. Amine **1** is based on the commercial neuraminidase inhibitor Tamiflu **2**, which binds adjacent to the hydrophobic pocket of interest, Figure 2. In a major advance on the previous work, they carried out the screening under conditions in which coupled products were only present in trace quantities, except for stabilised protein-binding combinations, which biased the equilibrium. The reactions were carried out in the presence of a very slow acting reductant such that significant coupled amine products were only observed for binding species. An important consideration was that whilst the reduced amine products are the observed amplified species, it is the transient imine which is the protein-binding species. The authors comment that whilst the amplified coupled amines tended to be higher affinity binders than combinations not amplified, there

Figure 2 (Top) active component of Tamiflu. **(Bottom)** reaction between core amine scaffold and series of aldehydes to probe the adjacent hydrophobic pocket.

were occasional exceptions where amines not selected had higher affinity that those selected. In an extension of their original work, Eliseev *et al*. carried out similar DCC experiments with ketones rather than aldehydes.[48]

Scott *et al*. probed the pantoate binding pocket of pantothenate synthetase using 5'-deoxy-5'-thioadenosine **3** as a non-covalent anchor fragment.[49] The DCL was composed of fragment **3** in addition to a number of other thiols, and the subsequent thiol-disulfide exchange monitored by HPLC. Comparison of the resulting protein-induced thermodynamic distribution to that in the absence of the template identified disulfide **4** as a favorable binding combination, Figure 3. Disulfide **4** was subsequently confirmed to bind to pantothenate synthetase with a $K_d = 210$ μM. Crystal structures of thioadenosine **3** and disulfide **4** indicated identical binding modes for the adenosine moiety in the pantoate pocket, as expected.

$$\begin{array}{ll} \mathbf{3} & R = H \\ \mathbf{4} & R = SCH_2Ph \end{array}$$
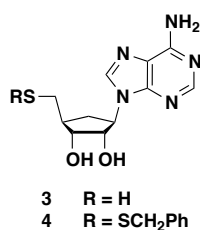
Figure 3 Thioadenosine **3** was incubated with a number of thiols in the presence and absence of pantothenate synthetase. Disulfide **4** was identified from the DCL as a thermodynamically stablised combination in the presence of the protein and demonstrated a moderate K_d of 210 μM.

In an impressive extension of protein DCC, Congreve *et al*. incubated DCLs with protein crystals and identified binding combinations by the resulting electron density maps after x-ray diffraction of the crystals.[50] They used this 'dynamic combinatorial crystallography' (DCX) to identify inhibitors of cdk2 with DCLs composed of hydrazines and isatins to generate the corresponding hydrazones. The major advantage of this compared to standard protein DCC is firstly that identification of the binding ligand is facile, and secondly that a detailed ligand binding mode is immediately obtained.

To use protein templated DCC as a method of site directed ligand discovery, a ligand adjacent to the pocket of interest must already be known. In addition, this ligand must be amenable to modification with a reactive group to allow reversible reaction with other fragments in the mixture. An elegant solution to this problem was discovered by Erlanson *et al*. as discussed in the following section.

1.3.2. Disulfide tethering

Pioneering work was carried out by Erlanson, Wells and colleagues, as part of Sunesis Pharmaceuticals, to develop a methodology for the site-directed discovery of protein-binding ligands. This methodology is an extension of protein DCC and has been termed disulfide tethering. A solvent exposed cysteine thiol (either native or engineered) on the surface of the protein of interest, in the vicinity (5-10 Å) of the target pocket, is allowed to react reversibly with a mixture of disulfide-modified fragments as an active consituent of the DCL. A thiol-disulfide equilibrium of protein-fragment adducts is generated. Any fragment within the mixture, which makes favourable interactions with the protein, is stabilised within the thermodynamic equilibrium at the expense of other protein-fragment adducts. Analysis of crude reaction mixtures by mass spectrometry allows the identification of favorable adducts, which can be deconvoluted to identify fragments with the highest binding affinity. The overall level of protein modification can be tuned by the addition of a reductant.

As an initial proof-of-concept for disulfide tethering, Erlanson *et al*. incubated a library of *ca*. 1200 disulfide-modified fragments in cocktails of up to 100 with the enzyme thymidylate synthase (TS).[51] Within this initial library, an N-tosyl D-proline fragment was observed to form a significant adduct with TS. Removal of the disulfide bond identified N-tosyl D-proline as a millimolar binder, and this initial hit was subjected to medicinal chemistry optimisation to increase affinity to the low micromolar region. Since this initial proof-of-concept work, tethering has been applied to a range of biological targets, as discussed in the following section.

Tethering with extenders - caspase-3

Cysteine aspartyl proteases (caspases) play key roles in cytokine maturation and apoptosis.[52] Caspase-3 has been suggested as a point for therapeutic investigation in a wide range of diseases such as Alzheimers, Parkinsons, sepsis and myocardial infarction. Caspase-3 was considered by Sunesis to provide an ideal starting point for their tethering based drug discovery as it has a nucleophilic cysteine (catalytic) in the active site pocket. Many inhibitors for caspase-3 are tetrapeptides, which contain an aspartyl residue that binds in a conserved aspartyl pocket within the active site. To probe the pocket from this aspartyl binding-site, Sunesis designed inhibitor **5** containing an arylacyloxymethylketone-modified aspartyl thioester.[53] Alkylation of the protein with arylacyloxymethylketone **5** and subsequent removal of the thioester to reveal the free thiol was successful, Figure 4.
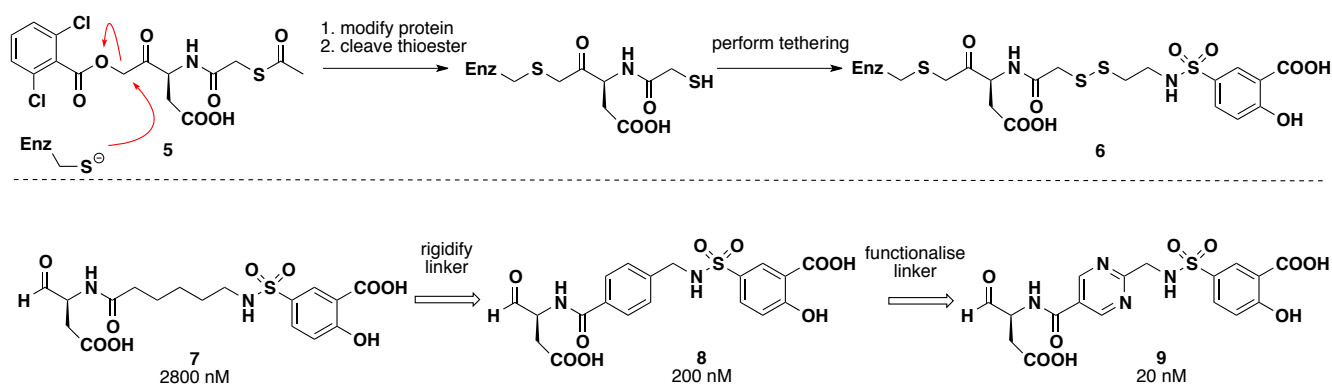
Figure 4 (Top) Caspase-3 was covalently modified with inhibitor **5**, and the thioacetate protecting group removed to reveal a free thiol for tethering experiments. Salicyclic acid derivative **6** was identified as a favourable binding combination. **(Bottom)** Replacement of the arylacyloxymethylketone with an aldehyde yielded low micromolar inhibitor **7**. Rigidification and functionalisation of the linker improved potency to 20 nM.

This modifed caspase-3 was then subjected to tethering experiments from which salicyclic acid derivative **6** was selected as the most prominent fragment hit. Replacement of the labile disulfide bond with an alkane and the
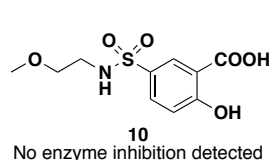
Figure 5

arylacyloxymethylketone with an aldehyde warhead generated sulfonamide **7** as a low micromolar inhibitor. Rigidification of the linker to give benzylsulfonamide **8** yielded a 10-fold improvement in affinity, and further functionalisation improved affinity by another 10-fold, yielding a 20 nM inhibitor, pyrimidine **9**. Presumably the aldehyde would have been replaced had the programme advanced towards the development of a caspase-3 clinical candidate. Fragment **10** could not be detected as an inhibitor of capsase-3 in a conventional enzyme activity assay, even when screened at high millimolar concentrations, indicating that it would probably not have been detected in a

conventional fragment screen, Figure 5. The same approach was applied to caspase-1 to identify a single digit nanomolar inhibitor.[54]

An allosteric pocket was identified in both caspase-3 and caspase-7 by screening 10,000 thiol-containing compounds against the native enzymes (which contain 5 cysteine residues).[55] Indole **11** and dichloroaryl **12** selectively modified cys264 (caspase-3) and cys290 (caspase-7), as identified by screening against a panel of cysteine mutants, Figure 6. These cysteine residues sit at the bottom of a deep cavity, 14 Å from the active site cysteine, and when modified with either indole **11** or dichloroaryl **12** inactivate the proteases. This work demonstrates the power of site directed drug discovery for the identification of novel allosteric pockets.
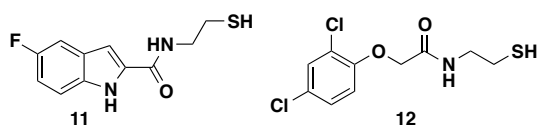
Figure 6 Thiols **11** and **12** identified as allosteric inhibitors of caspase-3 and caspase-7 *via* tethering.

Probing an adaptive binding site - interleukin 2

The cytokine interleukin-2 (IL-2) is a critical factor in the immune response, and has been linked to a number of immunodisorders.[56] IL-2 interacts with its heterotrimeric receptor (composed of three subunits α, β, and γ) to induce T-cell proliferation. Alkyne **13** was discovered by Hoffman La-Roche in 1997 to bind specifically and reversibly to IL-2 with an IC_{50} of 3 μM, Figure 7.[57] Alkyne **13** binds to IL-2 at the IL-2/IL-2Rα interface and disrupts the PPI. A crystal structure of alkyne **13** bound to IL-2, obtained by Sunesis, indicated that part of the IL-2/**13** binding pocket undergoes a striking transformation upon binding, where the flat unliganded surface in the apo structure undergoes significant side chain and loop movements to create a hydrophobic binding pocket.[58] To probe both the adaptive and rigid subsites of the IL-2/**13** binding interaction, Sunesis constructed a panel of 11 cysteine mutants of IL-2 in the vicinity of both pockets and screened a library of 7000 disulfide-modified fragments against each.[58] Mutants with a poor hit rate were found to target the rigid pocket, whereas mutants which demonstrated a high hit rate mapped fragments to the adaptive pocket. This adaptive site may therefore be more amenable to bind small drug-like molecules, although it would not have been identified from a crystal structure of the apo

Figure 7 Compound **13** was discovered by Roche in 1997 to bind to IL-2 in a pocket with two subsites, one highly adaptive and one rigid. Indole glyoxylate **14** was selected by mutant Y13C during disulfide tethering experiments, where the indole ring sits in the adaptive binding pocket occupied by the terminal phenyl ring in alkyne **13**. Merging the two compounds gave inhibitor **15**, which has a 2-fold improvement in binding affinity over alkyne **13**.

protein form. The adaptive site, which binds the biaryl alkyne motif in compound **13**, was found to have a high propensity for aromatic groups, and in accordance with this, indole glyoxylate **14** was observed to bind in this region when tethered to Y31C as identified by a crystal structure. Merging alkyne **13** and glyoxylate **14** to yield compound **15** led to a two-fold improvement in affinity from alkyne **13**, providing an early demonstration that tethering was able to discover fragments suitable for merging with a lead molecule to improve affinity.[59]

Tethering with breakaway extenders – protein tyrosine phosphatase 1B

Protein tyrosine phosphatase (PTP) enzymes remove a phosphate group from phosphotyrosine (pTyr) protein and peptide substrates, and are recognised as a challenging, but important target class in drug discovery.[60] Many PTP enzymes have a small, hydrophilic active site pocket designed to accommodate bisanionic pTyr, and tend not to bind drug-like molecules. PTP1B has been implicated as a target for the treatment of obesity and type II diabetes, but the associated challenges have prevented a pharmaceutically acceptable compound reaching clinical trials. Erlanson *et al*. applied disulfide tethering to identify a weak active site fragment binder of PTP1B.[61] The catalytic cysteine, at the bottom of the narrow active site channel in PTP1B, was considered inappropriate for disulfide tethering. The residues surrounding the active site pocket were considered crucial to maintain the finely tuned, delicate catalytic machinery.

Figure 8 Breakaway extender **16**.

This tethering problem led to the development by Sunesis of 'tethering with breakaway extenders'.[61] A cysteine was introduced far from the active site and subsequently modified with breakaway extender **16**, composed of a reactive bromoacetamide and a pTyr mimic, Figure 8. The pTyr mimic binds to the active site pocket protecting the active site cysteine from alkylation and positioning the bromoacetamide close to the mutant cysteine for covalent modification, Figure 9. Cleavage of the thioester with hydroxylamine places the thiol over the active site pocket for tethering screens. A library of *ca*. 15,000 disulfide-modified fragments were screened against the modified PTP1B to identify a pyrazine fragment as a millimolar inhibitor.

Figure 9 Tethering with 'breakaway extenders' developed by Sunesis to find fragments for PTP1B.

Aurora kinase – tethering with dynamic extenders

In an impressive extension of their previous work, Erlanson and colleagues developed 'tethering with dynamic extenders' to identify a low micromolar inhibitor of Aurora A kinase.[62] Aurora A plays a critical role in the regulation of mitosis and is thought to be an important target for drug development.[63] Tethering with dynamic extenders was developed as a means to probe both the purine binding site, and an adjacent adaptive binding pocket. Diaminopyrimidine, a known binder of the purine binding pocket, was modified with two disulfide appendages to give compound **17**, and incubated with a library of *ca*. 4500 disulfide-modified fragments under partially reducing conditions, Figure 10. The authors comment that due to the the stringent requirement for two disulfides to exist simultaneously, only very few hits were identified overall. Fragment **18** was identified as a hit, and upon replacement of the labile disulfide with a flexible alkyl chain, generated a diaminopyrimidine-**18** inhibitor with an IC$_{50}$ of 17 μM.

This impressive methodology has the potential to probe adaptive pockets to generate novel fragments once an inhibitor for an adjacent site is known. It also demonstrates potential to link fragments together, a non-trivial task.[64]
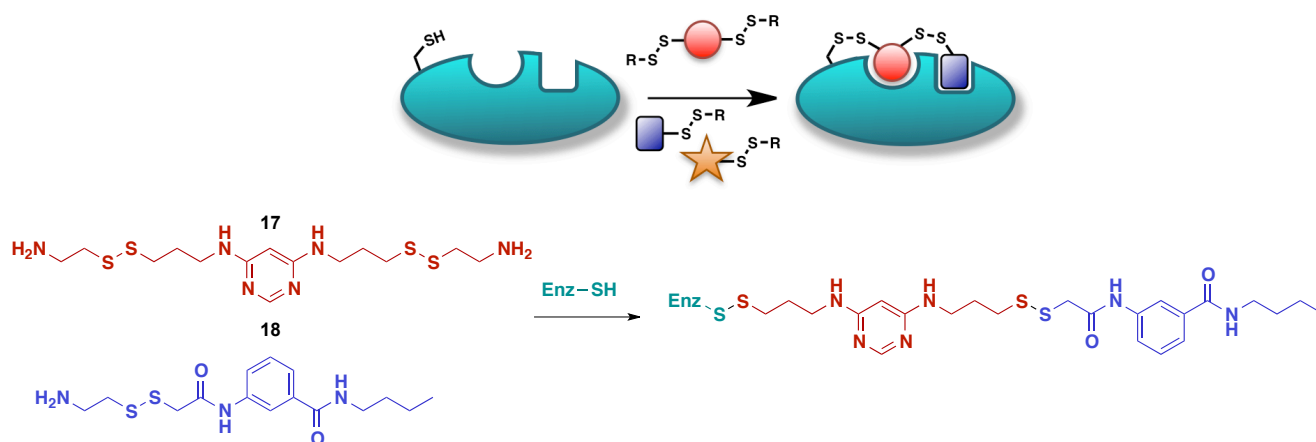
Figure 10 Tethering with dynamic extenders. Diaminopyrimidine **17** was incubated with mixtures of disulfides, of which disulfide **18** is an example, under partially reducing conditions in the presence of aurora A kinase. Favorable combinations were identified by mass spectrometry analysis of the crude mixtures. Aurora A kinase is represented by the cyan shape in the schematic, whilst the red circle represents the diaminopyrimidine and the purple square/yellow star represent disulfide-modified fragments.

Disadvantages of reversible covalent capture

Whilst the pioneering work reported by Sunesis led them to discover a number of active compounds, the practical difficulties in the implementation of disulfide tethering has prevented the use of the this methodology by others for the discovery of fragments. One of the biggest hurdles is perhaps the custom synthesis of unsymmetrical disulfides, which can rapidly disproportionate under certain conditions.[65] Published work by Sunesis describes the use of unsymmetrical disulfides with one side modified with a group to increase aqueous solubility and the other with a fragment. Additionally, high resolution mass spectrometry is needed to detect and resolve bound fragments, where care must be taken upon analysis not to peturb the rapidly equilibrating DCL. Furthermore, disulfide linked fragments identified by tethering must be resynthesised with a stable linker – an operation that may abrogate affinity due to the loss of the characteristic 90° disulfide dihedral bond angle.

Work was carried out previously* in an attempt to use disulfide tethering to identify an inhibitor of cdc25 phosphatase. Cdc25 phosphatases drive the cell cycle by dephosphorylation of substrate proteins, and have been identified as overexpressed in a significant number of cancers.[66-68] They are therefore considered as viable therapeutic targets, but despite a significant effort in the literature, only one pharmaceutical entity has entered clinical trials.[69] This is potentially due to the very small and narrow, hydrophilic active site pocket, which is particularly unsuitable to bind drug-like molecules.[70, 71] However, a hotspot over 20 Å from the active site pocket was reported for cdc25B as crucial for binding to cdk substrates, and may potentially represent a new pocket to target for cdc25-cdk inhibition.[72-74] Disulfide tethering was initially chosen as a means to target this pocket in a site specific manner, but difficulties were encountered. During the synthesis of unsymmetrical disulfides, it was noted that a significant number of compounds were highly labile, and rapidly led to statistical mixtures of products whilst as a solution in organic

---

* Carried out by RHN as part of MRes degree.

solvent, even in the absence of any additive such as acid or base, Equation 1. Synthesis of fragments for screening was therefore highly time-consuming.
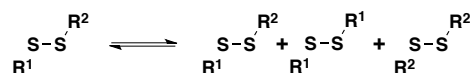
Equation 1 disulfide disproportionation.

Additionally, MALDI was the only mass spectrometry technique available at the time the experiments were conducted, but at the working MW of the protein ($ca.$ 23kDa) significant isotopic broadening prevented the accurate deconvolution of protein adducts, Figure 11. It was desirable for the DCL to be enzymatically digested to allow MALDI analysis of the resulting peptide-adducts, which would concomitantly identify the position of modification. However, this would have required an acidic quench of the DCL, which would have made the sample unsuitable for digestion by most proteolytic enzymes. An impressive desulfurisation reaction reported by Davis et $al.$ to generate a stable thioether from a disulfide was considered as a means to overcome this problem.[75] In their work, a thioether glycoprotein was generated from a disulfide glycoprotein by treatment with a phosphine in buffer. However, this was not pursued as the proposed mechanism for this reaction would require the protein to be severed from the fragment, rendering the final thioether mixture as an untrue representation of the original disulfide distribution.
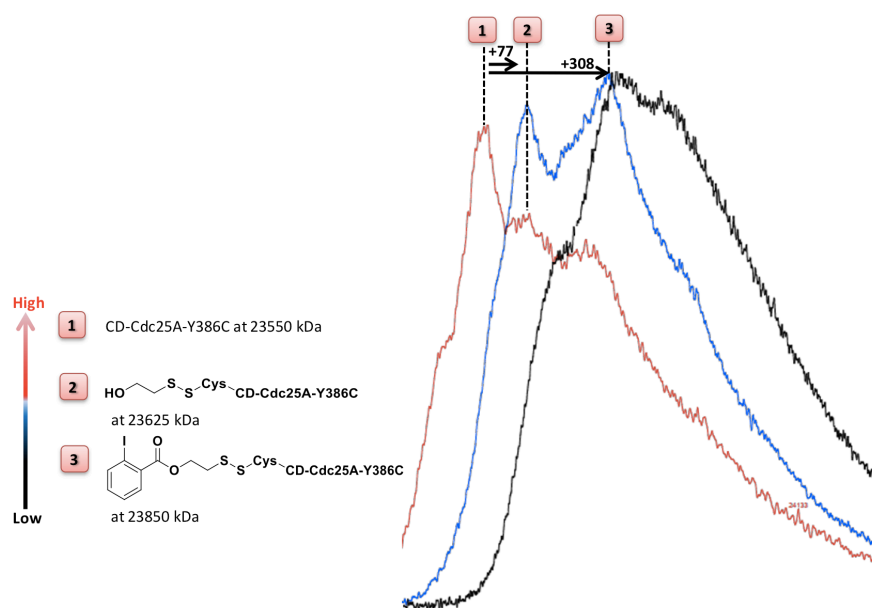
Figure 11 Representative spectrum obtained using MALDI for analysis of adducts by disulfide tethering.[*] The proportion of the protein present as an adduct was tuned by addition of a reductant. 'High' and 'low' indicate the concentration of βME in the sample. Red trace = 20 mM βME; blue trace = 0.2 mM βME; black trace = no βME. Catalytic domain of cdc25A Y386C is represented by CD-cdc25A-Y386C.

The work presented within this thesis describes a proof-of-concept for an *irreversible* fragment-capture methodology for the site-directed identification of fragments. This methodology will be referred to as 'kinetic template-guided tethering' (KTGT), and was initially designed to overcome the difficulties encountered during disulfide tethering. The

---

[*] Image generated and work carried out by R. H. Nonoo as part of MRes degree, 2008.[129]

concept is similar to that previously described for reversible tethering except that in KTGT, fragments are modified with a reactive electrophilic capture group for irreversible reaction with cysteine. In KTGT the capture group must be sufficiently unreactive that over the time course of the experiment, an adduct is only observed to form if the fragment binds to the protein and thereby increases the reaction rate by increased proximity. If the protein templates the reaction in this way, a stable adduct is formed and subsequently identified by mass spectrometry analysis. A suitable functional group should be stable to enzymatic digestion, to allow the use of MALDI to identify the location of binding adducts. The capture group should be easy to install synthetically, compatible with the aqueous screening conditions and highly selective for reaction with cysteine. After the identification of a hit fragment using KTGT, the capture group can be removed and the remaining fragment optimised using conventional medicinal chemistry. As an alternative, KTGT could be envisaged as a method for the discovery of irreversible covalent inhibitors. Such covalent inhibitors have traditionally been avoided by the pharmaceutical industry due to the potential for off-target effects, resulting in high toxicity. However, many drugs do act *via* an irreversible mechanism, and there has been a recent interest in covalent drugs.[76-78]

1.4. Evidence in support of a KTGT hypothesis

1.4.1. Activity based protein profiling and affinity labelling

KTGT can be considered to form a continuum with activity-based protein profiling (ABPP) and affinity labelling (AL), two techniques that are widely used to identify proteins that bind to a particular ligand. ABPP and AL both involve the design of a chemical probe to target specifically a particular enzyme family, but whereas ABPP uses the nucleophilic residue fundamental to the catalytic mechanism of action of an enzyme, AL targets non-catalytic residues. Chemical probes generally consist of three distinct functional parts: a reactive group for irreversible covalent modification of the protein of interest; a ligand to bind to the binding site of the required enzyme family; a tag for purification or identification of labelled enzymes. The chemical probe is added to a mixture of proteins, such as a crude cell extract, and those which are labelled are subsequently identified. As for KTGT, the warhead in both AL and ABPP must be sufficiently unreactive that selectivity for a particular enzyme class is high. The reaction only occurs upon binding of the ligand, bringing the reactive group into close proximity with the reactive site on the protein (usually a nucleophilic residue) and accelerating the reaction rate by increased proximity.

An interesting functional proteomic strategy was reported by Cravatt *et al*. in 2007, which made use of an ABPP probe specific for the serine hydrolases (SH) to identify selective SH carbamate inhibitors.[79] SHs are almost universally susceptible to active site serine modification by fluorophosphonate (FP) compounds. Such compounds have been conjugated to reporter molecules for use as ABPP probes of the serine hydrolases in a range of proteomes. Cravatt *et al*. preincubated the proteome from COS-7 cells expressing high levels of active SH ABHD6 individually with 55 carbamate ligands as potential SH inhibitors. This was followed by addition of a rhodamine tagged FP (FP-R) and subsequent analysis by in-gel fluorescence in comparison to control with no added inhibitor. This not only indicated which carbamates inhibited the desired ABHD6 SH, but also indicated for each inhibitor the degree of selectivity for inhibition between the different SHs.

The validity of KTGT was alluded to by D.A. Erlanson and S.K Hansen in 2008,[80] after Sames and colleagues demonstrated an epoxide as a suitable electrophile during work to develop a selective affinity probe.[81] Benzenesulfonamide, a potent nanomolar inhibitor of carbonic anhydrase II (CAII), was separately modified with twelve electrophiles including an epoxide, in addition to a fluorescent tag, to yield 12 chemical probes. These were individually incubated with a selection of proteins and subsequently analysed by in-gel fluoresence. Whereas promiscuous electrophiles such as a vinyl sulfone reacted non-selectively, the epoxide probe demonstrated a high selectivity for CAII over other proteins. Labelling by the epoxide probe was abolished in the presence of ethoxzolamide, a potent CAII inhibitor, indicating that modification by the epoxide probe was promoted by a molecular recognition event. Further studies indicated that the epoxide was modified by a histidine residue situated adjacent to the pocket.

1.4.2. Thermodynamic *vs* kinetic drug discovery: receptor accelerated synthesis

In receptor-accelerated synthesis (RAS), a protein brings two binding fragments, each decorated with complementary reactive functionality, into close proximity causing them to undergo an irreversible reaction that would not have occurred in solution. The two complementary functional groups are designed to react only slowly in the absence of a template, but upon binding to the receptor a significant increase in effective molarity makes the reaction pseudo intramolecular, causing it to proceed rapidly. Analysis of reaction mixtures in the presence and absence of the template, usually by LC-MS based techniques, quickly identifies binding combinations. In this way, the protein effectively assembles its own inhibitor from smaller building blocks, Figure 12. The irreversibility of the reaction in RAS is a key and fundamental difference that distinguishes it from DCC. Whereas protein templated DCC results in the amplification of the most thermodynamically stable species, RAS relies on chemistry for which a high kinetic barrier prevents covalent bond formation in solution in the absence of a template. By bringing the components together, the protein lowers the energetic barrier for reaction by stabilising the transition state. This necessitates a product-like transition state if the accelerated products are to be successful inhibitors.[82] Significant work has been carried out to determine that this kinetic rate acceleration corresponds to binding affinity in a number of cases, as will be discussed in the following section.
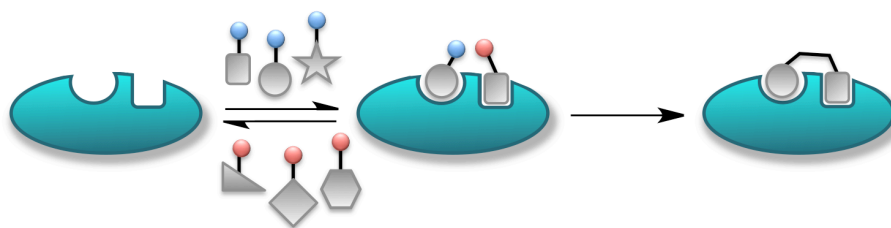
Figure 12 Schematic to illustrate receptor accelerated synthesis. The red and blue spheres represent functional groups able to react with one another once brought into close proximity by the 'template', represented in cyan. Reactive functional groups are brought into close proximity by the binding of ligands to the receptor.

Carnitine acetyltransferase – S_N2 reaction

RAS was conceptually proposed in the 1980s by Jencks who rationalised that enzymes generate a significant rate acceleration, relative to the untemplated reaction in solution, by decreasing the entropy of bound reactants.[83, 84] However, the very first example of RAS was reported in 1969 by Chase and Tubbs, who were interested in the enzyme carnitine acetyltransferase.[85, 86] They wanted to modify amino acids in the vicinity of the active site with either coenzyme A (CoA) or carnitine-based alkylating agents. However, they found that carnitine acetyltransferase was rapidly inhibited by bromoacetyl carnitine only after CoA was added to the reaction mixture, and analogously, by bromoacetyl-CoA only after the addition of carnitine, Figure 13. Based on a series of biochemical experiments, the authors were able to elucidate that, rather than modification of the protein, both carnitine and CoA formed a ternary complex with the enzyme. The bromoacetyl group was then rapidly transferred to carnitine, which subsequently reacted with the CoA thiol in a nucleophilic substitution reaction. The rate acceleration by the template was determined to be significant, such that formation of a CoA-carnitine adduct took more than 90 minutes in solution, but only seconds in the presence of the protein.
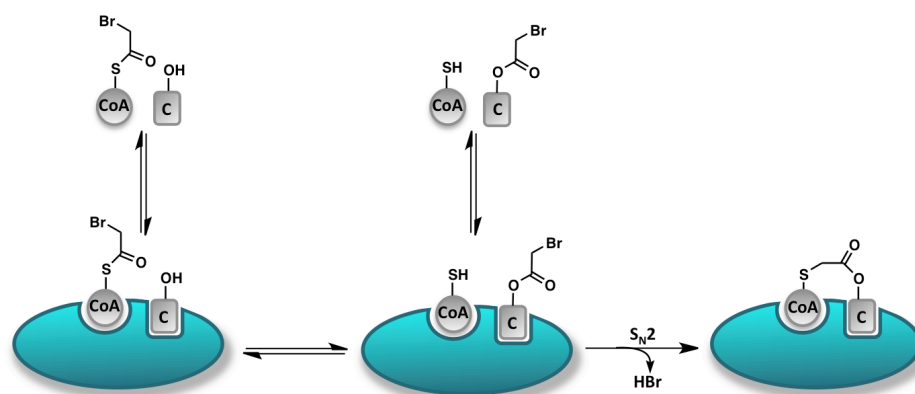
Figure 13 First reported example of RAS. CoA = Coenzyme A. C = carnitine. Carnitine acetyltransferase represented by the cyan ellipse.

Glycinamide ribonucleotide transformylase – S_N2 reaction

In 1991, Benkovic and colleagues reported the formation of a multisubstrate adduct inhibitor, synthesised *in situ* by a protein template.[87] They found that incubation of glycinamide ribonucleotide transformylase (GAR TFase) with its
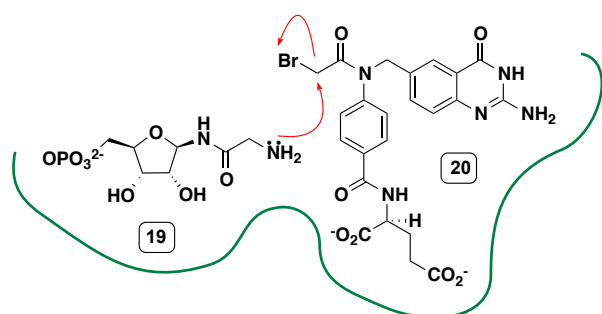
Figure 14 Templated reaction between β-GAR **19** and affinity label **20**. Green line schematically represents the protein pocket.

substrate glycinamide ribonucleotide (GAR) **19** and a folate-derived cofactor affinity label, N-10-(bromoacetyl)-dideazafolate **20**, led to the generation of a new inhibitor by a templated alkylation reaction, Figure 14. Although the natural cofactors for the protein have only micromolar affinities for GAR TFase, the adduct formed by reaction of GAR **19** and N-10-(bromoacetyl)-dideazafolate **20** demonstrates an impressive picomaolar affinity. In 1981, Jencks rationalised that the binding of a molecule A-B is often much greater than

the sum of the individual binding energies A and B.[84] This originates from an entropic penalty (ΔG^s), approximately independent of molecular size, which both A, B and A-B must overcome in order to bind to the protein. As the intrinsic binding energies of A (ΔG^i_A), and B (ΔG^i_B), are smaller than A-B (ΔG^i_{AB}), the binding of A-B is more favourable than the sum of A and B individually by an amount which corresponds to the entropic term, Figure 15.
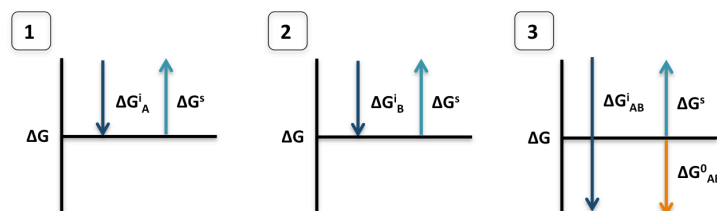
Figure 15 A simplified view of the balance of Gibbs free energies for binding of A, B and A-B to a protein. **1 and 2:** No binding is observed for ligands A or B (in this schematic) as the intrinsic binding energy (ΔG^i) is equal to the entropic penalty (ΔG^S), a term which is approximately independent of molecular weight. **3:** The intrinsic binding energy of A-B to the protein equals the sum of the intrisic binding energy of A and that of B. However, as the entropic penalty is approximately independent of molecular weight, a binding energy (ΔG^0_{AB}) is observed (orange arrow), which is equal to ΔG^S.

Whilst the GAR TFase inhibitor formed by reaction of GAR **19** and N-10-(bromoacetyl)-dideazafolate **20** had excellent binding affinity, the presence of the charged phosphate group prevented cellular uptake, resulting in poor bioavailability and preventing clinical development. As GAR TFase has the ability to assemble the drug *in situ* in the presence of the natural substrate GAR **19**, Benkovic and colleagues investigated the potential for folate analogues to act as prodrugs.[88, 89] N-10-(bromoacetyl)-dideazafolate **20** was found to be too reactive to be adopted for this purpose,

Figure 16

prompting a search for a suitable replacement folate analogue. Substitution of the α-bromo-amide with a dibromide functionality generated a compound which formed a high affinity adduct with natural substrate GAR **19** in the presence of enzyme, Figure 16. This was initially presumed to proceed *via* S_N2 bromide displacement, but upon generation of a crystal structure, a hydroxy group was observed in the place of the tertiary bro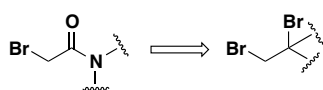mide. The authors proposed that fast generation of the bromonium ion, ring opening with water to form the bromohydrin, and subsequent displacement of the second bromide generated the epoxide as the active species for RAS.

Bovine carbonic anhydrase II – S_N2 reaction

Huc and Lehn utilised the displacement of an α-halogen by a thiol for their RAS approach, three decades after the initial report by Chase and Tubbs.[90] Sulfonamide **21**, a known inhibitor of bovine carbonic anhydrase (CA II), was incubated with binary mixtures of chlorides in the presence and absence of CA II. It was observed that the protein consistently accelerated the synthesis of the higher affinity inhibitor, an observation later confirmed by Kolb.[91] As an example, incubation of CA II with a binary mixture of chlorides **22** and **23** resulted in a 92 % yield of sulfide **24** and only an 8 % yield of sulfide **25**. However, in the absence of CA II, a 50 % yield of each sulfide was observed. The increase in the yield of sulfide **24** from 50 to 92 % is consistent with its affinity for CAII, which is 9-fold higher than sulfide **23**, Figure 17. This gives rise to a selectivity of *ca*. 0.2, i.e. the relative quantity of a binder to its closest

competing compound divided by the relative difference in binding constants.[92] This selectivity value is similar to that achieved with DCL chemistry.[92]
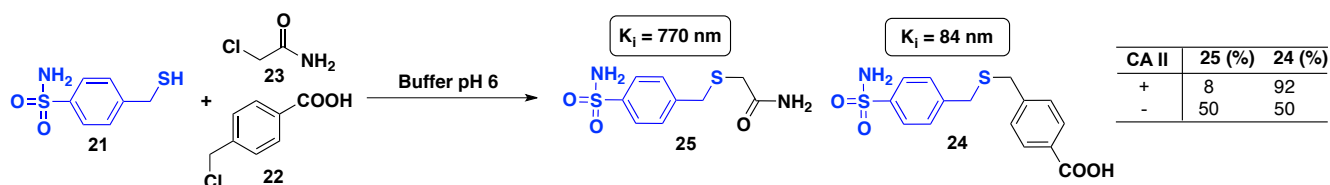

Figure 17 Receptor accelerated synthesis using carbonic anhydrase and known sulfonamide inhibitor **21**.

Kallikrein – nucleophilic aromatic substitution

The use of electrophilic aromatic substitution as the irreversible reaction in RAS, was demonstrated by Mosbach *et al*.[93] The protease kallikrein was incubated with a selection of four amines in addition to a substituted 4,6-dichlorotriazine. This led to the templated synthesis of the expected four products, with the rate acceleration of each product closely linked to its binding affinity. The amplification of each binder, relative to its closest competing compound, was *ca*. 1.5 times higher than their relative binding constants, giving rise to a selectivity of 1.5. Preincubation of kallikrein with high affinity inhibitor aprotinin significantly reduced the formation of S_NAr product. Interestingly, the templated reaction resulted in the formation of twice as much triazine **26** as its enantiomer triazine **27**, reflecting their binding constants of 33 and 47 µM respectively, Figure 18.
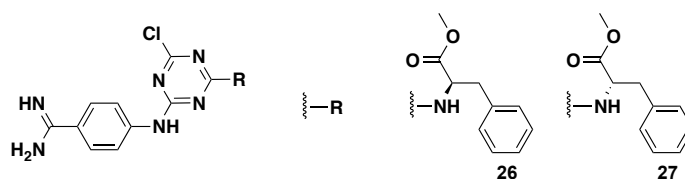
Figure 18 Enantiomeric inhibitors **26** and **27** synthesised using kallikrein as a template.

SIRT enzymes – S_N2 reaction

The catalytic mechanism of lysine deacetylation by the sirtuin (SIRT) enzymes was utilised by Suzuki and colleagues in the design of sirtuin-selective inhibitors.[94] The SIRT enzymes catalyse NAD^+-dependent deacetylation of lysine residues, resulting in the release of nicotinamide and O-acetyl-ADP-ribose, Figure 19.[94] Attack from the lysine amide oxygen onto the 1'-carbon of the ribose ring of NAD^+ displaces nicotinamide and results in the formation of an imido ester conjugate. The enzyme subsequently catalyses imido ester hydrolysis, releasing the free amine lysine residue. Coumarin-based inhibitor **28** was reported by Jung *et al*. to be deacetylated by SIRT1, and can be used as a substrate for fluorescence-based assays.[95] Introducing an electron withdrawing group into the α-position of the acetamide led to inhibitor **29**, an analogue of **28**. The electron withdrawing group was rationalised by Suzuki *et al*. to stabilise an anion at this position, and thereby increase the nucleophilicity of the α-carbon. Attack onto the NAD^+ ribose ring from the α-carbon then results in the formation of a highly thermodynamically stable C-C bond, generating *in situ* a stable, high affinity inhibitor which occupies both the NAD^+ and the acetylated lysine pockets. A number of anion stabilising

groups were investigated, including esters, ketones and sulfones amongst others. Use of an ethyl ester generated the highest affinity inhibitor, with IC_{50} of 3.9 µM and selectivity for SIRT1 over other SIRT enzymes.
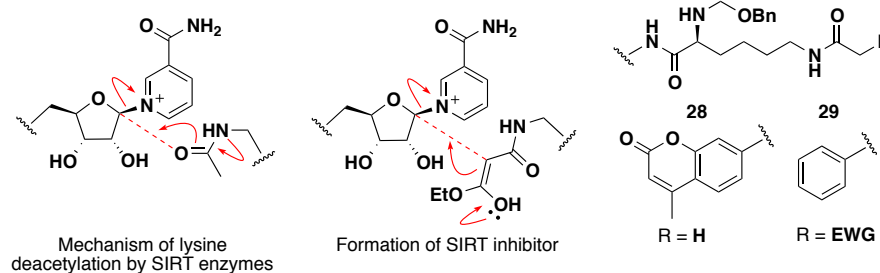
Figure 19 Comparison of the mechanism of NAD$^+$-dependent SIRT catalysed lysine deacetylation, and the approach to develop SIRT inhibitors by a receptor-accelerated synthesis.

Bcl-X$_L$ – sulfo-click reaction

Manetsch *et al*. developed a PPI inhibitor targeting Bcl-X$_L$ in an impressive demonstration of RAS.[96] Interuption of the interaction between anti-apoptotic Bcl-X$_L$ with pro-apoptotic protein partners is thought to induce apoptosis *via* initiation of a signalling cascade. Bcl-X$_L$ has therefore become an attractive target for the development of anticancer agents. In their work, Manetsch *et al*. utilise the reaction of a thioacid and sulfonyl azide to generate an amide, a reaction that they proposed as particularly suitable for RAS, Figure 20.[97, 98]
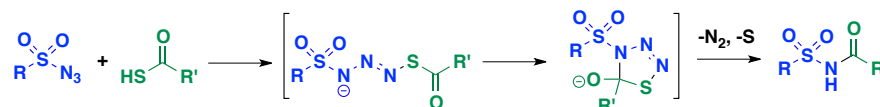
Figure 20 Mechanism for reaction of a sulfonyl azide with a thioacid to generate an amide, termed the 'sulfo-click' reaction.

Incubation of Bcl-X$_L$ with 6 sulfonyl azides and 3 thioacids in all possible 18 binary combinations led to the acceleration of only known inhibitor **30**, reported previously by Abbott to have a K_i of 19 nM, Figure 21.[99, 100] This rate accelerlation was dramatically reduced in the presence of BH3 peptides bak or bim, both known to interact with Bcl-X$_L$ at the PPI interface. Simultaneous incubation of Bcl-X$_L$ with all 6 azides and 1 thioacid impressively led to only the amplification of compound **30**, highlighting the potential for RAS approaches to be used in a high-throughput manner.
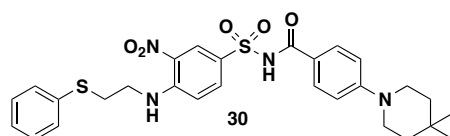
Figure 21

In an extension of this work, Manetsch *et al*. synthesised a larger library of thioacids and sulfonyl azides, and incubated them as previously in the presence and absence of Bcl-X$_L$ in 81 parallel binary experiments.[101] This identified three new acylsulfonamide inhibitors in addition to sulfonamide **30**. Mutagenesis of Bcl-X$_L$ residues predicted to be key for binding led to reduced amplification of the acylsulfonamide products. Including the 4 hit

compounds, 37 acylsulfonamides were synthesised and tested for their ability to disrupt the Bcl-X$_L$/Bak BH3 PPI. Strikingly, the 4 compounds identified during RAS experiments were the most potent compounds by a significant degree. Additionally, all thioacid and sulfonylazide building blocks were determined to be very weak inhibitors, indicating RAS as a powerful technique to build potent inhibitors from weakly binding building blocks. Both the reliability and the bioorthogonality of the reaction between thioacids and sulfonylazides led Liskamp to term it the 'sulfo-click'* reaction.[103]

Huisgen cycloaddition

A new strategy for RAS was introduced by Sharpless, who realised the potential of the azide-alkyne Huisgen cycloaddition as a bioorthogonal ligation reaction for use in RAS.[104] Whilst the work developed by Huc and Lehn could be envisaged to suffer from side reactions, such as a cysteine thiol reacting with one of the chloride substrates, a bioorgthogonal ligation reaction reacts independently of the myriad chemistry found in a biological system. Previous work that inspired Sharpless included that by Mock and colleagues, who elegantly demonstrated that cucurbituril, a nonadecacyclic cage, acted as an entropic trap for the azide and alkyne and kinetically enhanced the rate of the cycloaddition by 10^5-fold.[105] In addition, work by Bertozzi demonstrated the power of bioorthogonal reactions to probe biological systems.[106, 107]

The first biological target explored by Sharpless and colleagues in their investigation of RAS was acetylcholine esterase (AChE), which has two distinct binding pockets in close proximity to one another.[108-110] The catalytic pocket sits at the bottom of a 20 Å deep, narrow 'gorge' with a periheral pocket located adjacent to the rim. A number of ligands had previously been determined as site-specific inhibitors of AChE; tacrine specifically targets the catalytic pocket with a K$_d$ of 18 nM and propidium specifically binds at the peripheral pocket with a K$_d$ of 1.1 μM. The enzyme was incubated with a selection of 8 azide and alkyne-modified tacrine-based ligands, and 50 propidium-based ligands, also decorated with either azide or alkyne functionality in 189 parallel experiments. From this virtual library of 378 bivalent ligands (*syn* and *anti* products), AChE accelerated the rate of only six combinations. Interestingly, comparison with authentic samples revealed that the protein selectively accelerated the synthesis of only the *syn*-triazoles, which exhibited very low K$_d$ values between 33 fM to 3 pM. These were found to be 10-1000 times stronger than the corresponding *anti*-congeners, which have a more elongated form and a significantly compromised fit within the active site gorge. In addition, analysis of crystal structures of the bound ligands identified AChE to be in a previously unobserved conformation, suggesting that the RAS methodology has the potential to trap enzymes in unexpected low abundance conformations that may be missed by more conventional screening approaches, in addition to the identification of novel building block combinations.

Detailed studies were carried out by Sharpless and Kolb to determine the propensity of RAS to generate false negative and positive results.[91] 24 *anti*-substituted triazoles were synthesised, and their K$_d$ values against bovine carbonic anhydrase II (bCAII) determined. Those triazoles which were previously found to be generated by a templated bCAII

---

* Click reactions were introduced as a chemical philosophy by K. Barry Sharpless in 2001. Click reactions "must be modular, wide in scope, give very high yields, generate only inoffensive byproducts that can be removed by nonchromatographic methods, and be stereospecific (but not necessarily enantioselective)".[102]

synthesis were determined as potent subnanomolar inhibitors, whereas those from non-templated building block combinations were found to be poor inhibitors. This indicated that RAS is not susceptble to the generation of false positive results. However, there were a few bCAII inhibiting combinations which were not detected by RAS, indicating that this technique is susceptible to false negatives.

Work carried out with HIV-1 protease demonstrated that the building blocks used in RAS do not need to be high affinity binders.[111] Alkyne **31**, with an $IC_{50} > 100$ μM and azide **32** with an IC_{50} of 4 μM were incubated with the HIV protease as a template, Figure 22. This led to a 10-fold increase in the overall product formation over the background reaction, in addition to an increased regioisomeric ratio of 18:1 in favour of the *anti*-triazole **33** from the 2:1 background ratio. *Anti*-triazole **33** was determined to be an inhibitor of HIV-1 protease with an $IC_{50} = 6$ nM ($K_i = 1.7$ nM). During the course of this work, the authors also demonstrated the feasibility of multicomponent incubations, extending the scope of RAS as a useful tool in the development of protein inhibitors. Incubation of the HIV-1 protease with 5 alkynes and 1 azide led to the amplification of only one triazole product, which was detected by HPLC and mass spectrometry in single ion mode (LC-MS SIM).
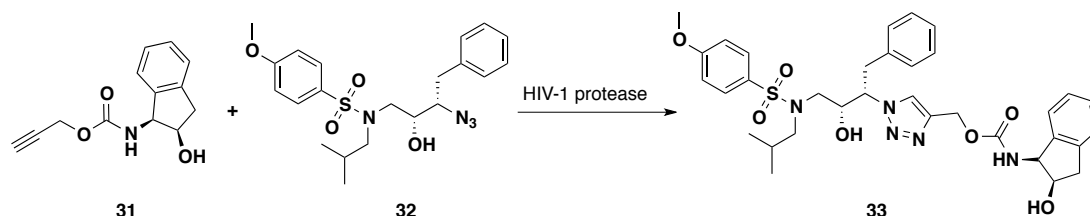
Figure 22 Alkyne **31** and azide **32** react in the presence of HIV-1 protease to generate *anti*-triazole **33** in an increased rate over the background reaction, and in increased selectivity.

RAS is a valuable addition to the arsenal of tools available for drug discovery. The suitability of the technique to identify potent inhibitors from weak binding building blocks suggests it may be valuable for fragment linking, which although conceptually simple, has proven extremely difficult in practice. The main disadvantage is that, in the absence of a known binder, RAS is not suitable for site-directed drug discovery.

1.5. The capture group in KTGT

The fundamental requirement for a suitable KTGT capture group was considered to be its rate of reaction with cysteine, which must be slow in the absence of a template, but amenable to a proximity induced rate acceleration. In addition, the reaction must be completely irreversible, compatible with aqueous solvent, selective for cysteine and inert to the myriad other functionality present under the screening conditions, and the capture group must be synthetically facile to install. Two functional groups, the acrylamide and the vinyl sulfonamide, were considered for use in KTGT as outlined in the following section.

1.5.1. Acrylamide

The suitability of the acrylamide functional group for KTGT is perhaps best illustrated by its presence in a number of kinase inhibitors which are currently in clinical trials.[112] Optimised inhibitors have been shown as rapid inactivators of the target kinase, whilst exhibiting impressive selectivity with respect to other kinases, other proteins more

generally and small molecule thiols such as glutathione and DTT. Such irreversible inhibitors have been shown to outperform their reversible counterparts both *in vitro* and in animal models.[113]

In work carried out by Meares *et al*. a known chelate ligand of the antibody CHA255 was modified with an acrylamide function group.[114] This was carried out in conjunction with a co-crystal structure, allowing the acrylamide to be added to a position on the ligand adjacent to a suitable cysteine thiol on the antibody. Addition of the acrylamide modified-ligand to raw tissue culture medium from cells expressing the recombinant antibody led to 50 % modification of CHA255 within 10 minutes, whereas modification of other protein thiols was negligible over a 2 h time period. This suggests the reactivity of the acrylamide is sufficiently low for the background reaction with endogenous nucleophiles to be negligible. In the presence of a protein template, a rapid reaction ensues.

An acrylamide functional group was also used by Belshaw *et al*. who engineered a mutant cysteine residue adjacent to the cyclosporin A binding site in cyclophilin A, in addition to modification of cyclosporin A with an acrylamide.[115] As for the antibody CHA255, this was also carried out with the guidance of receptor-ligand co-crystal structures to ensure the nucleophile and electrophile were suitably positioned for reaction acceleration. Impressively, the modified cyclosporin A was able to selectively modify mutant cyclophilin A in complex media such as Jurkat T-cell cytosolic extract. Addition of excess unmodified cyclosporin A completely abrogated affinity labelling, indicating that the acrylamide required the binding pocket to template the reaction.

Singh *et al*. reported an inhibitor of the viral protease HCV NS3/4A, which contained an acrylamide group to covalently modify a non catalytic cysteine residue.[116] The inhibitor demonstrated an IC_{50} against HCV NS3/4A of 2 nM whilst an analogue with the acrylamide Michael acceptor saturated was almost 1000 times less potent (IC_{50} = 1.1 µM). The acrylamide-inhibitor demonstated high selectivity for HCV NS3/4A over a panel of other proteases and in addition, demonstrated no nonspecific reactivity towards the small molecule thiol glutathione. Mass spectrometry analysis confirmed the formation of a single adduct between HCV NS3/4A and the inhibitor, suggesting the acrylamide was resistant to the other nucleophiles on the protein surface.

Fry *et al*. reported a novel class of acrylamide-modified quinazoline inhibitors against the epidermal growth factor receptor (EGFR).[113] Modification of a previously reported inhibitor **34**,[117] yielded acrylamide **35** and analogue acrylamide **36** as potent and selective, irreversible inhibitors of the EGFR, active both *in vivo* and *in vitro,* Figure 23.
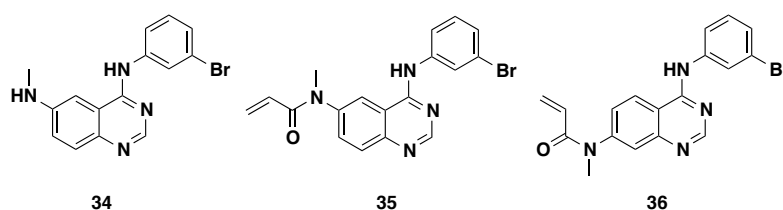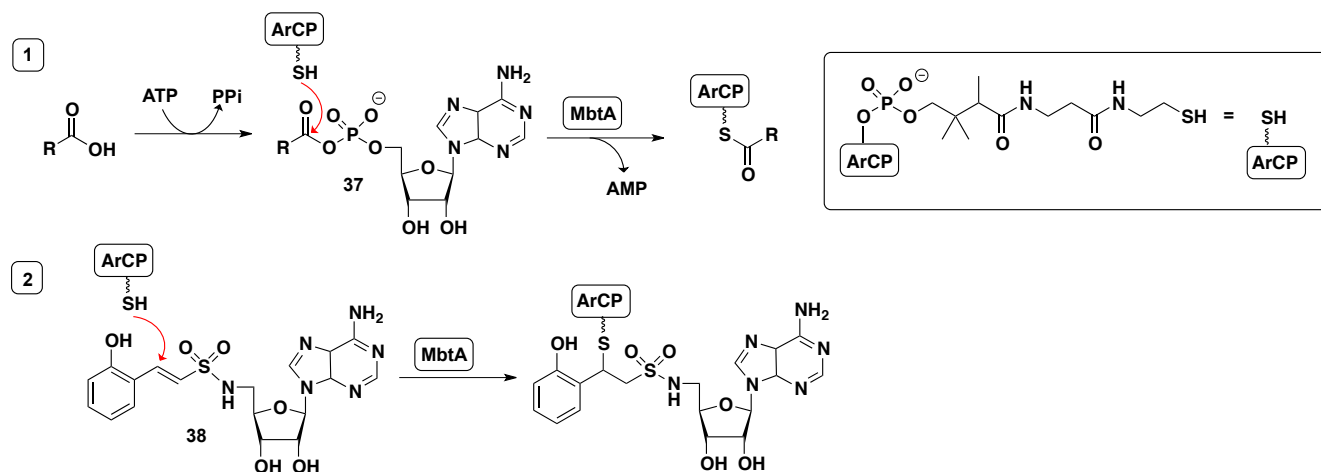

Figure 23

Alkylation by inhibitor **35** was selective for cys773 within the ATP pocket, despite the presence of four other cysteine residues. Both inhibitors **35** and **36** were found to be inactive against insulin, PDGF and basic FGF receptor tyrosine kinases, in addition to protein kinase C, with approximately 10^5-fold selectivities for EGFR. Docking studies indicated

that acrylamide **35** bound in the EGFR ATP pocket, bringing the β-carbon atom of the acrylamide to within a distance of 2.8 Å of the nucleophilic cys773 thiol atom. Interestingly, inhibitor **36** placed the acrylamide β-carbon atom at least 7 Å away according to the docking model, perhaps explaining why this inhibitor modifies the cysteine thiol with slower reaction kinetics. The authors suggest that the Michael addition to the acrylamide group in inhibitors **35** and **36** only occurs because of the increased proximity for the reaction, induced by binding in the ATP pocket.

1.5.2. Vinyl sulfonamide

In 2003, Roush *et al*. reported a study of the Michael addition rate of 2'-(phenylethyl)thiol to a range of Michael acceptors, including the vinyl sulfonamide[*].[118] The vinyl sulfonamide was found to be the least reactive, with the rate of thiol addition to phenyl vinyl sulfonate esters proceeding approximately 3000 times faster. This suggested the vinyl sulfonamide as a potential group for use in KTGT, as it is less likely to react non-selectively than other Michael acceptors. In addition to this work, vinyl sulfonamides have been reported to react 390 times faster with cysteine than with lysine at pH 8.1 in a phosphate buffer.[119]

Qiao *et al*. have demonstrated vinyl sulfonamides as mechanism-based affinity probes.[120] The adenylating enzyme MbtA selectively transfers the acyl group from acyladenylate intermediates **37** to aryl carrier proteins (ArCP), with loss of AMP, Figure 24. A vinyl sulfonamide acyladenylate analogue **38** was unreactive to Michael addition with the ArCP thiol in the absence of the MbtA enzyme. In the presence of MbtA, electrophile **38** binds to the enzyme, which templates the irreversible conjugate addition of the ArCP thiol.

Figure 24. 1. Adenylating enzyme MbtA catalyses the transfer of the acyl group from acyladenylate **37** to aryl carrier protein (ArCP). **2.** Conjugate addition of ArCP to vinyl sulfonamide-adenylate **38** only occurs in the presence of MbtA.

Vinyl sulfonamides have been described as providing a polarised and yet inert unsaturated bond, and are unreactive towards serine proteases, metalloproteases, non-active site cysteines and circulating thiols such as glutathione,[121] whilst being potent inhibitors of the cysteine proteases when embedded within a scaffold which confers affinity for the active site pocket.[122]

---

[*] This study did not include the acrylamide Michael acceptor.

1.6. Aim

The overall aim for this research was the development of a site-directed methodology for the discovery of low molecular weight protein-binding ligands. By screening mixtures of fragments with a reactive appendage against the protein target, binding ligands should be rapidly identified using mass spectrometry techniques. Covalent adducts formed should be stable to proteolytic digestion allowing the position of modification to be identified by analysis of the resulting peptides. Libraries of modified fragments should be amenable to rapid synthesis. Both the acrylamide and vinyl sulfonamide functional groups will be investigated for use in this methodology.

2. Preliminary work towards kinetic template-guided tethering

2.1. HPLC studies to determine reaction irreversibility

The instantaneous reaction between simple thiols and 2-cyanoacrylates at physiological pH was reported in the 1960s, but at this time the products could not be isolated or characterised.[123] This suggested that the conjugate addition to such electrophiles was reversible, and this was conclusively demonstrated by Serafimova *et al*. in 2012.[124] This reversibility was thought to arise from the increased acidity of the αC-H protons, and in accordance with this the Michael addition to acrylates, acrylonitriles and acrylamides was found to be irreversible, resulting in the generation of stable thioether bonds.[124] Surprisingly, the reaction between enones and thiols was found to be freely reversible under physiological conditions and was used by Greaney *et al*. to probe glutathione S-transferases using a dynamic combinatorial approach.[125, 126] The irreversibility of the Michael addition of thiols to vinyl sulfonamides and acrylamides is largely assumed within the literature. As discussed, acrylamides have been utilised as irreversible covalent warheads in kinase and non-kinase inhibitors,[127] five of which are currently in clincal trials, and vinyl sulfonamides have similarly been used as reactive functional groups to irreversibly inhibit the cysteine proteases.[120] However, a systematic study has not been reported that conclusively demonstrates the irreversibility of these reactions over the pH 8-11 range. This was considered important for their use in KTGT; An irreversible reaction ensures that the observed results represent a kinetic rate enhancement due to reduction of the reaction energy barrier upon fragment binding to protein, as opposed to a thermodynamic distribution as would be observed for DCC.

For both reactions, HPLC studies were undertaken using model thiols to investigate reaction irreversibility. A small collection of vinyl sulfonamides **39**-**45** and acrylamides **46**-**55** were synthesised to carry out proof-of-concept work, Figure 25.
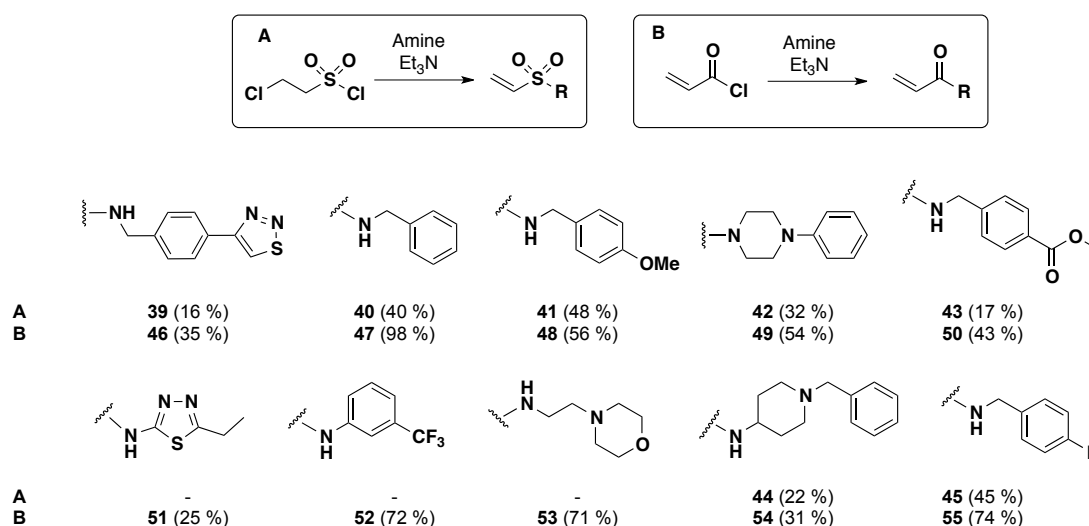

Figure 25 Synthesis of vinyl sulfonamides from the corresponding amine and 2-chloroethanesulfonyl chloride (A) and acrylamides from the corresponding amine and acryloyl chloride (B).

A subset of the collection included five benzylamines, four with *para* modifications. These were included on the basis that they should all demonstrate equivalent conjugate addition reactivity with the electrophilic moiety insulated from

the varying portion of the molecule by the benzylic methylene. Although these acrylamides/vinyl sulfonamides were synthesised for use in proof-concept studies, the amine fragments were chosen to be rule-of-three compliant such that the collection could be incorporated at a later time into a larger library.[8] The vinyl sulfonamides were synthesised from 2-chloroethanesulfonyl chloride and available amines in the presence of triethylamine base to effect the chloride displacement and elimination in one step. The acrylamides were synthesised, also in one step, from acryloyl chloride and available amines in the presence of triethylamine base.

To determine reaction irreversibility a procedure was employed as illustrated in Figure 26, whereby two different electrophiles (either vinyl sulfonamides or acrylamides) were reacted separately with a nucleophilic thiol and the reaction allowed to proceed until no futher changes were observed. A second electrophile was then added to each reaction and any further changes monitored over time. An irreversible reaction should yield two different reactant-product distributions whereas a reversible reaction should converge to a single thermodynamic distribution.
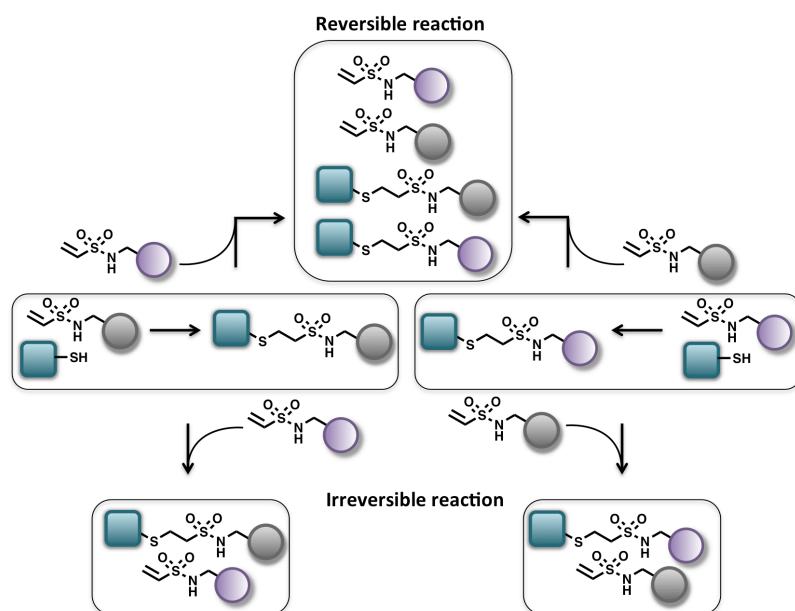
Figure 26 Schematic to illustrate the procedure adopted to test reaction irreversibility. Two electrophiles (either vinyl sulfonamide or acrylamide) were reacted separately with a nucleophile (model thiol) and the reaction allowed to proceed until no further changes were observed by HPLC. To each reaction was then added the second elecrophile. If the reaction is reversible (top) then both reactions should converge to the same thermodynamic distribution over time. If the reactions are irreversible then two separate distributions are generated.

Benzylmercaptan was initially chosen as the model thiol, due to its strong UV chromophore which allows it to be monitored by HPLC in addition to the electrophile. However, due to poor aqueous solubility at the concentrations required to generate reliable HPLC data, other thiols such as N-acetyl L-cysteine, glutathione and mercaptosuccinic acid were adopted. Whilst *N*-acetyl L-cysteine-vinyl sulfonamide conjugation addition products were facile to separate from starting vinyl sulfonamides by HPLC, many of the analogous acrylamide adducts were inseparable from their starting acrylamides despite extensive efforts to optimise solvent gradients. Mercaptosuccinic acid generated acrylamide-conjugate addition products which were significantly more polar than the starting acrylamides, presumably due to the additional polar carboxylic acid functionality. These mixtures were therefore more readily separated (see appendix I, p213, Figure 119). However, the reaction between acrylamides and mercaptosuccinic acid

was prohibitively slow. Reaction between acrylamides and glutathione proceeded at a more reasonable reaction rate and also gave separable products by HPLC. The gradual formation of disulfide over time using N-acetyl L-cysteine, glutathione or mercaptosuccinic acid cannot be measured by HPLC as neither compound has a suitable UV chromophore. Authentic samples of a selection of the conjugate addition products were synthesised, Scheme 1 and analysed by HPLC to confirm retention times.
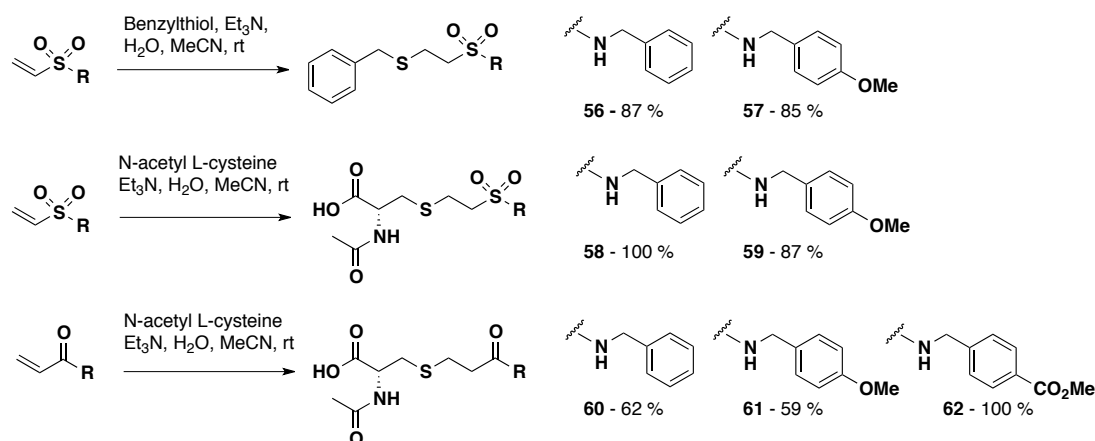

Scheme 1 Synthesis of vinyl sulfonamide and acrylamide conjugate addition products.

One equivalent of *N*-acetyl L-cysteine was added separately to both vinyl sulfonamides **40** (vial one) and **41** (vial two) in aqueous buffer, pH 8, and the reactions monitored by HPLC, Figure 27 and Figure 28. Both reactions were observed to proceed directly to products (confirmed using authentic samples of conjugate addition products) with no side-product formation. Neither reaction went to completion, presumably due to competing thiol oxidation to disulfide. After 460 min (vial one) or 320 min (vial two), one equivalent of vinyl sulfonamides **41** and **40** respectively were added to the mixtures and both reactions monitored for a further 850 min. Formation of a second conjugate addition product was not observed in either reaction, indicating complete irreversibility on this time scale. Two sets of acrylamide pairs **55/46** and **49/46** were used with glutathione as the model thiol to demonstrate the irreversibility of conjugate addition to acrylamide at pH 8, (data shown in appendix I, p213, Figure 120 and Figure 121). Irreversibility for both vinyl sulfonamide and acrylamide conjugate additions was also confirmed at pH 11. Using acrylamides **46** and **51**, the reaction with both glutathione and N-acetyl L-cysteine at pH 11 was determined to be irreversible over a 12 h time period (see appendix I, p214, Figure 122 and Figure 123). Vinyl sulfonamides **39** and **41** were used to determine reaction irreversibility between vinyl sulfonamide and N-acetyl L-cysteine at pH 11 (see appendix I, p215, Figure 124). Furthermore, an authentic sample of conjugate addition product **59** was added to vinyl sulfonamide **39** at pH 11, and irreversibility confirmed by the lack of formation of a second conjugate addition product or second acrylamide (see appendix I, p216, Figure 125).

It was noted during the course of these studies that acrylamides **51** and **52**, the only compounds conjugated to aromatic systems, both reacted very rapidly with glutathione compared to other acrylamides, with reactions gone to completion in approximately 5 min. The greater electron withdrawing nature of the ArN substituent, compared to ArCH$_2$N, increases the reactivity of the acrylamide towards Michael addition. This was assumed to render these acrylamides unsuitable for KTGT experiments due to the high expected background reaction.
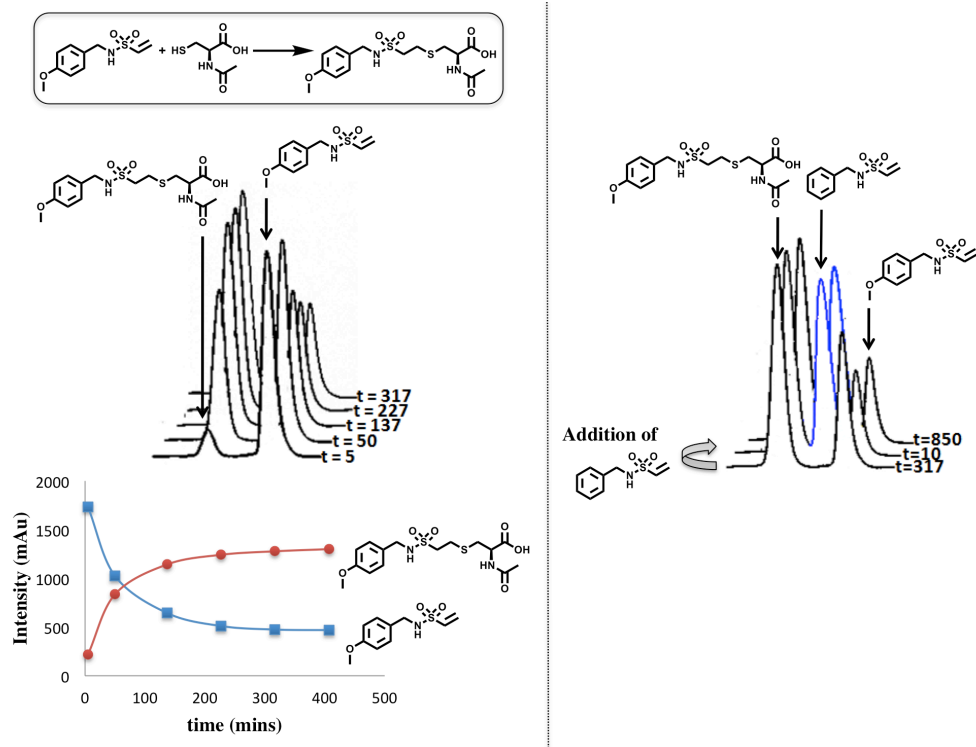
Figure 27 (Left hand side) Overlay of HPLC traces for the addition of vinyl sulfonamide **41** to *N*-acetyl L-cysteine. As expected, the peak due to vinyl sulfonamide **41** diminishes over time, and a new peak for the conjugate addition product **59** appears. **(Right hand side)** Overlay of HPLC trace just before addition of vinyl sulfonamide **40** and the HPLC traces 10 and 850 minutes after addition. Reactions were carried out in ammonium bicarbonate buffer (100 mM) pH 8. Time for each measurement is indicated in minutes.
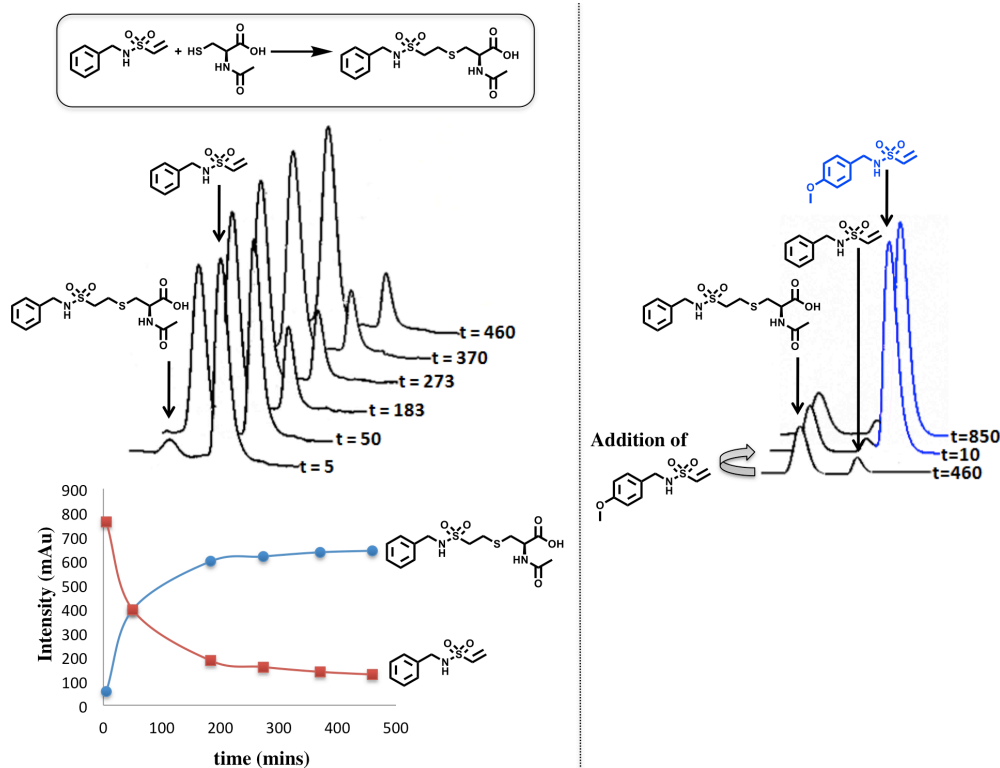
Figure 28 (Left hand side) Overlay of HPLC traces for the addition of vinyl sulfonamide **40** to *N*-acetyl L-cysteine. As expected, the peak due to vinyl sulfonamide **40** diminishes over time, and a new peak for the conjugate addition product **58** appears. **(Right hand side)** Overlay of the HPLC trace just before addition of vinyl sulfonamide **41** and the HPLC traces 10 and 850 minutes after addition. Reactions were carried out in ammonium bicarbonate buffer (100 mM) pH 8. Time for each measurement is indicated in minutes.

To summarise, HPLC studies confirmed the thiol-acrylamide and thiol-vinyl sulfonamide conjugate addition reactions to be irreversible at both pH 8 and pH 11 over the time scales monitored. Both electrophiles were converted smoothly to products with no side-product formation.

It was noted during the irreversibility studies that the acrylamides were generally significantly less reactive towards conjugate addition than the vinyl sulfonamides. This was conclusively shown for one vinyl sulfonamide/acrylamide pair, Figure 29. Vinyl sulfonamide **45** and acrylamide **55** were mixed separately with reduced glutathione and the reactions monitored by HPLC over time. The vinyl sulfonamide was observed to be significantly more reactive than the acrylamide.
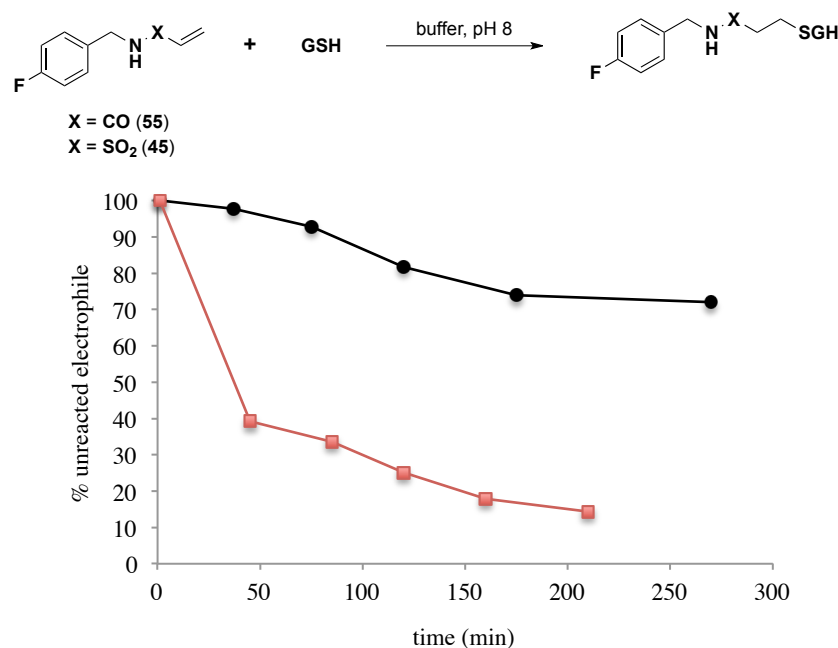

Figure 29 Comparison of the reactivity of the vinyl sulfonamide and acrylamide functional groups towards conjugate addition of reduced glutathione (GSH). Glutathione and electrophile were mixed at equimolar concentrations in an ammonium bicarbonate buffer (pH 8) and the reaction monitored by reverse phase HPLC. The area under the peak of the unreacted electrophile, normalised to the value at t = 0 min is plotted against time. Black trace represents reaction of acrylamide **55**, red trace represents reaction of vinyl sulfonamide **45**.

2.2. Initial attempts to develop KTGT using cdc25A

With the Michael addition of small molecule thiols to acrylamides and vinyl sulfonamides determined as irreversible under aqueous conditions, initial work in the use of these functional groups to identify inhibitors of cdc25 phosphatases was undertaken. Cdc25A has five native cysteine residues; cys430 (active site cysteine), cys441, cys476, cys384 and cys480, Figure 30. Examination of the cdc25A crystal structure (PDB code 1C25) indicated that cys430, cys441 and cys476 were solvent exposed and may therefore compromise tethering specificity. Of the residues surrounding the active site, tyr386 was well placed to tether fragments into the active site pocket, Figure 31.
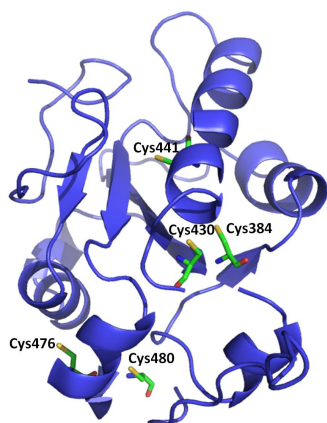
Figure 30 Crystal structure of native cdc25A (PDB 1C25) with all 5 cysteines highlighted. In cdc25A' cys430, cys441and cys476 have been mutated to serine. Cys384 and cys480 appear buried within the interior of the protein.
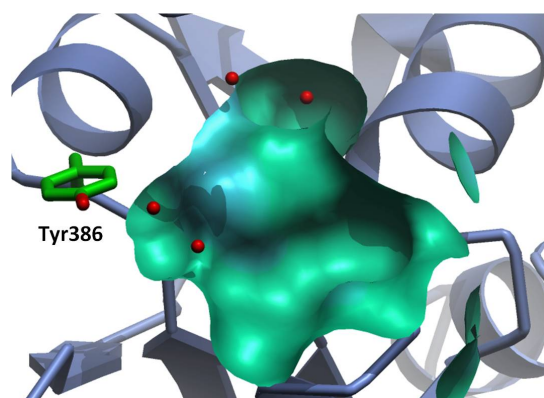
Figure 31 Active site pocket of cdc25A (green) with tyr386 highlighted. PDB code 1C25.

A quadruple cdc25A mutant of the catalytic domain was therefore required (cdc25A'), with the solvent exposed cysteines mutated to non-nucleophilic residues and with tyr386 mutated to cysteine. Such extensive mutation of native cysteine residues can cause disruption to the tertiary structure of the protein if key structural disulfide bridges are removed. In cdc25A, cys430 resides in close proximity to cys384, termed the 'backdoor cysteine', which functions to protect the active cys430 during oxidative stress by formation of a disulfide bond. This disulfide bond was therefore assumed to have no structural function, as the enzyme is active in its absence. Cys480 resides in close proximity to cys476 but these residues do not appear to form a disulfide bond in the cdc25A crystal structure. Disruption of disulfide bridges was therefore hypothesised not to cause a major structural change to cdc25A. There is no consensus amino acid substitution for cysteine;[128] alanine is thought to be the closest match in terms of hydrophobicity (for non-charged cysteine residues), whereas serine provides a closer size match. Serine residues were chosen to replace the solvent exposed cysteine groups.

The quadruple mutant DNA *cdc25A'* was generated by PCR from an available construct (pGEX-KG vector containing wild type *cdc25A*[*]) and cloned into a pET21a expression vector (pET21a-*cdc25A'*).[129]† Expression of the protein was carried out using *E. coli* BL21 (DE3) cells which were transformed with the plasmid by electroporation. After the required growth of the cells (usually to a volume of 2 L), expression was induced by addition of IPTG. Specifically, this induces expression of the T7 RNA polymerase, which begins rapid and extensive translation of the *cdc25A'* gene within the pET21a plasmid, which contains a T7 promoter region. Extremely high yields of the desired mutant cdc25A' protein were obtained using this expression system.

The cells were lysed by sonication and the desired protein extracted from the lysate using anionic beads composed of an insoluble resin with attached sulfopropyl groups. The protein was gradually eluted from the beads using an increasing linear NaCl gradient which disrupts protein-bead electrostatic interactions. As this protein is an inactive mutant with the active site cysteine mutated to serine, an activity assay could not be used to detect the cdc25A' in the fractions. Each fraction was therefore subjected to SDS PAGE, and the elution of cdc25A' visualised by staining for total protein with Coomassie blue, Figure 32. Fractions which contained cdc25A' were combined and concentrated using a 10 kDa centrifugal filter and the retentate centrifuged to remove the significant quantity of precipitation

---

* Generated by coworker J. C. Collins.
† Work previously carried out by R. H. Nonoo as part of MRes degree.

generated during the concentration process. The filtrate was subjected to further purification by gel filtration generating cdc25A' of reasonably high purity, Figure 32. The cdc25A' precipitate was re-dissolved in a TRIS-HCl buffer containing 6 M urea and dialysed into buffer with a gradually decreased concentration of urea over a 24 h period in accordance with standard literature protocols to re-fold precipitated protein. The protein obtained by this method was of higher purity than that obtained by gel filtration, Figure 32.
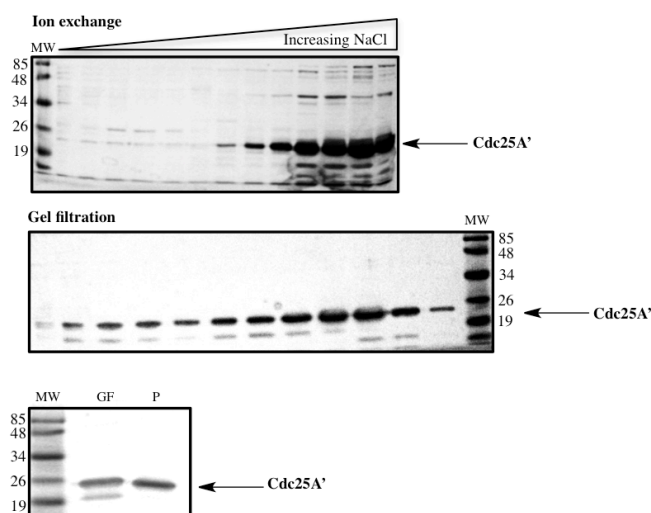
Figure 32 Purification of cdc25A' by ion exchange and either gel filtration (GF) or precipitation (P).

A thermal shift assay was used to determine whether the cdc25A' generated by precipitation was folded. This involved incubating the protein with a fluorescent reporter dye, Sypro Orange, which is effectively quenched in aqueous solution but upon interaction with the hydrophobic interior of protein begins to fluoresce with high quantum yield. This generates a 'melt curve', shown schematically in Figure 33, from which the protein T_M can be calculated from the first derivative. Cdc25A' (isolated by precipitation) generated a melt curve upon heating, although the T_M was observed to be *ca*. 5 °C lower than for active cdc25A triple cysteine mutant,[129]* Figure 34.
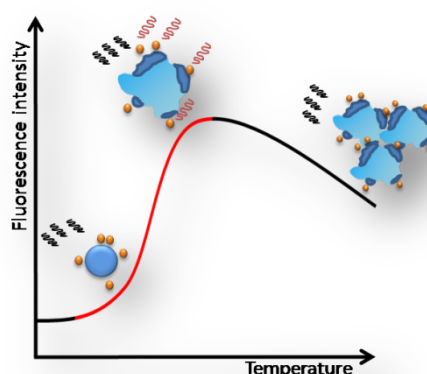

Figure 33 Depiction of a typical melt curve. The blue sphere represents a folded protein, the orange spheres represent the dye Sypro Orange and the dark blue patches represent hydrophobic regions exposed upon protein unfolding.

---

* Worked carried out by R. H. Nonoo as part of MRes degree.
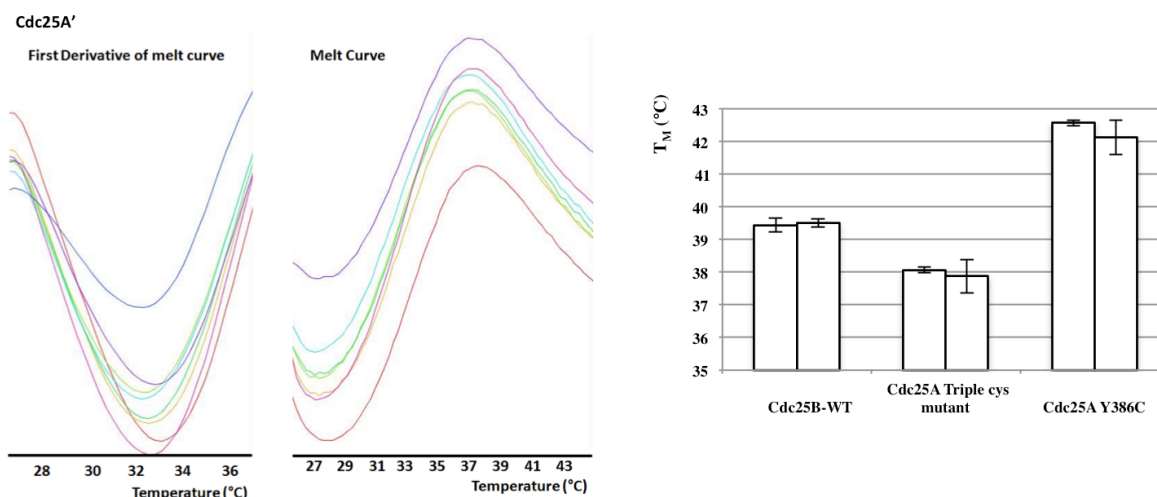
Figure 34 LHS Melt curve and its first derivative for cdc25A' (purified by the precipitation method) using 8 wells heated at a rate of 0.5 °C/min in the presence of the fluorescent dye Sypro Orange. As the protein is heated and begins to unfold, buried hydrophobic residues become solvent exposed and interact with the dye, which begins to fluoresce. The point at which the protein is half folded and half unfolded is represented by the melting temperature (T_M), which is calculated as the lowest point of the first derivative of the melt curve. **RHS** Bar chart to illustrate the T_M values for cdc25B-WT, cdc25A triple cys mutant and cdc25A Y386C.[*]

As previously discussed, the signal observed using MALDI spectroscopy for the catalytic domain of cdc25A Y386C (approximately 23,500 Da) was subject to significant isotopic broadening, and due to this effect, protein and protein-adduct peaks could not be resolved.[129]* A general protocol was therefore developed for digestion of the protein into low MW peptides prior to MS analysis, Figure 35. After incubation of the protein with acrylamide(s) or vinyl sulfonamide(s), excess electrophile was quenched by the addition of βME to prevent non-specific tethering during the digestion period. Digestion of the protein by the action of a proteolytic enzyme then generated a mixture of peptides with the retention of thioether bonds. Trypsin was chosen as the proteolytic enzyme for this work as it was commercially available in an autolytic-resistant form, thereby limiting contamination of spectra with non-cdc25A' enyzme fragments. Additionally, as tryspin is most efficient at pH 8 it was added directly to the protein-vinyl sulfonamide/acrylamide mixtures.
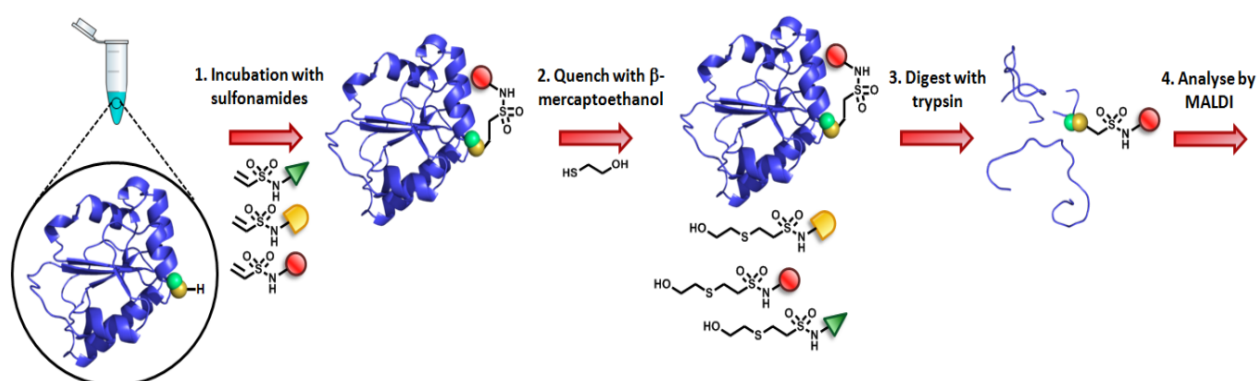

Figure 35 Schematic to illustrate the MALDI screening protocol. Cdc25A' was incubated with mixtures of either vinyl sulfonamides or acrylamides in an ammonium bicarbonate buffer (pH 8), to allow KTGT to occur. A large excess of βME was subsequently added to the mixture to quench the reaction. Trypsin was finally added to digest the protein into low MW peptides and the solvent was removed from the mixture. The peptide mixture was then analysed by MALDI MS.

---

[*] Work previously carried out by R. H. Nonoo as part of MRes thesis.

Trypsin cleaves proteins at the carboxyl side of arginine and lysine residues except when followed by proline. Digestion of cdc25A' by trypsin conveniently divides the three cysteine residues in the protein into three distinct peptides; peptide-994 (cys384), peptide-1296 (cys386) and peptide-2339 (cys480) where the peptide number refers to its mass in daltons. Using trypsin it was therefore possible not only to detect covalent adduct formation, but also to determine the tethering location. All tethering experiments were carried out in an ammonium bicarbonate buffer at pH 8 with the protein at a concentration of approximately 10 μM, as estimated using a Bradford assay. The volatility of ammonium bicarbonate allows its removal *in vacuo* prior to MS analysis. This was found to be a key criteria for the aqueous reaction medium as the presence of buffer molecules in samples for MS analysis has a highly detrimental effect on the quality of mass spectra.[130]

A typical MALDI spectrum obtained upon digestion of cdc25A' with the high MW peptides identified is shown in appendix III, p217, Figure 126. Initially cdc25A' (isolated by gel filtration rather than precipitation) was incubated with one vinyl sulfonamide (**39**, **40**, **41**, **43** or **45**) at 1.0, 0.5 or 0.1 mM for 10 min at room temperature, and quenched for 10 min at room temperature with 10 equivalents of βME before addition of tryspin. For all sulfonamides at all concentrations, large adducts were seen to both the 994 and 1296 peptides. No adducts were seen to the 2339 peptide, but for all cases, including the control with no added vinyl sulfonamide, the parent 2339 peptide was not observed either. When all 5 sulfonamides, **39**, **40**, **41**, **43** and **45** were incubated with the protein in the same mixture, with each sulfonamide at either 0.1 or 0.2 mM, with the same quench procedure, adducts to both the 994 and 1296 peptides were observed for all sulfonamides, Figure 36.
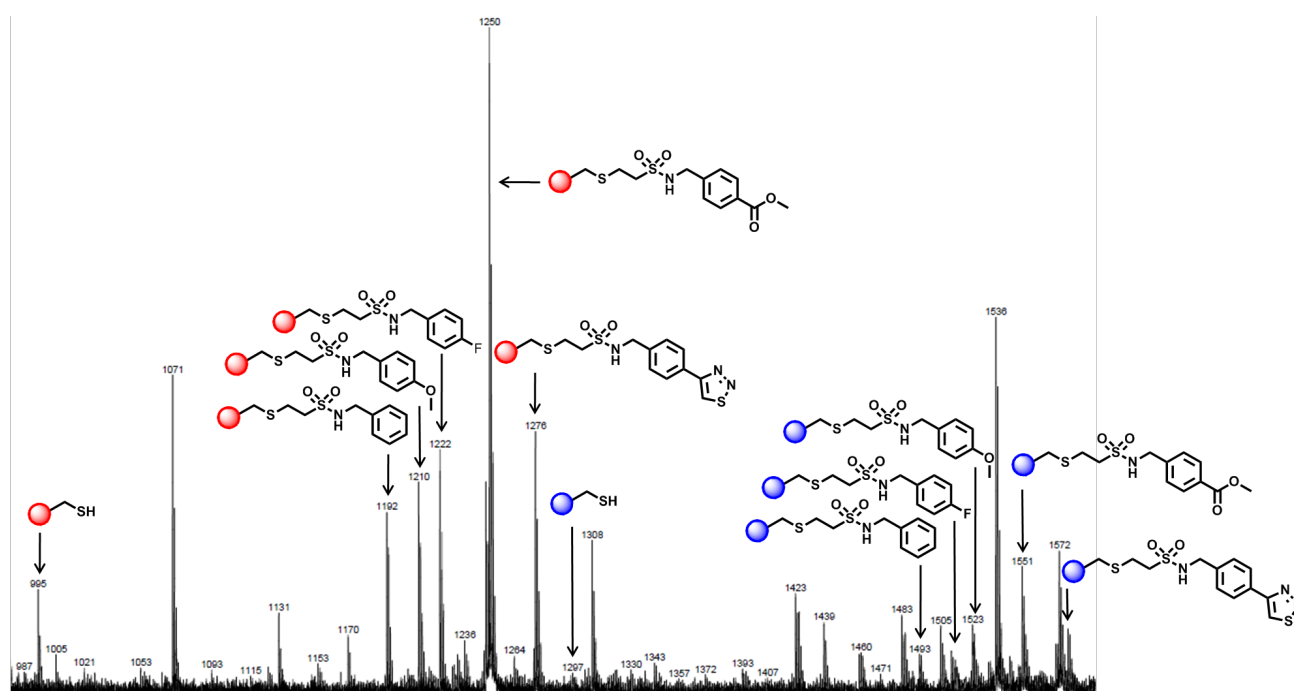
Figure 36 MALDI spectrum obtained after trypsin digestion of cdc25A'(gel filtration) preincubated with vinyl sulfonamides **39**, **40**, **41**, **43** and **45** each at 100 μM and quenched with 10 equivalents of βME.

All further experiments were carried out using the cdc25A' protein purified by precipitation, as this gave a strong peak for the peptide at 2339 and tethering at the third cysteine was therefore observed. This protein sample was also

significantly less contaminated, as indicated by SDS PAGE, and the obtained mass spectra were of higher quality. Experiments with five vinyl sulfonamides **39**, **40**, **41**, **43** and **45** incubated with the protein in one-pot were repeated with each vinyl sulfonamide at 1 and 20 μM, and with the same quench procedure. With each sulfonamide at 1 μM, no tethering to any cysteine was observed. However, with each sulfonamide at 20 μM, tethering was seen to all three cysteines, Figure 37.
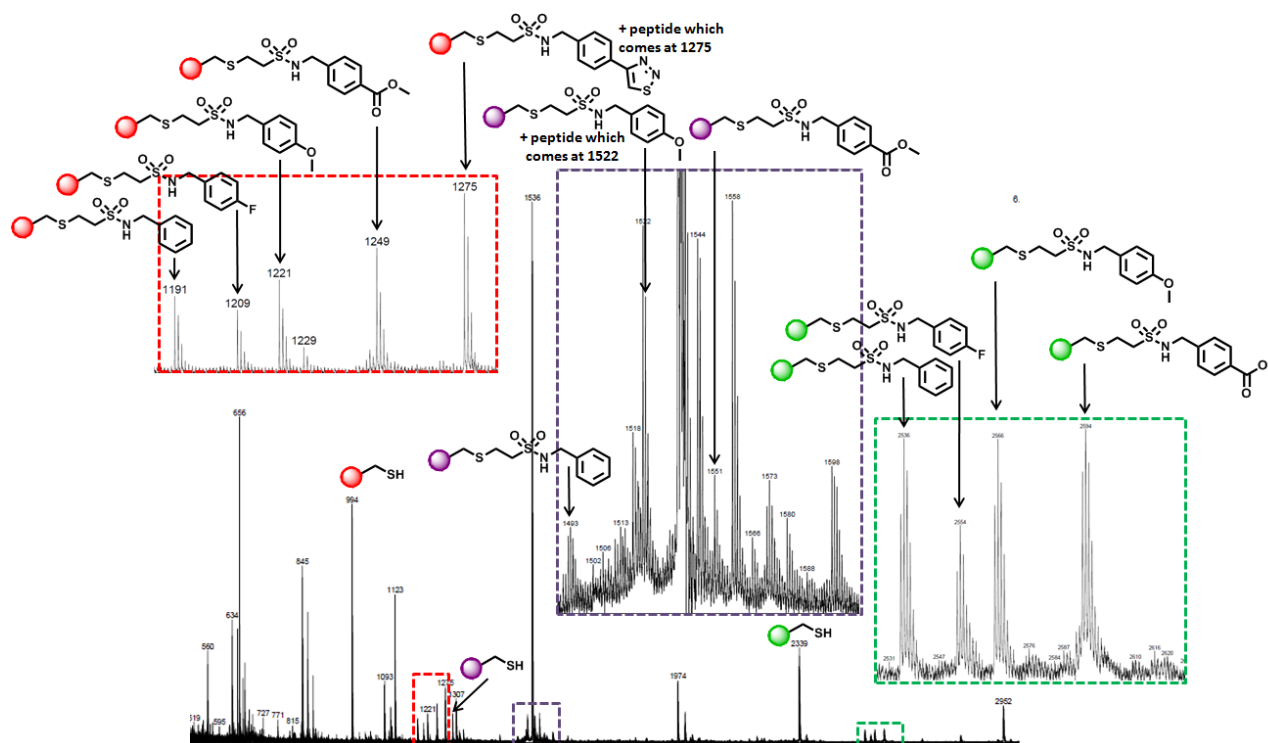
Figure 37 MALDI spectrum of cdc25A' incubated with 5 vinyl sulfonamides, **39**, **40**, **41**, **43** and **45** each at 20 μM and the mixture digested with tryspin. Adducts are seen to all three cysteines.

As Cys384 and Cys480 were hypothesised to be buried within the protein interior, tethering at these cysteine residues indicated that either the βME quench was not effective or that in fact these residues were solvent exposed in cdc25A'. Cdc25A' was incubated with sulfonamide **40** at 20 μM for 10 min at 4 °C and subsequently quenched with a large excess of βME (either 100, 500 or 1000 equivalents) at 4 °C for 16 h. Thermal shift 2 h after βME addition indicated that samples with 100 equivalents of βME contained folded protein, but those with either 500 or 1000 equivalents gave undefined melt curves indicating various degrees of protein unfolding, Figure 38. The samples were analysed by thermal shift again after 16 h, but all samples were completely unfolded (no melt curve). MALDI analysis of the digested samples indicated tethering to all three cysteines with 100 equivalents of βME, tethering to only the 994 and 1297 peptides with 500 equivalents of βME and tethering to only the 1297 peptide with 1000 equivalents of βME (although the adduct formed to the 1297 peptide after treatment with 1000 equivalents of βME was in very low yield), Figure 39. These results suggested that almost no tethering to the protein occurred within the allotted 10 min pre-quench incubation time due the lack of any significant adduct to the sample quenched with 1000 equivalents of βME. These experiments also indicated that under these conditions, 100-500 equivalents of βME was insufficient to effectively quench the remaining electrophile before background reaction with protein.
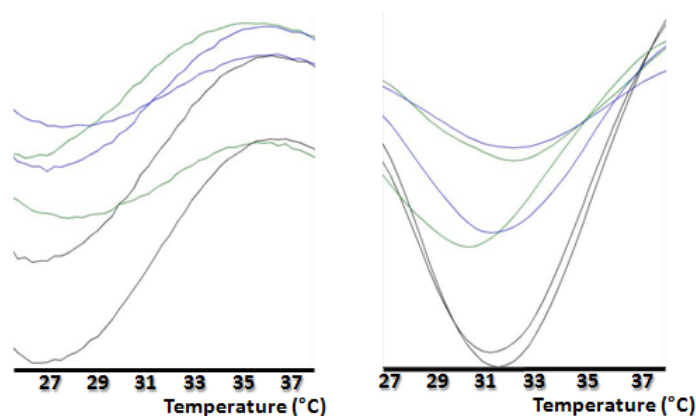
Figure 38 Left hand side: Thermal shift melt curves for cdc25A' incubated with sulfonamide **40** (20 μM) and either 100 equivalents of βME (black trace), 500 equivalents of βME (green trace) or 1000 equivalents of βME (blue trace). **Right hand side:** First derivative of the melt curves. All tests were run in duplicate.
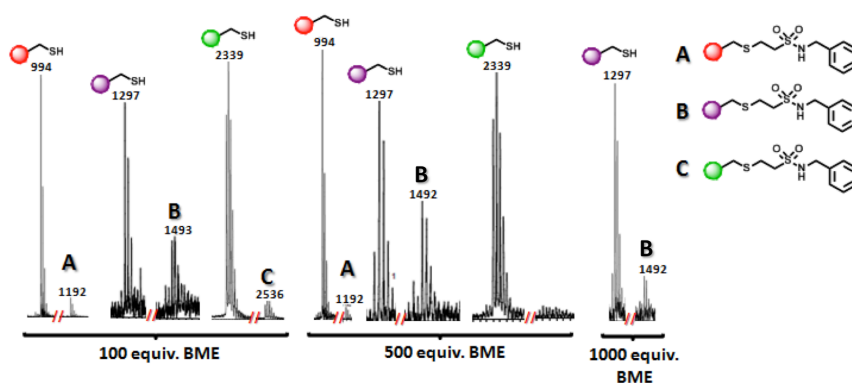
Figure 39 Tethering of vinyl sulfonamide **40** to cdc25A' at various concentrations of βME. Red sphere = peptide 994, purple sphere = peptide 1296, green sphere = peptide 2339.

2.3. Preliminary results for acrylamide tethering

When cdc25A' (isolated by precipitation) was incubated with acrylamide **47** (20 μM, 30 minutes, rt) and subsequently quenched with βME (1000 equivalents, 2h, rt), no significant adduct formation was seen with any of the three cysteine-containing peptides. However, when the same acrylamide was screened at 100 μM with the same quench procedure, low abundance adducts were seen to form with all three cysteines. This presumbly indicates that the addition of acrylamide **47** is not templated by the protein, such that upon increasing the acrylamide concentration, the background reaction at all three cysteines is increased.

2.4. Summary and conclusions

In this section of work, cdc25A' was incubated with vinyl sulfonamides and acrylamides and mixtures were digested proteolytically. Analysis of the resulting peptide mixtures by MALDI MS indicated that thioether bonds generated by conjugate addition reactions were stable to the proteolytic enzyme trypsin. Furthermore, up to five covalent adducts were resolved to three distinct peptides from the same sample, highlighting the powerful resolution obtained by MALDI at these low molecular weights. Extensive modification of all three cysteine residues indicated that either the quench with βME was ineffective or that the cysteine residues hypothesised to be buried were actually solvent

exposed, potentially due to the fluxional nature of the protein in solution. In either case, the observed modification of protein thiols with all electrophiles in the mixture, to approximately equal extents, indicated a non-templated background reaction and a lack of KTGT. It was decided that a model system with a positive control was required to validate the KTGT technique. This model system should be composed of a biomolecule with a known ligand to act as a positive control. If the biomolecule selects the known ligand from a pool of compounds using KTGT, this firstly provides a validation of the technique and secondly a set of conditions to use with the therapeutically useful target cdc25A'.

3. Thymidylate synthase as a model system for proof-of-concept studies

3.1. Introduction

Thymidylate synthase (TS) was chosen as the model system with which to validate KTGT. TS is a small (*ca*. 30 kDa), highly conserved enzyme which has been extensively studied within the literature. TS has been isolated from highly varied sources including bacteria, yeast, viruses, bacteriophage and vertebrates,[131] but much of the work to elucidate the structure and function of this enzyme has utilised either *Lactobacillus casei* or *Escherichia coli* TS, which share 82 % homology over the active site region.[132] TS catalyses the reductive methylation of deoxyuridine monophosphate (dUMP) by cofactor 5,10-methylenetetrahydrofolate (mTHF) to deoxythymidine monophosphate (dTMP), providing the sole *de novo* source of dTMP for DNA synthesis and repair in the cell, Figure 40 (A).[133] *E. coli* TS has five native cysteine residues, of which only the active site residue has been reported to be solvent exposed, Figure 40 (B).[51]
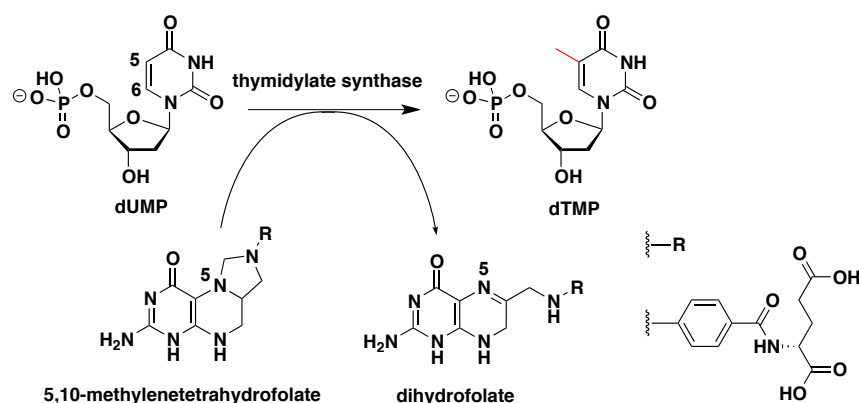
Figure 40 (A) Reductive methylation of dUMP to dTMP by TS. The new bond formed is shown in red.
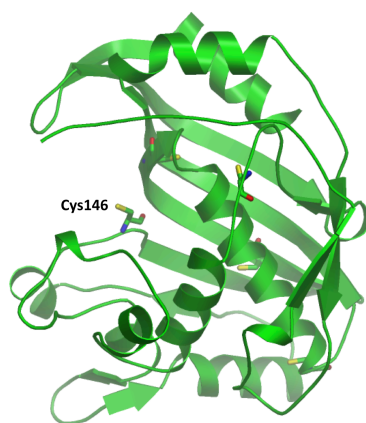
Figure 40 (B) Crystal structure of *E. coli* TS (1F4B) with cysteine residues highlighed. The solvent exposed active site cysteine 146 is labelled.

Native TS exists as a symmetric obligate dimer, where each monomer contains a deep active site cavity lined by the side chains of 25 residues, four of which are contibuted by the other subunit.[131] Of the 25 residues which line the active site pocket, 16 are invariant across 8 TS sequences.[131] Within the family of folate-utilising enzymes, TS is particularly unique due to the dual role played by its folate cofactor as both a one-carbon donor and a reductant. The catalytic mechanism for dTMP synthesis involves the initial formation of a ternary TS-dUMP-mTHF complex before attack of the TS active site cysteine (C146 in *E. coli*, C198 in *L. casei*) onto C6 of the dUMP pyrimidine ring, Scheme 2. The resulting enol(ate) attacks through the α-carbon onto mTHF which has been activated by formation of an imminium ion from the 1,1-diamine. Regeneration of the enolate and E1$_{CB}$ elimination of THF generates an exocyclic α,β-unsaturated alkene. This is reduced *in situ* by the already bound THF, which donates a hydride by pushing from the N5 lone pair, resulting in formation of the imine dihydrofolate (DHF). Conjugate addition of hydride onto the substrate generates the saturated system, from which a

final E1$_{CB}$ elimination of the enzyme releases dTMP. Structures of TS bound to mechanism based inhibitors, which mimic reaction intermediates[134-137] in addition to site directed mutagenesis studies to trap reaction intermediates[138, 139] have validated the described catalytic mode of action, which was initially proposed through a series of kinetic analyses and spectroscopic data.[140]
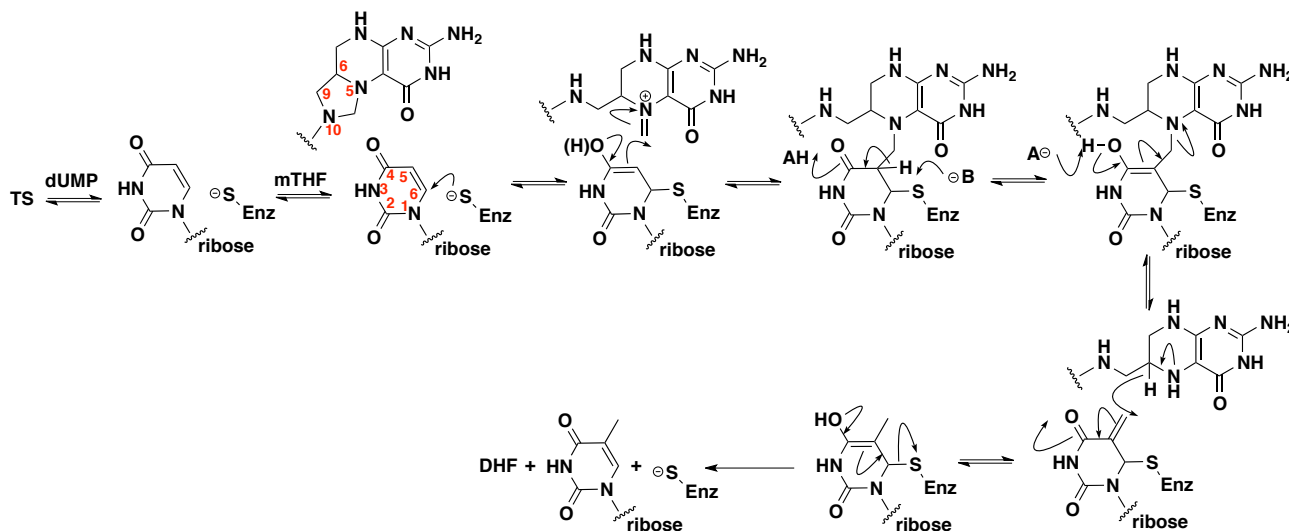
Scheme 2 Catalytic mechanism of action for TS.

The active site cysteine in TS has been postulated to have a surprisingly high pKa value of approximately 8.[141] Many catalytic cysteine residues have pKa values considerably lower than that of isolated cysteine, and are therefore often present as the more nucleophilic thiolate.[142] Such acidity is usually conferred by the environment set up by residues in the active site pocket. The high pKa of the active site cysteine in the apo TS enzyme is thought to act as a protective mechanism to guard the thiol from oxidation.[143] Generation of the thiolate is thought to occur upon dUMP substrate binding, which triggers a sequence of proton transfers resulting in thiol deprotonation by His207.[143] Before substrate binding, the basicity of His207 is reduced by neighbouring Arg126 whose cationic guanidinium moiety is stacked against the imidazole ring. Upon dUMP binding, the guanadinium moiety in Arg126 forms a hydrogen bond with the phosphate group of dUMP, neutralising the charge and raising the basicity of the local His residue, which then abstracts a proton from the catalytic cysteine to activate it as the thiolate for Michael addition to dUMP. It is thought that Ser167 is involved in this proton transfer, although the exact role this residue plays is currently unclear.[143, 144] Additionally, a role for Arg218 has been proposed in the activation of the active site cysteine.[131, 140, 145]

As TS provides the only intracellular *de novo* source of dTMP, it is crucial for DNA synthesis and repair. Selective inhibition of TS has been achieved by a number of compounds, many of which are substrate (e.g. 5-fluoro deoxyuridine monophosphate) or folate analogues (e.g. Raltitrexed), and lead to toxicity in actively dividing cells.[146] As such, TS is a critical target in the treatment of cancers such as ovarian, colorectal, breast, head and neck, pancreatic and gastric with significant achievements in the clinic to date.[146, 147] The substantial success of TS as a target in the development of anticancer therapeutics has led to a very thorough exploration of this protein within the literature. The availability of protocols for enzyme expression, purification, crystallisation and the wealth of available crystal

structure data encouraged the use of TS as a model system. In addition, TS has been used a number of times to validate other methods of drug discovery.[148-151]

Significantly, *E. coli* TS was used to generate an initial proof-of-concept for disulfide tethering by Erlanson *et al*.[51]
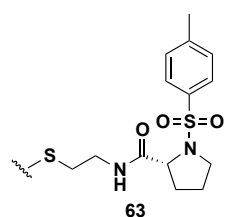

Figure 41

and was therefore considered to provide an excellent platform for proof-of-concept KTGT studies. Although TS has 5 native cysteine residues, in agreement with previous studies,[152] Erlanson *et al*. demonstrated that only the catalytic cysteine (C146) is solvent exposed.[51] Treatment of the native enzyme with the disulfide cystamine yielded complete, single modification, whereas no reaction at all was observed with TS mutant C146S. In their proof-of-concept, Erlanson *et al*. incubated TS with mixtures of up to 100 disulfides from a custom synthesised library and analysed the resulting distributions by mass spectrometry. They reported the selection of proline analogue **63** by TS, as identified by the high intensity disulfide adduct formed to this ligand at the expense of other protein-ligand adducts, Figure 41. Removal of the labile disulfide bond generated N-tosyl D-proline **64**, a millimolar

Figure 42 Overlaid crystal structures of proline analogue **63** tethered within the active site pocket of TS from mutant cysteine 143 (blue) (PDB code 1F4D) and wild type cysteine 146 (yellow) (PDB code 1F4C).

inhibitor of TS enzyme activity. Interestingly, proline-disulfide analogue **63** was found by the authors to be selected both by native TS and by a C146S L143S mutant but not by a C146S H147C mutant. This suggested that whilst there was some flexibility in the tethering location for this ligand, Figure 42, there was also some dependence on cysteine placement.

A total of 1200 disulfides were screened against TS using the mass spectrometry-based tethering assay, leading to the identification of some significant positive and negative SAR. The authors disclosed a selection of disulfide-modified ligands from this study, including N-methyl D-proline disulfide **65**, which was not selected by the enzyme. The original N-tosyl D-proline ligand **64** was optimised to give higher affinity ligand **66** by the replacement of the tosyl CH_3 with L-glutamic acid to incorporate part of the natural cofactor, improving affinity almost 50-fold.

In this work, the ligands originally reported by Erlanson *et al*. were modified for use as positive and negative controls in KTGT by the appendage of either acrylamide or vinyl sulfonamide functional groups, Figure 43
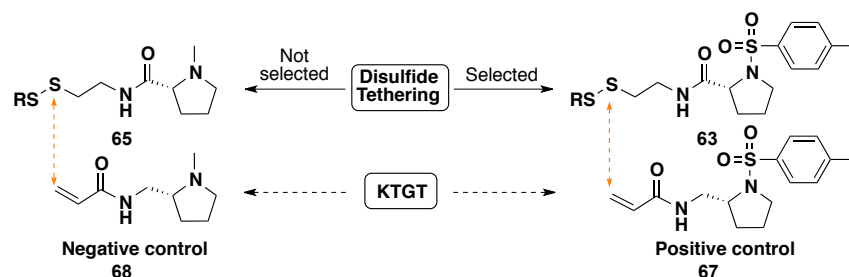

Figure 43 Ligands selected and not-selected by disulfide tethering[51] and their adaption for use as positive and negative controls respectively in KTGT by addition of either a vinyl sulfonamide or acrylamide group. Only acrylamide indicated in schematic.

The ligands were designed such that the electrophilic atom marking the point of covalent modification was kept consistent between both tethering types. The carbonyl adjacent to the pyrrolidine ring in disulfides **63** and **65** was moved to a new position two atoms further from the ring in positive control **67** and negative control **68** in order to place the acrylamide in the correct location. The proline-carbonyl in optimised ligand **66** was also moved in the same manner to yield higher affinity positive control **69** for KTGT, Figure 44. It was predicted that, due to the flexibility observed in the tethering location, these small molecular changes would not affect the ability of the compounds to act as appropriate controls.
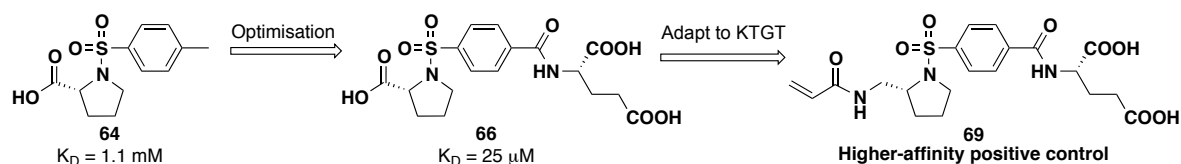
Figure 44 Optimisation of N-tosyl ᴅ-proline **64** to ᴅ-proline derivative **66** by Erlanson *et al*. improved affinity towards TS by almost 50-fold.[51] This micromolar inhibitor was modified for use in KTGT as a high affinity tethering control by the addition of a vinyl sulfonamide or acrylamide group. Only acrylamide **69** indicated in schematic.

The overall aim for work described within this chapter is to use *E. coli* TS to obtain a proof-of-concept for KTGT. This includes the following:

1. Cloning, expression and purification of *E. coli* TS.
2. The synthesis of appropriate positive and negative control ligands.
3. Demonstration that from a mixture of acrylamides or vinyl sulfonamides, TS selects only the positive and not the negative control ligand.
4. Digestion of TS-acrylamide/vinylsulfonamide adducts and MALDI MS analysis of the resulting peptide mixtures to identify the position of modification.

3. 2. Cloning, expression and purification of wild type *E. coli* thymidylate synthase

3.2.1. Cloning strategy

To generate high quantities of active TS enzyme, a pET/*E. coli* expression system was adopted. The pET vectors are particularly suitable for rapid, high level expression in bacteria due to the viral T7 promotor, which, along with a *lac* operator, flanks the gene of interest within the cloning region of the plasmid, Figure 45. The T7 promotor does not occur anywhere else within the prokaryotic genome and is highly specific for only the T7 RNA polymerase.[153] The *lacI* gene, also encoded within the pET plasmid, codes for the lac repressor protein which binds to the *lac* operator sequence, preventing transcription of the gene of interest. Expression of a desired recombinant protein using the pET vector must be carried out using a strain of *E. coli* which has been engineered to contain the gene for the T7 RNA polymerase. This is most often *E. coli* BL21 (DE3) in which the T7 RNA polymerase gene is flanked by a *lac* promotor and a *lac* operator sequence. Protein expression is only activated by the addition of IPTG which displaces the lac repressor protein from the *lac* operator and activates transcription of T7 RNA polymerase. T7 RNA polymerase then rapidly and profusely transcribes the gene inserted into the cloning region of the pET vector. The
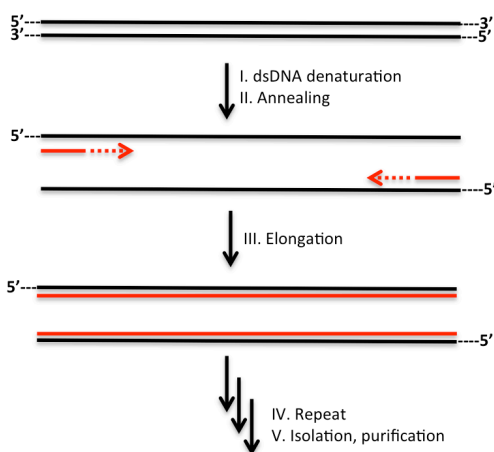
strong, constitutively active T7 promotor ensures that transcription continues as long as the T7 RNA polymerase is present. Expression of this gene increases rapidly as the quantity of mRNA increases, often until the protein of interest is the most dominant component of the cell, comprising more than 50 % of the total cell protein a few hours post-induction.
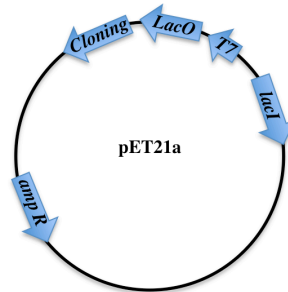
Figure 45 The pET21a vector which contains a multiple cloning region (see Appendix V) (cloning) preceded by the *lac* operator (*Lac*O) and the T7 promotor (T7). The plasmid also contains a gene to confer ampicillin resistance (*amp* R) and *lac*I which codes for the lac repressor protein.

To clone the *TS* gene into the pET21a expression vector, a two-step cloning stratgy was adopted. Difficulties were previously encountered cloning a DNA insert obtained by PCR directly into the pET21a plasmid, but were overcome using a 't-tailing' strategy.[*] This involved the addition of a deoxyadenosine (dA) to the 3' end of the original DNA insert and cloning into a pGEM-T vector, which has a single terminal deoxythymidine on each 3' end. The overhanging bases make this method more efficient than cloning with 'blunt ends' and subcloning from pGEM-T to pET21a is more efficient than from the PCR insert. The TS gene was amplified from whole *E. coli* BL21 (DE3) cells, which contain the sequence within their genome, using PCR, Figure 46. The insert generated by PCR was heated in the presence of a *Taq* DNA polymerase and dATP to effect the addition of an A base to the 3' ends. The t-tail insert was ligated

Figure 46 Schematic illustration of PCR.

into the pGEM-T vector using a T4 DNA ligase enzyme, Figure 47, but problems were encountered at this stage in the selection of colonies containing the insert. This is presumably as a small percentage of the commercial pGEM-T contains the non t-tailed vector, which can ligate itself to generate an empty vector.
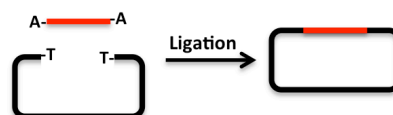
Figure 47 The desired successful ligation reaction between pGEM-T and the insert with overhanging A-bases.

A blue/white selection procedure was adopted to increase the probability of selecting transformants containing an insert. The transformed cells were grown in the presence of IPTG to induce gene transcription and 5-bromo-4-chloro-

---

[*] Work previously carried out by R. H. Nonoo during MRes.

3-indolyl-[β]-D-galactopyranoside (Xgal), which is converted to a bright blue product by the enzyme β-galactosidase, the product from the *LacZ* gene. β-Galactosidase functions as a homotetramer with tetramerisation dependent on the N-terminal 50 amino acids. *E. coli* DH5α cells used for cloning are only able to express a truncated form of β-galactosidase, which fails to tetramerise. The missing N-terminal sequence can be provided in trans from plasmids such as pGEM, leading to blue colonies after ampicillin selection. However, if the plasmid contains an insert, production of the N-terminal peptide is disrupted, tetramerisation of the *LacZ* gene product does not occur, and a white colony results. White colonies were selected, grown on a small scale, and the DNA isolated and digested to identify correct transformants. These were then grown on a larger scale and the DNA extracted, purified and sequenced to yield the desired pGEM-T-TS plasmid.

The cloning sites *EcoRI* and *NdeI* were used to subclone the insert from the pGEM-T vector to the pET21a expression vector. This cloning strategy was complicated by the presence of two further *NdeI* sites within the TS insert, Figure 48. A partial digest strategy was adopted in an effort to obtain the TS insert cut at only the desired *NdeI* site. The plasmid was fully digested with *EcoRI* over a one hour period in ten separate aliquots. Successively more dilute *NdeI* enzyme was subsequently titrated into each sample, and the digest allowed to proceed for 15 minutes. A fully digested *NdeI*/*EcoRI* sample was prepared as a control. The sample which contained *NdeI* at 5 x dilution gave a band at just above the 700 bases DNA ladder band as required for the correct insert. This digest was therefore repeated with four further samples of the pGEM-TS plasmid DNA in order to obtain a reasonable quantity of the digested insert. The insert was ligated into the cloning region of pET21a pre-digested with *NdeI*/*EcoRI*, and transformed into *E. coli* (DH5α) cells. Colonies were selected and grown overnight on a small scale and the DNA isolated and digested to identify correct transformants. These were then grown on a larger scale and the DNA isolated, purified and sequenced. However, the sequence indicated that the insert had been cut at two consecutive *NdeI* points (indicated in Figure 48 by asterisks), rather than the desired *NdeI* and *EcoRI* sites to give an insert of 563 bases rather than the desired 802 bases in a plasmid termed pET21a-TS$_{NdeI}$.

Figure 48 DNA sequence for the catalytic domain of TS with sites for selected restriction enzymes highlighted. The insert was found to be cut at two consecutive *NdeI* sites (indicated by an asterix) rather than the desired *NdeI* and *EcoRI* sites.

To complete the cloning, the pGEM-T-TS plasmid was cut with *EcoRI and AscI* whilst the pET21a plasmid containing the partial TS sequence was cut with *EcoRI* and *AscI*. The insert from the pGEM-TS digest was ligated into the *EcoRI*/*AscI* cut pET21a plasmid to give the full TS catalytic domain cloned into the pET21a expression vector (pET21a-TS), Figure 49, which was isolated, purified and sequenced.
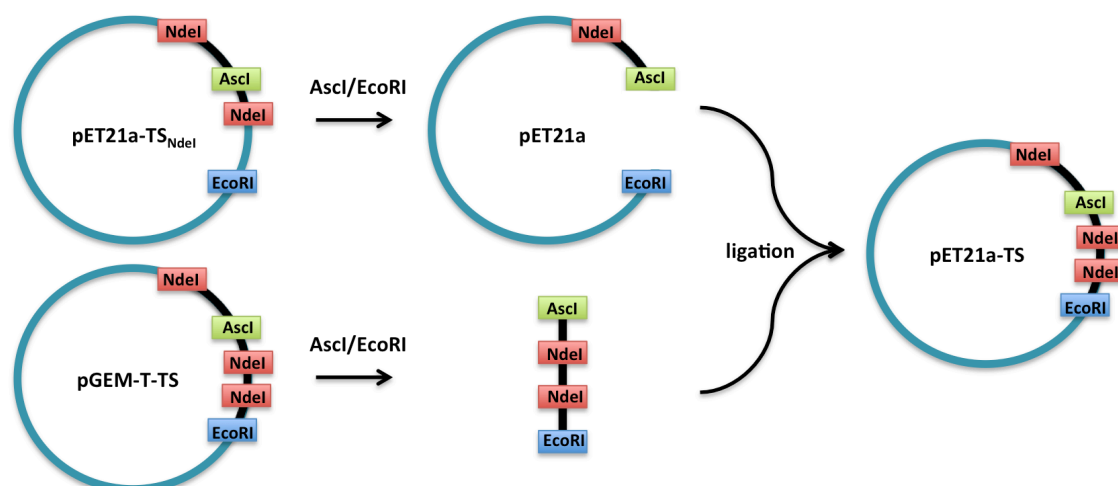
Figure 49 Schematic to illustrate the final TS cloning steps. pET21a-TS$_{NdeI}$ and pGEM-TS were both cut with AscI and EcoRI restriction enzymes and the insert from pGEM-TS ligated into the cut pET21a to generate the final desired pET21a-TS construct. The blue part of the circle represents the vector sequence and the black part of the circle represents the insert sequence.

3.2.2. Expression and purification

E. coli BL21-DE3 cells were transformed with the pET21a-TS vector by electroporation, grown and subsequently induced with IPTG. It was found that incubation at 37 °C rather than 18 °C after IPTG induction was optimal. After the induction period, analysis of the cells by SDS PAGE indicated a strong band for TS, Figure 50 (A). The purification was largely carried out in accordance with a literature protocol.[154] The cells were lysed by sonication and the nucleic acid removed by precipitation with streptomycin sulfate. Addition of ammonium sulfate to 50 % saturation yielded a precipitate which was mainly composed of other contaminant proteins, although some TS was evident (B). This precipitate was removed by centrifugation and the supernatant saturated to 80 % with ammonium sulfate. This yielded a second precipitate which contained the desired TS protein (B). The precipitate was dialysed into a potassium phosphate buffer and then bound to anion exchange cellulose beads (DE-52) pre-equilibrated in a potassium phosphate buffer. TS was eluted by increasing the concentration of NaCl in the buffer by stepwise increments. As the protein has a theoretical pI of 5.5 it harbours an overall negative charge during the purifcation procedure which is carried out in buffers of pH 7.5-8.0. The negatively charged protein binds strongly to the positively charged diethyl ammonium beads until displaced by salt ions. Fractions containing TS by SDS PAGE were combined and the protein precipitated by addition of ammonium sulfate to 80 % saturation. The precipitated protein was collected by centrifugation and stored at – 70 °C. The purity of the TS was increased by eluting the protein from the DE-52 beads through a thin walled glass column equipped with a frit. Application of buffer with increasing concentrations of salt generated more of a continous salt gradient, Figure 51.
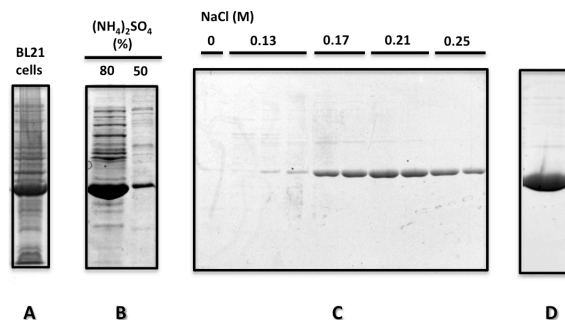
Figure 50 SDS PAGE of *E. coli* TS samples taken from various stages during purification. **A.** BL21 (DE3) cells transformed with pET21a-TS and induced with IPTG. **B.** Ammonium sulfate precipitation of crude extract to 50 % and 80 % as indicated. **C.** Ion exchange chromatography of dialysed 80 % ammonium sulfate extract. Wash NaCl concentrations (M) are indicated above each lane. **D.** Combined ion exchange extracts at 0.25 M NaCl after precipitation with ammonium sulfate to 80 % saturation, collection of the precipitate by centrifugation and resuspension in potassium phosphate buffer.
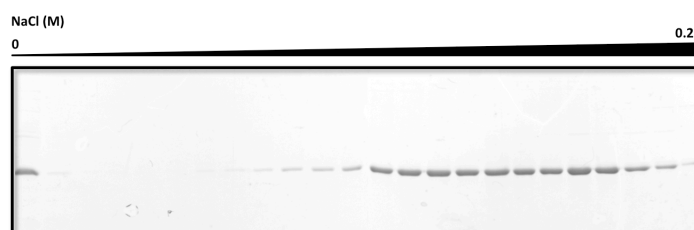
Figure 51 Elution of TS from beads through a thin glass walled column, generating more of a continous salt gradient. A band is seen for TS in the first fraction due to saturation of the resin.

A spectrophotometric assay was used to confirm that the purified TS had retained enzymatic activity. This assay, first reported by Wahba and Friedkin in 1961, is based on a marked spectral change at 340 nm which is observed when mTHF is converted to DHF.[155] mTHF is unstable and was therefore generated from tetrahydrofolate and formaldehyde *in situ* by a non-enzymatic reaction in accordance with the published procedure, Scheme 3. In the presence of a high concentration βME and an excess of formaldehyde, mTHF is reported to be stable for an hour at rt.[155] dUMP was added to a mixture of tetrahydrofolate, formaldehyde, magnesium chloride and purified TS and the absorbance measured over time at 340 nm. Absorbance at 340 nm was also measured for a reference sample, which was identical except for the absence of dUMP. The absorbance difference was calculated and plotted as a function of time to indicate that the TS enzyme was active, Figure 52.
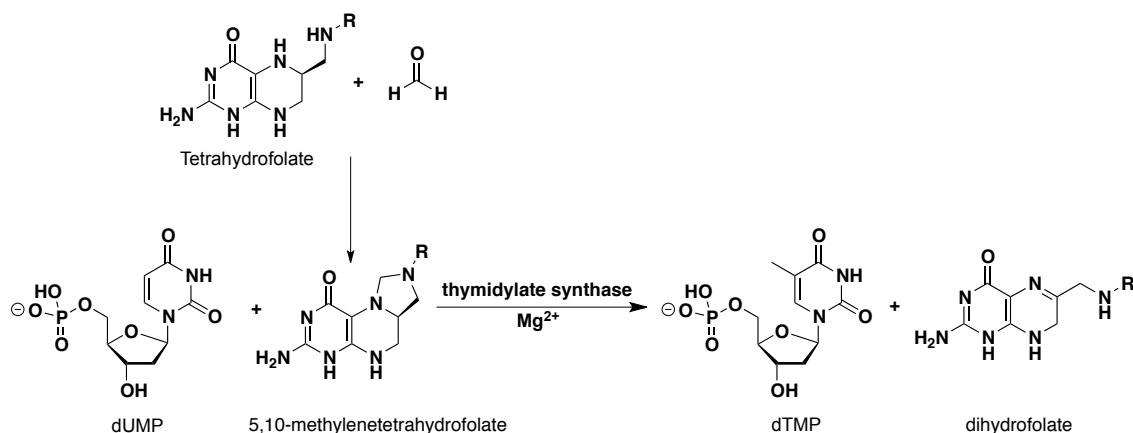
Scheme 3 Active TS catalyses the reductive methylation of dUMP to dTMP with concomitant conversion of 5,10-methylenetetrahydrofolate to dihydrofolate. 5,10-Methylenetetrahydrofolate was generated *in situ* from tetrahydrofolate and formaldehyde.
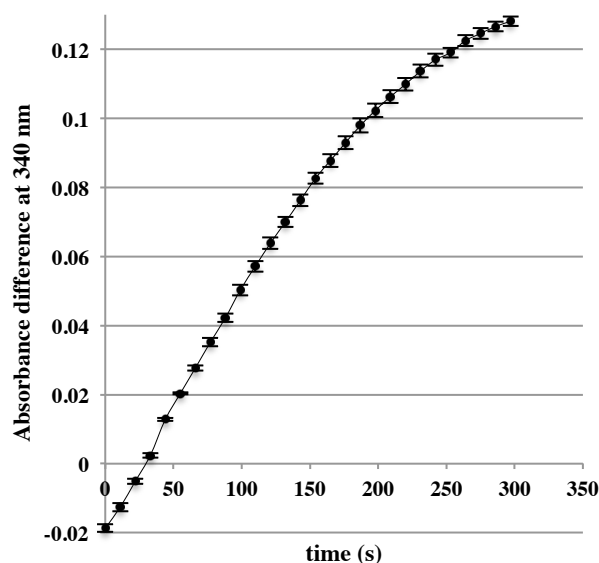
Figure 52 Absorbance difference measured at 340 nm as a function of time between two samples containing tetrahydrofolate, formaldehyde, magnesium chloride, purified TS and either dUMP or no dUMP (reference sample). Values are the average of 3 runs with error bars representing the standard devation. Conditions: 40 mM TRIS-HCl pH 7.5, 100 mM βME, 0.75 mM EDTA, 12 mM HCHO, 20 mM MgCl$_2$, 1 mM dUMP, 150 μM mTHF, 0.2 μM TS.

3.3. Ligand synthesis

To obtain a proof-of-concept for KTGT, a number of acrylamide and vinyl sulfonamide-modified control ligands were required, as summarised in Figure 53. These novel compounds were synthesised from chiral pool starting material D-proline, as discussed in the following section.
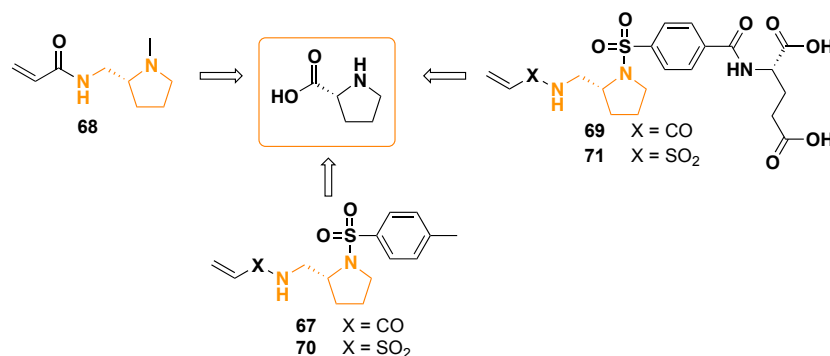
Figure 53 Both positive controls and the negative control were synthesised from D-proline.

3.3.1. Lower affinity positive control

It was envisaged that D-proline was a suitable chiral pool starting material to generate the desired positive control acrylamide **67** and vinyl sulfonamide **70**. As shown retrosynthetically in Scheme 4, reaction of primary amine **72** with acryloyl chloride or 2-chloroethanesulfonyl chloride generates the desired acrylamide **67** and vinyl sulfonamide **70** respectively in the final step. As divergence from the linear sequence occurs in the last step, the total number of steps to form both the vinyl sulfonamide and the acrylamide is minimised. Amine **72** is generated from tosylate **73** by displacement with azide and subsequent reduction. Bis-tosylation on both the N and O atoms after reduction of D-

proline to D-prolinol generates the desired N substitution and concomitantly modifies the alcohol for S_N2 displacement.
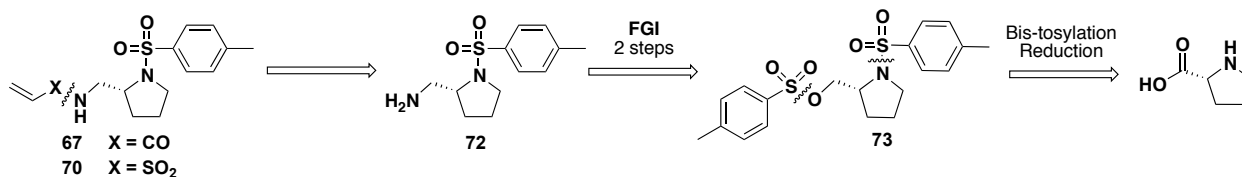
Scheme 4 Retrosynthesis from desired lower affinity positive control ligands acrylamide **67** and vinyl sulfonamide **70**.

The synthesis commenced with a one-step reduction of D-proline to D-prolinol using $LiAlH_4$ and bis-tosylation of the crude reduction product with *p*-toluenesulfonyl chloride. The use of triethylamine as the base and dichloromethane as the solvent for the tosylation step gave mainly the N-tosyl D-prolinol **74** with only a trace quantity of the required *N*,O-bis-tosyl **73**. Submitting this crude mono/bis mixture to tosylation with neat pyridine to act as a nucleophilic catalyst gave smooth conversion to the the desired D-pyrrolidine **73**, but in a poor 21 % isolated yield over the three steps, Table 1 (entry 1). The bis-tosylation reaction was improved with the use of neat pyridine as the solvent, generating the desired D-pyrrolidine **73** in a 49 % yield from D-proline over two steps (entry 2). It was considered that perhaps the yield for the reaction could be improved by tosylation in two separate steps, and treatment of the intermediate D-prolinol with only one equivalent of tosyl chloride and excess triethylamine in dichloromethane gave complete selectivity for N tosylation, although the yield was still moderate at 58 % from D-proline (entry 3).[*] The low isolated yield for the tosylation of the pyrrolidine N suggested that the $LiAlH_4$ reduction was sub-optimal, and as such, any future work should include an optimisation of this step.
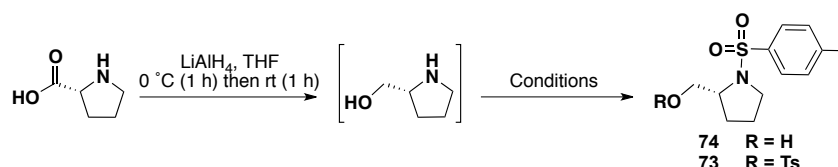
Entry	R	Conditions	Yield (%)
1	Ts	TsCl (4 eq.), Et₃N (4 eq.), CH₂Cl₂, rt, 12 h. *Then* TsCl (3 eq.), pyr, 16 h	21
2	Ts	TsCl (3 eq.), pyr, rt, 12 h	49
3	H	TsCl (1 eq.), Et₃N (3 eq.), CH₂Cl₂, rt, 7 h	58

Table 1 Reduction and tosylation of D-proline.

In agreement with this, the route was also started from the commercially available D-prolinol, which was treated with neat pyridine and tosyl chloride (3 equivalents) to furnish the desired bis-tosyl pyrrolidine **73** in quantitative yield, Table 2 (entry 1). Reducing the equivalents of tosyl chloride to 2.2 led to a significant reduction in isolated yield (entry 2).

---

[*] Selectivity for N was confirmed by oxidation of alcohol **74** to aldehyde **75** using Dess-Martin periodinane (yield 36 %).
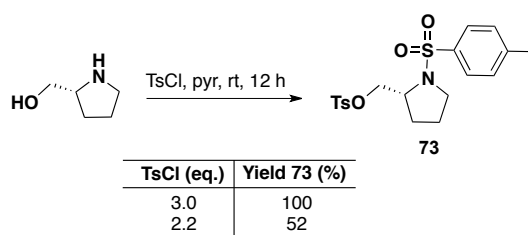
Table 2 Tosylation of D-prolinol.

An S_N2 displacement of the tosylate with azide took the bis-tosylpyrrolidine **73** to the azide **76** in 75 % yield. A subsequent Staudinger reduction of the azide was used to generate the amine **72**, which was initially taken straight on to reaction with acryloyl chloride without complete separation of the triphenylphosphine oxide impurity. This generated the desired acrylamide **67**, although in a poor 13 % yield over the two steps. Purification of the intermediate amine on silica led to a 49% isolated yield from the Staudinger reduction, but using a more successful alternative route, the azide **76** was hydrogenated to the amine using a Pd/C catalyst and H_2 (g) at atmospheric pressure. This proceeded in quantitative yield with facile isolation of the pure amine **72**. The amine was subsequently reacted with acryloyl chloride to generate the desired acrylamide **67** in a moderate 74 % yield or 2-chloroethanesulfonyl chloride to generate the vinyl sulfonamide **70** in a 42 % yield *via* displacement of the sulfonyl chloride and $E1_{CB}$ elimination of the second chloride. The overall route is summarised in Scheme 5.
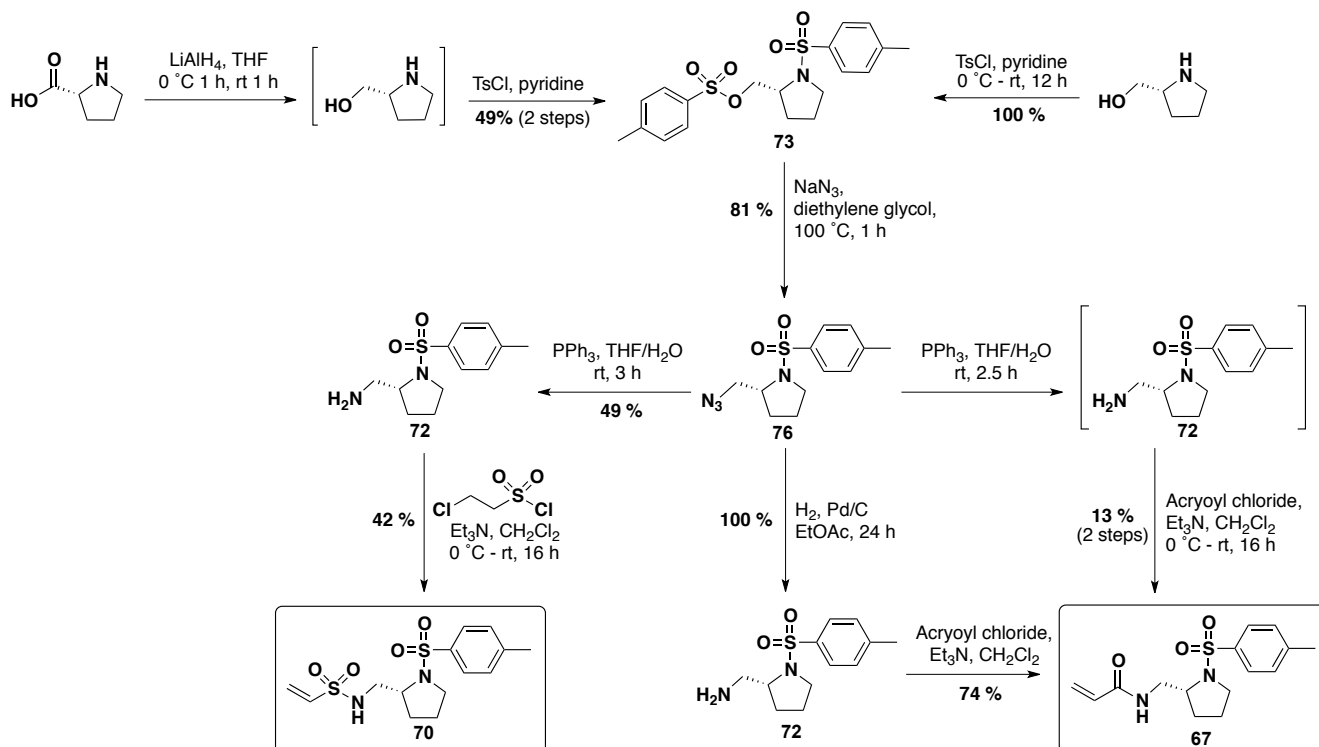
Scheme 5 Synthesis of the lower affinity positive controls acrylamide **67** and vinyl sulfonamide **70**.

3.3.2. Higher affinity positive control

To synthesise the higher affinity positive controls, a similar route to that described for the lower affinity postitive controls was envisaged, except that a functional handle was required at the *para* position of the N-substituted phenylsulfonamide for installation of the L-glutamic acid functionality at a later stage in the route, Equation 2.
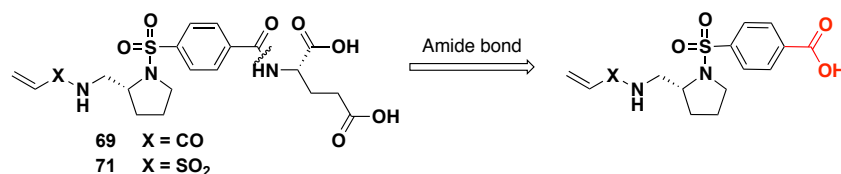
Equation 2

An initial attempt was made to bis-sulfonylate D-prolinol with 4-(chlorosulfonyl)benzoic acid, but difficulties were encountered during extraction from the aqueous layer after work up due to the polar nature of the product. It was anticipated that this would be a recurring problem with this route, and as such, the carboxylic acid was protected as the methyl ester **77**, Scheme 6. It was expected that an excess of the 4-(chlorosulfonyl)benzoic acid methyl ester **77** would react with D-prolinol to generate the bis-sulfonylated compound **78**. This reaction was carried out with Et$_3$N rather than pyridine as the base to prevent potential addition of the nucleophilic groups to the ester *via* nucleophilic pyridine catalysis. However, as previously observed, this caused the reaction at O to be significantly slower than at the more nucleophilic N, with the isolated yield of the bis-sulfonylated pyrrolidine **78** only 30 % in the presence of three equivalents of sulfonylchloride and triethylamine base after 16 h at rt. Reaction of D-prolinol with only one equivalent of sulfonyl chloride **77** gave complete selectivity for reaction at N, with isolated yields of 93-94 % of the N-sulfonyl prolinol **79** after 1 h at rt. The selectivity for N was confirmed by Dess-Martin oxidation of the alcohol **79** to the aldehyde **80**, Scheme 6.
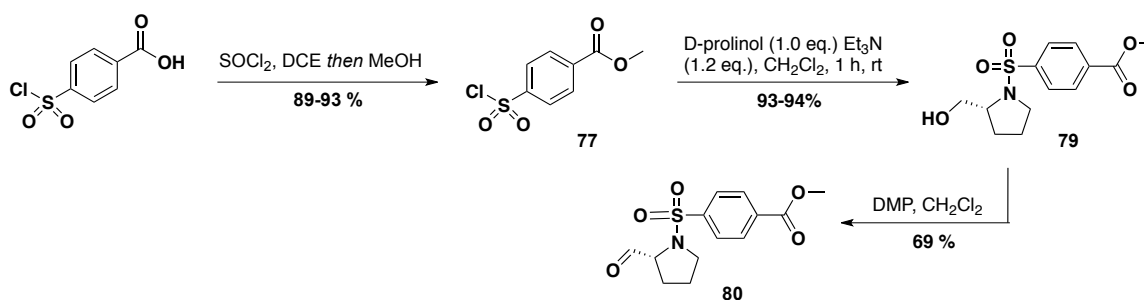
Scheme 6

Tosylation of sulfonamide **79** with 1.2 equivalents of both tosyl chloride and triethylamine went only partially to completion by TLC after 18 h at rt. Addition of a second equivalent of both tosyl chloride and triethylamine in an attempt to push the reaction to completion gave an 83 % isolated yield of pyrrolidine **81** after an additional 27 h, Table 3 (entry 1). Increasing the number of equivalents of both tosyl chloride and triethylamine to 3.0 led to completion of the reaction by TLC after 6 h and isolated yields for pyrrolidine **81** of 89-94 % (entry 2). This two-step sulfonylation reaction sequence allowed selective formation of sulfonamide **79** using the more expensive sulfonyl chloride **77** and subsequent formation of the sulfonyl ester with tosyl chloride to generate pyrrolidine **81**.
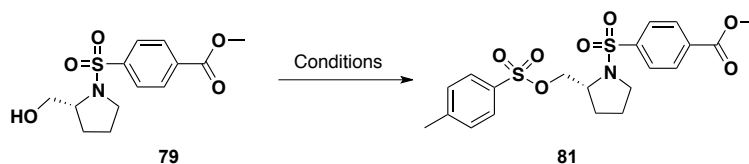
Entry	Conditions	Yield 81 (%)
1	TsCl (1.2 eq.), Et$_3$N (1.2 eq.), CH$_2$Cl$_2$, rt, 18 h *then* TsCl (1.0 eq.), Et$_3$N (1.0 eq.), rt, 27 h	83
2	TsCl (3.0 eq.), Et$_3$N (3.0 eq.), CH$_2$Cl$_2$, rt, 6 h	89-94

Table 3 Conditions for the tosylation of pyrrolidine **79**.

S$_N$2 displacement of tosylate **81** with azide could not be effected using the conditions employed to generate azide **76**, Table 4 (entry 1). However, by switching the solvent from diethylene glycol to DMF, the azide **82** was isolated in yields of 93-100 % (entry 2).
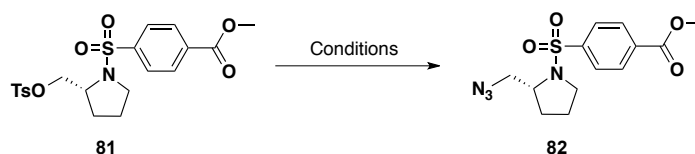
Entry	Azide synthesis conditions	Yield 82 (%)
1	NaN$_3$, diethylene glycol, 100 °C	0
2	NaN$_3$, DMF, 90 °C, 3 h	93-100

Table 4 Conditions for the synthesis of azide **82**.

A Staudinger reduction of the azide using PPh$_3$ and THF/H$_2$O generated the desired amine **83** although in a poor 48 % yield, Table 5 (entry 1). The low yield for this transformation may be due to the resistance of the intermediate iminophosphorane **84**, isolated as a side-product from this reaction, to hydrolysis. As hydrogenation of the azide **82** with a Pd/C catalyst generated the desired primary amine **83** reproducibly with yields between 96-100 % (entry 2), the Staudinger reduction was not further pursued.

Entry	Azide reduction conditions	Yield 83 (%)
1	PPh$_3$, THF, H$_2$O, 3 h	48
2	H$_2$, Pd/C, EtOAc, 24 h	96-100

Table 5 Conditions for the reduction of azide **82** to amine **83**.

Primary amine **83** was reacted with acryloyl chloride to give the desired acrylamide **85** in yields between 71-72 %, Scheme 7. Hydrolysis of the methyl ester using LiOH generated the desired carboxylic acid **86**, as a functional handle for installation of the L-glutamic acid, in excellent yields between 93-97 %.
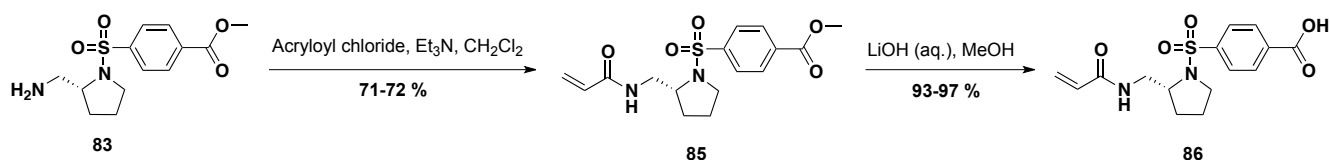
Scheme 7

An attempt was made to generate the acid chloride from carboxylic acid **86** using thionyl chloride. Quenching a drop of the reaction mixture with MeOH and subsequent TLC analysis indicated a mixture of products which did not include the desired ester. The crude reaction mixture was nevertheless added to a solution of L-glutamic acid in aqueous sodium bicarbonate in an attempt to form the desired amide using Schotten-Baumann conditions. Problems were encountered during the work up of this reaction, with no product extracted from the acidic aqueous layer, and it was therefore unknown at which stage this reaction had failed. Double-protection of the L-glutamic acid carboxylic acid groups as *tert*-butyl esters was desired to allow use of a carbodiimide coupling strategy, which would avoid generation of the acid chloride. The protected L-glutamic acid di-*tert*-butyl ester **87** was commercially available but expensive, and therefore attempts were made to synthesise it.

The protection of L-glutamic acid **88** to the di-*tert*-butyl ester **87** has been reported using isobutylene gas.[156] As this was unavailable at the time of synthesis, attempts were made to carry out this transformation using available reagents. Protection of amine **88** with a carbobenzyloxy (Z) group was initially carried out to add a UV chromophore for TLC analysis, to reduce any side-product formation and to aid with extraction from aqueous solvents. In addition, removal of the Z protecting group can be carried out orthogonally to the *tert*-butyl ester groups by hydrogenation. Z-L-glutamic acid **89** was generated in a 98 % yield, Scheme 8.

Z-L-glutamic acid **89** was treated with trifluoroacetic anhydride in THF at 0 °C for 30 min to activate the acid groups as mixed anhydrides. Subsequent addition of *tert*-butanol was expected to generate the desired esters but ¹H NMR of the crude reaction mixture indicated no conversion to the desired product. Treatment of Z-L-glutamic acid **89** with diisopropylcarbodiimide in the presence of DMAP resulted in the generation of only the mono-protected ester (20 % isolated yield) after 16 h reaction at rt. Reaction of Z-L-glutamic acid **89** with oxalyl chloride and subsequent addition of *tert*-butanol yielded none of the desired product, potentially due to unsuccessful generation of the acid chlorides as observed by methanol quench TLC analysis. It was decided that in order to progress more quickly with the synthesis, the L-glutamic acid di-*tert*-butyl ester **87** would be purchased.

Conditions
1. (CF₃CO)O, THF then *t*BuOH
2. *N,N*-Diisopropylcarbodiimide, DMAP, *t*BuOH, CH₂Cl₂
3. Oxalyl Chloride, DMF (cat.), toluene, then *t*BuOH
4. Oxalyl Chloride, DMF (cat.), THF, then *t*BuOH
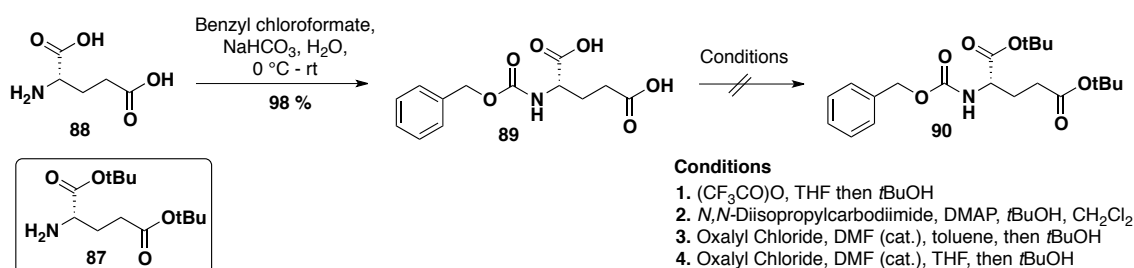
Scheme 8

The L-glutamic acid di-*tert*-butyl ester **87** was purchased as the HCl salt and reacted with carboxylic acid **86** using EDCI.HCl as the coupling reagent. Excess Et$_3$N was added to generate the free primary amine from the HCl salt *in situ*. However, under these conditions only a 4 % yield of the desired product **91** was obtained, Scheme 9. It was thought that this might be due to use of the HCl salt of the amine rather than the free amine. A literature reaction to couple *para*-nitrobenzoic acid with L-glutamic acid di-*tert*-butyl ester in the presence of EDC.HCl, HOBt and DCM/H$_2$O was carried out using L-glutamic acid di-*tert*-butyl ester HCl salt and an additional equivalent of triethylamine to determine whether the reported yield could be reproduced.[157] However, as only a 45 % yield of the desired product **92** was obtained in comparison to the 98 % reported yield, it was decided that the free amine as opposed to the salt should be used. The free amine was generated by a basic wash with NaHCO$_3$ and taken on to reaction with carboxylic acid **86** in the presence of EDC.HCl, HOBt and CH$_2$Cl$_2$/H$_2$O to achieve the amide **91** in a moderate yields of 53-74 %, Scheme 9. Intermediate **91** was deprotected with TFA in chloroform to give the final desired product **69** in 53 % yield (25 mg).
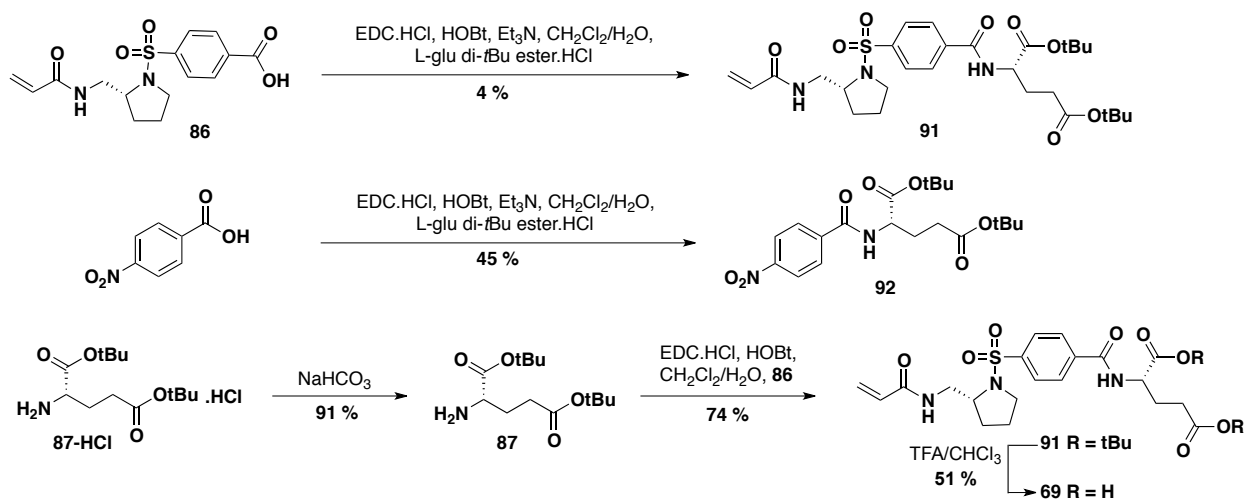
Scheme 9

The overall route reached the desired compound in only 9 steps, each in moderate-to-excellent yields. The vinyl sulfonamide higher affinity positive control ligand **71** was also synthesised from primary amine **83** as an common intermediate, Scheme 10. Treatment of amine **83** with 2-chloroethanesulfonyl chloride and triethylamine generated vinyl sulfonamide **93** in a modest 58 % yield. Hydrolysis of the ester with lithium hydroxide was facile, with isolation of the acid **94** achieved in quantitative yield. The coupling reaction between carboxylic acid **94** and di-*t*butyl L-glutamic acid **87** to yield di-ester **95** and the final deprotection step were both effected in high yields of 85 % and 94 % respectively to generate the final desired vinyl sulfonamide **71** (500 mg).
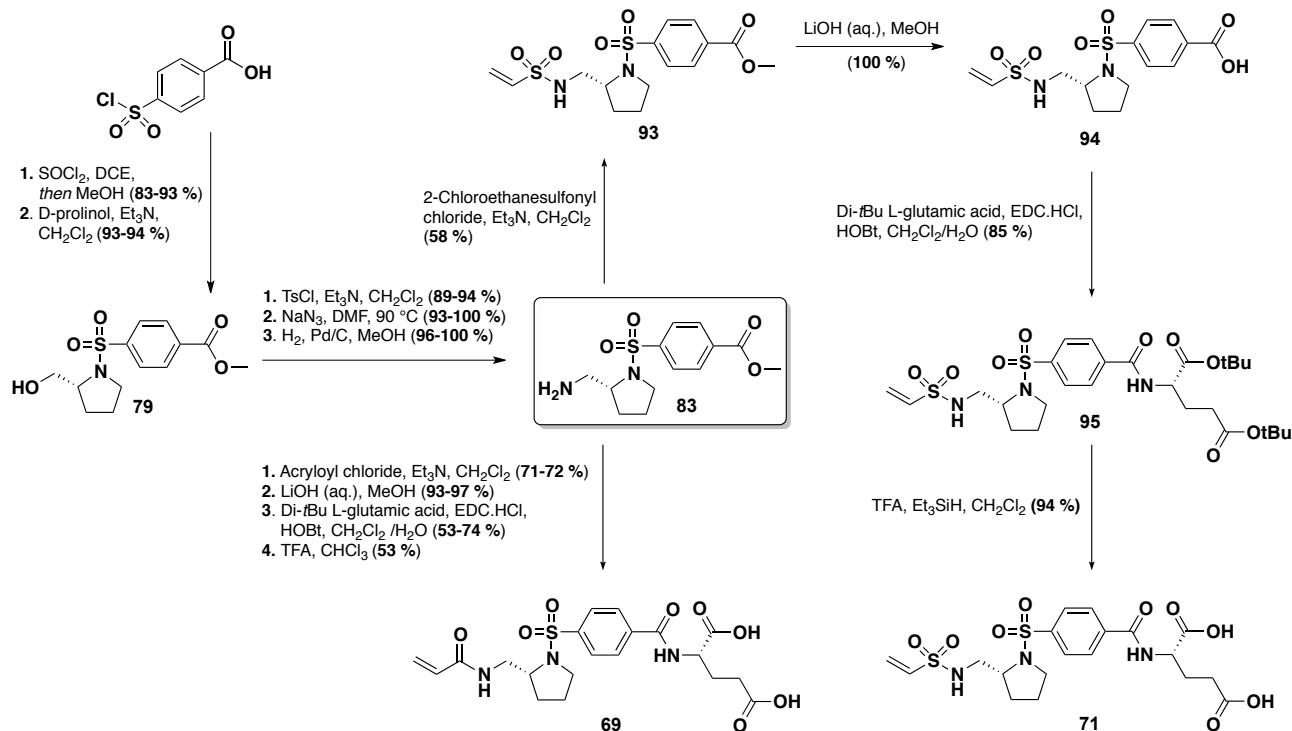
Scheme 10 Overall synthetic route to both acrylamide and vinyl sulfonamide-modified higher affinity positive control compounds. Amine **83**, a common intermediate in both routes, is highlighted.

Unfortunately, severe solubility problems were encountered with both final compounds acrylamide **69** and vinyl sulfonamide **71**. Both were found to be insoluble in all solvents tested, including DMSO, despite extended sonication and gentle heating. Attempts to generate salts from the corresponding acids in order to increase aqueous solubility were unsuccessful.

3.3.3. Negative control

A route to the desired negative control ligand **68** was designed as shown retrosynthetically in Scheme 11. In this route, the acrylamide is installed last, allowing divergence at the lastest point in the synthesis for the potential addition of other capture groups at a later point. The primary amine **96** is generated from N-methyl D-prolinol **97** in the three step tosylation-azide displacement-reduction sequence previously applied to positive controls. The N-methyl D-prolinol **97** is generated by a reductive amination of D-prolinol.

Scheme 11 Retrosynthetic analysis of negative control ligand **68**.

Eschweiler-Clarke reductive amination of D-prolinol using 37 % aqueous formaldehyde and formic acid furnished the desired N-methyl D-prolinol **97** in a moderate 66 % isolated yield after reflux for 20 h, Scheme 12. Although tosylation of N-methyl D-prolinol was successful, with the desired product **98** identified by ^{1}H NMR of the crude

reaction mixture, the mass recovery for the reaction was poor due to the difficulty in extraction of the product from the basic aqueous layer during reaction work up. In addition, the product was observed to undergo decomposition on silica during purification. It was considered at this point that taking the basic N-methyl pyrrolidine functionality through the synthesis would result in significant mass loss due to high aqueous solubility. To overcome this, it was decided that the synthesis would commence with a Boc protection of the pyrrolidine N, with the protecting group removed and the N methylated in the final two steps.
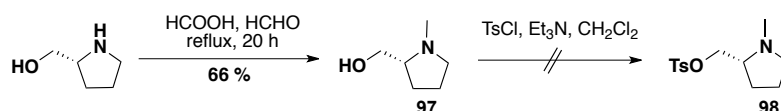
Scheme 12

Boc protection of D-prolinol was successful, generating the desired pyrrolidine **99** in a 73 % isolated yield. The synthetic route was also started from D-proline with a LiAlH$_4$ reduction and Boc-protection to yield intermediate **99**. Treatment of D-proline with LiAlH$_4$ for 1 h at 0 °C and subsequent Boc protection led to a 56 % isolated yield of **99**, Table 6 (entry 1). Increasing the LiAlH$_4$ reaction time to 1 h at 0 °C and 1 h at rt led to an increase of the the isolated yield of **99** to 68 % over the two steps (entry 2).

Entry	Conditions	Yield 99 (%)
1	0 °C (1 h)	56
2	0 °C (1 h) then rt (1 h)	68
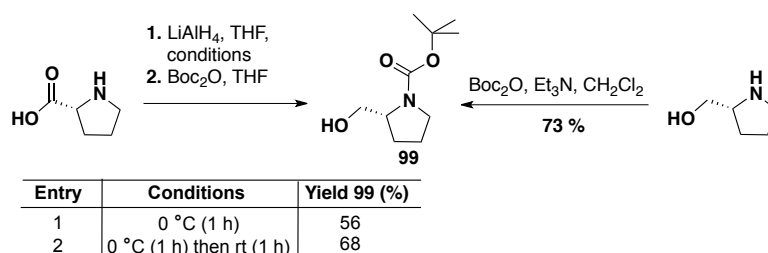
Table 6 Boc protection conditions.

The desired pyrrolidine **100** was generated in 89 % yield by tosylation of alcohol **99** with 1.2 equivalents of tosyl chloride in pyridine, Table 7 (entry 1). Changing the tosylation conditions to 3 equivalents of both tosyl chloride and triethylamine led to a quantitative yield of pyrrolidine **100** (entry 2).
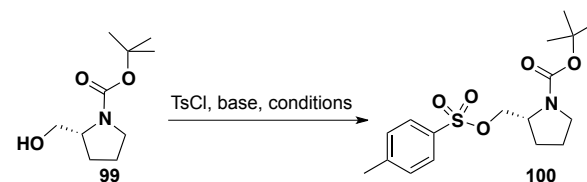
Entry	TsCl eq.	Temp (°C)	Time (h)	Base (eq.)	Yield 100 (%)
1	1.2	0	6	Pyridine (solvent)	89
2	3.0	rt	16	Et$_3$N (3.0)	100

Table 7 Conditions for the tosylation of pyrrolidine **99**.

S$_N$2 displacement of the tosylate was unsuccessful with 2.15 equivalents of azide in DMF, Table 8 (entry 1). Changing the solvent to DMSO and increasing the number of equivalents of azide to 6 led to the desired azide **101** in moderate yields of between 78-81 % (entry 2).

Table 8 Conditions for the synthesis of azide **101**.
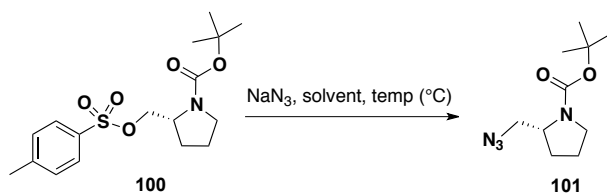
Entry	NaN₃ (eq.)	Temp (°C)	Solvent	Yield 101 (%)
1	2.15	90	DMF	0
2	6.0	65	DMSO	78-81

Hydrogenation of azide **101** using a Pd/C catalyst under an atmosphere of H_2 gas led to the desired amine **102** in high yields of between 75-100 %, Scheme 13. Reaction of the primary amine with acryloyl chloride generated N-Boc protected acrylamide **103** in moderate yields between 67-72 %, ready for the final Boc-group removal and reductive amination.
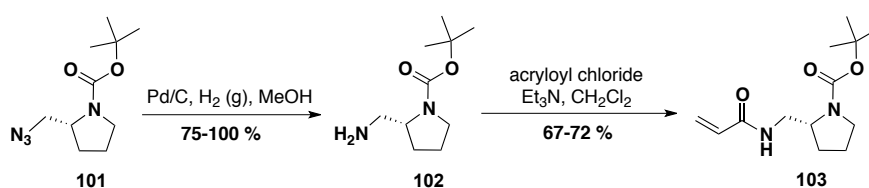
Scheme 13

Following treatment of N-Boc acrylamide **103** with TFA, ^{1}H NMR indicated a mixture of two acrylamides. However, column chromatography on silica to separate these compounds resulted in the isolation of only one compound, which had no olefinic protons by ^{1}H NMR. ^{13}C NMR and ^{1}H NMR were consistent with this product as the 5,7 fused bicyclic ring **104** resulting from a 7-endo-trig intramolecular conjugate addition of the free secondary amine at the acrylamide β-carbon, Scheme 14.
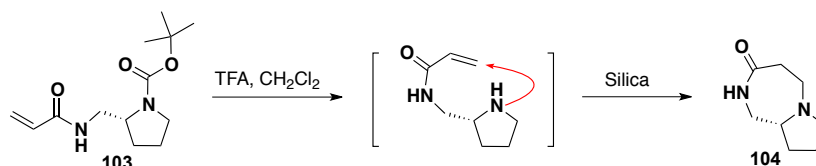
Scheme 14

The most intense peak obtained during electrospray mass spectrometry analysis had a mass consistent with dimer **104a** [2M + H]⁺, with a small peak with the mass of the 5,7 bicyclic ring **104**. The appearance of the dimer peak is likely to be explained by the formation of intermolecular H-bond bridges which are stable enough to stay intact during ionisation in the mass spectrometer, Figure 54. The observation of such intermolecular H-bond bridges by MS has been previously reported for similar structures.[158] If the presence of peak [2M + H]⁺ in the mass spectrum had been due to covalent dimer **104b**, then a peak for **104** [M + H]⁺ would probably not have been observed.
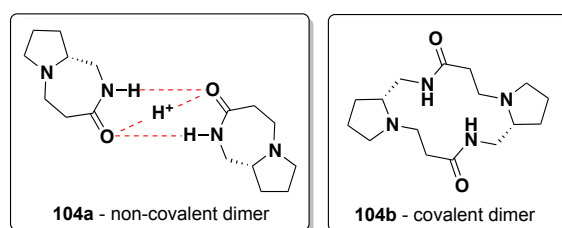
Figure 54

Protection strategy

With a gram quantity of the N-Boc protected pyrrolidine **103** in hand, a protecting group strategy to mask the acrylamide during the deprotection and reductive amination steps starting from this intermediate **103** was desired. It was considered that conjugate addition of a latent leaving group to the α,β-unsaturated amide would protect the acrylamide during the Boc-removal and reductive amination steps, before 'activation' of the of the leaving group and regeneration of the acrylamide. Substituted selenides and sulfides are obvious choices for this chemistry due to their high propensity for conjugate addition, and ease of removal by elimination after oxidation to the selenoxide or sulfoxide respectively. Both sulfoxide and selenoxide 2,3-*syn* eliminations proceed through planar 5-membered transition states, but the rate of this reaction is significantly higher for selenoxides which often fragment spontaneously at room temperature.[159] Sulfoxides often require heating to effect the desired elimination, the rate of which increases with increasing degree of double bond substitution.[160] Elimination from β-phenylsulfinyl carbonyls is favoured relative to the analogous α-phenylsulfinyl derivatives due to the increased acidity of the proton which is abstracted in the transition state. In addition, β-phenylsulfinyl carbonyl elimination does not lead to the development of positive charge adjacent to the carbonyl as the C-S bond breaks, an unfavorable situation which does occur in the analogous α-phenylsulfinyl elimination, Figure 55.[160]
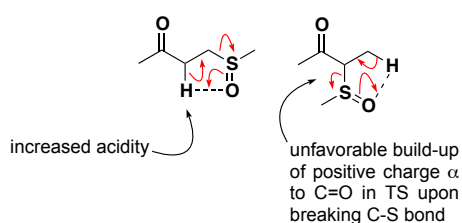
Figure 55 A comparison of the 2,3-*syn* elimination of α- and β-phenylsulfinyl carbonyls to generate the α,β-unsaturated carbonyls.

Murphy *et al*. used thiophenol to protect acrylamide **105** during the synthesis of Coerulescine and Horsfiline, Scheme 15.[161, 162] Thioether **106** was stable under the DIBAL-H reduction conditions to generate alcohol **107**, and oxidation to the sulfoxide and subsequent elimination regenerated the acrylamide **108**.
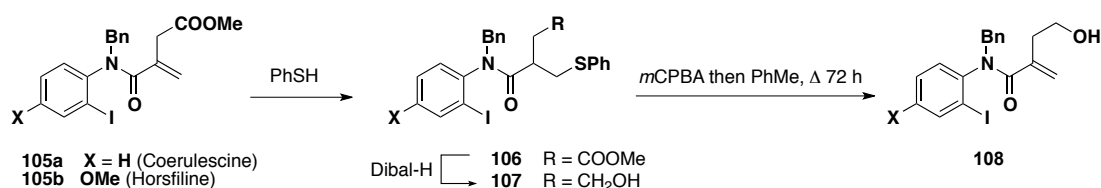
Scheme 15 Use of thiophenol as an acrylamide protecting group reported by Murphy *et al*. in their synthesis of Horsfiline and Coerulescine.

This thiophenol protecting group strategy was adopted to protect acrylamide **103** in the synthesis of negative control ligand **68**. A model acrylamide **47** was initially adopted to test the suitability of this strategy, Scheme 16. As the rate of sulfoxide 2,3-*syn* elimination can vary considerably depending on the degree of alkene substitution, it was important to establish conditions for elimination to generate the monosubstituted acrylamide. It was also crucial to establish the stability of the thioether to the acidic reductive amination conditions. 1,4-Addition of thiophenol to

acrylamide **47** generated the desired thioether **109** in a 41 % isolated yield. To test the stability of this to the Eschweiler-Clarke reductive amination conditions, thioether **109** was subjected to 24 h reflux in formic acid and 37 % aqueous formaldehyde, and whilst a few side-products were observed to form by TLC, the starting material was still the main component of the reaction mixture. Oxidation of the thioether to the sulfoxide **110** was effected in high yields using either *m*CPBA (89 %) in chloroform or sodium *meta*-periodate (85 %) in MeOH but not sodium *meta*-periodate in a mixture of MeOH and H_2O which returned only starting material, possibly due to its insolubility in the MeOH/H_2O mixture, Table 9. The sulfoxide was heated to reflux in chloroform in an attempt to effect the desired 2,3-*syn* elimination. However, even after 120 h the sulfoxide **110** remained as the major product by TLC although with a number of minor side-products. Pleasingly, treatment of thioether **109** with potassium *tert*-butoxide in THF gave complete conversion to the acrylamide **47** by elimination of thiophenolate with formation of no other side-product. A ^{1}H NMR yield of 74 % was obtained for this reaction after aqueous work up. As base treatment of thioether **109** led directly to the desired product in high yield and concomitantly removed one step from the linear sequence, the sulfoxide elimination was not further pursued.
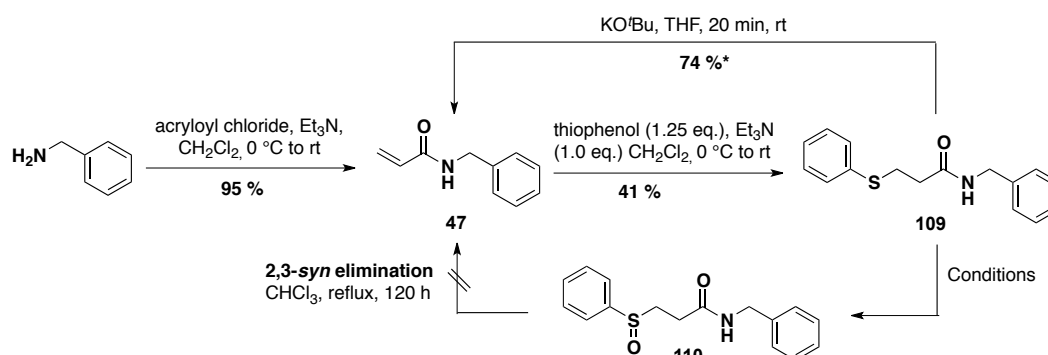
Scheme 16 Protecting group strategy using test substrate acrylamide **47**. *Yield estimated by ^{1}H NMR with tetramethylsilane as the internal standard.
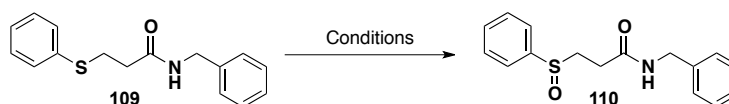
Entry	Conditions	Yield 110 (109) (%)
1	NaIO$_4$, MeOH, rt, 24 h	85
2	NaIO$_4$, MeOH/H$_2$O, rt, 2 h	0 (97)
3	*m*CPBA, CHCl$_3$, 0 °C, 2 h	89

Table 9 Conditions for the oxidation of sulfide **109** to sulfoxide **110**.

Treatment of the N-Boc pyrrolidine intermediate **103** with 2 equivalents of thiophenol and 1 equivalent of triethylamine in dichloromethane generated the desired thioether **111** in a poor 23 % isolated yield, Table 10 (entry 1). This was improved to 65 % by changing the solvent to THF and increasing both the equivalents of thiophenol and triethylamine to 3.2 and 4.5 respectively (entry 2). The Boc group was successfully removed in an excellent 97 % yield using 4 M HCl in dioxane to yield the desired amine **112** as the HCl salt.

Table 10 Conditions for the conjugate addition of thiophenol to acrylamide **103**.
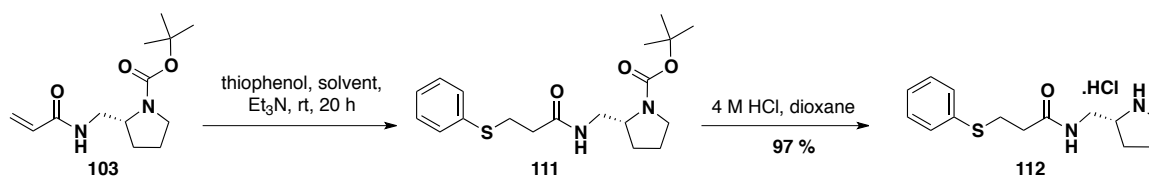
Entry	Solvent	Thiophenol (eq.)	Et$_3$N (eq.)	Yield 111 (%)
1	CH$_2$Cl$_2$	2.0	1.0	23
2	THF	3.2	4.5	65

An Eschweiler-Clarke reductive amination reaction to methylate the pyrrolidine N was unsuccessful, and resulted in decomposition, Table 11 (entry 1). The reductive amination was successfully carried out by refluxing the free amine in methanol and paraformaldehyde followed by reduction with sodium cyanoborohydride to generate N-methyl pyrrolidine **113** in a 97 % isolated yield (entry 2). Finally, the N-Me pyrrolidine thioether **113** was treated with potassium *tert*-butoxide to funish the final negative control ligand **68** in a moderate 52 % isolated yield.
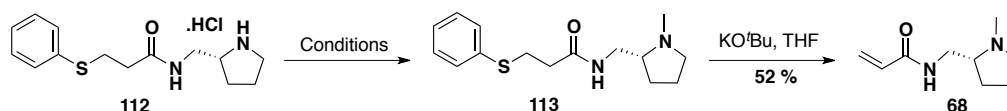
Entry	Conditions	Yield 113 (%)
1	Formaldehyde (37 % aq.), formic acid, reflux.	0
2	Paraformaldehyde, MeOH, reflux *then* NaCNBH$_3$	97

Table 11 Reductive amination conditions.

The Boc-deprotection of acrylamide intermediate **103**, which led to the formation of 5,7-bicyclic **104** as previously discussed, was thought to be an interesting reaction for further investigation. To test the effect of different Boc-deprotection reagents on this reaction, acrylamide **103** was treated with 2 M HCl in ether for 3 h. Analysis of the crude reaction mixture by ^{1}H NMR indicated that the reaction had gone to two products, consistent with the desired acrylamide and the 5,7-bicyclic system **104** in approximately a 1:1.25 ratio. This mixture was subjected to reductive amination conditions, Scheme 17, which surprisingly led to the isolation of dimer **114**. Formation of dimer **114** presumably results from successful reductive amination followed by intermolecular attack from the tertiary N onto the α,β-unsaturated bond of a second acrylamide. It is surprising that this occurs in preference to the intramolecular reaction. It may be the case that the intramolecular reaction is readily reversible, but then it is again surprising that this reversibility is not seen for the intermolecular reaction. Furthermore, it is curious that no further polymerisation occurred during this reaction, although this may account for the lost mass. It was hypothesised that treatment of intermediate **114** with strong base would effect the elimination of the tertiary amine leaving group, generating two molecules of the desired product. Indeed, addition of potassium *tert*-butoxide to dimer **114** generated the desired acrylamide **68** in yields between 58-82 %, providing a second route to the desired negative control ligand.
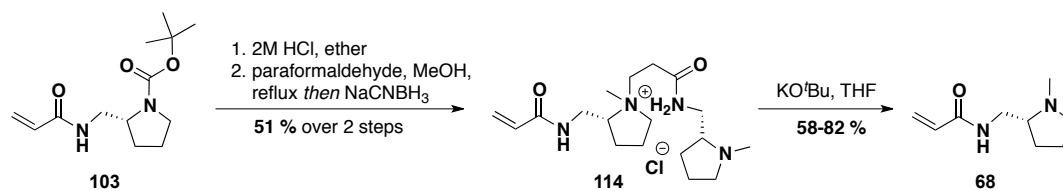
Scheme 17

In summary, the desired negative control ligand with an acrylamide appendage **68** was successfully synthesised using two synthetic routes, Scheme 18. The first route utilised a sulfide protecting group strategy, whereby addition of thiophenol to the acrylamide masked the reactive functionality during Boc-deprotection and reductive amination. This route reached the desired product in 9 steps from either D-proline or D-prolinol, with all steps achieved in moderate-to-high yields. The second route reached the desired product in 7 steps *via* generation of the unusual dimer intermediate **114**.
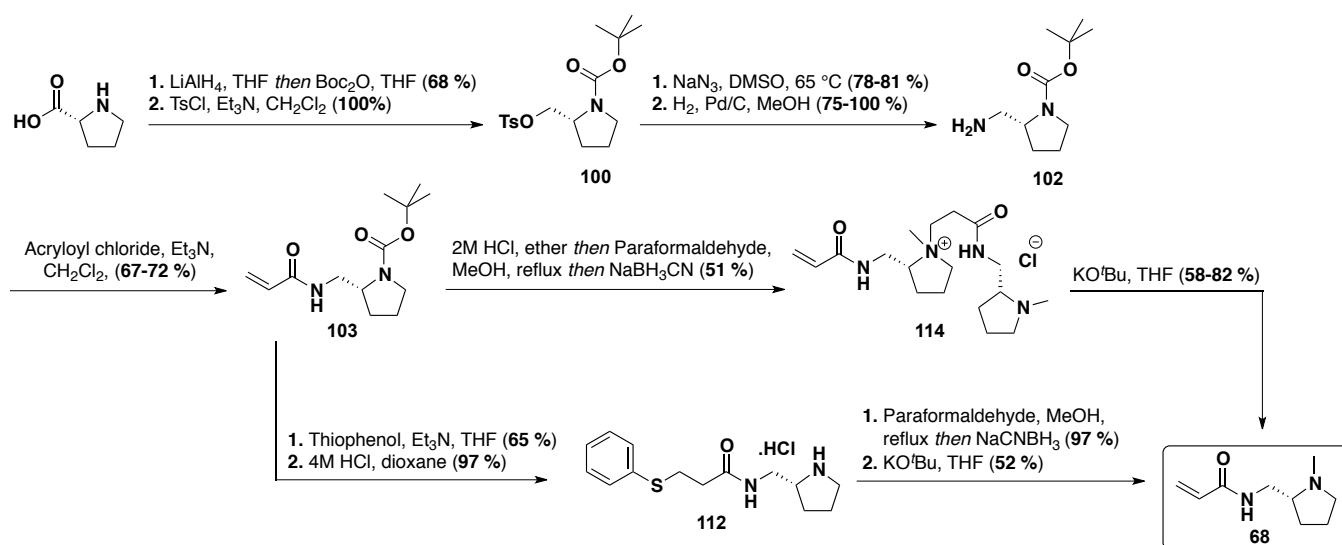
Scheme 18 Synthesis of negative control acrylamide **68**.

3.4. Acrylamides and kinetic template-guided tethering

3.4.1. Intrinsic ligand reactivity

An HPLC study was carried out to compare the intrinsic reactivity of positive control acrylamide **67** with a number of the 'dummy' acrylamides before protein screening. It was crucial that selection of the positive control from a mixture of acrylamides by the protein was due to a template-based rate enhancement rather than a high intrinsic reactivity. Binary mixtures of acrylamides, composed of the positive control with one dummy ligand, were incubated with an excess of reduced glutathione. Reactions were carried out in an aqueous ammonium bicarbonate buffer at pH 8, to mimic the conditions later used for protein screening, and aliquots taken for HPLC analysis at various time points. The concentrations of both acrylamides within the binary mixture were measured at these time points and the ratio plotted against time, Figure 56. Interestingly, the data identified the positive control acrylamide as the least intrinsically reactive in the mixture, although acrylamides **48**, **54** and **55** were observed to react only very slightly

faster. N-phenyl piperazine acrylamide **49** was identified to react significantly faster than the positive control and was expected to react promiscuously during protein screening. Conjugate addition of glutathione to acrylamide **51** was exceptionally fast with the reaction complete in less than one minute. Acrylamide **51** was therefore excluded from protein screening experiments on this basis. Acrylamide **49** was not excluded from protein screens as it was hoped to qualitatively indicate the degree of selection conferred by KTGT.
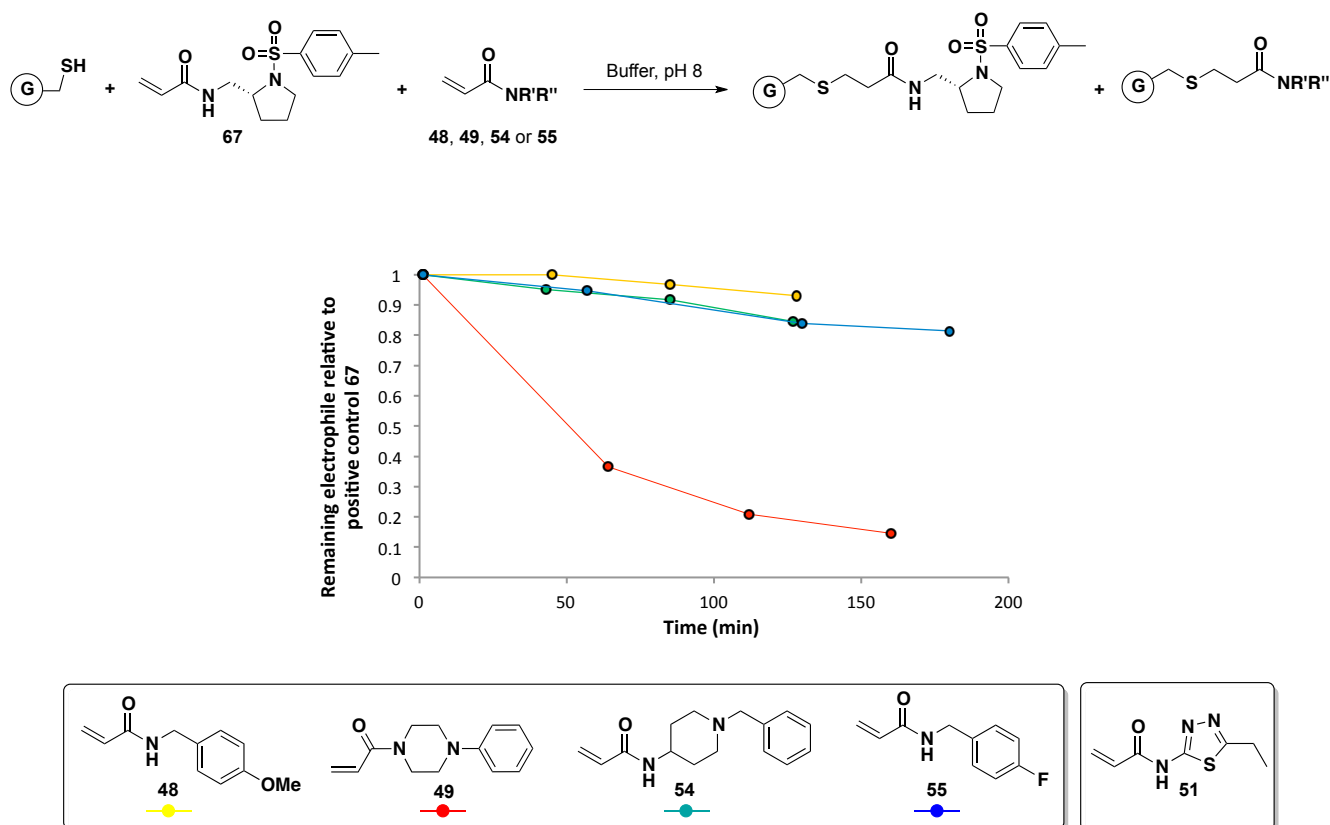
Figure 56 Relative Michael addition rates between the positive control and a series of 'dummy' acrylamides with reduced glutathione (G). Binary mixtures of acrylamides as indicated were incubated with an excess of reduced glutathione and the concentration of each remaining electrophile monitored over time by HPLC. The chart indicates [acrylamide]/[positive control **67**] against time.

3.4.2. Mass spectrometry analysis

Analysis of the complete thymidylate synthase catalytic domain (TS) by MALDI confirmed the unsuitability of this mass spectrometry technique for KTGT screening, Figure 57. The base of the singly charged protein peak spans a mass range of *ca*. 2000 Da, 10 times the mass of acrylamide-fragments. As discussed (Chapter two) attempts were previously made to develop a three-stage screening protocol for KTGT including incubation of protein with acrylamides, trypsin digestion of the crude mixture and subsequent analysis by MALDI. It was identified as crucial to fully quench the acrylamide before the addition of trypsin to prevent nonspecific untemplated tethering to peptide fragments during proteolysis. In order to develop such a procedure and to validate KTGT, TS was adopted as a model system due to the significant difficulties encountered with cdc25 which lacks a positive control. Before the use of TS in the development of a proteolytic procedure for analysis of KTGT using MALDI, a significant effort was applied to develop an electrospray ionisation (ESI) mass spectrometry protocol for analysis of full molecular weight TS. ESI would eliminate the additional variables conferred by the quench and proteolytic digestion, and would allow KTGT to

be observed *in situ*. The facilty for analysis of proteins by ESI had not been available during the previous studies conducted in chapter two.*
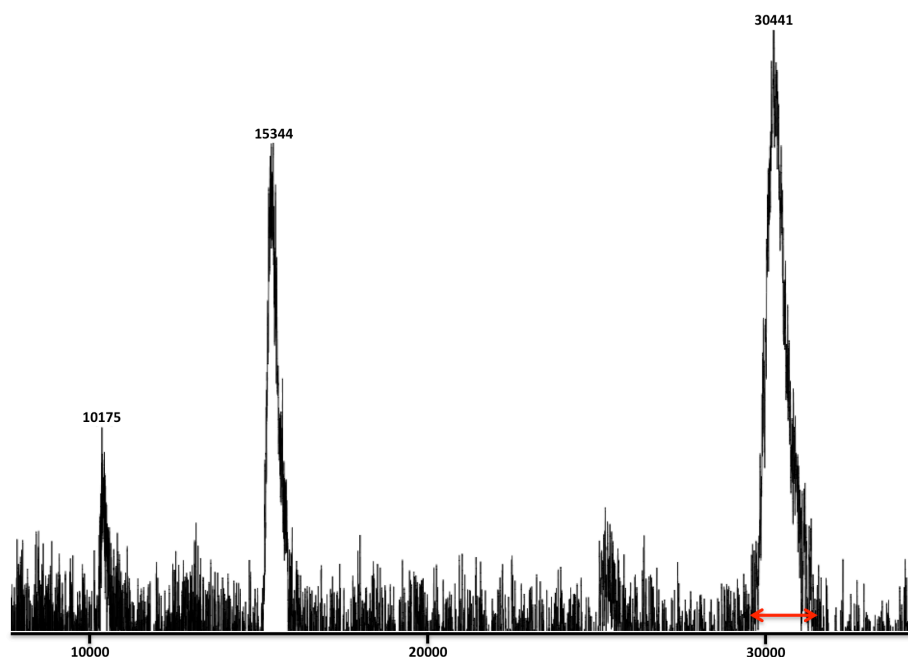
Figure 57 MALDI analysis of TS. The singly charged peak has a base width of approximately 2000 Da as indicated by the red arrow. The doubly and triply charged peaks are also evident from the spectrum.

Electrospray Ionisation MS and Matrix-Assisted Laser Desorption Ionisation MS

In general, mass spectrometers are composed of an ionisation source, a mass analyser and a detector. During ionisation, gas phase ions are generated from the analyte and are subsequently separated based on their *m/z* ratio by the mass analyser. Before the development of MALDI and ESI MS, there were a number of available methods for analyte ionisation (including electron ionisation (EI) and chemical ionisation (CI)), but none that were able to cause ionisation without analyte fragmentation. Both MALDI and ESI are soft ionisation methods – with ESI described as the most gentle ionisation technique available for MS[163] – in that minimum internal energy is transferred to the analyte, overcoming the propensity of the analyte to fragment.[164] Both methods are suitable for the analysis of high molecular weight biomolecules, including DNA, proteins, lipids and glycoconjugates.

In ESI MS, the sample is continuously sprayed into the ionisation source *via* a thin needle at which a high electrical potential is applied. This results in the formation of electrically charged droplets, a process which is termed nebulisation. The solvent evaporates from the charged droplets until the repulsive forces between the ions at the droplet surface exceed surface tension and the ions desorb into the gas phase. Generally, the ions generated by the ESI process remain intact (i.e. no fragmentation) and are multiply charged by protonation (in positive ion mode) or deprotonation (in negative ion mode). The peaks generated for the analyte therefore form an envelope along the *m/z*-axis where each peak represents the intact molecular species with particular charge. The molecular mass of the analyte can be determined from two adjacent peaks within this envelope by a technique termed 'mathematical charge deconvolution'. If the molecular mass of the analyte is termed M and the *m/z* ratios for two adjacent peaks

---

*Both MALDI and ESI ionisation sources were coupled time-of-flight (ToF) mass analysers for the work carried out in this thesis.

representing charge states (n)$^+$ and (n-1)$^+$ are termed m_1 and m_2 respectively then two simultaneous equations are generated, where $m_1 = (M + n)/n$ and $m_2 = [M + (n - 1)]/(n - 1)$ which can be solved for M and n. An accurate mass for the analyte is usually generated from the average mass calculated for each set of two adjacent peaks within an envelope. This manual interpretation of ESI spectra is challenging when mixtures of analytes are used, with each different species generating a distinct envelope of multiply charged peaks which interlace with each other and are difficult to distinguish. Deconvolution software, such as 'MaxEnt' developed by Waters, is usually required to deconvolute such spectra. ESI has no theoretical limit for the molecular weight of the analyte due to this multiple charging effect which lowers the m/z ratio to within the detection limit.

The observed charge state distribution (CSD) for analytes is affected by many factors and is a topic which has been intensely debated over the past two decades. Somewhat counterintuitively it has been shown that the analyte charge state (CS) observed in the gas phase does not correspond to that in the bulk solution.[165] In addition, the maximum CS in positive mode does not necessarily correspond to the number of basic sites (for proteins Lys, His, Arg and N-terminus) and in negative mode, acidic sites (Glu, Asp, Asn, Gln and C-terminus). Whitesides *et al*. suggest that this is due to a fundamental difference between solution and gas phase acidity/basicity.[166] In solution, the net charge of a protein depends on the number of ionisable groups, their pKa values and the pH of the solution. In the gas phase, the net charge depends on physical properties such as the molecular surface area and the Coulombic repulsion between charged sites on the protein surface.[166] A critical determinant of the CSD is the geometry and size of the analyte in question. For example, the CSD is narrower and the average CS is lower for a native protein in comparison to the same protein after denaturation. Upon denaturation, the spatially compact, native protein becomes extended and solvent exposed leading to the change in average CS and CSD, shown schematically for cytochrome C in Figure 58.[167] At pH 6.4, cytochrome C adopts its native, tightly folded conformation leading to a narrow CSD with the average CS as +8 observed in the positive ESI mass spectrum. Under denaturing conditions (pH 2.4), the protein is mainly in an unfolded state, leading to an increase in the average CS from +8 to +17 and an increase in the number of total charges present within the CSD. Folded and non-folded states can also be observed to co-exist in equilibrium with one another, Figure 58 pH 2.6. Similar observations were made by LeBlanc *et al*. upon heat denaturation of proteins,[168] whilst Loo *et al*. found the CSD to vary with the denaturing capacity of the solvent.[169] Covey *et al*. proposed that the maximum CS for a protein or peptide corresponds to the number of basic sites,[170] but although this often correlates reasonably well with observed results, there are also significant anomalies. For example, both actin and S4 ribosomal protein contain 46 basic sites.[171, 172] S4 ribosomal protein demonstrates a maximum CS of +30, which correlates well with the theories of both Covey and Whitesides. Actin, however, demonstrates a maximum charge state of +56 indicating that it can retain significantly more protons than it has basic sites.
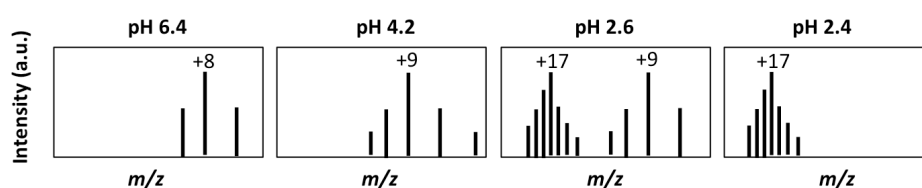
Figure 58 ESI mass spectra of cytochrome C at pH 6.4, pH 4.2, pH 2.6, and pH 2.3. pH adjusted by addition of hydrochloric acid to the protein in 0.5 mM ammonium acetate with 3 % MeOH. Image reproduced from work published by Konermann *et al*.[167]

In constrast to ESI, MALDI-MS usually results in the generation of only the singly charged molecular ion. Peaks due to the doubly and triply charged analyte may be observed in low intensity. The resolution achieved using MALDI usually decreases as the molecular weight of the analyte increases, due to isotopic broadening of the peak.

Both MALDI and ESI sources were coupled to time-of-flight mass analysers for the work carried out in this thesis. The purpose of the mass analyser within a mass spectrometer is to separate the gaseous ions based on their *m/z* values. There are currently four main mass analysers in use: Quadruple (Q), Quadruple ion trap (QIT), Time of Flight (ToF) and Fourier Transform Ion Cyclotron Resonance (FT-ICR).[164] The ToF mass analyser accelerates ions using an electric field of known strength. The kinetic energy transferred to ions with a particular charge is constant, resulting in a slower passage through the analyser for ions with higher mass.

Method development for ESI

The initial challenge in the development of a KTGT ESI screening procedure was to find conditions that would allow the ionisation of protein in the mass spectrometer. The protein must be in a solution of buffer with reducing agent during the incubation with acrylamide fragments. The buffer ensures that the pH is kept constant, irrespective of the acrylamide-fragments added, whilst also stabilising the folded state of the protein and the reducing agent prevents oxidation of the active site cysteine thiol. Such conditions require careful consideration, as buffers, salts and metal ions have the potential to interfere significantly with the quality of ESI spectra.[130]

In the initial protocol adopted, the TS pellet obtained from the protein purification was resuspended in TRIS-HCl buffer (20 mM), and dialysed for 48 h against the same buffer to remove any bound sulfate ions. The concentration of the resultant protein solution was then adjusted as required for KTGT experiments, and incubated with acrylamides. After the incubation period was complete, the aqueous solvent was removed *in vacuo* and the pellet redissolved in MeCN/H$_2$O (0.1 % TFA) (1:1) for MS analysis. As TRIS-HCl buffer is usually acceptable at, or below, concentrations of 100 mM,* it was the buffer of choice initially used to test this procedure. However, despite the low concentrations of TRIS-HCl buffer present, no multiply charged peaks to indicate protein were obtained. Use of the volatile buffer ammonium bicarbonate (50 mM) in this procedure rather than TRIS-HCl also failed to generate a protein electrospray spectrum.

To overcome this, a new strategy was adopted to remove the buffer ions. The protein was precipitated from a phosphate buffer by addition of ice-cold methanol, on the premise that whilst the protein precipitates, buffer and other organic molecules remain in solution. This method assumes that covalent attachment of a fragment to the active site cysteine does not affect the precipitation efficiency of the protein. To develop a protocol for this, some preliminary experiments were carried out. To analyse qualitatively how much protein from the original sample was precipitated over time, methanol was added to three identical samples. From one of the samples (lane 1, Figure 59) the protein precipitate was collected after 2 minutes on ice, whereas both the second and third samples (lanes 2, 3) were kept at -80 °C overnight after methanol addition with one (lane 2) washed with ice-cold methanol after the pellet was collected. Retention of protein after incubation overnight at -80 °C appeared to be almost quantitative, with only a

_____

* Personal communication with J. Barton, Imperial College Mass Spectrometry Technician.

small loss when a methanol wash was applied. However, precipitation of TS (using lane 3 conditions) and submission of the protein pellet to the ESI conditions[*] resulted in no multiply charged peaks.
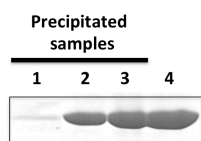
Figure 59 Qualitative analysis of the retention of protein during the precipitation protocol. **Lane 1** precipitation of protein by addition of 200 μL methanol (at -20 °C) to 20 μL TS in potassium phosphate for 2 minutes. Precipitate collected and dissolved in 20 μL phosphate buffer. **Lane 2** As for lane 1, but sample allowed to precipitate overnight at -80 °C, and subsequently washed with methanol (200 μL, -20 °C) before addition of phosphate buffer. **Lane 3** As for lane 2 but no methanol wash. **Lane 4** TS with no precipitation.

Adopting a third strategy, the buffer was changed to 10 mM ammonium bicarbonate, the ESI conditions were changed to MeOH/0.5 % aq. formic acid (1:1) rather than MeCN/0.1 % aq. TFA (1:1), and the solution was manually injected onto the spectrometer using a syringe pump, with data collected over a 3 minute period. This finally resulted in the generation of multiply charged peaks, which could be deconvoluted using MaxEnt to give the mass of the protein as 30410 Da as expected, Figure 60.
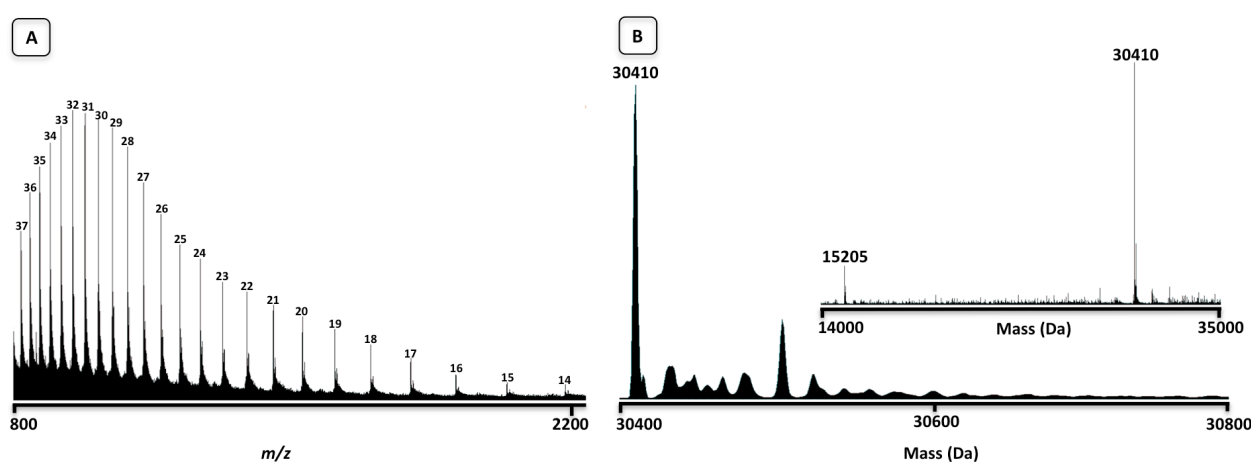
Figure 60 A typical spectrum obtained by positive mode ESI MS of thymidylate synthase. **A**. Raw data clearly demonstrates the expected envelope of multiply charged peaks. The charges have been labelled and range from + 37 to + 14 as calculated from the molecular mass (30409 Da) using $m = (M - n)/n$ as previously described. **B**. Deconvoluted spectrum (MaxEnt) in the mass range of interest (30400-30800 Da where tethered adducts are expected) and over the full range. The peak for singly charged thymidylate synthase is labelled (30409 Da) along with the peak for the doubly charged protein (15205 Da).

Conveniently, it was found that the 1:1 MeOH/0.1% aq. formic acid solvent mixture for MS could be added straight to the protein/ammonium bicarbonate solution [MeOH/0.1% formic acid/protein solution, 2:2:1 by volume] to achieve the same mass spectrum. The step to remove the buffer *in vacuo* was therefore removed from the protocol.

The final optimised protocol used for KTGT screening, Figure 61, was as follows. After purification of TS, ammonium sulfate was used to precipitate the protein, which was stored at -80 °C as a pellet until required. The pellet was then dissolved in ammonium bicarbonate (10 mM) and DTT (1 mM)[†] and dialysed for 48 h against 4 x 2 L changes of the same buffer. This very thorough dialysis was required to remove all bound sulfate ions.[‡] After dialysis the protein concentration was adjusted to 10 μM using a Bradford assay or Nanodrop, and stored at 4 °C for up to one month. Ligands were added to aliquots of the protein stock solution and after the set incubation time quenched with

---

[*] Pellet re-dissolved in acetonitrile:aqueous TFA (0.1 %).
[†] See appendix III, p219 for rationale behind DTT concentration.
[‡] See appendix III, Figure 129, p218 for spectrum obtained if dialysis is not thorough enough.

0.5 % formic acid and MeOH and the sample injected on to the electrospray mass spectrometer. Mass spectrometry results presented herein were obtained using this protocol.
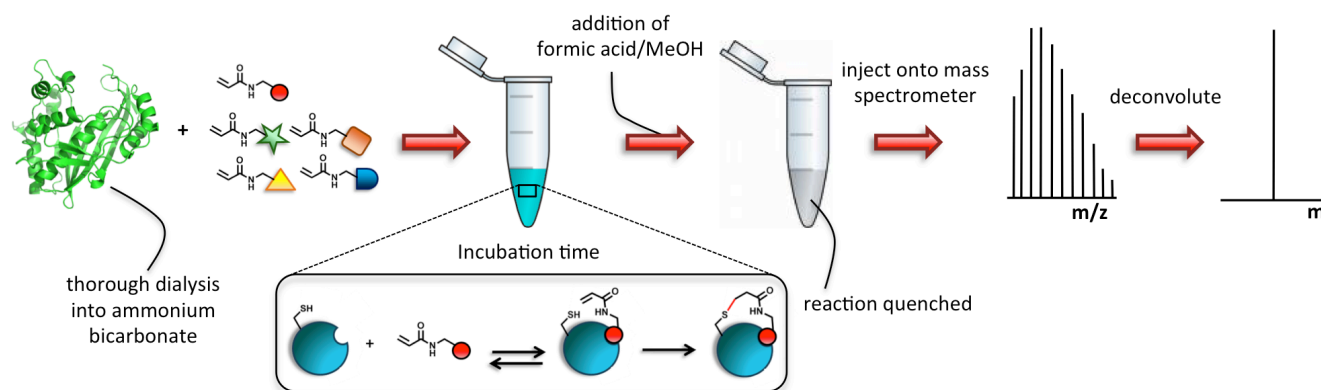
Figure 61 Optimised protocol for KTGT using ESI MS analysis. Before use, TS protein was dialysed thoroughly into an ammonium bicarbonate (10 mM) buffer to remove non-volatile buffer ions. The protein was then incubated with acrylamides/vinyl sulfonamides for a specific time at rt. A 1:1 formic acid (0.5 % aqueous)/MeOH mixture was subsequently added to prepare the solution for MS analysis and concomitantly to quench the reaction. The resulting mixture was injected onto the mass spectrometer at a rate of 20 μL/min, and data recorded for at least 3 min. The resulting envelope of multiply charged peaks was deconvoluted using Waters MaxEnt software.

Mass spectrometry experiments

Treatment of TS with an excess of iodoacetamide resulted in single and complete modification of the apo protein to the protein-acetamide adduct (protein + 57 Da) indicating only one surface exposed cysteine residue in agreement with reported experiments,[51] Figure 62.
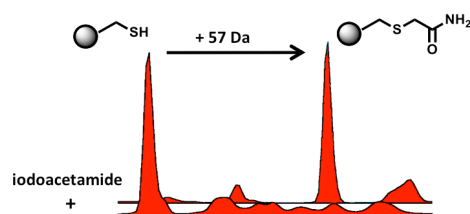
Figure 62 Front MS trace: apo TS. **Back MS trace:** TS (10 μM) after treatment with iodoacetamide (4 mM) for 10 min at rt. TS is shown as a grey sphere.

Treatment of TS with positive control acrylamide-fragment **67** led to single modification of the protein after 30 min at room temperature. The yield of the adduct formed within this time period was dependent on the concentration of acrylamide **67** applied, Figure 63. At 100 μM acrylamide **67**, only a low yielding adduct was observed to form during the 30 min incubation time, but on increasing the concentration to 200 and 400 μM, the yield of this adduct increased significantly. When TS was incubated with a mixture of acrylamide **67** and acrylamide **47** (in a 1:1 molar ratio), only positive control **67** was selected by the protein, even when both were applied at 400 μM (appendix III, p218, Figure 127).
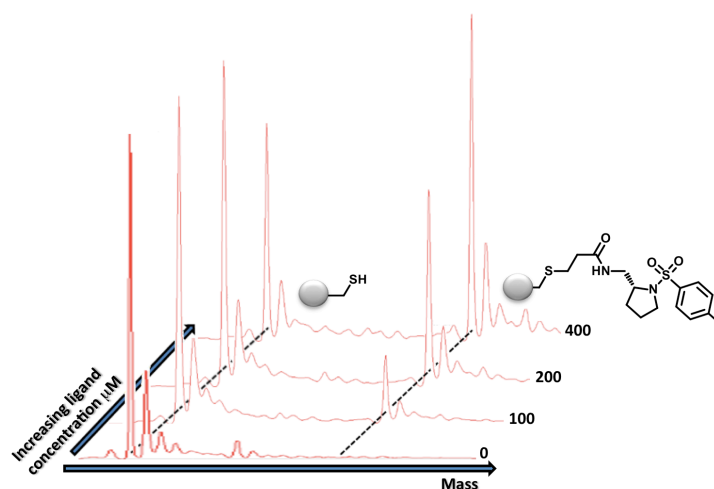
Figure 63 Overlaid mass spectra of TS incubated for 30 minutes with acrylamide ligand **67** at increasing final concentrations of 0, 100, 200 and 400 μM. The peak for TS is seen to diminish in favour of the TS-**67** adduct as the concentration of fragment **67** is increased.

The protein was subsequently incubated with mixtures of acrylamides, as indicated in Figure 64. Incubation of TS with mixture I at room temperature, with each acrylamide at 400 μM, resulted in modification of the apo protein with only acrylamide **67**, Figure 65. Complete modification of the apo protein with this positive control compound occurred before the formation of any other adduct, despite the presence of the more intrinsically reactive N-phenyl piperazine fragment **49**.

Mixture I	47, 48, 49, 55, 67
Mixture II	47, 48, 49, 55, 67, 68
Mixture III	47, 48, 49, 55, 67, 54, 119
Mixture IV	47, 48, 49, 55, 67, 54, 119, 46, 53
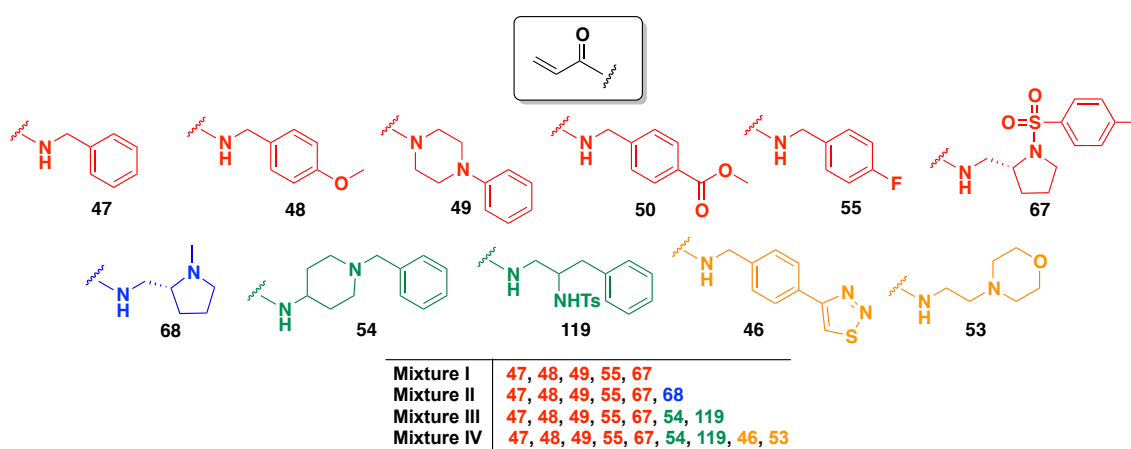
Figure 64 Acrylamide mixtures used in MS studies.
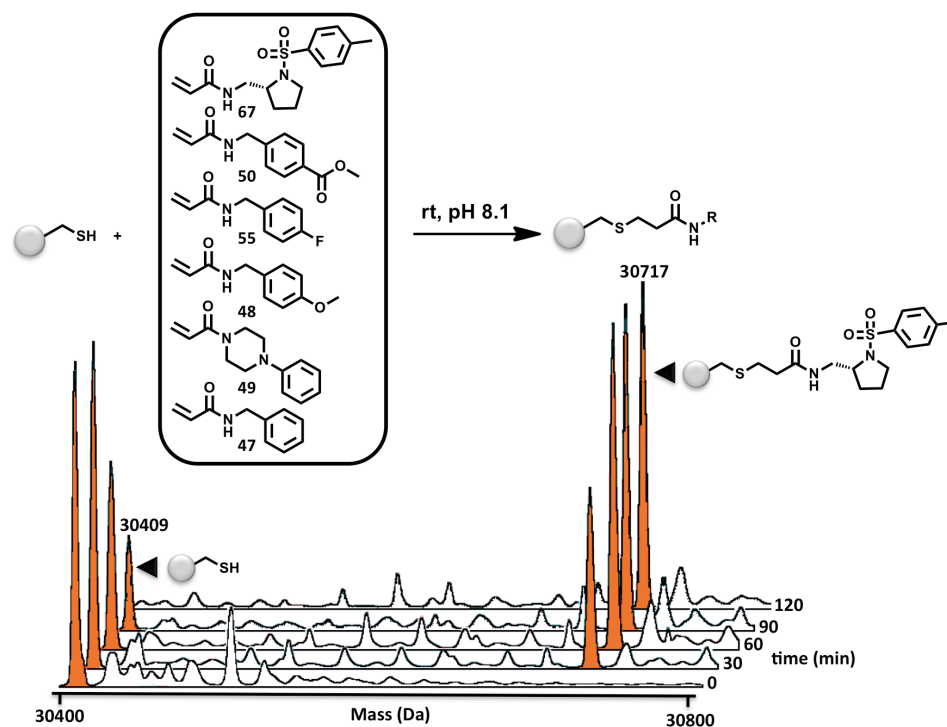
Figure 65 TS incubated with library of acrylamide-fragments, mixture I, each library member present at 400 μM and protein at 10 μM. Aliquots taken at the times indicated and analysed by electrospray MS. This indicated an increase in the concentration of the TS-**67** adduct at the expense of the apo protein, with no other TS adduct formed. Peaks corresponding to the protein and to the protein-**67** adduct are highlighted in orange.
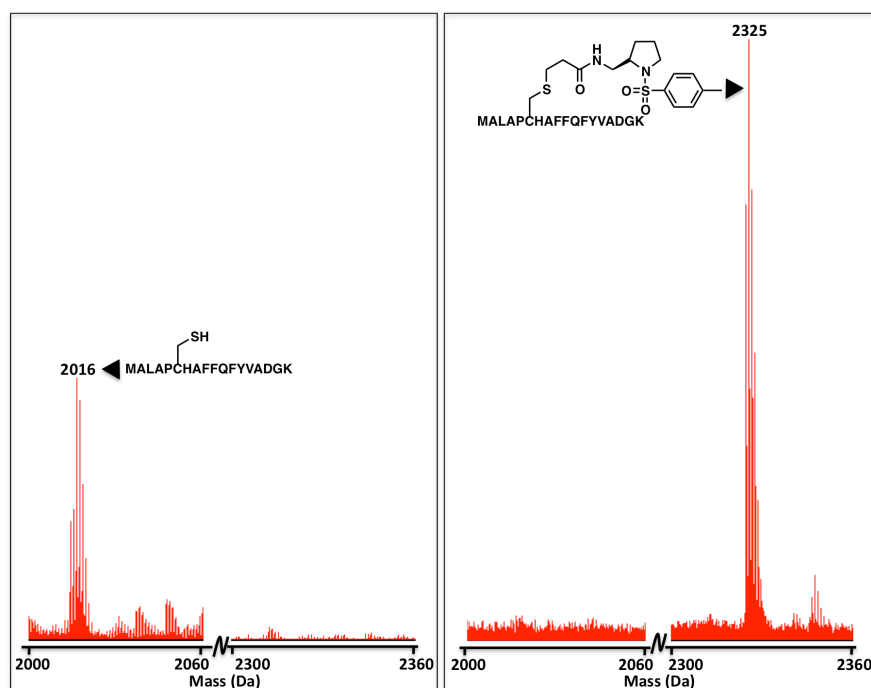
Figure 66 Trypsin digest and MALDI analysis of apo TS (left) and TS-**67** (right).

Complete modification of TS with acrylamide **67**, enzymatic digestion with trypsin and analysis of the peptide mixture using MALDI, localised the position of modification to the peptide containing the active site cysteine, Figure 66. Full modification of TS with iodoacetamide and incubation of the TS-acetamide adduct with acrylamide **67** resulted in no further modification of the protein. These experiments strongly suggested that modification of the protein had occurred at the expected surface exposed cysteine. The adduct formed between TS and positive control **67** was confirmed to be through a stable covalent bond; TS was fully modified with positive control **67** and subsequently washed thoroughly with an ammonium bicarbonate solution using a centrifuge filter to remove low molecular weight

entities but retain protein. Analysis of the resulting mixture by ESI MS indicated that the TS-**67** adduct had remained intact.

Fragment **47** was incubated with TS at 2.4 mM for 4 h and peaks corresponding to TS-**47** and the apo protein were observed (appendix III, p218, Figure 128). This indicated that other TS-fragment adducts were able to form under more forcing conditions and furthermore, that these were able to ionise in the ESI MS. Incubation of mixture II with papain and p97 resulted in the formation of no adduct, consistent with no kinetic-template-guided tethering, although both papain and p97 underwent full and single modification with iodoacetamide under the same conditions as TS, indicating the presence of a reactive solvent exposed cysteine thiol. As papain is a cysteine protease, and therefore designed to attack amide bonds, some tests were carried out to check the stability of the acrylamides in the presence of the enzyme. To a solution of papain in ammonium bicarbonate (pH 8), three acrylamides (**49**, **55** and **67**) were separately added from MeOH stock solutions. The stability of the acrylamides was monitored by TLC, indicating only a trace of side-product formation after 7 h. The experiment with **67** was repeated on a larger scale and analysed by ^{1}H NMR after 16 h, confirming the presence of only a trace of a side-product.

Surprisingly, when TS was incubated with mixture II, which contains negative control **68** in addition to the acrylamides in mixture I, formation of an adduct to both the positive and negative control compounds was observed. The TS-negative control adduct formed to a greater extent than the TS-positive control adduct, Figure 67.
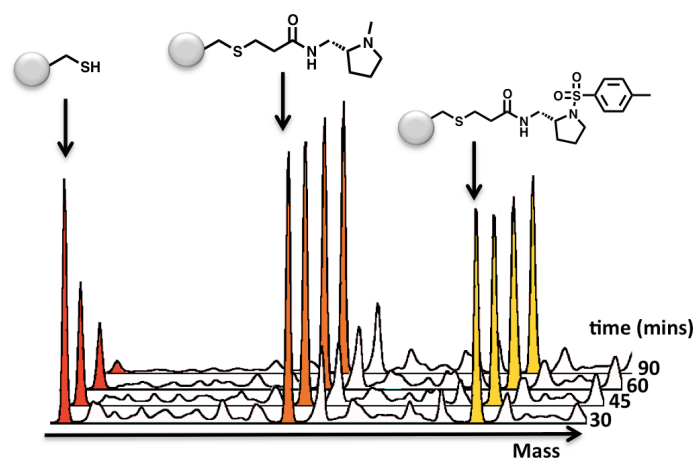
Figure 67 TS incubated with Mixture II (each acrylamide at a final concentration of 343 μM) in ammonium bicarbonate buffer (10 mM) at pH 8. Adducts to both the positive (yellow) and negative (orange) control are observed to form with the peak due to apo TS highlighted in red.

Unlike the positive control adduct, Figure 69, formation of the negative control adduct was strongly dependent on pH, Figure 68, with adduct formation at pH 8.1, but almost no formation at pH 7.2. Incubation of TS with mixture II at pH 7.2 for 60 minutes resulted in formation of an adduct only to the positive control **67**, with formation of an adduct to the negative control only visible after 120 minutes, Figure 70. When mixture II was incubated with papain at pH 8.1, no adduct was observed to form to any acrylamide, including the negative control compound **68**, suggesting that modification of TS by acrylamide **68** did not occur on the basis of a high intrinsic reactivity. The position of modification by negative control ligand **68** was confirmed at the catalytic cysteine in the same way as for the positive

control ligand. This included MALDI analysis after trypsin digestion and addition of acrylamide **68** to a solution of TS fully modified with one equivalent of iodoacetamide, which led to no further reaction.
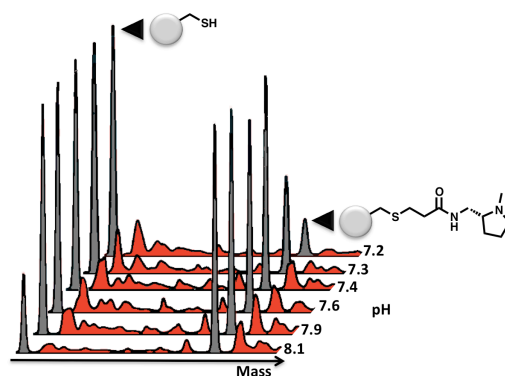
Figure 68 TS incubated with negative control compound **68** at 400 μM for 60 minutes at rt in the presence of formic acid, giving the pH values indicated.
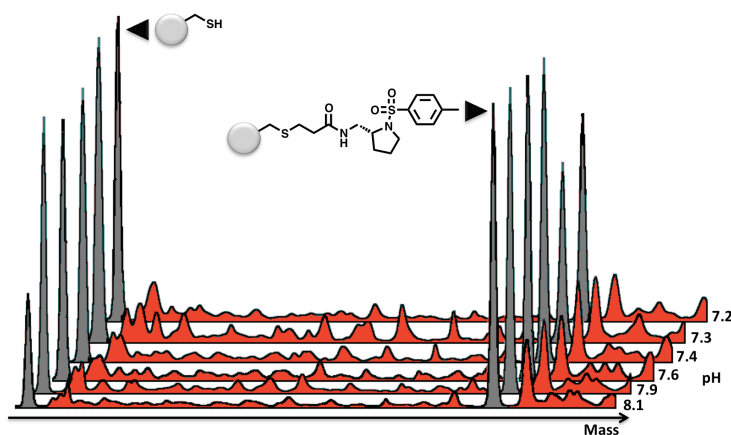
Figure 69 TS incubated with positive control compound **67** at 400 μM for 60 minutes at rt in the presence of formic acid, giving the pH values indicated.
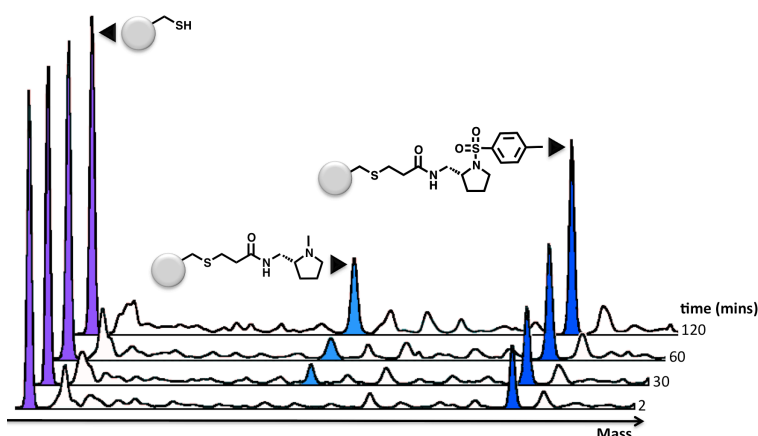
Figure 70 TS incubated with mixture II, each acrylamide at 300 μM, at pH 7.2. Aliquots taken for MS analysis at 2, 30, 60 and 120 minutes.

Disulfide tethering studies carried out by Erlanson *et al.*, whereby disulfide **65** was identified not to bind to TS, were carried out in aqueous solutions of pH 7.5.[51] It was considered that the basicity of the N-pyrrolidine in acrylamide

ligand **68** may have accounted for its selection by TS. The pKa of N-pyrrolidine is reported as 10.46 in aqueous solution,[173, 174] but the effect of the acrylamide moiety in **68**, or the amide in **65** on this value was unknown. Interestingly, the aqueous pKa values for a series of cyanoamines were available, Figure 71.[175] The tertiary amine in 1,5-substituted **115** has a basicity comparable to N-pyrrolidine, with pKa = 10.46. However, as the cyano group was brought closer to the amine in 1,2-substituted **116**, the effect on the basicity of the N was significant, bringing the pKa value down to 7.5 due to the destabilising electron withdrawing effect of the nitrile on the cationic charge at the protonated N. A further significant shift in basicity was observed for 1,1-substituted **117** with pKa = 4.5, although overlap between the N lone pair and the C-CN σ* orbital may contribute towards this. By comparison with this series of cyanoamines, the pKa of tertiary amine **68** was predicted to be *ca*. 7-8. Continuing this estimation, tertiary amine **65** was expected have a pKa value of *ca*. 4-5, although the validity of this particular estimate may be compromised by the lack of orbital overlap of the N lone pair with a low energy σ* orbital. On these assumptions, however, decreasing the pH from 8.1 to 7.2 leads to significant protonation of tertiary amine **68,** suggesting that it was the deprotonated form of this ligand which is selected by TS.
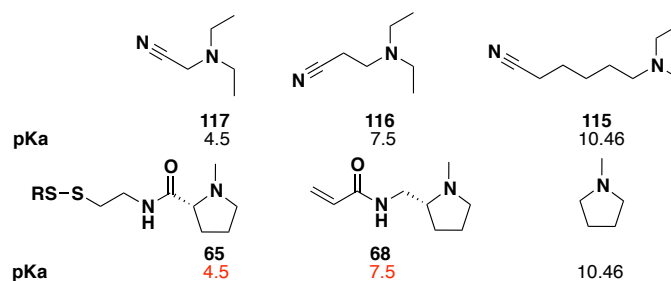
Figure 71 Reported pKa values (black),[173-175] and estimated pKa values (red).

Several mechanisms were considered to account for these observations as outlined below and summarised in Figure 72.

1. At *ca*. pH 8 and in a deprotonated state, pyrrolidine **68** may undergo an intramolecular cyclisation from the teriary N onto the acrylamide to form a 5,7-bicyclic ring system. This could in itself be a fragment binder, whilst also providing a site of electrophilic attack. As the pH is lowered, the tertiary amine becomes protonated and this cyclisation is prevented.

2. In its deprotonated state, ligand **68** may form hydrogen bonding interactions to residues within the protein pocket, an interaction which would not occur upon protonation.

3. The tertiary amine moiety within **68** may catalyse the addition of the catalytic thiol to the acrylamide by acting as a base to generate the thiolate. This seems highly plausible given that the active site cysteine, with a pKa of 8,[141] would be only partly deprotonated at pH 8.1 and the reaction would therefore be particularly susceptible to base-mediated acceleration. Similar rate-accelerated cysteine thiol-acrylamide Michael additions using a built-in tertiary amine have previously been previously reported.[112, 176]
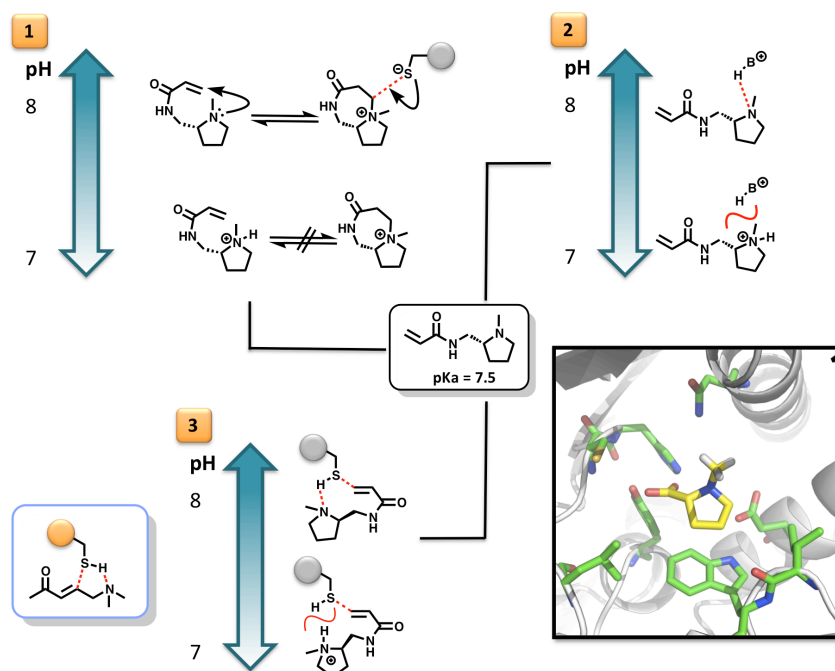
Figure 72 Three possible mechanistic explanations for the pH-dependent selection of negative control ligand **68** by TS. **1**. At pH 8 an intramolecular cyclisation occurs to form 5,7-bicyclic compound **104** which in itself is an electrophilic TS fragment binder. **2**. Deprotonated ligand **68** makes favourable interactions with a residue in the pocket of TS at pH 8, which are disrupted at pH 7 as the pyrrolidine becomes protonated. Image shows PDB file 1F4C altered using WebLabViewer to replace the N-tosyl with an N-methyl. Residues within 4 Å of the pyrrolidine ligand are highlighted, with the protein secondary structure in grey. Image generated using PyMol. **3**. At pH 8, the deprotonated pyrrolidine **68** is able to accelerate the addition of the catalytic cysteine to the acrylamide by intramolecular base-catalysis. Upon lowering the pH the pyrrolidine becomes protonated and therefore unable to catalyse the addition. Shown highlighted in the blue box: intramolecular base-catalysed addition of an acrylamide to a cysteine thiol reported by Wissner *et al*.[176]

3.4.3. Synthesis of a second negative control ligand

In their original disulfide tethering proof-of-concept, Erlanson *et al*. reported that, in addition to disulfide **65**, disulfide **118** was not selected by TS.[51] Ligand **119** was therefore designed and synthesized to replace acrylamide **68** as a negative control for KTGT, based on the disulfide-modified ligand originally reported, Figure 73.
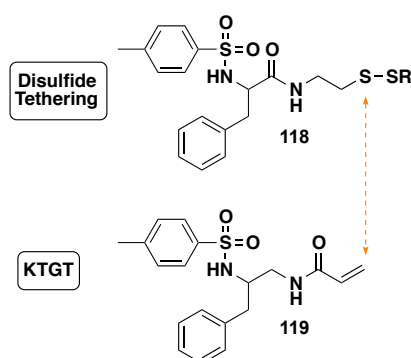
Figure 73 Design of an alternative negative control ligand by comparison with a ligand reported not to be selected by TS by Erlanson *et al*.[51] Dotted arrow compares the position of electrophilic attack for both ligands.

The synthetic route to novel compound **119** commenced with a Sharpless aziridination of allyl benzene using chloramine-T.3H$_2$O and catalytic trimethylphenyl ammonium tribromide (PTAB), Scheme 19.[177] The aziridine **120** was isolated as an inseparable mixture with an unidentified impurity and was taken straight on to the next step. The

ring opening was carried out using TMSN$_3$ to yield an inseparable mixture of both ring-opened regioisomers **121a/121b** in an 8:1 ratio in favour of the desired isomer **121a**. This mixture was hydrogenated using Pd\C catalyst and H$_2$ to give the mixture of amines **122a/122b** and subsequently treated with acryloyl chloride to give, after purification, the desired negative control ligand **119** in a 27 % yield over two steps. An unexpected side-product **123** was isolated in a 19 % yield from the final step of this reaction sequence, which was tentatively assigned as shown in Figure 74.
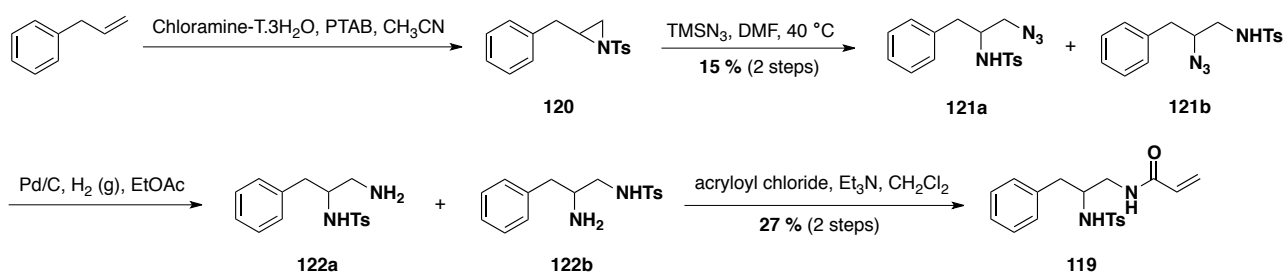
Scheme 19 Synthesis of negative control ligand **119**.
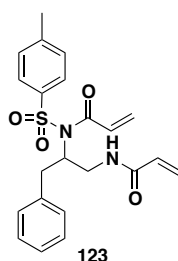
Figure 74 Isolated as a side-product after the treatment of amines **122a/122b** with acryloyl chloride.

Both compounds **119** and **123** have very similar R$_f$ values, leading to a close separation during purification on silica gel. The desired compound **119** was isolated in complete purity by ^{1}H NMR and TLC (with none of the side-product **123** observed), but this was not sufficient for KTGT experiments. Incubation of TS (10 μM) with 400 μM of acrylamide **119** for 20 min led to the formation of a significant adduct between TS and the impurity **123**, in addition to an unassigned adduct with a molecular weight 27 Da higher than than the TS-**123** adduct, Figure 75. The *N*-(sulfonamide)-acrylamide Michael acceptor within ligand **123** was likely to be highly reactive towards conjugate addition, such that contamination of the sample of acrylamide **119** with only a trace quantity of this reactive compound was significant enough to react with the catalytic cysteine. The contaminated sample of acrylamide **119** was subjected to further purification using a preparatory LC-MS to remove traces of reactive ligand **123**. Incubation
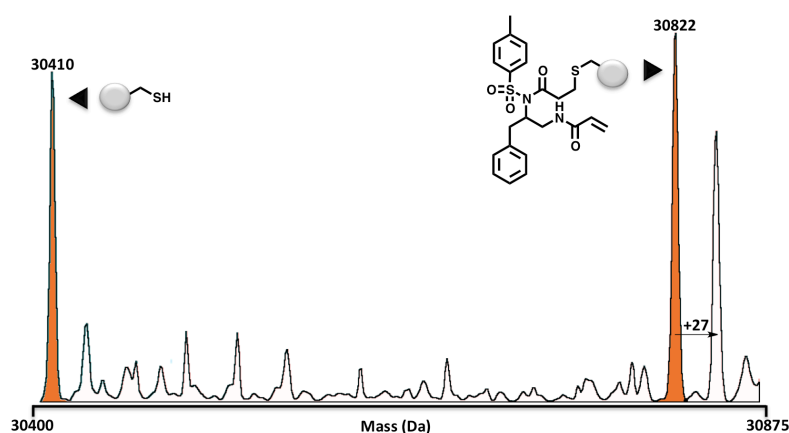
of TS with pure negative control compound **119** at 400 μM led to no modification of the protein, even after a 60 minute incubation period.

Figure 75 Deconvoluted ESI mass spectrum of a sample of TS (10 μM) incubated with acrylamide **119** (purified by column chromatography on silica) (400 μM) in an ammonium bicarbonate buffer (10 mM) with DTT (1 mM), pH 8, after 20 min incubation. A adduct to side-product **123** was observed as indicated.

Incubation of cdc25A with mixture IV with each acrylamide at 100 μM led to the formation of a low yielding adduct to negative control compound **119**, but not to any other acrylamide in the mixture, including the positive control **67**. Cdc25A was incubated with iodoacetamide to generate a cdc25A-acetamide adduct over time. The reaction was noted to be slower than with TS, papain or p97, which all went to completion within 10 min. The reaction between cdc25A and iodoacetamide went only to 25 % completion within 10 min, and to 65% after 60 min. This may be due to the very small and narrow active site pocket shielding the active site cysteine residue from the bulk solvent.

When TS was incubated with mixture III with each acrylamide at final concentration of 100 μM, no adduct was identified to form to negative control ligand **119** and an adduct was formed, as expected, to positive control compound **67**. However, a further adduct was also observed to form with N-benzylpiperidine acrylamide **54**, Figure 76. When TS was incubated with a slightly larger library, mixture IV, still only adducts to positive control **67** and N-benzylpiperidine acrylamide **54** were formed. The adduct to N-benzylpiperidine acrylamide **54** was localised to the active site cysteine, as was previously carried out for positive control **67** and negative control **68**, using MALDI after trypsin digest and addition to TS after full modification with iodoacetamide. TS and N-benzylpiperidine acrylamide **54** were identified to form a stable covalent bond in the same manner as was carried out for positive control **67**. TS was fully modified with N-benzylpiperidine acrylamide **54** and the mixture subjected to thorough washing through a centrifuge filter. Subsequent analysis by ESI MS indicated that the TS-**54** adduct was still intact.
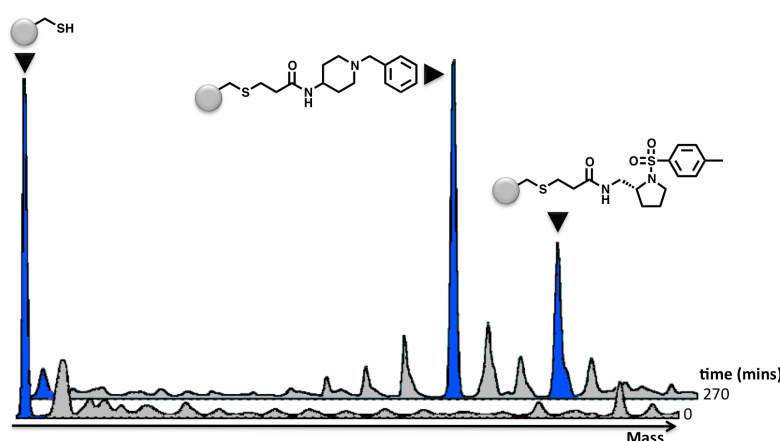
Figure 76 TS (10 μM) in ammonium bicarbonate (10 mM), DTT (1mM), pH 8, incubated with mixture III, each acrylamide at 100 μM, and analysis at 270 min.

As this fragment contains a basic amine, with a pKa value of approximately the same value as for negative control **68**,[178, 179] it was considered that it may act *via* a similar base-catalysed intramolecular thiol deprotonation mechanism, Figure 77. Whilst this could not be ruled out, this ligand did not show a tethering dependence on pH between 8.1 – 7.2 as was observed for negative control **68**. The molecular similarity between positive control **67** and piperidine ligand **54** suggested that perhaps N-benzylpiperidine acrylamide **54** was actually a fragment binder of TS. Additionally, the N-benzyl piperidine motif was found embedded within a series of ligands reported as TS inhibitors.[180] The spectrophotometric assay, originally reported by Wahba and Friedkin, and previously used to confirm TS activity, was used to measure the binding affinity for the fragments used in the acrylamide-tethering studies. The aim of this work

was to confirm acrylamide **67** as a positive control and to elucidate the binding affinity of the N-benzyl piperidine fragment **54** in addition to a selection of the other ligands.
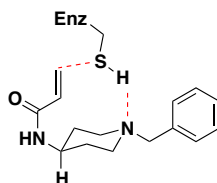
Figure 77 Acrylamide **54** may react with TS *via* an intramolecular deprotonation of the cysteine thiol.

3.4.4. Synthesis of non-tethering control ligands and spectrophotometric assay

A series of non-tethering ligands was required to quantify binding to the active site pocket. These were synthesised from the respective amine and either acetyl chloride or acetic anhydride, Figure 78. N-tosyl D-proline **64**, synthesised from D-proline and tosyl chloride (Equation 3), was used as a control with a known K_i value.[51]

X	R^1	R^2	Yield (%)	Method
124	H	CH_2p-FC_6H_4	69	a
125	H	CH_2p-$(OMe)C_6H_4$	59	a
126	-	N-phenyl piperazine	58	a
127	H	4-(N-benzyl)piperidine	90	c
128	H	CH_2-2-(N-tosyl)-D-pyrrolidine	68	b
129	H	CH_2Ph	71	c
130	H	CH_2p-$CO_2MeC_6H_4$	65	d
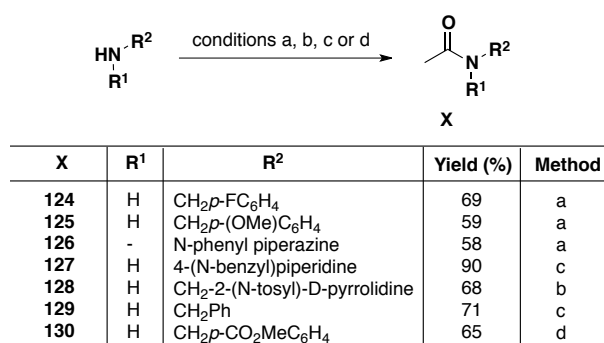
Figure 78 a. AcCl, Et_3N, Et_2O **b.** AcCl, Et_3N, CH_2Cl_2 **c.** Ac_2O, CH_2Cl_2 **d.** AcCl, Et_3N, THF.
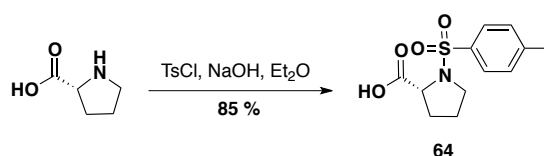
Equation 3

Thymidylate synthase (TS) catalyses the methylation and subsequent reduction of dUMP using mTHF as a cofactor for both steps, resulting in the production of dTMP and DHF as previously discussed. The sequential mechanism proposed for this reaction involves the initial binding of the substrate dUMP before binding of the cofactor mTHF. Once substrate and cofactor are bound, methylation and reduction reactions occur sequentially before the release of dihydrofolate and subsequently thymidylate. N-tosyl D-proline inhibitor **64** was determined as competitive with only dUMP by Erlanson *et al*.[51] This is perhaps initially counterintuitive when the crystal structure of this ligand bound to TS is examined, as the ligand clearly overlaps with both the dUMP and mTHF binding sites, Figure 79. This is presumably due to the sequential order of TS catalysis, in which if dUMP is unable to bind then mTHF is also unable to bind. In steady state Michaelis Menten enzyme kinetics, the K_M value equals the concentration of substrate required to generate an initial velocity equal to half the maximum velocity (V_{max}). Ideally, when using an assay to measure IC_{50}

values for competitive inhibitors, substrate concentrations equal to their K_M values are used to ensure that the inhibitor is not out-competed by the enzyme substrate. If higher substrate concentrations are used, higher inhibitor concentrations are required in order to be able to monitor inhibition. The K_M values for dUMP and mTHF from the literature vary from 0.2-5.0 μM and 14-15 μM respectively. Ideally, therefore, in this assay the concentration of dUMP used would be *ca*. 2 μM.
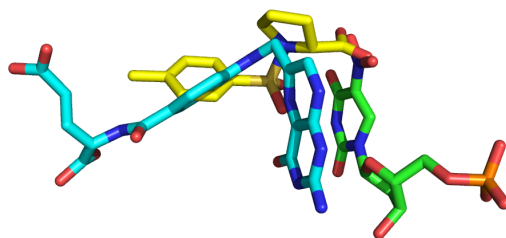
Figure 79 Overlay of two crystal structures: *N*-tosyl D-proline (carbons in yellow) bound in the active site of TS (PDB code 1F4C) and mTHF (carbons in cyan) and dUMP (carbons in green) bound in the active site of TS (PDB code 3BHL).

Unfortunately, due to technical limitations, sensitivity at the required 340 nm wavelength was too low to screen at dUMP K_M concentrations. To get an accurate and reliable measure of the initial enzyme velocity, a 0.1 unit change in absorbance over time was required, which meant a minimum dUMP concentration of 20 μM. Below 20 μM dUMP, the quantity of DHF formed during the course of the reaction was too low to detect. Using the Cheng-Prussoff equation to relate IC_{50} to K_i, a dUMP concentration of approximately 10 x K_M yields IC_{50} values that are *ca*. 10 x K_i values. Using fragment inhibitors with intrinsically low affinity (high K_i values) led to practical difficulties using the spectrophotometric assay.

To generate an IC_{50} curve for N-tosyl D-proline **64**, a range of log[inhibitor] concentrations between 0.5 - 1.2 were screened against the enzyme (0.1 μM) with mTHF (150 μM) and dUMP (20 μM) at 25 °C. The enzyme was preincubated with the inhibitor for 15 min prior to addition of substrates. Initial velocities were calculated by fitting a linear trendline to the initial portion of the curve and taking the gradient as a fraction of the initial velocity of the uninhibited reaction. This generated a sigmoidal dose-response curve with an IC_{50} value of 10.4 ± 0.1 mM, which is an order of magnitude higher than the reported K_i value (1.1 mM ± 0.25 mM) as expected, Figure 80. Using the Cheng-Prussoff equation and an experimentally determined K_M value for dUMP,[181] the IC_{50} was converted into a K_i value of 0.59 ± 0.06 mM, in reasonable agreement with the literature.[51]
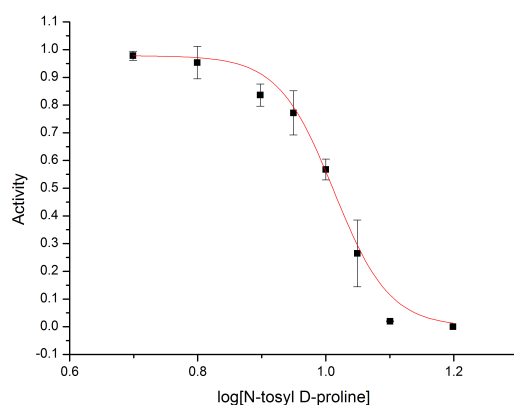
Figure 80 IC_{50} curve for N-tosyl D-proline **64**. Points are the average of three repeats and error bars represent the standard deviation. Sigmoidal curve generated using OriginPro 8.5 software.

Applying the same method to generate an IC_{50} value for positive control acetamide **128** failed due to poor solubility at the high concentrations required. In an attempt to overcome this, the percentage of DMSO was increased from 4 to 8 % and samples were both pre-incubated and assayed at 30 °C rather than 25 °C. These conditions conferred sufficient aqueous solubility that acetamide **128** could be dissolved at all the required concentrations. Unfortunately, even under these conditions, acetamide **128** crystallised from the solution during the course of the assay leading to an unexpected, rapid increase in absorbance at 340 nm over time, Figure 81. All other compounds retained greater than 70 % enzyme activity at 40 mM, except for N-benzyl piperidine acetamide **127**, which only retained 66 % activity at 30 mM. An IC_{50} value for inhibitor **127** greater than 30 mM implies that this compound is a very weak TS fragment binder with a $K_i > 3$ mM. The weak affinity of acetamide **127** for TS may suggest that tethering to acrylamide fragment **54** occurs by an intramolecular base-mediated rate acceleration rather than a template-based effect.
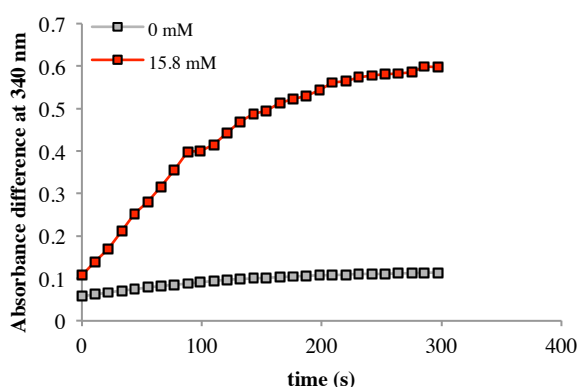
Figure 81 Screening of positive control acetamide **128** at 15.8 mM. Red data points show the absorbance difference at 340 nm over time in the presence of acetamide **128** at 15.8 mM, grey data points show absorbance difference at 340 nm over time for the protein in the absence of the inhibitor. Assay carried out at 30 °C. Samples preincubated at 30 °C for 8 minutes prior to assay.

3.4.5. Thermofluor®

It was considered that a qualitative measure of binding affinity for positive control acetamide **128** to TS might be obtainable through a more sensitive biophysical screen such as Thermofluor®. This fluorescence-based thermal shift assay is a general method to measure ligand-induced stabilisation of protein. The protein is heated in the presence of a dye such as Sypro Orange, as previously described (p39), resulting in the generation of a melt curve. The melting temperature (T_m) for the protein is calculated as the minimum point in the first derivative of the melt curve, and is expected to increase in the presence of a binding ligand. Reported T_m stabilisations for binding fragments are usually expected to be about 0.5 °C.[182] TS was heated in the presence of Sypro Orange to generate a melt curve, Figure 82. Unfortunately, no increase in T_m value was achieved in the presence of known fragment inhibitor N-tosyl D-proline **64**, even up to fragment concentrations of 10 mM. Thermofluor was therefore concluded not to be suitable for the identification of fragment binders to TS.

Figure 82 Melt curve for thymidylate synthase.

3.4.5. Competition studies

To determine whether the observed adduct formation with N-benzyl piperidine acrylamide **54** and positive control **67** was a template-dependent effect or not, a series of competition studies were carried out, Figure 83. Pre-incubation of TS with N-tosyl D-proline **64** before addition of acrylamides was expected to block the active site pocket, slowing down the rate of adduct formation relative to a control tethering experiment. TS was preincubated with either 4 mM N-tosyl D-proline **64** or 4 mM formic acid as a pH control. After a 15 minute preincubation period, acrylamides **54** or **67** were added to the sample and aliquots taken for MS analysis over a 20 minute period. Acrylamide **67** demonstrated no tethering to TS after preincubation with N-tosyl D-proline **64,** whereas tethering did occur after preincubation with formic acid. Likewise for N-benzyl piperidine acrylamide **54**, the tethering observed after preincubation with formic acid was significantly reduced after preincubation with N-tosyl D-proline **64**, Figure 84. These results indicated that the active site pocket was indeed required to template the Michael addition reaction.
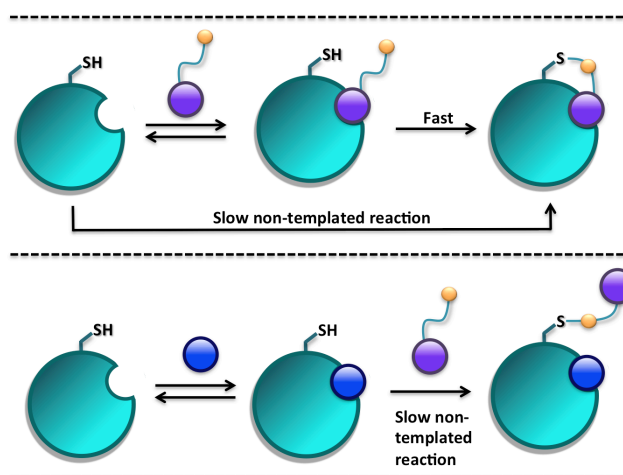
Figure 83 Schematic to illustrate competition tethering experiments.
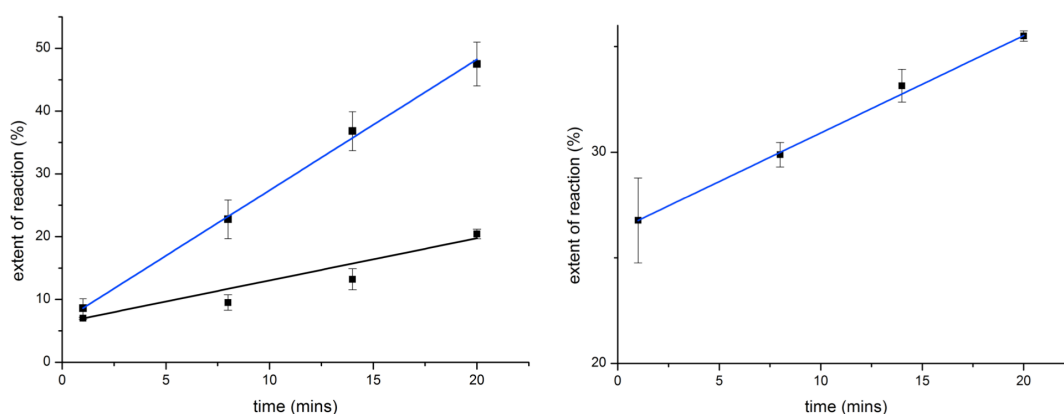
Figure 84 (Left hand side) TS preincubated with either 4 mM formic acid (blue graph) or 4 mM N-tosyl D-proline **64** (black graph) for 15 minutes before addition of N-benzyl piperidine acrylamide **54** at 400 μM. **(Right hand side)** TS incubated with 4 mM formic acid for 15 minutes before addition of positive control acrylamide **67** at 400 μM. When TS was preincubated with N-tosyl D-proline **64** there was no reaction with acrylamide **67** within the 20 minute incubation period. Each graph is an average of 3 repeats where the error bars represent the standard deviation. The average pH values for the different solutions: pH(TS/formic acid/**54**) = 7.05; pH(TS/formic acid/**67**) = 6.94; pH(TS/**64/54**) = 7.17; pH(TS/**64/67**) = 7.12.

A crystal structure of N-tosyl D-proline bound to the protein obtained by Erlanson *et al*.[51] indicated that whilst the pocket was blocked, the active site cysteine was available and still solvent exposed, Figure 85. This was a necessary requirement for the competition study to be able to differentiate between the non-templated and the templated reaction. In an attempt to show that the pocket was blocked whilst the cysteine was solvent exposed, the protein was incubated with iodoacetamide in the presence of either N-tosyl D-proline **64** or formic acid. A low concentration of iodoacetamide (100 µM) was used in this study to ensure a slow enough rate of reaction for measurements to be taken over a 20 min period. In the presence of formic acid, the iodoacetamide modified the protein to approximately 50 % conversion over the 20 min analysis time as expected. Interestingly however, in the presence of N-tosyl D-proline **64** no reaction with iodoacetamide was observed. It was considered initially that this might be due to a reaction between the iodoacetamide and the N-tosyl D-proline, but after 300 minutes, the protein was completely present as an acetamide adduct. It was also considered that upon binding of the N-tosyl D-proline **64**, the protein adopts a different conformation where the cysteine is blocked. A comparison of the apo (1F4B) and bound (1F4C) crystal structures indicated that this was not the case, although this did not give any information about the tertiary protein structure in solution. Unfortunately, the significant reduction in rate of acetamide-adduct formation rendered by the pre-incubation with N-tosyl D-proline **64** suggested that no meaningful result could be gained from competition studies of this nature with this protein.
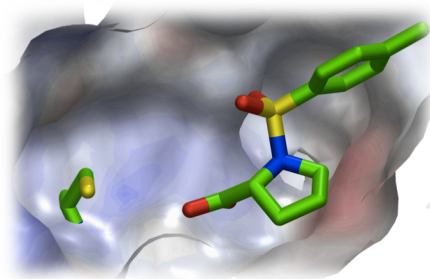
Figure 85 N-tosyl D-proline bound to TS. Active site cys146 is highlighted. PDB code 1F4C. Image generated using AstexViewer.

3.4.6. Reaction irreversiblility

Although extensive HPLC studies had been carried out to demonstrate the irreversibility of the thiol-acrylamide/vinyl sulfonamide Michael addition reaction using small molecule thiols, an ESI MS study was carried out using the protein to confirm irreversibility under the TS-tethering conditions. The method used in this study is illustrated schematically in Figure 86. TS was fully modified separately with two acrylamides **54** and **67**, by treatment with each acrylamide at 400 µM for 3.5 h at room temperature under the standard screening conditions. After this time, acrylamide **54** was added to the TS-**67** sample and acrylamide **67** was added to the TS-**54** sample, with both new acrylamides added to 400 µM final concentration. After 1 h the samples were analysed by ESI MS, which indicated complete

Figure 86 Schematic to illustrate the irreversibility method.

reaction irreversibility by the formation of no new TS-acrylamide adduct, Figure 87.
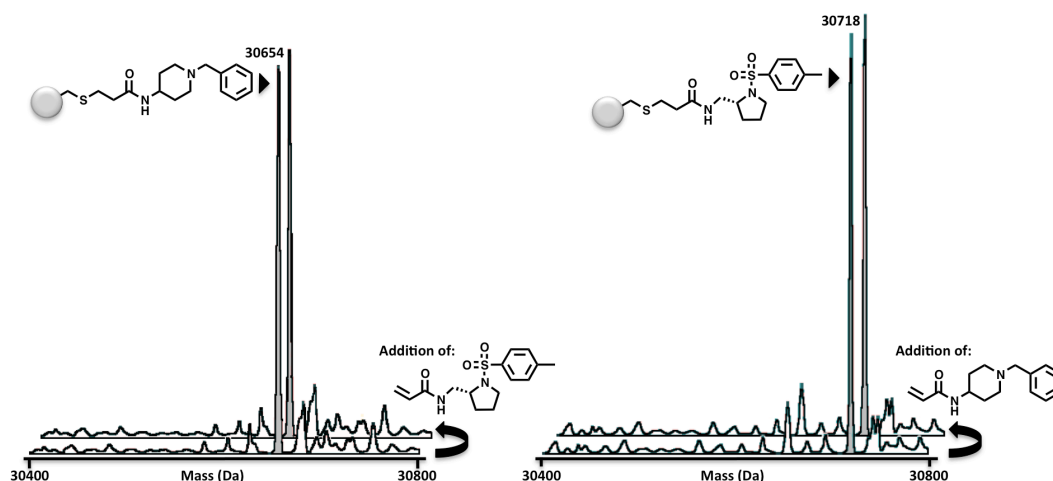
Figure 87 Left hand side: Incubation of TS (10 μM) with acrylamide **54** (400 μM) for 3.5 h and analysis by ESI MS indicated complete modification of the protein. Addition of acrylamide **67** (400 μM) to the TS-**54** adduct and analysis by ESI MS after 1 h indicated no formation of a second adduct. **Right hand side:** Incubation of TS (10 μM) with acrylamide **67** (400 μM) for 3.5 h and analysis by ESI MS indicated complete modification of the protein. Addition of acrylamide **54** (400 μM) to the TS-**67** adduct and analysis by ESI MS after 1 h indicated no formation of a second adduct.

3.5. Vinyl sulfonamides and kinetic template-guided tethering

As the vinyl sulfonamides were identified as significantly more reactive than the acrylamides towards conjugate addition (Chapter Two), it was assumed that the level of background reaction would be too high for the use of this functional group in KTGT. Work was carried out in an attempt to either prove or disprove this hypothesis. To account for this higher intrinsic reactivity of the vinyl sulfonamides, screening was carried out at 10 μM rather than 400 μM. TS was incubated with a mixture of 4 vinyl sulfonamides, **41**, **43**, **44** and **70** each at 10 μM and the sample analysed after 2, 10, 30 and 120 min, Figure 88. Interestingly this resulted in the selection of only positive control **70**, with no adduct formed to the N-benzyl piperidine fragment previously identified. The reversibility of vinyl sulfonamide addition to TS was examined using the same method as for the acrylamides. TS was fully modified with either vinyl sulfonamide **44** or **70**, and subsequently incubated with the second sulfonamide, indicating that the reaction was completely irreversible over the 120 minute time period examined.
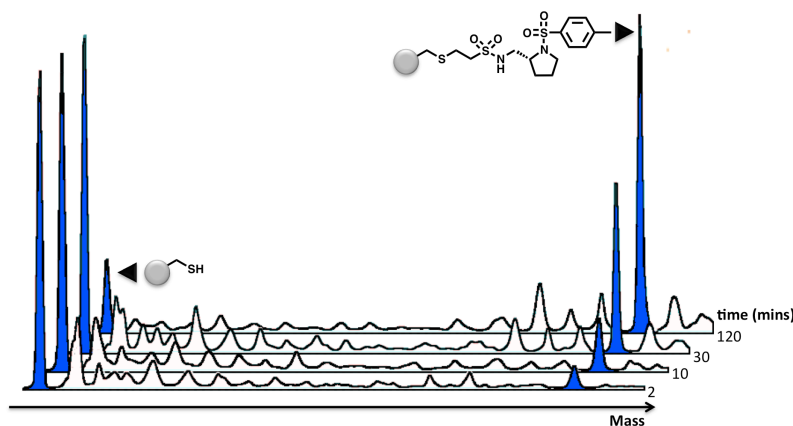
Figure 88 TS incubated with 4 vinyl sulfonamides, each at 10 μM, and analysis by ESI MS carried out at 2, 10, 30 and 120 minutes.

3.5. Summary and conclusions

TS was adopted as a model protein to develop a proof-of-concept for KTGT. A number of positive and negative control ligands were designed and synthesised and TS was cloned, expressed and purified. A reliable, robust and facile method was developed for the incubation of ligands with protein prior to analysis by ESI MS. Using iodoacetamide, TS was shown to have only one surface exposed cysteine thiol in agreement with that previously reported. Using the developed method, TS was incubated with a mixture of acrylamides including the positive control **67** and piperazine acrylamide **49** with a high intrinsic reactivity. Analysis by ESI MS indicated modification of the protein by only the positive control ligand **67** and not the more reactive ligand **49**, providing an initial proof-of-concept for KTGT. Incubation with N-methyl pyrrolidine negative control compound **68** led to unexpected modification of the protein, which may be due to intramolecular base-catalysis by the tertiary amine. Ligand **54**, containing a tertiary amine functionality, was also unexpectedly found to modify the protein, an effect which may also be due to a similar base catalysis. Ligand **54** was identified as a weak fragment binder of TS using an enzymatic spectrophotometric assay. Incubation of TS with a mixture of vinyl sulfonamides led to modification of the protein with only the positive control **70**, suggesting that this functionality is also potentially suitable for KTGT experiments. Protein-acrylamide adducts were stable to proteolytic digestion, allowing the position of modification to be identified by MALDI MS of the crude peptide mixtures. Reaction of the protein with both acrylamides and vinyl sulfonamides was found to be completely irreversible as expected. No further work is carried out with the vinyl sulfonamides in this thesis, but this certainly represents an area with scope for future studies. The acrylamide KTGT work described in this chapter was published in 2012.[183]

4. Design of a linker for acrylamide-based KTGT

4.1. Introduction and aim

To develop KTGT into a general strategy for the discovery of protein-binding ligands, an important consideration was the design of a structural element to separate the acrylamide from the fragment. The purpose of this linker was twofold: to isolate the acrylamide from the fragment to ensure identical kinetic reactivity across the library members and to allow the acrylamide some flexibility to find the local cysteine thiol after fragment binding, Figure 89. The key challenge during this work was the design of such a linker without loss of the effective molarity induced by the template.
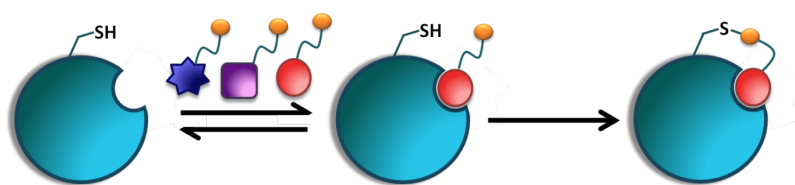
Figure 89 Schematic to illustrate KTGT with a flexible linker.

Work published by Whitesides *et al*. in 2007 examined the change in effective molarity (M_{eff}) with linker length for intramolecular protein-ligand binding in a related system.[184] Adopting human carbonic anhydrase (hCA) as a model system, a benzene sulfonamide ligand was covalently tethered to the protein surface, in the vicinity of the binding pocket, by linkers of various lengths comprised of oligo(ethylene glycol) units (n = 0, 2, 5, 10 and 20), Figure 90.
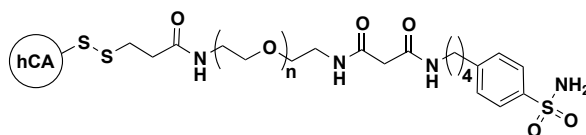
Figure 90 Human carbonic anhydrase (hCA) was modified covalently with a known aryl sulfonamide binder *via* oligo(ethyleneglycol) tethers of various lengths n = 0, 2, 5, 10 and 20.

Whitesides *et al*. calculated the effective molarity for binding of the ligand to the protein according to Equation 4, where K_d^{inter} represents the affinity of the untethered ligand for the protein, and K_d^{intra} represents the affinity of the tethered ligand for the protein.

$$M_{eff} = K_d^{inter}/K_d^{intra}$$

Equation 4

K_d^{intra} was calculated according to Equation 5, which was derived from the thermodynamic cycle shown in Figure 91.

$$K_d^{intra} = K_d^{Ethox}/K_d^{comp, Ethox}$$

Equation 5

Ethoxzolamide (Ethox), Figure 92, binds to hCA and quenches intrinsic protein fluorescence, which derives from tryptophan residues, offering a spectrophotometric method to follow binding. Incubation of hCA (modified with the benzene sulfonamide ligand *via* various linker lengths) with varying concentrations of Ethox allowed calculation of the dissociation constant for the competing Ethox ligand ($K_d^{comp, Ethox}$).
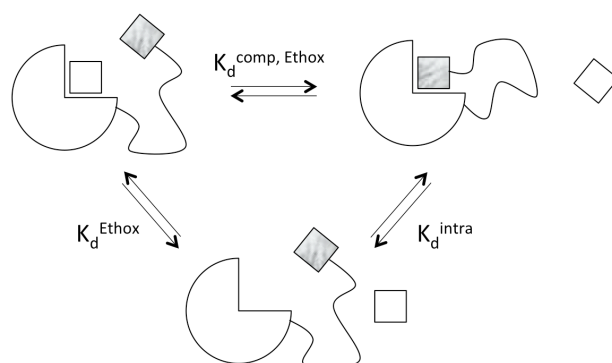
Figure 91 Thermodynamic cycle used by whitesides *et al*. to calculate K_d^{intra}, utilising the observed dissociation constant ($K_d^{comp, Ethox}$) for competing ligand Ethox (shown as a white square). $K_d^{intra} = K_d^{Ethox} / K_d^{comp, Ethox}$.
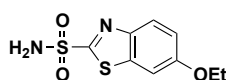
Figure 92 Ethoxzolamide (Ethox).

Whitesides *et al*. previously argued that flexible oligomers should not be suitable as linkers in multivalent ligands due to the severe loss of conformational entropy when the linker becomes bound at both ends.[185] The results obtained using hCA as a model system contradicted this hypothesis. With the number (n) of oligo(ethyleneglycol) units n = 2, the linker was at an optimal length and the effective molarity was highest, Figure 93 scenario 2. Surprisingly, as the linker length was increased beyond the optimal value, only a weak dependency on length was observed with an 8-fold decrease in M_{eff} from n = 2 to n = 20, scenario 3. When n = 0, the linker was too short to allow unconstrained ligand binding and the effective molarity was < 1, scenario 1. The authors proposed this to be qualitatively in accordance with a model that treats the linker as a random-coil polymer, which retains significant conformational mobility once bound, and only contributes entropically to the thermodynamics of the system. The weak dependence on linker length led the authors to suggest that the most effective strategy for the design of multivalent ligands is to connect the two moieties by a flexible linker, which is significantly longer than the distance between the two sites. This was in agreement with a thermodynamic analysis published by Kane in 2010.[186]
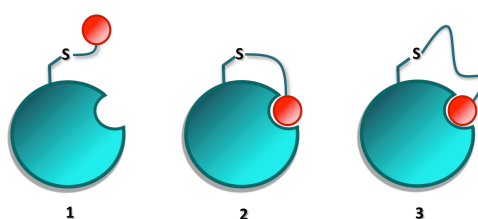
Figure 93 Three scenarios observed by Whitesides *et al*. **1.** The linker length is too short to allow the ligand to reach the binding pocket and the effective molarity is < 1. **2.** The linker is exactly the right length to allow the ligand to reach the pocket and the effective molarity is highest. **3.** The linker is longer than the distance between the tether point and the pocket, but the effective molarity is only moderately reduced.

In a very interesting report, Blaustein *et al*. tethered triethylamine to *Shaker* K$^+$ channels *via* flexible linkers of various lengths.[187] A maleimde group was used as a functional handle to attach the linker to the channel by reaction with a solvent exposed cysteine residue. The variant of *Shaker* channel used in these experiments had a high affinity external triethylamine pocket, which caused block of the channel upon binding, Figure 94. When the linker was too short to allow the triethylamine ligand to reach the pore, no significant block of the channel was observed as expected. A

significant jump in ion channel block was observed when the linker length was increased from 11 to 12 Å, with the quaternary ammonium now able to reach the pore. Surprisingly however, as the linker length was further increased, blockage of the ion channel also continued to increase. The authors suggest that longer linkers are able to adopt a greater number of conformations that result in binding, whereas the shorter linker must adopt the improbable, fully extended conformation to achieve this.
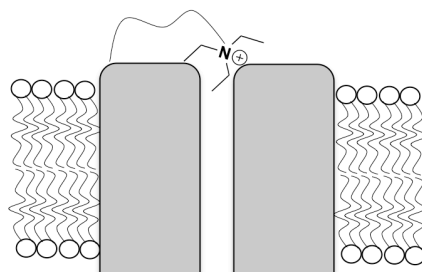
Figure 94 Schematic to illustrate the *Shaker* K⁺ channel with a tethered triethylamine ligand.

A thorough kinetic analysis of this work was later published by Blaustein.[188] Interestingly, he reported that not only did tethered blockers of longer length achieve greater block of the ion channel, but that these linkers also covalently modified the solvent exposed cysteine *at a faster rate*. Blaustein proposed that, just as the longer linkers result in a higher concentration of triethylamine at the pore, and therefore greater block of the channel, the same longer linkers (before covalent attachment) bind the triethylamine pocket and result in a higher concentration of maleimide near the reactive cysteine. Interestingly, longer linkers were observed to react with the channel *via* biphasic kinetics when there was more than one reactive cysteine in the vicinity of the pore. Reaction with the first cysteine was observed to be much faster due to binding of the triethylamine group and resultant increase in maleimide concentration at the first cysteine. With the triethylamine moiety now efficiently blocking the pore, all further reactions proceed at the slower rate of background reaction. Shorter linkers that demonstrated only a partial block of the pore reacted with single phase kinetics.

Although the papers published by Whitesides and Blaustein reported different observed changes in effective molarity with linker length, both sets of results suggest that the use of a long and flexible linker is a justifiable strategy for multivalent ligands. This was thought to be particularly suitable for KTGT where a library of compounds would ideally be screened against a range of proteins where the distance between the nucleophilic protein capture atom and the fragment pocket would vary slightly. For each system, the linker would confer the required flexibility for the acrylamide to react with the cysteine thiol after fragment binding, Figure 95 scenario 3, in addition to normalising the intrinsic kinetic reactivity across the fragment library. Without the incorporation of a linker into fragments for KTGT, it was considered that a significant number of false negatives might result, due to fragment binding in a conformation with the acrylamide unable to reach the reactive cysteine thiol, Figure 95 scenario 1.

Thymidylate synthase was used once again as the model system for this work. The overall aim was to design and synthesise a library of acrylamide-linker-fragments, including the positive and negative controls, and to demonstrate selection of only the positive control fragment by the protein.
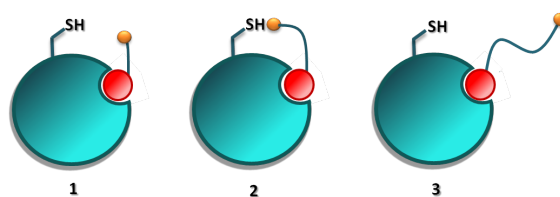
Figure 95 Three scenarios for KTGT which vary by linker length. **1**. The linker length is too short to reach the cysteine such that the effective molarity is 0. **2**. When the linker length is exactly right the effective molarity is highest. **3**. Multivalent systems with long flexible linkers lose effective molarity with length only slowly.

4.2. Linker design

The distance between the carboxylic acid oxygen atom in N-tosyl D-proline fragment **64** and the sulfur atom from C146 in TS is 0.37 nm, as determined using an available crystal structure (PDB code 1F4E), Figure 96.[*] When this fragment is tethered to C146 *via* a disulfide linkage (PDB code 1F4C), the distance between the amide NH and the sulfur atom is 0.47 nm,[*] suggesting the linker as almost exactly the right length. In order to probe the importance of linker length for KTGT, a linker in excess of the approximately ideal 0.4 nm length was required. A linker spanning a maximum length of *ca*. 3.5 times this distance was therefore designed, Figure 96. The linker was comprised of 2.5 ethylene glycol units, with the amine fragment attached to the linker *via* a carboxylic acid handle, Figure 97. Oligo(ethylene glycol) units were chosen to constitute the linker as these confer a solubility advantage over a hydrocarbon chain, have been found not to interact non-selectively with protein surfaces[189] and are a common moiety in multivalent ligands.[23]
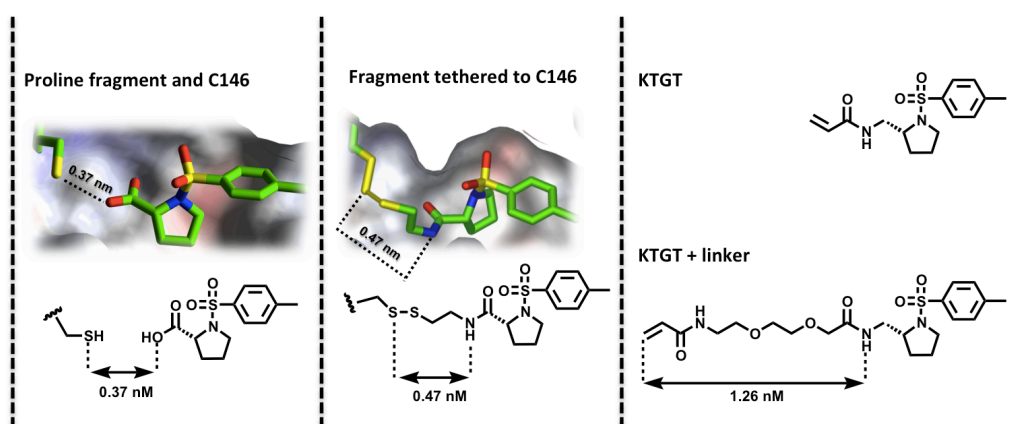
Figure 96 Design of a linker for KTGT. **Left hand side:** Crystal structure (PDB code 1F4E) of WT-TS with N-tosyl D-proline bound in the active site pocket. The distance between the active site cysteine sulfur atom and the oxygen atom from the carboxyl group in the proline ligand is highlighted (0.37 nm). **Middle:** Crystal structure (PDB code 1F4C) of WT-TS covalently modified with N-tosyl D-proline *via* a disulfide linkage. The distance between the cysteine sulfur and the oxygen atom in the ligand is highlighted (0.47 nm). Images were generated using AstexViewer. **Right hand side:** Comparison of KTGT and KTGT with a linker. The linker spans a maximum distance of approximately 1.26 nm, calculated using ChemBio3D Ultra.
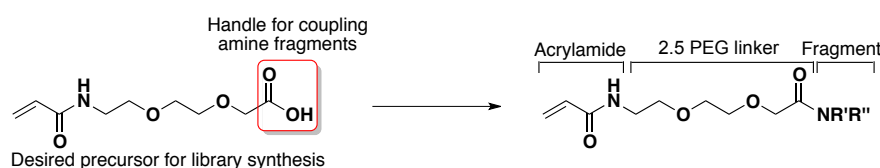
Figure 97 Acrylamide-linker-fragment design.

---

[*] Measured using AstexViewer software.

4.3. Synthetic route one

The initial strategy developed to synthesise a PEG-modified acrylamide library was based on a retrosynthetic analysis shown in Scheme 20. The amide bond forming reaction to couple amine fragments to the common intermediate carboxylic acid **131** is carried out in the ultimate step to diversify the synthesis at the latest possible point. The carboxylic acid required for this final step was thought to be obtainable from alcohol **132** by reaction with a haloacetic acid. It was considered at this step that the haloacetic acid may require protection, firstly due to the requirement for the use of strong base to effect the S_N2 reaction, and secondly as the carboxylic acid **131** was anticipated to be highly polar and therefore potentially problematic to isolate. Disconnection of the acrylamide C-N bond gives commercially available 2-(2-aminoethoxy)ethane **133** as the starting point for the synthesis.
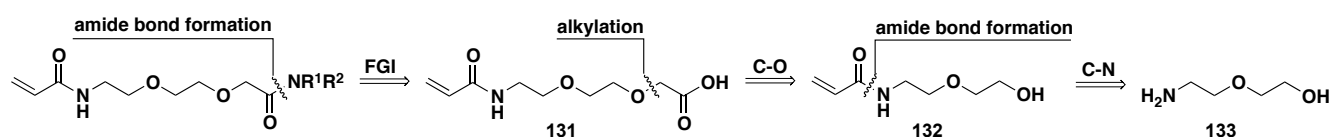
Scheme 20 Retrosynthetic analysis to reach library of acrylamide-linker-fragments.

It was initially anticipated that only poor chemoselectivity for the N over the O in the acetylation of 2-(2-aminoethoxy)ethane **133** would be possible, and this amino-alcohol was therefore reacted with an excess of acryloyl chloride to acetylate both nucleophilic atoms. Basic cleavage of the ester bond with aqueous LiOH during work up then generated the desired carboxylic acid. Unfortunately, the acid was highly water soluble and could not be extracted in a reasonable yield from the aqueous layer. This was overcome by reacting 2-(2-aminoethoxy)ethane with one equivalent of acryloyl chloride, which pleasingly gave reasonable selectively for the more nucleophilic nitrogen. By omitting an aqueous workup and passing the crude reaction mixture straight through a silica column, the desired acrylamide **132** was isolated in a moderate 67 % yield.

Tert-butyl protected chloroacetic acid was initially chosen as the electrophile for the alkylation of acrylamide **132**. Protection as an ester was chosen to aid isolation by decreasing the polarity of the final compound. A *tert*-butyl group was chosen as the ester substituent to prevent transesterification with the nucleophilic alcohol rather than the desired alkylation. Triethylamine was initially chosen as the base in the alkylation step to avoid generation of the alkoxide, which was anticipated to attack the acrylamide either intra- or intermolecularly. With triethylamine as the base, there was no reaction with chloroacetic acid *tert*-butyl ester after 3 h at 70 °C, Table 12 (entry 1). Using a stronger base, potassium butoxide, a 6 % isolated yield of the desired product **134** was obtained after reaction for 12 h at rt, with a significant quantity of starting material left as indicated by TLC (entry 2). Use of a stronger base (NaH) and 12 h reflux in THF led to the generation of none of the desired product by TLC (entry 3). Treatment of alcohol **132** with the α-bromo rather than α-chloro ester in the presence of potassium *tert*-butoxide and THF increased the yield of this reaction to 20 %, presumably due to the increased ability of the α-haloester to undergo S_N2 displacement. Repeating this reaction, but reversing the order of addition such that the α-bromo ester was added to the reaction mixture before the potassium *tert*-butoxide base, increased the yield of this reaction to 28 % (entry 4). Reaction of α-bromo acetic acid with alcohol **132** in the presence of potassium *tert*-butoxide led to none of the alkylated product **131** (entry 5). A

large batch of acrylamide **132** was synthesised to further optimise these reactions, but this was observed to polymerise under vacuum. The low yields encountered throughout this synthesis may be due to polymerisation side reactions.

Entry	R	X	Base	Yield (%)
1	^tBu	Cl	Et$_3$N	0
2	^tBu	Cl	KO^{t}Bu	6
3	^tBu	Cl	NaH	0
4	^tBu	Br	KO^{t}Bu	28*
5	H	Br	KO^{t}Bu	0
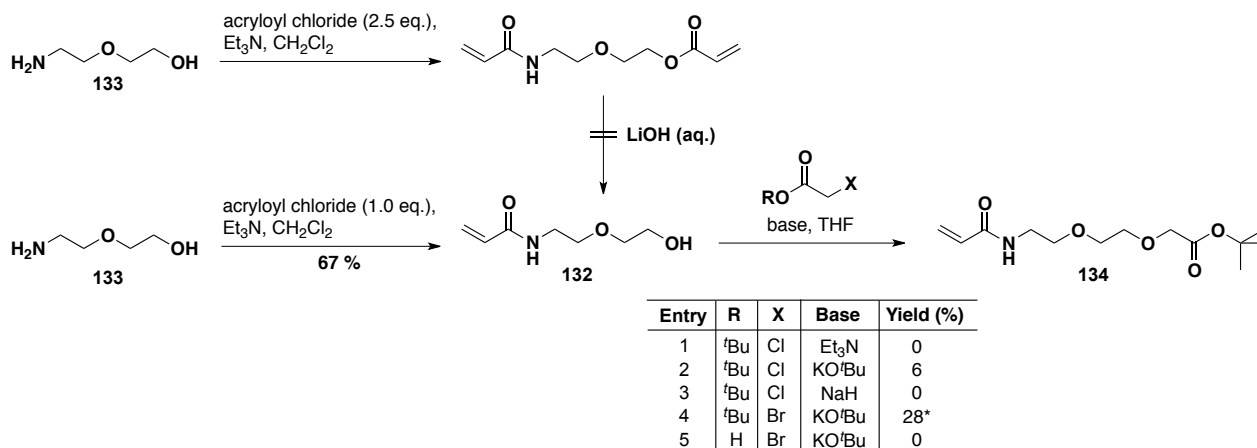
Table 12 Conditions for the alkylation of alcohol **132**. An asterix indicates reversed order of addition such that the base is added to the mixture of the alcohol and the alkylating agent.

An attempt was made to selectively alkylate alcohol **133** to ether **135** in the presence of the primary amine by full deprotonation using one equivalent of NaH and subsequent addition of the chloroacetic acid *tert*-butyl ester, Equation 6. After reaction with chloroacetic acid *tert*-butyl ester at 70 °C for 1 h, a new product was evident by TLC analysis although significant quantities of both starting materials were still present. An attempt was made to isolate this new product but it could not be extracted from the aqueous layer during work up.
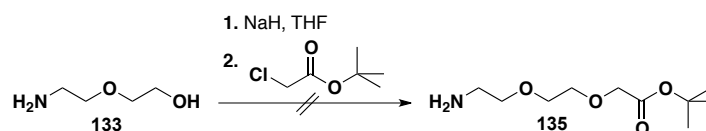
Equation 6

As a new protection strategy, a literature synthesis was adopted to dibenzylate 2-(2-aminoethoxy)ethanol, alkylate the free alcohol with α-bromoacetic acid, and remove the N-benzyl groups using hydrogenolysis with a palladium on charcoal catalyst, Scheme 21.[190] At this point, reaction of the resulting amine **138** with acryloyl chloride did not yield any of the desired acrylamide **131**. The carboxylic acid was thought to be problematic here due to potential reaction with acryloyl chloride to generate an anhydride, leading to a number of other side reactions.
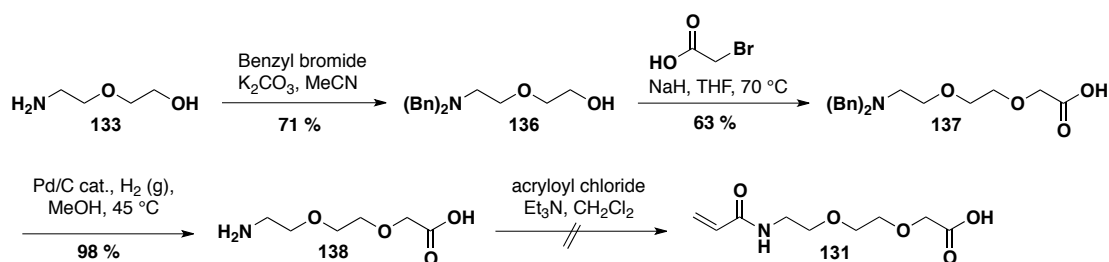
Scheme 21

To overcome this, it was desirable for the carboxylic acid to be protected as the *tert*-butyl ester. N-dibenzyl 2-(2-aminoethoxy)ethane **136** was treated with chloroacetic acid *tert*-butyl ester and NaH and refluxed in THF, but this failed to generate any of the desired ester **139**, Table 13 (entry 1). Repeating this reaction at room temperature led to the isolation of carboxylic acid **137** (47 % yield) rather than the desired ester (entry 2). The use of bromoacetic acid *tert*-butyl ester with NaH base led to the disappearance of the starting material by TLC after 2 h, but gave only a 21 % isolated yield of ester **139** (entry 3). The presence of significant material on the baseline for this reaction suggested formation of the carboxylic acid. However, upon repeating this reaction with a 12 h rather than 2 h stirring time, a 57 % isolated yield of the desired product **139** was obtained (entry 4). The yield for this reaction was significantly improved by stirring at 0 °C rather than room temperature, leading to a 68 % isolated yield for ester **139** after 2.5 h (entry 5) and a 75 % yield after 3 h (entry 6).
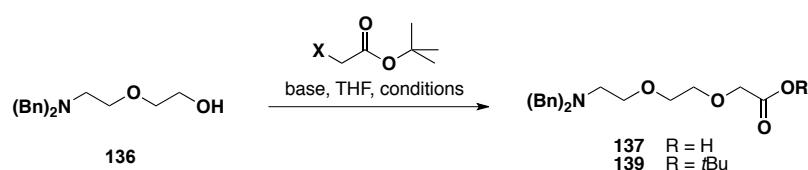
Entry	X	Base	Temp (°C)	Time (h)	Yield 139 (%)	Yield 137 (%)
1	Cl	NaH	0 to reflux	12	0	*
2	Cl	NaH	rt	12	0	47
3	Br	NaH	rt	2	21	*
4	Br	KO^{t}Bu	rt	12	57	*
5	Br	KO^{t}Bu	0	2.5	68	*
6	Br	KO^{t}Bu	0	3	75	*

*Product not isolated

Table 13 Conditions for the alkylation of alcohol **136**.

Using the hydrogenolysis conditions which worked almost quantitatively to take dibenzyl amine **137** to the free amine **138** resulted in the removal of only one benzyl group from ester **139**, Table 14 (entry 1). This was initially a surprising result as the two hydrogenolysis substrates, carboxylic acid **137** and ester **139**, differ only at the end of the molecule furthest from the reacting centre. However, it is well documented that the product amine from N-debenzylation reactions can poison the palladium catalyst, an effect which can be minimised by the addition of acid.[191] The absence of the carboxylic acid in ester **139** leads to poisoning of the catalyst by the di-debenzylated amine product, effectively halting the reaction. Addition of an acid such as acetic acid may have provided a simple solution to convert ester **139** directly to primary amine **135**. However, treatment of the mono-benzylamine **140** with Pearlman's catalyst Pd(OH)$_2$ under an atmosphere of H$_2$ (g) for 3 days resulted in generation of the desired primary amine **135** in 100 % yield (entry 2). It was also found that primary amine **135** could be generated straight from the dibenzylated amine **139** with Pearlman's catalyst and ammonium formate as the hydrogen transfer agent in refluxing methanol for 24 h (entry 3).
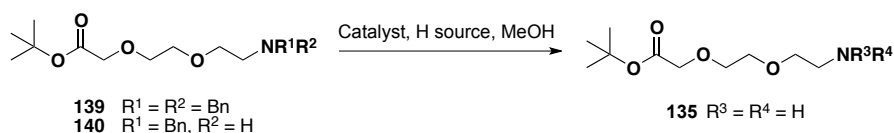

Entry	R^1	R^2	R^3	R^4	Cat.	H source	Time (h)	Temp (°C)	Yield (%)
1	Bn	Bn	Bn	H	Pd/C	H$_2$ (g) 1 atm	20	45	100
2	Bn	H	H	H	Pd(OH)$_2$	H$_2$ (g) 1 atm	72	rt	100
3	Bn	Bn	H	H	Pd(OH)$_2$	NH$_4$.HCO$_2$	24	75	100

Table 14 Hydrogenolysis conditions.

The resulting amine was reacted with acryloyl chloride to generate the acrylamide **134**, albeit in a disappointing 22 % yield, Scheme 22. Attempted deprotection of *tert*-butyl protected carboxylic acid **134** in 4M HCl in dioxane was unsuccessful.
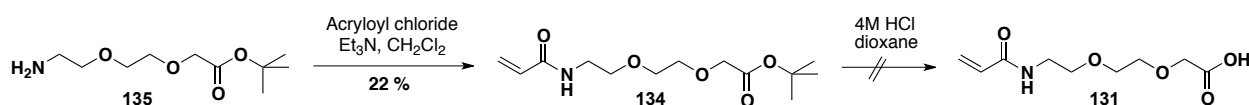
Scheme 22

4.4. Summary of attempts to use route one

2-(2-Aminoethoxy)ethane **133** was reacted selectively at N to generate acrylamide **132** in moderate 67 % yield, Scheme 23. Attempts to react this with chloroacetic acid *tert*-butyl ester to generate the desired *tert*-butyl protected library synthesis precursor **134** were unsuccessful. Use of the α-bromoacetic acid *tert*-butyl ester led to the successful alkylation of alcohol **132** to ether **134**, albeit in poor 28 % yield. The reaction between alcohol **132** and α-bromoacetic acid was unsuccessful. The intermediate acrylamide **132** was found to polymerise under vacuum, precluding large scale synthesis of this compound. Polymerisation was considered a potential problem in the alkyation reactions due to the presence of the nucleophilic alcohol and the electrophilic acrylamide within the same molecule. Direct alkylation of the alcohol **133** to generate amine **135**, in an attempt to overcome this problem, was unsuccessful. Protection of amine **133** as the dibenzyl amine, alkylation with bromoacetic acid to generate carboxylic acid **137** and facile hydrogenation of the benzyl groups led to intermediate amine **138**. At this point, generation of the desired acrylamide from amine **138** was unsuccessful, potentially due to generation of an anhydride and other side reactions. It was thought that this could be overcome by protection of the carboxylic acid as the ester, and generation of the *tert*-butyl ester **135** was successful, although optimised deprotection conditions were then required to remove the benzyl groups. Amine **135** was taken onto the acrylamide **134**, albeit in low 22 % yield, but it was found that the *tert*-butyl ester group in acrylamide **134** could not be removed. The acrylamide was considered to be highly problematic within this synthetic route, and a protecting strategy to overcome this was therefore investigated.
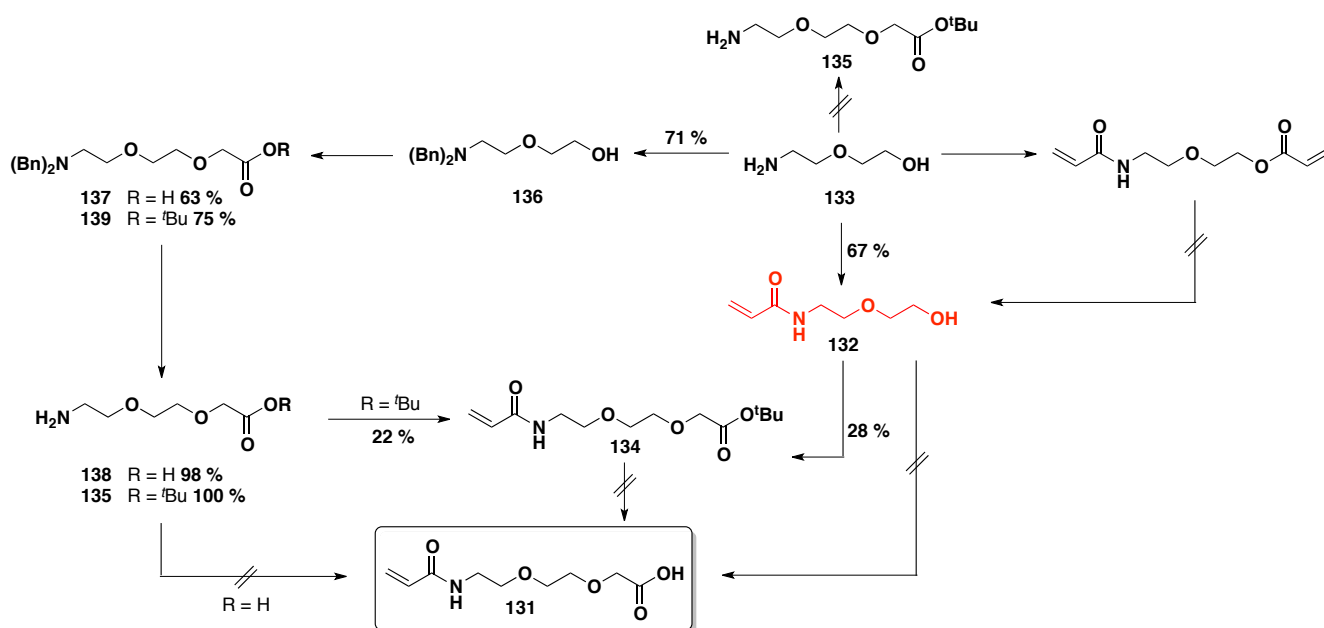
Scheme 23 Summary of attempts to reach the desired carboxylic acid **131**. Intermediate **132** highlighted in red was found to polymerise under vacuum.

4.5. Synthetic route two

It was decided that a protection strategy was required with the electrophilic acrylamide generated in a late step to avoid polymerisation. Furthermore, the final deprotection reaction should avoid strongly basic or acidic conditions to prevent side reactions. Finally, the protecting group should confer some degree of hydrophobicity to help with purification and isolation. An α-phenylselenide was chosen for this purpose, and a retrosynthesis to reach the desired compounds using this protecting group is shown in Scheme 24. The acrylamide is generated in the final step by oxidation of the selenium and *in situ* retro-ene to eliminate phenyl selenenic acid. It was envisaged that the α-phenylselanyl amide would be stable through the amide bond formation and alkylation steps. A literature method was available for the preparation of 2-phenylselanyl-propionic acid **142** from ethyl 2-bromopropionate **141**, which is commercially available.
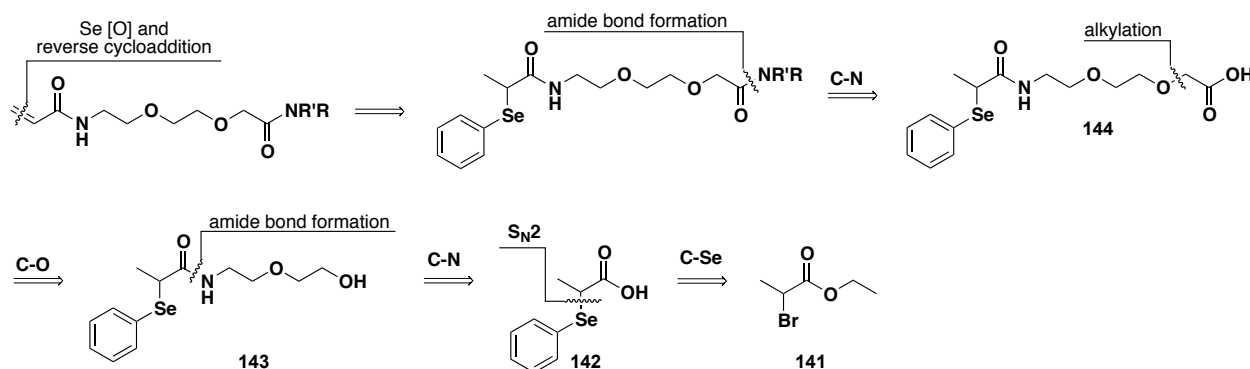
Scheme 24 Second generation retrosynthetic analysis to reach desired acrylamide-PEG linker-fragments for KTGT.

Starting from the commercially available α-bromoethyl ester **141**, the α-phenylseleno acid **142** was generated by an S_N2 displacement of the bromide by phenyl selenide, generated by an *in situ* reduction of diphenyl diselenide, in excellent yields between 87-94 %, Scheme 25. Basic hydrolysis of the ester in aqueous KOH furnished the carboxylic acid **145** in yields between 72-81 %. Treatment of carboxylic acid **145** with oxalyl chloride and catalytic DMF generated the acid chloride, which was quenched *in situ* with 1.5 equivalents of 2-(2-aminoethoxy)ethane **133** to yield the desired amide **143** in a moderate 63 % yield, in addition to the di-acetylated side-product **146** in 14 % yield.
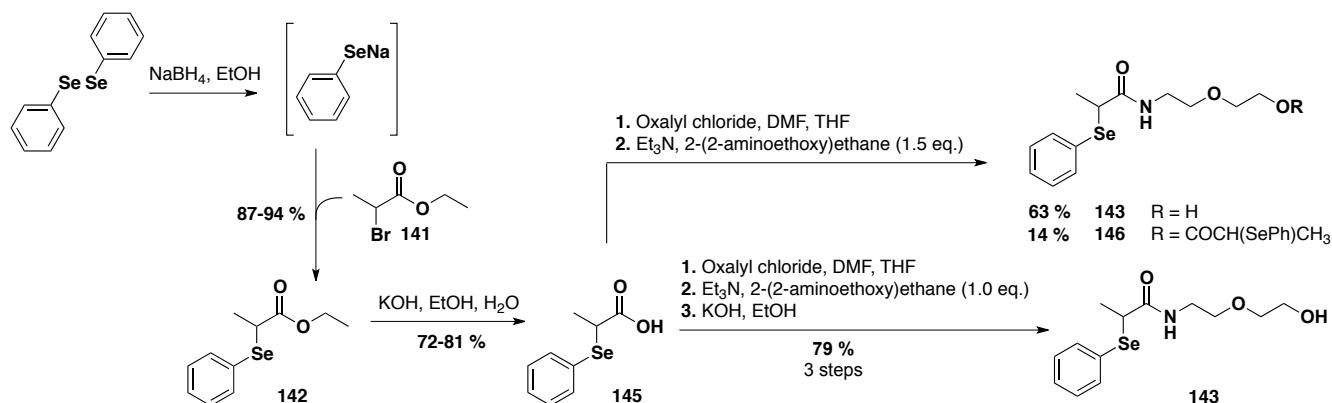
Scheme 25

The yield of **143** was improved to 79 % by treatment of the crude reaction mixture with aqueous KOH in EtOH to hydrolyse the ester, Scheme 25. Extraction of the basic aqueous layer during work up furnished alcohol **143** in high

purity, removing the need for column chromatography. Additionally, carboxylic acid **145** was recovered from the reaction in high purity by acidification of the aqueous layer and further extraction.

Reaction of the N-acetylated alcohol **143** with *tert*-butyl bromoacetate and KO^{t}Bu in THF, conditions which were previously successful for this type of alkylation, led to degradation by TLC and isolation of none of the desired product **147**, Table 15 (entry 1). The reaction was attempted with benzyl bromoacetate, KO^{t}Bu and THF as a hydrogenation deprotection step was thought to be favourable over an acidic hydrolysis step, which previously caused problems. However, only starting material was recovered from the reaction with none of the desired product **148** (entry 2). Refluxing the N-acetylated alcohol **143** in THF with α-bromoacetic acid and NaH for 3 days also gave no reaction, with analysis of the crude reaction mixture by ^{1}H NMR indicating mainly starting material (entry 3).
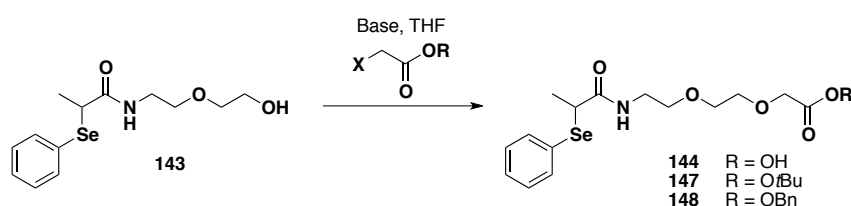
Entry	R	X	Base	Time (h)	Temp (°C)	Yield (%)
1	tBu	Br	KO^{t}Bu	12	0 to rt	0
2	CH$_2$Ph	Br	KO^{t}Bu	6	0 to rt	0
3	H	Br	NaH	72	reflux	0
4	H	I	NaH	0.5	rt	trace
5	H	I	NaH	0.5	rt	62*
6	H	I	NaH	16	rt	63*

*Iodoacetic acid recrystallised before use.

Table 15 Conditions for the alkylation of intermediate **143**.

The quality of the NaH used in this reaction, in addition to two other sources, was checked using a literature allylation of benzyl alcohol with allyl bromide, reported to go to 99 % yield.[192] The three sources of NaH gave conversions of 60, 60 and 61 % to the desired ether **149**, Equation 7, indicating that the quality of the NaH was almost certainly not responsible for the 0 % yield achieved for the alkylation of alcohol **143**. Changing α-bromoacetic acid to α-iodoacetic acid led to a trace of the desired product **144** using NaH as the base, Table 15 (entry 4). Recrystallisation of the iodoacetic acid immediately prior to reaction increased the yield of carboxylic acid **144** significantly to a moderate 62 % (entry 5). Increasing the reaction time from 30 min to 16 h did not significantly improve the yield (entry 6).
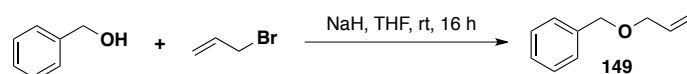
Equation 7 Test allylation reaction. Conversions to ether **149** of 60, 60 and 61 % were achieved using three different sources of NaH.

With the desired intermediate **144** in hand, the next stage in the synthetic sequence involved the derivatisation of the carboxylic acid with amine fragments. As this step forms the point of divergence in the sequence and therefore has to be repeated for each fragment, high yielding reactions with minimal byproducts were desired. Treatment of carboxylic **144** with oxalyl chloride and DMF (cat.) in THF at rt led to degradation as observed by methanol quench TLC analysis, which indicated 4 products. The mixture was nevertheless treated with benzylamine and triethylamine, but

only diphenyl diselenide was isolated from the reaction mixture (31 % yield). Lowering the temperature for the formation of the acid chloride to 0 °C still indicated the same degradation by MeOH quench and subsequent TLC analysis. As an alternative to acid chloride formation, a series of N,N'-dicyclohexylcarbodiimide (DCC) coupling reactions were attempted. Although removal of the N,N'-dicyclohexylurea byproduct is often tricky by column chromatography, the insolubility of the urea in acetonitrile reported by a coworker allows separation from products, which are freely soluble. It was found in practice, however, that the urea was sparingly soluble in acetonitrile such that significant numbers of washings were required to gain complete purity, even though this step was often carried out after column chromatography. Both amides **150** and **151** were extensively purified, but were still contaminated by the urea **152**, with molar ratios (product:**152**) of 3:2 and 2:1 respectively, as calculated by ^{1}H NMR, Table 16 (entries 1-2). Amides **153**-**155** were successfully separated from the urea byproduct to give the desired products in moderate-to-good yields between 54 - 91% (entries 3 – 5).

Entry	X	R^1	R^2	Yield X (%)	X:152
1	**150**	H	4-(N-benzyl)piperidine	-	3:2
2	**151**	-	N-phenyl piperazine	-	2:1
3	**153**	H	$CH_2pOMeC_6H_4$	69	-
4	**154**	H	CH_2Ph	91	-
5	**155**	H	CH_2p-FC_6H_4	54	-
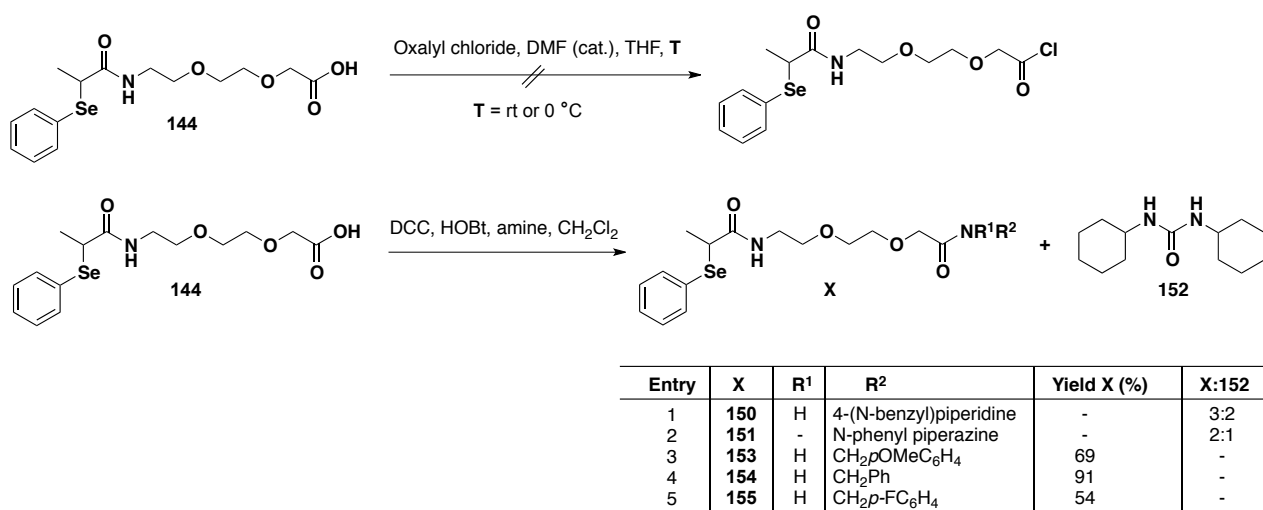
Table 16 Coupling carboxylic acid **144** to amine fragments.

A novel amide-bond forming method recently published by Allen *et al*. was adopted to form the desired amides without the requirement for extensive purification.[193] The acid and the amine were refluxed in toluene overnight with a ZrCp$_2$Cl$_2$ Lewis acid catalyst to yield, in most cases, the desired amide as the only product in 100 % conversion. Purification often required only a filtration to remove solid impurities. To illustrate the superiority of the zirconocene dichloride method, the synthesis of amide **155** was carried out using both methods. The DCC-coupling reaction and the zirconocene dichloride reflux, gave yields of 54 % and 94 % respectively. The DCC-coupling method required two purifications using silica gel chromatography and three acetonitrile washes to remove the contaminating urea, whereas the zirconocene method required only filtration of the crude reaction mixture to remove solid impurities, and led to the isolation of amide **155** in high purity. Oxidation of the selenium with sodium *meta*-periodate led to *in situ* elimination, yielding the final desired compounds and the phenyl selenenic acid by-product. An overall summary of the route is shown in Scheme 26.
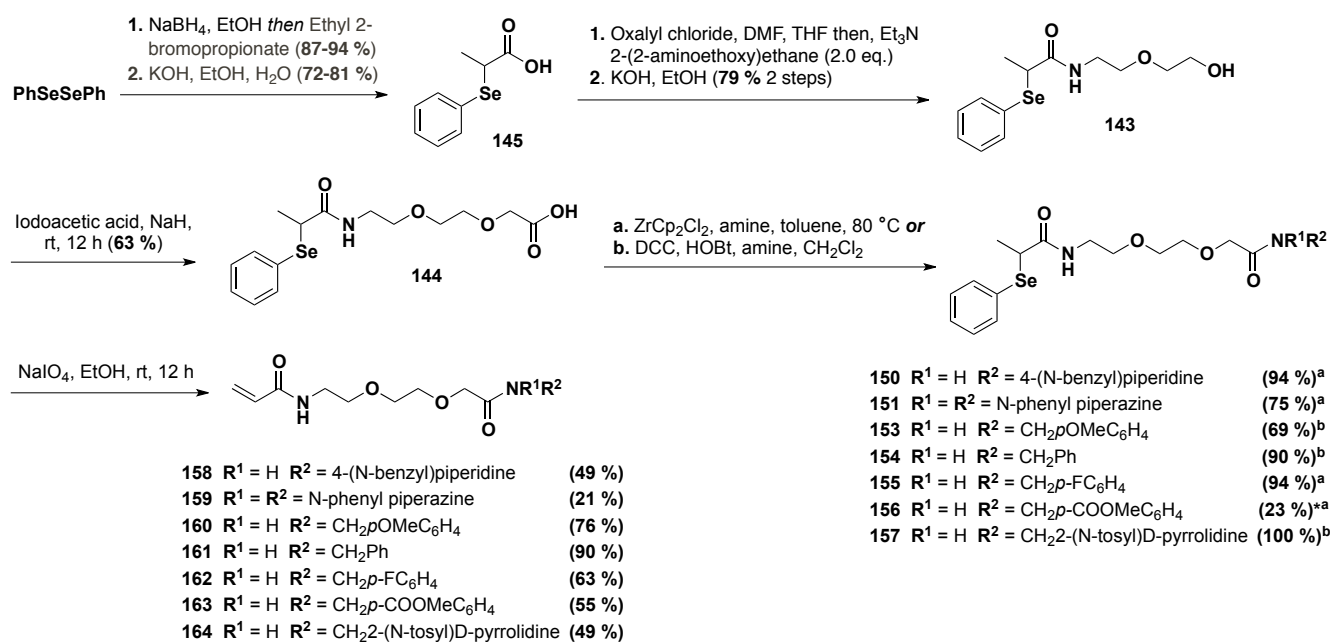
Scheme 26 Overall synthetic route to desired acrylamide-PEG linker-fragments for KTGT. *Using the HCl salt of the amine.

4.6. Mass spectrometry screening and intrinsic reactivity

Incubation of TS with positive control PEG-linked acrylamide **164** at a final concentration of 400 μM led to very slow generation of a TS-**164** adduct, Figure 98. Modification of TS with positive control PEG-linked acrylamide **164** proceeded at a rate approximately 20 times slower than with initial positive control acrylamide **67**. Incubation of TS with a mixture of 6 PEG-linked acrylamide fragments (**158**-**160** and **162**-**164**)*, each at 400 μM final concentration for 180 min, led to slow adduct formation with each acrylamide, with no enhanced binding to the positive control **164**, Figure 99. This slow rate of modification probably represents the rate of background reaction.
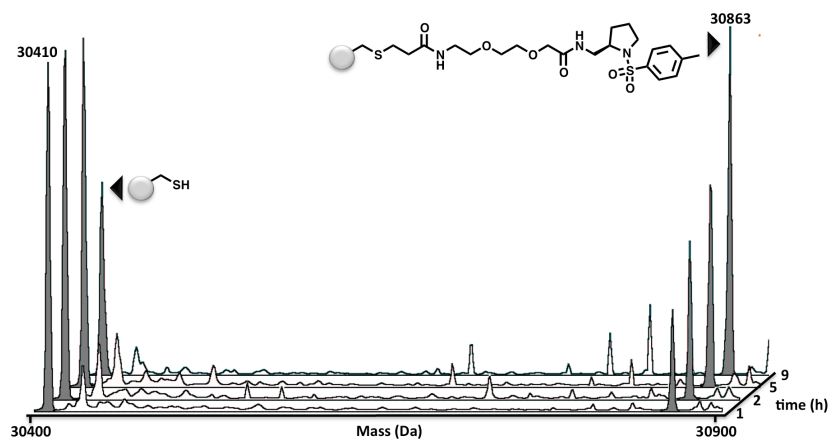
Figure 98 TS (10 μM) in ammonium bicarbonate (10 mM) and DTT (1 mM) at pH 8 incubated at rt with positive control PEG-linked acrylamide **164** at 400 μM final concentration from a stock solution in MeOH. Aliquots taken for ESI MS analysis at 1, 2, 5 and 9 h.

---

* Acrylamide **161** had to be excluded on the basis of poor aqueous solubility.
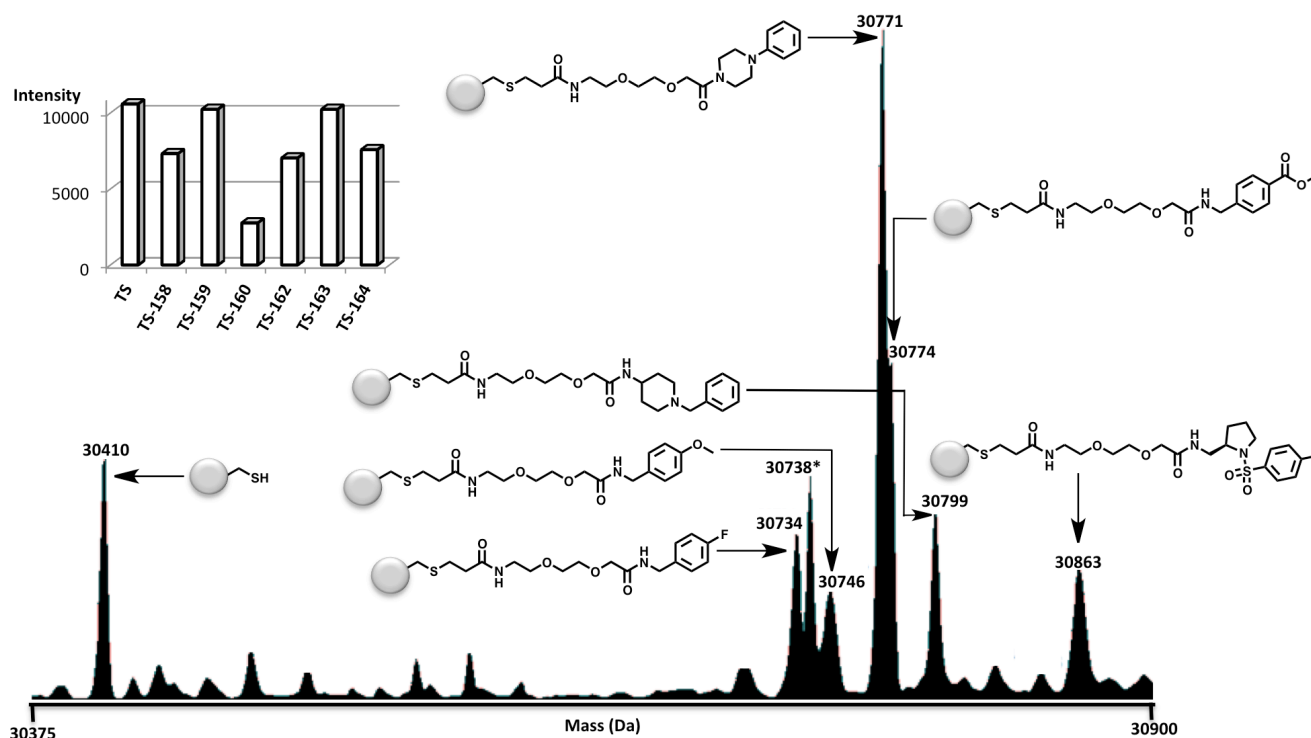
Figure 99 TS (10 μM) in ammonium bicarbonate (10 mM) and DTT (1 mM) at pH 8 incubated at rt with a mixture of 6 acrylamides **158**, **159**, **160**, **162**, **163**, **164** each at 400 μM for 180 min. All major adduct peaks are assigned by mass (Da). **LHS** chart indicates the intensity for each peak, integrated using MaxEnt. The intensity for the peak at 30771/30774 Da was divided in half, as the contribution from each acrylamide was unknown.

An HPLC study was carried out to determine the intrinsic reactivity of the PEG-linked acrylamide fragments in comparison to positive control **67**, using glutathione as the model thiol. As shown in Figure 100, PEG-linked acrylamides **164** and **159** both demonstrated a slower intrinsic reactivity than positive control **67**, with *ca.* 70-78 % remaining electrophile 180 min after glutathione treatment for **67** and 84-96/90-95 % remaining electrophile for **164** and **159** respectively.[*]
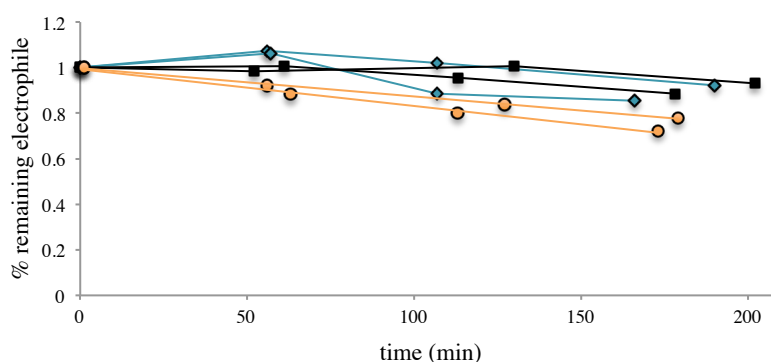
Figure 100 Rate of reaction of acrylamides **164** (blue traces, diamonds), **159** (black traces, squares), **67** (orange traces, circles) with reduced glutathione in ammonium bicarbonate (100 mM) pH 8 (measured as three separate reactions). Acrylamides at 1 mM and glutathione at 5 mM. Reactions monitored by HPLC in the presence of 4-aminobenzamide (0.5 mM) as an internal standard. All reactions were run in duplicate, with both traces indicated on the chart. Data is relative to internal standard and normalised to intensity at t = 0 min. Data for acrylamide **67** has been fit with a linear trendline whereas the data for acrylamides **159** and **164** are represented as straight marked scatter plots.

---

[*]Remaining electrophile at 180 min calculated by fitting a linear trendline to each set of data, and calculating the Y values at X = 180 min.

The data for both PEG-linked acrylamides **164** and **159** was significantly more unreliable than that for positive control acrylamide **67**, Figure 100. Linear trendlines fitted to the data for PEG-acrylamides **159** and **164** gave R^2 values of 0.50, 0.84 and 0.65, 0.42 respectively, whereas the the R^2 values for the data for acrylamide **67** were 0.99 and 1.0.[*] It may be that the PEG-linked acrylamides form micelle or other type aggregates in solution, which firstly obscure the acrylamide from the solution, resulting in very slow reaction with thiols, and secondly interfere with the UV absortion intensity leading to unreliable HPLC data.

4.7. A new strategy for linker design

To rapidly ascertain a more effective linker structure and length, a new strategy was adopted involving the synthesis of acrylamide-linker-fragments modified with only the negative and positive control fragments. A successful linker should allow the selection of only the positive control from a mixture of both fragments, a strategy that overcomes the necessity for the highly time consuming synthesis of a larger set of acrylamide-linker-fragments at the initial test stage. This strategy required access to gram quantites of both the positive and negative control amine fragments. This was possible for amine **72** using the previously developed route (Chapter 3, p55, Scheme 5). However, the route previously used to synthesise amine **122a** (Chapter 3, p79, Scheme 19) was not suitable for the synthesis of significant quantites of material. This route involved three synthetic steps, commencing with an aziridination of allyl benzene, subsequent aziridine ring-opening and a final hydrogenation. Problems encountered during this synthesis included the aziridination step, which resulted in the isolation of aziridine **120** as an inseparable mixture with an unidentified impurity, and the aziridine ring-opening, which yielded a mixture of inseparable regioisomers **121a** and **121b**. During this previous work, the regioisomeric mixture was taken through the rest of the synthetic route as the mixture and separated after the final step. To access gram quantites of the pure negative control amine fragment **122a**, an optimisation of this route was required.

During optimisation of the first step, a set of recrystallisation trials and column chromatography conditions were investigated. Under optimised solvent conditions, an R_f separation of 0.08 was achieved by TLC between the aziridine **120** and the unwanted impurity. The impurity was therefore removed using a very wide silica packed column, to yield the desired pure aziridine **120** in yields of between 39-43 %. It was also found that recrystallisation from ether furnished the desired aziridine **120**, although the yield was lower at 27 %.

In the prior synthesis, ring-opening of the aziridine with $TMSN_3$ generated a regioisomeric mixture of azides **121a** and **121b** (8:1 selectivity in favour of the desired isomer **121a** with ring-opening at the less hindered position), in a poor 32 % overall yield, Table 17 (entry 1). Ring-opening of aziridine **120** with sodium azide in an acetonitrile:water mixture was reported with to proceed with complete regioselectivity in 98 % yield by Bisai *et al*. in 2003.[194] However, adopting a procedure similar to that reported led to the isolation of a 1:5 mixture of regiosomers, with selectivity for the desired isomer **121a** (entry 2). Perhaps the lower regioselectivity was a feature of the reduced steric bulk of the nucleophile compared to $TMSN_3$. Many aziridine ring-opening reactions with trimethylsilyl-nucleophiles are catalysed by Lewis acids, which activate the aziridine towards nucleophilic attack, Figure 101. These reactions

---

[*]As only a small percentage of the electrophile reacts during HPLC analysis, the data is linear as it represents the initial reaction rate.

often result in mixtures of regioisomers, depending on the aziridine substitution. Hou *et al*. developed an aziridine ring-opening based on activation of the nucleophile rather than the aziridine. Treatment of TMSCN with TBAF generated the activated ammonium cyanide nucleophile *in situ*, Figure 101.[195] Inspired by this work, Minakata *et al*. developed a highly regioselective aziridine ring-opening by activating TMS-nucleophiles with a Lewis base.[196] The authors proposed that the Lewis base TMEDA coordinates to the silicon atom to generate either 5- or 6-coordinate silicon (depending on solvent coordination), which increases the nucleophilicity of the Si-nucleophile bond. Regioselectivity is presumably increased by the steric bulk of the nucleophile, promoting attack at the less hindererd site.
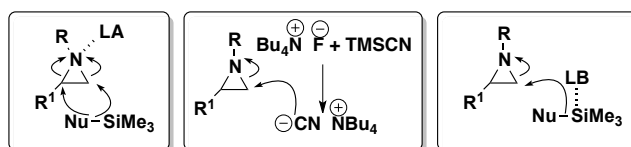
Figure 101 Catalysed TMS-nucleophile aziridine ring-opening reactions. **LHS** Lewis acid promoted ring-opening. **Middle** work by Hou *et al*. to activate the nucleophile. **RHS** Lewis base promoted ring-opening.

Treatment of the aziridine **120** with TMSN$_3$ in the presence of catalytic TMEDA gave a significantly higher regioselectivity of **121a/121b**, 21:1 (entry 3). Unfortunately, upon scaling this reaction up from 0.3 to 13 mmol, none of the desired product could be isolated. The highly Lewis basic tris(2,4,6-trimethoxyphenyl)phosphine (TTMPP) was reported to catalyse the ring-opening of aziridines by trimethylsilyl-nucleophiles in a highly regioselective manner in 2009 by Matsukawa *et al*.[197] The use of catalytic TTMPP rather than TMEDA for ring-opening of aziridine **120** resulted in complete regioselectivity for the desired isomer on a small scale, although the reaction did not proceed satisfactorily within the 1 hour reported in the literature (entry 4). Increasing the reaction time to 5 h gave an 88 % conversion to product (entry 5), which increased to 100 % after 7.5 h (entry 6). This reaction was amenable to scale up from 0.5 to 2.5 mmol, although the isolated yield was slightly diminished to 55 % (entry 7).
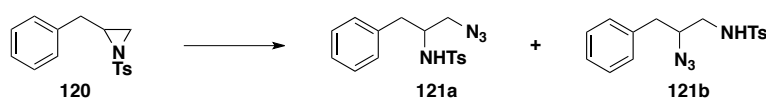
Entry	Nucleophile	Solvent	Catalyst	Time (h)	Temp (°C)	Regioselectivity (121a:121b)	Conversion (%)
1	TMSN$_3$	DMF	none	16	40	8:1	32[c]
2	NaN$_3$	MeCN:H$_2$O (9:1)	none	24	80	5:1	100
3	TMSN$_3$	MeCN	TMEDA[a]	24	rt	21:1	84
4	TMSN$_3$	DMF	TTMPP[b]	1	rt	**a** only	28
5	TMSN$_3$	DMF	TTMPP[b]	5	rt	25:1	88
6	TMSN$_3$	DMF	TTMPP[b]	7.5	rt	**a** only	100 (70[c])
7	TMSN$_3$	DMF	TTMPP[b]	7.5	rt	**a** only	55[cd]

[a]20 mol %
[b]10 mol %
[c]isolated yield
[d]2.5 mmol scale

Table 17 Optimisation of the azido aziridine ring-opening. Conversions determined by ^{1}H NMR.

Treatment of the pure azide **121a** with Pd/C (cat.) under an atmosphere of H$_2$ (g) effected the desired hydrogenation to

Figure 102

amine **122a** in quantitative yield, Scheme 27. In the previous synthetic route, treatment of the mixture of amine regioisomers with acryloyl chloride at rt led to the desired acrylamide **119** in a poor 26 % yield, in addition to an unexpected and subsequently problematic side-product **123** in a 19 % yield, Figure 102. Addition of acryloyl chloride to pure amine **122a** at 0 °C, rather than rt, furnished the
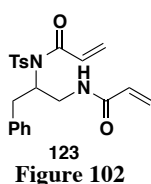
desired negative control **119** in a 56 % isolated yield, with no formation of the undesired reactive Michael acceptor **123**. The optimised route to the desired negative control acrylamide **119** is shown in Scheme 27.
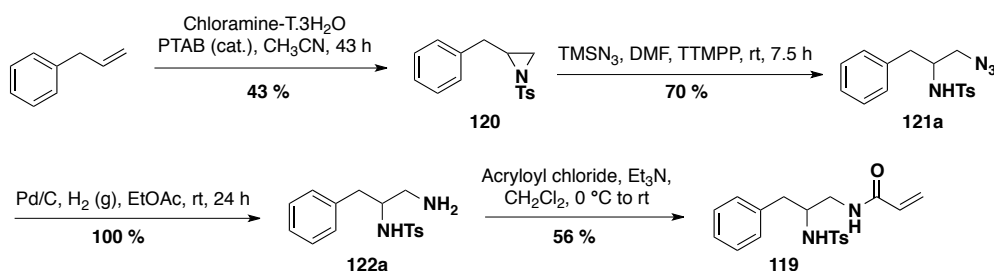
Scheme 27 Optimised synthesis of negative control amine **119**.

It was desirable for a number of linker lengths to be investigated, varying in length and flexibility. Natural units such as glycine, β-alanine and γ-aminobutyric acid conveniently provide an amine for generation of the acrylamide and a carboxylic acid as a handle with which to couple amine fragments, with both functionalities separated by varying carbon spacers. Additionally, a number of di-amines with short carbon spacers are commercially available and were considered as more flexible linkers suitable for coupling to a carboxylic acid fragment. Such a linker would be suitable for coupling to the original carboxylic acid N-tosyl D-proline **64** fragment reported by Erlanson *et al.*[51] rather than the positive control amine **67**, and would therefore provide an interesting comparison between linker types. Some attempts were made to investigate glycine, β-alanine, and 1,3-diaminopropane as linkers for use in KTGT as discussed in the following section.

4.7.1. Glycine

Glycine was investigated as a linker during the early stages of the KTGT project with cdc25A as the target protein. A series of small heterocyclic fragments tethered to the active site cysteine *via* a glycine spacer were predicted to bind favourably in the small active site binding pocket, as determined by manual docking using an available crystal structure, Figure 103. Synthesis of acrylamide **165** was facile using Schotten-Baumann type conditions, but problems were encountered taking carboxylic acid **165** on to further reaction with amines, Scheme 28. The problems encountered during the synthesis were likely to be due to polymerisation with the acrylamide, as previously discussed for other synthetic routes. This suggested that for the synthesis of acrylamide-linker-fragments, the acrylamide should remain protected until the final step.
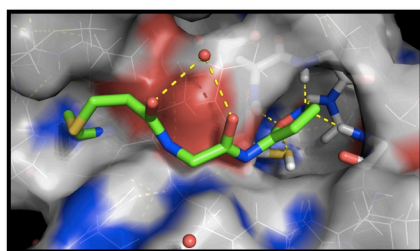
Figure 103 Structure **167** manually tethered from tyr386 using the cdc25A crystal structure (PDB code 1C25) and WebLabViewer software. The glycine linker makes an interaction with a bound water molecule and the isoxazole fragment makes a number of interactions within the active site pocket.
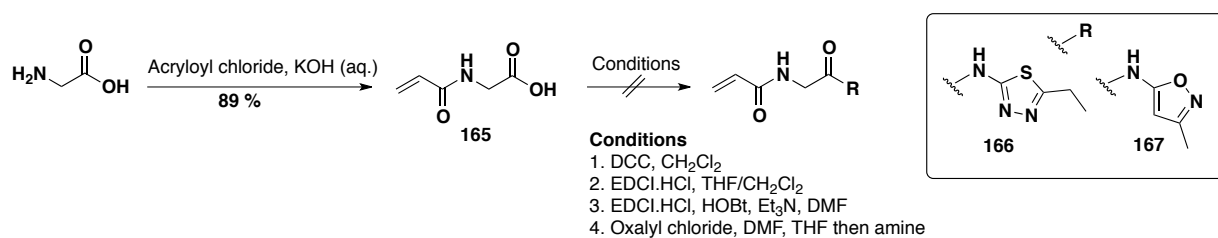
Scheme 28 Attempted synthesis of glycine linked acrylamide-fragments.

4.7.2. β-Alanine

The first linker length to be thoroughly investigated for KTGT was β-alanine, which provides a two-carbon spacer between the acrylamide and the fragment, Figure 104. As this is a significantly shorter length than that employed in the previous PEG-linker it was hoped that effective molarity would be retained, whilst still providing some flexibility.
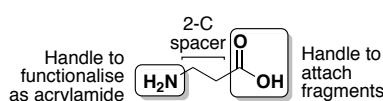
Figure 104 β-alanine linker.

Synthesis of β-alanine modified acrylamide-fragments

As outlined retrosynthetically in Scheme 29, the acrylamide was taken through the synthesis protected as an α-phenylselenide in a manner analogous to the PEG-linker synthesis. Deprotection in the final step by oxidation of the selenium and *in situ* elimination generates the desired acrylamide. The amine fragment is coupled to the linker in the penultimate step in order to diverge the synthesis at the latest possible point. The precursor for this coupling reaction, carboxylic acid **168**, is synthesised from commercially available β-alanine and the previously synthesised carboxylic acid **145**.
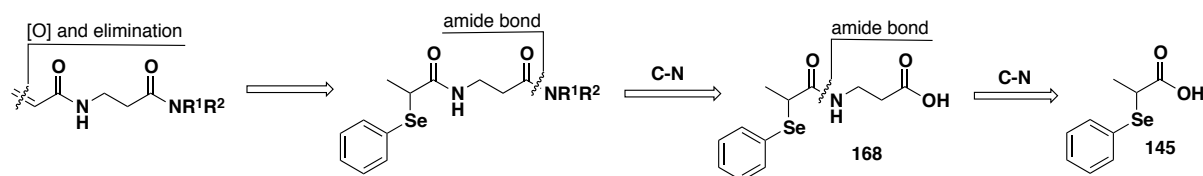
Scheme 29 Retrosynthesis for acrylamide-fragments with β-alanine spacer.

The synthetic route commenced with commercially available β-alanine methyl ester **169**, with the ester protecting group to prevent reaction of the alanine carboxylic acid during the first step. Treatment of α-selenide carboxylic acid **145** with oxalyl chloride and catalytic DMF in THF, with subsequent addition of β-alanine methyl ester and triethylamine led to generation of the desired amide **170** in isolated yields of between 61-65 %, Scheme 30. Hydrolysis of the ester furnished the desired carboxylic acid **168** in excellent isolated yields of between 94-100 %. Before coupling of carboxylic acid **168** with either the positive or negative control amines, a test reaction was carried out using N-phenylpiperazine **171**. Treatment of carboxylic acid **168** with amine **171** and zirconocene dichloride in toluene led to a moderate isolated yield of 65 % for the desired amide **172**. Oxidation of the selenium and *in situ* elimination led to the final acrylamide-fragment **173** in 48 % yield. Treatment of intermediate acid **168** with positive control amine **67** using the same zirconocene dichloride reflux conditions generated the desired amide **174** in 44 %

yield, with subsequent deprotection furnishing the desired compound **175** for screening in an excellent 94 % yield. Coupling of intermediate acid **168** with negative control amine **119** yielded the desired acrylamide **177** upon oxidation and elimination, although in only 18 % over the two steps.
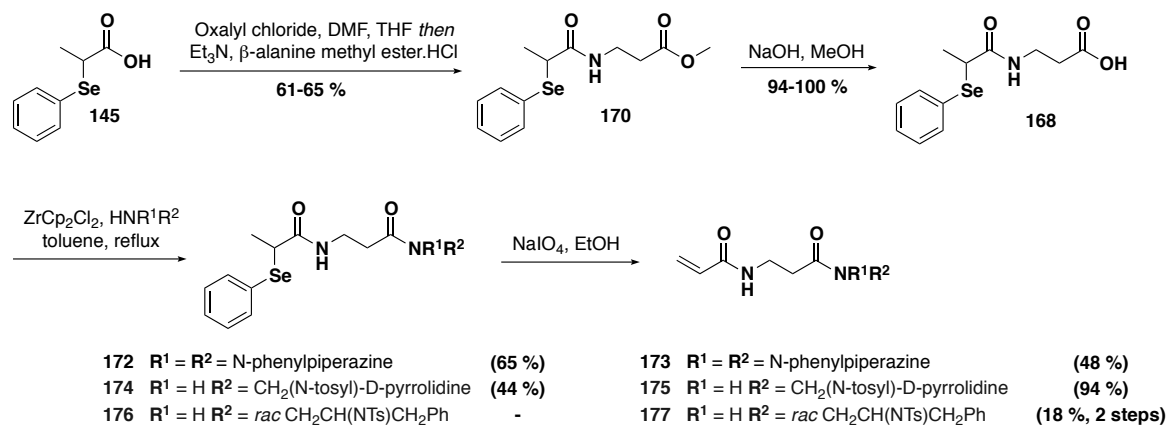
Scheme 30 Synthesis of a set of acrylamide-fragments with a β-alanine linker.

An HPLC study was carried out to ascertain the intrinsic reactivity of the positive and negative β-alanine modified acrylamides, using reduced glutathione as the model thiol. As shown in Figure 105, both ligands reacted at a very similar rate (red and black traces for positive **175** and negative **177** ligands respectively) with both reactions slightly faster than that of the positive control **67** (blue trace). The percentage of electrophile which reacted per minute was calculated as 0.16 ± 0.2 and 0.19 ± 0.2 for the positive and negative control ligands **175** and **177** respectively, whereas that for positive control **67** was 0.14 ± 0.3.[*] As only a small percentage of the acrylamide reacts during this experiment, the data sets can be fitted with linear trendlines, which represent initial reaction rates.
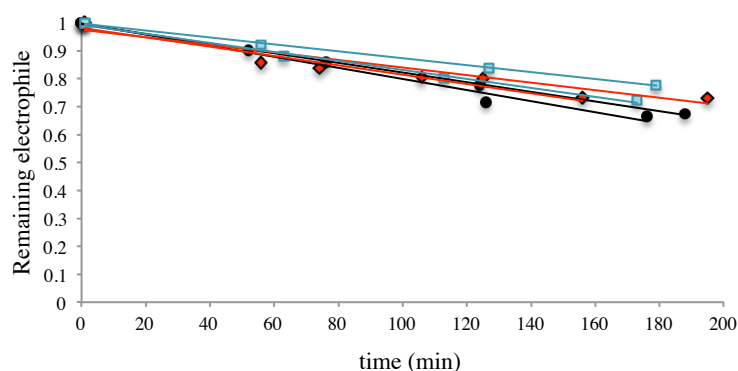
Figure 105 Rate of reaction of acrylamides **67** (blue trace, squares), **175** (red trace, diamonds), **177** (black trace, circles) with glutathione in ammonium bicarbonate (100 mM) pH 8 (measured as three separate reactions). Acrylamides at 1 mM and glutathione at 5 mM. Reactions monitored by HPLC in the presence of 4-aminobenzamide (0.5 mM) as an internal standard. All reactions were run in duplicate, with both traces indicated on the chart. Data is relative to internal standard and normalised to intensity at t = 0 min.

Incubation of TS with a mixture of both positive and negative β-alanine-linked acrylamides **175** and **177**, with each acrylamide at 100 μM, led to modification of the protein with both ligands over time, Figure 106. Reducing the

---

[*] Calculated from the average gradient of linear trendlines fit to two data sets. Error represents the standard deviation.

concentration of both acrylamides to 10 μM (stoichiometric with the protein), in an attempt to reduce the background reaction, led to no modification of the protein with either acrylamide, even after a 900 min incubation period. Increasing the concentration of each acrylamide to 200 μM led to generation of adducts with both ligands, although at a faster rate. As indicated in Figure 107, the rate of modification of TS with positive control **175** was faster than with negative control **177**, at both 100 and 200 μM ligand concentrations. As positive control acrylamide **175** was found to have a slightly lower intrinsic reactivity than negative control acrylamide **177**, this suggests that a kinetic template-guided tethering effect accounts for the faster modification of protein thiol with positive control **175**, whereas adduct formation between TS and negative control **177** is likely to represent the non-templated background reaction rate.
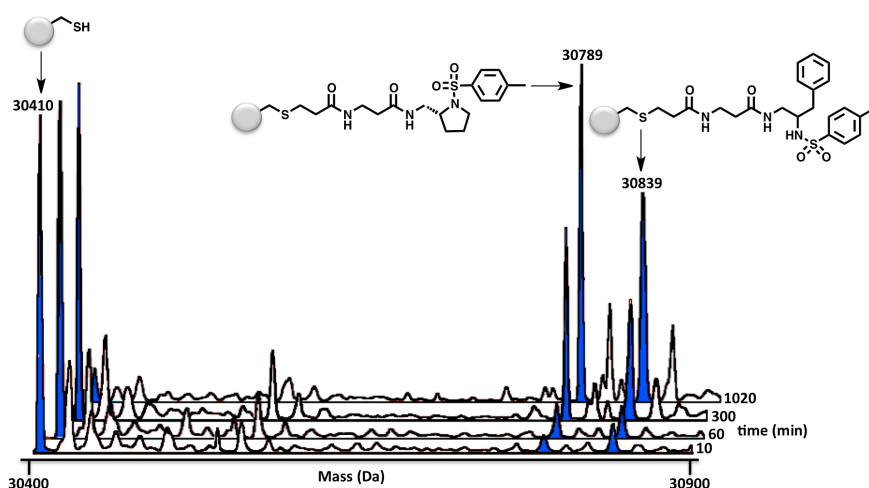
Figure 106 TS (10 μM) in ammonium bicarbonate (10 mM) and DTT (1 mM) pH 8, with acrylamides **175** and **177** each at a final concentration of 100 μM. Aliquots from the main reaction taken for ESI MS analysis at 10, 60 300 and 1020 min.
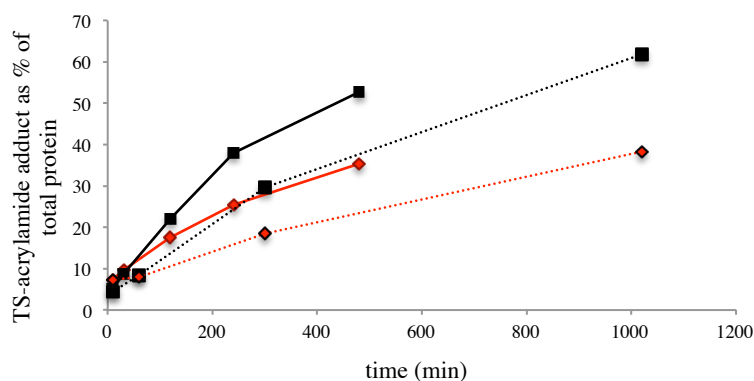
Figure 107 Analysis of data from Figure 106 in addition to data generated with acrylamides at 200 μM. Chart shows formation of protein-acrylamide adducts over time normalised to total protein. Black traces (squares) represent positive control **175**, red traces (diamonds) represent negative control **177**, with full lines indicating acrylamides at 200 μM final concentration and dotted lines indicating acrylamides at 100 μM final concentration. Integrals for peaks were obtained after deconvolution of raw data using MaxEnt software. Integrals were normalised to the sum of the total protein.

It was also considered that a favourable interaction between the linker and the protein surface might itself template the reaction, leading to a higher rate of background reaction for both fragments. The β-alanine linker was considered to potentially interact with the protein surface either through the direct formation of intermolecular H-bonds or by the formation of an intramolecular H-bond, generating a 6-membered ring fragment binder, Equation 8. To rule out the

formation of such favorable interactions, an acrylamide connected to the β-alanine linker, but without the fragment was desired. A propyl unit was considered to provide a good substitution for the N-tosyl D-proline fragment, Figure 108.
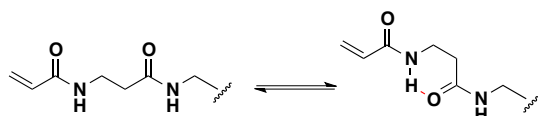
Equation 8 An intramolecular H-bond within the β-alanine linker generates a 6 m ring, which was considered a potential TS binder.
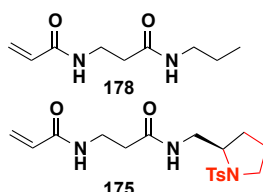
Figure 108 Compound **178** was desired as a control for the β-alanine linker.

Initial protection of β-alanine with a Z-group to generate Z-protected alanine **179** was carried out to protect the amine during amide synthesis. However, reaction of alanine **179** with N-propylamine under a range of conditions failed to generate the desired amide, Scheme 31. It was considered that the primary amide would also be suitable as the control compound for this experiment, and generation of this using ethyl chloroformate, with an aqueous ammonia quench furnished the desired product **180**. Removal of the Z-group was facile to give amine **181**, but reaction of this with acryloyl chloride under the conditions used to synthesise acrylamide **165** did not yield the desired acrylamide **182**.
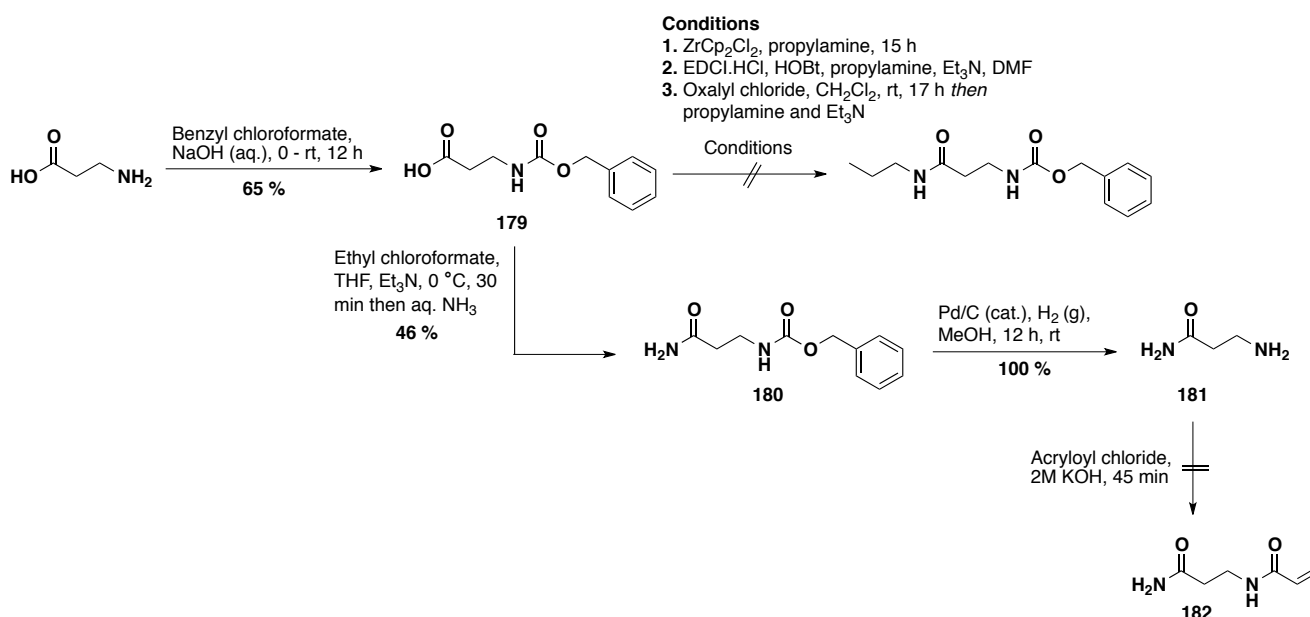
Scheme 31 Attempted synthesis of a screening control for the β-alanine linker.

However, reaction of acrylamide **183**[*] with ethyl chloroformate, and a subsequent ammonia quench led to the desired amide **182**, albeit in a poor 6 % yield, Equation 9. Screening of acrylamide **182** against TS to control for the effect of the linker should form part of the future work for this project.

---

[*] Synthesised by Masters student Madeline Ross.
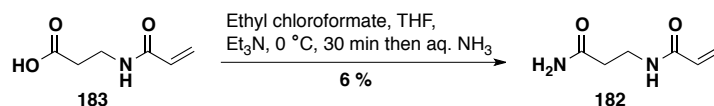
Equation 9

4.7.3. 1,3-Diaminopropane

Alkyl diamine spacers were considered as potentially suitable for use in KTGT to link the acrylamide and the fragment. In comparison to the β-alanine linker, a 1,3-diaminopropane linker has a greater flexibility due to the replacement of the sp^2 centre with an sp^3 centre. A diamine linker would be suitable for coupling to fragments with a carboxylic acid handle, rather than the amines that were required for coupling to the β-alanine, Figure 109.
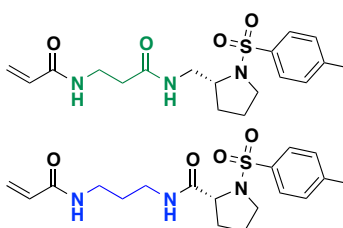
Figure 109 Comparison between the β-alanine (green) and the 1,3-diamine linker (blue).

Some initial work towards the synthesis of acrylamide-fragments with a 1,3-diamine linker was carried out. Initial attempts to sythesise the desired acrylamides modified with this linker and the positive and negative fragments began with attempts to mono-protect the diamine. Monoprotection with either a Boc or a Cbz protecting group was unsuccessful, with mono-Cbz protection leading to isolation of only the di-protected amine **184**, Scheme 32. It has been proposed that the reaction between acid chlorides and alkyl diamines is so rapid that upon addition of one drop of the reagent to the diamine, the reaction is complete at the point of contact.[198] Therefore, before mixing has occurred, complete formation of the di-acylated product has taken place. Christensen *et al*. proposed benzylphenylcarbonate **185** as a less reactive acylating agent suitable for the monoprotection of polyamines.[199] Synthesis of carbonate **185** was completed using the reported literature procedure, but its use in the mono-protection of 1,3-diaminopropane to amine **186** was unsuccessful.
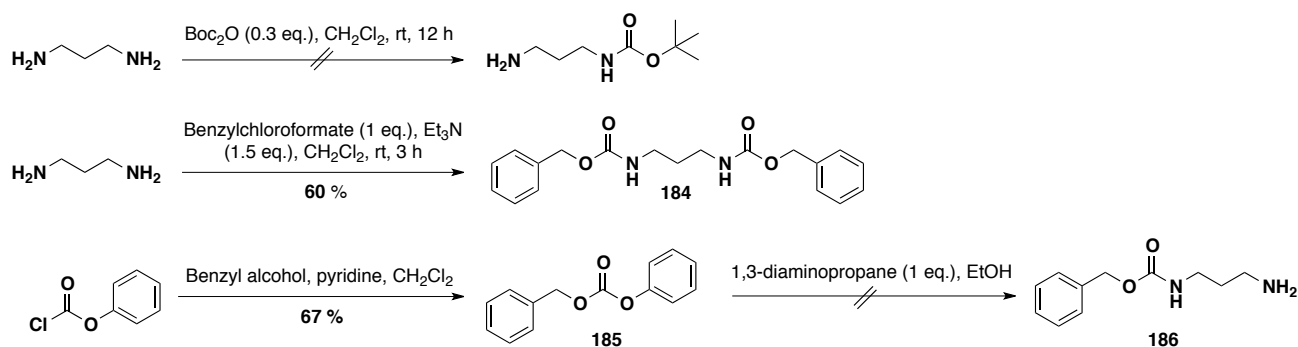
Scheme 32 Unsuccessful attempts to mono-acylate 1,3-diaminopropane.

Applying a different strategy, ten equivalents of the diamine were refluxed in the presence of N-tosyl phenylalanine **187** and zirconocene dichloride, Scheme 33. Assuming that reaction with one amine does not affect the reactivity of the second amine, the major product from this reaction should have been the mono-amide **188**. However, this was actually only isolated in a 24 % yield, with the di-amide **189** isolated in a 52 % yield. Reaction of the mono-amide **188** with acryloyl chloride was unsuccessful.
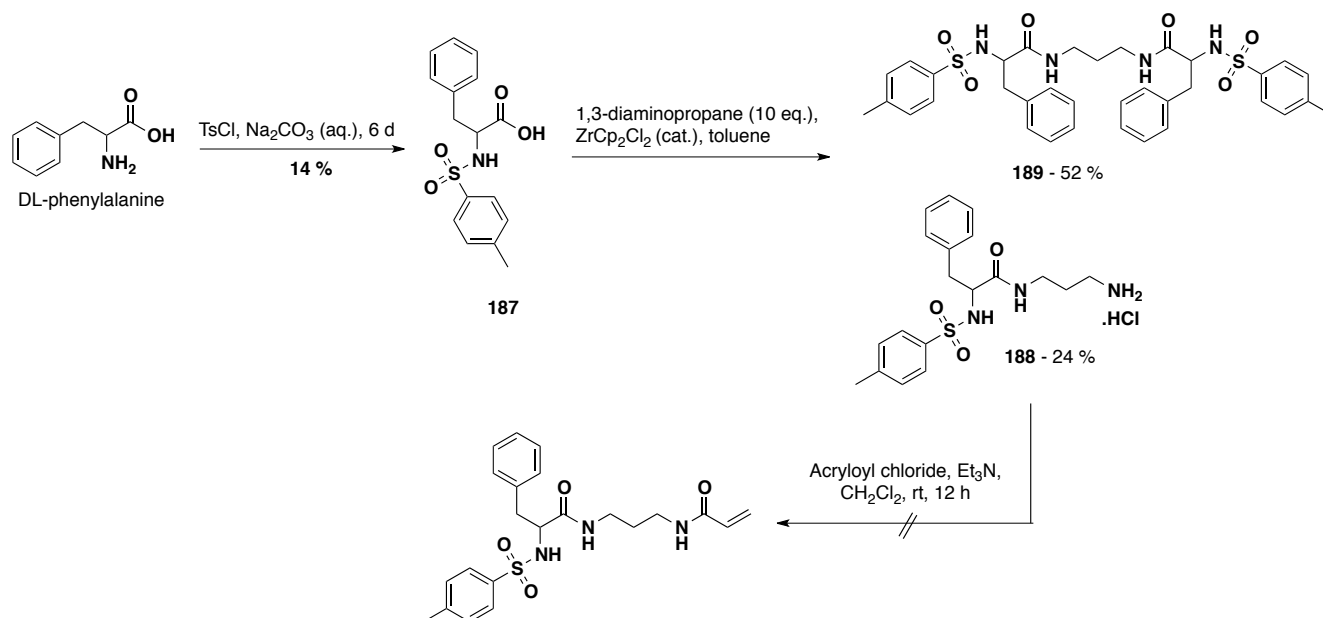
Scheme 33 Attempts to synthesise a 1,3-diamino-acrylamide linker modified with the negative control ligand.

4.8. Conclusions and further work

It was desirable to incorporate a linker into KTGT in order to normalise acrylamide reactivity across the library, and to allow fragments the flexibility to bind across a range of protein systems. The incorporation of linkers that are longer than the exact distance between the binding points of two multivalent ligands has been deemed a justifiable strategy by Whitesides *et al*. due to the slow loss of effective molarity with length.[184] Work by Blaustein *et al*. also suggested this as an effective strategy, with longer linkers thought to have a greater number of binding conformations that shorter ones, which must adopt more improbable, fully extended conformations.[188]

In this work, the use of a linker composed of 2.5 PEG units led to a very slow modification of the protein, with loss of the templated reaction for the positive control. The linker may have been too long and flexible, such that upon binding of the positive control ligand, no increase in effective molarity of the acrylamide at the cysteine thiol occurred. As the cysteine resides so close to the pocket in this system, the long linker may have resulted in placement of the acrylamide too far from the reactive thiol. Alternatively, the overall slow rate of reaction of these PEG-linked acrylamides with the small molecule thiol glutathione may suggest some sequestration of the acrylamide by the water soluble PEG-linker in aqueous solvents.

Changing the linker to a β-alanine unit led to the observation of a KTGT effect, with formation of an adduct to TS with the less intrinsically reactive positive control proceeding at a faster rate than with the negative control. Attempts to synthesise positive and negative acrylamides incorporating the slightly more flexible 1,3-diamine linker were made but not completed. It was unknown whether the more flexible linker would confer an advantage by allowing the reaction to take place with reduced strain, or whether the additional loss of entropy upon reaction would make this linker less favorable.

Future work for this project should include cloning and expression of a TS mutant with the cysteine moved to a location outside the pocket. Incubation of this mutant with a library of acrylamides modified with the 2.5 PEG unit linker might lead to some interesting results. Further work should be carried out with this TS mutant to see how linker length and rigidity affect reaction rate. It would be interesting to compare the acrylamide and vinyl sulfonamide functional groups with respect to the linker chemistry.

5. Conclusions and future work for kinetic template-guided tethering

The aim of this project was the development of a novel methodology for the site-directed discovery of protein-binding fragments. Early work included the investigation of acrylamide and vinyl sulfonamide functionalities as potential capture groups for use in this method. The reaction of each capture group with small molecule thiols was monitored in a series of HPLC experiments and shown to be irreversible. A protocol was developed for the analysis of protein-ligand adducts using MALDI mass spectrometry and a quadruple mutant of cdc25A with one surface exposed cysteine. The results obtained from this work were difficult to interpret, and it was concluded that a model system was required for proof-of-concept studies.

Thmidylate synthase was adopted as the model system, with a number of compounds available for use as controls from earlier work published by Erlanson *et al*.[51] The synthesis of positive controls and higher affinity positive controls with acrylamide and vinyl sulfonamide appendages was successfully completed. The synthesis of a negative control with an acrylamide appendage was successful. TS was cloned, expressed and purified, and a protocol was developed to observe protein and protein-adducts using ESI mass spectrometry. Both vinyl sulfonamide and acrylamide capture groups were demonstrated to select only the positive control ligand from certain mixtures during screening against TS. The design of library members was shown to need special consideration, and basic amines are probably best avoided. It was considered that the basic amine in the acrylamide-modified negative control led to its selection by TS by an intramolecular base catalysis. A second negative control ligand with an acrylamide appendage was synthesised, and shown not to be selected by TS. A further compound **54** with a basic amine was found to be selected by TS. Of the ligands used in this study, N-benzyl piperidine **54** was found to be the best inhibitor of TS, although with a very weak K_i of greater than 3 mM. It might be that this compound is also selected by TS by a base-promoted intramolecular rate acceleration. This compound was not selected by TS when modified with a vinyl sulfonamide. Control proteins papain, p97 and cdc25 were shown to have a reactive cysteine thiol by modification with iodoacetamide, but did not select the positive control acrylamide. The described methodology rapidly identified binding ligands *via* the formation of an adduct, which was stable to proteolytic digestion. This allowed identification of the position of modification by MALDI analysis of the resulting peptides. Further work should include an investigation of the vinyl sulfonamide group for use in KTGT.

In the final chapter, an attempt was made to develop a linker unit to insulate the acrylamide from the fragment, and therefore normalise reactivity to conjugate addition across the library. It was also hoped that the linker would allow the acrylamide greater flexibility to react with the nucleophilic thiol upon fragment binding. The synthesis of a library of compounds containing an acrylamide and a fragment connected by 2.5 PEG units was successful using a phenylseleno protecting group. However, this connecting structural element was found to be unsuitable for KTGT, with no rate acceleration observed for reaction with the acrylamide-positive control. A β-alanine linker was shown to be more appropriate with a small rate acceleration observed for adduct formation to the positive control over the negative control. As future work for this part of the project, it would be interesting to investigate a shorter linker such as glycine, in addition to to probing the effect of moving the reactive cysteine further from the binding site. Furthermore, it would be useful to probe the effect of the linker length on vinyl sulfonamide-based KTGT.

Future work for this project should include the synthesis of a larger library of suitable fragments and application of KTGT to a therapeutically useful target.

6. Design and synthesis of a chemical probe to dissect the cellular signalling cascade leading to cyclin D1 degradation after DNA damage

6.1. Introduction

6.1.1. The Eukaryotic cell cycle

The mammalian cell cycle is composed of four main phases; gap 1 (G1), synthesis (S), G2 and mitosis (M), which result in the exact duplication of genetic material and cell division (cytokinesis).[200] The cell cycle is tightly regulated by a complex network of proteins in which the serine/threonine cyclin-dependent kinases (cdks) play a fundamental role, Figure 110.[201] Monomeric cdks have only negligible activity as kinases and require binding of a cyclin subunit as an initial activation step.[202] Activated heterodimeric cdk-cyclin units act to phosphorylate substrate proteins, which then drive the cell cycle through the key transition points. With the exception of the D-type cyclins, the expression of cyclins is oscillatory throughout the cell cycle, providing a means to regulate cdk activity in a phase-specific manner. D-type cyclins (D1, D2 and D3) are expressed in response to growth factors, and in combination with their cdk binding partners, cdk 4 and 6, are critical for the entry of cells into the cell cycle and for G1-S phase progression.[203, 204] Cdk4/6-cyclin D complexes phosphorylate the retinoblastoma (rb) family of proteins which then release E2F transcription factors that activate many genes required for cell cycle progression, including cyclins A and E.[205-209] Cdk2-cyclin E complexes further phosphorylate rb proteins in mid-late G1, causing complete disruption of their interaction with E2Fs.[210, 211] Cdk2-cyclin E complexes in late G1 and cdk2-cyclin A complexes in S-phase activate DNA synthesis,[212-214] whilst cdk1-cyclin A and cdk1-cyclin B complexes activate and drive the cell through mitosis.[215-217] Cyclin degradation occurs in a ubiquitin-dependent manner throughout the cell cycle once each particular cyclin has played its required role.[218]
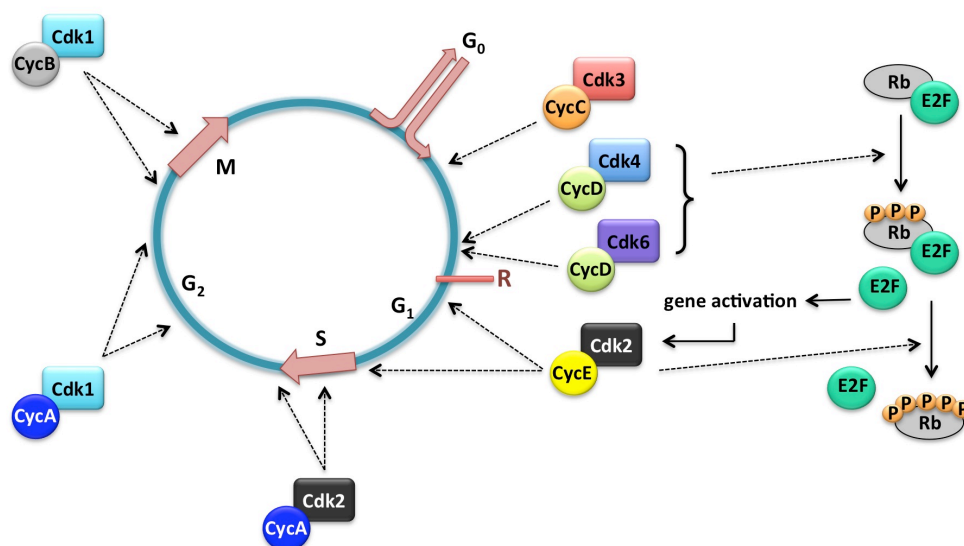
Figure 110 The role played by the cdk-cyclin complexes in the cell cycle. The phases of the cell cycle G_0, G_1, S, G_2 and M refer to quiescence, gap1, DNA synthesis, gap2 and mitosis respectively. Phosphorylation of the retinoblastoma protein (Rb) by the cdk-cyclin complexes leads to release of E2F transcription factors and subsequent DNA synthesis of target genes, including cyclins A and E.

6.1.2. Cyclin D1 and the DNA damage response

The integrity of the genome is constantly challenged by agents such as ultraviolet (UV) light, reactive oxygen species (ROS) and ionising radiation (IR). DNA lesions must be rapidly detected by the cell and a response quickly mounted to either stall cell cycle progression to enable DNA repair or to coordinate cell death.[219] The cell has three regulatory pathways, G1/S, intra-S and G2/M, termed DNA damage checkpoints, which control cell cycle progression after DNA damage in order to preserve genomic integrity.[220] Rapid cell cycle arrest at G1, initiated by ubiquitin-mediated degradation of cyclin D1, is an important part of the DNA damage response, as activation of the G1/S checkpoint prevents the replication of damaged DNA in S phase.[221-223] Cyclin D1 is often found to be overexpressed in human cancers and can have a highly detrimental impact if not correctly regulated following the DNA damage response.[224] Understanding the function and regulation of cyclin D1 on a molecular level is therefore of fundamental importance.

Phosphorylation of cyclin D1 on Thr286, which marks the protein for ubiquitination and proteolytic degradation under both normal cell conditions and under genotoxic stress, can be carried out by a number of kinases. Glycogen synthase kinase (GSK) 3β has been shown to implement this phosphorylation of cyclin D1 under conditions of mitogen deprivation[221] and in response to genotoxic stress.[222] IKKα, which along with IKKβ and IKKγ subunits constitutes the IKK complex, has also been shown to destabilise cyclin D1 through phosphorylation of Thr286.[225] The IKK complex also plays a central role in the regulation of NF-kB transcription factors, which activate a number of genes including *cyclin D1*.[226] NF-kB transcription factors are held inactive in the cytoplasm by IkB proteins. Phosphorylation of IkBα protein on serine residues 32 and 36 by IKK marks it for ubiquitin-mediated proteasomal degradation and releases NF-kB which translocates from the cytoplasm to the nucleus to implement gene activation.[227] DNA damage can initiate the degradation of IkBα protein by the IKK complex, releasing NF-kB and initiating NF-kB signalling cascades.[228, 229] The reported downregulation of cyclin D1 following DNA damage and the effect on this by IKK is yet to be fully understood.
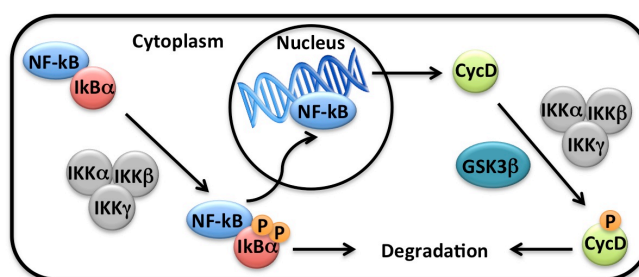
Figure 111 The role played by NF-kB, IkBα, and the IKK complex in the regulation of cyclic D1 in the cell.

6.1.3. Previous work

Two novel inhibitors **190** and **191**, Figure 112, were reported by Pierce *et al*. to irreversibly inhibit TNFα induced phosphorylation of IkBα, leading to decreased NF-kB released from the cytoplasm into the nucleus.[230] This led to an observed anti-inflammatory effect *in vivo* due to the decreased transcription of NF-kB target genes, including those of adhesion molecules such as E-selectin, intercellular adhesion molecule-1 and vascular cell adhesion molecule-1. The

Mann group was interested in elucidating the effect of NF-kB signalling on the regulation of cyclin D1 levels following DNA damage and the reported inhibition of IkBα phosphorylation and therefore of NF-kB transcription factors by vinyl sulfone **190** suggested this compound as a potentially useful tool to probe this. It was found that treatment of U2OS cells with genotoxic agents (UV, IR, 4-nitroquinoline 1-oxide (4NQO) and H_2O_2) led to a reduction in cyclin D1 levels as expected.[231] Interestingly, pre-treatment of cells with vinyl sulfones **190** or **191** attenuated this reduction, Figure 113. Cells treated with vinyl sulfone **190** in the absence of DNA damaging agents exhibited a reduction in cyclin D1 relative to control cells, potentially due a reduction in transcription of *cyclin D1* by NF-kB. Sulfone **190** was found not to be a general inhibitor of proteolysis.
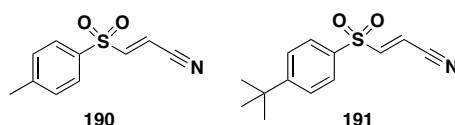
Figure 112

The role of the IKK complex in the response of cells to inhibitor **190** after DNA damage was also investigated.[231] IKKα kinase has been suggested to phosphorylate cyclin D1 at Thr286, leading to cyclin D1 ubiquitination and degradation by the proteasome. However, cells lacking IKKα, IKKβ or both exhibited a cyclin D1 response similar to wild-type cells. Inhibitor **190** was able to attenuate the degradation of cyclin D1 induced by 4NQO exposure in wild-type, IKKα null, IKKβ null and double knock out 3T3 cells, indicating that the attenuation of cyclin D1 after DNA damage is, at least in part, independent of the IKK pathway.
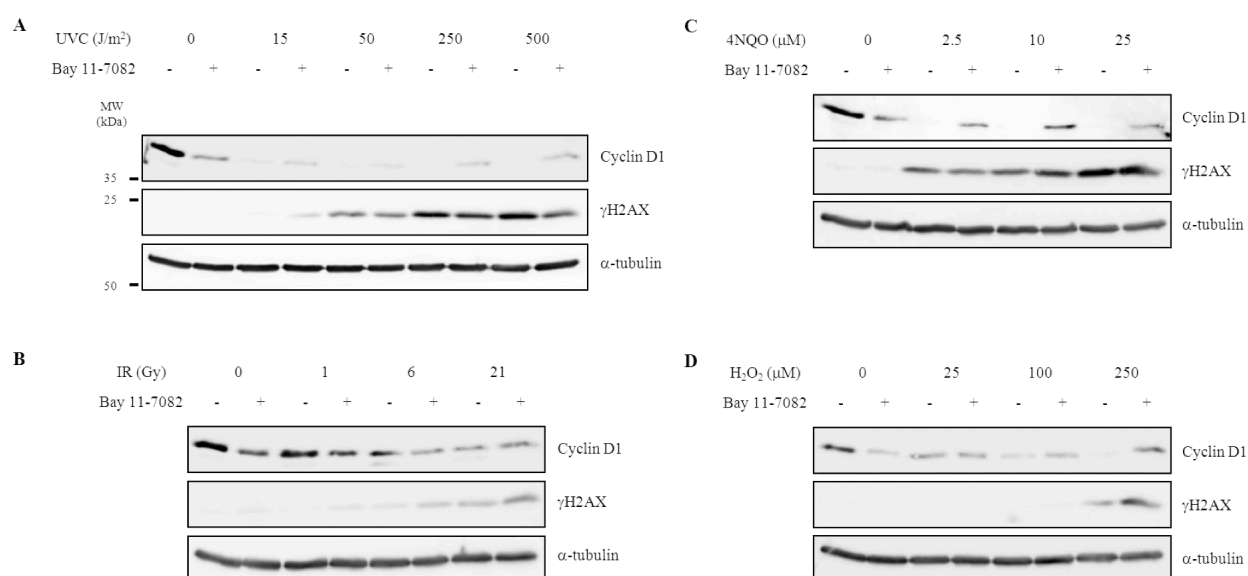
Figure 113 U2OS cells were exposed to DNA damaging agents to analyse of the effect of inhibitor **190** on cyclin D1 expression. Cells were treated with different doses of ultraviolet C radiation (UVC, A), ionizing radiation (IR, B), 4NQO (C) and H_2O_2 (D) in the absence or presence of 5mM inhibitor **190**. Cells were lysed 3h post-exposure and whole cell lysates were resolved by SDS-PAGE and analysed by immunoblotting against cyclin D1, phospho-histone H2A variant (ser139) (γH2AX) (marker to assess the degree of the DNA damage response mounted by the cell) and α-tubulin (loading control). Results are representative of two independent experiments. MW as per Protein Molecular Weight Marker. Work carried out and figure generated by Alexandra Duarte, PhD Thesis 2012.[231]

6.1.4. The chemical proteomics approach to compound-based target elucidation

To identify the molecular target(s) of inhibitors **190** and **191** and therefore potentially elucidate the mechanism responsible for the attenuation in cyclin D1 reduction after DNA damage, a chemical proteomic strategy was considered.[232, 233] The field of proteomics aims to identify the structure, function, expression, localisation, regulation and interaction partners of every single protein produced by the genome.[234] Within the field of proteomics, chemical proteomics employs the use of a carefully designed chemical probe to achieve some of these goals.[235] Chemical probes are designed to bind specifically and covalently to a protein (or protein class) to facilitate its identification from complex cellular extracts. Probes that target catalytic nucleophilic residues in enzyme active site pockets are termed activity-based probes (ABPs) to reflect the necessity for the enzyme to be active in order to be captured. Probes which target non-catalytic residues are termed affinity-based probes (AFBP). Chemical probes are usually composed of an analytical tag (often a fluorophore, radiolabel or biotin group) connected to the reactive inhibitor by a linker. The biotin or fluorescent group conjugated to the mechanism-based inhibitor often confers poor pharmacokinetic properties to the probe, in addition to potentially affecting the binding affinity of the inhibitor.[236] Such bulky probes are often added to cell lysates, as they are unable in most cases to permeate cell membranes, and the analytical tag is used to isolate or identify bound proteins by either in-gel fluorescence, streptavidin-biotin pull down, or mass spectrometry-based techniques.

The development of two-step labelling strategies independently by the Cravatt and Overkleeft groups in 2003 provided a means to overcome the limitation of cell permeability.[237, 238] Two-step labelling strategies involve the addition of a mechanism-based enzyme inhibitor, conjugated to a small latent bioorthogonal handle, to live cells where the inhibitor binds to target biomolecule(s). A bioorthogonal ligation reaction is then used to attach an analytical tag to the inhibitor after the cell has been lysed. Bioorthogonal reactions must fulfil two stringent requirements; they must proceed rapidly under physiological conditions and be inert to the myriad of other functionality present in the cell.

The Staudinger ligation, a modification of the classic Staudinger reduction, was employed by the Overkleeft group who used an azide-modified vinyl sulfone to target proteasomes within the cell, with subsequent capture by a biotinylated trialkylphosphine probe.[238] The trialkylphosphine used in this reaction is a slight modification of triphenylphosphine with one of the phenyl groups containing a stratgically placed *ortho* methylester. After formation of the aza-ylide, key intramolecular amide formation with displacement of methanol occurs, preventing hydrolysis of the ylide to the amine and phosphine oxide. Subsequent hydrolysis generates the stable ligation product, Figure 114.

An alternate use for the azide in bioorthogonal ligation chemistry is the Cu(I)-catalysed azide-alkyne 1,3-dipolar cycloaddition (CuAAC). This reaction is a variant of the initial Huisgen triazole synthesis which is typically quite a slow reaction.[102] Sharpless[239] and Meldal[240] reported the addition of a Cu(I) catalyst to significantly increase the reaction rate, and the bioothogonality of this reaction was demonstrated by Finn *et al*. in 2003.[241] CuAAC was first utilised in a two-step labelling procedure by the Cravatt group who used an azide-conjugated phenylsulfonate ester to modify several enzymes in live cells.[237] An alkyne-modified rhodamine fluorophore was added to cell lysates to conjugate the fluorophore to the enzymes, which were subsequently separated using gel electrophoresis and visualised

using fluorescence scanning. The Cravatt group has since used this procedure to profile human breast cancer cells[242] and the P450 cytochrome enzyme family *in vivo*.[243] The CuAAC mediated two step labelling procedure is reported to be more efficient with the azide conjugated to the analytical tag and the alkyne to the electrophilic inhibitor, due to nonspecific modification of proteins with the alkyne-rhodamine tag, but not the azide-rhodamine tag in the presence of Cu(I). [242]
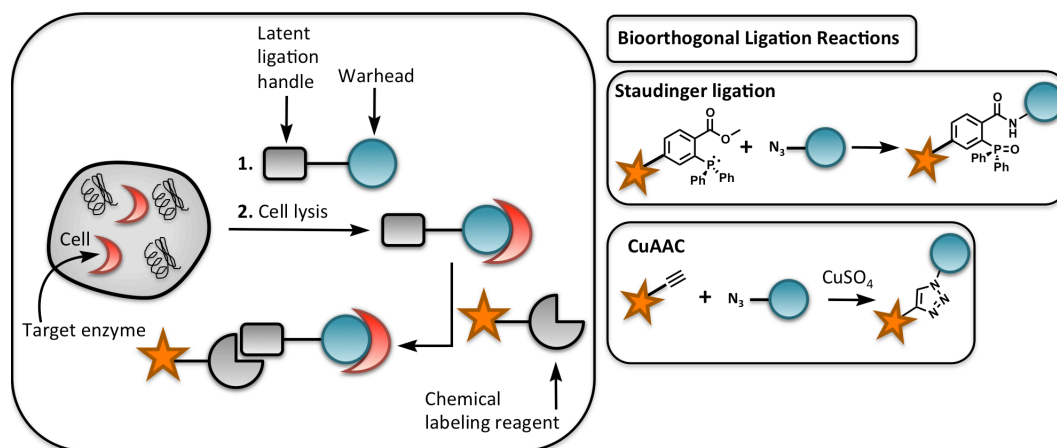
Figure 114 Illustration of the 2-step labelling strategy and bioorthogonal ligation reactions.

6.1.5. Design of the chemical probe

A two-step chemical ligation strategy was thought to be particularly suitable for this project. Introduction of a small latent ligation site minimises disruption to the size and shape of the original inhibitor and furthermore, should not significantly alter the cell permeability. The CuAAC reaction was hypothesised to be more suitable than the Staudinger chemistry due to the small size of the alkyne in comparison to the trialkylphosphine. Both compound **190** and related inhibitor **191** were postulated to exert their irreversible mechanism of action through the formation of an irreversible covalent bond to their target biomolecules *via* the unsual 3-sulfonylacrylonitrile electrophile. It was therefore critical to leave this functionality intact in the chemical probe. As both methyl and *tert*butyl groups are tolerated on the phenyl ring at the *para* position, this was thought to be the position with greatest degree of flexibility and therefore suitability for installation of the alkyne, Figure 115. With the alkyne combined with the electrophilic inhibitor, the analytical tag requires an azide modification. This avoids addition of an alkyne-modified analytical tag to cellular extracts, which as previously discussed, leads to nonspecific protein modification and increased background reaction. The overall aim of this section of work was to develop a synthetic route to chemical probe **192** and to synthesise enough material to use in chemical proteomic experiments.
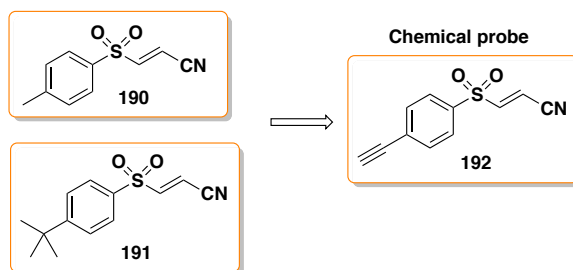
Figure 115 Design of the chemical probe **192** from literature inhibitors **190** and **191**.

6.2. Synthesis of the alkyne-tagged chemical Probe

6.2.1. Synthetic route one

A retrosynthetic analysis to reach novel compound **192** was designed as shown in Scheme 34. The acrylonitrile functional group was expected to be an exceptionally good Michael acceptor and the synthetic route was therefore designed to install it in the final step using oxidation of α-selenide **193** and subsequent *in situ* 2,3-*syn* elimination of phenylselenenic acid. The route included a key 'selenosulfonation' of acrylonitrile to install the α-selenide **193** from selenosulfone **194**. Aromatic sulfonation of phenylacetylene was expected to yield a mixture of *ortho/para* substituted products.
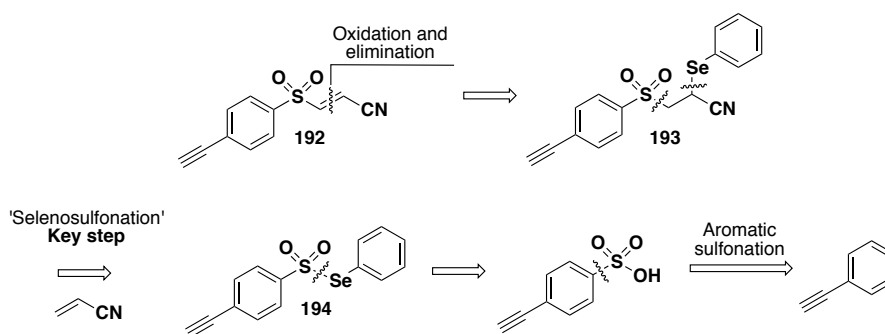
Scheme 34 Initial retrosynthetic analysis to reach desired chemical probe **192**.

The aromatic sulfonation of phenylacetylene was an unprecedented transformation. Chlorosulfonic acid was chosen as the sulfonylating agent with which to attempt this reaction due to the range of successful examples in the literature.[244] Additionally, as chlorosulfonic acid is a more powerful sulfonylating agent than sulfuric acid, mild conditions can often be used to effect the desired reaction.[244] Upon addition of chlorosulfonic acid to phenylacetylene in chloroform at 0 °C a thick, black slurry was instantaneously generated with a number of products visible by TLC. Attempts to isolate the products using column chromatography led to degradation. Addition of the chlorosulfonic acid at -78 °C did not improve the reaction, and the alkyne was considered likely to be the source of the problem, perhaps leading to polymerisation side reactions. The sulfonation of bromobenzene using the same reagent was therefore attempted as this reaction is known with chlorobenzene,[244] and the bromine provides a handle for installation of the alkyne later in the synthesis. However, treatment of bromobenzene with chlorosulfonic acid resulted in the isolation of only diaryl sulfone **195** from the reaction mixture, Equation 10. Diaryl sulfones are known side-products of this reaction, and are thought to arise by reaction of the desired arylsulfonic acid with the starting aromatic.[244]
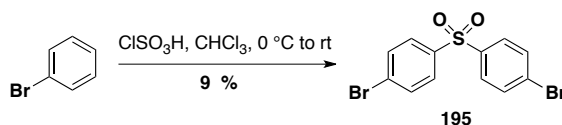
Equation 10

As 4-bromobenzenesulfonyl chloride **196** was commercially available, it was purchased as the starting point for the synthetic route. Reaction of this sulfonyl chloride with hydrazine hydrate furnished the intermediate sulfonyl

hydrazide **197** in 91 % yield. The sulfonylhydrazide was subsequently oxidized with benzene seleninic acid to generate selenosulfonate **198** in a moderate 74 % yield, Scheme 35. The reaction mechanism for this transformation, proposed by Back *et al*.[245] involves initial attack from the terminal sulfonylhydrazine N onto selenium with displacement of water, Scheme 36. Elimination of selenenic acid generates the sulfonyldiazene, which then reacts with the selenenic acid at the terminal N. Entropically favorable extrusion of N_2 generates the desired selenosulfonate.
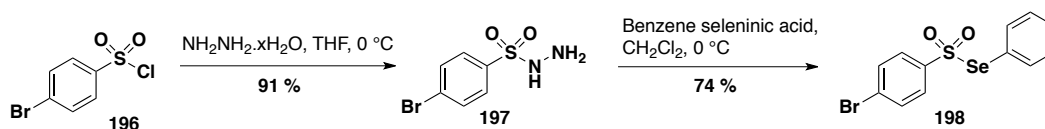
Scheme 35
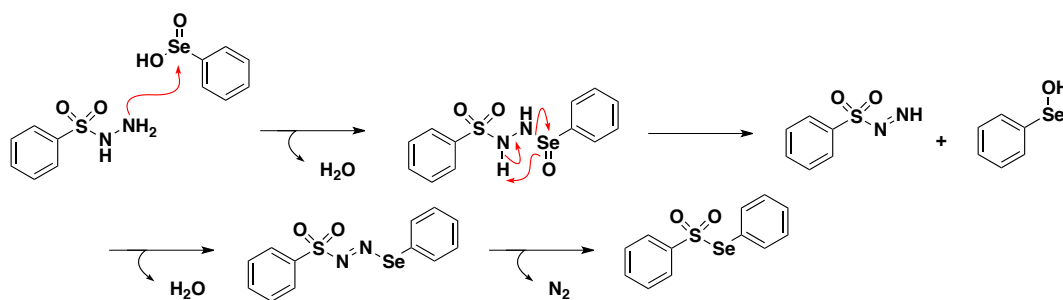
Scheme 36 Mechanism proposed by Back *et al*. for formation of sulfur-selenide intermediate.[245]

With the selenosulfonate intermediate **198** in hand, the key step for this reaction sequence was attempted. A reaction mechanism, proposed by Back and Collins, for the selenosulfonation reaction is shown in Scheme 37.[246] Initial homolysis of the Se-S bond generates two radical species, the sulfonyl radical, which is subsequently trapped by attack at the β-position of acrylonitrile, and the phenyl selenyl radical. The resulting alkyl radical attacks the selenium atom of a second molecule of starting selenosulfonate to generate the desired product and a sulfonyl radical to propagate the chain. The literature conditions for this reaction require refluxing of the two reaction components in chloroform, with the radical reaction initiated by heat.[246] The only example in the literature of the selenosulfonation of acrylonitrile employs R = *p*-tolyl,[246] and examples for the selenosulfonation of other olefins with aryl R groups include only R = phenyl, *p*-tolyl.[247-250] It was therefore unknown whether the aryl-bromide substituent would be tolerated.
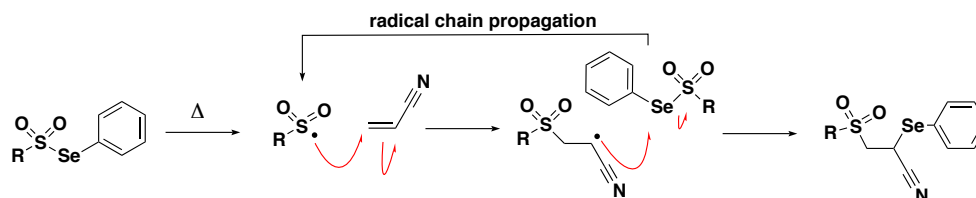
Scheme 37 Mechanism proposed by Back for the selenosulfonation of acrylonitrile.

Following the literature conditions, the starting selenosulfonate **198** was refluxed in chloroform with one equivalent of acrylonitrile, but this led to an almost quantitative yield of diphenyl diselenide. This presumably results from the dimerisation of the initially generated phenylselenyl radical. The reaction was repeated in anhydrous, degassed chloroform with two equivalents of acrylonitrile to trap the sulfonyl radical more effectively and with gradual heating

over a longer period of time to more slowly initiate the radical reaction, but only starting material **198** and diphenyl diselenide were identified in the reaction mixture. Changing the solvent from chloroform to toluene with reflux at higher temperature gave no improvement in this reaction. It was noted that the starting material was unstable over the course of a few days in solvent at rt in the presence of light, with decomposition to diphenyl diselenide by TLC, indicating that this S-Se bond is susceptible to photolysis. Photolysis has been reported as an alternative method to intiate selenosulfonation reactions.[249]

The use of DABCO to catalyse similar selenosulfonation reactions has been reported in the literature with α,β-unsaturated ketones rather than acrylonitriles.[251] Presumably the mechanism for this reaction involves 1,4-conjugate addition of the tertiary amine catalyst onto the unsaturated ketone, followed by attack of the enolate through the carbon onto the selenium with loss of the sulfonate anion. $E1_{CB}$ elimination of the amine catalyst then regenerates the electrophilic α,β-unsaturated bond, which is subsequently attacked by the sulfonate anion to generate the desired selenosulfonation product. This reaction was attempted with acrylonitrile and selenosulfonate **198**, but none of the desired product **199** and a 75 % yield of diphenyldiselenide was isolated from the reaction mixture, Equation 11.
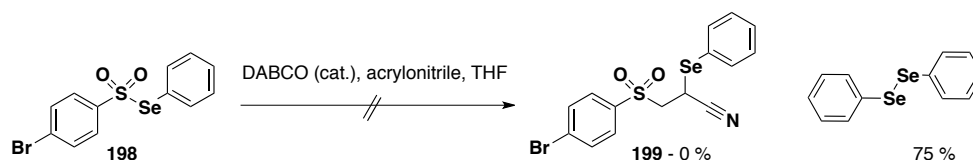
Equation 11

During their efforts to develop desulfitative Heck reactions between readily available sulfonyl chlorides and olefins, the Vogel group reported that the corresponding vinyl sulfones were accessed at lower reaction temperatures.[252] Reaction between 4-chlorophenylsulfonyl chloride and styrene gave an impressive 60 % yield of the corresponding vinyl sulfone, demonstrating excellent selectivity over the aryl chloride bond, which agrees with the reported greater reactivity of sulfonyl chlorides towards oxidative addition compared with the analogous bromides and chlorides.[253, 254] This indicated that there was reasonable precedent for the analogous Heck reaction between 4-bromophenylsulfonyl chloride **196** and acrylonitrile, but the desired product **200** was only isolated in only 5 % yield along with the sulfonic acid **201** in 3 % yield, Equation 12.
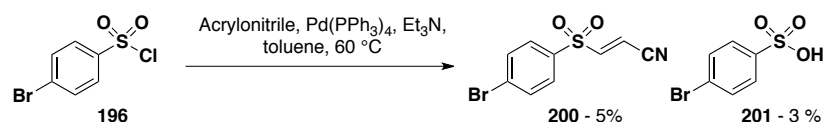
Equation 12

The desired 3-sulfonylacrylonitrile **200** was obtained in an improved yield *via* generation of the sodium sulfinate salt **202** from 4-bromosulfonyl chloride **196** and subsequent reaction with 2,3-dibromopropionitrile, Scheme 38.[255]
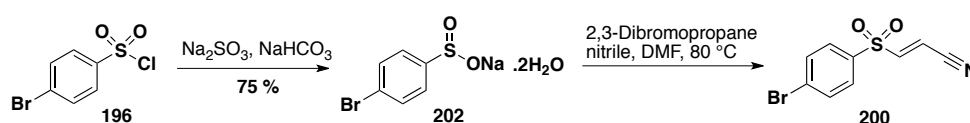
Scheme 38

The authors suggest the mechanism for this reaction involves initial dehydrobromination mediated by a sulfinate anion, conjugate addition of a second sulfinate anion, S_N2 displacement of the second bromide and a final elimination of sulfinic acid to generate the desired vinyl sulfone, Figure 116, mechanism 1. However, as they report scope for the reaction including R_1 = alkyl and phenyl, the second step of this mechanism seems unlikely. Although the polar aprotic DMF solvent favours the S_N2 reaction, this is still moderately unfavorable at the secondary carbon. The reaction may be more likely to proceed *via* an initial S_N2 displacement of the primary halogen, followed by an $E1_{CB}$ elimination of the second bromide, mechanism 2.
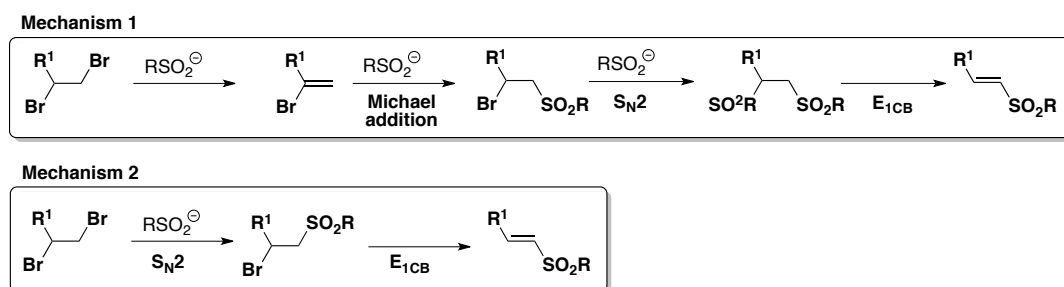
Figure 116 Possible mechanisms for the addition of aryl sodium sulfinate to 2,3-dibromo substrates.

An 80 % isolated yield was quoted by the authors for the addition of sodium phenylsulfinate to 2,3-dibromopropionitrile.[255] The use of these conditions with the sodium 4-bromophenylsulfinate substrate, with 1.5 eq. of the sulfinate and a 10 h reaction time, gave only a 37 % isolated yield of the desired vinyl sulfone **200**, although pleasingly with complete selectivity for the *trans* isomer, Table 18 (entry 1). Using 1.5 equivalents and a 3 h reaction time, a slightly reduced yield of 25 % (^{1}H NMR yield) was obtained (entry 2). Decreasing the number of equivalents of sulfinate to 1.1 decreased the yield to 25 % after 10 h (entry 3), whilst increasing the equivalents to 3.0 led to consumption of starting material by TLC after only 1 h, although this gave an isolated yield of only 44 % (entry 4). With 1.7 equivalents, the starting material was consumed after 1.5 h, although this only gave a 16 % isolated yield (entry 5). As 3 equivalents of sulfinate and a 1 h reaction time gave the highest isolated yield, the reaction was repeated with 3 equivalents and left for 3 hours. However, ^{1}H NMR analysis identified that no product remained in the crude reaction mixture after this time (entry 6). On attempting to increase the reaction scale to 8mmol, only a 3 % yield of the product was isolated (entry 7) indicating that perhaps the reaction is not particularly amenable to scale up.
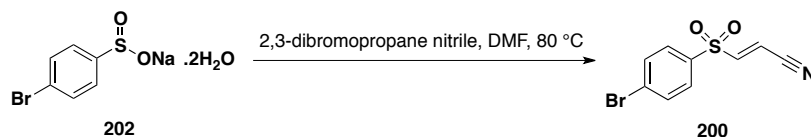
Entry No.	Eq. **202**	time (h)	Yield **200** (%)
1	1.5	10	37
2	1.5	3	25*
3	1.1	10	25
4	**3.0**	**1.0**	**44**
5	1.7	1.5	16
6	3.0	3	0*
7	1.6	8	3**

Table 18 Conditions to synthesise 3-sulfonylacrylonitrile **200**. *Yield estimated by ^{1}H NMR yield with 1,3,5-trimethoxybenzene internal standard. ** 8 mmol scale. Highest yielding reaction conditions highlighted in bold (entry 4).

Despite the low yields for generation of acrylonitrile **200**, enough material was obtained to test the subsequent Sonogashira step. Although rate determining oxidative insertion of Pd(0) into iodoarene C-I bonds is faster than for the corresponding bromides, the starting bromoarene **200** was anticipated to be activated to oxidative addition of Pd(0) by the electron withdrawing sulfone. Conditions which have been reported previously for the Sonogashira coupling of electron deficient 4-bromobenzonitrile with TMS-acetylene were initially employed to convert bromoarene **200** to the TMS-protected acetylene **203**, Table 19 (entry 1).[256] Two equivalents of TMS-acetylene were used in this procedure, presumably due to the expected copper mediated Glaser-Hay homodimerisation side reaction, which usually occurs upon incomplete exclusion of oxygen.[257] However, despite only obtaining 17 % isolated yield of the TMS-acetylene homodimer, none of the desired product was obtained. The use of Et$_3$N base as the solvent for the reaction with gentle heating at 50 °C (entry 2) resulted in precipitation of a thick black solid, potentially containing the catalytically inactive palladium black, and resulting in a poor mass recovery. A procedure reported by Krause for the Sonogashira reaction of a range of activated bromoarenes was next applied to this transformation (entry 3).[258] In this procedure, triphenylphosphine is added to stabilize the palladium catalyst and the copper (I) iodide is added 20 minutes after the other reagents. However, this actually resulted in an increase in the isolated yield of the TMS homodimer to 34 % whilst some starting material but none of the desired acetylene product was isolated. Using conditions reported for the successful Sonogashira reaction between 4-bromophenyl(methyl)sulfone and TMS-acetylene, arylbromide **200** was treated with Et$_3$N/CH$_2$Cl$_2$ (1:1), 5 mol % of CuI and of Pd(PPh$_3$)$_2$Cl$_2$ and 2 equivalents of TMS-acetylene (entry 4).[259] However, after 14 h at rt no conversion to product was indicated by ^{1}H NMR of the crude reaction mixture and the starting material was re-isolated in an 82 % yield. For these reactions, no formal degassing of solvents was carried out, although the reaction was always purged thoroughly with argon by subjecting the flask to multiple vacuum-argon cycles.
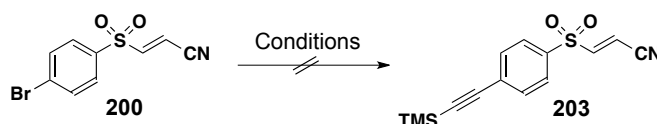
Entry	Pd(PPh$_3$)$_2$Cl$_2$ mol%	CuI mol %	Solvent	Base (eq.)	TMS-acetylene eq.	Time (h)	Temp (°C)	Ligand
1	10	10	THF/Et$_3$N (4:1)	n/a	2.0	16	rt	No
2	5	5	Et$_3$N	n/a	1.2	7	50	No
3	5	1.2*	THF	Et$_3$N (1.5)	1.5	22	rt	PPh$_3$
4	5	5	CH$_2$CH$_2$/Et$_3$N (1:1)	n/a	2.0	14	rt	No

Table 19 Attempted Sonogashira to generate TMS-acetylene **203** from bromoarene **200**. *The CuI was added to the reaction mixture 20 minutes after the other reagents.

A new set of Sonogashira conditions were adopted with the solvents sparged with argon for 10 min before use in the reaction. The reaction was initially tested on known substrate 4-cyano-3-fluorobromobenzene **204**, which gave the desired TMS-acetylene **205** in a pleasing 72 % isolated yield, Scheme 39. Upon addition of Et$_3$N to the reaction mixture, a very distinct colour change, as reported, from bright yellow to black was observed to indicate the necessary reduction of Pd(II) to Pd(0).[260] Application of the same conditions to aryl bromide **200** gave no distinct colour change. Analysis of the crude reaction mixture by ^{1}H NMR indictated the TMS-acetylene dimer, but no starting material and no product with olefinic protons. It was considered that perhaps in this reaction, the palladium

coordinates across the unusual 3-sulfonylacrylonitrile system, leading to the stabilisation of Pd(II), consistent with the lack of colour change, and no generation of the desired Sonogashira product.
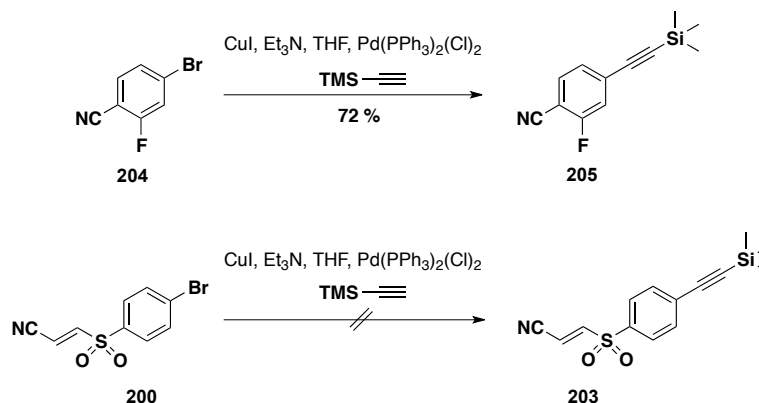
Scheme 39

An 'aromatic Finklestein' reaction, reported by Buchwald in 2002, was adopted in an attempt to synthesise the iodoarene from the bromoarene, on the basis that the Sonogashira reaction may prove more successful with the more reactive C-I bond.[261] Unfortunately, the excellent yields reported by Buchwald for this transformation could not be repeated using either using either catalytic *trans*-racemic-diamine **207** or *N,N'*-dimethylethylenediamine ligand with either aryl bromide **200** or known substrate 5-bromoindole, Scheme 40.
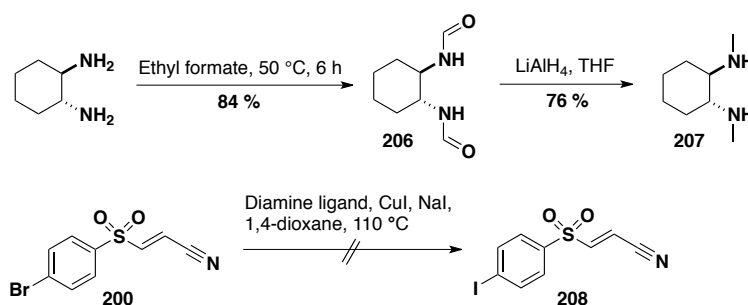
Scheme 40

It was decided that a new route to the desired chemical probe was required to avoid intermediate **200**, which was not amenable to Pd or Cu catalysed reactions. It was thought that conjugate addition of phenylthiolate or benzeneselenide to sulfonyl acrylonitrile **200** might protect the olefin during the Sonogashira couping whilst also providing a handle for removal by oxidation and elimination. However, selectivity issues beween conjugate addition of the thiol/selenide to the olefin and aromatic substitution were anticipated, along with potential interference between sulfide/selenide and metal catalyst and so this reaction pathway was not pursued.

Returning to a retrosynthesis similar to that outlined in Scheme 34, an attempt was made to generate 4-TMS-acetylenebenzenesulfonyl chloride **208**, on the basis that this would provide the necessary functionality to generate the sulfonate salt **209**, and a subsequent addition to 2,3-dibromopropanenitrile and TMS-deprotection would yield the desired chemical probe **192**. Selective coupling of the Ar-I bond of 4-iodobromobenzene **210** with TMS-aceylene generated bromoarene **211** in an excellent 96 % yield, Scheme 41. Halogen-lithium exchange using nBuLi and quench

with sulfonylchloride was hoped to yield arylsulfonyl chloride **208**. However, this generated multiple products which were too difficult to separate using column chromatography, due to their high solubility in n-hexane. Changing the quench from sulfonyl chloride to sulfur dioxide gas pleasingly led directly to the lithium sulfinate salt **212.** Although reaction of sulfinate **212** with 2,3-dibromopropionitrile did not generate any of the desired acrylonitrile **203**, conjugate addition of sulfinate **212** to 2-chloroacrylonitrile and *in situ* elimination of HCl under the reaction conditions led directly to the desired acrylonitrile **203**, a reaction that is unreported in the literature. A yield of only 16 % was achieved for this reaction but no further optimisation was carried out due to the concurrent success of a second synthetic route.
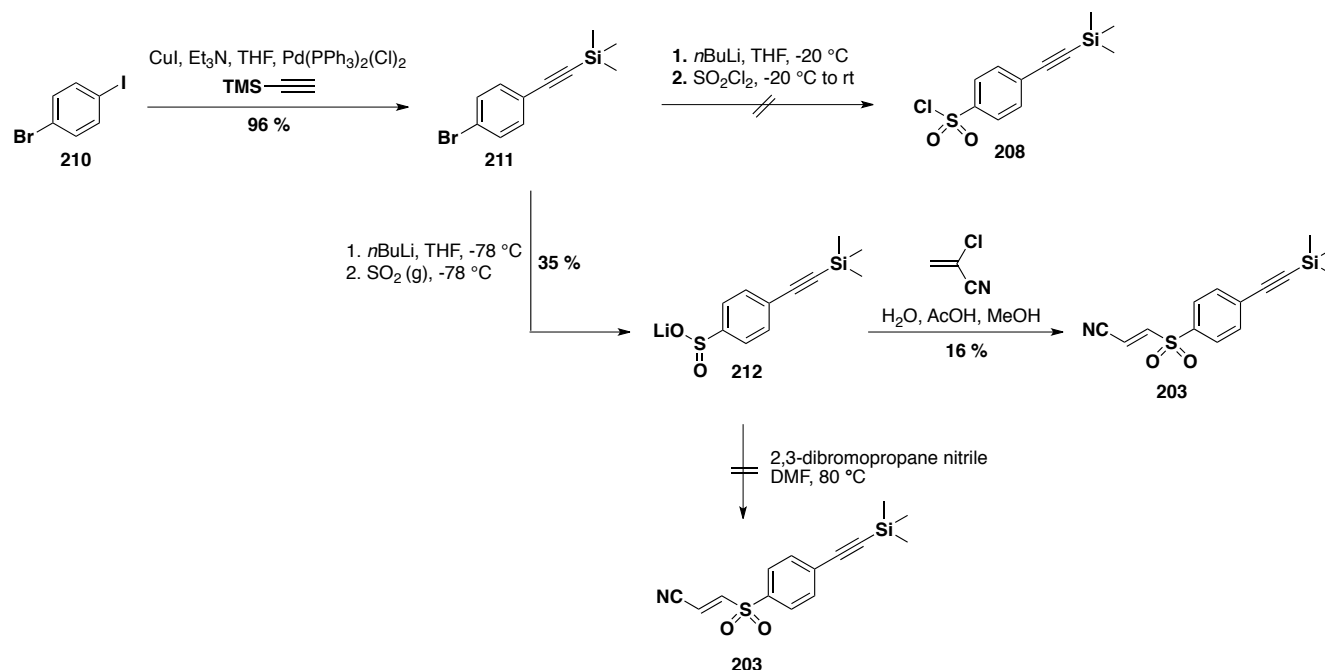
Scheme 41 Synthesis of TMS-protected chemical probe **203** from 4-iodobromobenzene **210**.

6.2.2. Synthetic route two

It was hypothesised that the 3-sulfonylacrylonitrile moiety within intermediate **200** rendered this compound unsuitable as a substrate for metal-catalysed reactions. It was predicted that the saturated 3-sulfonylpropionitrile analogue would not be susceptible to the same problems and could be desaturated using a number of methods later in the synthetic route.

Synthesis of starting bromoarene **213** for the Sonogasira reaction was facile using a conjugate addition of sulfinate salt **202** to acrylonitrile.[262] Application of the Sonogashira conditions used to generate aryl-TMS-alkynes **205** or **211** led to a poor 15 % yield of desired TMS-acetylene **214**, with 67 % recovery of starting material, Table 20 (entry 1). However, upon gentle heating with an increased reaction time, a significant improvement to yield 66-68 % of the desired aryl-TMS-acetylene **214** was achieved (entry 2). In order to generate the 3-sulfonylacrylonitrile from the saturated 3-sulfonylpropionitrile system, two strategies were considered; α-selenation, oxidation and *in situ* elimination and dehydrogenation.
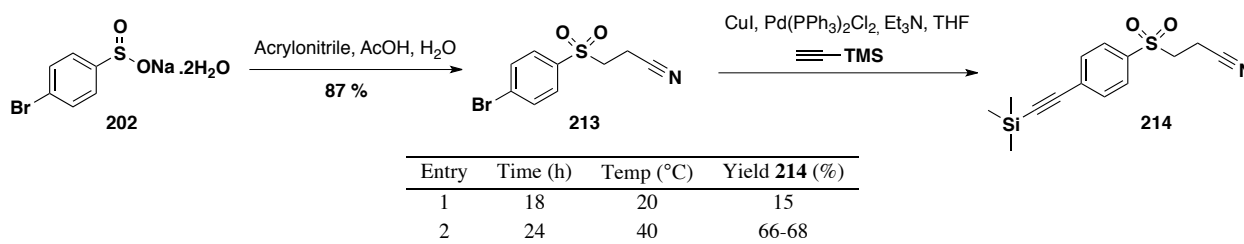
Table 20 Conditions for the Sonogashira reaction of arylbromide 213 to generate TMS-acetylene 214.

Entry	Time (h)	Temp (°C)	Yield 214 (%)
1	18	20	15
2	24	40	66-68

Whilst there are currently no methods available to dehydrogenate alkyl sulfones or alkyl nitriles to vinyl sulfones or acrylonitriles respectively in one step, a number of one step dehydrogenations have been reported to take carbonyl groups to the the corresponding α,β-unsaturated compounds. These include the use of 2,3-dichloro-5,6-dicyano-1,4-benzoquinone (DDQ),[263, 264] Chloranil[265] and *o*-iodobenzoic acid (IBX).[266, 267] IBX was reported as a highly efficient reagent to effect the dehydrogenation of ketones by K.C. Nicolaou in 2002.[266] It was suggested that this reaction proceeded *via* a single electron transfer (SET) mechanism and it was considered that cyano-sulfone 214 may be more susceptible to such oxidation given the high degree of conjugation and therefore thermodynamic stability this desaturation would confer. The IBX reagent 215 was synthesised from 2-iodobenzoic acid and oxone in water using a procedure reported by Santagostino, Scheme 42.[268] IBX made by this method is proposed to pose much less of an explosion risk compared with that synthesised using potassium bromate.[266, 269] Using the Santagostino method, pure IBX was isolated as a precipitate from the reaction in a moderate 76 % yield. A second crystalline solid was observed to form within the filtrate over a 24 h period, which upon isolation was identified as pure iodosobenzoic acid (IBA) 216, previously unreported as a side product in this reaction. Heating cyano-sulfone 214 with IBX in DMSO at 85 °C for 30 min led to complete recovery of starting material, whilst heating for longer periods led to slow degradation and formation of a complex mixture.
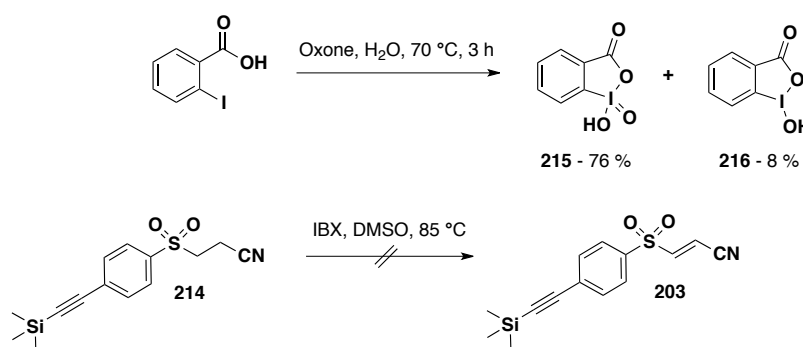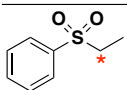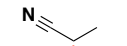
Scheme 42 Synthesis of IBX 215 and attempted oxidation of cyano-sulfone 214.

Development of α-selenation conditions

The α-selenation of saturated sulfones or nitriles and subsequent oxidation and elimination has been previously reported as a strategy to generate vinyl sulfones[270-273] and acrylonitriles[274, 275] respectively. However, there is no reported example of the α-selenation of the 1,3-sulfonylnitrile system required here. As an initial test reaction to accomplish the desired α-selenation, 1,3-sulfonylnitrile 214 was added to LDA (generated *in situ* from iPr₂NH and

nBuLi) to effect the deprotonation and PhSeCl was added to quench the anion in a subsequent step, Table 21 (entry 1). It was expected that a mixture of selenides would result from this reaction with possible deprotonation α to either the nitrile or the sulfone. Although exact pKa values for the relevant protons in 1,3-sulfonylnitrile **214** are unknown, examination of other substrates indicates that they are probably fairly similar, Figure 117.[276] However, the reaction led only to the recovery of starting material (63 %), diphenyl diselenide and diaryl selenide **217** (17 %). Diaryl selenide **217** presumably results from the fast elimination of SO$_2$ from the α-nitrile anion, resulting in the aryl lithium which is then quenched upon addition of the selenide electrophile. 1,3-Sulfonylnitrile **214** was treated with LiHMDS in the presence of PhSeCl in an attempt to quench the anion before decomposition (entry 2). Pleasingly, this led to the formation of a small quantity of an α-selenation product **218** (8 %), along with the recovery of significant starting material **214** (59 %). Diphenyl diselenide and diaryselenide **217**, were identified as components of the reaction mixture by TLC.

	pKa (DMSO)
	31.0
	32.5

Figure 117 pKa values for protons α to sulfone or nitrile, indicated by asterix.

There were a number of problems associated with this reaction. Firstly, a side reaction between PhSeCl and LiHMDS occurs, leading to the generation of the poorly electrophilic diphenyl diselenide, and using up the base within the reaction mixture. Degradation to the aryl lithium occurs if the reaction is carried out in the absence of the electrophilic selenium source, and to some extent even in the presence of the selenium source leading to the observed degradation product **217**. To test the stability of sulfone **214** to basic conditions it was stirred with NaH in THF for 15 min, after which time there was no remaining starting material, and none of the degradation products could be identified by ^{1}H NMR. Repeating this in the presence of N-(phenylseleno)phthalimide (NPSP) led to the generation of diphenyl diselenide and the recovery of starting material (entry 3). Treatment of a mixture of diphenyl diselenide and sulfone **214** with LiHMDS gave no reaction at all, rather than either the degradation product **217** or the desired α-selenide (entry 5). Treatment of 1,3-sulfonylnitrile **214** with LiHMDS followed by PhSeCl led to the complete formation of degradation product **217** with no starting material remaining by TLC (entry 4). It was considered that perhaps a weak base could be used to carry out this reaction, but addition of Et$_3$N to a solution of PhSeCl and 1,3-sulfonylnitrile **214** led to only the formation of diphenyl diselenide and the recovery of starting material (entry 6).

Interestingly, addition of LiHMDS to NPSP in CH$_2$Cl$_2$ followed by addition of sulfone **214** led to the generation of 22 % of the desired product **218** with 51 % recovered starting material (entry 7). The addition of LiHMDS to a mixture of NPSP and **214** led to generation of only diphenyl diselenide and starting material (entries 8 and 9). The conditions for both these reactions involved addition of reagents at -78 °C with at least 30 min stirring at this temperature and subsequent warming to rt before addition of an aqueous quench. In an attempt to understand this reaction, 1,3-sulfonylnitrile **214**, as a solution in CH$_2$Cl$_2$, was treated with LiHMDS at -78 °C and quenched with D$_2$O at either -78 °C or 5 min after warming to rt. Unfortunately, these experiments were inconclusive with no deuterium incorporation observed by ^{1}H NMR for either quench temperature. This may be due to an effect similar to that reported previously by Seebach, where incomplete deuterium incorporation was observed upon quenching lithium enolates generated by strong secondary amine bases.[277] Despite the anomalies observed with this reaction, enough material was brought through to test the remaining steps in the synthetic sequence.
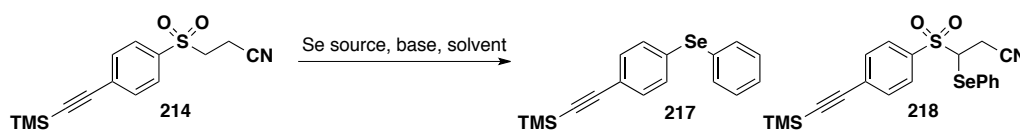
Entry No.	214 addn order	Base	Se Source	Solvent	214	217	218	DPDS
1	2	LDA (1)	PhSeCl (3)	THF	63	17	0	Y
2	**1**	**LiHMDS (3)**	**PhSeCl (2)**	**THF**	**59**	**Y**	**8**	**Y**
3	2	NaH (1)	NPSP (2)	THF	Y	N	N	Y
4	1	LiHMDS (2)	PhSeCl (3)	THF	N	Y	N	Y
5	1	LiHMDS (2)	DPDS (1)	THF	Y	N	N	Y
6	1	Et$_3$N (2)	PhSeCl (1)	CH$_2$Cl$_2$	Y	N	N	Y
7	**3**	**LiHMDS (2)**	**NPSP (1)**	**CH$_2$Cl$_2$**	**51**	**N**	**22**	**Y**
8	1	LiHMDS (2)	NPSP (1)	CH$_2$Cl$_2$	Y	N	N	Y
9	2	LiHMDS (3)	NPSP (1)	CH$_2$Cl$_2$	Y	N	N	Y

Table 21 Reaction conditions tested to effect the α-selenation of 1,3-sulfonylnitrile **214**. Numbers in brackets indicate the order of addition to the reaction mixture. Diphenyl diselenide (DPDS) observed by TLC.

A decision was made to remove the TMS-protecting group from α-selenide **218** before revealing the acrylonitrile, to prevent Michael addition under the aqueous basic TMS-deprotection reaction conditions. However, treatment with potassium carbonate in MeOH to effect the TMS-deprotection led to the decomposition of α-selenide **218** to the *cis* and *trans* alkenes **219** and **220**, Equation 13. These results confirmed that the selenide was α to the sulfone as opposed to the cyano group and suggested that in the previous α-selenation reaction, generation of the α-cyano anion led to rapid degradation to form selenide **217** unlike the α-sulfone anion, which was stable enough to react with the selenium electrophile.
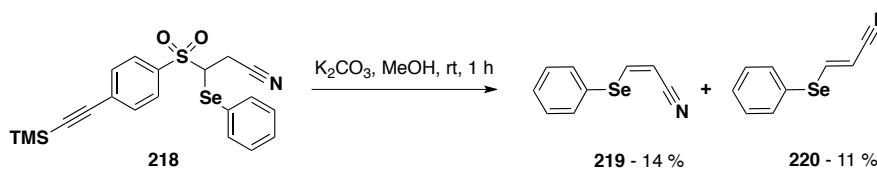
Equation 13

The more readily accessible sulfone **214** was used to optimise the deprotection conditions, in anticipation that 1,3-sulfonylnitrile **214** and α-selenide **218** would demonstrate similar base sensitivity. Treatment of 1,3-sulfonylnitrile **214** with 1.0 M TBAF in THF at 0 °C led to rapid degradation, Table 22 (entry 1). However, significant improvement was observed using only one equivalent of TBAF in a THF solution, giving a 55 % isolated yield of the terminal alkyne **221** (entry 2).
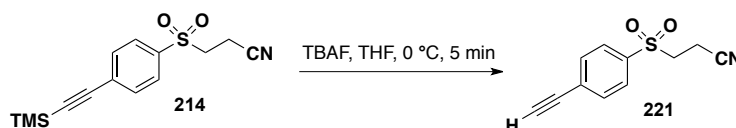
Entry	[TBAF] (M)	Yield **214** (%)
1	1.0	0
2	0.07 (1 eq.)	55

Table 22 Optimisation of TMS deprotection using test substrate 1,3-sulfonylnitrile **214**.

Despite the assumption that 1,3-sulfonylnitrile **214** and α-selenide **218** would be similarly sensitive to base, application of the successful deprotection conditions to α-selenide **218** led to rapid degradation, Equation 14.
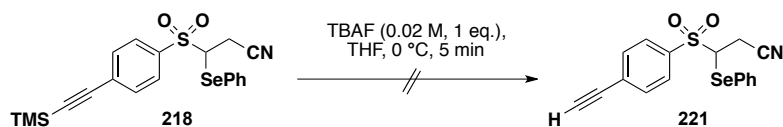
Equation 14 Attempted deprotection of α-selenide **218**.

To avoid elimination across the 3-seleno-3-sulfonylpropane nitrile system or degradation during the TMS-deprotection, the acrylonitrile was generated in the step prior to TMS-removal. Treatment of α-selenide **218** with sodium (*meta*)periodate in EtOH led to only a 25 % ^{1}H NMR conversion of the selenide to the desired acrylonitrile **203** after 16 h at rt, although no other side products were generated. Alternatively, oxidation of α-selenide **218** with *m*CPBA gave a slightly improved 36 % isolated yield of the desired sulfonylacrylonitrile **203** after 4 h, with recovery of 33 % starting material. Addition of 1 equivalent of TBAF to a solution of sulfonylacrylonitrile **203** in THF led to very rapid decomposition, again presumably due to the basic conditions generated by TBAF, Table 23 (entry 1). Deprotection of sulfonylacrylonitrile **203** was successfully carried out by buffering the solution with AcOH (0.35 M), yielding the desired chemical probe **192** in a moderate 48 % yield (entry 2).
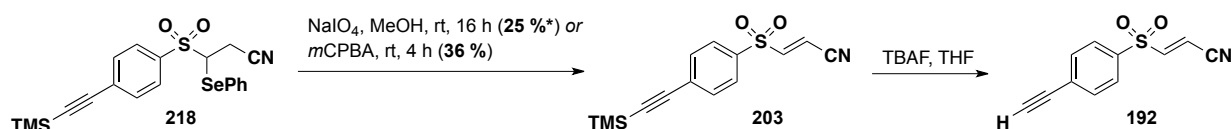
Entry	[TBAF] (M)	[AcOH] (M)	Temp (°C)	time (min)	Yield **192** (%)
1	0.04 (1 eq.)	0	0	5	0
2	0.02 (1 eq.)	0.35	0 to rt	95	48

Table 23 Optimisation of TMS deprotection of substrate **203**. *Conversion by ^{1}H NMR.

6.3. Summary

A small molecule with interesting cellular activity has been adapted as a chemical probe in order to identify its cellular target(s). Two concise synthetic routes to the target compound have been developed, Scheme 43, and enough material has been produced to carry out the desired biochemical screening. The first synthetic route, which reaches the desired synthetic target in only 4 steps, commenced with a C-I bond selective Sonogashira reaction, using commercially available 4-bromo-iodobenzene to install the TMS-acetylene in an excellent 96 % yield. Lithium-halogen exchange and sulfur dioxide quench generated lithium sulfinate salt **212**. A conjugate addition to 2-chloroacrylonitrile and *in situ* elimination generated the desired acrylonitrile **203** before TMS deprotection to yield the final chemical probe. The second route reaches the desired synthetic target in 6 steps starting from the commercially available 4-bromosulfonyl chloride **196**. Reduction to sodium sulfinate salt **202** using sodium sulfinate and sodium bicarbonate, and subsequent Michael addition of the sulfinate onto acrylonitrile through the S atom, generated bromoarene **213** as a precursor for the Sonogashira reaction. The Sonogashira coupling reaction was optimised from 15 to 66-68 %, and although the subsequent α-selenation reaction proved problematic, the desired α-selenide **218** was

successfully generated in a 22 % yield. Oxidation of the selenide and concomitant *syn* elimination generated the desired sulfonylacrylonitrile **203**, which was deprotected with a solution of TBAF buffered with AcOH to yield the desired alkyne chemical probe **192** in a moderate 48 % yield.
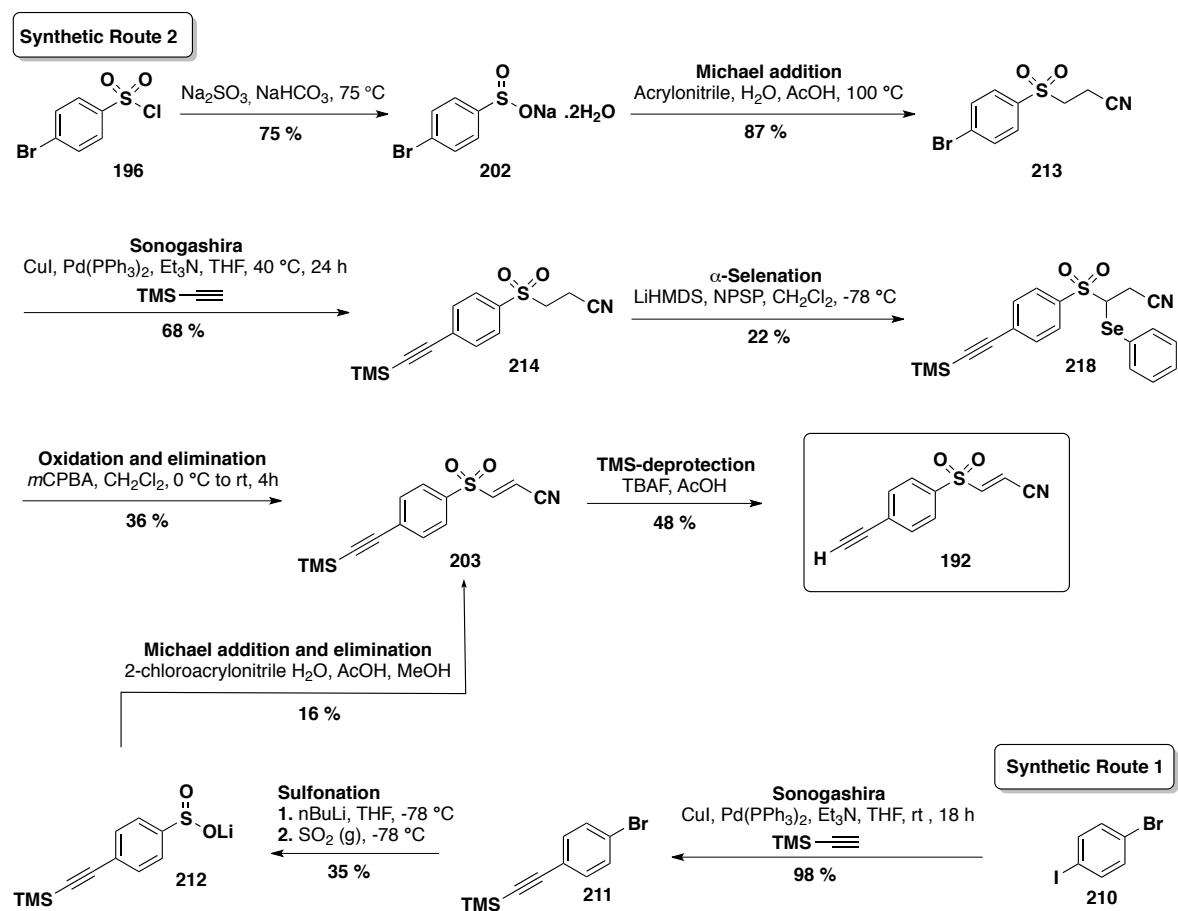
Scheme 43 Summary of the two synthetic routes developed to reach chemical probe **192**.

Future work

Future work should include chemical proteomics experiments to investigate the cellular targets of inhibitors **190** and **191** using chemical probe **192**. Initial experiments conducted with inhibitors **190** or **191** should be repeated with compound **192** to check that the chemical probe has the same effect on cyclin D1 after DNA damage. If this is the case, after addition of probe **192** to cells, and generation of the cell lysate, a fluorophore attached to an azide and a source of Cu(I) should be added to initiate the Cu-catalysed Huisgen cycloaddition. Subjection of the cell lysate to SDS PAGE and subsequent analysis by in-gel fluorescence allows identification of proteins modified with probe **192**. If the fluorophore is conjugated to biotin, the tagged proteins can be enriched by streptavidin-biotin purification before analysis by in-gel fluorescence. Mass spectrometry techniques such as liquid chromatography tandem-mass spectrometry (LC-MS/MS) can be used to identify labelled proteins.

7. Biochemistry materials and methods

Materials

Tetrahydrofolate, dUMP, Sypro Orange and Bradford reagent were purchased from Sigma-Aldrich. Sypro Orange was purchased as a 5000 x solution in DMSO. All reagents were used as commercially supplied. p97 was kindly supplied by Prof. Paul Freemont. Papain and carbonic anhydrase were purchased as lyophilised powders from Sigma-Aldrich and were stored at -20 °C.

Buffer constitutions

Buffer A	25 mM TRIS-HCl pH 7.5, 2 mM DTT, 1 mM EDTA
Cdc25 assay buffer	100 mM TRIS-HCl pH 8, 150 mM NaCl, 1 mM EDTA, 0.1 % βME, 400 μM OMFP
Coomassie destain solution	10 % (*v/v*) AcOH, 10% (*v/v*) MeOH
Coomassie stain solution	0.4 % (*w/v*) Coomassie brilliant blue dye R-250, 10 % (*v/v*) AcOH, 10% (*v/v*) MeOH
GeneClean wash solution	50 mM NaCl, 10 mM TRIS-HCl pH 7.5, 2.5 mM EDTA, 50 % (*v/v*) EtOH
KOD Buffer 1	1.2 M TRIS-HCl, 100 mM KCl, 60 mM $(NH_4)_2SO_4$, 1% (v/v) Triton X-100, 0.01% (w/v) BSA, pH 8.0
KOD DNA polymerase	2.5 U μL^{-1} KOD, 50 mM TRIS-HCl, 50 mM KCl, 1 mM DTT, 0.1 mM EDTA, 50% (*v/v*) glycerol, 0.1% (*v/v*) NP40, 0.1% (*v/v*) Tween, pH 8.0
LB	1% (*w/v*) bactotryptone, 1% (*w/v*) NaCl, 0.5% (*w/v*) bactoyeast extract, pH 7.0
5 x SDS Loading buffer	160 mM TRIS-HCl, 24% (v/v) glycerol, 5% (w/v) SDS, 12.5% (v/v) βME, 0.1% (w/v) bromophenol blue, pH 6.8
SDS PAGE stacking gel	0.1% (*v/v*) SDS, 5% (*v/v*) acrylamide, 0.1 M TRIS-HCl, pH 6.8
SDS PAGE resolving gel	0.2% (v/v) SDS, 10% (v/v) acrylamide, 0.4 M TRIS-HCl, pH 8.8
SDS running buffer	7.8 mM TRIS-HCl, 80 mM glycine, 10% (v/v) MeOH, 10% (w/v) SDS
Solution II	0.2 M NaOH, 1% SDS
Solution III	3 M KOAc, 5 M glacial acetic acid
TAE	40 mM TRIS-acetate, 1 mM EDTA, pH 8.0
5 x TAE loading buffer	TAE + 0.04% (*w/v*) bromophenol blue, 2.5% (*w/v*) ficoll
Taq PCR buffer	100 mM TRIS-HCl, 500 mM KCl, 0.8% (v/v) NP40, pH 8.8
Trypsin reconstitution buffer	50 mM acetic acid

Recombinant DNA techniques

Transformation of bacterial cells via electroporation

Competent *E. coli* DH5α or BL21 (DE3) cells were taken from -80 °C storage and thawed on ice before addition of plasmid DNA (1 μL). The cells were transferred to a chilled 2 mm gap cuvette (Geneflow) and subjected to electroporation at a capacitance of 25200 mFD and 22,000-23,000 Volts using a BioRad Gene Pulser. LB culture medium (1 mL) was added to the electroporated cells and 900 μL of the LB removed after centrifugation (13000 rpm, 1 s). The cells were resuspended in the remaining LB medium, spread onto LB agar medium supplemented with ampicilin and incubated at 37 °C for 15-20 h to select transformants.

Agarose gel electrophoresis

 1 % agarose gels were made up with 1 x TAE buffer containing ethidium bromide (1 μL/mL). Electrophoresis of samples was carried out by applying 80 mA of constant current through the gel (45-60 min). DNA was visualised using UV-A (non-preparative samples) or UV-C (preparative samples) and for preparative samples the required DNA bands excised and extracted using GeneClean or Jetsorb (<500 bases) DNA purification procedures.

GeneClean DNA purification

Sodium iodide (500 mL, 6M) was added to the excised agarose gel band containing DNA and the mixture heated at 65 °C for 5 min. A suspension of silica (5 μL) was added and the mixture kept on ice for 5 min, before brief centrifugation (13000 rpm). The supernatant was removed and the pellet washed three times with ice cold Gene clean wash solution before resuspension in milli Q. The resulting suspension was incubated at 65 °C for 5 min, centrifuged (13000 rpm) and the supernatant retained.

Genomed Jetsorb Purification

Buffer A1 (300 μL) and Jetsorb bead suspension (10 μL) were added to the excised agarose gel band containing DNA and the mixture incubated at 65 °C for 15 min, with mixing every 3 min. The resulting sample was centrifuged (13000 rpm, 30 s), the supernatant removed and the pellet washed with buffer A1 (300 μL) and buffer A2 (300 μL). The dry pellet was then resuspended in sterile Milli Q water (20 μL), incubated at 65 °C for 5 min and centrifuged to give the desired solution of DNA.

DNA ligation

Ligations were carried out in a 20 μL volume in 0.5M TRIS-HCl pH 7.6, 10 mM $MgCl_2$, 10 mM DTT and 50 μg/ml BSA with 10 ng digested vector, 500 ng digested insert and T4 DNA ligase. Samples were left at room temperature for at least 1 h.

Enzymatic digestion of DNA

DNA digests were carried out in a total volume of 20 μL with 8-10 μg DNA (inserts) or 0.5 μg DNA (plasmids), 2 μL enzyme and 2 μL of appropriate 10 x buffer. Samples were incubated for 1 h at 37 °C. 4 μL 5 x TAE loading buffer was added and samples run on a 1 % (*w/v*) agarose gel.

Two step PCR reaction

A mixture of the DNA template (1 µL), the 5'-primer (1 ug) and the 3'-primer (1 µg), the oligonucleotides containing the mutation (each 1 µg), *Thermococcus kodakaraensis* (KOD1) DNA polymerase (2.5 µL), 2 mM dNTPs (2.5 µL), 25 mM $MgCl_2$ (2 µL) and KOD Buffer 1 (2.5 µL) as commercially supplied (Novagen) was made up to 50 µL with sterile water and subjected to PCR conditions dictated by the properties of the oligonucleotides used (containing denaturation, annealing and ligation steps with 25-50 cycles). The resulting mixtures were separated by agarose gel electrophoresis.

T-tailing

Gene-cleaned or Jetsorb-cleaned PCR DNA fragments (6 µL) were subjected to heating at 72 °C for 20 min in the presence of *Taq* DNA polymerase (1 µL), 1 mM dATP, 2.5 mM $MgCl_2$ and 10 x PCR buffer in a total volume of 20 µL. The product was purified by the GeneClean or Jetsorb procedures and ligated into pGEM-T (Promega).

DNA Sequencing

Plasmids were sequenced commercially by COGENICS.

Preparation of plasmid DNA

Small scale (mini-prep)

Single colonies were picked and shaken in LB medium supplemented with ampicilin (2 mL) at 37 °C for a minimum of 8 h. 1.5 mL of each culture was centrifuged (13000 rpm) and the supernatant removed. Each pellet was re-suspended in milli Q water (100 µL) by vortexing. The cells were lysed by addition of Solution II (200 µL) and then immediately neutralised by addition of Solution III (150 µL). After centrifugation (3 min, 13000 rpm) the supernatants were retained and nucleic acid precipitated by addition of EtOH (1 mL). The mixtures were centrifuged (3 min, 13000 rpm) and the supernatant removed. Milli Q water (50 µL) was added, with care taken not to over-vortex the pellet and the solutions centrifuged (1 min, 13000 rpm) before analytical enzymatic digestion.

Large scale (maxi-prep)

The remaining culture (*ca*. 0.5 mL) from Mini-Prep containing the required plasmid was transferred to ampicillin-supplemented LB (200 mL) and shaken at 37 °C for 16 h. After centrifugation (5000 rpm, 4 °C, 5 min) the supernatant was removed and the pellet re-suspended in milli Q water (10 mL) by vortexing. The cells were lysed by addition of Solution II (20 mL) and the mixture neutralised by addition of Solution III (15 mL). The lysate was centrifuged (9000 rpm, 4 °C, 5 min) to remove contaminants and the filtered supernatant retained. Isopropanol (45 mL) was added to precipitate nucleic acid and the pellet obtained by centrifugation (9000 rpm, 4 °C, 5 min). The dry pellet was re-suspended in milli Q water (3 mL) and ice-cold LiCl (4 mL) and kept on ice for 5 min to precipitate high molecular weight RNA. The mixtures were centrifuged (13000 rpm, 5 min) and EtOH (14 mL) added to the supernatant to precipitate nucleic acid. The mixtures were left on ice for 5 min and centrifuged (5000 rpm, 4 °C, 5 min) and the supernatant discarded. The dry pellet was re-suspended in milli Q water (500 µL) and small molecular weight RNA digested with RNase A (10 µL) for 15 min at 37 °C. DNA was precipitated by addition of 2.5 M NaCl, 20 % PEG-4000 solution (600 µL) and the mixture kept on ice for 5 min, centrifuged (13000 rpm, 5 min) and the

supernatant removed. The pellet was re-suspended in milli Q water (500 μL) by vortexing, and the contaminating protein denatured with 1:1 (v/v) phenol/chloroform and the aqueous layer separated by centrifugation (13000, 5 min) and subsequently extracted with chloroform to remove traces of phenol. 3M NaOAc, pH 5.2 (50 μL) and EtOH (1 mL) were added to precipitate the DNA plasmid. The suspension was centrifuged (13000 rpm, 5 min), the supernatant removed and the pellet dissolved in milli Q water to give a concentration of 1 μg/μL, as determined by UV (260 nm, Pharmacia LKB UltroSpec III). A 10 μL aliquot from all Maxi preps was sent was for sequencing.

Measure of DNA concentration

DNA obtained from Maxi-Prep (5 μL) was added to a quartz cuvette containing milli Q (1 mL), and the absorbance at 260 nm measured relative to milli Q water using a Pharmacia LKB UltroSpec III. The DNA concentration (μg/μL) was calculated as absorbance x 5.

General protein Analysis

Determination of concentration by Bradford assay

Various dilutions of the protein stock solution (5 μL) were mixed with 250 μL Bradford reagent/H$_2$O, 1:4 (*v/v*) in a clear 96-well plate (TC Microwell 96F, Nunc). The optical density (OD) was measured at 595 nm (Spectramax 340 PC, Molecular Devices) and the protein concentration determined from a standard curve generated using solutions of known concentrations of BSA. All samples were run in triplicate.

SDS polyacrylamide gel electrophoresis

Samples were mixed with an equal volume of 2 x SDS loading buffer and subjected to electrophoresis at 200 V for *ca*. 1 h with SDS running buffer. Gels comprised a 4 % stacking gel and a 10 % resolving gel and were polymerised using 50 μL ammonium persulfate as a radical initiator and 50 μL tetramethylethylenediamine as a radical catalyst and allowed to set for at least 30 minutes at rt before use.

InstantBlue™ staining

SDS-PAGE gels were stained with InstantBlue™ (Expedeon) with gentle rocking for 20 minutes to visualise protein.

Coomassie staining

SDS PAGE gels were incubated at rt for 1 h with gentle rocking in Coomassie Blue staining solution preheated to 60 °C. Stained gels were washed once with water followed by incubation with de-stain solution at rt for *ca*. 12 h with gentle rocking.

Reconstitution of trypsin for protein digestion

Lyophilised sequencing grade modified Trypsin was purchased from Promega in 20 μg aliquots. Aliquots were resuspended in the supplied Trypsin reconstitution buffer to 0.5 μg/μL and the reconstituted enzyme stored at -70 °C.

Cdc25A Y386C C441S C430S C476S (cdc25A')

Cloning

The catalytic domain (residues 335-538) was constructed using the two step PCR amplification procedure, using the standard PCR components. The primers 5' GAATTCAGAGCTTCTTCAGACGACTGTACATCTCC 3' and 5' GTTATCATCGACTGTCGATGTCCATATGAATACGAG 3' were used to construct the 3' end, and the primers 5' GGATCCCTTATAGGAGACTTCTCCAAGGGTTATC 3' and 5' CTCGTATTCATATGGACATCGACAGTCGA-TGATAAC 3' were used to construct the 5' end and plasmid cdc25A C441S C430S C476S (triple mutant) was used as the template. Both PCR amplification steps used 25 cycles with denaturation at 98°C for 15 s, annealing at 79 °C for 1 min and ligation at 72 °C for 50 s. An adenosine base was added to the 3' ends of the final PCR product using the standard t-tailing conditions. The construct was ligated into the pGEM-T vector, and the resulting plasmid transformed into *E. coli* DH5α (genotype F⁻ endA1 glnV44 thi-1 recA1 relA1 gyrA96 deoR nupG Φ80d*lacZ*ΔM15 Δ(*lacZYA-argF*)U169, hsdR17(r$_K^-$ m$_K^+$), λ–) cells. 12 single colonies were selected and grown overnight at 37°C in LB supplemented with ampicillin (2 mL). A Mini-Prep was carried out to extract the DNA from the cells, and these were digested with *Bam*HI and *Eco*RI to identify cells transformed with the correct plasmid. Cells correctly transformed were grown overnight at 37°C in LB supplemented with ampicillin (200 mL), and a Maxi-Prep carried out to isolate the plasmid (0.25 μg/μL). Following digestion with *Bam*HI and *Eco*RI the construct was subcloned into the *Bam*HI and *Eco*RI sites of the pET21a vector and the plasmid isolated by Maxi-Prep.

Expression

pET21a containing the catalytic domain of cdc25A' was transformed into *E. coli* BL21 (DE3) (genotype F⁻ ompT gal dcm lon hsdS$_B$(r$_B^-$ m$_B^-$) λ(DE3 [lacI lacUV5-T7 gene 1 ind1 sam7 nin5])) cells, and a single colony grown overnight at 37°C in LB supplemented with ampicillin (2 mL). This was scaled up to 200 mL of media and incubated at 37°C for 12 hours, and finally to 2000 mL and incubated for a further 1 hour. Protein expression was then induced by the addition of IPTG to a final concentration of 1 μM. The cells were shaken overnight at 18°C, and harvested by centrifugation at 5000 rpm for 5 min at 4°C.

Purification by ion exchange chromatography and gel filtration

The cells overexpressing cdc25A' were resuspended in Buffer A, and lysed by sonication (2 x 18W, 30 s). Following centrifugation (9000 rpm, 4°C, 20 min) the cleared lysate was bound to 8 mL of SP-Sepharose beads equilibrated in Buffer A. Cdc25A' was eluted with a NaCl gradient (0.05-0.50 M) in Buffer A at 4°C using a thin glass walled column with a frit. The collected fractions were run by SDS PAGE and those with a band at the correct molecular weight identified. Fractions were cleared of precipitate by centrifugation and the cleared solution concentrated and purified further by gel filtration using a GE Pharmacia AKTA purifier with a Sephadex-300 column. The precipitate collected from the fractions was redissolved in TRIS-HCl (25 mM), EDTA (1 mM), urea (6 M) and dialysed over 48 h at 4 °C into TRIS-HCl (25 mM), EDTA (1 mM) with no urea *via* TRIS-HCl (25 mM), EDTA (1 mM) with 3 M and 1 M urea respectively.

Cdc25 fluorescence based activity assay

Cdc25A assay buffer (190 µL), was added to the appropriate wells of a 96-well microfluor black plate (Fischer Scientific). 10 µL from each fraction collected from an ion exchange chromatography column purification was added to each well and the fluorescence measured (Cary Eclipse software) using Ex/Em, 471/530 nm.

Thymidylate Synthase

Cloning

The primers 5' CATATGAAACAGTATTTAGAACTGATGC 3' and 5' GAATTCAGATAGCCACCGGCGCTTTA-ATGCC 3' were used in PCR amplification with *E. coli* (BL21-DE3) cells for 25 cycles with denaturation at 98 °C, annealing at 55 °C and ligation at 72 °C. An adenosine base was added to the 3' ends of the final PCR product using the standard t-tailing conditions. The construct was ligated into the pGEM-T vector, and the resulting plasmid transformed into *E. coli* DH5α cells. 12 single colonies were selected and grown overnight at 37°C in LB supplemented with ampicillin (2 mL). A Mini-Prep was carried out to extract the DNA from the cells, and these were digested with *Pvu*I to identify cells transformed with the correct plasmid. Cells correctly transformed were grown overnight at 37°C in LB supplemented with ampicillin (200 mL), and a Maxi-Prep carried out to isolate the plasmid (0.62 µg/µL), pGEM-TS. Following digestion with *Nde*I, the construct was cloned into the *Nde*I site of the pET21a vector, and the resulting plasmid transformed into *E. coli* DH5α cells. 12 single colonies were selected and grown overnight at 37°C in LB supplemented with ampicillin (2 mL). A Mini-Prep was carried out to extract the DNA from the cells, and these were digested with *Pst*I to identify cells transformed with the correct plasmid. Cells correctly transformed were grown overnight at 37°C in LB supplemented with ampicillin (200 mL), and a Maxi-Prep carried out to isolate the plasmid (0.06 µg/mL), pET21a-TS$_{NdeI}$. The plasmid pGEM-TS was then digested with *Asc*I and *Eco*RI and the insert cloned into pET21a-TS$_{NdeI}$ pre-digested with *Asc*I and *Eco*RI. The resulting plasmid was transformed into *E. coli* DH5α cells. 12 single colonies were selected and grown overnight at 37°C in LB supplemented with ampicillin (2 mL). A Mini-Prep was carried out to extract the DNA from the cells, correct transformants grown overnight in LB supplemented with ampicillin (200 mL) and a Maxi-Prep carried out to isolate the final plasmid, pET21a-TS.

Expression

pET21a containing the catalytic domain of TS was transformed into *E. coli* BL21 (DE3) cells, and a single colony grown overnight at 37°C in LB supplemented with ampicillin (2 mL). This was scaled up to 200 mL and incubated at 37°C for 12 hours, and finally to 1000 mL and incubated for a further 1 hour at 37°C. Protein expression was then induced by the addition of IPTG to a final concentration of 1 µM. The cells were shaken overnight at 37 °C, and harvested by centrifugation (5000 rpm, 20 min, 4°C). The pellet was washed twice with 10 mM TRIS-HCl (pH 7.5), 10 mM MgCl$_2$, and the cells stored at -80 °C until required.

Purification

The pellet was resuspended in 20 mM TRIS-HCl (pH 7.5), 10 mM MgCl$_2$, 5 mM DTT (100 mL) and sonicated twice for 30 s at 18 W, with cooling on ice. The solution was centrifuged (9000 rpm, 20 min, 4 °C) and the supernatant

collected. 5 % streptomycin sulfate (15 mL/100 mL of the supernatant fraction) (*v/v*) was added and stirred for 10 min at 4 °C. The resulting nucleic acid precipitate was removed by centrifugation (9000 rpm, 30 min, 4 °C). Solid ammonium sulfate was added to the resulting supernatant fraction to 50 % saturation and the solution stirred at 4 °C for 10 min. The resulting precipitate was collected by centrifugation (9000 rpm, 20 min, 4 °C) and discarded and solid ammonium sulfate added to the supernatant fraction to increase saturation to 80 %. After stirring at 4 °C for 10 min the resulting precipitate was collected by centrifugation (9000 rpm, 4 °C, 20 min) and stored at -80 °C prior to further purification. The ammonium sulfate pellet was thawed, dissolved in 20 mM TRIS-HCl pH 7.5, 1 mM DTT (40 mL) and loaded onto DE-52 beads pre-equilibrated with 20 mM TRIS-HCl pH 7.5, 1 mM DTT. The protein was spun with the beads at 4 °C for at least 1 h. The beads were loaded into a thin glass column equipped with a frit and a tap. 20 mM TRIS-HCl pH 7.5, 1 mM DTT (20 mL) was passed through the beads, followed by 20 mL portions of the same buffer containing an increasing concentration of NaCl from 0.13 to 0.25 M, whilst fractions of 2-3 mL were collected. Fractions containing TS were combined and ammonium sulfate added to 80 % saturation with stirring for 10 min at 4 °C to precipitate the protein. The protein was collected by centrifugation (5000 rpm, 4°C, 60 min) and stored at -80 °C until required.

Spectrophotometric assay

The purified TS pellet was thawed, dissolved in 25 mM potassium phosphate, pH 7.5 or 10 mM ammonium bicarbonate, 1 mM DTT and dialysed for 48 h against 4 x 2 L changes of the same buffer respectively. The protein concentration was measured using a Bradford assay. The appropriate amount of protein was then added to mixture I (40 mM TRIS-HCl (pH 7.6), 100 mM βME, 1 mM EDTA, 25 mM MgCl$_2$, 15 mM formaldehyde) to make the final protein concentration 0.2 mg/mL. 10 mL of 16 mM tetrahydrofolate in mixture I and 10 μL of 4.6 mM dUMP in mixture I were added to the solution to give a final volume of 1 mL. A second sample with no dUMP was also prepared as a reference. Absorbance was then measured at 340 nm over a 20 minute period using a Cary spectrophotometer for both samples and the absorbancy difference plotted as a function of time.

Spectrophotometric assay to determine IC$_{50}$ values

Initial reaction rates were measured spectrophotometrically at 25 °C by the increase in absorbance at 340 nm due to the enzymatic generation of dihydrofolate from methylene tetrahydrofolate. Reaction mixtures contained 40 mM TRIS-HCl (pH 7.5), 20 mM MgCl$_2$, 100 mM βME, 12 mM formaldehyde, 750 μM EDTA, 20 μM dUMP, 150 μM tetrahydrofolate, 100 nM thymidylate synthase, 0.1 % Tween-20 and 4 % DMSO. Enzymatic reaction was initiated by the addition of a methylene tetrahydrofolate and dUMP mixture. Final reaction volumes were 1 mL and 3 x 250 μL added to multiwell plate to run samples in triplicate. A sample containing no dUMP was used as a reference for all runs. Reactions were monitored over a five minute period with readings every 11 seconds. Initial reaction rate was calculated as the gradient of the initial linear portion. Buffers and dUMP/methylene tetrahydrofolate stock solutions were made up freshly on the day of use and kept on ice. Data was collected in a 96-well transparent Sterilin plate using a SpectraMax 340PC Absorbance Microplate Reader. Data was fitted to a non-linear sigmoidal curve with iterations until convergence using OriginPro 8.5. IC$_{50}$ values were obtained from dose-response curves using average velocites of three separate runs with IC$_{50}$ errors determined from the standard error of the three separate IC$_{50}$ values.

Errors on dose-response curves were standard errors calculated from the velocities of the three separate runs at each point.

Hydrolytic stability of acrylamides in the presence of papain

Mini tests for TLC analysis

To 10 μM papain in ammonium bicarbonate (10 mM), DTT (1 mM) was added one acrylamide (**49**, **55** and **67**) from a 60 mM stock solution in MeOH to give a final acrylamide concentration of 2.5 μM. Identical samples with the papain omitted were used as controls. Samples were analysed by TLC initially and after 7 h (1:1 EtOAc/n-hex). After 7 hours incubation, the original acrylamides were still present as the main organic component by TLC for both + papain and - papain samples. There was also a small spot on the baseline of the plate for all + papain samples but not for - papain samples which may correspond to hydrolysed acrylamide.

Preparative test

To 10 μM papain in ammonium bicarbonate (10 mM), DTT (1 mM) was added acrylamide **67** to a final concentration of 2.5 mM and a total sample volume of 4.5 mL. After incubation at rt for 16 h the solvent was removed from the sample under a high vacuum and the resulting residue analysed by TLC and NMR, to indicate the acrylamide present with only a trace of the hydrolysis products.

8. HPLC, Mass spectrometry and Thermofluor methods

HPLC Experiments

Irreversibility tests for addition of thiol to vinyl sulfonamide and acrylamide

A spherisorb 5μ C18 316 x 4 mm column was used with either an Agilent HPLC machine equipped with single UV/vis detection at 254 nm or a JASCO HPLC machine with a UV-2077 plus 4-l intelligent UV/Vis detector. The mobile phases were HPLC grade water (0.1 % TFA) and acetonitrile, degassed using either a Hewlett Packard 1100 Series G1322A degasser or a JASCO DG-2080-53 3 line degasser. Solvents were passed through the HPLC at a rate of between 0.5-0.7 mL/min. Injections were 2 μL. An example method to monitor the conjugate addition of thiol to vinyl sulfonamide is as follows. Samples were run in 100 mM ammonium bicarbonate at pH 7.95 with 10 % total DMSO and acrylamides/vinyl sulfonamides generally present at 1 mM. Stock solutions of thiols in H_2O were always prepared on the day of use and kept at 4 °C.

An example HPLC method is as follows:

time (mins)	% MeCN	% 0.1% TFA
0	5	95
20	36	64
25	95	5
30	95	5
35	5	95
45	5	95

Comparision of reaction rate for conjugate addition of thiol to acrylamide-fragments

A Phenomenex Luna 5μ C18 250 x 4.60 mm column was used with a LaserChrom HPLC machine equipped with single UV/vis detection at 240 nm. The mobile phases were HPLC grade water (0.1 % TFA) and acetonitrile (0.1 % TFA) or methanol (0.1 % TFA), degassed using a LaserChrom CSI6150 vacuum degasser. Injections were 2 μL. Recipe to make up samples: 980 μL ammonium bicarbonate (100 mM) at pH 7.95, 2 μL acrylamide 1 at 0.5 M in DMSO, 2 μL acrylamide 2 at 0.5 M in DMSO, 6 μL DMSO, 10 μL freshly prepared reduced glutathione at 0.5 M in H_2O.

An example HPLC method is as follows:

time (mins)	% MeCN	% 0.1% TFA
0	5	95
5	5	95
25	35	65

Comparison of reaction rate for conjugate addition of thiol to vinyl sulfonamide and acrylamide

A Phenomenex Luna 5μ C18 250 x 4.60 mm column was used with a LaserChrom HPLC machine equipped with single UV/vis detection at 254 or 225 nm. The mobile phases were HPLC grade water (0.1 % formic acid) and methanol, degassed using a LaserChrom CSI6150 vacuum degasser. Injections were 2 μL. Recipe to make up samples: 980 μL ammonium bicarbonate (100 mM) at pH 7.95, 10 μL acrylamide or vinyl sulfonamide at 0.5 M in DMSO, 10 μL glutathione at 0.5 M in H_2O. Acrylamides monitored at λ = 254 nm, vinyl sulfonamides at λ = 225 nm.

Vinyl sulfonamides do not absorb at 254 nm when at a concentration of 5 mM. Acrylamides absorb too strongly at 225 nm at 5 mM, such that they reach the limit of the detector.

HPLC method:

time (mins)	% MeOH	% 0.1% formic acid
0	10	90
5	10	90
20	60	40
30	90	10

Reaction of acrylamides with reduced glutathione in the presence of an internal standard

A Phenomenex Luna 5μ C18 250 x 4.60 mm column was used with a LaserChrom HPLC machine equipped with single UV/vis detection at 254 nm. The mobile phases were HPLC grade water (0.1 % formic acid) and methanol (0.1 % formic acid), degassed using a LaserChrom CSI6150 vacuum degasser. Injections were 2 μL. Recipe to make up samples: 979 μL ammonium bicarbonate (100 mM) pH 7.95, 1 μL 4-amino benzylamide (0.5 M in DMSO), 10 μL ligand (0.1 M in DMSO), 10 μL freshly prepared reduced glutathione (0.5 M in H_2O).

HPLC method:

time (mins)	% MeOH (0.1 % formic acid)	% H_2O (0.1 % formic acid)
0	5	95
5	5	95
35	95	5
40	95	5

Thermal shift experiments

Thermal denaturations were carried out in sealed, fast optical MicroAmp 96-well plates (Applied Biosystems) using an Applied Biosystems StepOne Plus Real-Time PCR System. The system contains a Peltier-based thermal cycling system for rapid heating/cooling and monitors fluorescence using an LED-based optical system. The 96-well plates were heated from 25-65 °C at a ramp of 0.5 °C per minute. Fluorescence was monitored at the emission wavelength of FAM dye (Ex/Em: 495/520 nm) or SYBR green dye (Ex/Em: 497/520 nm), which overlaps with the emission from Sypro Orange (Ex/Em: 470/569 nm). Samples were composed of 100 μM protein (15 μL), Sypro Orange (2000 x dilution of commerical stock with sterilised Milli Q water) (5 μL) or protein (14 μL), Sypro Orange (2000 x dilution of commerical stock with sterilised Milli Q water) (5 μL) and organic ligand (1 μL) at various concentrations from DMSO stock solution.

Analysis of protein by Electrospray or MALDI MS

Preparation of TS for ESI or MALDI MS

The ammonium sulfate TS pellet was allowed to thaw on ice before addition of 10 mM ammonium bicarbonate, 1 mM DTT, pH 8. The protein was then dialysed for 48 h against 4 x 2 L changes of the same buffer. The dialysate was centrifuged to remove any insoluble impurities and the concentration adjusted to 10 μM using a Bradford assay. The protein solution was then stored at 4 °C ready for use.

Analysis of TS samples by MALDI MS

10 μM TS (in ammonium bicarbonate (10 mM), DTT (1 mM)) (192 μL) was added to organic compound **54**, **67** or **68** (from stock solution at 10 mM in MeOH) (8 μL) and the solutions allowed to react at rt for 2 h. The resulting solutions were washed through a spin filter to remove any unreacted organic compound and concentrated to 25 μL total sample volume. Reconstituted trypsin (2 μL) was added to the sample before incubation at 37 °C for 4 h. To prepare the trypsinised solution for MALDI analysis, 0.5 % formic acid and MeCN were added to the sample to give 1:1 aqueous/organic and an overall 2.4 x dilution. The sample was then mixed thoroughly with a matrix, α-cyano 4-hydroxy cinnamic acid (v/v, 1:1), and 1 μL of this solution added to the target plate and allowed to dry. MALDI spectrometry was carried out using a Micromass MALDI micro MX which has a laser desorption ion source coupled to a time-of-flight analyser. Pulsed laser energy was fired at the target in the UV range (337 nm) and either fired randomly, or focused on the centre of the target. The method used detected positive ions in the 1000-4000 Da range.

Analysis of cdc25A' samples by MALDI

Cdc25A' was dialysed from storage buffer (TRIS-HCl (25 mM), EDTA (1mM) with 50 % glycerol) into ammonium bicarbonate (50 mM, pH 8) or TRIS-HCl (50 mM, pH 8) buffers prior to experiment. Acrylamides or sulfonamides were added to protein samples from stock solutions in acetonitrile or methanol to give 4 % overall organic solvent. βME was added to protein samples from freshly prepared stock solutions in ammonium bicarbonate or TRIS-HCl buffer. For digestion, reconstituted trypsin (2 μL) was added to protein samples (usually 25 μL) and samples incubated overnight at 37 °C. The aqueous buffer from samples was removed *in vacuo* and the sample diluted to approximately 0.1 mg/mL with acetonitrile/water (0.1 % TFA), 1:1. The sample was then mixed with a matrix, α-cyano 4-hydroxy cinnamic acid (v/v, 1:1), and 1 μL of this solution added to the target plate and allowed to dry. MALDI spectrometry was carried out using a Micromass MALDI micro MX which has a laser desorption ion source coupled to a time-of-flight analyser. Pulsed laser energy was fired at the target in the UV range (337 nm) and either fired randomly, or focused on the centre of the target. The method used detected positive ions in the 300-5000 Da range.

General procedure for protein analysis by electrospray MS

Protein at a concentration of 10 μM in ammonium bicarbonate (10 mM), DTT (1 mM) and acrylamide from stock solution in MeOH (to give maximum 4 % MeOH) were incubated at rt. To a 25 μL aliquot of the reaction, 0.5 % formic acid (50 μL) and MeOH (50 μL) were added and the mixture loaded into a syringe (Hamilton microsyringe). A syringe driver was used to inject the sample onto the mass spectrometer at 30 μL/min and data collected in the m/z range 900-3000. Spectra were deconvoluted with Maximum Entropy software from Waters. A Micromass LCT Premier was used to obtain all ESI mass spectrometry data. This instrument has an electrospray ionisation source coupled to a time-of-flight analyser, and was operated in W reflectron mode. A Waters 1525μ LC pump was used to deliver the mobile phase to the source.

9. Organic chemistry experimental

General Procedures

NMR Spectroscopy

^{1}H NMR spectra were recorded on a Bruker AV400 spectrometer operating at 400 MHz in deuterated solvents as indicated. All spectra were referenced to solvent as indicated and peaks labelled as s (singlet), d (doublet), t (triplet), q (quartet), multiplet (m), b (broad). All chemical shifts (δ) are quoted in parts per million (ppm). Coupling constants (*J*) for ^{1}H NMR spectroscopy are given in Hz. ^{13}C NMR spectra were recorded on a Bruker AV400 spectrometer operating at 101 MHz in deuterated solvents as indicated. All spectra were referenced to solvent as indicated.

Infrared spectroscopy

IR spectra were recorded as thin films or compressed solids on a Perkin Elmer Spectrum 100 FT-IR spectrometer with Universal ATR Sampling Accessory.

Mass spectrometry

Low resolution mass spectra (*m/z*) were recorded on either VG 707E, VG Autospec Q, VG platform or VG Prospec spectrometers. Only molecular ions (M$^+$) and major fragmentation peaks are reported. High resolution mass spectra were recorded on a VG prospec spectrometer.

Melting Points

Melting points were determined on a Reichert microscope melting point apparatus.

Silica Chromatography

Analytical thin layer chromatography (TLC) was performed on glass backed plates pre-coated with silica (0.2 mm, 60 F$_{524}$). Compounds were visualised by UV at 254 nm, potassium permanganate stain (potassium permanganate (3 g), potassium carbonate (20 g), 5 % aqueous sodium hydroxide solution (5 mL) and water (300 mL)) or ninhydrin stain. Retention factor (R$_f$) values are quoted with respected to the solvent system used to develop the plate. Flash column chromatography was performed on silica gel (Merck Kieselgel 60 F$_{254}$ 230-400 mesh) eluting with solvents as described.

Solvents and reagents

Anhydrous Toluene, THF, CH$_2$Cl$_2$ and MeOH were obtained from a PureSoIv^{TM} solvent purification system (Innovative Technologies Inc.). Commercial anhydrous grade DMF, DMSO and MeCN were used without further purification. Where specified, solvents were degassed by sparging with argon for 30 min. All other reagents were used as commercially supplied and handled in accordance with COSHH regulations. Petroleum ether refers to the fraction which boils between 40-60 °C.

General

All reactions were carried out in either oven-dried or flame-dried glassware under an argon atmosphere with magnetic stirring. Room temperature is taken to be 20 °C. Compound names were generated using CS ChemDraw Ultra 6.0.

9.1. Vinyl sulfonamide/acrylamide library and derivatives

Ethenesulfonic acid 4-[1,2,3]thiadiazol-4-yl-benzylamide **39**
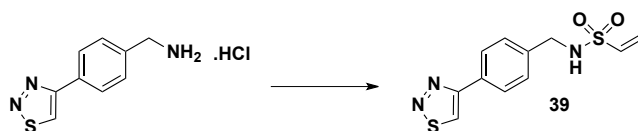
2-Chloroethanesulfonyl chloride (23 μL, 0.22 mmol, 1 eq.) was added to a stirred solution of 4-(1,2,3-thiadiazole-4-yl)benzylamine HCl salt (50 mg, 0.22 mmol, 1 eq.) and Et$_3$N (107 μL, 0.77 mmol, 3.5 eq.) in CH$_2$Cl$_2$ (1 mL) at 0 °C. Stirring was continued at 0 °C for 1.5 h and at rt for 0.5 h, before dilution with CH$_2$Cl$_2$ (10 mL). The diluted reaction mixture was washed with brine (2 x 10 mL), dried over MgSO$_4$, filtered and concentrated *in vacuo*. The crude mixture was purified by flash chromatography on silica (EtOAc/n-hexane, 2:1) to isolate the desired vinyl sulfonamide **39** (10 mg, 16 %) as a white powder, mp = 117-120 °C; R$_f$ = 0.3 (EtOAc/n-hexane, 2:1); ν$_{max}$ /cm^{-1} 3270, 3066, 1147, 1424, 1319, 1224, 1138, 1073, 1068, 968, 938, 813; δ$_H$ (400 MHz, CDCl$_3$) 8.67 (1H, s, thiadiazole-H), 8.02 (2H, d, *J* 7.0, Ar*H*), 7.47 (2H, d, *J* 7.0, Ar*H*), 6.52 (1H, dd, *J* 10.4, *J* 17.4, NHSO$_2$C*H*CH$_2$), 6.28 (1H, d, *J* 17.4, NHSO$_2$CHC*H$_2$ cis* to SO$_2$), 5.95 (1H, d, *J* 10.4, NHSO$_2$CHC*H$_2$ trans* to SO$_2$), 4.90 (1H, bt, *J* 6.0, N*H*), 4.28 (2H, d, *J* 6.0, NHC*H$_2$*); δ$_C$ (101 MHz, CDCl$_3$) 162.4, 138.0, 136.1, 130.7, 130.5, 128.8, 127.9, 127.2, 46.9; *m/z* (CI) 282 [MH]$^+$, 299 [MNH$_4$]$^+$; found: [MNH$_4$]$^+$, 299.0640 C$_{11}$H$_{15}$N$_4$O$_2$S$_2$ requires 299.0636 Δ 1.2 ppm.

Ethenesulfonic acid benzylamide **40**
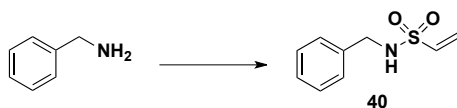
To a solution of benzylamine (0.22 mL, 2.0 mmol, 1 eq.) and chloroethanesulfonyl chloride (0.21 mL, 2.0 mmol, 1 eq.) in anhydrous CH$_2$Cl$_2$ (30 mL) at 0 °C was added Et$_3$N (0.60 mL, 4.2 mmol, 2.1 eq.) dropwise. The reaction mixture was warmed to rt and stirred for 3 h, the solvent evaporated *in vacuo* to 15 mL and the white precipitate Et$_3$NHCl salt removed by filtration. The filtrate was purified on silica (EtOAc/n-hexane, 1:1) and (EtOAc/n-hexane, 3:7) to yield the desired vinyl sulfonamide **40** (156.3 mg, 40 %) as a colourless oil; R$_f$ = 0.22 (EtOAc/n-hexane, 3:7); ν$_{max}$ /cm^{-1} 3291, 1497, 1456, 1425, 1386, 1322, 1142, 1084, 1060, 1028, 971, 841, 734, 698, 657; δ$_H$ (400 MHz, CDCl$_3$) 7.35-7.26 (5H, m, Ph), 6.44 (1H, dd, *J* 16.5, *J* 9.9, SO$_2$C*H*CH$_2$), 6.17 (1H, d, *J* 16.5, SO$_2$CHC*H$_2$ cis* to SO$_2$), 5.85 (1H, d, *J* 9.9, SO$_2$CHC*H$_2$ trans* to SO$_2$), 5.30 (1H, bt, *J* 6.3, N*H*), 4.15 (2H, d, *J* 6.3, PhC*H$_2$*); δ$_C$ (101 MHz, CDCl$_3$) 136.7, 135.8, 128.6, 127.9, 127.8, 126.6, 46.8; *m/z* (CI) 215 [MNH$_4$]$^+$; found [MNH$_4$]$^+$ 215.0859 C$_9$H$_{15}$N$_2$O$_2$S requires 215.0854, Δ 2.2 ppm. Data in agreement with literature values.[278]

Ethenesulfonic acid 4-methoxy-benzylamide **41**
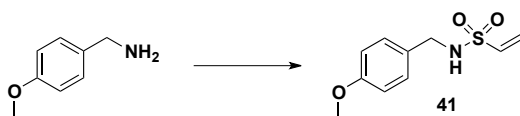
2-Chloroethanesulfonyl chloride (0.21 mL, 2.1 mmol, 1.0 eq.) was added dropwise to a stirred solution of 4-methoxy-benzylamine (0.27 mL, 2.1 mmol, 1.0 eq.) and Et$_3$N (1.00 mL, 7.3 mmol, 3.5 eq.) in CH$_2$Cl$_2$ (10 mL) at 0 °C. After addition, stirring was continued at 0 °C for 2 h. The mixture was diluted with CH$_2$Cl$_2$ (10 mL), washed with brine (2 x 5 mL), dried over MgSO$_4$ and the solvent removed *in vacuo* to yield a yellow oil which was purified on silica (EtOAc/n-hexane, 3:7) to yield the desired vinyl sulfonamide **41** (230.3 mg, 48 %) as a white solid, mp = 71-73 °C; R$_f$ = 0.22 (EtOAc/n-hexane, 3:7); ν_{max} /cm^{-1} 3287, 1514, 1316, 1247, 1175, 1138, 1030, 979, 960, 868, 816, 753, 661; δ_H (400 MHz, CDCl$_3$) 7.22 (2H, d, *J* 9.0, Ar*H2'*), 6.84 (2H, d, *J* 9.0, Ar*H3'*), 6.43 (1H, dd, *J* 16.0, *J* 9.0, SO$_2$C*H*CH$_2$), 6.17 (1H, d, *J* 16.0, SO$_2$CHC*H$_2$ cis* to SO$_2$), 5.87 (1H, d, *J* 9.0, SO$_2$CHC*H$_2$ trans* to SO$_2$), 5.17 (1H, bt, *J* 6.0, N*H*), 4.09 (2H, d, *J* 6.0, ArC*H$_2$*NH), 3.77 (3H, s, ArC*H$_3$*); δ_C (101 MHz, CDCl$_3$) 159.2, 135.9, 129.3, 128.7, 126.6, 114.0, 55.3, 46.4; *m/z* (CI) 245 [MNH$_4$]$^+$; found [MNH$_4$]$^+$, 245.0960 C$_{10}$H$_{17}$N$_2$O$_3$S requires 245.0960, Δ 0 ppm.

1-Ethenesulfonyl-4-phenyl-piperazine **42**
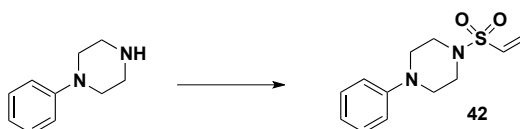
2-Chloroethanesulfonyl chloride (0.31 mL, 3.0 mmol, 1 eq.) was added dropwise to a stirred solution of 1-phenylpiperazine (0.46 mL, 3.0 mmol, 1 eq.) and Et$_3$N (1.46 mL, 0.5 mmol, 3.5 eq.) in CH$_2$Cl$_2$ (10 mL) at 0 °C under argon. The solution was stirred at 0 °C for 1 h and at rt overnight. The reaction mixture was diluted with CH$_2$Cl$_2$ washed with brine, dried over MgSO$_4$, filtered and concentrated *in vacuo*. The crude yellow solid was purified by flash column chromatography on silica (EtOAc/n-hex, 2:3) to yield the desired vinyl sulfonamide **42** (241.3 mg, 32 %) as a white powder, mp = 125-127 °C; R$_f$ = 0.31 (EtOAc/n-hex, 2:3); ν_{max} /cm^{-1} 1597, 1495, 1448, 1381, 1336, 1325, 1269, 1232, 1150, 1117, 972, 759; δ_H (400 MHz, CDCl$_3$) 7.34-7.30 (2H, m, Ar*H*), 6.98-6.94 (3H, m, Ar*H*), 6.50 (1H, dd, *J* 16.8, *J* 10.5, NHSO$_2$C*H*CH$_2$), 6.32 (1H, d, *J* 16.8, NHSO$_2$CHC*H$_2$ cis* to SO$_2$), 6.12 (1H, d, *J* 10.5, NHSO$_2$CHC*H$_2$ trans* to SO$_2$), 3.37-3.29 (8H, m, piperazine-*H*); δ_C (101 MHz, CDCl$_3$) 150.7, 132.3, 129.4, 129.4, 121.1, 117.1, 49.5, 45.7; *m/z* (ESI) 253 [MH]$^+$; found: [MH]$^+$, 253.1023 C$_{12}$H$_{17}$N$_2$O$_2$S requires 253.1011, Δ 4.7 ppm.

4-(Ethenesulfonylamino-methyl)-benzoic acid methyl ester **43**
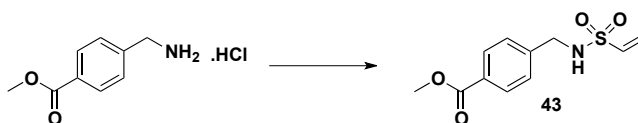
To a solution of methyl 4-(aminomethyl)benzoate HCl salt (200 mg, 1 mmol, 1 eq.) in CH$_2$Cl$_2$ (4 mL) at rt was added pyridine (0.12 mL, 1.5 mmol, 1.5 eq.), DMAP (12.2 mg, 0.1 mmol, 0.1 eq.), triethylamine (0.15 mL, 1.1 mmol, 1.1 eq.) and 2-chloroethanesulfonyl chloride (0.1 mL, 1 mmol, 1 eq.) to give a bright yellow solution which quickly

turned pink. The resulting mixture was stirred at rt for 5 min before dilution with EtOAc (20 mL). The organic phase was washed with 2N HCl (2 x 20 mL), dried (MgSO$_4$) and concentrated *in vacuo*. The residue was dissolved in CH$_2$Cl$_2$ (4 mL) and triethylamine (0.4 mL, excess) and the resulting bright yellow solution stirred at rt for 16 h. The reaction was diluted with EtOAc and the organic phase washed with aq. HCl (2N), brine, dried (MgSO$_4$) and concentrated *in vacuo*. The crude mixture was purified by flash chromatography on silica (EtOAc/n-hexane, 1:1) to give the desired sulfonamide **43** (43.6 mg, 17 %) as a white solid, mp = 66-68 °C; R$_f$ = 0.29 (EtOAc/n-hexane, 1:1); ν_{max} /cm^{-1} 3284, 1718, 1435, 1328, 1283, 1148, 1111; δ_H (400 MHz, CDCl$_3$) 8.01 (2H, d, *J* 8.3, Ar*H*), 7.40 (2H, d, *J* 8.3, Ar*H*), 6.49 (1H, dd, *J* 9.6, *J* 16.0, NHSO$_2$C*H*CH$_2$), 6.26 (1H, d, *J* 16.0, NHSO$_2$CHC*H$_2$ cis* to *SO$_2$*), 5.94 (1H, d, *J* 9.6, NHSO$_2$CHC*H$_2$ trans* to *SO$_2$*), 4.82 (1H, bs, N*H*), 4.27 (2H, d, *J* 6.4, NHC*H$_2$*Ar), 3.91 (3H, s, OC*H$_3$*); δ_C (101 MHz, CDCl$_3$) 166.8, 141.8, 136.1, 130.2, 130.0, 127.9, 127.3, 52.4, 46.8; *m/z* (CI) 273 [MNH$_4$]$^+$; found: [MNH$_4$]$^+$, 273.0911 C$_{11}$H$_{17}$N$_2$O$_4$S requires 273.0909. Δ 0.7 ppm. Data in agreement with literature values.[279]

Ethenesulfonic acid (1-benzyl-piperidin-4-yl)-amide **44**
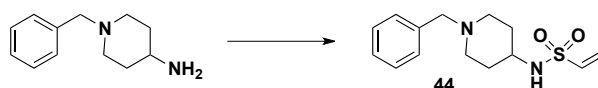
2-Chloroethanesulfonyl chloride (0.21 mL, 2 mmol, 1 eq.) was added dropwise to a stirred solution of 4-aminobenzylpiperidine (0.41 mL, 2 mmol, 1 eq.) and triethylamine (0.97 mL, 7.0 mmol, 3.5 eq.) in CH$_2$Cl$_2$ (10 mL) at 0 °C under argon. After addition, stirring was continued at 0 °C for 1 h and at rt overnight. The reaction mixture was diluted with CH$_2$Cl$_2$, poured into aq. NH$_4$Cl (2 M), the layers separated and the organic layer dried over MgSO$_4$, filtered and the solvent removed *in vacuo*. The resulting crude oil was triturated in ether to remove insoluble impurities to yield the desired vinyl sulfonamide **44** (125 mg, 22 %) as a clear oil. ν_{max} /cm^{-1} 3276, 2802, 2761, 1328, 1153, 1073, 970, 907, 735; δ_H (400 MHz, CDCl$_3$) 7.35-7.25 (5H, m, Ar*H*), 6.57 (1H, dd, *J* 15.7, *J* 10.0, NHSO$_2$C*H*CH$_2$), 6.26 (1H, d, *J* 15.7, NHSO$_2$CHC*H$_2$ cis* to *SO$_2$*), 5.91 (1H, d, *J* 10.0, NHSO$_2$CHC*H$_2$ trans* to *SO$_2$*), 3.51 (2H, s, ArC*H$_2$*), 3.22 (1H, m, SO$_2$NHC*H*), 2.81 (2H, bd, *J* 12.0, piperidine-*H*), 2.11 (2H, bt, *J* 11.0, piperidine-*H*), 1.95 (2H, dd, *J* 12.0, *J* 4.0, piperidine-*H*), 1.61 (2H, qd, *J* 12.0, *J* 4.0, piperidine-*H*); δ_C (101 MHz, CDCl$_3$) 138.2, 137.2, 129.1, 128.3, 127.1, 125.8, 62.9, 51.9, 50.9, 33.3; *m/z* (ESI) 281 [MH]$^+$; found: [MH]$^+$, 281.1324 C$_{14}$H$_{21}$N$_2$O$_2$S requires 281.1324, Δ 0 ppm.

Ethenesulfonic acid 4-fluoro-benzylamide **45**
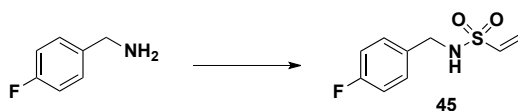
2-Chloroethanesulfonyl chloride (0.21 mL, 2.1 mmol, 1 eq.) was added dropwise to a solution of 4-fluorobenzylamine (262.8 mg, 2.1 mmol, 1 eq.) and triethylamine (1 mL, 7.35 mmol, 3.5 eq.) in CH$_2$Cl$_2$ (10 mL) at 0 °C. After addition, stirring was continued at 0 °C for 1 h and at rt overnight. The mixture was diluted with CH$_2$Cl$_2$ (10 mL), washed with brine (2 x 10 mL), dried over MgSO$_4$, filtered and concentrated *in vacuo*. The crude yellow oil was purified using flash chromatography on silica (gradient elution EtOAc/n-hexane, 3:7 to EtOAc/n-hexane, 1:1) to give the desired

vinyl sulfonamide **45** (205.6 mg, 45 %) as a white solid, mp = 52-55 °C; ν_{max} /cm^{-1} 3291 (b), 1606, 1510, 1428, 1387, 1325, 1222, 1146, 1061, 972, 833; δ_H (400 MHz, CDCl$_3$) 7.29-7.27 (2H, m, Ar*H*), 7.06-7.01 (2H, m, Ar*H*), 6.47 (1H, dd, *J* 17.5, *J* 10.0, SO$_2$C*H*CH$_2$), 6.25 (1H, d, *J* 17.5, SO$_2$CHC*H*$_2$ *cis* to SO$_2$), 5.94 (1H, d, *J* 10.0, SO$_2$CHC*H*$_2$ *trans* to SO$_2$), 4.67 (1H, bs, N*H*), 4.18 (2H, d, *J* 6.0, ArNHC*H*$_2$); δ_C (101 MHz, CDCl$_3$) 162.6 (d, *J* 243, ArC4'), 136.0, 132.3, 129.7 (d, *J* 9, ArC2'), 127.0, 115.7 (d, *J* 18, ArC3'), 46.5; *m/z* (CI) 233 [MNH$_4$]$^+$; found: [MNH$_4$]$^+$, 233.0763 C$_9$H$_{14}$N$_2$O$_2$SF requires 233.0760, Δ 1.3 ppm.

N-(4-[1,2,3]Thiadiazol-4-yl-phenyl)-acrylamide **46**
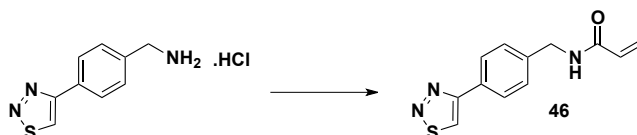
To a solution of 4-(1,2,3-thiadiazol-4-yl)benzylamine HCl salt (100.0 mg, 0.44 mmol, 1.0 eq.) in CH$_2$Cl$_2$ (1 mL) at 0 °C was added Et$_3$N (0.13 mL, 0.92 mmol, 2.1 eq.) and acryloyl chloride (0.04 mL, 0.48 mmol, 1.1 eq.) and the mixture stirred at rt for 4 h. The reaction was quenched with sat. NaHCO$_3$, extracted with CH$_2$Cl$_2$ (x 3), dried over MgSO$_4$ and the solvent removed *in vacuo*. The crude residue was purified on silica (EtOAc/n-hexane, 3:2) to yield the desired acrylamide **46** (37.8 mg, 35 %) as a white solid, mp = 190-193 °C; R$_f$ = 0.27 (EtOAc/n-hexane, 3:2); ν_{max} /cm^{-1} 2926, 2855, 2397, 1652, 1616, 1461, 1454, 1224, 800; δ_H (400 MHz, MeOD) 9.24 (1H, s, thiadiazole-*H*), 8.08 (2H, d, *J* 8.9, Ar*H3*'), 7.47 (2H, d, *J* 8.9, Ar*H2*'), 6.36-6.25 (2H, m, NHCOCHC*H*$_2$), 5.71 (1H, dd, *J* 8.8, *J* 3.1, NHCOC*H*CH$_2$), 4.55 (2H, s, CH$_2$); δ_C (101 MHz, MeOD) 166.7, 162.4, 139.9, 131.3, 130.5, 129.9, 128.0, 127.1, 125.7, 42.4; *m/z* (CI) 246 [MH]$^+$, 263 [MNH$_4$]$^+$; found [MH]$^+$ 246.0705 C$_{12}$H$_{12}$N$_3$OS requires 246.0701, Δ 1.6 ppm.

N-Benzyl-acrylamide **47**
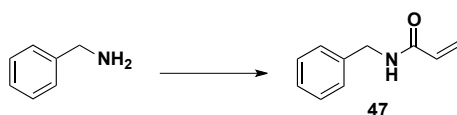
To a solution of benzylamine (0.22 mL, 2.0 mmol, 1.0 eq.) in CH$_2$Cl$_2$ (5 mL) at 0 °C was added Et$_3$N (0.31 mL, 2.2 mmol, 1.1 eq.) and acryloyl chloride (0.18 mL, 2.2 mmol, 1.1 eq.) and the mixture stirred at rt for 1 h. The reaction was quenched with sat. NaHCO$_3$ and extracted with CH$_2$Cl$_2$ (3 x 20 mL). The organics were combined and dried (MgSO$_4$) and the solvent removed *in vacuo*. The crude mixture was purified on silica (gradient elution, EtOAc/petroleum ether 40-60, 3:7 to 100 % EtOAc) to yield the desired acrylamide (316.6 mg, 98 %) as a white solid, mp = 68-70 °C; R$_f$ = 0.18 (EtOAc/petroleum ether 40-60, 3:7); ν_{max} /cm^{-1} 3284, 1651, 1623, 1610, 1557, 1533, 1495, 1455, 1407, 1238, 1075, 1027, 996, 956, 743, 692; δ_H (400 MHz, CDCl$_3$) 7.38-7.29 (5H, m, Ph), 6.35 (1H, dd, *J* 17.0, *J* 1.3, NHCOCHC*H*$_2$ *cis* to C=O), 6.15 (1H, dd, *J* 10.3, *J* 17.0, NHCOC*H*CH$_2$), 6.02 (1H, bs, N*H*), 5.69 (1H, dd, *J* 1.3, *J* 10.3, NHCOCHC*H*$_2$ *trans* to C=O), 4.54 (2H, d, *J* 5.8, ArC*H*$_2$NH); δ_C (101 MHz, CDCl$_3$) 165.4, 138.0, 130.6, 128.8, 128.0, 127.7, 126.9, 43.7; *m/z* (CI) 162 [MH]$^+$; found [MH]$^+$ 162.0910 C$_{10}$H$_{12}$NO requires 162.0919, Δ 5.6 ppm. Data in agreement with literature values.[280]

N-(4-Methoxy-benzyl)-acrylamide **48**
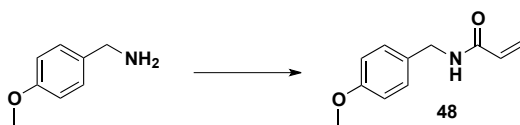
To a solution of *p*-methoxybenzylamine (0.26 mL, 2.0 mmol, 1.0 eq.) in CH_2Cl_2 (5 mL) at 0 °C was added Et_3N (0.31 mL, 2.2 mmol, 1.1 eq.) and acryloyl chloride (0.18 mL, 2.2 mmol, 1.1 eq.) and the mixture stirred at rt for 1 h. The reaction was quenched with sat. $NaHCO_3$, extracted with CH_2Cl_2 (20 mL x 3), the combined organic extracts dried ($MgSO_4$) and the solvent removed *in vacuo*. The crude product was purified on silica (EtOAc/petroleum ether 40-60, 2:3) to give the desired amide (213.8 mg, 56 %) as a white powder, mp = 100-103 °C; R_f = 0.23 (EtOAc/petroleum ether 40-60, 2:3); ν_{max} /cm^{-1} 3244, 1665, 1650, 1611, 1549, 1511, 1464, 1456, 1444, 1409, 1301, 1244, 1221, 1176, 1111, 1029, 983, 968, 831, 817, 755, 569; δ_H (400 MHz, CDCl$_3$) 7.23 (2H, d, *J* 9.0, Ar*H*), 6.87 (2H, d, *J* 9.0, Ar*H*), 6.32 (1H, dd, *J* 1.3, *J* 17.1, NHCOCHC*H*$_2$ *cis* to C=O), 6.09 (1H, dd, *J* 10.3, *J* 17.1, NHCOC*H*CH$_2$), 5.80 (1H, bs, N*H*), 5.66 (1H, dd, *J* 1.3, *J* 10.3, NHCOCHC*H*$_2$ *trans* to C=O), 4.46 (2H, d, *J* 6.0, ArC*H*$_2$NH), 3.80 (3H, s, OC*H*$_3$); δ_C (101 MHz, CDCl$_3$) 165.6, 159.0, 130.9, 130.3, 129.2, 126.5, 114.0, 55.3, 43.1; *m/z* (CI) 192 [MH]$^+$, 209 [MNH$_4$]$^+$; found [MH]$^+$ 192.1025 $C_{11}H_{14}NO_2$ requires 192.1025, Δ 0 ppm. Data in agreement with literature values.[281]

1-(4-Phenyl-piperazin-1-yl)-propenone **49**
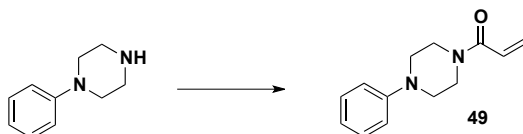
To a solution of 1-phenyl piperazine (0.61 mL, 4.0 mmol, 1 eq.) in CH_2Cl_2 (10 mL) at 0 °C under argon was added triethylamine (0.83 mL, 6.0 mmol, 1.5 eq.) and acryloyl chloride (0.36 mL, 4.4 mmol, 1.1 eq.) and the reaction mixture stirred at rt for 2 h. The reaction mixture was poured into aq. NH$_4$Cl (2M) (20 mL), extracted with CH_2Cl_2 (x 3), the combined organics dried over MgSO$_4$, filtered and the solvent removed *in vacuo*. The crude orange oil was purified by flash column chromatography on silica (EtOAc/n-hexane, 85:15) to give the desired acrylamide (465.4 mg, 54 %) as a white powder, mp = 73-74 °C; R_f = 0.45 (EtOAc/n-hex, 19:1); ν_{max} /cm^{-1} 1638, 1604, 1497, 1456, 1439, 1385, 1329, 1312, 1226, 1204, 1154, 1036, 1029, 968, 945, 901, 789, 771, 697; δ_H (400 MHz, CDCl$_3$) 7.31 (2H, t, *J* 8.0, Ph), 6.97-6.92 (3H, m, Ph), 6.64 (1H, dd, *J* 10.8, *J* 16.7, NHCOC*H*CH$_2$), 6.36 (1H, dd, *J* 16.7, *J* 1.7, NHCOCHC*H*$_2$ *cis* to C=O), 5.76 (1H, dd, *J* 10.8, *J* 1.7, NHCOCHC*H*$_2$ *trans* to C=O), 3.88-3.74 (4H, m, piperazine-*H*), 3.23-3.20 (4H, m, piperazine-*H*); δ_C (101 MHz, CDCl$_3$) 165.4, 150.9, 129.3, 128.2, 127.3, 120.7, 116.7, 49.9, 49.4, 45.7, 41.9; *m/z* (CI) 217 [MH]$^+$; found: [MH]$^+$, 217.1350 $C_{13}H_{17}N_2O$ requires 217.1341, Δ 4.2 ppm.

4-(Acryloylamino-methyl)-benzoic acid methyl ester **50**
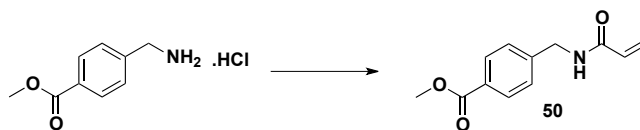
To a solution of methyl 4-(aminomethyl)-benzoate HCl salt (322.0 mg, 1.6 mmol, 1.0 eq.) in CH_2Cl_2 (2 mL) at 0 °C was added Et_3N (0.47 mL, 3.36 mmol, 2.1 eq.) and acryloyl chloride (0.14 mL, 1.8 mmol, 1.1 eq.) and the mixture stirred at rt for 4 h. The reaction was quenched with sat. $NaHCO_3$, extracted with CH_2Cl_2 (x 3), dried over $MgSO_4$ and the solvent removed *in vacuo*. The crude yellow oil was purified on silica (EtOAc/n-pentane, 2:3) to give the desired product (150.5 mg, 43 %) as a white solid, mp = 114-116 °C; R_f = 0.20 (EtOAc/n-pentane, 2:3); ν_{max} /cm^{-1} 3273, 1718, 1652, 1621, 1555, 1437, 1412, 1278, 1246, 1107, 965, 754, 708; δ_H (400 MHz, CDCl$_3$) 7.86 (2H, d, *J* 7.0, Ar*H2'*), 7.34 (1H, bt, N*H*), 7.23 (2H, d, *J* 7.0, Ar*H3'*), 6.25-6.15 (2H, m, NHCOCHC*H$_2$*), 5.58 (1H, dd, *J* 8.3, *J* 3.5, NHCOC*H*CH$_2$), 4.42 (2H, d, *J* 6.7, C*H$_2$*), 3.84 (3H, s, C*H$_3$*); δ_C (101 MHz, CDCl$_3$) 166.9, 166.0, 143.6, 130.6, 129.8, 129.0, 127.3, 126.7, 52.1, 43.0; *m/z* (CI) 220 [MH]$^+$, 237 [MNH$_4$]$^+$; found [MH]$^+$ 220.0970 C$_{12}$H$_{14}$NO$_3$ requires 220.0974, Δ 1.8 ppm.

N-(5-Ethyl-[1,3,4]thiadiazol-2-yl)-acrylamide **51**
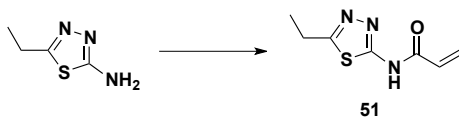
To a solution of 5-ethyl-[1,3,4]thiadiazol-2-ylamine (206.5 mg, 1.60 mmol, 1.0 eq.) in CH_2Cl_2 (2 mL) was added Et_3N (0.24 mL, 1.76 mmol, 1.1 eq.), the solution cooled to 0 °C and acryloyl chloride (0.14 mL, 1.76, 1.1 eq.) added dropwise. The mixture was stirred at rt overnight, and subsequently quenched with $NaHCO_3$, extracted with CH_2Cl_2 (x 3), dried over $MgSO_4$ and the solvent removed *in vacuo*. The crude residue was purified on silica (EtOAc/n-hexane, 3:2) to give the desired acrylamide **51** (72.1 mg, 25 %) as a white solid, mp = 194-198 °C; R_f = 0.20 (CH$_2$Cl$_2$/MeOH, 97:3); ν_{max} /cm^{-1} 1683, 1559, 1401, 1323, 1289, 1198, 982, 968, 936, 836, 794, 710, 682; δ_H (400 MHz, CDCl$_3$) 6.91 (1H, dd, *J* 17.2, *J* 10.0, NHCOC*H*CH$_2$), 6.68 (1H, dd, *J* 1.4, *J* 17.2, NHCOCHC*H$_2$ cis* to C=O), 6.01 (1H, dd, *J* 10.0, *J* 1.4, NHCOCHC*H$_2$ trans* to C=O), 3.10 (2H, q, *J* 7.7, C*H$_2$*), 1.44 (3H, t, *J* 7.7, C*H$_3$*); δ_C (101 MHz, CDCl$_3$) 167.0, 163.7, 160.8, 131.3, 129.3, 23.7, 14.2; *m/z* (ESI) 184 [MH]$^+$; found [MH]$^+$ 184.0552 C$_7$H$_{10}$N$_3$OS requires 184.0545, Δ 3.8 ppm.

N-(3-Trifluoromethyl-phenyl)-acrylamide **52**
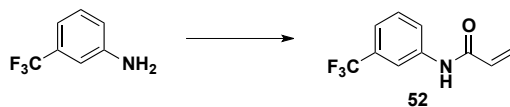
To a solution of 3-(trifluoromethyl)-aniline (0.5 mL, 4.0 mmol, 1 eq.) in CH_2Cl_2 (10 mL) at 0 °C under argon was added triethylamine (0.83 mL, 6.0 mmol, 1.5 eq.) and acryloyl chloride (0.36 mL, 4.4 mmol, 1.1 eq.) and the reaction

mixture stirred at 0 °C for 15 min and then at rt for 1 h. The reaction mixture was poured into aq. NH₄Cl (2M) (20 mL), extracted with CH_2Cl_2 (x 3) and the combined organics dried over $MgSO_4$, filtered and concentrated *in vacuo*. The crude yellow oil was purified by flash column chromatography on silica (EtOAc/n-hexane, 35:65) to yield the desired acrylamide **52** (617.3 mg, 72 %) as a white solid, mp = 82-83 °C. R_f = 0.61 (EtOAc/n-hexane, 1:1); ν_{max} /cm⁻¹ 1668, 1626, 1557, 1494, 1408, 1334, 1177, 1161, 1111, 1098, 1070, 963, 880, 794, 721, 695; δ_H (400 MHz, CDCl₃) 8.02 (1H, bs, N*H*), 7.91 (1H, s, Ar*H2'*), 7.81 (1H, d, *J* 8.0, Ar*H6'*), 7.45 (1H, t, *J* 8.0, Ar*H5'*), 7.39 (1H, d, *J* 8.0, Ar*H4'*), 6.48 (1H, dd, *J* 16.0, *J* 1.0, NHCOCHC*H₂ cis* to C=O), 6.32 (1H, dd, *J* 16.0, *J* 10.0, NHCOC*H*CH₂), 5.82 (1H, dd, *J* 10.0, *J* 1.0, NHCOCHC*H₂ trans* to C=O); δ_C (101 MHz, CDCl₃) 164.0, 138.3, 131.9, 131.6, 131.2, 130.9, 130.7, 129.6, 128.7, 125.2, 122.5, 121.2, 116.9; *m/z* (CI) 216 [MH]⁺ 233 [MNH₄]⁺; found: [MH]⁺, 216.0645 $C_{10}H_9NOF_3$ requires 216.0636, Δ 4.1 ppm.

N-(2-Morpholin-4-yl-ethyl)-acrylamide **53**
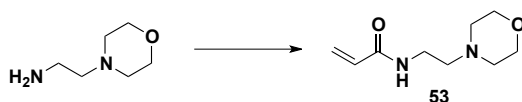
To a solution of 4-(2-aminoethyl)morpholine (0.66 mL, 5.0 mmol, 1.0 eq.) in anhydrous CH_2Cl_2 (25 mL) at 0 °C under argon was added Et₃N (1.04 mL, 7.5 mmol, 1.5 eq.) and acryloyl chloride (0.45 mL, 5.5 mmol, 1.1 eq.) and the resulting bright yellow solution warmed to rt and stirred for 1 h. The reaction mixture was poured in H_2O and extracted with CH_2Cl_2 (x 3). The aqueous layer was basified with 20 % saturated NaOH to pH 12 and further extracted with CH_2Cl_2. Combined organics were dried over $MgSO_4$, filtered and the solvent removed *in vacuo*. The crude yellow solid was purified on silica (EtOAc/MeOH, 4:1) to yield the desired acrylamide (651.8 mg, 71 %) as a white solid, mp = 96-97 °C; R_f = 0.32 (EtOAc/MeOH, 4:1); ν_{max} /cm⁻¹ 3283, 3097, 2973, 2958, 2941, 2917, 2892, 2858, 2813, 2790, 2777, 2769, 1655, 1627, 1565, 1450, 1413, 1303, 1282, 1263, 1244, 1169, 1149, 1134, 1115, 1092, 1013, 1002, 977, 914, 867, 734; δ_H (400 MHz, CDCl₃) 6.25 (1H, dd, *J* 1.5, *J* 17.0, C*H₂*CHCONH *cis* to C=O), 6.14 (1H, bs, N*H*), 6.10 (1H, dd, *J* 10.2, *J* 17.0, CH₂C*H*CONH), 5.61 (1H, dd, *J* 1.5, *J* 10.2, C*H₂*CHCONH *trans* to C=O), 3.68 (4H, t, *J* 4.6, morpholine-*H2'*), 3.41 (2H, q, *J* 5.7, NHC*H₂*), 2.49 (2H, t, *J* 6.0, NHCH₂C*H₂*), 2.43 (4H, m, morpholine-*H3'*); δ_C (101 MHz, CDCl₃) 165.6, 131.0, 126.5, 67.1, 57.1, 53.5, 35.8; *m/z* (ESI) 185 [MH]⁺; found [MH]⁺ 185.1285 $C_9H_{17}N_2O_2$ requires 185.1290, Δ 2.7 ppm.

N-(1-Benzyl-piperidin-4-yl)-acrylamide **54**
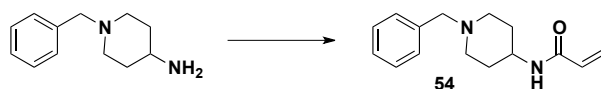
To a solution of 4-amino-N-benzyl piperidine (0.40 mL, 1.98 mmol, 1.0 eq.) in CH_2Cl_2 (10 mL) at 0 °C under argon was added Et₃N (0.41 mL, 2.98 mmol, 1.5 eq.) and acryloyl chloride (0.18 mL, 2.18 mmol, 1.1 eq.). The reaction mixture was stirred for 1 h, poured into aq. NH₄Cl (20 mL) and extracted with CH_2Cl_2 (x 1) and the organic layer dried over $MgSO_4$, filtered and the solvent removed *in vacuo*. The crude yellow oil was triturated in ether to yield the desired acrylamide **54** (148.9 mg, 31 %) as a white solid, mp = 115-116 °C; ν_{max} /cm⁻¹ 3299, 1656, 1626, 1539, 1233,

981, 943, 731, 695; δ_H (400 MHz, CDCl$_3$) 7.36-7.25 (5H, m, Ph), 6.30 (1H, dd, *J* 17.0, *J* 1.4, NHCOCHC*H$_2$ cis* to C=O), 6.10 (1H, dd, *J* 17.0, *J* 10.2, NHCOC*H*CH$_2$), 5.65 (1H, dd, *J* 10.2, *J* 1.4, NHCOC*H*CH$_2$ *trans* to C=O), 3.96-3.86 (1H, m, NHC*H*), 3.53 (2H, s, PhC*H$_2$*), 2.87-2.84 (2H, m, piperidine-*H*), 2.16 (2H, td, *J* 12.0, *J* 1.5, piperidine-*H*), 1.98-1.94 (2H, m, piperidine-*H*), 1.52 (2H, qd, *J* 12.0, *J* 4.0, piperidine-*H*); δ_C (101 MHz, CDCl$_3$) 164.9, 138.4, 131.2, 129.2, 128.4, 127.2, 126.5, 63.2, 52.4, 46.7, 32.3; *m/z* (ESI) 245 [MH]$^+$; found: [MH]$^+$, 245.1654 C$_{15}$H$_{21}$N$_2$O requires 245.1654, Δ 0 ppm.

N-(4-Fluoro-benzyl)-acrylamide **55**
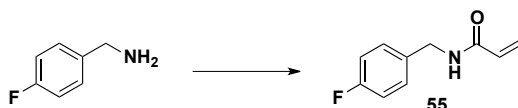
To a solution of 4-fluorobenzylamine (200.0 mg, 1.60 mmol, 1.0 eq.) in CH$_2$Cl$_2$ (5 mL) at 0 °C was added Et$_3$N (0.24 mL, 1.76 mmol, 1.1 eq.) and acryloyl chloride (0.14 mL, 1.76 mmol, 1.1 eq.) and the mixture stirred at rt for 1 h. The reaction was quenched with sat. NaHCO$_3$ and extracted with CH$_2$Cl$_2$ (3 x 20 mL). The organics were combined and dried over MgSO$_4$, filtered and the solvent removed *in vacuo*. The crude mixture was purified on silica (gradient elution, EtOAc/n-pentane, 2:3 to 100 % EtOAc) to yield the desired acrylamide **55** (210.9 mg, 74 %) as a white powder, mp = 119-121 °C; R$_f$ = 0.19 (EtOAc/n-hexane, 2:3); ν_{max} /cm^{-1} 3270, 1654, 1621, 1545, 1509, 1214, 1159, 981, 951, 850, 826, 804, 698; δ_H (400 MHz, CDCl$_3$) 7.24-7.20 (2H, m, Ar*H2'*), 7.00-6.95 (2H, m, Ar*H3'*), 6.41 (1H, bs, N*H*), 6.27 (1H, dd, *J* 17.1, *J* 1.7, NHCOCHC*H$_2$ cis* to C=O), 6.12 (1H, dd, *J* 10.3, *J* 17.1, NHCOC*H*CH$_2$), 5.63 (1H, dd, *J* 10.3, *J* 1.7, NHCOCHC*H$_2$ trans* to C=O), 4.42 (2H, d, *J* 5.8, ArC*H$_2$*NH); δ_C (101 MHz, CDCl$_3$) 165.6, 162.3 (d, *J* 246), 134.0 (d, *J* 2), 130.6, 129.7 (d, *J* 8), 127.2, 115.7 (d, *J* 22), 43.1; *m/z* (CI) 180 [MH]$^+$, 197 [MNH$_4$]$^+$; found [MH]$^+$ 180.0820 C$_{10}$H$_{11}$NOF requires 180.0825, Δ 2.8 ppm.

2-Benzylsulfanyl-ethanesulfonic acid benzylamide **56**
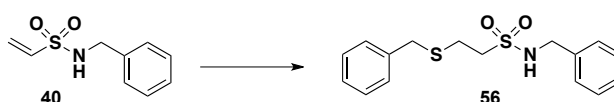
To a solution of vinyl sulfonamide **40** (60 mg, 0.30 mmol, 1 eq.) in MeCN (6 mL) and water (1 mL), benzylthiol (45 mg, 0.37 mmol, 1.2 eq.) and Et$_3$N (36.9 mg, 0.37 mmol, 1.2 eq.) were added, and the mixture stirred at rt for 1 h. The acetonitrile was removed *in vacuo*, water (10 mL) added to the resultant slurry, and this extracted with CH$_2$Cl$_2$ (2 x 10 mL). Combined organics were dried over MgSO$_4$, filtered and the solvent removed *in vacuo* to yield the desired sulfonamide **56** (83.9 mg, 87 %) as a white solid, mp = 96-99 °C; R$_f$ = 0.53 (EtOAc/n-hexane, 1:1); ν_{max} /cm^{-1} 3294, 1455, 1429, 1324, 1304, 1145, 1134, 1065, 855, 698; δ_H (400 MHz, CDCl$_3$) 7.41-7.28 (10H, m, Ar*H*), 5.00 (1H, t, *J* 6.0, N*H*), 4.22 (2H, d, *J* 6.0, NHC*H$_2$*), 3.68 (2H, s, SC*H$_2$*Ph), 3.06 (2H, t, *J* 8.0, SO$_2$C*H$_2$*), 2.76 (2H, t, *J* 8.0, SO$_2$CH$_2$C*H$_2$*); δ_C (101 MHz, CDCl$_3$) 137.5, 136.8, 128.9, 128.9, 128.8, 128.2, 128.0, 127.5, 52.8, 47.1, 36.5, 24.8; *m/z* (CI) 339 [MNH$_4$]$^+$, 322 [MH]$^+$; found: [MH]$^+$, 322.0921 C$_{16}$H$_{20}$NO$_2$S$_2$ requires 322.0935, Δ 4.3 ppm.

2-Benzylsulfanyl-ethanesulfonic acid 4-methoxy-benzylamide **57**
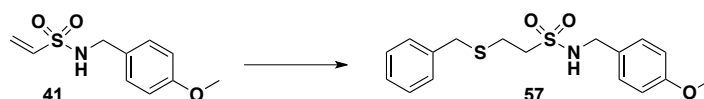
To a stirred solution of vinyl sulfonamide **41** (50 mg, 0.22 mmol, 1 eq.) in MeCN (6 mL) and water (1 mL), benzylthiol (32.8 mg, 0.26 mmol, 1.2 eq.) and Et$_3$N (26.7 mg, 0.26 mmol, 1.2 eq.) were added, and the mixture stirred at rt for 1 h. The MeCN was removed *in vacuo*, and the resultant slurry diluted with additional water (5 mL) and extracted with diethylether (2 x 10 mL). The combined organics were dried (MgSO$_4$) and concentrated *in vacuo* to give the desired sulfonamide **57** (65.4 mg, 85 %) as a white solid, mp = 91-95 °C; R$_f$ = 0.47 (EtOAc/n-hexane, 1:1); ν_{max} /cm^{-1} 3296, 1614, 1515, 1454, 1321, 1300, 1257, 1145, 1133, 1120, 1043, 1029, 845, 816, 698; δ_H (400 MHz, CDCl$_3$) 7.35-7.23 (7H, m, Ar*H*), 6.90 (2H, d, *J* 7.3, Ar*H*) 4.87 (1H, t, *J* 5.5, N*H*), 4.15 (2H, d, *J* 5.5, NHC*H$_2$*), 3.81 (3H, s, OC*H$_3$*), 3.68 (2H, s, SC*H$_2$*Ph), 3.05 (2H, t, *J* 7.3, SO$_2$C*H$_2$*), 2.75 (2H, t, *J* 7.3, SO$_2$CH$_2$C*H$_2$*); δ_C (101 MHz, CDCl$_3$) 159.5, 137.5, 129.4, 128.9, 128.8, 128.8, 127.5, 114.3, 55.4, 52.8, 46.7, 36.6, 24.9; *m/z* (CI) 369 [MNH$_4$]$^+$, 352 [MH]$^+$; found: [MH]$^+$, 352.1038 C$_{17}$H$_{22}$NO$_3$S$_2$ requires 352.1041, Δ 0.9 ppm.

(R)-3-(2-Benzylsulfamoyl-ethylsulfanyl)-2-carboxyamino-propionic acid **58**
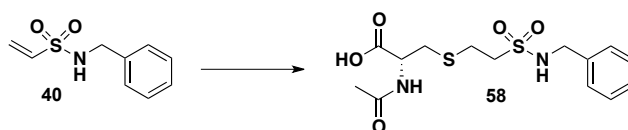
Method 1: To a stirred solution of vinyl sulfonamide **40** (50 mg, 0.25 mmol, 1 eq.) in acetonitrile (6 mL) and water (6 mL), *N*-acetyl L-cysteine (49.7 mg, 0.30 mmol, 1.2 eq.) and triethylamine (61.6 mg, 0.60 mmol, 2.4 eq.) were added, the mixture stirred at rt for 1 h, and the acetonitrile removed *in vacuo*. The resultant slurry was acidified to pH 3 with aq. HCl (2N), extracted with EtOAc (3 x 10 mL), and the combined organics dried (MgSO$_4$). The solvent was removed *in vacuo* and the crude product purified by flash chromatography on silica (gradient elution, 100 % CH$_2$Cl$_2$ to 100 % MeOH) to give the desired sulfonamide **58** (83 mg, 92 %) as a white powder.

Method 2: To a stirred solution of vinyl sulfonamide **40** (26.8 mg, 0.136 mmol, 1 eq.) at rt in acetonitrile (1 mL) was added *N*-acetyl L-cysteine (22.2 mg, 0.136 mmol, 1 eq.) in acetonitrile: water 1:1, and triethylamine (33.0 mg, 0.326 mmol, 2.4 eq.) in acetonitrile (2 mL). Stirring was continued at rt for 9 hours before the acetonitrile was removed *in vacuo*, and the resulting slurry acidified to pH 3 with aq. HCl (2N). The resulting white precipitate was filtered under reduced pressure and subsequently washed with aq. HCl (2N) and ether to yield the desired sulfonamide **58** (49 mg, 100 %) as a white powder.

Mp = 115-120 °C; R$_f$ = 0 (EtOAc/n-hexane, 3:2); ν_{max} /cm^{-1} 3298 (b), 1603, 1419, 1325, 1146; δ_H (400 MHz, DMSO-d$_6$) 12.87 (1H, bs, COO*H*), 8.27 (1H, d, *J* 8.6, N*H*Ac), 7.76 (1H, t, *J* 6.4, N*H*SO$_2$), 7.37-7.25 (5H, m, ArH), 4.40-4.35 (1H, m, AcNHC*H*), 4.16 (2H, d, *J* 6.4, ArC*H$_2$*NHSO$_2$), 3.20-3.15 (2H, m, SO$_2$C*H$_2$*), 2.89 (1H, dd, *J* 14.0, *J* 4.0, SO$_2$CH$_2$CH$_2$SC*H$_2$*), 2.78-2.69 (3H, m, SO$_2$CH$_2$C*H$_2$* (1H) and SO$_2$CH$_2$CH$_2$SC*H$_2$* (2H)), 1.86 (3H, s, NHCOOC*H$_3$*); δ_C

(101 MHz, DMSO-d$_6$) 173.2, 168.7, 138.5, 128.4, 127.6, 127.2, 53.9, 52.1, 45.9, 34.7, 25.1, 22.9; *m/z* (ESI) 383 [MNa]$^+$, 361 [MH]$^+$; found [MH]$^+$ 361.0877 C$_{14}$H$_{21}$N$_2$O$_5$S$_2$ requires 361.0892, Δ 4.2 ppm.

(R)-2-Carboxyamino-3-[2-(4-methoxy-benzylsulfamoyl)-ethylsulfanyl]-propionic acid **59**
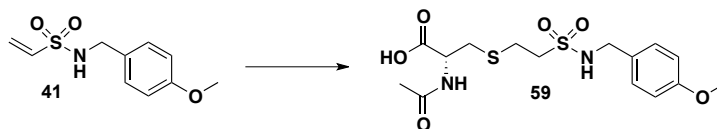
To a stirred solution of vinyl sulfonamide **41** (50.0 mg, 0.22 mmol, 1.0 eq.) in MeCN (6 mL) and water (1 mL), *N*-acetyl L-cysteine (43.1 mg, 0.26 mmol, 1.2 eq.) and Et$_3$N (55.7 mg, 0.55 mmol, 2.5 eq.) were added and the mixture stirred at rt for 1 h. The MeCN was removed *in vacuo*, water (10 mL) added to the resultant slurry, the aqueous solution acidified to pH 2 with aq. HCl (2N) and extracted with EtOAc (3 x 10 mL). The combined organics were dried over MgSO$_4$, filtered and the solvent removed *in vacuo* to yield the desired sulfonamide **59** (75.2 mg, 87 %) as a white solid, mp = 100-105 °C; R$_f$ = 0 (EtOAc/n-hexane, 3:2); ν$_{max}$ /cm^{-1} 3299 (b), 1702, 1611, 1541, 1515, 1428, 1331, 1322, 1304, 1246, 1146, 1026, 818; δ$_H$ (400 MHz, DMSO-d$_6$) 8.26 (1H, d, *J* 8.6, AcN*H*CH), 7.65 (1H, t, *J* 5.7, SO$_2$N*H*), 7.25 (2H, d, *J* 8.6, Ar*H2'*), 6.90 (2H, d, *J* 8.6, Ar*H3'*), 4.38-4.34 (1H, m, AcNHC*H*), 4.08 (2H, d, *J* 5.7, SO$_2$NHC*H$_2$*), 3.73 (3H, s, OC*H$_3$*), 3.16-3.12 (2H, m, SO$_2$C*H$_2$*), 2.89 (1H, dd, *J* 13.0, *J* 5.0, SO$_2$CH$_2$CH$_2$SC*H$_2$*), 2.77-2.69 (3H, m, SO$_2$CH$_2$C*H$_2$* (2H) and SO$_2$CH$_2$CH$_2$SC*H$_2$* (1H)), 1.86 (3H, s, NHCOC*H$_3$*); δ$_C$ (101 MHz, DMSO-d$_6$) 172.3, 169.7, 158.8, 130.4, 129.3, 113.9, 55.3, 52.2, 52.1, 45.7, 33.3, 25.3, 22.6; *m/z* (ESI) 413 [MNa]$^+$, 391 [MH]$^+$; found [MH]$^+$ 391.0979 C$_{15}$H$_{23}$N$_2$O$_6$S$_2$ requires 391.0998, Δ 4.9 ppm.

(R)-2-Acetylamino-3-(2-benzylcarbamoyl-ethylsulfanyl)-propionic acid **60**
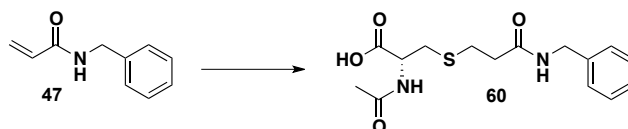
To a solution of acrylamide **47** (25 mg, 0.16 mmol, 1.0 eq.) in acetonitrile (1 mL) under argon was added *N*-acetyl L-cysteine (25.3, 0.16 mmol, 1.0 eq.) in H$_2$O (1 mL) and triethylamine (0.11 mL, 0.78 mmol, 5 eq.) and the mixture stirred at rt for 72 h. The reaction mixture was washed with EtOAc and the solvent removed from the aqueous layer to yield the desired thioether **60** (41.2, 62 %) as a clear oil; R$_f$ = 0 (100 % EtOAc); ν$_{max}$ /cm^{-1} 3280, 1646, 1606, 1556, 1455, 1379; δ$_H$ (400 MHz, MeOD) 7.34-7.21 (5H, m, Ar*H*), 4.44 (1H, dd, *J* 7.1, *J* 4.7, HOOCC*H*), 4.38 (2H, s, PhC*H$_2$*NH), 3.11 (1H, dd, *J* 13.3, *J* 4.7, HOOCCH(NHCOCH$_3$)C*H$_2$*), 2.88-2.83 (3H, m, SC*H$_2$*CH$_2$CONH and HOOCCH(NHCOCH$_3$)C*H$_2$*), 2.54 (2H, td, *J* 6.6, *J* 1.6, SCH$_2$C*H$_2$*CONH), 1.98 (3H, s, NHCOC*H$_3$*); δ$_C$ (101 MHz, MeOD) 176.6, 174.0, 172.8, 139.9, 129.5, 128.6, 128.2, 55.4, 48.8, 37.3, 35.5, 29.1, 22.7; *m/z* (ESI) 325 [MH]$^+$; found: [MH]$^+$, 325.1222. C$_{15}$H$_{21}$N$_2$O$_4$S requires 325.1222, Δ 0 ppm.

(R)-2-Acetylamino-3-[2-(4-methoxy-benzylcarbamoyl)-ethylsulfanyl]-propionic acid **61**
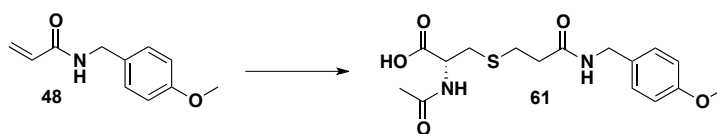
To a solution of acrylamide **48** (25 mg, 0.131 mmol, 1.0 eq.) in MeCN (1 mL) under argon was added *N*-acetyl L-cysteine (21.3 mg, 0.131 mmol, 1.0 eq.) in H_2O (1 mL) and Et_3N (0.18 mL, 1.31 mmol, 10 eq.) and the mixture stirred at rt for 16 h. The MeCN was removed *in vacuo* and the aqueous layer was acidified to pH 1 with aq. HCl (2N) and extracted with EtOAc (x 3), chloroform (x 3) and chloroform/EtOH, 2:1 (x 1). The organics were combined, dried over $MgSO_4$, filtered and the solvent removed *in vacuo* to yield the desired thioether **61** (27.7 mg, 60 %) as a clear oil; $R_f = 0$ (100 % EtOAc); ν_{max} /cm^{-1} 3276, 2827, 1648, 1548, 1514, 1421, 1375, 1301, 1249, 1179, 1032; δ_H (400 MHz, MeOD); 7.24 (2H, d, *J* 8.6, Ar*H2'*), 6.89 (2H, d, *J* 8.6, Ar*H3'*), 4.62 (1H, dd, *J* 8.0, *J* 4.7, HOOCC*H*), 4.33 (2H, s, ArC*H₂*), 3.79 (3H, s, ArOC*H₃*), 3.07 (1H, dd, *J* 13.9, *J* 4.7, HOOCCH(NHCOCH₃)C*H₂*), 2.91-2.85 (3H, m, SC*H₂*CH₂CONH and HOOCCH(NHCOCH₃)C*H₂*), 2.53 (2H, t, *J* 7.2, SCH₂C*H₂*CONH), 2.01 (3H, s, NHCOC*H₃*); δ_C (101 MHz, MeOD) 172.4, 172.3, 172.0, 159.0, 130.4, 128.6, 113.5, 54.3, 52.4, 42.3, 35.8, 33.2, 27.9, 21.0; *m/z* (ESI) 355 [MH]⁺, 377 [MNa]⁺; found: [MH]⁺, 355.1322 $C_{16}H_{23}N_2O_5S$ requires 355.1328, Δ 1.7 ppm.

(R)-4-([3-(2-Acetylamino-2-carboxy-ethylsulfanyl)-propionylamino]-methyl)-benzoic acid methyl ester **62**
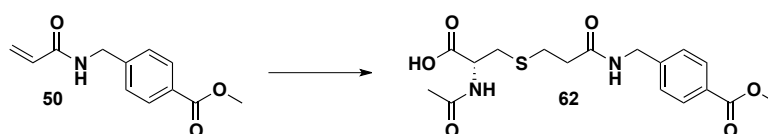
To a solution of acrylamide **50** (25 mg, 0.114 mmol, 1.0 eq.) in acetonitrile (1 mL) was added *N*-acetyl L-cysteine (18.6 mg, 0.114 mmol, 1.0 eq.) in H_2O (1 mL) and triethylamine (0.16 mL, 1.14 mmol, 10 eq.) and the mixture stirred at rt for 16 h. The acetonitrile was removed *in vacuo*, the aqueous layer was acidifed to pH 1 with aq. HCl (2N) and extracted with EtOAc (x 6). The combined organics were dried ($MgSO_4$) and the solvent removed *in vacuo* to yield the desired thioether **62** (44 mg, 100 %) as a clear oil; $R_f = 0$ (100 % EtOAc); ν_{max} /cm^{-1} 3305, 1720, 1650, 1616, 1548, 1434, 1417, 1377, 1285, 1114; δ_H (400 MHz, MeOD); 7.98 (2H, d, *J* 8.2, Ar*H3'*), 7.43 (2H, d, *J* 8.2, Ar*H2'*), 4.64 (1H, m, HOOCC*H*), 4.47 (2H, s, ArC*H₂*NHCO), 3.90 (3H, s, COOC*H₃*), 3.08 (1H, dd, *J* 4.9, *J* 14.2, HOOCCH(NHCOCH₃)C*H₂*), 2.93-2.87 (3H, m, SC*H₂*CH₂CONH and HOOCCH(NHCOCH₃)C*H₂*), 2.58 (2H, t, *J* 7.1, SCH₂C*H₂*CONH), 2.02 (3H, s, NHCOC*H₃*); δ_C (101 MHz, MeOD) 174.1, 173.4, 168.4, 145.6, 131.0, 130.7, 130.1, 128.5, 53.7, 52.6, 43.8, 37.1, 34.6, 29.2, 22.4; *m/z* (ESI) 383 [MH]⁺, 405 [MNa]⁺; found [MH]⁺ 383.1275 $C_{17}H_{23}N_2O_6S$ requires 383.1277, Δ 0.5 ppm.

9.2. Pyrrolidine analogues

1-(Toluene-4-sulfonyl)-(R)-pyrrolidine-2-carboxylic acid **64**
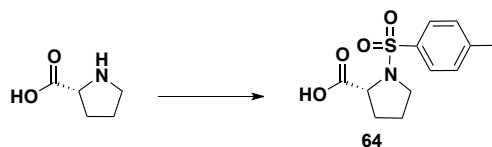
D-proline (300 mg, 2.61 mmol, 1.0 eq.) was dissolved in aqueous 2 M NaOH (2.6 mL, 5.21 mmol, 2.0 eq.) at 0 °C. A solution of TsCl (497.6 mg, 2.61 mmol, 1.0 eq.) in Et$_2$O (3 mL) was added dropwise with stirring over 10 min. The solution was stirred at rt overnight. The ethereal solution was separated and the aqueous solution acidified to pH 2 with aqueous 1 M HCl. The aqueous layer was extracted with EtOAc (x 3) and combined EtOAc extracts dried over MgSO$_4$, filtered and concentrated *in vacuo*. The crude clear oil was washed with CHCl$_3$ (x 5) to remove traces of EtOAc to yield the desired N-tosyl D-proline **64** (597.3 mg, 85 %) as a clear oil which solidified at -20 °C to a white solid, mp = 46-48 °C; R_f = 0 (100 % EtOAc); $[\alpha]^{24}_D$ = + 77.0 (*c* = 1.27, CHCl$_3$); ν_{max} /cm^{-1} 1722, 1337, 1197, 1154, 1092, 1010, 911, 815, 729, 661, 589; δ_H (400 MHz, CDCl$_3$) 7.77 (2H, d, *J* 8.0, Ar*H*), 7.35 (2H, d, *J* 8.0, Ar*H*), 4.26 (1H, dd, *J* 3.6, *J* 8.2, HOOCC*H*), 3.55-3.50 (1H, m, pyrrolidine-*H5'*), 3.28-3.22 (1H, m, pyrrolidine-*H5'*), 2.45 (3H, s, ArC*H$_3$*), 2.19-2.14 (1H, m, pyrrolidine-*H3'*), 2.00-1.87 (2H, m, pyrrolidine-*H3'* and pyrrolidine-*H4'*), 1.79-1.70 (1H, m, pyrrolidine-*H4'*); δ_C (101 MHz, CDCl$_3$) 177.4, 144.1, 134.5, 130.0, 127.6, 60.5, 48.8, 30.9, 24.7, 21.6; *m/z* (ESI) 270 [MH]$^+$; found [MH]$^+$ 270.0796 C$_{12}$H$_{16}$NO$_4$S requires 270.0800, Δ 1.5 ppm.

N-[1-(Toluene-4-sulfonyl)-(R)-pyrrolidin-2-ylmethyl]-acrylamide **67**

Method one *Staudinger reduction*
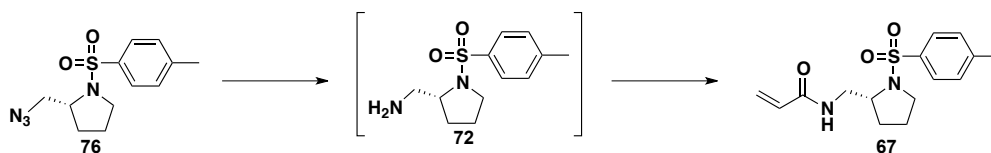
Triphenylphosphine (187.3 mg, 0.714 mmol, 2 eq.) was added to a solution of azide **76** (100 mg, 0.357 mmol, 1 eq.) in THF/H$_2$O (2.5 mL/0.25 mL). The mixture was stirred at rt for 2.5 h. 1M HCl (1 mL) was added and the aqueous layer washed with Et$_2$O (x 3). The aqueous layer was basified with 2N NaOH to pH 12-14 and extracted with EtOAc (x 5). The combined EtOAc layers were washed with brine, dried over MgSO$_4$, filtered and concentrated *in vacuo*. To a solution of the crude amine **72** (80 mg, 0.315 mmol, 1 eq.) in CH$_2$Cl$_2$ (2 mL) at 0 °C under argon was added triethylamine, (0.07 mL, 0.519 mmol, 1.5 eq.) and acryloyl chloride (0.03 mL, 0.346 mmol, 1.1 eq.) and the reaction stirred at 0 °C (15 min) and then at rt overnight. The reaction mixture was poured into aqueous 2M NH$_4$Cl and extracted with CH$_2$Cl$_2$, dried over MgSO$_4$, filtered and concentrated *in vacuo*. The crude yellow oil was purified by flash column chromatography on silica (EtOAc/n-hex, 4:1) to give the desired acrylamide **67** (14.2 mg, 13 %) as a clear oil.

Method 2 *Hydrogenation*
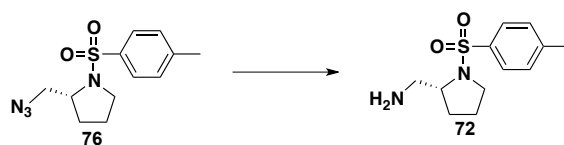
To a solution of azide **76** (700 mg, 2.50 mmol, 1.0 equiv.) in EtOAc (23 mL) under argon was added Pd/C (121 mg, cat.) and the mixture stirred at rt under a H_2 atmosphere for 24 h. The reaction mixture was filtered over celite, washed through with EtOAc and MeOH and the solvent removed under reduced pressure. The crude residue was purified on silica (10 % MeOH/CH_2Cl_2 to 100 % MeOH) to yield the desired amine **72** (532.9 mg, 84 %) as a clear oil.
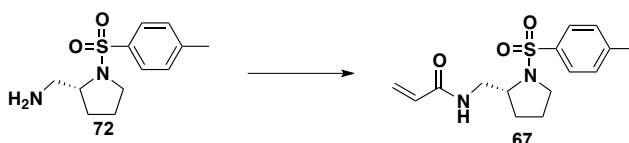
To a solution of amine **72** (242.0 mg, 0.95 mmol, 1.0 equiv.) in anhydrous CH_2Cl_2 (7 mL) at 0 °C under argon was added Et_3N (0.20 mL, 1.43 mmol, 1.5 equiv.) and acryloyl chloride (0.12 mL, 1.43 mmol, 1.5 equiv.) and the resulting solution stirred at 0 °C for 15 min and at rt overnight. The reaction mixture was poured into 2M aqueous NH_4Cl and extracted with CH_2Cl_2 (x 3), dried over Na_2SO_4, filtered and the solvent removed *in vacuo*. The crude residue was purified on silica (4:1, EtOAc/n-hex) to yield the desired acrylamide **67** (216.3 mg, 74 %) as a clear oil.

R_f = 0.4 (n-Hex/EtOAc, 4:1); $[\alpha]^{18}_D$ = + 67.7 (*c* = 0.41, $CHCl_3$); ν_{max} /cm^{-1} 1662, 1627, 1599, 1540, 1342, 1158, 1093, 989, 817, 666; δ_H (400 MHz, $CDCl_3$) 7.73 (2H, d, *J* 8.1, Ar*H*), 7.36 (2H, d, *J* 8.1, Ar*H*), 6.33 (1H, dd, *J* 17.3, *J* 1.6, NHCOCHC*H₂ cis* to C=O), 6.21 (1H, dd, *J* 17.3, *J* 9.7, NHCOC*H*CH₂), 5.69 (1H, dd, *J* 9.7, *J* 1.6, NHCOCHC*H₂ trans* to C=O), 3.78-3.72 (1H, m, pyrrolidine-*H2'*), 3.64-3.58 (1H, m, pyrrolidine-C*H₂*), 3.50-3.45 (1H, m, pyrrolidine-C*H₂*), 3.39-3.33 (1H, m, pyrrolidine-*H5'*), 3.30-3.23 (1H, m, pyrrolidine-*H5'*), 2.46 (3H, s, ArC*H₃*), 1.88-1.47 (4H, m, pyrrolidine-*H3'* and pyrrolidine-*H4'*); δ_C (101 MHz, $CDCl_3$) 166.1, 144.0, 133.8, 131.1, 129.9, 127.6, 126.2, 59.6, 49.7, 44.0, 29.9, 24.2, 21.6; *m/z* (CI) 309 [MH]$^+$, 326 [MNH₄]$^+$; HRMS (ESI) found: [MH]$^+$, 309.1266 $C_{15}H_{21}N_2O_3S$ requires 309.1273, Δ 2.3 ppm.

(R)-N-(1-Methyl-pyrrolidin-2-ylmethyl)-acrylamide **68**
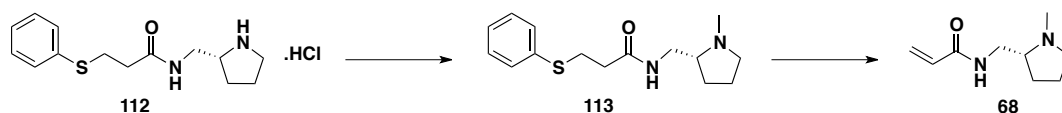
To amine **112** (37.3 mg, 0.12 mmol, 1.0 eq.) and paraformaldehyde (13.0 mg, 0.43 mmol, 3.5 eq.) was added MeOH (4 mL) and the suspension heated at reflux for 20 min. The resulting cloudy white suspension was cooled to 0 °C and $NaCNBH_3$ (77.9 mg, 1.24 mmol, 10 eq.) added. The reaction was warmed to rt and stirred overnight. To the colourless solution was added 10 % $NaHCO_3$ (1 mL) to quench the reaction. The resulting mixture was washed with $CHCl_3$ (x 1) and the organic layer dried over Na_2SO_4, filtered and the solvent removed *in vacuo*. The crude residue was washed

with 1:1 THF/MeOH (2 x 25 mL) and dried under high vacuum to yield the desired *N*-methyl pyrrolidine **113** (33.6 mg, 97 %) which was taken straight onto the next step. δ_H (400 MHz, CDCl$_3$) 7.39-7.36 (2H, m, Ar*H*), 7.33-7.29 (2H, m, Ar*H*), 7.24-7.19 (1H, m, Ar*H*), 6.19 (1H, bs, N*H*), 3.61 (1H, ddd, *J* 13.7, *J* 7.7, *J* 2.8, NHC*H*$_2$), 3.24 (2H, t, *J* 7.2, SC*H*$_2$), 3.14-3.04 (2H, m, NHC*H*$_2$ and pyrrolidine-*H2'*), 2.52 (2H, t, *J* 7.2, SCH$_2$C*H*$_2$), 2.45-2.39 (1H, m, pyrrolidine-*H5'*), 2.33 (3H, s, NC*H*$_3$), 2.28-2.22 (1H, m, pyrrolidine-*H5'*), 1.94-1.84 (1H, m, pyrolidine-*H3'*), 1.75-1.55 (3H, m, pyrrolidine-*H3'* and pyrrolidine-*H4'*).

To the *N*-methyl pyrrolidine thioether **113** (33.6 mg, 0.12 mmol, 1.0 equiv.) was added KO^{t}Bu as a 1.0 M solution in THF (Sigma-Alrich, SureSeal) (1.0 mL, 1.0 mmol, 9.4 eq.) at rt under argon. After 3 h the reaction mixture was loaded onto a silica column (3:7, MeOH/CH$_2$Cl$_2$) to yield the desired *N*-methyl pyrrolidine acrylamide **68** (10.5 mg, 52 %) as a clear oil. R_f = 0.17 (3:7, MeOH/CH$_2$Cl$_2$); $[\alpha]^{24}_D$ = + 72.0 (*c* = 0.67, MeOH); ν_{max} /cm^{-1}; 1662, 1627, 1606, 1554, 1457, 1410, 1245, 985, 957; δ_H (400 MHz, MeOD) 6.30-6.19 (2H, m, C*H*$_2$CHCONH *cis* to C=O and CH$_2$C*H*CONH), 5.67 (1H, dd, *J* 8.8, *J* 3.6, C*H*$_2$CHCONH *trans* to C=O), 3.56 (1H, dd, *J* 13.0, *J* 4.3, NHC*H*$_2$), 3.18 (1H, dd, *J* 13.0, *J* 7.3, NHC*H*$_2$), 3.08 (1H, quintet, *J* 4.8, pyrrolidine-*H2'*), 2.49-2.44 (1H, m, pyrrolidine-*H5'*), 2.42 (3H, s, NC*H*$_3$), 2.31 (1H, dd, q, *J* 9.0, pyrrolidine-*H5'*), 2.04-1.95 (1H, m, pyrrolidine-*H4'*), 1.80-1.73 (2H, m, pyrrolidine-*H4'* and -*H3'*), 1.65-1.56 (1H, m, pyrrolidine-*H3'*); δ_C (101 MHz, CDCl$_3$) 168.5, 132.1, 127.0, 66.7, 58.3, 42.8, 41.2, 30.1, 23.1; *m/z* (ESI) 169 [MH]$^+$; found [MH]$^+$ 169.1335 C$_9$H$_{17}$N$_2$O requires 169.1341, Δ 3.5 ppm.

(R)-N-(1-Methyl-pyrrolidin-2-ylmethyl)-acrylamide **68**
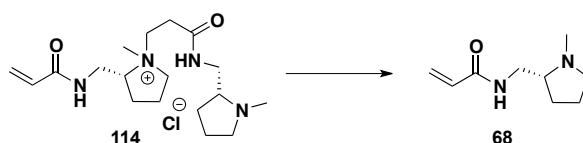
To acrylamide **114** (107.7 mg, 0.29 mmol, 1.0 eq.) was added KO^{t}Bu as 1.0 M solution in THF (Sigma-Aldrich, SureSeal, 2.90 mL, 2.90 mmol, 10 eq.) at rt under an atmosphere of argon. The reaction mixture was stirred at rt for 1 h before addition of sat. aq. NaHCO$_3$ and the layers separated. The aqueous layer was further washed with ether (x 1) and combined organics were dried over MgSO$_4$, filtered and the solvent removed *in vacuo*. The crude residue was purified on silica (CH$_2$Cl$_2$/MeOH, 7:3) to yield the desired acrylamide **68** (56.6 mg, 58 %) as a clear oil. Data in agreement with above.

2-(S)-[4-[2-(R)-(Acryloylamino-methyl)-pyrrolidine-1-sulfonyl]-benzoylamino]-pentanedioic acid **69**
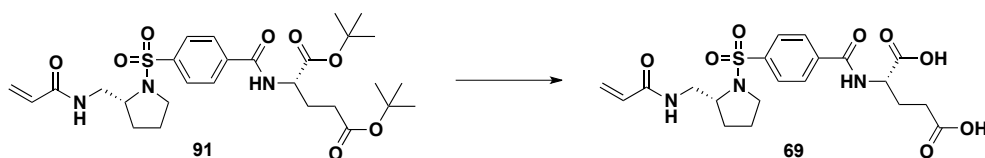
A solution of acrylamide **91** (58.2 mg, 0.10 mmol, 1 eq.) in CHCl$_3$ (3.75 mL) at 0 °C was treated with trifluoroacetic acid (3 mL). The reaction mixture was allowed to warm to rt and stirred for 72 h. The solvent was removed *in vacuo* and the resulting brown residue triturated with ether. The tan coloured precipitate was filtered, washed on the filter paper with cold ether and dried under high vacuum to yield the desired acrylamide **69** (24.7 mg, 53 %) as a tan

coloured powder. R_f = 0 (100 % EtOAc); ν_{max} /cm⁻¹ 1717, 1649, 1625, 1601, 1540, 1448, 1437, 1411, 1399, 1336, 1291, 1247, 1199, 1152, 1092, 1046, 1013, 986, 932, 857, 804, 762, 734, 697; δ_H (400 MHz, MeOD) 8.08 (2H, d, *J* 7.6, Ar*H*), 8.01 (2H, d, *J* 7.6, Ar*H*), 6.34-6.23 (2H, m, C*H₂*CHCONH *cis* to C=O and CH₂C*H*CONH), 5.71 (1H, dd, *J* 9.5, *J* 3.8, CH₂CHCONH *trans* to C=O), 4.69 (1H, bs, ArCONHC*H*), 3.87-3.81 (1H, m, pyrrolidine-*H2'*), 3.62-3.57 (1H, m, CH₂CHCONHC*H₂*), 3.53-3.47 (1H, m, CH₂CHCONHC*H₂*), 3.44-3.38 (1H, m, pyrrolidine-*H5'*), 3.30-3.23 (1H, m, pyrrolidine-*H5'*), 2.52 (2H, t, *J* 6.1, HOOCC*H₂*), 2.39-2.33 (1H, m, HOOCCH₂C*H₂*), 2.18-2.09 (1H, m, HOOCCH₂C*H₂*), 1.91-1.82 (1H, m, pyrrolidine-*H3'*), 1.75-1.70 (1H, m, pyrrolidine-*H3'*), 1.60-1.50 (2H, m, pyrrolidine-*H4'*); *m/z* (ESI) 468 [MH]⁺; found: [MH]⁺, 468.1444 C₂₀H₂₆N₃O₈S requires 468.1441, Δ 0.6 ppm.

(R)-Ethenesulfonic acid [1-(toluene-4-sulfonyl)-pyrrolidin-2-ylmethyl]-amide **70**
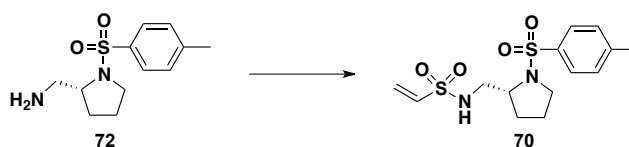
2-Chloroethanesulfonyl chloride (0.08 mL, 0.75 mmol, 1.0 eq.) was added dropwise to a stirred solution of amine **72** (190 mg, 0.75 mmol, 1.0 eq.) and triethylamine (0.36 mL, 2.61 mmol, 3.5 eq.) in dry CH₂Cl₂ (4 mL) at 0 °C under argon. After addition, stirring was continued at 0 °C for 1 h and at rt overnight. The mixture was diluted with CH₂Cl₂, washed with brine, dried over MgSO₄, filtered and concentrated *in vacuo*. The crude brown amorphous solid was purified by flash column chromatography on silica (EtOAc/n-hex, 1:1) to yield the desired vinyl sulfonamide **70** (108.5 mg, 42 %) as a clear oil. R_f = 0.34 (EtOAc/n-hex, 1:1); $[\alpha]^{20}_D$ = +109.1 (*c* = 0.37, CHCl₃); ν_{max} /cm⁻¹ 1598, 1495, 1451, 1428, 1384, 1328, 1255, 1200, 1149, 1091, 1040, 972, 915, 867, 817, 729, 663; δ_H (400 MHz, CDCl₃) 7.71 (2H, d, *J* 8.3, Ar*H*), 7.34 (2H, d, *J* 8.3, Ar*H*), 6.60 (1H, dd, *J* 9.7, *J* 16.6, NHSO₂C*H*CH₂), 6.26 (1H, d, *J* 16.6, NHSO₂CHC*H₂ cis* to C=O), 5.98 (1H, d, *J* 9.7, NHSO₂CHC*H₂ trans* to C=O), 5.36 (1H, t, *J* 5.5, N*H*), 3.70-3.64 (1H, m, pyrrolidine-*H2'*), 3.47-3.41 (1H, m, pyrrolidine-*H5'*), 3.26-3.13 (3H, m, pyrrolidine-*H5'* and pyrrolidine-C*H₂*), 2.43 (3H, s, ArC*H₃*), 1.84-1.76 (2H, m, pyrrolidine-*H3'*), 1.72-1.61 (1H, m, pyrrolidine-*H4'*), 1.50-1.41 (1H, m, pyrrolidine-*H4'*); δ_C (101 MHz, CDCl₃) 144.2, 135.9, 133.5, 130.0, 127.7, 126.8, 59.4, 50.0, 47.4, 29.6, 24.1, 21.7; *m/z* (CI) 345 [MH]⁺, 362 [MNH₄]⁺; found: [MH]⁺, 345.0943 C₁₄H₂₁N₂O₄S₂ requires 345.0943, Δ 0 ppm.

2-(S)-(4-[2-(R)-(Ethenesulfonylamino-methyl)-pyrrolidine-1-sulfonyl]-benzoylamino)-pentanedioic acid **71**
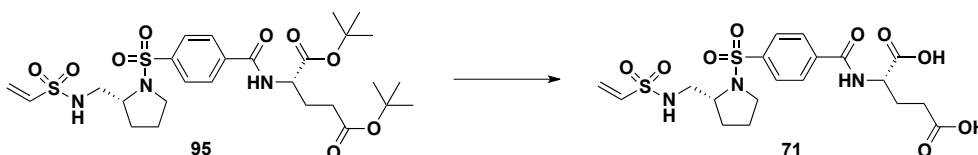
To a solution of sulfonamide **95** (651.6 mg, 1.06 mmol, 1 equiv.) in anhydrous CH₂Cl₂ (20 mL) was added TFA (15 mL) and Et₃SiH (0.84 mL, 5.28 mmol, 5 equiv.) at 0 °C under argon. The reaction was allowed to warm to rt and stirred for 4 days. The solvent was removed *in vacuo* and ether added to the brown residue. The resulting tan coloured precipitate was filtered under reduced pressure and washed thoroughly on the filter paper with ether to give the desired vinyl sulfonamide **71** (500.0 mg, 94 %) as a tan coloured powder, mp = 135-140 °C; R_f = 0 (100 % EtOAc);

ν_{max} /cm^{-1} 1707, 1642, 1603, 1544, 1420, 1324, 1200, 1143, 1090, 855, 799, 733, 616; δ_H (400 MHz, DMSO-d$_6$) 12.50 (2H, bs, COO*H*), 8.86 (1H, bs, ArCHN*H*), 8.10 (2H, d, *J* 7.3, Ar*H*), 7.91 (2H, d, *J* 7.3, Ar*H*), 7.52 (1H, t, *J* 5.5, SO$_2$N*H*), 6.74 (1H, dd, *J* 9.0, *J* 18.2, NHSO$_2$C*H*CH$_2$), 6.07 (1H, d, *J* 18.2, NHSO$_2$CHCH$_2$ *cis* to sulfonamide), 6.02 (1H, d, *J* 9.0, NHSO$_2$CHCH$_2$ *trans* to sulfonamide), 4.41 (1H, bs, ArCONHC*H*), 3.60-3.56 (1H, m, pyrrolidine-*H2'*), 3.38-3.33 (1H, m, pyrrolidine-*H5'*), 3.13-3.15 (1H, m, pyrrolidine-*H5'*), 3.04-3.10 (1H, m, SO$_2$NHC*H*$_2$), 2.89-2.82 (1H, m, SO$_2$NHC*H*$_2$), 2.38 (2H, bs, C*H*$_2$COOH), 2.12 (1H, bs, C*H*$_2$CH$_2$COOH), 1.97 (1H, bs, C*H*$_2$CH$_2$COOH), 1.78-1.71 (2H, m, pyrrolidine-*H4'*), 1.49-1.39 (2H, m, pyrrolidine-*H3'*); *m/z* (ESI) 504 [MH]$^+$, 526 [MNa]$^+$; found: [MH]$^+$, 504.1117 C$_{19}$H$_{26}$N$_3$O$_9$S$_2$ requires 504.1110, Δ 1.4 ppm.

(R)-[1-(Toluene-4-sulfonyl)-pyrrolidin-2-yl]-methylamine **72**
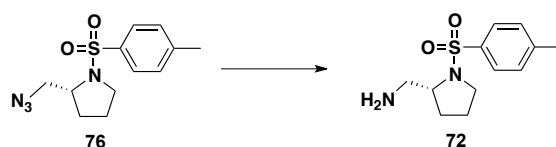
Triphenylphosphine (748.6 mg, 2.85 mmol, 2 eq.) was added to a solution of azide **76** (400 mg, 1.43 mmol, 1 eq.) in THF/H$_2$O (10/1 mL) and the mixture stirred for 3 h at rt under argon. 1 M HCl (4 mL) was added to the reaction and the aqueous layer washed with Et$_2$O (x 3). The aqueous layer was basified with 2N NaOH to pH 12-14 and extracted with EtOAc (x 5). The combined EtOAc layers were dried over MgSO$_4$, filtered and concentrated *in vacuo*. The crude yellow oil was purified by flash column chromatography on silica (gradient elution CH$_2$Cl$_2$/MeOH, 9:1 to 100 % MeOH) to yield the desired amine **72** (190 mg, 52 %) as a light yellow oil. R$_f$ = 0 (EtOAc/n-hex, 1:1); $[\alpha]^{21}_D$ = +147.4 (*c* = 0.38, CHCl$_3$); ν_{max} /cm^{-1} 2953, 2869, 1335, 1154, 1090, 816, 662; δ_H (400 MHz, CDCl$_3$) 7.64 (2H, d, *J* 8.0, Ar*H*), 7.24 (2H, d, *J* 8.0, Ar*H*), 3.55-3.50 (1H, m, pyrrolidine-*H2'*), 3.34-3.28 (1H, m, pyrrolidine-*H5'*), 3.16-3.10 (1H, m, pyrrolidine-*H5'*), 2.75 (2H, d, *J* 5.5, pyrrolidine-C*H*$_2$), 2.34 (3H, s, ArC*H*$_3$), 1.72-1.33 (4H, m, pyrrolidine-*H3'* and pyrrolidine-*H4'*); δ_C (101 MHz, CDCl$_3$) 143.4, 134.2, 129.6, 127.4, 62.4, 49.3, 46.4, 28.9, 24.0, 21.4; *m/z* (CI) 255 [MH]$^+$; found: [MH]$^+$, 255.1170 C$_{12}$H$_{19}$N$_2$O$_2$S requires 255.1167, Δ 1.2 ppm.

(R)-Toluene-4-sulfonic acid 1-(toluene-4-sulfonyl)-pyrrolidin-2-ylmethyl ester **73**

Method one: *from* D-*proline*
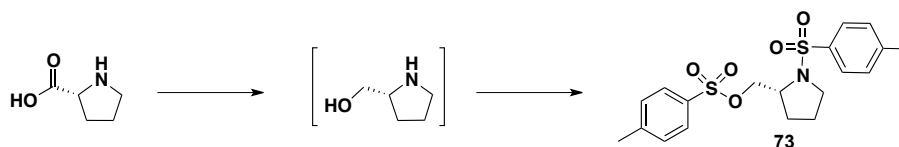
LiAlH$_4$ (516 mg, 12.88 mmol, 1.5 eq.) was cooled to 0 °C under argon before addition of anhydrous THF (16 mL) and D-proline (1.00 g, 8.69 mmol, 1.0 eq.) portionwise as a solid. The resultant mixture was stirred at 0 °C for 1 h and at rt for 1 h. 20 % aqueous NaOH (2 mL) was added dropwise with vigorous evolution of H$_2$ (g). The resultant white precipitate was filtered through celite under reduced pressure and the filtrate dried over Na$_2$SO$_4$, filtered and the solvent removed *in vacuo*. To the resultant yellow oil at 0 °C under argon was added a solution of TsCl (4.97 g, 26.07

mmol, 3.0 eq.) in pyridine (8 mL) dropwise. The resulting black solution was warmed to rt and stirred overnight. The reaction mixture was poured into H_2O and extracted with CH_2Cl_2 (x 3). Combined organics were washed with 1M HCl (x 3), dried over $MgSO_4$, filtered and the solvent removed *in vacuo*. The crude black residue was purified on silica (EtOAc/n-hex, 1:3) to yield the desired bis tosylate **73** (1.76 g, 49 %) as a white solid.

Method 2: *from D-prolinol*
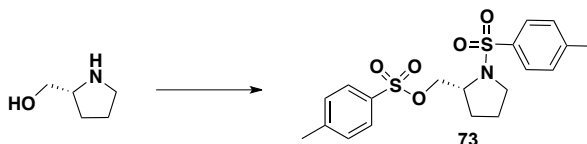
To a solution of *p*-toluenesulfonyl chloride (2.90 g, 15.2 mmol, 3.0 eq.) in dry pyridine (5.2 mL) at 0 °C under argon was added D-prolinol (0.50 mL, 5.1 mmol, 1.0 eq.) dropwise and the mixture allowed to warm to rt and stirred for 12 h. The solution was poured into ice-water and extracted with CH_2Cl_2 (x 4). The combined organics were dried over $MgSO_4$, filtered and the solvent removed *in vacuo*. The crude red oil was purified by flash column chromatography on silica (EtOAc/n-hexane, 2:3) to give the bis-tosylated D-prolinol **73** (1.93 g, 100 %) as a white solid, mp = 94-96 °C; R_f = 0.28 (EtOAc/n-pentane, 1:3); $[\alpha]^{22}_D$ = + 108.1 (*c* = 1.17, CHCl₃); ν_{max} /cm⁻¹ 1599, 1454, 1345, 1189, 1175, 1158, 1094, 1044, 967, 908, 730; δ_H (400 MHz, CDCl₃) 7.78 (2H, d, *J* 8.5, Ar*H*), 7.62 (2H, d, *J* 8.5, Ar*H*), 7.35 (2H, d, *J* 8.5, Ar*H*), 7.28 (2H, d, *J* 8.5, Ar*H*), 4.24 (1H, dd, *J* 3.2, *J* 10.5, TsOC*H₂*), 3.95 (1H, dd, *J* 6.3, *J* 10.5, TsOC*H₂*), 3.73-3.67 (1H, m, pyrrolidine-*H2'*), 3.37-3.32 (1H, m, pyrrolidine-*H5'*), 3.04-2.98 (1H, m, pyrrolidine-*H5'*), 2.42 (3H, s, ArC*H₃*), 2.38 (3H, s, ArCH₃), 1.82-1.69 (2H, m, pyrrolidine-*H4'*), 1.62-1.46 (2H, m, pyrrolidine-*H3'*); δ_C (101 MHz, CDCl₃) 145.1, 143.9, 133.4, 130.0, 129.8, 129.8, 127.9, 127.5, 71.5, 57.6, 49.3, 28.5, 23.7, 21.6, 21.5; *m/z* (CI) 410 [MH]⁺, 427 [MNH₄]⁺; found: [MH]⁺, 410.1087 $C_{19}H_{24}NO_5S_2$ requires 410.1096, Δ 2.2 ppm.

(R)-[1-(Toluene-4-sulfonyl)-pyrrolidin-2-yl]-methanol **74**
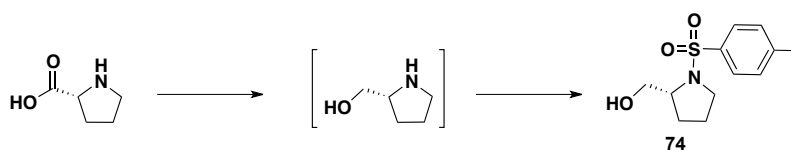
To D-proline (200 mg, 1.74 mmol, 1.0 eq.) in anhydrous THF (1 mL) at 0 °C under argon was added $LiAlH_4$ as a 1.0 M solution in THF (Sigma-Aldrich, SureSeal) (2.6 mL, 2.61 mmol, 1.5 eq.) The reaction mixture was stirred at 0 °C for one hour and at rt for one hour. 20 % aqueous NaOH (0.40 mL) was added dropwise to give vigorous evolution of hydrogen gas and a thick white precipitate. The mixture was filtered through celite, dried over Na_2SO_4 and concentrated to approximately 20 mL. TsCl (332 mg, 1.74 mmol, 1.0 eq.) in anhydrous THF (3 mL) was added dropwise and the resulting brown solution stirred at rt for 7 h. The reaction was quenched with brine and extracted with Et_2O (x 1).The organic layer was dried over Na_2SO_4, filtered and the solvent removed *in vacuo*. The resulting crude brown residue was purified on silica (1:1, n-hexane/EtOAc) to yield the desired N-tosylate D-prolinol **74** (256 mg, 58 %) as a white solid, mp = 89-91 °C; R_f = 0.19 (1:1, EtOAc/n-hexane); $[\alpha]^{20}_D$ = + 58.1 (*c* = 0.87, CHCl₃); ν_{max} /cm⁻¹ 3464 (b), 2956, 2874, 1339, 1157, 1092, 1044, 817, 665, 588; δ_H (400 MHz, CDCl₃) 7.71 (2H, d, *J* 8.2, Ar*H*),

7.31 (2H, d, *J* 8.2, Ar*H*), 3.70-3.57 (3H, m, HOC*H₂* and pyrrolidine-*H2'*), 3.46-3.40 (1H, m, pyrrolidine-*H5'*), 3.27-3.20 (1H, m, pyrrolidine-*H5'*), 2.41 (s, 3H, ArC*H₃*), 1.82-1.72 (1H, m, pyrrolidine-*H4'*), 1.68-1.63 (2H, m, pyrrolidine-*H4'* and -*H3'*), 1.46-1.37 (1H, m, pyrrolidine-*H3'*); δ_C (101 MHz, CDCl₃) 144.0, 134.1, 130.0, 127.8, 66.1, 62.1, 50.3, 29.1, 24.5, 21.7; *m/z* (ESI) 256 [MH]⁺; found [MH]⁺ 256.0998 $C_{12}H_{18}NO_3S$ requires 256.1007, Δ 3.5 ppm.

(R)-1-(Toluene-4-sulfonyl)-pyrrolidine-2-carbaldehyde **75**
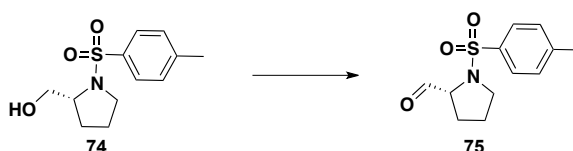
To D-prolinol **74** (125.8 mg, 0.49 mmol, 1.0 eq.) and Dess-Martin periodinane (523.3 mg, 1.23 mmol, 2.5 eq.) at 0 °C was added anhydrous CH₂Cl₂ (3.0 mL) and the mixture stirred at rt for 1.5 h. The mixture was diluted with CH₂Cl₂ and washed with saturated aq. NaHCO₃ (x 2) and saturated aq. Na₂S₂O₃ and the aqueous layer extracted with CH₂Cl₂ (x 1). The organic layer was washed with saturated Na₂S₂O₃, dried over anhydrous Na₂SO₄, filtered and the solvent removed *in vacuo*. The crude product was purified on silica (1:1, EtOAc/n-hex) to yield the desired aldehyde **75** (44.3 mg, 36 %) as a white solid, mp = 135-137 °C; $[\alpha]^{28}_D$ = + 206.2 (*c* = 2.90, CHCl₃); ν_{max} /cm⁻¹ 1732, 1338, 1158, 1093, 906, 727, 663, 588; δ_H (400 MHz, CDCl₃) 9.70 (1H, d, *J* 2.0, aldehyde-*H*), 7.74 (2H, d, *J* 8.2, Ar*H*), 7.37 (2H, d, *J* 8.2, Ar*H*), 3.86-3.83 (1H, m, pyrrolidine-*H2'*), 3.59-3.55 (1H, m, pyrrolidine-*H5'*), 3.24-3.18 (1H, m, pyrrolidine-*H5'*), 2.46 (3H, s, ArC*H₃*), 2.11-2.04 (1H, m, pyrrolidine-*H4'*), 1.89-1.79 (2H, m, pyrrolidine-*H4'* and pyrrolidine-*H3'*), 1.71-1.62 (1H, pyrrolidine-*H3'*). δ_C (101 MHz, CDCl₃) 200.4, 144.4, 133.6, 130.1, 127.9, 66.7, 49.3, 27.7, 24.8, 21.7; *m/z* (ESI) 254 [MH]⁺; found [MH]⁺ 254.0843 $C_{12}H_{16}NO_3S$ requires 254.0851, Δ 3.1 ppm.

(R)-2-Azidomethyl-1-(toluene-4-sulfonyl)-pyrrolidine **76**
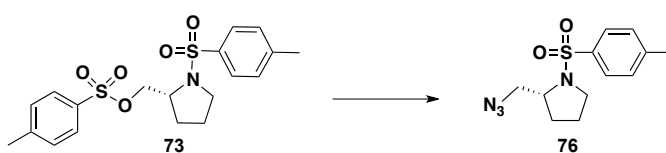
A mixture of bis-tosylate **73** (1.085 g, 2.65 mmol, 1 eq.) and sodium azide (397.6 mg, 6.12 mmol, 2.15 eq.) in diethylene glycol (4.2 mL) was stirred and heated at 100 °C for 1h. The solution was cooled to 60 °C and diluted slowly with iced water (5.2 mL). The resulting white precipitate was filtered and washed thoroughly with cold water. The crude white solid was recrystallised from ethanol/water to give the desired azide **76** (556.5 mg, 76 %) as long white needles, mp = 82-84 °C; R_f = 0.64 (EtOAc/n-hex, 1:1); $[\alpha]^{26}_D$ = + 89.7 (*c* = 1.36, CHCl₃); ν_{max} /cm⁻¹ 2102, 2078, 1342, 1330, 1311, 1292, 1204, 1158, 1094, 1052, 1028, 975, 826, 722; δ_H (400 MHz, CDCl₃) 7.75 (2H, d, *J* 7.9, Ar*H*), 7.36 (2H, d, *J* 7.9, Ar*H*), 3.72-3.69 (1H, m, pyrrolidine-*H2'*), 3.60-3.45 (3H, m, C*H₂*N₃ and pyrrolidine-*H5'*), 3.20-3.14 (1H, m, pyrrolidine-*H5'*), 2.46 (3H, s, ArC*H₃*), 1.94-1.52 (4H, m, pyrrolidine-*H3'* and pyrrolidine-*H4'*); δ_C (101 MHz, CDCl₃) 144.0, 134.2, 130.0, 127.8, 59.1, 55.4, 49.7, 29.5, 24.2, 21.7; *m/z* (CI) 281 [MH]⁺, 298 [MNH₄]⁺; found: [MH]⁺, 281.1072 $C_{12}H_{17}N_4O_2S$ requires 281.1072, Δ 0 ppm.

4-Chlorosulfonyl-benzoic acid methyl ester **77**
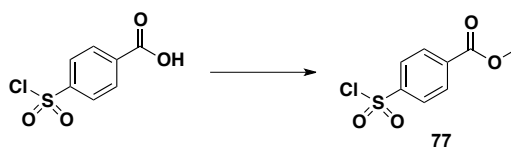
A procedure reported by Winans *et al.* was used.[282] 4-Chlorosulfonyl benzoic acid (5.0 g, 23 mmol, 1 eq.) was suspended in thionyl chloride (20 mL) and dichloroethane (10 mL) and the mixture heated to reflux for 1 h. The reaction mixture was concentrated *in vacuo* to a light brown solid which was chilled on ice before addition of ice cold methanol (40 mL). The resulting mixture was stirred at 0 °C for 5 min and at rt for 10 min before addition of ice cold H_2O (40 mL). The resulting white precipitate was filtered under reduced pressure, washed with ice cold H_2O and dried under vacuum to yield the desired methyl ester **77** (5.0 g, 93 %) as a white solid, mp = 64-66 °C; R_f = 0.69 (EtOAc/n-hex, 1:1); δ_H (400 MHz, CDCl$_3$) 8.30 (2H, d, *J* 8.5, Ar*H*), 8.14 (2H, d, *J* 8.5, Ar*H*), 4.01 (3H, s, OC*H$_3$*); δ_C (101 MHz, CDCl$_3$) 165.1, 147.6, 136.2, 131.1, 127.3, 53.2. Data in agreement with literature values.[282]

4-methyl ester benzenesulfonic acid 1-(R)-(4-methyl ester-benzenesulfonyl)-pyrrolidin-2-ylmethyl ester **78**
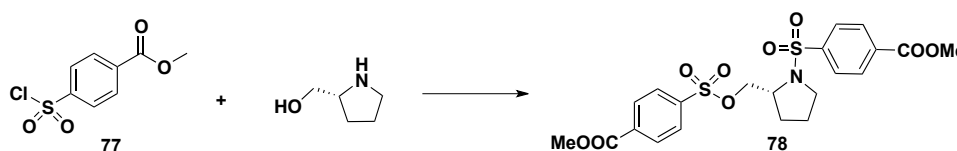
To a solution of 4-chlorosulfonyl-benzoic acid methyl ester **77** (713.4 mg, 3.04 mmol, 3 eq.) in anhydrous CH_2Cl_2 (5 mL) was added triethylamine (0.42 mL, 3.04 mmol, 3 eq.) and D-prolinol (0.1 mL, 1.013 mmol, 1 eq.) at 0 °C under argon, and the mixture stirred at rt overnight. The reaction was quenched with H_2O and extracted with CH_2Cl_2 (x 2), dried over MgSO$_4$, filtered and the solvent removed *in vacuo*. The crude white solid was purified by flash column chromatography on silica (EtOAc/n-hex, 1:1) to yield the desired bis-sulfonylated pyrrolidine **78** (152.8 mg, 30 %) as a white solid, mp = 184-185 °C; R_f = 0.33 (EtOAc/n-hex, 1:1); $[\alpha]^{20}_D$ = + 96.8 (*c* = 3.1, CHCl$_3$); ν_{max} /cm^{-1} 1718, 1435, 1401, 1367, 1348, 1275, 1183, 1163, 1109, 1091, 1014, 986, 966, 907, 859, 791, 765, 733, 694; δ_H (400 MHz, CDCl$_3$) 8.20 (2H, d, *J* 8.5, Ar*H*), 8.13 (2H, d, *J* 8.5, Ar*H*), 7.97 (2H, d, *J* 8.5, Ar*H*), 7.79 (2H, d, *J* 8.5, Ar*H*), 4.26 (1H, dd, *J* 10.0, *J* 7.0, ArSO$_3$C*H$_2$*), 4.03 (1H, dd, *J* 10.0, *J* 7.0, ArSO$_3$C*H$_2$*), 3.94 (1H, s, OC*H$_3$*), 3.92 (1H, s, OC*H$_3$*), 3.73-3.69 (1H, m, pyrrolidine-*H*), 3.40-3.34 (1H, m, pyrrolidine-*H*), 3.05-2.98 (1H, m, pyrrolidine-*H*), 1.87-1.74 (2H, m, pyrrolidine-*H*), 1.65-1.48 (2H, m, pyrrolidine-*H*); δ_C (101 MHz, CDCl$_3$) 165.5, 165.3, 140.3, 139.4, 135.1, 134.2, 130.6, 130.4, 128.1, 127.5, 71.9, 57.8, 52.8, 52.7, 49.4, 28.6, 23.8; *m/z* (ESI) 498 [MH]$^+$; found: [MH]$^+$, 498.0874 $C_{21}H_{24}NO_9S_2$ requires 498.0893, Δ 3.8 ppm.

4-(2-(R)-Hydroxymethyl-pyrrolidine-1-sulfonyl)-benzoic acid methyl ester **79**
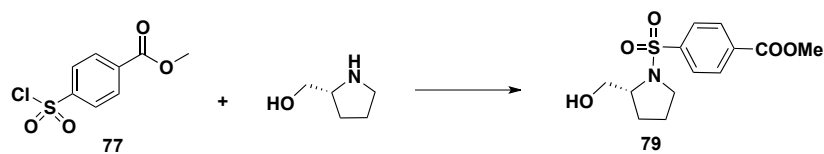
To a solution of sulfonyl chloride **77** (1.90 g, 8.12 mmol, 1.0 eq.) in anhydrous CH_2Cl_2 (15.8 mL) was added D-prolinol (0.80 mL, 8.12 mmol, 1.0 eq.) and triethylamine (1.35 mL, 9.74 mmol, 1.2 eq.) at 0 °C under argon and the mixture stirred at rt for 1 h. The reaction was quenched with H_2O and extracted with CH_2Cl_2 (x 2). The combined organics were washed with 2N HCl, dried over $MgSO_4$, filtered and the solvent removed *in vacuo* to give the desired pyrrolidine **79** (2.28 g, 94 %) as a white solid, mp = 86-88 °C; R_f = 0.19 (EtOAc/n-hex, 1:1); $[\alpha]^{20}_D$ = + 53.0 (c = 1.43, $CHCl_3$); ν_{max} /cm^{-1} 3468, 1725, 1445, 1437, 1399, 1337, 1284, 1197, 1156, 1108, 1091, 1038, 1012, 987, 857, 808, 761, 734, 693; δ_H (400 MHz, $CDCl_3$) 8.18 (2H, d, J 8.3, Ar*H*), 7.90 (2H, d, J 8.3, Ar*H*), 3.94 (3H, s, OC*H₃*), 3.71-3.59 (3H, m, pyrrolidine-C*H₂*OH and pyrrolidine-*H*), 3.50-3.44 (1H, m, pyrrolidine-*H*), 3.26-3.20 (1H, m, pyrrolidine-*H*), 2.39 (1H, bs, O*H*), 1.85-1.59 (3H, m, pyrrolidine-*H*), 1.48-1.38 (1H, m, pyrrolidine-*H*); δ_C (101 MHz, $CDCl_3$) 165.8, 141.0, 134.3, 130.6, 127.8, 65.9, 62.2, 52.9, 50.2, 29.0, 24.4; *m/z* (ESI) 300 [MH]$^+$; found: [MH]$^+$, 300.0902 $C_{13}H_{18}NO_5S$ requires 300.0906, Δ 1.3 ppm.

4-(2-(R)-Formyl-pyrrolidine-1-sulfonyl)-benzoic acid methyl ester **80**
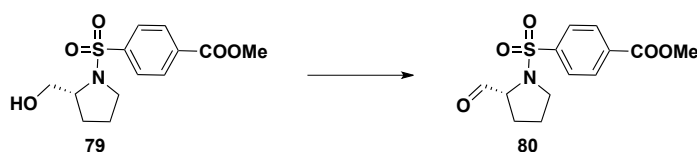
To a solution of alcohol **79** (50 mg, 0.17 mmol, 1 eq.) in CH_2Cl_2 (1.5 mL) was added Dess-Martin periodinane (85 mg, 0.20 mmol, 1.2 eq.) at 0 °C and the mixture stirred at rt for 1.5 h. To the mixture was added sat. $NaHCO_3$ aq. and the aqueous layer extracted with CH_2Cl_2 (x 2). The combined organics were washed with brine (x 1) and dried over $MgSO_4$, filtered and the solvent removed *in vacuo*. The crude clear oil was purified by flash column chromatography on silica (EtOAc/n-hex, 2:3) to yield the desired aldehyde **80** (34 mg, 69 %) as a white solid, mp = 107-109 °C; R_f = 0.8 (100 % EtOAc); $[\alpha]^{26}_D$ = + 157.6 (c = 1.57, $CHCl_3$); ν_{max} /cm^{-1} 1726, 1437, 1400, 1349, 1977, 1160, 1110, 1091, 766, 733, 695; δ_H (400 MHz, $CDCl_3$) 9.64 (1H, d, J 2.2, aldehyde-*H*), 8.18 (2H, d, J 8.9, Ar*H*), 7.88 (2H, d, J 8.9, Ar*H*), 3.93 (3H, s, OC*H₃*), 3.88-3.84 (1H, m, pyrrolidine-*H*), 3.58-3.53 (1H, m, pyrrolidine-*H*), 3.21-3.15 (1H, m, pyrrolidine-*H*), 2.08-2.00 (1H, m, pyrrolidine-*H*), 1.86-1.76 (2H, m, pyrrolidine-*H*), 1.68-1.60 (1H, m, pyrrolidine-*H*); δ_C (101 MHz, $CDCl_3$) 199.5, 165.5, 140.5, 134.4, 130.5, 127.6, 66.6, 52.8, 49.2, 27.6, 24.7; *m/z* (CI) 298 [MH]$^+$, 315 [MNH$_4$]$^+$; HRMS (ESI) found: [MH]$^+$, 298.0751 $C_{13}H_{16}NO_5S$ requires 298.0749, Δ 0.7 ppm.

4-[2-(R)-(Toluene-4-sulfonyloxymethyl)-pyrrolidine-1-sulfonyl]-benzoic acid methyl ester **81**
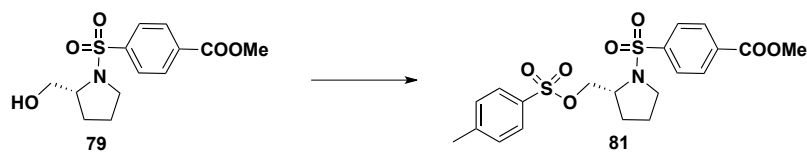
To a solution of alcohol **79** (1.74 g, 5.8 mmol, 1.0 eq.) and *p*-toluene sulfonyl chloride (3.32 g, 17.4 mmol, 3.0 eq.) in anhydrous CH_2Cl_2 (10 mL) at 0 °C under argon was added triethylamine (2.42 mL, 17.4 mmol, 3.0 eq.) and the mixture stirred at rt for 6 h. The reaction mixture was poured into aqueous 2N HCl and extracted with CH_2Cl_2 (x 1). The organic layer was dried over $MgSO_4$, filtered and the solvent removed *in vacuo*. The crude solid was purified by flash column chromatography on silica (7:3, n-hex/EtOAc) to yield the desired bis-sulfone **81** (2.35 mg, 89 %) as a white solid, mp = 124-125 °C; $[\alpha]^{20}_D$ = + 97.1 (*c* = 1.4, $CHCl_3$); R_f = 0.31 (EtOAc/n-hex, 3:7); ν_{max} /cm^{-1} 1720, 1598, 1435, 1403, 1360, 1345, 1279, 1189, 1160, 1112, 1092, 1052, 1016, 1003, 994, 963, 907, 845, 814, 783, 765, 734, 696, 666; δ_H (400 MHz, $CDCl_3$) 8.15 (2H, d, *J* 8.1, Ar*H*), 7.82 (2H, d, *J* 8.1, Ar*H*), 7.79 (2H, d, *J* 8.1, Ar*H*), 7.36 (2H, d, *J* 8.1, Ar*H*), 4.22 (1H, dd, *J* 10.5, *J* 3.4, pyrrolidine-C*H$_2$*), 3.97-3.93 (1H, m, pyrrolidine-C*H$_2$*), 3.94 (3H, s, ArCO$_2$C*H$_3$*), 3.77-3.72 (1H, m, pyrrolidine-*H*), 3.42-3.38 (1H, m, pyrrolidine-*H*), 3.07-3.01 (1H, m, pyrrolidine-*H*), 2.45 (3H, s, ArC*H$_3$*), 1.91-1.76 (2H, m, pyrrolidine-*H*), 1.66-1.51 (2H, m, pyrrolidine-*H*); δ_C (101 MHz, $CDCl_3$) 165.8, 145.4, 140.7, 134.4, 132.7, 130.6, 130.2, 128.2, 127.7, 71.4, 58.1, 52.9, 49.6, 28.8, 24.0, 21.9; *m/z* (ESI) 454 [MH]$^+$, 476 [MNa]$^+$; found: [MH]$^+$, 454.1006 $C_{20}H_{24}NO_7S_2$ requires 454.0994, Δ 2.6 ppm.

4-(2-(R)-Azidomethyl-pyrrolidine-1-sulfonyl)-benzoic acid methyl ester **82**
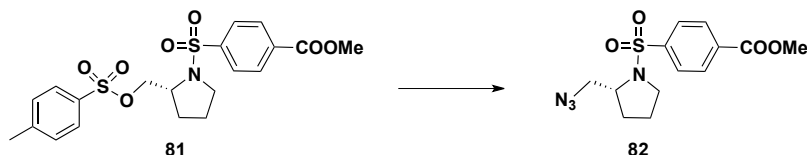
A solution of pyrrolidine **81** (200 mg, 0.44 mmol, 1 eq.) and NaN_3 (61.6 mg, 0.95 mmol, 2.15 eq.) in DMF (5 mL) was heated with stirring to 50 °C for 1.5 h and to 90 °C for 3h. The reaction mixture was diluted with 2M aq. NH_4Cl and extracted with EtOAc (x 3). The combined organics were dried over $MgSO_4$, filtered and the solvent removed *in vacuo* to yield the desired azide **82** (133.7 mg, 94 %) as a white powder, mp = 61-62 °C; $[\alpha]^{23}_D$ = + 101.3 (*c* = 1.0, $CHCl_3$); R_f = 0.56 (EtOAc/n-hex, 1:1); ν_{max} /cm^{-1} 2101, 1727, 1437, 1400, 1350, 1278, 1199, 1161, 1109, 1090, 1044, 1016, 990, 766, 742, 734, 695, 620, 580; δ_H (400 MHz, $CDCl_3$) 8.18 (2H, d, *J* 8.3, Ar*H*), 7.90 (2H, d, *J* 8.3, Ar*H*), 3.94 (3H, s, OC*H$_3$*), 3.73-3.68 (1H, m, pyrrolidine-*H*), 3.56-3.44 (3H, m, pyrrolidine-*H* and pyrrolidine-C*H$_2$*), 3.18-3.12 (1H, m, pyrrolidine-*H*), 1.92-1.77 (2H, m, pyrrolidine-*H*), 1.70-1.49 (2H, m, pyrrolidine-*H*); δ_C (101 MHz, $CDCl_3$) 165.8, 141.1, 134.3, 130.6, 127.7, 59.3, 55.3, 52.9, 49.7, 29.5, 24.3; *m/z* (ESI) 325 [MH]; found: [MH]$^+$, 325.0956 $C_{13}H_{17}N_4O_4S$ requires 325.0971, Δ 4.6 ppm.

4-(2-(R)-Aminomethyl-pyrrolidine-1-sulfonyl)-benzoic acid methyl ester **83**
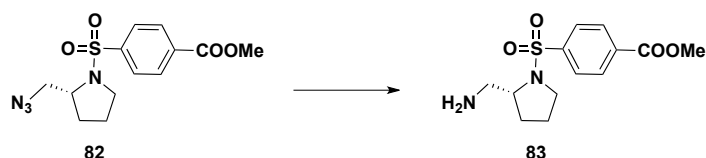
Method One: *Staudinger Reduction*

Triphenylphosphine (161.7 mg, 0.62 mmol, 2 eq.) was added to a solution of azide **82** (100 mg, 0.31 mmol, 1 eq.) in THF/H$_2$O (2.5/0.25 mL). The mixture was stirred at rt for 3h before removal of the solvent *in vacuo*. The crude mixture was purified by flash column chromatography on silica (CH$_2$Cl$_2$/MeOH, 9:1) to yield the desired amine **83** (44.8 mg, 48 %) as a clear oil. The intermediate iminophosphorane **84** was also isolated (40.7 mg, 24 %) as a clear oil.

Method Two: *Hydrogenation*

To a solution of azide **82** (109 mg, 0.34 mmol, 1 eq.) in EtOAc (3 mL) was added Pd/C (15 mg, cat.). The mixture was stirred at rt under a H$_2$ balloon for 24 h, then filtered through celite and the filter cake washed with EtOAc and MeOH. Removal of the solvent under reduced pressure yielded the desired amine **83** (102.5 mg, quant.) as a clear oil.

$[\alpha]^{23}_D$ = + 59.3 (c = 1.1, CHCl$_3$); R$_f$ = 0 (EtOAc/n-hex, 1:1); ν_{max} /cm^{-1} 1728, 1437, 1400, 1344, 1282, 1197, 1162, 1111, 1090, 1015, 990, 767, 733, 696, 623, 581; δ_H (400 MHz, CDCl$_3$) 8.12 (2H, d, *J* 8.5, Ar*H*), 7.85 (2H, d, *J* 8.5, Ar*H*) 3.89 (3H, s, OC*H$_3$*), 3.60-3.54 (1H, m, pyrrolidine-*H*), 3.40-3.35 (1H, m, pyrrolidine-*H*), 3.18-3.12 (1H, m, pyrrolidine-*H*), 2.83-2.75 (2H, m, H$_2$NC*H$_2$*), (2H, bs, N*H$_2$*), 1.79-1.70 (1H, m, pyrrolidine-*H*), 1.68-1.60 (1H, m, pyrrolidine-*H*), 1.54-1.47 (1H, m, pyrrolidine-*H*), 1.45-1.36 (1H, m, pyrrolidine-*H*); δ_C (101 MHz, CDCl$_3$) 165.7, 141.4, 134.0, 130.4, 127.6, 62.6, 52.8, 49.5, 46.4, 29.1, 24.2; *m/z* (ESI) 299 [MH]$^+$; found: [MH]$^+$, 299.1059 C$_{13}$H$_{19}$N$_2$O$_4$S requires 299.1066, Δ 2.3 ppm.

4-(2-(R)-(triphenylphosphineimine)methyl-pyrrolidine-1-sulfonyl)-benzoic acid methyl ester **84**
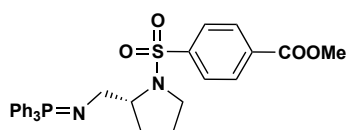
R$_f$ = 0 (EtOAc/n-hex, 1:1); δ_H (400 MHz, CDCl$_3$) 8.12 (2H, d, *J* 8.5, Ar*H*), 7.94-7.88 (6H, m, Ar*H*), 7.83-7.79 (3H, m, Ar*H*), 7.72-7.68 (6H, m, Ar*H*), 7.62 (2H, d, *J* 8.5, Ar*H*), 3.97 (3H, s, C*H$_3$*), 3.50-3.30 (3H, m), 2.95 (1H, td, *J* 9.5, *J* 6.6), 2.59-2.53 (1H, m), 1.97-1.89 (2H, m), 1.57-1.47 (2H, m); *m/z* (ESI) 559 [MH]$^+$; found: [MH]$^+$, 559.1810 C$_{31}$H$_{32}$N$_2$O$_4$SP requires 559.1820, Δ 1.8 ppm.

4-[2-(R)-(Acryloylamino-methyl)-pyrrolidine-1-sulfonyl]-benzoic acid methyl ester **85**
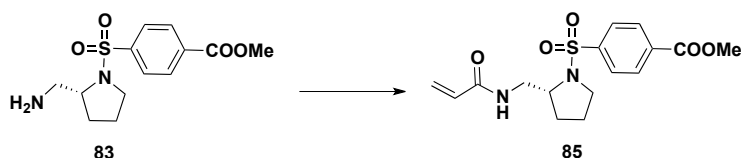
To a solution of amine **83** (615.8 mg, 2.06 mmol, 1.0 eq.) in anhydrous CH$_2$Cl$_2$ (12 mL) at 0 °C under argon was added Et$_3$N (0.43 mL, 3.09 mmol, 1.5 eq.) and acryloyl chloride (0.18 mL, 2.27 mmol, 1.1 eq.) and the resulting yellow solution stirred at 0 °C for 15 min and at rt for 22 h. The reaction mixture was poured into aqueous NH$_4$Cl (2 M), extracted with CH$_2$Cl$_2$ (x 3), dried over MgSO$_4$, filtered and concentrated *in vacuo*. The crude product was purified on silica (EtOAc/n-hex, 4:1) to yield the desired acrylamide **85** (524.1 mg, 72 %) as a clear oil. $[\alpha]^{26}_D$ = +105.4 (*c* = 1.1, CHCl$_3$); R$_f$ = 0.34 (EtOAc/n-hex, 4:1); ν_{max} /cm^{-1} 1729, 1661, 1627, 1604, 1540, 1437, 1401, 1349, 1281, 1162, 1110, 1091, 1045, 1016, 989, 963, 766, 734, 696, 622, 609, 580, 573; δ_H (400 MHz, CDCl$_3$) 8.16 (2H, d, *J* 8.5, Ar*H*), 7.87 (2H, d, *J* 8.5, Ar*H*), 6.71 (1H, bt, *J* 4.0, N*H*), 6.27 (1H, dd, *J* 1.7, *J* 16.7, COCHC*H$_2$* *cis* to C=O), 6.15 (1H, dd, *J* 16.7, *J* 10.0, COC*H*CH$_2$), 5.63 (1H, dd, *J* 10.0, *J* 1.7, COCHC*H$_2$* *trans* to C=O), 3.93 (3H, s, OC*H$_3$*), 3.75-3.69 (1H, m, pyrrolidine-*H2'*), 3.59-3.53 (1H, m, NHC*H$_2$*), 3.48-3.42 (1H, m, NHC*H$_2$*), 3.38-3.31 (1H, m, pyrrolidine-*H5'*), 3.23-3.16 (1H, m, pyrrolidine-*H5'*), 1.84-1.41 (4H, m, pyrrolidine-*H3'* and pyrrolidine-*H4'*); δ_C (101 MHz, CDCl$_3$) 166.1, 165.5, 140.6, 134.3, 131.1, 130.5, 127.6, 126.4, 59.9, 52.7, 49.7, 43.8, 29.8, 24.1; *m/z* (ESI) 353 [MH]$^+$, 375 [MNa]$^+$; found: [MH]$^+$, 353.1168 C$_{16}$H$_{21}$N$_2$O$_5$S requires 353.1171, Δ 0.8 ppm.

4-[2-(R)-(Acryloylamino-methyl)-pyrrolidine-1-sulfonyl]-benzoic acid **86**
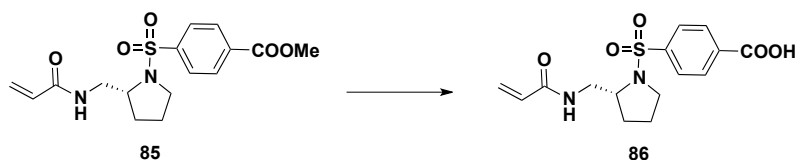
To a solution of ester **85** (500 mg, 1.42 mmol, 1 eq.) in MeOH (10 mL) was added aqueous 2M LiOH (10 mL). The reaction mixture was stirred at rt for 10 minutes and the MeOH removed *in vacuo*. The aqueous solution was acidified to pH 2 with HCl (2N) and extracted with EtOAc (x 3). The combined organics were dried over MgSO$_4$, filtered and the solvent removed *in vacuo*. The crude compound was purified on silica (CH$_2$Cl$_2$, 20 % MeOH) and subsequently triturated in n-hexane/EtOAc/MeOH, 1:1:1 to yield the desired carboxylic acid **86** (447.4 mg, 93 %) as a white solid, mp > 230 °C; $[\alpha]^{21}_D$ = + 90.0 (*c* = 0.27, CH$_3$CH$_2$OH); R$_f$ = 0 (100 % EtOAc); ν_{max} /cm^{-1} 1657, 1596, 1551, 1460, 1404, 1334, 1300, 1255, 1201, 1161, 1139, 1090, 1046, 1013, 984, 869, 856, 803, 782, 730, 699, 617, 578; δ_H (400 MHz, DMSO-d$_6$) 8.38 (1H, bt, N*H*), 8.12 (2H, d, *J* 7.5, Ar*H*), 7.78 (2H, d, *J* 7.5, Ar*H*), 6.27 (1H, dd, *J* 10.0, *J* 17.5, NHCOC*H*CH$_2$), 6.09 (1H, d, *J* 17.5, NHCOCHC*H$_2$* *cis* to C=O), 5.59 (1H, d, *J* 10.0, NHCOCHC*H$_2$* *trans* to C=O), 3.68-3.62 (1H, m, pyrrolidine-*H*), 3.53-3.32 (2H, m, NHC*H$_2$*), 3.21-3.15 (1H, m, pyrrolidine-*H*), 3.11-3.05 (1H, m, pyrrolidine-*H*), 1.75-1.69 (1H, m, pyrrolidine-*H*), 1.62-1.59 (1H, m, pyrrolidine-*H*), 1.39-1.27 (2H, m, pyrrolidine-*H*); δ_C (101 MHz, DMSO-d$_6$) 169.1, 164.9, 142.6, 137.2, 131.7, 129.8, 126.7, 125.2, 59.1, 49.1, 42.9, 28.3, 23.2; *m/z* (ESI) 339 [MH]$^+$; found: [MH]$^+$, 339.1023 C$_{15}$H$_{19}$N$_2$O$_5$S requires 339.1015, Δ 2.4 ppm.

N-benzyloxycarbonyl-(L)-glutamic acid **89**
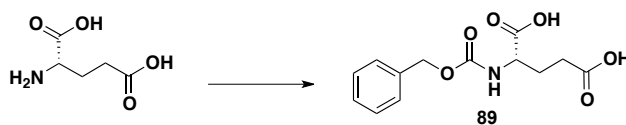
To a solution of NaHCO$_3$ (5.0 g, 59.6 mmol, 4.4 eq.) in H$_2$O (150 mL) was added L-glutamic acid (2.0 g, 13.6 mmol, 1 eq.) and benzyl chloroformate (3.70 g, 21.6 mmol, 1.6 eq.) at 0 °C and the mixture stirred at rt for 24 h. Ether (150 mL) was added to the reaction mixture and the layers separated. The aqueous layer was acidified to pH 1 with 2N HCl and extracted with EtOAc (x 3), and the combined EtOAc organics dried over MgSO$_4$, filtered and concentrated *in vacuo* to yield the desired Cbz-protected L-glutamic acid **89** (3.73 g, 98 %) as a white solid, mp = 114-116 °C; [a]$^{22}_D$ = - 13.3 (*c* = 0.75, CH$_3$CH$_2$OH); ν_{max} /cm^{-1} 3297, 1699, 1685, 1547, 1526, 1419, 1298, 1255, 1229, 1214, 1181, 1168, 1051, 1015, 952, 945, 910, 903, 868, 786, 779, 753, 734, 721, 694; δ_H (400 MHz, DMSO-d$_6$) 12.40 (2H, bs, COO*H*), 7.59 (1H, d, *J* 8.0, N*H*), 7.39-7.21 (5H, m, Ar*H*), 5.03 (2H, s, ArC*H$_2$*), 4.04-3.97 (1H, m, ZNHC*H*), 2.37-2.23 (2H, m, C*H$_2$*COOH), 2.01-1.91 (1H, m, C*H$_2$*CH$_2$COOH), 1.80-1.71 (1H, m, C*H$_2$*CH$_2$COOH); δ_C (101 MHz, DMSO-d$_6$) 173.7, 173.6, 156.2, 137.0, 128.4, 127.8, 127.7, 65.4, 53.0, 30.1, 26.1; *m/z* (ESI) 282 [MH]$^+$, 304 [MNa]$^+$; found: [MH]$^+$, 282.0982 C$_{13}$H$_{16}$NO$_6$ requires 282.0978, Δ 1.4 ppm.

2-(S)-[4-[2-(R)-(Acryloylamino-methyl)-pyrrolidine-1-sulfonyl]-benzoylamino]-pentanedioic acid ditertbutyl ester **91**
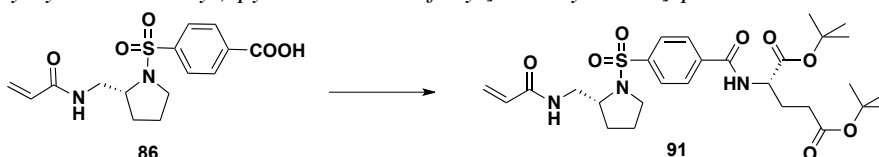
Di-*tert*butyl L-glutamate HCl salt was dissolved in EtOAc and washed with saturated NaHCO$_3$ (x 1). The organic layer was dried over MgSO$_4$, filtered and the solvent removed *in vacuo* to yield the desired amine as the free base, as a clear oil.

To a solution of carboxylic acid **86** (544.2 mg, 1.61 mmol, 1.2 eq.) in CH$_2$Cl$_2$ (6 mL) was added H$_2$O (13.5 mL), di-*tert* butyl L-glutamate (348.2 mg, 1.34 mmol, 1.0 eq.) in CH$_2$Cl$_2$ (7.5 mL) and HOBt (217.5 mg, 1.61 mmol, 1.2 eq.). The reaction was cooled to 0 °C and 1,3-dimethylaminopropyl-3-ethylcarbodiimide HCl (308.6 mg, 1.61 mmol, 1.2 eq.) was added. The reaction was allowed to warm to 14 °C over 5 h, then stirred at rt for 60 h, diluted with H$_2$O and extracted with CH$_2$Cl$_2$. Combined organics were dried over MgSO$_4$ and the solvent removed *in vacuo*. The crude product was purified by flash column chromatography on silica (1:1, EtOAc/n-hex) to yield the desired acrylamide **91** (572.3 mg, 74 %) as a clear oil, R$_f$ = 0.48 (7:3, EtOAc/n-hex); [α]$^{20}_D$ = +88.8 (*c* = 0.65, CHCl$_3$); ν_{max} /cm^{-1} 1731, 1661, 1628, 1602, 1540, 1485, 1452, 1394, 1368, 1346, 1290, 1248, 1201, 1151, 1103, 754; δ_H (400 MHz, CDCl$_3$) 7.96 (2H, d, *J* 8.6, Ar*H*), 7.83 (2H, d, *J* 8.6, Ar*H*), 7.44 (1H, d, *J* 7.5, ArCON*H*), 6.78 (1H, t, *J* 4.8, N*H*CH$_2$), 6.26 (1H, dd, *J* 17.1, *J* 1.9, C*H$_2$*CHCONH *cis* to C=O), 6.15 (1H, dd, *J* 17.1, *J* 9.5, CH$_2$C*H*CONH), 5.62 (1H, dd, *J* 9.5, *J* 1.9, C*H$_2$*CHCONH *trans* to C=O), 4.59 (1H, ddd, *J* 7.8, *J* 7.5, *J* 4.7, ArCONHC*H*), 3.72-3.66 (1H, m, pyrrolidine-*H2'*), 3.56-3.50 (1H, m, CH$_2$CHCONHC*H$_2$*), 3.45-3.40 (1H, m, CH$_2$CHCONHC*H$_2$*), 3.37-3.30 (1H, m, pyrrolidine-*H5'*), 3.18-3.12 (1H, m, pyrrolidine-*H5'*), 2.45-2.28 (2H, m, *t*BuOOCC*H$_2$*), 2.22-2.14 (1H, m, *t*BuOOCCH$_2$C*H$_2$*), 2.08-1.99 (1H, m, *t*BuOOCCH$_2$C*H$_2$*), 1.82-1.48 (4H, m, pyrrolidine-*H3'* and pyrrolidine-*H4'*), 1.45 (9H, s, *t*Bu), 1.38 (9H, s,

*t*Bu); δ_C (101 MHz, CDCl₃) 173.1, 171.1, 166.3, 165.6, 139.5, 138.3, 131.1, 128.3, 127.8, 126.6, 82.8, 81.4, 60.0, 53.5, 49.8, 44.0, 31.8, 29.9, 28.2, 28.2, 27.0, 24.2; *m/z* (ESI) 580 [MH]⁺, 602 [MNa]⁺; found: [MH]⁺, 580.2687 C₂₈H₄₂N₃O₈S requires 580.2693, Δ 1.0 ppm.

2-(S)-(4-Nitro-benzoylamino)-pentanedioic acid di-tert-butyl ester **92**
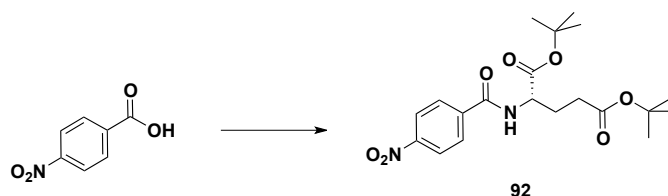
To a solution of 4-nitrobenzoic acid (24.7 mg, 0.148 mmol, 1.0 eq.) in CH₂Cl₂ (1.5 mL) was added H₂O (1.5 mL), di-*tert*butyl L-glutamate hydrochloride salt (43.8 mg, 0.148 mmol, 1.0 eq.), Et₃N (62 μL, 0.444 mmol, 3.0 eq.) and 1-hydroxybenzotriazole (20.0 mg, 0.148 mmol, 1.0 eq.). The reaction mixture was cooled to 0 °C and 1-ethyl-3-(3-dimethylaminopropyl)carbodiimide hydrochloride (31.2 mg, 0.163 mmol, 1.1 eq.) was added. The reaction was allowed to warm to rt and stirred for 24 h before dilution with H₂O and extraction with CH₂Cl₂. The combined organics were dried over MgSO₄, filtered and the solvent removed *in vacuo*. The crude product was purified on silica (EtOAc/n-hex, 1:1) to yield the desired nitrobenzene **92** (27.0 mg, 45 %) as a clear oil. R_f = 0.8 (EtOAc/n-hex, 1:1); [α]²¹_D = +1.66 (c = 1.21, CHCl₃); ν_max /cm⁻¹ 1730, 1672, 1652, 1603, 1527, 1488, 1455, 1393, 1368, 1346, 1300, 1256, 1150, 1110, 870, 845, 720; δ_H (400 MHz, CDCl₃) 8.28-8.25 (2H, m, Ar*H3'*), 8.00-7.97 (2H, m, Ar*H2'*), 7.42 (1H, d, *J* 6.7, N*H*), 4.63-4.58 (1H, m, NHC*H*), 2.48-2.03 (4H, m, C*H₂*C*H₂*), 1.47 (9H, s, *t*Bu), 1.40 (9H, s, *t*Bu); δ_C (101 MHz, CDCl₃) 173.3, 171.0, 165.2, 149.9, 139.7, 128.6, 124.0, 82.9, 81.5, 53.6, 31.9, 28.3, 28.2, 27.0; *m/z* (ESI) 409 [MH]⁺; found: [MH]⁺, 409.1976 C₂₀H₂₉N₂O₇ requires 409.1975, Δ 0.2 ppm.

4-[2-(R)-(Ethenesulfonylamino-methyl)-pyrrolidine-1-sulfonyl]-benzoic acid methyl ester **93**
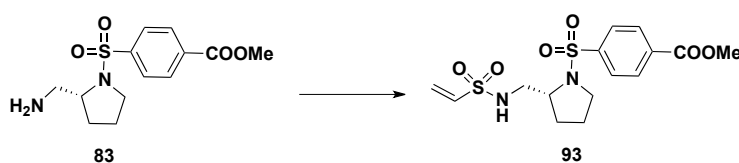
2-Chloroethanesulfonyl chloride (0.47 mL, 4.45 mmol, 1 eq.) was added dropwise to a stirred solution of amine **83** (1.328 g, 4.45 mmol, 1 eq.) and Et₃N (1.86 mL, 13.35 mmol, 3.5 eq.) in anhydrous CH₂Cl₂ (10 mL) at 0 °C under argon. After addition, stirring was continued at 0 °C for 1 h and at rt overnight. The mixture was diluted with CH₂Cl₂, washed with brine, dried over MgSO₄, filtered and the solvent removed *in vacuo*. The crude product was purified on silica (EtOAc/n-hex, 1:1) to yield the desired vinyl sulfonamide **93** (1.01 g, 58 %) as a white solid, mp = 111-113 °C; R_f = 0.21 (EtOAc/n-hex, 1:1); [α]²²_D = +95.5 (c = 6.20, CHCl₃); ν_max /cm⁻¹ 1726, 1436, 1400, 1332, 1280, 1200, 1152, 1110, 1090, 1016, 971, 766, 734, 696, 621, 581, 555; δ_H (400 MHz, CDCl₃) 8.15 (2H, d, *J* 8.0, Ar*H*), 7.86 (2H, d, *J* 8.0, Ar*H*), 6.54 (1H, dd, *J* 10.0, *J* 16.0, CH₂C*H*SO₂NH), 6.21 (1H, d, *J* 16.0, C*H₂*CHSO₂NH *cis* to SO₂), 5.94 (1H, d, *J* 10.0, C*H₂*CHSO₂NH *trans* to SO₂), 5.29 (1H, t, *J* 6.4, N*H*), 3.91 (3H, s, OC*H₃*), 3.66-3.61 (1H, m, pyrrolidine-*H2'*), 3.44-3.40 (1H, m, SO₂NHC*H₂*), 3.21-3.10 (3H, m, SO₂NHC*H₂* and pyrrolidine-*H5'*), 1.84-1.73 (2H, m, pyrrolidine-

H4'), 1.66-1.55 (1H, m, pyrrolidine-*H3'*), 1.46-1.37 (1H, m, pyrrolidine-*H3'*); δ_C (101 MHz, CDCl$_3$); 165.6, 140.3, 135.7, 134.3, 130.5, 127.6, 126.9, 59.6, 52.8, 49.9, 47.2, 29.4, 24.0; *m/z* (ESI) 389 [MH]$^+$ 411 [MNa]$^+$; found: [MH]$^+$, 389.0836 C$_{15}$H$_{21}$N$_2$O$_6$S$_2$ requires 389.0841, Δ 1.3 ppm.

4-[2-(R)-(Ethenesulfonylamino-methyl)-pyrrolidine-1-sulfonyl]-benzoic acid **94**
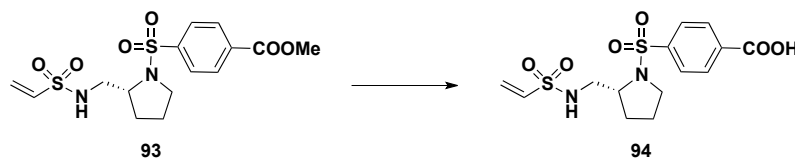
To a solution of vinyl sulfonamide **93** (1.0 g, 2.6 mmol, 1 eq.) in THF (10 mL) was added 2M LiOH (10 mL) at 0 °C. The reaction mixture was allowed to warm to rt and stirred for a further 10 min. The THF was removed *in vacuo* and the basic aqueous solution acidified to pH 2 with 2N HCl. The resulting thick white precipitate was filtered under gravity and washed thoroughly with cold ether to yield the desired carboxylic acid **94** (975.0 mg, 100 %) as a white solid, mp = 164-167 °C ; R$_f$ = 0 (100 % EtOAc); [α]$^{23}_D$ = + 98.0 (*c* = 1.00, MeOH); ν_{max} /cm^{-1} 1691, 1602, 1573, 1425, 1402, 1385, 1345, 1314, 1285, 1140, 1159, 1149, 1126, 1113, 1086, 1038, 1015, 995, 979, 966, 932, 862, 771, 716, 690, 659, 618, 575; δ_H (400 MHz, MeOD) 8.26 (2H, d, *J* 8.4, Ar*H*), 8.00 (2H, d, *J* 8.4, Ar*H*), 6.70 (1H, dd, *J* 15.7, *J* 9.8, SO$_2$C*H*CH$_2$), 6.22 (1H, d, *J* 15.7, SO$_2$CHC*H$_2$* cis to SO$_2$), 6.04 (1H, d, *J* 9.8, SO$_2$CHC*H$_2$* trans to SO$_2$), 3.75-3.69 (1H, m, pyrrolidine-*H2'*), 3.52-3.46 (1H, m, NHC*H$_2$*), 3.32-3.28 (1H, dd, *J* 13.5, *J* 3.9, pyrrolidine-*H5'*), 3.30 (1H, m, NHC*H$_2$*), 3.05 (1H, dd, *J* 13.5, *J* 8.4, pyrrolidine-*H5'*), 1.94-1.82 (2H, m, pyrrolidine-*H4'*), 1.66-1.50 (2H, m, pyrrolidine-*H3'*); δ_C (101 MHz, MeOD) 166.7, 140.4, 136.1, 134.8, 130.2, 127.5, 125.4, 59.7, 49.5, 46.6, 28.4, 23.2; *m/z* (ESI) 375 [MH]$^+$; found: [MH]$^+$, 375.0687 C$_{14}$H$_{19}$N$_2$O$_6$S$_2$ requires 375.0685, Δ 0.5 ppm.

2-(S)-(4-[2-(R)-(Ethenesulfonylamino-methyl)-pyrrolidine-1-sulfonyl]-benzoylamino)-pentanedioic acid di-tert-butyl ester **95**
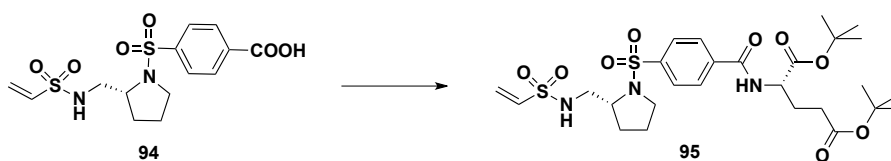
Di-*tert*butyl L-glutamate.HCl was dissolved in EtOAc and washed with saturated NaHCO$_3$ (x 1). The organic layer was dried over MgSO$_4$ and the solvent removed *in vacuo* to give the desired amine.

To a solution of carboxylic acid **94** (603.1 mg, 1.61 mmol, 1.2 equiv.) in CH$_2$Cl$_2$ (6 mL) was added H$_2$O (13.5 mL), di*tert*butyl L-glutamate (348.2 mg, 1.34 mmol, 1.0 equiv.) in CH$_2$Cl$_2$ (7.5 mL) and HOBt (217.5 mg, 1.61 mmol, 1.2 equiv.). The reaction was cooled to 0 °C and EDC.HCl (308.6 mg, 1.61 mmol, 1.2 equiv.) was added. The reaction was allowed to warm to rt and stirred for 70 h, diluted with brine and extracted with CH$_2$Cl$_2$ (x 3). Combined organics were dried over MgSO$_4$, filtered and the solvent removed *in vacuo*. The crude was purified on silica (100 % EtOAc) to yield the desired vinyl sulfonamide **95** (698.4 mg, 85 %) as an oily white solid, mp = 57-59 °C; [α]$^{25}_D$ = +49.7 (*c* = 1.05, CHCl$_3$); R$_f$ = 0.71 (EtOAc/n-hex, 4:1); ν_{max} /cm^{-1} 1728, 1658, 1535, 1368, 1334, 1254, 1150, 1096, 846, 733,

622; δ_H (400 MHz, CDCl$_3$) 7.99 (2H, d, *J* 7.7, Ar*H*), 7.87 (2H, d, *J* 7.7, Ar*H*), 7.37 (1H, d, *J* 6.2, CON*H*), 6.56 (1H, dd, *J* 9.2, *J* 15.4, SO$_2$C*H*CH$_2$), 6.24 (1H, d, *J* 15.4, SO$_2$CHC*H$_2$* *cis* to SO$_2$), 5.97 (1H, d, *J* 9.2, SO$_2$CHC*H$_2$* *trans* to SO$_2$), 5.10 (1H, t, *J* 6.7, SO$_2$N*H*), 4.63-4.58 (1H, m, ArCONHC*H*), 3.64-3.59 (1H, m, pyrrolidine-*H2'*), 3.47-3.43 (1H, m, SO$_2$NHC*H$_2$*), 3.25-3.22 (1H, m, SO$_2$NHC*H$_2$*), 3.19-3.11 (2H, m, pyrrolidine-*H5'*), 2.48-2.30 (2H, m, *t*BuOOCC*H$_2$*CH$_2$), 2.25-2.16 (1H, m, *t*BuOOCCH$_2$C*H$_2$*), 2.11-2.04 (1H, m, *t*BuOOCCH$_2$C*H$_2$*), 1.87-1.76 (2H, m, pyrrolidine-*H4'*), 1.71-1.62 (2H, m, pyrrolidine-*H3'*); δ_C (101 MHz, MeOD) 173.3, 171.1, 165.6, 139.1, 138.5, 135.9, 128.4, 128.0, 127.2, 82.9, 81.5, 77.4, 59.8, 50.2, 47.4, 31.9, 29.8, 28.3, 28.2, 27.1, 24.2; *m/z* (ESI) 616 [MH]$^+$, 638 [MNa]$^+$; found: [MH]$^+$, 616.2353 C$_{27}$H$_{42}$N$_3$O$_9$S$_2$ requires 616.2362, Δ 1.5 ppm.

(R)-(1-Methylpyrrolidin-2-yl)-methanol **97**

A procedure reported by Zhu *et al*. was used with some modifications.[283] D-prolinol (0.50 mL, 5.12 mmol, 1.0 equiv.) was added to formic acid (1 mL) at 0 °C followed by 37 % aqueous formaldehyde (0.75 mL). The reaction mixture was warmed to reflux whereby a vigorous evolution of carbon dioxide was observed. The mixture was stirred at reflux for 20 h before acidification with 5N HCl (1.25 mL) and evaporation *in vacuo* to afford a yellow gum. The residue was dissolved in a minimum quantity of saturated NaOH and extracted with chloroform (x 6). The combined organic extracts were dried over MgSO$_4$, filtered and the solvent removed *in vacuo* to leave the desired methylated prolinol **97** (389.5 mg, 66 %) as a clear oil. δ_H (400 MHz, CDCl$_3$) 4.21 (1H, bs, O*H*), 3.41 (1H, dd, *J* 3.6, *J* 10.9, pyrrolidine-C*H$_2$*), 3.29 (1H, dd, *J* 3.6, *J* 10.9, pyrrolidine-C*H$_2$*), 2.90-2.86 (1H, m, pyrrolidine-*H2'*), 2.18 (3H, s, NC*H$_3$*), 2.17-2.13 (1H, m, pyrrolidine-*H5'*), 2.10-1.99 (1H, m, pyrrolidine-*H5'*), 1.76-1.49 (4H, m, pyrrolidine-*H4'* and pyrrolidine-*H3'*); δ_C (101 MHz, CDCl$_3$) 66.6, 62.3, 57.5, 41.0, 27.4, 22.9. *m/z* (CI) 116 [MH]$^+$; found [MH]$^+$ 116.1068 C$_6$H$_{14}$NO requires 116.1075, Δ 6.0 ppm.

2-(R)-Hydroxymethyl-pyrrolidine-1-carboxylic acid tert-butyl ester **99**

Method one *from* D-*proline*
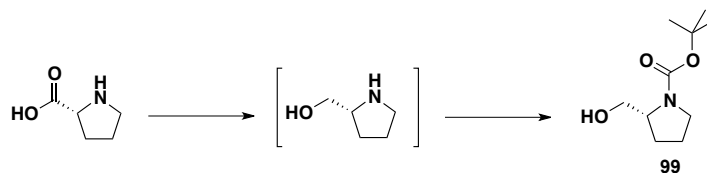
The method of Pericàs *et al*.[284] was used with some small modifications. To D-proline (1.00 g, 8.69 mmol, 1.0 eq.) in anhydrous THF (3 mL) at 0 °C under argon was added LiAlH$_4$ as a 1.0 M solution in THF (Sigma-Aldrich, SureSeal) (13.0 mL, 13.0 mmol, 1.5 eq.) with vigorous effervescence. The reaction mixture was stirred for one hour at 0 °C and for one hour at rt to give a cloudy grey solution. 20 % aqueous NaOH (2 mL) was added with vigorous effervescence to give a thick white precipitate. The mixture was filtered through celite, dried over Na$_2$SO$_4$ and concentrated to approximately 30 mL before addition of Boc$_2$O (2.85 g, 13.0 mmol, 1.5 eq.) in anhydrous THF (6 mL) dropwise. The

resulting bright orange solution was stirred at rt overnight. NaHCO$_3$ was added and the reaction mixture extracted with Et$_2$O (x 3). Combined organics were dried over Na$_2$SO$_4$, filtered and the solvent removed *in vacuo*. The crude orange oil was purified on silica (1:1, n-hexane/EtOAc) and dried under high vacuum to yield the desired N-Boc D-prolinol **99** (1.19 g, 68 %) as a white powder.

Method two *from D-prolinol*
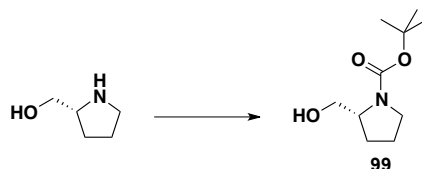
To a solution of D-prolinol (0.40 mL, 4.10 mmol, 1.0 equiv.) and triethylamine (0.64 mL, 4.61 mmol, 1.1 equiv.) in anhydrous CH$_2$Cl$_2$ (5 mL) under argon at 0 °C was added di-*tert*butyl dicarbonate (1.06 g, 4.61 mmol, 1.1 equiv.) in CH$_2$Cl$_2$ (3.5 mL) and the mixture warmed to rt and stirred for 16 h. The reaction mixture was quenched with NaHCO$_3$ and the organic layer washed with brine (x 1) and dried over MgSO$_4$. The solvent was removed *in vacuo* to yield the desired N-Boc D-Prolinol **99** (603.0 mg, 73 %) as a clear oil which solidified under vacuum to a white solid.

R_f = 0.38 (2:1, EtOAc/n-nex); $[\alpha]^{20}_D$ = + 42.4 (*c* = 0.61, CHCl$_3$); ν_{max} /cm^{-1} 3400 (b), 2974, 2876, 1692, 1669, 1395, 1367, 1166, 1125, 1107, 1052; δ_H (400 MHz, CDCl$_3$) 3.95-3.89 (1H, m, pyrrolidine-*H2'*), 3.62-3.53 (2H, m, pyrrolidine-*H5'*), 3.46-3.40 (1H, m, pyrrolidine-C*H$_2$*), 3.31-3.52 (1H, m, pyrrolidine-C*H$_2$*), 2.02-1.94 (1H, m, pyrrolidine-*H*), 1.86-1.70 (2H, m, pyrrolidine-*H*), 1.60-1.54 (1H, bm, pyrrolidine-*H*), 1.44 (9H, s, *t*Bu); δ_C (101 MHz, CDCl$_3$) 157.5, 80.4, 67.9, 60.4, 47.7, 28.9, 28.7, 24.2. Data in agreement with literature values.[285]

(R)-2-(Toluene-4-sulfonyloxymethyl)-pyrrolidine-1-carboxylic acid tert-butyl ester **100**
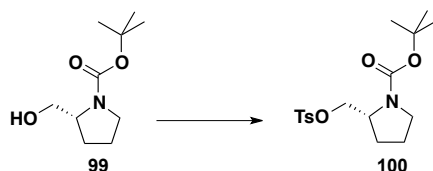
To a solution of N-Boc D-prolinol **99** (552.3 mg, 2.74 mmol, 1.0 equiv.) in anhydrous CH$_2$Cl$_2$ (5 mL) was added tosyl chloride (1.57 g, 8.23 mmol, 3.0 equiv.) and triethylamine (1.14 mL, 8.23 mmol, 3.0 equiv.) and the reaction stirred under argon at rt for 16 h. The reaction mixture was poured into brine and extracted with CH$_2$Cl$_2$ (x 3). Combined organics were dried over MgSO$_4$, filtered and the solvent removed *in vacuo*. The crude oil was purified on silica (4:1, n-hex/EtOAc) to yield the desired tosylated pyrrolidine **100** (996 mg, 100 %) as a colourless oil. R_f = 0.29 (3:1, n-hex/EtOAc); $[\alpha]^{20}_D$ = + 44.0 (*c* = 1.41, CHCl$_3$); ν_{max} /cm^{-1} 2974, 1691, 1392, 1363, 1174, 1097, 968, 815, 666; δ_H (400 MHz, CDCl$_3$) 7.75 (2H, d, *J* 8.2, Ar*H*), 7.38-7.35 (2H, bm, Ar*H*), 4.12-3.89 (3H, m, TsOC*H$_2$* and pyrrolidine-*H2'*), 3.37-3.30 (2H, m, pyrrolidine-*H5'*), 2.47 (3H, s, ArC*H$_3$*), 1.98-1.72 (4H, m, pyrrolidine-*H3'* and pyrrolidine-*H4'*), 1.37 (3H, s, *t*Bu), 1.33 (6H, s, *t*Bu); δ_C (101 MHz, CDCl$_3$, isomers) 154.5, 145.1, 133.1, 130.1, 128.1, 80.1, 79.8, 70.1,

55.7, 47.1, 46.7, 28.5, 27.8, 24.0, 23.0, 21.8; *m/z* (ESI) 378 [MNa]$^+$; found [MNa]$^+$ 378.1345 C$_{17}$H$_{25}$NO$_5$SNa requires: 378.1351, Δ 1.6 ppm. Data in agreement with literature values.[286]

(R)-2-Azidomethyl-pyrrolidine-1-carboxylic acid tert-butyl ester **101**
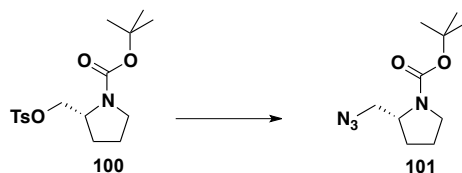
Tosylate **100** (375 mg, 1.06 mmol, 1.0 equiv.) was dissolved in anhydrous DMSO (12 mL) and NaN$_3$ (411 mg, 6.33 mmol, 6.0 equiv.) was added. The reaction was heated to 65 °C and stirred for 19 h under an atmosphere of argon. The reaction was diluted with Et$_2$O (20 mL) and washed with H$_2$O (16 mL x 3) and brine (1 x 8 mL), dried over MgSO$_4$, filtered and the solvent removed *in vacuo* to yield the desired azide **101** (187.6 mg, 78 %) as a clear oil. R$_f$ = 0.75 (100 % EtOAc); $[\alpha]^{19}_D$ = + 47.9 (*c* = 2.38, CHCl$_3$); ν_{max} /cm^{-1} 2974, 2881, 2100, 1693, 1392, 1366, 1165, 1106; δ_H (400 MHz, CDCl$_3$) 3.90 (1H, bm, pyrrolidine-*H2'*), 3.55-3.34 (4H, bm, pyrrolidine-*H5'* and N$_3$C*H$_2$*), 2.03-1.73 (4H, bm, pyrrolidine-*H3'* and pyrrolidine-*H4'*), 1.44 (9H, s, C(C*H$_3$*)$_3$); δ_C (101 MHz, CDCl$_3$, isomers) 154.7, 79.9, 56.7, 54.0, 52.9, 47.2, 46.9, 29.6, 28.7, 24.0, 23.2. Data in agreement with literature values.[287]

(R)-2-Aminomethyl-pyrrolidine-1-carboxylic acid tert-butyl ester **102**
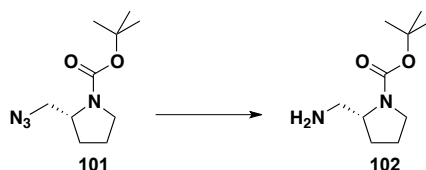
To Boc-azidomethylpyrrolidine **101** (188 mg, 0.83 mmol, 1.0 equiv.) dissolved in MeOH (5 mL) was added 10 % Pd/C (16 mg, cat.) and the reaction mixture stirred for 24 h under an atmosphere of H$_2$ (g). The reaction mixture was filtered through celite, washed through with MeOH and the solvent evaporated from the filtrate *in vacuo* to yield the desired amine **102** (157.9 mg, 95 %) as a clear oil. R$_f$ = 0 (100 % EtOAc); $[\alpha]^{23}_D$ = + 54.0 (*c* = 0.93, MeOH); ν_{max} /cm^{-1} 2975, 1692, 1397, 1366, 1171, 1112; δ_H (400 MHz, MeOD) 3.89-3.76 (1H, bm, pyrrolidine-*H2'*), 3.42-3.34 (2H, bm, pyrrolidine-*H5'*), 2.91-2.87 (1H, bm, H$_2$NC*H$_2$*), 2.78-2.65 (1H, bm, H$_2$NC*H$_2$*), 2.06-1.81 (4H, bm, pyrrolidine-*H3'*, pyrrolidine-*H4'*), 1.47 (9H, s, OC(C*H$_3$*)$_3$); δ_C (101 MHz, MeOD, isomers) 156.9, 156.6, 81.1, 80.8, 60.7, 60.6, 48.2, 47.8, 45.5, 29.8, 29.5, 29.0, 24.7, 24.0; *m/z* (ESI) 201 [MH]$^+$; found [MH]$^+$ 201.1602 C$_{10}$H$_{21}$N$_2$O$_2$ requires 201.1603, Δ 0.5 ppm. Data in agreement with literature values.[287]

(R)-2-(Acryloylamino-methyl)-pyrrolidine-1-carboxylic acid tert-butyl ester **103**
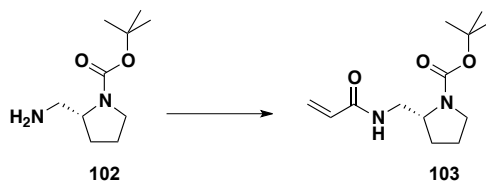
To a solution of amine **102** (138.8 mg, 0.69 mmol, 1.0 equiv.) in anhydrous CH_2Cl_2 (4 mL) at 0 °C under argon was added Et_3N (0.14 mL, 1.035 mmol, 1.5 equiv.) and acryloyl chloride (0.10 mL, 1.23 mmol, 1.8 equiv.) and the resulting light yellow solution stirred at 0 °C for 15 min and at rt for 20 h. The resulting bright yellow solution was poured into aqueous NH_4Cl (2M) and extracted with CH_2Cl_2 (x 2). Combined organics were dried over $MgSO_4$, filtered and the solvent removed *in vacuo*. The crude yellow residue was purified on silica (gradient EtOAc/n-hex, 1:1 to EtOAc/n-hex, 1:0) to yield the desired acrylamide **103** (127.2 mg, 72 %) as a yellow oil. R_f = 0.41 (100 % EtOAc); $[\alpha]^{20}_D$ = + 68.4 (c = 1.17, $CHCl_3$); v_{max} /cm^{-1} 3293 (b), 2972, 1693, 1662, 1627, 1548, 1395, 1366, 1246, 1169, 1111; δ_H (400 MHz, $CDCl_3$) 7.65 (1H, bs, N*H*), 6.10-5.95 (2H, m, C*H*$_2$CHCON *cis* to C=O and CH$_2$C*H*CONH), 5.45 (1H, d, *J* 8.9, C*H*$_2$CHCONH *trans* to C=O), 3.96-3.74 (1H, bm, pyrrolidine-*H2'*), 3.35-3.05 (4H, bm NHC*H*$_2$ and pyrrolidine-*H5'*), 1.91-1.62 (4H, bm, pyrrolidine-*H3'* and pyrrolidine-*H4'*), 1.33 (9H, s, OC(C*H*$_3$)$_3$); δ_C (101 MHz, $CDCl_3$) 166.0, 156.7, 131.5, 125.2, 80.0, 56.2, 47.0, 45.8, 29.3, 28.4, 23.8; *m/z* (ESI) 277 [MNa]$^+$; found [MNa]$^+$ 277.1521 $C_{13}H_{22}N_2O_3Na$ requires 277.1528, Δ 2.5 ppm.

(R)-Octahydro-pyrrolo[1,2-a][1,4]diazepin-3-one **104**
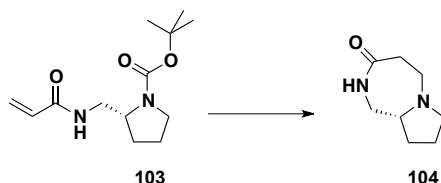
N-Boc pyrrolidine **103** (120 mg, 0.48 mmol, 1 eq.) was dissolved in a 1:1 mixture of TFA and CH_2Cl_2 (3 mL) and the solution stirred at room temperature for 30 min. The solvent was removed *in vacuo*, the pH adjusted to pH 8 with sat. aq. $NaHCO_3$ and the aqueous phase extracted with CH_2Cl_2 (x 3). Combined organics were dried over Na_2SO_4, filtered and the solvent removed *in vacuo*. The crude mixture was passed through a column of silica with MeOH to isolate bicyclic structure **104** (7.9 mg, 11%) as a white solid. v_{max} /cm^{-1} 1645, 1540, 730; δ_H (400 MHz, $CDCl_3$) 8.70 (1H, br m, N*H*), 3.74-3.68 (1H, m), 3.31 (1H, bt, *J* 8.0), 3.23-3.12 (2H, m), 2.69-2.59 (2H, m), 2.40 (1H, dt, *J* 17.2 *J* 3.1), 2.30 (1H, dt, *J* 12.2 *J* 3.6), 2.22-2.16 (1H, m), 1.98-1.83 (2H, m), 1.74-1.61 (2H, m); δ_C (101 MHz, $CDCl_3$) 173.1, 63.1, 53.0, 49.9, 38.4, 33.8, 27.3, 22.7; *m/z* (ESI) 155 [M+H], 309 [2M+H]$^+$; found [2M+H]$^+$ 309.2273 $C_{16}H_{29}N_4O_2$ requires 309.2291, Δ 5.8 ppm. *m/z* (EI) 308 [2M]$^+$; found [2M]$^+$ 308.2207 $C_{16}H_{28}N_4O_2$ requires 308.2212, Δ 1.6 ppm.

N-Benzyl-3-phenylsulfanyl-propionamide **109**
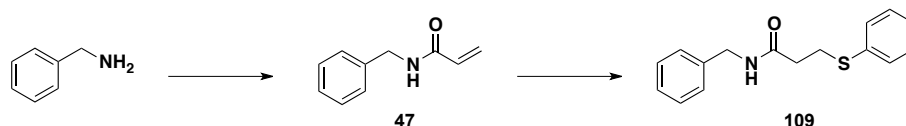
To a solution of benzylamine (0.44 mL, 4.0 mmol, 1.0 eq.) in anhydrous CH_2Cl_2 (10 mL) at 0 °C was added Et_3N (0.62 mL, 4.4 mmol, 1.1 eq.) and acryloyl chloride (0.36 mL, 4.4 mmol, 1.1 eq.) and the cloudy white mixture stirred at rt for 1 h. The reaction was quenched with aqueous NH_4Cl (2 M), acidified to pH 2 with 2N HCl and extracted with CH_2Cl_2 (x 3). The combined organics were dried over $MgSO_4$, filtered and the solvent removed *in vacuo* to yield the desired acrylamide **47** (691 mg, > 95 % pure), which was taken straight on to the next step.

To a solution of the benzyl acrylamide **47** (640 mg, 3.97 mmol, 1.0 equiv) in anhydrous CH_2Cl_2 (1 mL) at 0 °C was added Et_3N (0.55 mL, 3.97 mmol, 1.0 equiv.) and thiophenol (0.51 mL, 4.96 mmol, 1.25 equiv.) and the bright yellow solution warmed to rt resulting in the production of a thick precipitate. Stirring was continued for a further 5 min before addition of further anhydrous CH_2Cl_2 (5 mL). Stirring was continued at rt for another 10 min before the reaction mixture was diluted with CH_2Cl_2 and washed with 5 % NaOH (x 3), 1 N HCl (x 1), sat. $NaHCO_3$ (x 1) and brine (x 2). The organic layer was dried over $MgSO_4$, filtered and the solvent removed *in vacuo* to yield a crude white solid. This was recrystallised from CH_2Cl_2 and the filtrate subjected to a second recrystallisation from CH_2Cl_2 to yield the desired thioether **109** (446mg, 41 %) as a grey crystalline solid, mp = 115-122 °C; R_f = 0.31 (EtOAc/n-hex, 1:1); v_{max} /cm^{-1} 3273, 1639, 1553, 1479, 1452, 1437, 1428, 1373, 1354, 1278, 1235, 1183, 1092, 1070, 1023, 733, 687; δ_H (400 MHz, CDCl$_3$) 7.34-7.24 (9H, m, Ar*H*), 7.18 (1H, tt, *J* 1.0, *J* 7.3, Ar*H*), 5.75 (1H, bs, N*H*), 4.42 (2H, d, *J* 6.2, NHC*H$_2$*), 3.24 (2H, t, *J* 7.7, NHCOC*H$_2$*CH$_2$S), 2.49 (2H, t, *J* 7.7, NHCOCH$_2$C*H$_2$*S); δ_C (101 MHz, DMSO-d$_6$) 170.1, 139.4, 136.0, 129.1, 128.3, 128.1, 127.2, 126.8, 125.7, 42.1, 34.9, 28.2; *m/z* (ESI) 294 [MNa]$^+$, 272 [MH]$^+$; found [MH]$^+$ 272.1105 $C_{16}H_{18}NOS$ requires 272.1109, Δ 1.5 ppm.

(±)-3-Benzenesulfinyl-N-benzyl-propionamide **110**
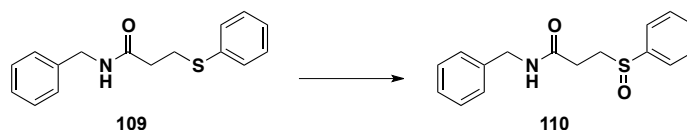
To thioether **109** (200 mg, 0.74 mmol, 1.0 eq.) and sodium *meta*periodate (252 mg, 1.18 mmol, 1.6 eq.) was added MeOH (4 mL) at 0 °C and the suspension stirred rapidly at rt for 24 h. H_2O was added to the reaction mixture and the aqueous layer extracted with CHCl$_3$ (x 3). Combined organics were dried over Na_2SO_4, filtered and the solvent removed *in vacuo*. The crude product was purified on silica (100 % EtOAc) to yield the desired sulfoxide **110** (180 mg, 85 %) as a white solid, mp = 93-96 °C; R_f = 0.29 (100 % EtOAc); v_{max} /cm^{-1} 3283, 3064, 2921, 1651, 1548, 1444, 1250, 1085, 1034, 998, 747, 693; δ_H (400 MHz, CDCl$_3$) 7.62 (1H, bt, *J* 5.8, N*H*), 7.52-7.46 (5H, m, Ar*H*), 7.29-7.18 (5H, m, Ar*H*), 4.39 (1H, dd, *J* 5.8, *J* 15.6, ArC*H$_2$*), 4.33 (1H, dd, *J* 5.8, *J* 15.6, ArC*H$_2$*), 3.27-3.19 (1H, m, SOC*H$_2$*), 2.93-2.86 (1H, m, SOC*H$_2$*), 2.82-2.75 (1H, m, SOCH$_2$C*H$_2$*), 2.56-2.49 (1H, m, SOCH$_2$C*H$_2$*); δ_C (101 MHz, CDCl$_3$)

170.0, 142.8, 138.3, 131.1, 129.3, 128.6, 127.8, 127.3, 123.9, 52.1, 43.6, 28.3; m/z (ESI) 310 [MNa]$^+$, 288 [MH]$^+$; found [MH]$^+$ 288.1045 $C_{16}H_{18}NO_2S$ requires 288.1058, Δ 4.5 ppm.

2-(R)-[(3-Phenylsulfanyl-propionylamino)-methyl]-pyrrolidine-1-carboxylic acid tert-butyl ester **111**
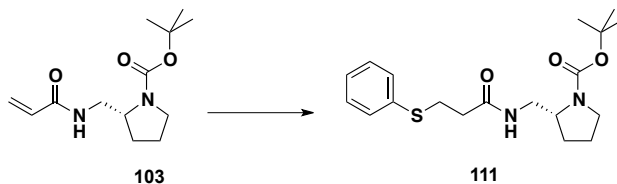
To acrylamide **103** (293.0 mg, 1.15 mmol, 1.0 eq.) in THF (10 mL) was added thiophenol (0.38 mL, 3.69 mmol, 3.2 eq.) and triethylamine (0.72 mL, 5.18 mmol, 4.5 eq.) and the reaction stirred at rt for 20 h. The solvent was removed *in vacuo* and the crude yellow oil purified on silica (EtOAc/n-hex, 1:1) to yield the desired thioether **111** (272.2 mg, 65 %) as a clear oil. $R_f = 0.70$ (100 % EtOAc); $[\alpha]^{22}_D = + 20.1$ ($c = 14.2$, CHCl$_3$); ν_{max} /cm^{-1} 3309, 2972, 1689, 1650, 1480, 1392, 1365, 1344, 1254, 1165, 1133, 1108, 737, 691; δ_H (400 MHz, CDCl$_3$) 7.47 (1H, bs, N*H*), 7.30 (2H, d, *J* 7.2, Ar*H2'*), 7.21 (2H, t, *J* 7.2, Ar*H3'*), 7.12 (1H, t, *J* 7.2, Ar*H4'*), 3.97-3.93 (1H, m, pyrrolidine-*H2'*), 3.42-3.23 (3H, m, NHC*H2* and pyrrolidine-*H5'*), 3.20-3.08 (3H, m, pyrrolidine-*H5'* and ArSC*H2*), 2.48-2.36 (2H, m, ArSCH$_2$C*H2*), 1.98-1.74 (3H, m, pyrrolidine-*H3'* and pyrrolidine-*H4'*), 1.64-1.55 (1H, m, pyrrolidine-*H3'*), 1.39 (9H, s, *t*Bu); δ_C (101 MHz, CDCl$_3$) 171.1, 156.8, 135.8, 129.6, 129.0, 126.3, 80.1, 56.3, 47.2, 46.1, 36.4, 29.5, 29.5, 28.5, 24.0; m/z (ESI) 387 [MNa]$^+$; found [MH]$^+$ 365.1894 $C_{19}H_{29}N_2O_3S$ requires 365.1899, Δ 1.4 ppm.

(R)-3-Phenylsulfanyl-N-pyrrolidin-2-ylmethyl-propionamide **112**
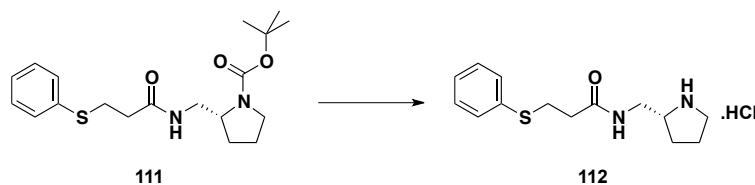
Thioether **111** (213.4 mg, 0.59 mmol, 1.0 eq.) was dissolved in 4M HCl in dioxane (2.0 mL) and the reaction stirred at rt for 50 min until complete by TLC. The solvent was removed under reduced pressure and the residue washed thoroughly with CHCl$_3$ to yield the desired amine **112** (172.9 mg, 97 %) as a clear oil. $R_f = 0$ (100 % EtOAc); $[\alpha]^{22}_D = + 52.0$ ($c = 3.0$, CHCl$_3$); ν_{max} /cm^{-1} 3321 (b), 2931, 2756, 1651, 1549, 1481, 1439, 1368, 1261, 741, 692; δ_H (400 MHz, CDCl$_3$) 9.78 (1H, bs, N*H*), 9.08 (1H, bs, N*H*), 8.15 (1H, bs, N*H*), 7.30 (2H, d, *J* 7.5, Ar*H2'*), 7.23 (2H, t, *J* 7.5, Ar*H3'*), 7.13 (1H, t, *J* 7.5, Ar*H4'*), 3.79 (1H, bs, pyrrolidine-*H2'*), 3.57 (2H, bs, NHC*H2*), 3.24 (2H, bs, ArSC*H2*), 3.18 (2H, bs, pyrrolidine-*H5'*), 2.58 (2H, bs, ArSCH$_2$C*H2*), 2.03-1.93 (3H, m, pyrrolidine-*H3'* and pyrrolidine-*H4'*), 1.76 (1H, bs, pyrrolidine-*H3'*); δ_C (101 MHz, CDCl$_3$) 173.1, 135.6, 129.3, 129.1, 126.3, 60.8, 45.3, 40.1, 35.9, 29.4, 27.4, 24.1; m/z (ESI) 265 [MH]$^+$; found [MH]$^+$ 265.1376 $C_{14}H_{21}N_2OS$ requires 265.1375, Δ 0.4 ppm.

(R,R)-N-(1-Methyl-1-(2-[(1-methyl-pyrrolidin-2-ylmethyl)-carbamoyl]-ethyl)-pyrrolidin-2-ylmethyl)-acrylamide **114**
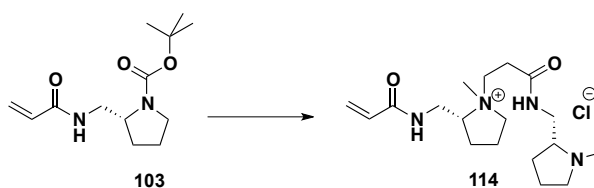
N-boc pyrrolidine **103** (356.9 mg, 1.40 mmol, 1.0 eq.) was stirred in HCl (2.0 M in ether, Sigma-Aldrich, SureSeal) (20 mL) for 3 h. The solvent was removed *in vacuo* and the product dried under high vacuum. To the resulting residue was added paraformaldehyde (147.1 mg, 4.9 mmol, 3.5 eq.) and MeOH (20 mL) and the mixture heated to reflux for 20 min. The solution was cooled to 0 °C and NaBH$_3$CN (879.8 mg, 14.0 mmol, 10 eq.) was added all at once. The reaction mixture was warmed to rt and stirred overnight. 10% aqueous NaHCO$_3$ (11 mL) was added to quench the reaction and the mixture washed with CHCl$_3$ (x 3). Combined organics were dried over MgSO$_4$, filtered and the solvent removed *in vacuo*. The residue was washed with THF/MeOH, 1:1 (2 x 10 mL) to remove any traces of the borate esters. The crude yellow oil was purified on silica (CH$_2$Cl$_2$/MeOH, 7:3) to yield the acrylamide **114** (134.6 mg, 52 %) as a clear oil. $[\alpha]^{22}_D$ = + 84.5 (c = 0.95, MeOH); R$_f$ = 0.18 (CH$_2$Cl$_2$/MeOH, 7:3); ν_{max} /cm^{-1} 1654, 1623, 1555, 1456, 1121, 979; δ_H (500 MHz, MeOD, HSQC, NOESY) 6.28 (1H, dd, J 13.7, J 7.4, CH$_2$CHCONH), 6.22 (1H, dd, J 13.7, J 2.1, CH$_2$CHCONH *cis* to C=O), 5.66 (1H, dd, J 7.4, J 2.1, CH$_2$CHCONH *trans* to C=O), 3.80 (2H, t, J 4.9, NCH$_2$CH$_2$CONH), 3.56 (1H, dd, J 10.8, J 3.2, NHCH$_2$), 3.51 (1H, dd, J 10.8, J 3.2, NHCH$_2$), 3.18 (1H, dd, J 10.8, J 5.8, NHCH$_2$), 3.12 (1H, dd, J 10.8, J 5.8, NHCH$_2$), 3.09-3.06 (2H, m, pyrrolidine-*H2'*), 2.67 (2H, t, J 4.9, NCH$_2$CH$_2$CONH), 2.48-2.42 (2H, m, pyrrolidine-*H5'*), 2.42 (3H, s, NCH$_3$), 2.41 (3H, s, NCH$_3$), 2.33-2.28 (2H, m, pyrrolidine-*H5'*), 2.02-1.95 (2H, m, pyrrolidine-*H3'*), 1.79-1.73 (4H, m, pyrrolidine-*H3'* and pyrrolidine-*H4'*), 1.64-1.57 (2H, m, pyrrolidine-*H4'*); δ_C (500 MHz, MeOD) 172.5, 168.2, 132.0, 126.7, 66.5, 66.5, 58.2, 58.1, 48.8, 48.7, 42.6, 41.2, 41.1, 41.1, 39.9, 29.9, 29.8, 22.9; *m/z* (ESI) 373 [MH]$^+$, 337 [M-Cl]$^+$; found [M-Cl]$^+$ 337.2593 C$_{18}$H$_{33}$N$_4$O$_2$ requires 337.2604, Δ 3.3 ppm.

9.3. Negative control two

Synthesis as a mixture of regioisomers

(±)-2-Benzyl-1-(toluene-4-sulfonyl)-aziridine **120**
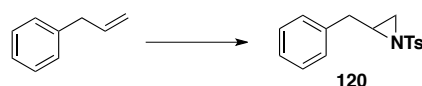
A procedure reported by Sharpless *et al*. was used with some modifications.[177] To a solution of allyl benzene (4.0 mL, 30 mmol, 1.0 eq.) and chloramine-T trihydrate (9.30 g, 33 mmol, 1.1 eq.) in MeCN (150 mL) was added trimethylphenylammonium tribromide (1.11 g, 3.0 mmol, 0.1 eq.) and the yellow reaction mixture stirred vigorously at rt under argon for 43 h. The solvent was removed from the reaction *in vacuo* and the crude residue partitioned between EtOAc and brine. The layers were separated and the aq. layer washed with EtOAc (x 1). Combined organics were dried over MgSO$_4$, filtered and the solvent removed *in vacuo*. The crude orange oil (10.2 g) was purified on silica (EtOAc/n-hex, 1:4) to yield the desired aziridine **120** (3.74 g, 43 %) as a white solid, mp = 64-66 °C; δ_H (400

MHz, CDCl$_3$) 7.69 (2H, d, J 8.2, tol-$H3'$), 7.20 (2H, d, J 8.2, tol-$H2'$), 7.17-7.14 (3H, m, Ph), 7.05-7.03 (2H, m, Ph), 2.96-2.92 (1H, m, PhCH$_2$CH), 2.81 (1H, dd, J 5.2, J 14.5, PhCH_2), 2.71 (1H, d, J 7.1, PhCH$_2$CH(NTs)CH_2), 2.67 (1H, dd, J 7.2, J 14.5, PhCH_2), 2.41 (3H, s, ArCH_3), 2.16 (1H, d, J 4.5, PhCH$_2$CH(NTs)CH_2); δ_C (101 MHz, CDCl$_3$) 144.3, 137.0, 134.8, 129.6, 128.7, 128.5, 127.9, 126.5, 41.2, 37.5, 32.8, 21.6; m/z (ESI) 288 [MH]$^+$; found [MH]$^+$ 288.1047 C$_{16}$H$_{18}$NO$_2$S requires 288.1058, Δ 3.8 ppm. Data in agreement with literature values.[288]

(±)-N-(1-Azidomethyl-2-phenyl-ethyl)-4-methyl-benzenesulfonamide **121a** *and (±)-N-(2-Azido-3-phenyl-propyl)-4-methyl-benzenesulfonamide* **121b**
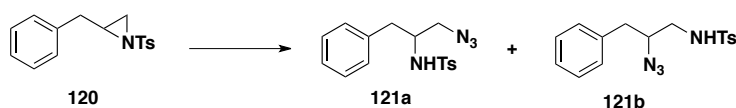
Trimethylsilyl azide (0.21 mL, 1.60 mmol, 1.0 eq.) was added to N-tosyl aziridine **120** (459.2 mg, 1.60 mmol, 1.0 eq.) in DMF (13 mL) under an atmosphere of argon and the colourless solution stirred at 40 °C for 16 h. The reaction mixture was then allowed to cool to rt, diluted with EtOAc and washed with H$_2$O (x 6). The organic layer was dried over MgSO$_4$, filtered and the solvent removed *in vacuo*. The crude clear oil was purified on silica (n-hex/EtOAc, 4:1) and the resulting mixture repurified on silica (n-hex/Et$_2$O, 1:1) to give azides **121a** and **121b** (170.0 mg, 32%) as a colourless oil as an inseparable mixture of regioisomers (8:1). δ_H (400 MHz, CDCl$_3$) 7.73 (2H$_b$, d, J 8.2, tol-$H2'$), 7.63 (2H$_a$, d, J 8.3, tol-$H2'$), 7.32-7.27 (5H$_b$, m, Ph), 7.23-7.19 (5H$_a$, m, Ph), 7.14-7.12 (2H$_b$, m, tol-$H3'$), 7.01-6.98 (2H$_a$, m, tol-$H3'$), 5.27 (1H$_b$, t, J 6.4, TsNH), 5.13 (1H$_a$, d, J 7.7, TsNH), 4.19-4.12 (1H$_b$, m, N$_3$CH), 3.57-3.49 (1H$_a$, m, TsNHCH), 3.38-3.28 (2H$_a$, m, N$_3$CH_2), 3.26-3.17 (2H$_b$, m, TsNHCH_2), 3.07 (1H$_b$, dd, J 7.8, J 14.2, PhCH_2), 2.81-2.67 (2H$_a$, m, PhCH_2), 2.44 (3H$_b$, s, ArCH_3), 2.41 (3H$_a$, s, ArCH_3).

(±)-N-[3-Phenyl-2-(toluene-4-sulfonylamino)-propyl]-acrylamide **119**
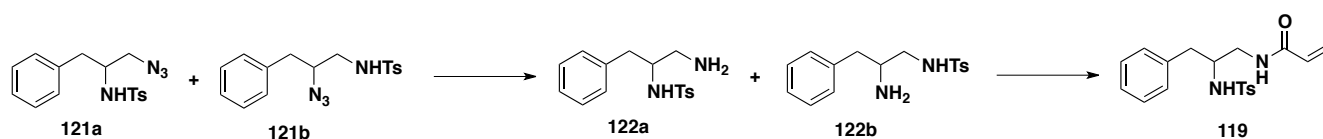
To a solution of azides **121a** and **121b** (165.3 mg, 0.50 mmol, 1.0 eq.) in EtOAc (5 mL) under an argon atmosphere was added palladium on carbon (30 mg, cat.) and the mixture stirred under a H$_2$ atmosphere for 18 h at rt. The reaction mixture was filtered through celite and the solvent removed from the filtrate *in vacuo* to yield an inseparable mixture of amines **122a** and **122b.** To the crude mixture of amines (109.4 mg, 0.36 mmol, 1.0 eq.) in anhydrous CH$_2$Cl$_2$ (1.8 mL) under argon at rt was added Et$_3$N (0.08 mL, 0.50 mmol, 1.5 eq.) and acryloyl chloride (0.03 mL, 0.4 mmol, 1.1 eq.). The resulting pale yellow solution was stirred at rt for 4 h before dilution with CH$_2$Cl$_2$ and addition of H$_2$O. The layers were separated and the aqueous layer further washed with CH$_2$Cl$_2$ (x 1). Combined organics were dried over MgSO$_4$, filtered and the solvent removed *in vacuo*. The crude mixture was purified on silica (1:1, EtOAc/n-hex) to yield the desired acrylamide **119** (41.9 mg, 26 %) as a white powder and the bis-Michael acceptor **123** (28.2 mg, 19 %) as a clear oil. A small portion of the desired acrylamide was repurified using a prep LC-MS (1:1 MeOH/H$_2$O to 100 % MeOH) to give the desired acrylamide **119** as a white solid in high purity for screening.

(±)-N-[3-Phenyl-2-(toluene-4-sulfonylamino)-propyl]-acrylamide **119**

119
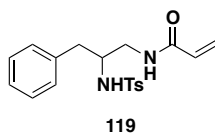
Mp 119-120 °C; R_f = 0.11 (1:1 EtOAc/n-hexane); ν_{max} /cm^{-1} 2925, 1662, 1626, 1601, 1543, 1496, 1455, 1430, 1408, 1324, 1306, 1290, 1245, 1158, 1091, 978; δ_H (400 MHz, CDCl$_3$) 7.56 (2H, d, *J* 8.2, tol-*H2'*), 7.20-7.17 (5H, m, Ph), 6.98-6.96 (2H, m, tol-*H3'*), 6.26 (1H, dd, *J* 17.0, *J* 1.2, C*H$_2$*CHCONH *cis* to C=O), 6.22 (1H, bt, acrylamide-N*H*), 6.03 (1H, dd, *J* 17.0, *J* 10.3, CH$_2$C*H*CONH), 5.65 (1H, dd, *J* 1.2, *J* 10.3, C*H$_2$*CHCONH *trans* to C=O), 5.26 (1H, d, *J* 6.5, sulfonamide-N*H*), 3.51-3.31 (3H, m, NHC*H$_2$CH*), 2.73 (2H, d, *J* 6.8, PhC*H$_2$*), 2.40 (3H, s, ArC*H$_3$*); δ_C (101 MHz, CDCl$_3$) 166.6, 143.4, 136.7, 136.3, 130.6, 129.8, 129.2, 128.8, 127.0, 126.9, 126.9, 55.7, 43.2, 39.7, 21.5; *m/z* (ESI) 359 [MH]$^+$; found [MH]$^+$ 359.1427 C$_{19}$H$_{23}$N$_2$O$_3$S requires 359.1429, Δ 0.6 ppm.

(±)-N-[2-(acryloyl(toluene-4-sulfonyl)amino)-3-phenylpropyl]acrylamide **123**

123
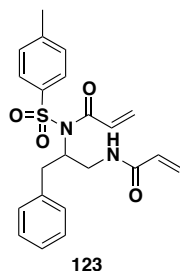
R_f = 0.19 (1:1 EtOAc/n-hexane); δ_H (400 MHz, CDCl$_3$) 7.39 (2H, d, *J* 8.3, tol-*H3'*), 7.22-7.20 (3H, m, Ph), 7.16 (2H, d, *J* 8.3, tol-*H2'*), 7.09-7.06 (2H, m, Ph), 6.67 (1H, dd, *J* 16.6, *J* 10.4, NC(O)C*H*CH$_2$), 6.32 (1H, dd, *J* 16.6, *J* 1.2, NC(O)CHC*H$_2$ cis* to C=O), 6.22 (1H, dd, *J* 17.0, *J* 1.2, NC(O)CHC*H$_2$ cis* to C=O), 6.13 (1H, bt, *J* 5.5, N*H*), 6.02 (1H, dd, *J* 17.0, *J* 10.4, NC(O)C*H*CH$_2$), 5.70 (1H, dd, *J* 10.4, *J* 1.2, NC(O)CHC*H$_2$ trans* to C=O), 5.61 (1H, dd, *J* 10.4, *J* 1.2, NC(O)CHC*H$_2$ trans* to C=O), 4.70-4.63 (1H, m, PhCH$_2$C*H*), 4.03 (1H, ddd, *J* 14.3, *J* 8.4, *J* 6.5, PhCH$_2$CHC*H$_2$*NH), 3.71 (1H, dt, *J* 14.3, *J* 5.0, PhCH$_2$CHC*H$_2$*NH), 3.28 (1H, dd, *J* 13.8, *J* 8.5, PhC*H$_2$*), 3.13 (1H, dd, *J* 13.8, *J* 6.8, PhC*H$_2$*), 2.39 (3H, s, ArC*H$_3$*); δ_C (101 MHz, CDCl$_3$) 167.2, 165.9, 144.9, 137.9, 136.4, 130.9, 130.7, 130.1, 130.0, 129.4, 128.9, 127.6, 126.9, 126.5, 62.4, 42.1, 37.0, 21.7; *m/z* (ESI) 413 [MH]$^+$, 435 [MNa]$^+$; found [MH]$^+$ 413.1518 C$_{22}$H$_{25}$N$_2$O$_4$S requires 413.1535, Δ 4.1 ppm.

Regioselective synthesis

(±)-N-(1-Azidomethyl-2-phenyl-ethyl)-4-methyl-benzenesulfonamide **121a**

120　　　　**121a**
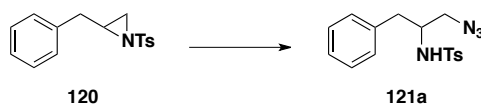
A procedure reported by Maksukawa *et al*. was used with some modifications.[197] To a solution of tris(2,4,6-trimethoxyphenyl)phosphine (26.6 mg, 0.05 mmol, 0.1 eq.) and aziridine **120** (143.7 mg, 0.50 mmol, 1.0 eq.) in

anhydrous DMF (1 mL) was added trimethylsilyl azide (0.1 mL, 0.75 mmol, 1.5 eq.) at rt and the reaction stirred for 7.5 h before addition of H_2O (2 mL). The resulting mixture was extracted with EtOAc (x 1) and the organic layer washed with H_2O (x 5) to remove the remaining DMF. The crude residue was purified on silica (EtOAc/n-hexane, 1:4) to yield the desired azide **121a** (114.8 mg, 70 %) as a clear oil, as a single regioisomer. R_f = 0.34 (EtOAc/n-hexane, 1:4); ν_{max} /cm^{-1} 2101 (N$_3$), 1664, 1604, 1578, 1447, 1330, 1293, 1252, 1227, 1157, 1126, 1089, 965, 816, 729, 697; δ_H (400 MHz, CDCl$_3$) 7.63 (2H, d, J 8.3, tol-$H3'$), 7.23-7.18 (5H, m, ArH), 7.02-6.98 (2H, m, ArH), 5.09 (1H, d, J 7.8, NH), 3.57-3.49 (1H, m, CHNHSO$_2$tol), 3.36 (1H, dd, J 12.3, J 4.9, N$_3$CH_2), 3.30 (1H, dd, J 12.3, J 4.2, N$_3$CH_2), 2.77 (1H, dd, J 13.8, J 7.4, PhCH_2), 2.69 (1H, dd, J 13.8, J 6.9, PhCH_2), 2.41 (3H, s, PhCH_3); δ_C (101 MHz, CDCl$_3$) 143.5, 137.1, 136.3, 129.8, 129.2, 128.8, 127.0, 126.9, 54.5, 53.8, 38.6, 21.6; m/z (ESI) 331 [MH]$^+$; found [MH]$^+$ 331.1230 C$_{16}$H$_{19}$N$_4$O$_2$S requires 331.1229, Δ 0.3 ppm. Data in agreement with literature values.[196]

(±)-N-(1-aminomethyl-2-phenyl-ethyl)-4-methyl-benzenesulfonamide **122a**
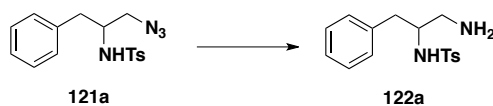
To a solution of azide **121a** (456.5 mg, 1.38 mmol, 1.0 eq.) in EtOAc (13 mL) under argon was added Pd/C (80 mg, cat.) and the mixture stirred under an H_2 atmosphere for 24 h. The reaction mixture was filtered through celite and the solvent removed *in vacuo* to yield the desired amine **122a** (419.3 mg, 100 %) as a clear oil. R_f = 0 (4:1, n-hex/EtOAc); ν_{max} /cm^{-1} 3060, 3029, 2924, 2866, 1599, 1496, 1455, 1320, 1304, 1289, 1151, 1091, 952, 813, 733, 699; δ_H (400 MHz, CDCl$_3$) 7.65 (2H, d, J 8.0, tol-$H2'$), 7.12 (2H, d, J 8.0, tol-$H3'$), 7.06-7.05 (3H, m, Ph), 6.94-6.92 (2H, m, Ph), 5.39 (3H, bs, NH), 3.59-3.53 (1H, bm, TsHNCH), 2.99-2.87 (2H, m, NH$_2$CH_2), 2.68 (2H, d, J 6.4, PhCH_2), 2.34 (3H, s, ArCH_3); δ_C (101 MHz, CDCl$_3$) 143.0, 137.5, 137.0, 129.6, 129.2, 128.4, 127.0, 126.4, 55.7, 43.9, 38.7, 21.5; m/z (ESI) 305 [MH]$^+$; found [MH]$^+$ 305.1315 C$_{16}$H$_{21}$N$_2$O$_2$S requires 305.1324, Δ 2.9 ppm.

(±)-N-[3-Phenyl-2-(toluene-4-sulfonylamino)-propyl]-acrylamide **119**
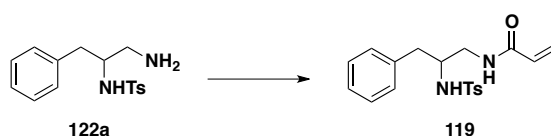
To a rapidly stirred solution of amine **122a** (80 mg, 0.26 mmol, 1.0 eq.) and Et$_3$N (54.2 µL, 0.39 mmol, 1.5 eq.) in anhydrous CH$_2$Cl$_2$ (3.5 mL) at 0 °C was added acryloyl chloride (21.4 µL, 0.26 mmol, 1.0 eq.) and the reaction mixture stirred at 0 °C for 1 h before warming to rt and stirring for a further 13 h. The solvent was removed from the reaction mixture *in vacuo* and the clear oil purified on silica (1:1, EtOAc/n-hex) to yield the desired acrylamide **119** (52.6 mg, 56 %) as a clear oil. Data in agreement with above.

9.4. Non-tethering control ligands

N-(4-Fluoro-benzyl)-acetamide **124**
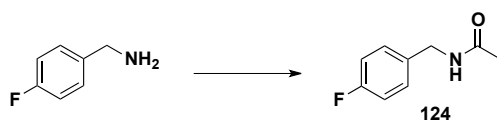
To a solution of *p*-fluorobenzylamine (0.50 mL, 4.37 mmol, 1.0 equiv.) in Et$_2$O (13 mL) was added Et$_3$N (1.22 mL, 8.75 mmol, 2.0 equiv.) and the solution cooled to 0 °C. Acetyl chloride (0.62 mL, 8.75 mmol, 2.0 equiv.) was added dropwise and the resulting thick white precipitate stirred at 0 °C for 5 min and at rt for 10 min. The mixture was filtered under reduced pressure and the filter cake washed with Et$_2$O. The crude solid was purified on silica (100 % EtOAc) to yield the desired acetamide **124** (501.6 mg, 69 %) as a white powder, mp = 98-99 °C. R$_f$ = 0.33 (100 % EtOAc); ν_{max} /cm^{-1} 3286, 1637, 1552, 1509, 1465, 1432, 1419, 1374, 1355, 1304, 1281, 1214, 1160, 1092, 1018, 852, 835, 827, 762, 726, 707, 600; δ_H (400 MHz, CDCl$_3$) 7.23-7.18 (2H, m, Ar*H2'*), 7.00-6.94 (2H, m, Ar*H3'*), 5.99 (1H, bs, N*H*), 4.35 (2H, d, *J* 5.6, C*H$_2$*Ar), 1.98 (3H, s, C*H$_3$*); δ_C (101 MHz, CDCl$_3$) 170.2, 162.4 (d, *J* 245, Ar*C4'*), 134.3, 129.7 (d, *J* 9, Ar*C2'*), 115.7 (d, *J* 22, Ar*C3'*), 43.2, 23.4; *m/z* (ESI) 168 [MH]$^+$; found [MH]$^+$ 168.0824 C$_9$H$_{11}$NOF requires 168.0825, Δ 0.6 ppm. Data in agreement with literature values.[289]

N-(4-Methoxy-benzyl)-acetamide **125**
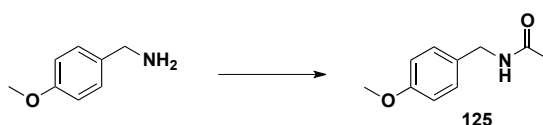
To a solution of *p*-methoxybenzylamine (0.50 mL, 3.83 mmol, 1.0 eq.) in Et$_2$O (11.5 mL) was added Et$_3$N (1.06 mL, 7.65 mmol, 2.0 eq.) and the mixture cooled to 0 °C. Acetyl chloride (0.54 mL, 7.65 mmol, 2.0 eq.) was added dropwise to give immediate precipitation of a white solid. The reaction mixture was warmed to rt and stirred for a further 5 min. The reaction mixture was filtered under reduced pressure and the filter cake washed with Et$_2$O. The crude light tan solid was purified on silica (gradient elution 1:1 to 1:0 EtOAc/n-hexane) to yield the desired amide **125** (402.2 mg, 59 %) as a white solid, mp = 97-99 °C. R$_f$ = 0.25 (100 % EtOAc); ν_{max} /cm^{-1} 3281, 1628, 1611, 1552, 1500, 1465, 1368, 1289, 1250, 1229, 1173, 1110, 1094, 1014, 807, 755, 746, 624, 603; δ_H (400 MHz, MeOD) 7.21-7.18 (2H, m, Ar*H2'*), 6.88-6.85 (2H, m, Ar*H3'*), 4.27 (2H, s, NHC*H$_2$*), 3.76 (3H, s, ArOC*H$_3$*), 1.96 (3H, s, NHCOC*H$_3$*); δ_C (101 MHz, MeOD) 173.1, 160.6, 132.1, 130.1, 115.1, 55.8, 43.9, 22.7; *m/z* (ESI) 180 [MH]$^+$; found [MH]$^+$ 180.1028 C$_{10}$H$_{14}$NO$_2$ requires 180.1025, Δ 1.7 ppm. Data in agreement with literature values.[290]

1-(4-Phenyl-piperazin-1-yl)-ethanone **126**
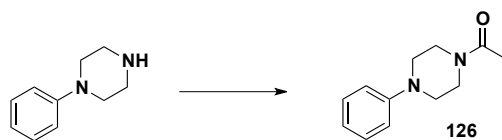
To a solution of N-phenyl piperazine (0.50 mL, 3.27 mmol, 1.0 eq.) in Et$_2$O (10 mL) was added Et$_3$N (0.91 mL, 6.55 mmol, 2.0 eq.) and the mixture cooled to 0 °C. Acetyl chloride (0.47 mL, 6.55 mmol, 2.0 eq.) was added dropwise to give immediate precipitation of a white solid. The mixture was warmed to rt and stirred for a further 5 min, filtered under reduced pressure and the filter cake washed with Et$_2$O and dried under high vacuum. The crude yellow solid was purified on silica (100 % EtOAc) to yield the desired amide **126** (384.9 mg, 58 %) as a crystalline white solid, mp = 89-91 °C. R$_f$ = 0.31 (100 % EtOAc); ν$_{max}$ /cm^{-1} 2819, 1624, 1598, 1496, 1443, 1428, 1387, 1343, 1279, 1227, 1158, 1001, 976, 908, 769, 699, 588; δ$_H$ (400 MHz, MeOD) 7.27-7.22 (2H, m, Ar*H3'*), 7.00-6.97 (2H, m, Ar*H2'*), 6.89-6.84 (1H, m, Ar*H4'*), 3.73 (2H, t, *J* 5.0, piperazine-*H3'*), 3.68 (2H, t, *J* 5.0, piperazine-*H3'*), 3.18 (2H, t, *J* 5.0, piperazine-*H2'*), 3.13 (2H, t, *J* 5.0, piperazine-*H2'*), 2.14 (3H, s, C*H3*); δ$_C$ (101 MHz, MeOD) 171.8, 152.7, 130.3, 121.8, 118.1, 51.2, 50.8, 47.6, 42.9, 21.3; *m/z* (ESI) 205 [MH]$^+$; found [MH]$^+$ 205.1341 C$_{12}$H$_{17}$N$_2$O requires 205.1341, Δ 0 ppm. Data in agreement with literature values.[291]

(±)-N-(1-Benzyl-piperidin-4-yl)-acetamide **127**
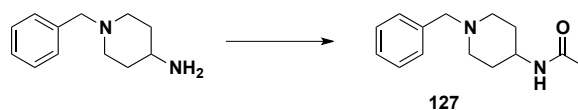
To 4-amino-*N*-benzyl piperadine (0.50 mL, 2.45 mmol, 1.00 eq.) in anhydrous CH$_2$Cl$_2$ (1.5 mL) at rt, under argon, was added acetic anhydride (0.24 mL, 2.57 mmol, 1.05 eq.) dropwise to bring to solution to reflux. The reaction was then refluxed for 1 h before cooling on ice and addition of 20 % aqueous NaOH. The layers were separated and the organic layer dried over MgSO$_4$, filtered and the solvent removed *in vacuo*. The crude white solid was purified on silica (gradient elution, 2 % MeOH to 20 % MeOH in CH$_2$Cl$_2$) to yield the desired amide **127** (514.6 mg, 90 %) as a white solid, mp = 144-145 °C. R$_f$ = 0.29 (CH$_2$Cl$_2$/MeOH, 24:1); ν$_{max}$ /cm^{-1} 3263, 3082, 2940, 2806, 2762, 1633, 1557, 1494, 1453, 1445, 1431, 1364, 1324, 1307, 1293, 1265, 1244, 1142, 1125, 1110, 1101, 1074, 1028, 1013, 982, 971, 793, 738, 699, 613, 592; δ$_H$ (400 MHz, CDCl$_3$) 7.35-7.24 (5H, m, Ar*H*), 5.66 (1H, bd, *J* 7.4, N*H*), 3.85-3.75 (1H, m, HNC*H*), 3.50 (2H, s, ArC*H2*), 2.85-2.82 (2H, m, piperidine-*H2'*), 2.15-2.09 (2H, m, piperidine-*H2'*), 1.97 (3H, s, NHCOC*H3*), 1.92-1.89 (2H, m, piperadine-*H3'*), 1.52-1.42 (2H, m, piperadine-*H3'*); δ$_C$ (101 MHz, CDCl$_3$) 100.5, 92.6, 90.3, 90.1, 89.8, 73.7, 80.0, 69.6, 65.9, 63.8; *m/z* (ESI) 233 [MH]$^+$; found [MH]$^+$ 233.1652 C$_{14}$H$_{21}$N$_2$O requires 233.1654, Δ 0.9 ppm. Data in agreement with literature values.[292]

N-[1-(Toluene-4-sulfonyl)-(R)-pyrrolidin-2-ylmethyl]-acetamide **128**
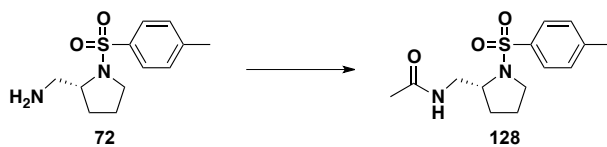
To a solution of amine **72** (187.7 mg, 0.74 mmol, 1.0 eq.) and Et$_3$N (0.12 mL, 0.89 mmol, 1.2 eq.) in anhydrous CH$_2$Cl$_2$ (5 mL) at 0 °C was added acetyl chloride (0.06 mL, 0.89 mmol, 1.2 eq.) dropwise and the reaction stirred at 0 °C for 1 h. The reaction mixture was poured into brine and extracted with CH$_2$Cl$_2$ (x 2), dried over Na$_2$SO$_4$, filtered and the solvent removed *in vacuo*. The crude product was purified on silica (100 % EtOAc) to give the desired acetamide **128** (148.0 mg, 68 %) as a white powder, mp = 171-174 °C; [α]$^{24}_D$ = + 90.0 (*c* = 0.67, CHCl$_3$); R$_f$ = 0.29 (100 % EtOAc); ν_{max} /cm^{-1} 3298, 1658, 1637, 1570, 1339, 1308, 1290, 1253, 1198, 1156, 1106, 1040, 977, 818, 727, 709, 662, 602, 584; δ_H (400 MHz, CDCl$_3$) 7.68 (2H, d, *J* 8.9, Ar*H3'*), 7.31 (2H, d, *J* 8.9, Ar*H2'*), 6.57 (1H, bs, N*H*), 3.70-3.64 (1H, m, pyrrolidine-*H2'*), 3.50-3.39 (2H, m, NHC*H$_2$*), 3.23-3.16 (2H, m, pyrrolidine-*H5'*), 2.42 (3H, s, ArC*H$_3$*), 2.02 (3H, s, C*H$_3$*CONH), 1.79-1.72 (1H, m, pyrrolidine-*H4'*), 1.61-1.41 (3H, m, pyrrolidine-*H3'* and pyrrolidine-*H4'*); δ_C (101 MHz, CDCl$_3$) 171.0, 144.2, 133.9, 130.1, 127.8, 59.7, 49.9, 44.2, 30.0, 24.3, 23.5, 21.8; *m/z* (ESI) 297 [MH]$^+$, 319 [MNa]$^+$; found [MH]$^+$ 297.1263 C$_{14}$H$_{21}$N$_2$O$_3$S requires 297.1273, Δ 3.4 ppm.

N-Benzyl-acetamide **129**
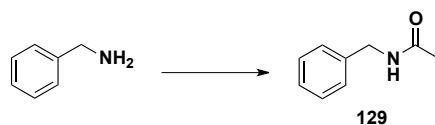
To benzylamine (0.50 mL, 4.58 mmol, 1.00 eq.) in anhydrous CH$_2$Cl$_2$ (3 mL) at rt under argon was added acetic anhydride (0.45 mL, 4.81 mmol, 1.05 eq.) dropwise bringing the reaction mixture to reflux. The colourless solution was further refluxed for 3 h before cooling on ice and addition of 20 % NaOH (aq.) dropwise. The aqueous and organic layers were separated and the aqueous layer extracted with CH$_2$Cl$_2$ (x 1). Combined organics were dried over MgSO$_4$, filtered and the solvent removed *in vacuo*. The crude white solid was purified on silica (100 % EtOAc) to yield the desired acetamide **129** (512.6 mg, 71 %) as a white solid, mp = 64-65 °C; R$_f$ = 0.38 (100 % EtOAc); ν_{max} /cm^{-1} 3294, 1640, 1632, 1543, 1498, 1452, 1375, 1353, 1280, 748, 716, 692; δ_H (400 MHz, CDCl$_3$) 7.35-7.26 (5H, m, Ar*H*), 6.43 (1H, bs, N*H*), 4.39 (2H, d, *J* 5.6, C*H$_2$*), 1.98 (3H, s, C*H$_3$*); δ_C (101 MHz, CDCl$_3$) 170.2, 138.4, 128.7, 127.8, 127.4, 43.6, 23.1; *m/z* (ESI) 150 [MH]$^+$; found [MH]$^+$ 150.0916 C$_9$H$_{12}$NO requires 150.0919, Δ 2.0 ppm. Data in agreement with literature values.[293]

4-(Acetylamino-methyl)-benzoic acid methyl ester **130**
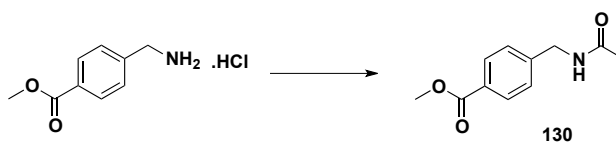
To a solution of methyl 4-(aminomethyl) benzoate hydrochloride (1.00 g, 4.96 mmol, 1.0 eq.) in anhydrous THF (20 mL) under argon was added Et$_3$N (2.4 mL, 17.36 mmol, 3.5 eq.) and the mixture cooled to 0 °C before addition of acetyl chloride (0.35 mL, 4.96 mmol, 1.0 eq.) dropwise. The thick white precipitate was stirred for 24 h at rt before addition of 1 M HCl (aq.) and the mixture extracted with EtOAc (x 2). Combined organics were dried over MgSO$_4$, filtered and the solvent removed *in vacuo*. The crude white solid was purified on silica (EtOAc/n-hexane, 4:1) to yield the desired acetamide **130** (666.7 mg, 65%) as a white powder. A small portion was recrystallised from EtOAc/n-hexane to yield the desired acetamide **130** as colourless crystals, mp = 112-115 °C; R$_f$ = 0.26 (EtOAc/n-hexane, 4:1); ν_{max} /cm^{-1} 3271 (NH), 1721 (ester C=O), 1643, 1632, 1612, 1555, 1435, 1416, 1378, 1274, 1236, 1194, 1181, 1171, 1112, 1106, 1019, 752, 697; δ_H (400 MHz, CDCl$_3$) 7.95 (2H, d, *J* 8.2, Ar*H2'*), 7.29 (2H, d, *J* 8.2, Ar*H3'*), 4.44 (2H, d, *J* 5.9, ArC*H$_2$*), 3.87 (3H, s, COOC*H$_3$*), 2.01 (3H, s, NHCOC*H$_3$*); δ_C (101 MHz, CDCl$_3$) 170.2, 166.9, 143.7, 130.1, 129.4, 127.6, 52.2, 43.4, 23.3; *m/z* (ESI) 208 [MH]$^+$; found [MH]$^+$ 208.0963 C$_{11}$H$_{14}$NO$_3$ requires 208.0974, Δ 5.3 ppm.

9.5. Oligo(ethyleneglycol) linker

N-[2-(2-Hydroxy-ethoxy)-ethyl]-acrylamide **132**
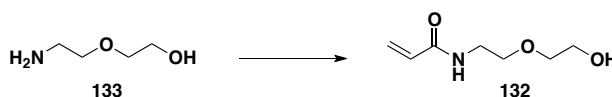
To 2-(2-aminoethoxy)ethanol **133** (0.50 mL, 4.98 mmol, 1.0 eq.) in anhydrous CH$_2$Cl$_2$ (5 mL) at 0 °C was added acryloyl chloride (0.40 mL, 4.98 mmol, 1.0 eq.) and triethylamine (0.69 mL, 4.98 mmol, 1.0 equiv.) and the reaction mixture stirred at 0 °C for 15 min and at rt overnight. The solvent was removed from the reaction mixture and the crude residue purified on silica (100 % EtOAc) to yield the desired acrylamide **132** (527.2 mg, 67 %) as a clear oil. R$_f$ = 0.13 (100 % EtOAc); ν_{max} /cm^{-1} 3282 (b), 2928, 2874, 1656, 1642, 1547, 1456, 1410, 1351, 1317, 1247, 1121, 1062, 985, 961, 886, 805; δ_H (400 MHz, CDCl$_3$) 7.41 (1H, bt, *J* 4.9, N*H*), 6.16 (1H, dd, *J* 17.1, *J* 2.4, C*H$_2$*CHONH *cis* to C=O), 6.07 (1H, dd, *J* 17.1, *J* 10.0, CH$_2$C*H*ONH), 5.49 (1H, dd, *J* 10.0, *J* 2.4, C*H$_2$*CHONH *trans* to C=O), 4.26 (1H, bs, O*H*), 3.61-3.59 (2H, m, OCH$_2$C*H$_2$*OH), 3.48-3.44 (4H, m, OC*H$_2$*CH$_2$NH and OC*H$_2$*CH$_2$OH), 3.42-3.38 (2H, m, OCH$_2$C*H$_2$*NH); δ_C (101 MHz, CDCl$_3$) 166.2, 130.7, 126.3, 72.2, 69.5, 61.3, 39.3; *m/z* (ESI) 182 [MNa]$^+$; found [MNa]$^+$ 182.0790 C$_7$H$_{13}$NO$_3$Na requires 182.0793, Δ 1.6 ppm.

[2-(2-Acryloylamino-ethoxy)-ethoxy]-acetic acid tert-butyl ester **134**
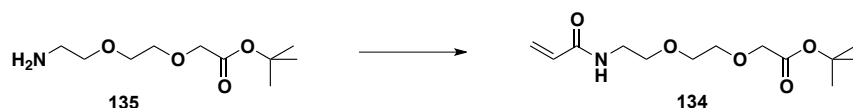
To amine **135** (100 mg, 0.46 mmol, 1.0 eq.) in anhydrous CH_2Cl_2 (5 mL) at 0 °C was added acryloyl chloride (0.06 mL, 0.69 mmol, 1.5 eq.) and triethylamine (0.10 mL, 0.69 mmol, 1.5 eq.) and the bright yellow reaction mixture stirred under argon at 0 °C for 15 min and at rt overnight. H_2O was added to the reaction mixture and the layers separated. The organic layer was dried over $MgSO_4$, filtered and the solvent removed *in vacuo*. The crude residue was purified on silica (100 % EtOAc) to give the desired acrylamide **134** (27.2 mg, 22 %) as a clear oil. R_f = 0.37 (100 % EtOAc); ν_{max} /cm^{-1} 1745, 1661, 1628, 1540, 1369, 1230, 1145, 1120; δ_H (400 MHz, CDCl$_3$) 6.54 (1H, bs, N*H*), 6.26 (1H, dd, *J* 17.3, *J* 1.8, CH$_2$CHCONH *cis* to C=O), 6.15 (1H, dd, *J* 17.3, *J* 10.0, CH$_2$C*H*CONH), 5.57 (1H, dd, *J* 10.0, *J* 1.8, CH$_2$CHCONH trans to C=O), 3.98 (2H, s, OC*H*$_2$COO^{t}Bu), 3.67-3.62 (4H, m, C*H*$_2$), 3.61-3.58 (2H, m, C*H*$_2$), 3.54-3.49 (2H, m, C*H*$_2$), 1.45 (9H, s, *t*Bu); δ_C (101 MHz, CDCl$_3$) 169.7, 165.7, 131.1, 126.1, 81.9, 70.8, 70.0, 69.8, 68.9, 39.2, 28.1; *m/z* (ESI) 296 [MNa]$^+$; found [MNa]$^+$ 296.1469 C$_{13}$H$_{23}$NO$_5$Na requires 296.1474, Δ 1.7 ppm.

[2-(2-Amino-ethoxy)-ethoxy]-acetic acid tert-butyl ester **135**

Method One: *from monobenzylated amine* **140**
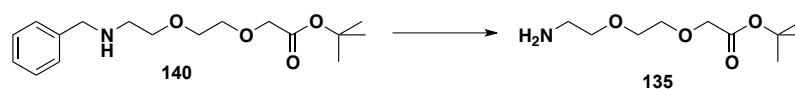
To monobenzylamine **140** (1.38 g, 4.5 mmol, 1.0 eq.) in MeOH (25 mL) under argon was added Pd(OH)$_2$/C (313 mg, cat.) all at once, and the mixture stirred at rt under a H$_2$ (g) atmosphere for 3 days. The reaction mixture was filtered through celite and the solvent removed *in vacuo* to yield the desired amine **135** (1.0 g, 100 %) as a yellow oil.

Method Two: *from dibenzylated amine* **139**
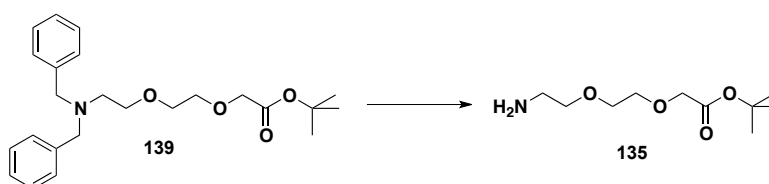
A mixture of dibenzylamine **139** (100 mg, 0.25 mmol, 1.0 eq.), Pd(OH)$_2$/C (25 mg, cat.) and NH$_4$.HCO$_2$ (71.3 mg, 1.13 mmol, 4.5 eq.) in MeOH (5 mL) was heated to 75 °C for 24 h. The reaction mixture was allowed to cool to rt, filtered through celite and the solvent removed *in vacuo* to yield the desired amine **135** (55.0 mg, 100 %) as a clear oil. R_f = 0 (100 % EtOAc); ν_{max} /cm^{-1} 3399 (NH), 2513, 1735, 1457, 1370, 1240, 1141, 1112; δ_H (400 MHz, MeOD) 4.08 (2H, s, N*H*$_2$), 3.78-3.72 (8H, m, 3 x C*H*$_2$ and OC*H*$_2$COO*t*Bu), 3.18-3.15 (2H, m, C*H*$_2$), 1.52 (9H, s, *t*Bu); δ_C (101 MHz, MeOD) 170.3, 81.6, 70.4, 69.8, 69.0, 68.3, 39.9, 27.0; *m/z* (ESI) 220 [MH]$^+$; found [MH]$^+$ 220.1548 C$_{10}$H$_{22}$NO$_4$ requires 220.1549, Δ 0.5 ppm.

2-(2-Dibenzylamino-ethoxy)-ethanol **136**
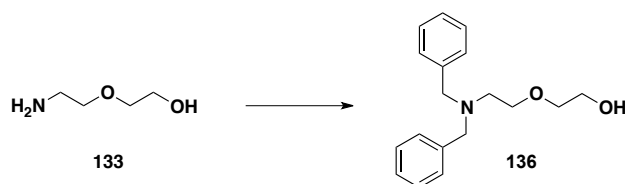
A procedure reported by Visintin *et al*. was used with some modifications.[190] A mixture of 2-(2-aminoethoxy)ethanol (5.00 mL, 49.8 mmol, 1.0 eq.), potassium carbonate (17.21 g, 124.5 mmol, 2.5 eq.) and benzyl bromide (11.83 mL, 99.6 mmol, 2.0 eq.) in MeCN (250 mL) was stirred at 50 °C for 20 h. The solid was filtered under reduced pressure and the solvent removed from the filtrate. The residue was dissolved in HCl (0.1 M) and washed with EtOAc (2 x 25 mL). The aqueous layer was basified with NaOH and extracted with CH_2Cl_2 (4 x 25 mL). The combined CH_2Cl_2 layers were washed with H_2O (x 1), added to the EtOAc layers, and combined organics dried over $MgSO_4$, filtered and the solvent removed *in vacuo* to yield the desired dibenzylamino alcohol **136** (10.10 g, 71 %) as a clear oil. R_f = 0.64 (100 % EtOAc); ν_{max} /cm^{-1} 1495, 1453, 1367, 1244, 1119, 1049, 1027, 744, 732, 696; δ_H (400 MHz, CDCl$_3$) 7.50 (4H, d, *J* 7.6, Ar*H2'*), 7.43 (4H, t, *J* 7.6, Ar*H3'*), 7.34 (2H, t, *J* 7.6, Ar*H4'*), 3.76-3.74 (6H, m, ArC*H$_2$*N and OCH$_2$C*H$_2$*OH), 3.67 (2H, t, *J* 6.2, NCH$_2$C*H$_2$*O), 3.55 (2H, t, *J* 4.9, HOCH$_2$C*H$_2$*O), 3.35 (1H, bs, OH) 2.80 (2H, t, *J* 6.2, NC*H$_2$*CH$_2$O); δ_C (101 MHz, CDCl$_3$) 139.2, 128.8, 128.2, 126.9, 72.1, 69.4, 61.6, 58.8, 52.8; *m/z* (ESI) 286 [MH]$^+$; found [MH]$^+$ 286.1805 $C_{18}H_{24}NO_2$ requires 286.1807, Δ 0.7 ppm.

[2-(2-Dibenzylamino-ethoxy)-ethoxy]-acetic acid **137**
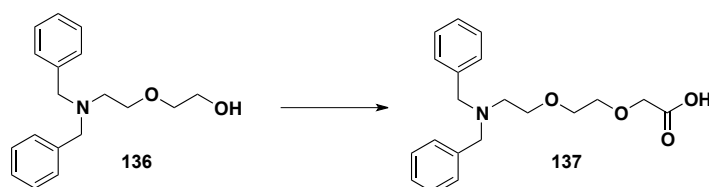
A procedure reported by Visintin *et al*. was used with some modifications.[190] 2-[(Dibenzylamino)ethoxy]ethanol **136** (2.00 g, 7.0 mmol, 1.0 eq.) was dissolved in anhydrous THF (15 mL) before cooling to 0 °C and addition of NaH (1.12 g, 28.0 mmol, 4.0 eq.) portionwise followed by α-bromoacetic acid (1.46 g, 10.5 mmol, 1.5 eq.) and the suspension refluxed under argon overnight. Water (0.5 mL) was added dropwise and the reaction stirred for a further 5 min before addition of further water (15 mL) and extraction with Et$_2$O:n-hexane (1:1) (16 mL x 2). The aqueous layer was acidified to pH 2-3 with 1M HCl and extracted with Et$_2$O (7 mL x 3). The aqueous layer was then basified to pH 6-7 with saturated NaOH and then saturated with NaCl before extraction with CH_2Cl_2 (4 x 20 mL) and CHCl$_3$ (4 x 20 mL). Chlorinated organics were combined and the solvent removed *in vacuo* to give the desired carboxylic acid **137** (1.53 g, 63 %) as an oily white solid. R_f = 0 (100 % EtOAc); ν_{max} /cm^{-1} 3400 (b), 1601, 1495, 1454, 1427, 1324, 1250, 1108, 1028, 751, 736, 700; δ_H (400 MHz, MeOD) 7.49-7.47 (4H, m, Ar*H2'*), 7.41-7.33 (6H, m, Ar*H3'* and Ar*H4'*), 4.07 (4H, s, ArC*H$_2$*N), 3.93 (2H, s, OC*H$_2$*COOH), 3.67 (2H, t, *J* 5.7, NCH$_2$C*H$_2$*O), 3.63-3.56 (4H, m, OC*H$_2$*C*H$_2$*O), 2.99 (2H, t, *J* 5.7, NC*H$_2$*CH$_2$O); δ_C (101 MHz, MeOD) 177.3, 135.6, 131.6, 130.0, 129.8, 79.6, 71.3, 71.2, 68.1, 59.6, 53.1; *m/z* (ESI) 344 [MH]$^+$; found [MH]$^+$ 344.1848 $C_{20}H_{26}NO_4$ requires 344.1862, Δ 4.1 ppm.

[2-(2-Amino-ethoxy)-ethoxy]-acetic acid **138**
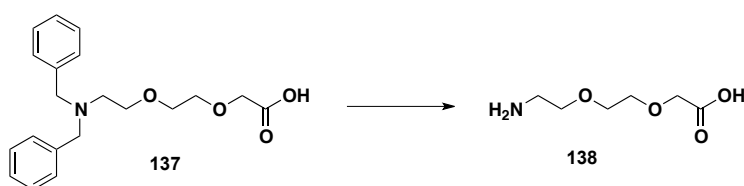
A procedure reported by Visintin *et al.* was used with some modifications.[190] Dibenzyl amine **137** (1.42 g, 4.12 mmol, 1.0 eq.) was dissolved in MeOH (17 mL), palladium on carbon (10 %) (710 mg, cat.) was added and the mixture stirred under a H_2 atmosphere for 20 h at 45 °C. The reaction mixture was filtered through celite and the solvent removed *in vacuo*. The crude residue was dried under high vacuum to yield the desired amine **138** (657 mg, 98 %) as a white residue. R_f = 0 (100 % EtOAc); ν_{max} /cm^{-1} 3370 (b), 2918, 1586, 1411, 1323, 1094, 1026, 704; δ_H (400 MHz, MeOD) 3.90 (2H, s, OCH_2COOH), 3.71-3.65 (6H, m, OCH_2CH_2OCH_2CH_2NH$_2$), 3.07 (2H, t, *J* 5.0, H$_2$NCH_2); δ_C (101 MHz, MeOD) 178.0, 71.6, 71.0, 71.0, 69.3, 40.7; *m/z* (ESI) 164 [MH]$^+$; found [MH]$^+$ 164.0916 $C_6H_{14}NO_4$ requires 164.0923, Δ 4.3 ppm.

(2-(2-[Benzyl-(2-methylene-pent-3-enyl)-amino]-ethoxy)-ethoxy)-acetic acid tert-butyl ester **139**
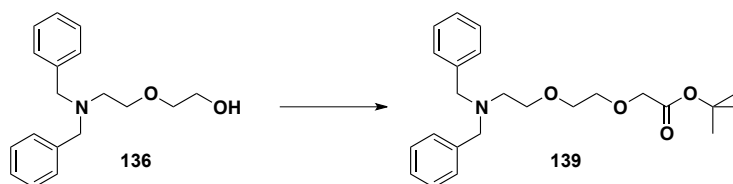
To a solution of alcohol **136** (2.10 mL, 8.18 mmol, 1.0 eq.) in anhydrous THF (12 mL) at 0 °C was added KO^{t}Bu (1.0 M solution in THF, Sigma-Aldrich SureSeal, 12.26 mL, 12.26 mmol, 1.5 eq.) and bromo-acetic acid *tert*-butyl ester (1.81 mL, 12.26 mmol, 1.5 eq.) and the thick yellow suspension stirred at 0 °C for 3 h. H_2O (5 mL) was added to quench the reaction before addition of further H_2O and CH_2Cl_2. The layers were separated and the aqueous layer washed with further CH_2Cl_2. Combined organics were dried over $MgSO_4$, filtered and the solvent removed *in vacuo*. Purification of the crude product on silica (n-hex/EtOAc, 3:1), combination of appropriate fractions, and repurification of the partially pure product on silica (n-hex/EtOAc, 5:1) yielded the desired *tert*butyl ester **139** (2.44 g, 75 %) as a clear oil. R_f = 0.41 (n-hex/EtOAc, 3:1); ν_{max} /cm^{-1} 1747, 1495, 1454, 1367, 1301, 1249, 1226, 1141, 1116, 1028, 844, 744, 733, 698; δ_H (400 MHz, CDCl$_3$) 7.40 (4H, d, *J* 7.3, Ar*H2'*), 7.33 (4H, t, *J* 7.3, Ar*H3'*), 7.25 (2H, t, *J* 7.3, Ar*H4'*), 4.04 (2H, s, OCH_2COOtBu), 3.71-3.69 (2H, m, CH_2), 3.68 (4H, s, ArCH_2N), 3.63-3.59 (4H, m, CH_2), 2.73 (2H, t, *J* 6.3, NCH_2CH_2O), 1.50 (9H, s, tBu); δ_C (101 MHz, CDCl$_3$) 176.6, 146.7, 135.6, 135.1, 133.7, 88.4, 84.3, 83.9, 83.6, 75.9, 65.8, 59.6, 35.0; *m/z* (ESI) 400 [MH]$^+$, 422 [MNa]$^+$; found [MH]$^+$ 400.2481 $C_{24}H_{34}NO_4$ requires 400.2488, Δ 1.7 ppm.

[2-(2-Benzylamino-ethoxy)-ethoxy]-acetic acid tert-butyl ester **140**
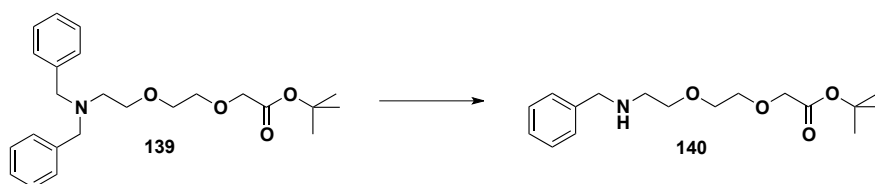
To dibenzylamine **139** (2.44 g, 6.1 mmol, 1.0 eq.) in MeOH (25 mL) under argon was added Pd/C (740 mg, cat.) and the mixture stirred for 20 h at 45 °C under an atmosphere of H_2 (g). The reaction mixture was filtered through celite and the solvent removed *in vacuo* to yield the monobenzylated amine **140** (1.9 g, 100 %) as a white wax. $R_f = 0.81$ (CH_2Cl_2/MeOH, 2:1); δ_H (400 MHz, MeOD) 7.53-7.45 (5H, m, Ar*H*), 4.27 (2H, s, NHC*H*$_2$Ph), 4.04 (2H, s, OC*H*$_2$COO*t*Bu), 3.81-3.79 (2H, m, C*H*$_2$), 3.72-3.70 (4H, m, 2 x C*H*$_2$), 3.27-3.25 (2H, m, CH$_2$), 1.47 (9H, s, *t*Bu); δ_C (101 MHz, MeOD) 170.3, 131.1, 129.7, 129.3, 128.9, 81.8, 70.4, 69.7, 68.1, 65.2, 50.7, 46.6, 26.9.

(±)-2-Phenylselanyl-propionic acid ethyl ester **142**
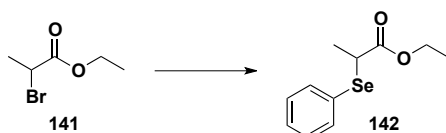
Using an adaption of a literature method,[294] NaBH$_4$ (454 mg, 12 mmol, 3.00 equiv.) was added portionwise to a solution of diphenyldiselenide (1.25 g, 4.0 mmol, 1.00 eq.) in EtOH (30 mL) at 0 °C to give vigorous evolution of H_2 (g). The resulting bright yellow precipitate was stirred at 0 °C under argon to give a cloudy grey suspension. Ethyl 2-(bromo)propionate **141** (1.30 mL, 10.0 mmol, 1.25 eq.) was added dropwise and the mixture stirred at 0 °C for 1 h and allowed to warm to rt. The reaction was quenched by dropwise addition of water and extracted with ether. The ether layer was washed with water, brine, dried over MgSO$_4$, filtered and the solvent removed *in vacuo*. The crude residue was purified on silica (n-hex/EtOAc, 4:1) to yield the desired ester **142** (1.78 g, 87 %) as a clear oil. $R_f = 0.47$ (EtOAc/n-hex, 1:5); ν_{max} /cm^{-1} 1725, 1477, 1439, 1369, 1325, 1254, 1207, 1145, 1066, 1057, 1021, 740, 692; δ_H (400 MHz, CDCl$_3$) 7.59-7.57 (2H, m, Ar*H*), 7.34-7.24 (3H, m, Ar*H*), 4.07 (2H, q, *J* 7.3, COOC*H*$_2$CH$_3$), 3.75 (1H, q, *J* 7.0, EtOCOC*H*), 1.52 (3H, d, *J* 7.0, EtOCOCH(SePh)C*H*$_3$), 1.15 (3H, t, *J* 7.3, COOCH$_2$C*H*$_3$); δ_C (101 MHz, CDCl$_3$) 173.7, 136.0, 129.2, 128.7, 128.1, 61.2, 37.6, 17.8, 14.2; *m/z* (CI) 276 [MNH$_4$]$^+$. Data in agreement with literature values.[294]

(±)-N-[2-(2-Hydroxy-ethoxy)-ethyl]-2-phenylselanyl-propionamide **143**

Method One
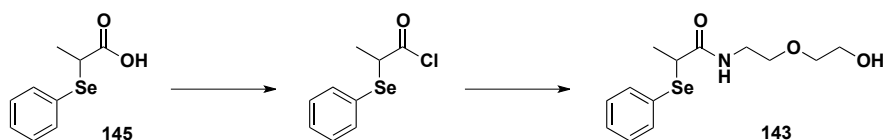
To a solution of carboxylic acid **145** (103.9 mg, 0.45 mmol, 1.00 eq.) in anhydrous THF (1 mL) was added oxalyl chloride (0.04 mL, 0.48 mmol, 1.05 eq.) and a drop of DMF (cat.) and the reaction stirred at room temperature under argon for 10 minutes, at which point all effervescence ceased. The resultant mixture was added dropwise to a stirred solution of 2-(2-aminoethoxy)ethanol (0.07 mL, 0.68 mmol, 1.5 eq.) and Et$_3$N (0.16 mL, 1.13 mmol, 2.5 eq.) in THF (1 mL) to give vigorous evolution of gas. The resulting thick white precipitate was stirred under argon at rt for 3 h before loading directly onto a silica column (100 % EtOAc) to give the desired amide **143** (88.2 mg, 63 %) as a clear oil and bis-acetylated **146** (15.9 mg, 14 %) as a yellow oil.

(±)-N-[2-(2-Hydroxy-ethoxy)-ethyl]-2-phenylselanyl-propionamide **143**
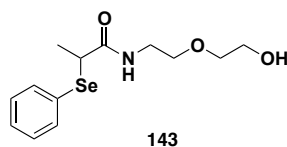
R$_f$ = 0.19 (100 % EtOAc); ν$_{max}$ /cm^{-1} 3291 (b), 1643, 1546, 1477, 1438, 1371, 1351, 1245, 1122, 1064, 1022, 886, 739, 691; δ$_H$ (400 MHz, CDCl$_3$) 7.56-7.55 (2H, m, Ar*H*), 7.33-7.26 (3H, m, Ar*H*), 6.63 (1H, bt, N*H*), 3.77 (1H, q, *J* 7.2, NHCOC*H*), 3.69 (2H, t, *J* 4.4, C*H$_2$*), 3.51-3.49 (2H, m, C*H$_2$*), 3.46-3.45 (2H, m, C*H$_2$*), 3.41-3.38 (2H, m, C*H$_2$*), 2.74 (1H, bs, O*H*), 1.58 (3H, d, *J* 7.2, C*H$_3$*); δ$_C$ (101 MHz, MeOD) 172.8, 134.9, 129.3, 128.5, 128.4, 72.3, 69.8, 61.8, 40.8, 39.7, 18.4; *m/z* (ESI) 318 [MH]$^+$, 340 [MNH$_4$]$^+$; found [MH]$^+$ 318.0616 C$_{13}$H$_{20}$NO$_3$^{80}Se requires 318.0608, Δ 2.5 ppm.

(±)-2-Phenylselanyl-propionic acid 2-[2-(2-phenylselanyl-propionylamino)-ethoxy]-ethyl ester **146**
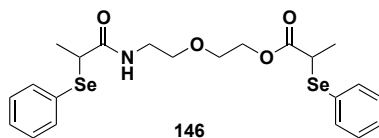
R$_f$ = 0.19 (100 % EtOAc); δ$_H$ (400 MHz, CDCl$_3$) 7.64-7.55 (4H, m, Ar*H*), 7.38-7.27 (6H, m, Ar*H*), 6.40 (1H, s, N*H*), 4.20 (2H, m, C*H$_2$*), 3.38-3.74 (2H, m, CH$_3$C*H*(SePh)CONH and CH$_3$C*H*(SePh)COO), 3.56-3.52 (2H m, C*H$_2$*), 3.45-3.35 (4H, m, C*H$_2$*), 1.61-1.54 (6H, m, 2 x C*H$_3$*).

Method Two
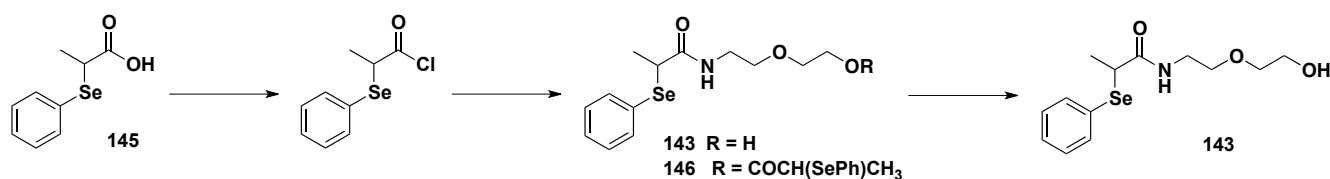
To a solution of carboxylic acid **145** (11.26 g, 49.1 mmol, 1.0 eq.) in anhydrous THF (75 mL) under argon at 0 °C was added oxalyl chloride (4.2 mL, 49.1 mmol, 1.0 eq.) dropwise and a few drops of DMF (cat.) and the reaction allowed to warm to rt and stirred for 2 h.

To a stirred solution of 2-(2-aminoethoxy)ethanol (9.9 mL, 98.3 mmol, 2.0 eq.) in THF (75 mL) at 0 °C under argon was added Et$_3$N (10.2 mL, 73.7, 1.5 eq.) and the acid chloride solution dropwise. The thick white precipitate was stirred overnight before quenching by dropwise addition of H$_2$O. The layers were separated and the aqueous further washed with CH$_2$Cl$_2$ (x 3). Combined organics were dried over MgSO$_4$, filtered and the solvent removed *in vacuo*. The resulting yellow oil was dissolved in EtOH (100 mL) before addition of 30 % aqueous KOH (100 mL) dropwise and stirring at rt for 15 min. The EtOH was removed *in vacuo* and the aqueous layer washed with CH$_2$Cl$_2$ (x 2). Combined organics were washed with 5 % aq. KOH, dried over MgSO$_4$, filtered and the solvent removed *in vacuo* to give the desired amide **143** (12.19 g, 79 %) as a clear oil. Data in agreement with above.

(±)-(2-[2-(2-Phenylselanyl-propionylamino)-ethoxy]-ethoxy)-acetic acid **144**
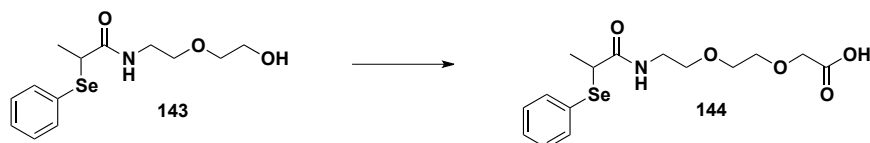
To a solution of alcohol **143** (798.8 mg, 2.53 mmol, 1.1 eq.) and freshly recrystallised iodoacetic acid (427.0 mg, 2.30 mmol, 1.0 eq.) in anhydrous THF (20 mL) was added 60% NaH in mineral oil (368.0 mg, 9.20 mmol, 4.0 eq.) portionwise and the reaction stirred at rt for 16 h. The white suspension was quenched with H$_2$O (8 mL) and extracted with Et$_2$O (x 4) and CH$_2$Cl$_2$ (x 3). The aqueous layer was acidified to pH 1 with 1 M aqueous HCl and extracted with Et$_2$O (x 6). Combined organics were dried over MgSO$_4$, filtered and the solvent removed *in vacuo*. The crude residue was dissolved in CH$_2$Cl$_2$, dried over MgSO$_4$, filtered and the solvent removed *in vacuo* to yield the desired carboxylic acid **144** (537 mg, 63 %) as a yellow oil. R_f = 0 (100 % EtOAc); ν_{max} /cm^{-1} 1730, 1634, 1533, 1437, 1372, 1356, 1213, 1147, 1107, 1022, 741, 692; δ_H (400 MHz, CDCl$_3$) 10.11 (1H, bs, COO*H*), 7.58-7.55 (2H, m, Ar*H*), 7.33-7.26 (3H, m, Ar*H*), 6.71 (1H, bt, *J* 5.4, N*H*), 4.14 (2H, s, HOOCC*H$_2$*), 3.84 (1H, q, *J* 7.4, CH$_3$C*H*(SePh)CONH), 3.70-3.68 (2H, m, C*H$_2$*), 3.60-3.59 (2H, m, C*H$_2$*), 3.49-3.47 (2H, m, C*H$_2$*), 3.41-3.39 (2H, m, C*H$_2$*), 1.61-1.56 (3H, d, *J* 7.4 C*H$_3$*CH(SePh)CONH); δ_C (101 MHz, CDCl$_3$) 173.2, 173.1, 134.9, 129.2, 128.3, 128.3, 71.0, 70.1, 69.7, 68.4, 40.5, 39.6, 18.2; *m/z* (ESI) 376 [MH]$^+$, 398 [MNa]$^+$; found [MH]$^+$ 376.0661 C$_{15}$H$_{22}$NO$_5$^{80}Se requires 376.0663, Δ 0.5 ppm.

(±)-2-Phenylselanyl-propionic acid **145**
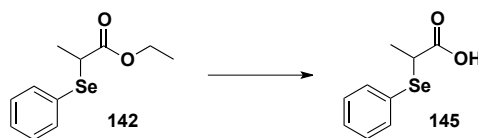
KOH (30 % aqueous, 40 mL) was added to a solution of ester **142** (1.77 g, 6.88 mmol, 1.0 eq.) in EtOH (40 mL) at rt. After 1 h, H_2O and ether were added to the reaction mixture and the layers separated. The aqueous layer was acidified to pH 1 with conc. HCl and extracted with ether (x 2). Combined organics from both extractions were dried over $MgSO_4$, filtered and the solvent removed *in vacuo* to yield the desired carboxylic acid **145** (1.28 g, 81 %) as a white crystalline solid, mp = 46-48 °C. R_f = 0 (100 % EtOAc); ν_{max} /cm^{-1} 1683, 1473, 1449, 1428, 1378, 1330, 1299, 1243, 1078, 1062, 1019, 999, 948, 910, 861, 734, 686, 662, 576; δ_H (400 MHz, MeOD) 7.62-7.60 (2H, m, Ar*H*), 7.36-7.28 (3H, m, Ar*H*), 3.77 (1H, q, *J* 7.1, HOOC*H*), 1.49 (3H, d, *J* 7.1, C*H₃*); δ_C (101 MHz, MeOD) 177.3, 136.7, 130.2, 129.6, 129.5, 38.7, 18.5; *m/z* (ESI) 157 [PhSe]$^-$, 229 [M-H]$^-$; found [M-H]$^-$ 228.9776 $C_9H_9O_2Se$ requires 228.9768, Δ 3.5 ppm.

Allyloxymethyl-benzene **149**
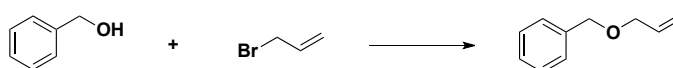
A procedure reported by Westwood *et al.* was used.[192] To a suspension of NaH (160 mg, 4.00 mmol, 1.1 eq.) in anhydrous THF (4 mL) was added benzyl alcohol (0.38 mL, 3.64 mmol, 1.0 eq.) and the reaction stirred at rt under argon for 2 h. Allyl bromide (0.35 mL, 4.00 mmol, 1.1 eq.) was then added dropwise and the suspension stirred overnight at rt. The reaction was quenched with H_2O and extracted with Et_2O (x 3). Combined organics were dried over $MgSO_4$, filtered and the solvent removed *in vacuo*. Coversion to product was measured using the benzyl CH_2 peaks in the ^{1}H NMR for starting material and product. Conversions of 60, 61 and 61 % were measured for the three sources of NaH tested with recovered masses of 475.3, 489.9 and 486.1 mg respectively. δ_H (400 MHz, CDCl$_3$) 7.39-7.28 (10 H, m, Ar*H* (benzyl alcohol) and Ar*H* (**149**)), 6.04-6.95 (1H, m, OCH$_2$C*H*), 5.35 (1H, dq, *J* 17.4, *J* 1.7, OCH$_2$CHC*H₂ cis* to CH$_2$O (**149**)), 5.25 (1H, dq, *J* 10.2, *J* 1.2, OCH$_2$CHC*H₂ trans* to CH$_2$O (**149**)), 4.63 (2H, s, PhC*H₂* (benzyl alcohol)), 4.55 (2H, s, PhC*H₂* (**149**)), 4.06 (2H, dt, *J* 5.6, *J* 1.3, OC*H₂*CHCH$_2$ (**149**)). Data in agreement with literature values.[295]

(±)-N-(2-(2-[(1-Benzyl-piperidin-4-ylcarbamoyl)-methoxy]-ethoxy)-ethyl)-2-phenylselanyl-propionamide **150**
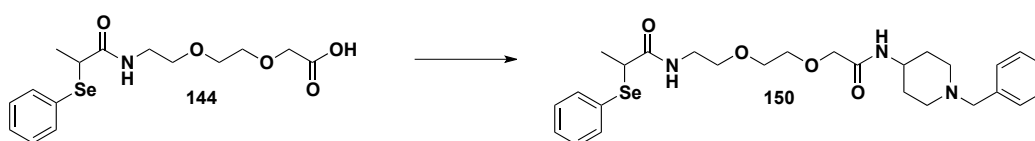
A solution of carboxylic acid **144** (415.0 mg, 1.11 mmol, 1.0 eq.), 4-aminobenzyl piperidine (0.23 mL, 1.11 mmol, 1.0 eq.) and bis(cyclopentadienyl)zirconium(IV) dichloride (16.0 mg, 5 mol%) in anhydrous toluene (30 mL) was

heated at reflux under argon for 12 h. The reaction mixture was allowed to cool to rt and filtered. The solvent was removed from the filtrate to yield the desired amide **150** (567.7 mg, 94 %) as a yellow oil. R_f = 0.53 (CH$_2$Cl$_2$/MeOH, 9:1); ν_{max} /cm^{-1} 3294 (NH), 2939, 2807, 2243, 1657, 1629, 1533, 1452, 1241, 1138, 1104, 985, 909, 726, 698; δ_H (400 MHz, CDCl$_3$, mixture of diastereomers) 7.55-7.53 (2H, m, Ar*H*), 7.31-7.20 (6H, m, Ar*H*), 6.66-6.64 (2H, m, Ar*H*), 3.94 (2H, s, OC*H$_2$*CONH), 3.86-3.76 (1H, m, piperidine-*H4'*), 3.79 (1H, q, *J* 7.1, CH$_3$C*H*(SePh)CONH), 3.62-3.59 (2H, m, C*H$_2$*), 3.55-3.52 (2H, m, C*H$_2$*), 3.47 (2H, s, piperidine-NC*H$_2$*Ar), 3.47-3.45 (2H, m, C*H$_2$*), 3.42-3.38 (2H, m, C*H$_2$*), 2.81-2.79 (2H, m, piperidine-*H2'*), 2.11-2.06 (2H, m, piperidine-*H2'*), 1.88-1.85 (2H, m, piperidine-*H3'*), 1.57 (3H, d, *J* 7.1, C*H$_3$*CH(SePh)CONH), 1.51-1.42 (2H, m, piperidine-*H3'*); δ_C (101 MHz, CDCl$_3$) 172.5, 169.1, 138.3, 134.6, 129.2, 129.0, 128.4, 128.2, 128.2, 127.0, 70.8, 70.5, 70.1, 69.8, 63.0, 52.2, 46.0, 40.5, 39.4, 32.2, 18.4; *m/z* (ESI) 548 [MH]$^+$, 570 [MNa]$^+$; found [MH]$^+$ 548.2015 C$_{27}$H$_{38}$N$_3$O$_4$^{80}Se requires 548.2028, Δ 2.4 ppm.

(±)-N-(2-(2-[2-Oxo-2-(4-phenyl-piperazin-1-yl)-ethoxy]-ethoxy)-ethyl)-2-phenylselanyl-propionamide **151**
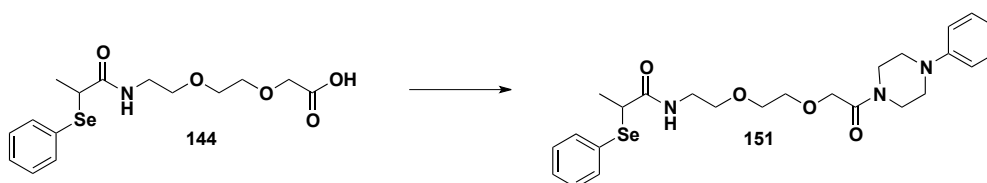
A solution of carboxylic acid **144** (414.0 mg, 1.11 mmol, 1.0 eq.), bis(cyclopentadienyl)zirconium(IV) dichloride (16.2 mg, 5 mol%) and N-phenylpiperazine (0.17 mL, 1.11 mmol, 1.0 eq.) in anhydrous toluene (30 mL) was heated to reflux under argon for 24 h. The pink coloured solution was filtered under reduced pressure and the solvent removed from the filtrate *in vacuo*. The crude residue was purified on silica (CH$_2$Cl$_2$/MeOH, 19:1) to yield the desired amide **151** (429.8 mg, 75 %) as a yellow oil. R_f = 0.28 (CH$_2$Cl$_2$/MeOH, 19:1); ν_{max} /cm^{-1} 3298 (NH), 2917, 2865, 2822, 1641 (C=O), 1598, 1541, 1496, 1476, 1437, 1229, 1149, 1117, 1097, 1023, 758, 742, 691; δ_H (400 MHz, CDCl$_3$) 7.58-7.56 (2H, m, Ar*H*), 7.32-7.25 (4H, m, Ar*H*), 6.93-6.90 (4H, m, Ar*H*), 4.24 (2H, s, OC*H$_2$*CON), 3.85 (1H, q, *J* 7.2, CH$_3$C*H*(SePh)CONH), 3.75-3.72 (2H, m, C*H$_2$*), 3.69-3.66 (2H, m, C*H$_2$*), 3.64-3.59 (4H, m, C*H$_2$*), 3.52-3.45 (2H, m, C*H$_2$*), 3.43-3.39 (2H, m, C*H$_2$*), 3.18-3.13 (4H, m, C*H$_2$*), 1.59 (3H, d, *J* 7.2, C*H$_3$*CH(SePh)CONH); δ_C (101 MHz, CDCl$_3$, dept90, dept135, hmqc) 172.5 (C), 167.6 (C), 150.7 (C), 134.7 (CH), 129.2 (CH), 129.0 (CH), 128.4 (C), 128.0 (CH), 120.5 (CH), 116.5 (CH), 70.5 (CH$_2$), 70.1 (CH$_2$), 69.6 (CH$_2$), 49.6 (CH$_2$), 49.2 (CH$_2$), 44.7 (CH$_2$), 41.6 (CH$_2$), 40.4 (CH), 39.4 (CH$_2$), 18.4 (CH$_3$); *m/z* (ESI) 520 [MH]$^+$, 542 [MNa]$^+$; found [MH]$^+$ 520.1691 C$_{25}$H$_{34}$N$_3$O$_4$^{80}Se requires 520.1715, Δ 4.6 ppm.

(±)-N-(2-(2-[(4-Methoxy-benzylcarbamoyl)-methoxy]-ethoxy)-ethyl)-2-phenylselanyl-propionamide **153**
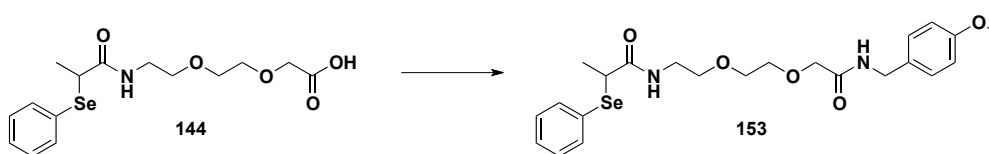
To a solution of carboxylic acid **144** (362.6 mg, 0.97 mmol, 1.0 eq.), DCC (299.2 mg, 1.45 mmol, 1.5 eq.) and HOBt (261.8 mg, 1.94 mmol, 2 eq.) in anhydrous CH$_2$Cl$_2$ (10 mL) under argon was added *p*-methoxybenzyl amine (0.15

mL, 1.16 mmol, 1.2 eq.) and the reaction stirred at rt for 3 h. The reaction mixture was filtered and the solvent removed from the filtrate *in vacuo*. The crude residue was resuspended in acetonitrile and filtered. The solvent was removed from the filtrate and the residue dissolved in CH_2Cl_2 and washed with 1 M HCl (x 1), sat. aq. $NaHCO_3$ (x 1), dried over $MgSO_4$, filtered and the solvent removed *in vacuo*. The crude residue was purified on silica (CH_2Cl_2/MeOH, 19:1) and the resulting product suspended in acetonitrile and filtered. The solvent was removed from the filtrate to yield the desired amide **153** (330.7 mg, 69 %) as a clear oil. R_f = 0.50 (CH_2Cl_2/MeOH, 9:1); v_{max} /cm^{-1} 3304 (NH), 2929, 2869, 1646 (C=O), 1612, 1532, 1512, 1476, 1456, 1437, 1244, 1176, 1109, 1031, 815, 740, 692; δ_H (400 MHz, CDCl$_3$) 7.51-7.48 (2H, m, Ar*H*), 7.29-7.15 (5H, m, Ar*H*), 6.82-6.79 (2H, m, Ar*H*), 6.47 (1H, bt, *J* 5.2, N*H*), 4.37-4.35 (2H, m, ArC*H$_2$*), 3.97 (2H, s, OC*H$_2$*CONH), 3.73 (3H, s, OC*H$_3$*), 3.69 (1H, q, *J* 7.2, CH$_3$C*H*(SePh)CONH), 3.59-3.57 (2H, m, C*H$_2$*), 3.48-3.46 (2H, m, C*H$_2$*), 3.34-3.31 (2H, m, C*H$_2$*), 3.23 (2H, q, *J* 3.9, C*H$_2$*), 1.51 (3H, d, *J* 7.2, C*H$_3$*CH(SePh)CONH); δ_C (101 MHz, CDCl$_3$, dept135, dept90) 171.9 (C), 169.1 (C), 158.2 (C), 134.0 (CH), 131.4 (C), 129.1 (CH), 128.7 (CH), 128.7 (C), 127.7 (CH), 113.6 (CH), 70.2 (CH$_2$), 70.0 (CH$_2$), 69.4 (CH$_2$), 68.9 (CH$_2$), 55.0 (CH$_3$), 41.1 (CH$_2$), 39.5 (CH), 38.7 (CH$_2$), 18.8 (CH$_3$); *m/z* (ESI) 495 [MH]$^+$, 517 [MNa]$^+$; found [MH]$^+$ 495.1390 C$_{23}$H$_{31}$N$_2$O$_5$Se requires 495.1398, Δ 1.6 ppm.

(±)-N-(2-[2-(Benzylcarbamoyl-methoxy)-ethoxy]-ethyl)-2-phenylselanyl-propionamide **154**
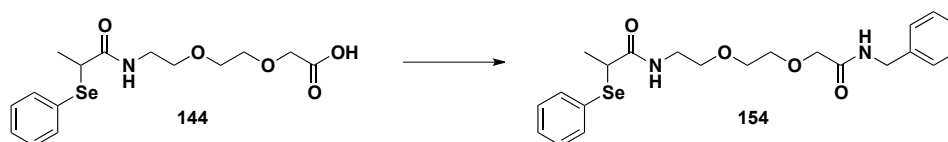
To carboxylic acid **144** (227.8 mg, 0.61 mmol, 1.0 eq.), DCC (188.4 mg, 0.91 mmol, 1.5 eq.) and HOBt (164.8 mg, 1.22 mmol, 2.0 eq.) in anhydrous CH_2Cl_2 (20 mL) was added benzylamine (0.08 mL, 0.73 mmol, 1.2 eq.) and the mixture stirred at rt for 3 h. The reaction mixture was filtered under reduced pressure and the filtrate washed with 1M aqueous HCl, sat. $NaHCO_3$, dried over $MgSO_4$, filtered and the solvent removed *in vacuo*. The crude residue was purified on silica (gradient elution, 100 % CH_2Cl_2 to 95:5 CH_2Cl_2/MeOH) and the resulting residue suspended in MeCN and filtered to remove the urea. The desired amide **154** (256.9 mg, 91 %) was isolated as a clear oil. R_f = 0.48 (CH_2Cl_2/MeOH, 9:1); v_{max} /cm^{-1} 1638, 1454, 1436, 1356, 1248, 1106, 1022, 1000, 739, 693; δ_H (400 MHz, CDCl$_3$) 7.53-7.50 (2H, m, Ar*H*), 7.33-7.22 (8H, m, Ar*H*), 4.45 (2H, s, OC*H$_2$*CONH), 4.02 (2H, s, NHC*H$_2$*Ph), 3.69 (1H, q, *J* 7.2, CH$_3$C*H*(SePh)CONH), 3.62-3.60 (2H, m, C*H$_2$*), 3.51-3.49 (2H, m, C*H$_2$*), 3.34 (2H, t, *J* 5.2, C*H$_2$*), 3.24-3.21 (2H, m, C*H$_2$*), 1.53 (3H, d, *J* 7.2, C*H$_3$*CH(SePh)CONH); δ_C (101 MHz, MeOD) 172.3, 169.8, 138.0, 134.6, 129.2, 128.7, 128.4, 128.2, 127.7, 127.5, 70.9, 70.5, 70.0, 69.7, 42.7, 40.4, 39.2, 18.3; *m/z* (ESI) 465 [MH]$^+$; found [MH]$^+$ 465.1288 C$_{22}$H$_{29}$N$_2$O$_4$Se requires 465.1293, Δ 1.1 ppm.

(±)-N-(2-(2-[(4-Fluoro-benzylcarbamoyl)-methoxy]-ethoxy)-ethyl)-2-phenylselanyl-propionamide **155**
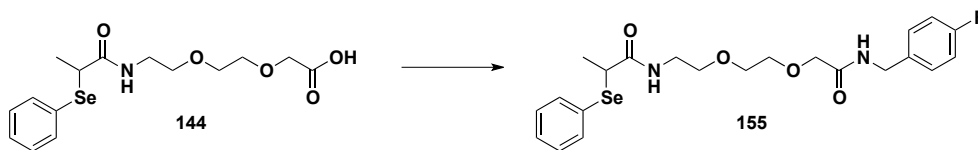
A solution of carboxylic acid **144** (434.4 mg, 1.16 mmol, 1.0 eq.), *p*-fluorobenzylamine (0.13 mL, 1.16 mmol, 1.0 eq.) and bis(cyclopentadienyl)zirconium(IV) dichloride (17 mg, 5 mol%) in anhydrous toluene (30 mL) was heated to reflux under argon for 4 h. The reaction mixture was allowed to cool to rt and filtered. The solvent was removed from the filtrate to yield the desired amide **155** (525.2 mg, 94 %) as a clear oil. R_f = 0.14 (CH$_2$Cl$_2$/MeOH, 19:1); ν_{max} /cm^{-1} 3304 (NH), 3068, 2925, 2866, 1646 (C=O), 1531 (NH), 1508 (NH), 1437, 1219, 1100 (C-F), 824, 740, 692; δ_H (400 MHz, CDCl$_3$) 7.56-7.52 (2H, m, Ar*H*), 7.33-7.23 (5H, m, Ar*H*), 7.18 (1H, bt, N*H*), 7.04-6.98 (2H, m, Ar*H*), 6.40 (1H, bt, N*H*), 4.49-4.40 (2H, m, ArC*H$_2$*), 4.05 (2H, s, NHCOC*H$_2$*O), 3.74 (1H, q, *J* 7.1, C*H$_3$*CH(SePh)CONH), 3.66-3.64 (2H, m, C*H$_2$*), 3.55-3.53 (2H, m, C*H$_2$*), 3.40 (2H, t, *J* 5.0, C*H$_2$*), 3.36-3.26 (2H, m, C*H$_2$*), 1.57 (3H, d, *J* 7.1, CH$_3$C*H*(SePh)CONH); δ_C (101 MHz, CDCl$_3$) 172.4, 169.9, 163.3, 160.9, 134.5, 134.0, 129.5, 129.4, 129.2, 128.3, 128.2, 115.6, 115.4, 70.9, 70.5, 70.0, 69.8, 42.0, 40.6, 39.4, 18.3; *m/z* (ESI) 483 [MH]$^+$, 505 [MNa]$^+$; found [MH]$^+$ 483.1221 C$_{22}$H$_{28}$N$_2$O$_4$FSe requires 483.1198, Δ 4.8 ppm.

(±)-4-[(2-(2-[2-(2-Phenylselanyl-propionylamino)-ethoxy]-ethoxy)-acetylamino)-methyl]-benzoic acid methyl ester **156**
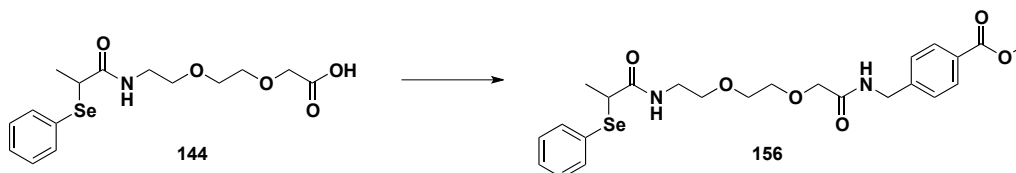
A solution of carboxylic acid **144** (390.0 mg, 1.04 mmol, 1.0 eq.), methyl 4-(aminomethyl)benzoate hydrochloride (209.7 mg, 1.04 mmol, 1.0 eq.) and bis(cyclopentadienyl)zirconium(IV) dichloride (15.2 mg, 5 mol%) in anhydrous toluene (30 mL) was heated at reflux under argon for 12 h. The reaction mixture was allowed to cool to rt and filtered. The crude residue was purified on silica (CH$_2$Cl$_2$/MeOH, 19:1) and re-purified on silica (CH$_2$Cl$_2$/MeOH, 97:3) to yield the desired amide **156** (123.3 mg, 23 %) as a brown oil. R_f = 0.22 (CH$_2$Cl$_2$/MeOH, 19:1); ν_{max} /cm^{-1} 3308 (b), 2921, 1718, 1648, 1612, 1529, 1435, 1416, 1278, 1105; δ_H (400 MHz, CDCl$_3$) 7.98 (2H, d, *J* 8.3, Ar*H*), 7.52-7.50 (2H, m, Ar*H*), 7.36-7.23 (5H, m, Ar*H*), 6.39 (1H, bt, *J* 5.8, N*H*), 4.57-4.47 (2H, m, CONHC*H$_2$*Ar), 4.05 (2H, s, OC*H$_2$*CONH), 3.90 (3H, s, ArCOOC*H$_3$*), 3.71 (1H, q, *J* 7.1, PhSeC*H*), 3.66-3.64 (2H, m, C*H$_2$*), 3.55-3.52 (2H, m, C*H$_2$*), 3.38 (2H, t, *J* 5.4, C*H$_2$*), 3.31-3.26 (2H, m, C*H$_2$*), 1.54 (3H, d, *J* 7.1, CH$_3$C*H*(SePh)CONH); δ_C (101 MHz, CDCl$_3$) 172.4, 170.0, 166.8, 143.4, 134.6, 130.0, 129.3, 129.2, 128.3, 128.2, 127.5, 71.0, 70.6, 70.0, 69.8, 52.2, 42.4, 40.6, 39.4, 18.3; *m/z* (ESI) 523 [MH]$^+$, 545 [MNa]$^+$; found [MH]$^+$ 523.1356 C$_{24}$H$_{31}$N$_2$O$_6$^{80}Se requires 523.1347, Δ 1.7 ppm.

(±)-N-(2-[2-(([1-(Toluene-4-sulfonyl)-pyrrolidin-2-(R)-ylmethyl]-carbamoyl)-methoxy)-ethoxy]-ethyl)-acrylamide **157**
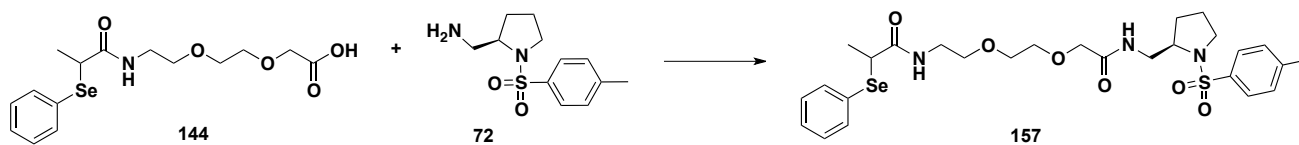
A solution of carboxylic acid **144** (89.5 mg, 0.24 mmol, 1.0 eq.), amine **72** (60.8 mg, 0.24 mmol, 1.0 eq.) and bis(cyclopentadienyl)zirconium(IV) dichloride (3.5 mg, 5 mol%) in anhydrous toluene (25 mL) was refluxed for 18 h under argon. The mixture was allowed to cool and filtered under reduced pressure. The solvent was removed from the filtrate *in vacuo* to yield the desired amide **157** (159.6 mg, 100 %) as a clear oil. $[\alpha]^{21}_D$ = + 39.3 (*c* = 10.64, CHCl$_3$); R$_f$ = 0.65 (CH$_2$Cl$_2$/MeOH, 9:1); ν_{max} /cm^{-1} 3329 (NH), 2925, 2876, 1657 (C=O), 1535, 1341, 1158, 1108, 1093, 664; δ_H (400 MHz, CDCl$_3$) 7.66 (2H, d, *J* 7.7, tol *H3'*), 7.57-7.53 (3H, m, SeAr*H*), 7.30 (2H, d, *J* 7.7, tol H2'), 7.25-7.23 (2H, m, SeAr*H*), 6.73-6.69 (1H, bm, N*H*), 4.00 (2H, s, OC*H*$_2$CONH), 3.83-3.77 (1H, m, CH$_3$C*H*(SePh)CONH), 3.76-3.70 (1H, m, pyrrolidine-*H2'*), 3.68-3.63 (2H, m, OC*H*$_2$CH$_2$O), 3.61-3.58 (2H, m, OC*H*$_2$CH$_2$O), 3.54-3.46 (3H, m, NC*H*$_2$CH$_2$O), 3.44-3.27 (4H, m, NC*H*$_2$CH$_2$O and pyrrolidine-C*H*$_2$NH and pyrrolidine-*H5'*), 3.19-3.12 (1H, m, pyrrolidine-*H5'*), 2.40 (3H, s, ArC*H*$_3$), 1.80-1.70 (1H, m, pyrrolidine-*H4'*), 1.64-1.56 (2H, m, pyrrolidine-*H4'* and pyrrolidine-*H3'*), 1.54 (3H, d, *J* 7.1, C*H*$_3$CH(SePh)CONH), 1.47-1.38 (1H, m, pyrrolidine-*H3'*); δ_C (101 MHz, CDCl$_3$) 172.6, 170.6, 143.9, 134.7, 133.7, 129.8, 129.0, 128.5, 128.0, 127.5, 71.1, 70.6, 70.0, 69.8, 59.5, 49.4, 43.2, 40.4, 39.4, 29.5, 24.0, 21.5, 18.3; *m/z* (ESI) 612 [MH]$^+$, 634 [MNa]$^+$; found [MH]$^+$ 612.1648 C$_{27}$H$_{38}$N$_3$O$_6$S^{80}Se requires 612.1647, Δ 0.2 ppm.

(±)-N-(2-(2-[(1-Benzyl-piperidin-4-ylcarbamoyl)-methoxy]-ethoxy)-ethyl)-acrylamide **158**
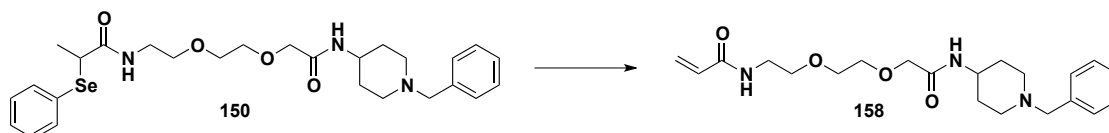
Selenide **150** (415.8 mg, 0.76 mmol, 1.0 eq.) and sodium (*meta*)periodate (260.3 mg, 1.22 mmol, 1.6 eq.) were stirred in MeOH (2 mL) at rt overnight. To the resulting off-white precipitate was added H$_2$O (8 mL) and the reaction mixture extracted with CH$_2$Cl$_2$ (x 2). The combined CH$_2$Cl$_2$ layers were washed with 1 M HCl (aq.) and the aqueous layers combined and basified to pH 14 with sat. aq. NaOH. The basic aqueous layer was extracted with EtOAc (x 3) and combined organics dried over MgSO$_4$, filtered and the solvent removed *in vacuo*. The crude clear oil was purified on basic alumina (CH$_2$Cl$_2$/MeOH, 49:1) to yield the desired acrylamide **158** (145.2 mg, 49 %) as a clear oil. R$_f$ = 0.24 (CH$_2$Cl$_2$/MeOH, 49:1); ν_{max} /cm^{-1} 3294, 2939, 1657, 1629, 1533, 1104, 909, 726, 698; δ_H (400 MHz, CDCl$_3$) 7.31-7.20 (5H, m, Ar*H*), 6.72-6.67 (2H, bm, N*H*), 6.28 (1H, dd, *J* 1.8, *J* 16.8, C*H*$_2$CHCONH *cis* to C=O), 6.15 (1H, dd, *J* 10.1, *J* 16.8, CH$_2$C*H*CONH), 5.59 (1H, dd, *J* 1.8, *J* 10.1, C*H*$_2$CHCONH *trans* to C=O), 3.95 (2H, s, OC*H*$_2$CONH), 3.87-3.77 (1H, m, piperidine-*H4'*), 3.66-3.64 (2H, m, C*H*$_2$), 3.61-3.57 (4H, m, 2 x C*H*$_2$), 3.54-3.50 (2H, m, C*H*$_2$), 3.47 (2H, s, piperidine-NC*H*$_2$Ar), 2.84-2.79 (2H, m, piperidine-*H2'*), 2.11-2.05 (2H, m, piperidine-*H2'*), 1.90-1.84 (2H, m, piperidine-*H3'*), 1.48 (2H, qd, *J* 11.4, *J* 3.8, piperidine-*H3'*); δ_C (101 MHz, CDCl$_3$) 169.2, 165.7, 138.2, 130.7, 129.0,

128.2, 127.0, 126.4, 70.9, 70.6, 70.2, 69.9, 63.0, 52.2, 45.9, 39.2, 32.2; *m/z* (ESI) 390 [MH]$^+$, 412 [MNa]$^+$; found [MH]$^+$ 390.2389 C$_{21}$H$_{32}$N$_3$O$_4$ requires 390.2393, Δ 1.0 ppm.

N-(2-(2-[2-Oxo-2-(4-phenyl-piperazin-1-yl)-ethoxy]-ethoxy)-ethyl)-acrylamide **159**
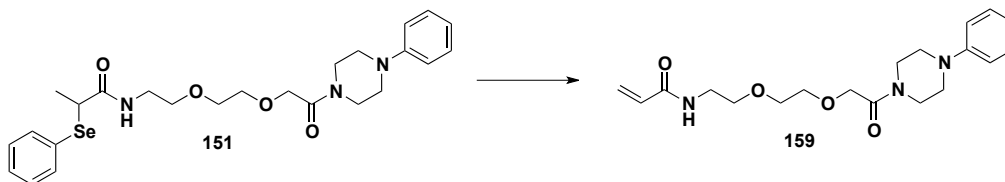
To selenide **151** (421.9 mg, 0.81 mmol, 1.0 eq.) and sodium (*meta*)periodate (278.5 mg, 1.30 mmol, 1.6 eq.) was added EtOH (3 mL) and the orange solution stirred for 18 h at rt. To the resulting thick off-white precipitate was added H$_2$O and the mixture extracted with CH$_2$Cl$_2$ (x 3). Combined organics were dried over MgSO$_4$, filtered and the solvent removed *in vacuo*. The crude orange oil was purified on silica (EtOAc/MeOH, 19:1) and re-purified on silica (EtOAc/MeOH, 9:1) to yield the desired acrylamide **159** (62.3 mg, 21 %) as a yellow oil. R$_f$ = 0.13 (EtOAc/MeOH, 19:1); ν_{max} /cm^{-1} 3286, 2863, 1647, 1627, 1598, 1543, 1495, 1442, 1229, 1115, 1098, 1025, 991, 759, 693; δ_H (400 MHz, CDCl$_3$) 7.32-7.31 (2H, m, Ar*H*), 6.96-6.91 (3H, m, Ar*H*), 6.32 (1H, dd, *J* 17.1, *J* 2.3, CH$_2$CHCONH *cis* to C=O), 6.24 (1H, dd, *J* 9.5, *J* 17.1, CH$_2$C*H*CONH), 5.61 (1H, dd, *J* 9.5, *J* 2.3, C*H$_2$*CHCONH *trans* to C=O), 4.29 (2H, s, OC*H$_2$*CONH), 3.81-3.78 (2H, m, C*H$_2$*), 3.74-3.71 (2H, m, C*H$_2$*), 3.69-3.65 (4H, m, C*H$_2$*), 3.63 (2H, t, *J* 4.8, C*H$_2$*), 3.57-3.53 (2H, m, C*H$_2$*), 3.21-3.17 (4H, m, C*H$_2$*); δ_C (101 MHz, CDCl$_3$) 167.9, 165.8, 150.9, 131.1, 129.3, 126.1, 120.8, 116.8, 70.7, 70.4, 70.2, 69.9, 49.9, 49.5, 44.9, 41.9, 39.4; *m/z* (ESI) 362 [MH]$^+$, 382 [MNa]$^+$; found [MH]$^+$ 362.2067 C$_{19}$H$_{28}$N$_3$O$_4$ requires 362.2080, Δ 3.6 ppm.

N-(2-(2-[(4-Methoxy-benzylcarbamoyl)-methoxy]-ethoxy)-ethyl)-acrylamide **160**
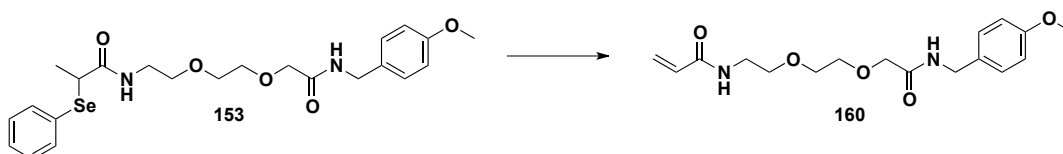
A solution of selenide **153** (307.7 mg, 0.62 mmol, 1.0 eq.) and sodium (*meta*)periodate (213.4 mg, 1.0 mmol, 1.6 eq.) in EtOH (2 mL) was stirred vigorously overnight. To the resulting yellow precipitate was added H$_2$O (8 mL) and the mixture extracted with CH$_2$Cl$_2$ (x 3). Combined organics were dried over MgSO$_4$, filtered and the solvent removed *in vacuo*. The crude mixture was purified on silica (29:1, CH$_2$Cl$_2$:MeOH) to yield a mixture of the desired acrylamide **160** with the starting material **153**. To the mixture was added sodium meta periodate (213.4 mg, 1.0 mmol, 1.6 eq.) and EtOH (2 mL) and the mixture stirred vigorously overnight. To the resulting thick white precipitate was added H$_2$O (8 mL) and the aqueous layer extracted with CH$_2$Cl$_2$ (x 3). Combined organics were dried over MgSO$_4$, filtered and the solvent removed *in vacuo*. The crude residue was purified on silica (29:1, CH$_2$Cl$_2$/MeOH) to yield the desired acrylamide **160** (157.5 mg, 76 %) as a clear oil which crystallised upon standing to yield a white waxy solid, mp = 70-71 °C; R$_f$ = 0.14 (CH$_2$Cl$_2$/MeOH, 29:1); ν_{max} /cm^{-1} 3294, 2929, 1655, 1627, 1611, 1535, 1512, 1244, 1109, 1031, 987, 958, 808, 728; δ_H (400 MHz, CDCl$_3$) 7.22 (2H, d, *J* 8.6, Ar*H*), 7.08 (1H, bs, N*H*) 6.86 (2H, d, *J* 8.6 Ar*H*), 6.26 (1H,

dd, *J* 1.6, *J* 17.0, C*H*₂CHCONH *cis* to C=O), 6.05 (1H, dd, *J* 17.0, *J* 10.3, CH₂C*H*CONH), 5.89 (1H, bs, N*H*), 5.62 (1H, dd, *J* 10.3, *J* 1.6, CH₂CHCON*H* *trans* to C=O), 4.42 (2H, d, *J* 5.8, ArC*H*₂NHCO), 4.05 (2H, s, OC*H*₂CONH), 3.78 (3H, s, ArOC*H*₃), 3.68-3.66 (2H, m, C*H*₂), 3.58-3.56 (2H, m, C*H*₂), 3.47 (2H, t, *J* 5.0, C*H*₂), 3.41-3.38 (2H, m, C*H*₂); δ_C (101 MHz, CDCl₃) 170.0, 165.6, 159.2, 130.8, 130.2, 129.3, 126.7, 114.2, 71.1, 70.8, 70.3, 70.1, 55.4, 42.5, 39.3; *m/z* (ESI) 337 [MH]⁺, 359 [MNa]⁺; found [MH]⁺ 337.1767 C₁₇H₂₅N₂O₅ requires 337.1763, Δ 1.2 ppm.

N-(2-[2-(Benzylcarbamoyl-methoxy)-ethoxy]-ethyl)-acrylamide **161**
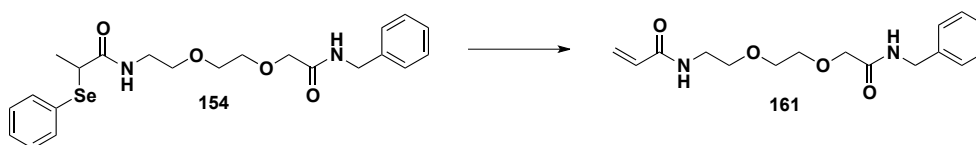
To selenide **154** (194.8 mg, 0.42 mmol, 1.0 eq.) and NaIO₄ (143.9 mg, 0.67 mmol, 1.6 eq.) was added EtOH (1.5 mL) and the clear solution rapidly stirred for 24 h at rt. The resulting thick white precipitate was diluted with H₂O and washed with CH₂Cl₂ (x 3). Combined organics were dried over MgSO₄, filtered and the solvent removed *in vacuo*. The crude yellow oil was purified on silica (100 % EtOAc) to yield the desired acrylamide **161** (115.8 mg, 90 %) as a clear oil. R*f* = 0.18 (100 % EtOAc); ν_{max} /cm⁻¹ 1655, 1627, 1536, 1245, 1107, 700; δ_H (400 MHz, CDCl₃) 7.38-7.26 (5H, m, Ar*H*), 6.26 (1H, dd, *J* 16.5, *J* 1.1, *H*₂CCHCONH *cis* to C=O), 6.21 (1H, bs, N*H*), 6.07 (1H, dd, *J* 9.9, *J* 16.5, H₂CC*H*CONH), 5.50 (1H, dd, *J* 9.9, *J* 1.1, *H*₂CCHCONH *trans* to C=O), 4.49 (2H, d, *J* 6.4, ArC*H*₂NHCO), 4.07 (2H, s, OC*H*₂CONH), 3.69-3.67 (2H, m, C*H*₂), 3.59-3.57 (2H, m, C*H*₂), 3.48 (2H, t, *J* 5.1, C*H*₂), 3.41-3.37 (2H, m, C*H*₂); δ_C (101 MHz, CDCl₃) 170.2, 165.8, 138.1, 130.8, 128.9, 127.9, 127.7, 126.4, 71.1, 70.7, 70.3, 70.0, 43.0, 39.2; *m/z* (ESI) 307 [MH]⁺, 329 [MNa]⁺; found [MH]⁺ 307.1653 C₁₆H₂₃N₂O₄ requires 307.1658, Δ 1.6 ppm.

N-(2-(2-[(4-Fluoro-benzylcarbamoyl)-methoxy]-ethoxy)-ethyl)-acrylamide **162**
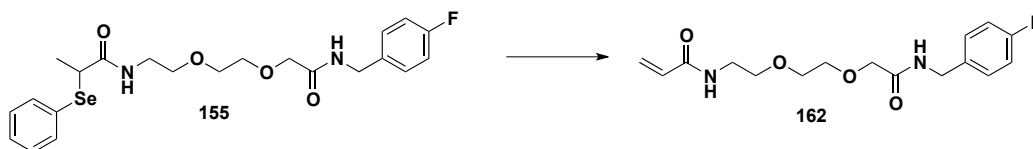
A solution of selenide **155** (525.2 mg, 1.09 mmol, 1.0 eq.) and sodium (*meta*)periodate (373.4 mg, 1.75 mmol, 1.6 eq.) in EtOH (3 mL) was stirred vigorously overnight. To the resulting thick white precipitate was added H₂O and the mixture extracted with CH₂Cl₂ (x 3). Combined organics were dried over MgSO₄, filtered and the solvent removed *in vacuo*. The crude residue was purified on silica (EtOAc/MeOH, 9:1) to yield the desired acrylamide **162** (221.0 mg, 63 %) as a clear oil. R*f* = 0.41 (EtOAc/MeOH, 9:1); ν_{max} /cm⁻¹ 3297 (NH), 3075, 2929, 2873, 1657 (C=O), 1628, 1606, 1538, 1510, 1221, 1110; δ_H (400 MHz, CDCl₃) 7.25 (1H, bs, N*H*), 7.22-7.18 (2H, m, Ar*H*), 6.97-6.91 (2H, m, Ar*H*), 6.40 (1H, bs, N*H*), 6.19 (1H, dd, *J* 16.9, *J* 1.7, C*H*₂CHCONH *cis* to C=O), 6.04 (1H, dd, *J* 10.3, *J* 16.9, CH₂C*H*CONH), 5.54 (1H, dd, *J* 10.3, *J* 1.7, C*H*₂CHCONH *trans* to C=O), 4.38 (2H, d, *J* 6.0, NHC*H*₂Ar), 3.98 (2H, s, OC*H*₂CONH), 3.62-3.59 (2H, m, C*H*₂), 3.56-3.52 (2H, m, C*H*₂), 3.45 (2H, t, *J* 5.2, C*H*₂), 3.38-3.35 (2H, m, C*H*₂); δ_C (101 MHz, CDCl₃) 170.0, 165.7, 163.3, 160.9, 134.0, 134.0, 130.7, 129.4, 129.4, 126.4, 115.6, 115.4, 71.0, 70.6, 70.1,

69.8, 42.0, 39.1; *m/z* (ESI) 325 [MH]⁺, 347 [MNa]⁺; found [MH]⁺ 325.1567 $C_{16}H_{22}N_2O_4F$ requires 325.1564, Δ 0.9 ppm.

4-((2-[2-(2-Acryloylamino-ethoxy)-ethoxy]-acetylamino)-methyl)-benzoic acid methyl ester **163**
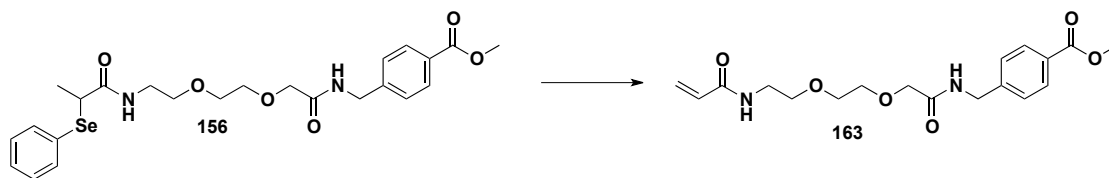
To selenide **156** (123.3 mg, 0.22 mmol, 1.0 eq.) and sodium (*meta*)periodate (76.4 mg, 0.35 mmol, 1.6 eq.) was added EtOH (1 mL) and the orange solution stirred at rt for 36 h. To the resulting thick yellow precipitate was added H_2O and the mixture extracted with CH_2Cl_2 (x 3). Combined organics were dried over $MgSO_4$, filtered and the solvent removed *in vacuo*. The resulting residue was purified on silica (EtOAc/MeOH, 9:1) and subsequently re-purified on silica (EtOAc/MeOH, 4:1) to yield the desired acrylamide **163** (44.1 mg, 55 %) as a clear oil. R_f = 0.32 (EtOAc/MeOH, 9:1); ν_{max} /cm⁻¹ 3298, 1718, 1656, 1532, 1278, 1107; δ_H (400 MHz, CDCl₃) 7.98 (2H, d, *J* 8.0, Ar*H*), 7.34 (2H, d, *J* 8.0, Ar*H*), 7.29 (1H, bs, N*H*), 6.23 (1H, dd, *J* 16.9, *J* 1.5, C*H₂*CHCONH *cis* to C=O), 6.06 (1H, bs, N*H*), 6.03 (1H, dd, *J* 16.9, *J* 10.3, CH₂C*H*CONH), 5.58 (1H, dd, *J* 10.3, *J* 1.5, C*H₂*CHCONH *trans* to C=O), 4.53 (2H, d, *J* 6.3, CONHC*H₂*Ar), 4.06 (2H, s, OC*H₂*CONH), 3.89 (3H, s, ArCOOC*H₃*), 3.69-3.67 (2H, m, C*H₂*), 3.60-3.58 (2H, m, C*H₂*), 3.49 (2H, t, *J* 5.2, C*H₂*), 3.43-3.39 (2H, m, C*H₂*); δ_C (101 MHz, CDCl₃) 170.3, 166.8, 165.7, 143.4, 130.7, 130.1, 129.5, 127.6, 126.7, 71.1, 70.7, 70.3, 70.0, 52.2, 42.5, 39.2; *m/z* (ESI) 365 [MH]⁺, 387 [MNa]⁺; found [MH]⁺ 365.1704 $C_{18}H_{25}N_2O_6$ requires 365.1713 Δ 2.5 ppm.

(R)-N-(2-[2-((([1-(Toluene-4-sulfonyl)-pyrrolidin-2-ylmethyl]-carbamoyl}-methoxy)-ethoxy]-ethyl)-acrylamide **164**
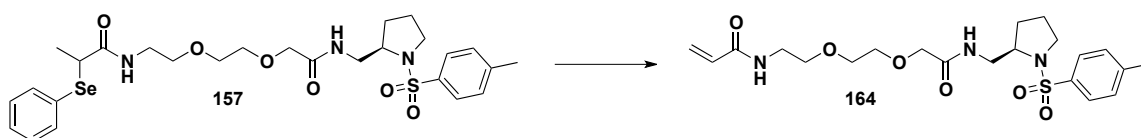
Selenide **157** (159.6mg, 0.26 mmol, 1.0 eq.) and sodium (*meta*)periodate (89.5 mg, 0.42 mmol, 1.6 eq.) were stirred vigorously in EtOH (2 mL) for 16 h. To the resulting thick white precipitate was added H_2O and the mixture extracted with CH_2Cl_2 (x 3). Combined organics were dried over $MgSO_4$, filtered and the solvent removed *in vacuo*. The crude residue was purified on silica (EtOAc/MeOH, 9:1) to yield the desired acrylamide **164** (57.2 mg, 49 %) as a clear oil. $[\alpha]^{22}_D$ = + 44.9 (*c* = 0.71, CHCl₃); R_f = 0.29 (EtOAc/MeOH, 9:1); ν_{max} /cm⁻¹ 3301 (NH), 2929, 2873, 1658, 1627, 1532, 1340, 1243, 1156, 1106, 1092, 1040, 987, 817, 663; δ_H (400 MHz, CDCl₃) 7.65 (2H, d, *J* 8.2, tol *H3'*), 7.59 (1H, bt, *J* 4.8, N*H*), 7.29 (2H, d, *J* 8.2, tol *H2'*), 6.62 (1H, bs, N*H*), 6.24 (1H, dd, *J* 17.0, *J* 2.1, C*H₂*CHCONH *cis* to C=O), 16.15 (1H, dd, *J* 17.0, *J* 9.8, CH₂C*H*CONH), 5.54 (1H, dd, *J* 9.8, *J* 2.1, C*H₂*CHCONH *trans* to C=O), 4.01 (2H, s, OC*H₂*CONH), 3.76-3.68 (3H, m), 3.66-3.44 (7H, m), 3.40-3.26 (2H, m), 3.19-3.13 (1H, m), 2.39 (3H, s, ArC*H₃*), 1.79-1.69 (1H, m, pyrrolidine-*H4'*), 1.64-1.49 (2H, m, pyrrolidine-*H4'* and pyrrolidine-*H3'*), 1.46-1.37 (1H, m, pyrrolidine-*H3'*); δ_C (101 MHz, CDCl₃) 171.0, 165.9, 144.2, 133.8, 131.2, 130.1, 127.7, 126.3, 71.4, 70.8, 70.3,

70.2, 59.8, 49.6, 43.4, 39.4, 29.7, 24.3, 21.7; m/z (ESI) 454 [MH]$^+$, 476 [MNa]$^+$; found [MH]$^+$ 454.1995 $C_{21}H_{32}N_3O_6S$ requires 454.2012, Δ 3.7 ppm.

9.6. Glycine, β-alanine and 1,3-diaminopropane linkers

N-Acryloylglycine **165**

To a solution of glycine (2.00 g, 26.64 mmol, 1.0 eq.) in KOH (2M) (28.0 mL, 55.94 mmol, 2.1 eq.) at 0 °C was added acryloyl chloride (2.6 mL, 31.97 mmol, 1.2 eq.) dropwise, with vigorous stirring. The solution was stirred at rt for 45 min and subsequently washed with ether (20 mL x 2). The aqueous layer was then acidified to pH 3 by addition of aq. HCl (2N) and extracted with ethyl acetate (6 x 20 mL). The combined EtOAc extractions were dried over MgSO$_4$, filtered and the solvent removed *in vacuo* to yield the desired acrylamide **165** (3.05 g, 89 %) as a white powder, mp = 119-121 °C; R$_f$ = 0 (100 % EtOAc); ν_{max}/cm^{-1} 3321, 1720, 1649, 1611, 1549, 1226; δ_H (400 MHz, DMSO-d$_6$) 12.61 (1H, bs, O*H*), 8.43 (1H, bt, *J* 5.5, N*H*), 6.29 (1H, dd, *J* 9.4, *J* 15.9, NHCOC*H*CH$_2$), 6.10 (1H, dd, *J* 2.4, *J* 15.9, NHCOCHC*H$_2$ cis* to C=O), 5.62 (1H, dd, *J* 2.4, *J* 9.4, NHCOCHC*H$_2$ trans* to C=O), 3.83 (2H, d, *J* 5.5, NHC*H$_2$*); δ_C (101 MHz, DMSO-d$_6$) 171.26, 164.92, 131.32, 125.73, 40.65; m/z (CI) 147 [MNH$_4$]$^+$, 130 [MH]$^+$; found: [MNH$_4$]$^+$, 147.0772 $C_5H_{11}N_2O_3$ requires 147.0770, Δ 1.6 ppm. Data in agreement with literature values.[296]

(±)-3-(2-Phenylselanyl-propionylamino)-propionic acid **168**
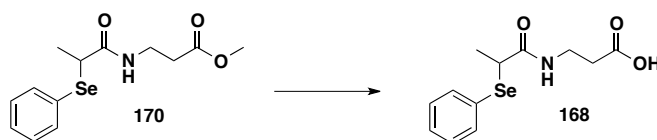
To a solution of methyl ester **170** (985.4 mg, 3.14 mmol, 1.0 eq.) in MeOH (7 mL) was added 1 M NaOH (7 mL) and the reaction stirred at rt overnight. The MeOH was removed *in vacuo* and the aqueous residue acidified with 1 M HCl and extracted with EtOAc. Combined organics were dried over MgSO$_4$, filtered and the solvent removed *in vacuo* to yield the desired carboxylic acid **168** (947.3 mg, 100 %) as a yellow oil. R$_f$ = 0 (EtOAc/n-hexane, 1:1); ν_{max} /cm^{-1} 1715 (C=O carboxylic acid), 1638 (amide), 1537, 1438, 1193; δ_H (400 MHz, CDCl$_3$) 9.60 (1H, bs, O*H*), 7.56-7.54 (2H, m, Ph), 7.35-7.27 (3H, m, Ph), 6.72 (1H, bt, *J* 6.0, N*H*), 3.79 (1H, q, *J* 7.1, CH$_3$C*H*(SePh)), 3.47 (2H, q, *J* 6.0, NHC*H$_2$*), 2.48 (2H, t, *J* 6.0, NHCH$_2$C*H$_2$*), 1.59 (3H, d, *J* 7.1, C*H$_3$*CH(SePh)); δ_C (101 MHz, CDCl$_3$) 176.7, 173.2, 134.9, 129.4, 128.5, 128.1, 40.6, 35.1, 33.7, 18.2; m/z (ESI) 301 [MH]$^+$; found [MH]$^+$ 301.0219 $C_{12}H_{15}O_3NSe$ requires 301.0212, Δ 0.4 ppm.

(±)-3-(2-Phenylselanyl-propionylamino)-propionic acid methyl ester **170**
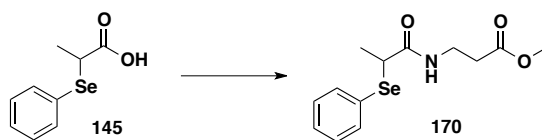
To a solution of α-selenide **145** (250.0 mg, 1.09 mmol, 1.0 eq.) in anhydrous THF (3 mL) at 0 °C under argon was added oxalyl chloride (0.10 mL, 1.14 mmol, 1.05 eq.) and DMF (2 drops, cat.) and the light yellow solution stirred at rt for 110 min. To the reaction mixture was added β-alanine methyl ester hydrochloride (304.3 mg, 2.18 mmol, 2.0 eq.) all at once, Et$_3$N (0.53 mL, 3.82 mmol, 3.5 eq.) dropwise (care - vigorous evolution of HCl gas) and THF (5 mL) to aid stirring. The thick yellow precipitate was stirred for 24 h at rt before dilution with ether. The organic layer was washed with brine (x 1), dried over MgSO$_4$ and the solvent removed *in vacuo*. The crude yellow oil (258.4 mg) was purified on silica (EtOAc/n-hexane, 1:1) to yield the desired ester **170** (210.1 mg, 61 %) as a clear oil. R$_f$ = 0.3 (EtOAc/n-hexane, 1:1); ν$_{max}$ /cm^{-1} 3297 (NH), 1736 (ester), 1646 (amide), 1544, 1438,1368, 1242, 1198, 1174, 742, 692; δ$_H$ (400 MHz, CDCl$_3$) 7.52-7.50 (2H, m, Ph), 7.30-7.22 (3H, m, Ph), 6.62 (1H, bt, *J* 6.1, N*H*), 3.73 (1H, q, *J* 7.1, CH$_3$C*H*(SePh)), 3.63 (3H, s, COOC*H*$_3$), 3.42 (2H, q, *J* 6.1, NHC*H*$_2$), 2.39 (2H, t, *J* 6.1, NHCH$_2$C*H*$_2$), 1.55 (3H, d, *J* 7.1, C*H*$_3$CH(SePh)); δ$_C$ (101 MHz, CDCl$_3$) 172.8, 172.3, 134.6, 129.2, 128.3, 128.2, 51.7, 40.6, 35.1, 33.6, 18.2; *m/z* (ESI) 315 [MH]$^+$; found [MH]$^+$ 315.0361 C$_{13}$H$_{17}$O$_3$NSe requires 315.0368, Δ 2.2 ppm.

(±)-N-[3-Oxo-3-(4-phenyl-piperazin-1-yl)-propyl]-2-phenylselanyl-propionamide **172**
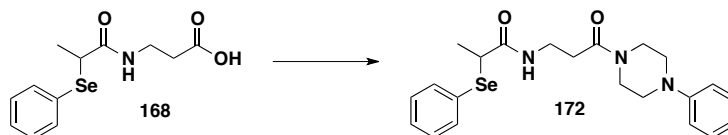
To a solution of carboxylic acid **168** (123.2 mg, 0.41 mmol, 1.0 eq.) and zirconocene dichloride (6.0 mg, 0.02 mmol, 5 mol %) in anhydrous toluene (10 mL) was added N-phenyl piperazine (0.06 mL, 0.41 mmol, 1.0 eq.) and the mixture heated to reflux. After 24 h the resulting orange solution was cooled to rt and filtered, and the solvent removed from the filtrate *in vacuo*. The resulting crude orange oil was purified on silica (100 % EtOAc) to yield the desired amide **172** (118.1 mg, 65 %) as a clear oil. R$_f$ = 0.44 (EtOAc/n-hexane, 1:1 on neutral alumina); ν$_{max}$ /cm^{-1} 3308 (NH), 1639 (amide), 1599, 1497, 1439,1230, 1024, 759, 742, 692; δ$_H$ (400 MHz, CDCl$_3$) 7.56-7.54 (2H, m, Ph), 7.32-7.24 (5H, m, Ph), 6.95-6.88 (3H, m, Ph), 6.87 (1H, bt, *J* 5.8, N*H*), 3.78-3.73 (3H, m, CH$_3$C*H*(SePh) and 2H piperazine), 3.56-3.45 (4H, m, NHC*H*$_2$ and 2H piperazine), 3.17-3.13 (4H, m, 4H piperazine), 2.45-2.42 (2H, m, NHCH$_2$C*H*$_2$), 1.62-1.57 (3H, m, C*H*$_3$CH(SePh)); δ$_C$ (101 MHz, CDCl$_3$) 172.4, 169.9, 150.7, 134.6, 129.3, 129.1, 128.6, 128.1, 120.8, 116.7, 49.7, 49.4, 45.2, 41.4, 40.8, 35.3, 32.7, 18.3; *m/z* (ESI) 468 [MNa]$^+$; found [MNa]$^+$ 468.1163 C$_{22}$H$_{27}$N$_3$O$_2$NaSe requires 468.1166, Δ 0.6 ppm.

N-[3-Oxo-3-(4-phenyl-piperazin-1-yl)-propyl]-acrylamide **173**
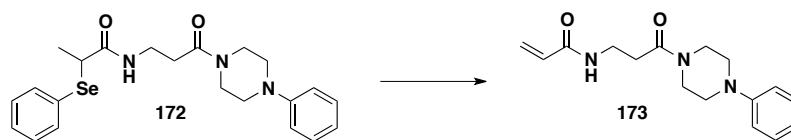
To α-selenide **172** (113.4 mg, 0.26 mmol, 1.0 eq.) and NaIO$_4$ (186 mg, 0.41 mmol, 3.3 eq.) was added EtOH (1 mL) and the suspension rapidly stirred at rt for 10 h before dilution with CH$_2$Cl$_2$ and brine. The layers were separated and the aqueous layer washed with CH$_2$Cl$_2$ (x 2). Combined organics were dried over MgSO$_4$, filtered and the solvent removed *in vacuo*. The crude oil (176.1 mg) was purified on silica (100 % EtOAc) and the resulting residue repurified on silica (EtOAc:MeOH, 19:1). The obtained residue was dissolved in CH$_2$Cl$_2$ and washed with 1 M HCl (x 3). Combined aqueous layers were basified with saturated NaOH (aq.) and extracted with CH$_2$Cl$_2$ (x 3) and EtOAc (x 1). Combined organics from the basic extraction were dried over MgSO$_4$, filtered and the solvent removed *in vacuo*. The residue was purified on silica (gradient elution EtOAc to EtOAc/MeOH, 19:1) to yield the desired acrylamide **173** (36.0 mg, 48 %) as a white powder, mp = 105-107 °C; R$_f$ = 0.27 (100 % EtOAc); ν$_{max}$ /cm^{-1} 3297, 1621, 1598, 1496, 1440, 1228, 1211, 1025, 991, 760, 694; δ$_H$ (400 MHz, CD$_2$Cl$_2$) 7.29-7.24 (2H, m, Ph), 6.93-6.91 (2H, m, Ph), 6.90-6.85 (1H, m, Ph), 6.66 (1H, bs, N*H*), 6.20 (1H, dd, *J* 17.0, *J* 2.1, C*H*$_2$CHCONH *cis* to C=O), 6.11 (1H, dd, *J* 17.0, *J* 9.8, CH$_2$C*H*CONH), 5.58 (1H, dd, *J* 9.8, *J* 2.1, C*H*$_2$CHCONH *trans* to C=O), 3.75 (2H, t, *J* 5.2, 2H piperazine), 3.62-3.56 (4H, m, 4H piperazine), 3.16-3.12 (4H, m, 2H piperazine and NHC*H*$_2$), 2.59 (2H, t, *J* 5.7, NHCH$_2$C*H*$_2$); δ$_C$ (101 MHz, CD$_2$Cl$_2$) 170.5, 165.6, 165.5, 151.7, 131.9, 131.9, 129.7, 126.0, 120.7, 117.0, 50.0, 49.8, 45.7, 41.9, 35.6, 35.4, 33.3; *m/z* (ESI) 310 [MNa]$^+$; found [MNa]$^+$ 310.1528 C$_{16}$H$_{21}$N$_3$O$_2$Na requires 310.1531, Δ 1.0 ppm.

(±)-2-Phenylselanyl-N-(2-(R)-([1-(toluene-4-sulfonyl)-pyrrolidin-2-ylmethyl]-carbamoyl)-ethyl)-propionamide **174**
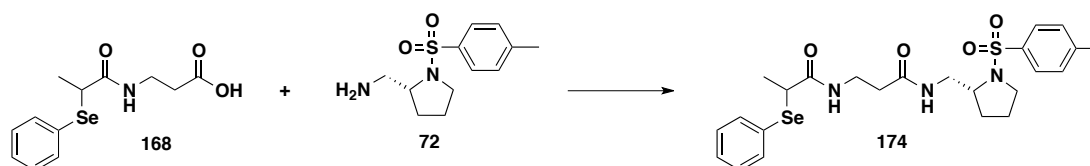
A solution of amine **72** (563.9 mg, 1.89 mmol, 1.0 eq.), carboxylic acid **168** (567.3 mg, 1.89 mmol, 1.0 eq.) and zirconocene dichloride (28 mg, 5 mol %) was refluxed in toluene (60 mL) for 17 h. The reaction was allowed to cool to rt, the solvent removed *in vacuo* and the resultant brown oil purified on silica (100 % EtOAc) twice to give the desired amide **174** (443.4mg, 44 %) as a white foam as an inseparable mixture of diastereoisomers. R$_f$ = 0.39 (100 % EtOAc); ν$_{max}$ /cm^{-1} 3301 (NH), 1646 (amide), 1537, 1446, 1338, 1156, 1093, 747, 664; δ$_H$ (400 MHz, CDCl$_3$) 7.62 (2H, d, *J* 8.1, tol *H3'*), 7.48 (2H, td, *J* 7.7, *J* 1.5, Ar*H*), 7.25-7.15 (5H, m, Ar*H*), 6.99-6.94 (1H, m, N*H*), 6.86-6.81 (1H, m, N*H*), 3.74-3.67 (2H, m), 3.47-3.32 (4H, m), 3.20-3.08 (2H, m), 2.34 (3H, s, tol C*H*$_3$), 2.34-2.28 (2H, m), 1.73-1.64 (1H, m, pyrrolidine), 1.55-1.35 (3H, m, pyrrolidine), 1.48 (3H, d, *J* 7.0, C*H*$_3$CH(SePh)); δ$_C$ (101 MHz, CDCl$_3$) 172.4, 172.3, 171.9, 171.8, 143.8, 134.9, 134.8, 133.6, 129.8, 129.0, 128.3, 128.2, 128.0, 128.0, 127.4, 59.3, 59.3, 49.3, 43.7, 43.6, 40.5, 40.5, 35.7, 35.3, 35.3, 29.2, 23.9, 21.4, 18.3, 18.2; *m/z* (EI) 537 [M]$^+$, 382 [M-SO$_2$tol]$^+$, 224 [M-SO$_2$tol-SePh]$^+$, 155 [SO$_2$tol]$^+$; found [M]$^+$ 537.1199 C$_{24}$H$_{31}$O$_4$N$_3$SSe requires 537.1195, Δ 0.8 ppm.

(R)-N-(2-([1-(Toluene-4-sulfonyl)-pyrrolidin-2-ylmethyl]-carbamoyl)-ethyl)-acrylamide **175**
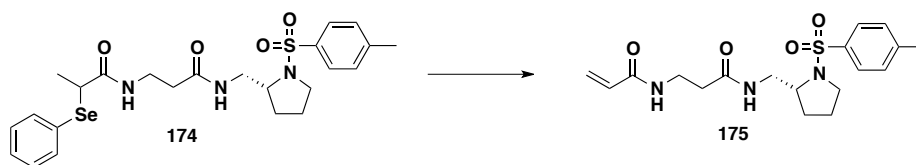
To α-(phenyl)selenide **174** (413.2 mg, 0.77 mmol, 1.0 eq.) and NaIO$_4$ (263.3 mg, 1.23 mmol, 1.6 eq.) was added EtOH (6 mL) and the suspension stirred rapidly at rt for 90 h. The thick yellow precipitate was diluted with CH$_2$Cl$_2$ and washed with H$_2$O. The aqueous layer was further washed with CH$_2$Cl$_2$ (x 1) and the organic layers combined, dried over MgSO$_4$ and the solvent removed *in vacuo*. The crude residue was purified on silica (gradient elution, EtOAc to EtOAc/MeOH, 9:1) to yield the desired acrylamide **175** (276.5 mg, 94 %) as a clear oil. [α]$^{27}_D$ = + 67.4 (*c* = 8.37, CHCl$_3$); R$_f$ = 0.13 (100 % EtOAc); ν$_{max}$ /cm^{-1} 3290 (NH), 1654, 1627, 1539, 1339, 1156, 1092, 752, 664; δ$_H$ (400 MHz, CDCl$_3$) 7.59 (2H, d, *J* 8.1, tosyl Ar*H3'*), 7.21 (2H, d, *J* 8.1, tosyl Ar*H2'*), 7.16 (2H, bt, *J* 5.4, 2 x N*H*), 6.16-6.04 (2H, m, C*H$_2$*CHCONH *cis* to C=O and CH$_2$C*H*CONH), 5.46 (1H, dd, *J* 2.6, *J* 9.1, C*H$_2$*CHCONH *trans* to C=O), 3.71-3.66 (1H, m), 3.59-3.46 (2H, m), 3.36-3.28 (2H, m), 3.21-3.15 (1H, m), 3.09-3.03 (1H, m), 2.43 (2H, t, *J* 6.1, C*H$_2$*CONH), 2.31 (3H, s, tosyl C*H$_3$*), 1.72-1.62 (1H, m), 1.53-1.45 (1H, m), 1.42-1.31 (2H, m); δ$_C$ (101 MHz, CDCl$_3$) 172.1, 165.7, 143.8, 133.6, 131.0, 129.7, 127.3, 125.8, 59.2, 49.2, 43.6, 35.6, 35.5, 29.0, 23.8, 21.3; *m/z* (ESI) 402 [MNa]$^+$, 380 [MH]$^+$; found [MNa]$^+$ 402.1472 C$_{18}$H$_{25}$O$_4$N$_3$SNa requires 402.1463, Δ 2.2 ppm.

(±)-N-(2-[3-phenyl-2-(toluene-4-sulfonylamino)propylcarbamoyl]-ethyl)-acrylamide **177**
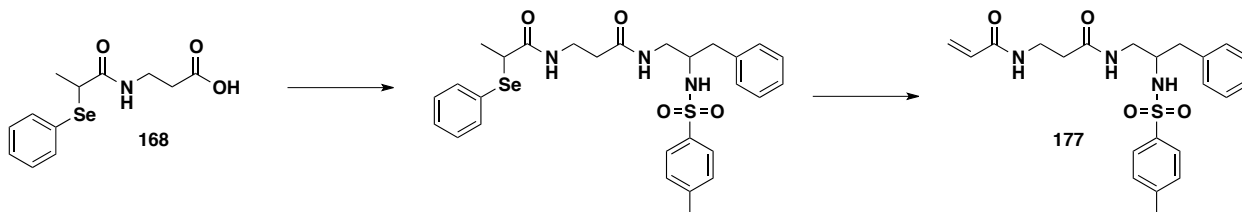
To carboxylic acid **168** (334.0 mg, 1.11 mmol, 1.0 eq.) and zirconocene (16.2 mg, 5 mol%) was added amine **121a** (339.0 mg, 1.11 mmol, 1 eq.) in anhydrous toluene (25 mL) and the mixture refluxed for 17 h. The reaction mixture was allowed to cool to rt, filtered to remove insoluble and the solvent removed *in vacuo*. The crude brown residue (501 mg) was purified on silica (gradient elution EtOAc/n-hex, 1:1 to EtOAc/MeOH, 9:1). Relevant fractions were combined and the solvent removed *in vacuo* to yield the desired amide **176** as a 1:1 mixture of diastereoisomers (151.1 mg) as a clear oil. To this was added NaIO$_4$ (88 mg, 0.41 mmol, 1.6 eq.) and the mixture stirred vigourously in EtOH (3 mL) for 24 h. The reaction mixture was diluted with CH$_2$CH$_2$ (10 mL) and washed with H$_2$O (10 mL). The aqueous layer was washed with CH$_2$CH$_2$ (10 mL) and the combined organics dried over MgSO$_4$, filtered and the solvent removed *in vacuo*. The crude yellow oil (164.6 mg) was purified on silica (gradient elution EtOAc to EtOAc/MeOH, 9:1) to yield the desired acrylamide **177** (86.8 mg, 18 % over 2 steps) as a clear oil. R$_f$ = 0.22 (100 % EtOAc); ν$_{max}$ /cm^{-1} 3287, 1656, 1626, 1599, 1539, 1498, 1454, 1429, 1321, 1288, 1241, 1154, 1091, 982, 813, 732, 701, 664; δ$_H$ (400 MHz, CDCl$_3$) 7.56 (2H, d, *J* 8.2, tolyl *H3'*), 7.16 (2H, d, *J* 8.2, tolyl *H2'*), 7.12-7.03 (5H, m, Ph), 6.96-6.94 (2H, m, N*H*), 6.26-6.13 (3H, m, C*H$_2$*CHCONH *cis* to C=O and CH$_2$C*H*CONH and N*H*), 5.57 (1H, dd, *J* 9.1,

J 2.8, C*H*₂CHCONH *trans* to C=O), 3.65 (3H, m), 3.30-3.21 (2H, m), 2.63 (2H, d, *J* 6.9, PhC*H*₂), 2.42-2.40 (2H, m), 2.37 (3H, s, ArC*H*₃); δ_C (101 MHz, CDCl₃) 173.0, 166.2, 143.3, 137.7, 136.9, 131.1, 129.7, 129.3, 128.6, 126.8, 126.7, 126.5, 55.7, 43.2, 39.5, 35.9, 35.8, 21.6; *m/z* (ESI) 430 [MH]⁺, 452 [MNa]⁺; found [MNa]⁺ 452.1610 C₂₂H₂₇O₄N₃SNa requires 452.1620, Δ 2.2 ppm.

3-Benzyloxycarbonylaminopropionic acid **179**
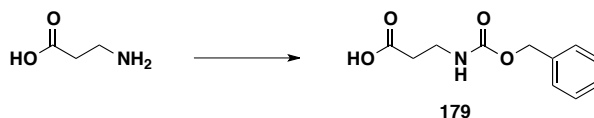
Benzyl chloroformate (0.79 mL, 5.5 mmol, 1.1 eq.) was added dropwise to a solution of β-alanine (445 mg, 5 mmol, 1 eq.) in 2M NaOH (5 mL) at 0 °C and the mixture allowed to warm to rt and stirred vigorously for 12 h. The reaction mixture was washed with ether (x 3), acidified to pH 5 with conc. aq. HCl and washed with EtOAc (x 1). The organic EtOAc layer was dried over MgSO₄, filtered and the solvent removed *in vacuo* to yield the desired carbamate **179** (729.6 mg, 65 %) as a white crystalline powder, mp = 98-101 °C; ν_{max} /cm⁻¹ 3330, 1682, 1531, 1320, 1261, 1247, 1216, 1027, 949, 728, 695; δ_H (400 MHz, MeOH) 7.39-7.26 (5H, m, Ph), 5.07 (2H, s, C*H*₂Ph), 3.39-3.35 (2H, m, C*H*₂NH), 2.50 (2H, t, *J* 6.8, C*H*₂CH₂NH); δ_C (101 MHz, MeOH) 175.5, 158.9, 138.5, 129.6, 129.1, 128.9, 67.6, 38.0, 35.3; *m/z* (ESI) 222 [M-H]⁻; found [M-H]⁻ 222.0763 C₁₁H₁₂NO₄ requires 222.0766, Δ 1.4 ppm. Data in agreement with literature values.[297]

(2-Carbamoylethyl)carbamic acid benzyl ester **180**
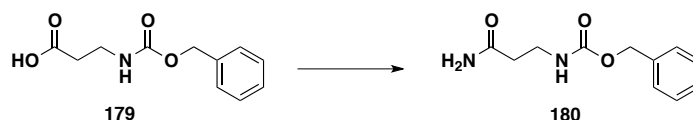
To a solution of Cbz-protected β-alanine **179** (251.9 mg, 1.13 mmol, 1.0 eq.) in anhydrous THF (1.6 mL) at 0 °C under Ar was added anhydrous Et₃N (0.16 mL, 1.13 mmol, 1.0 eq.) and ethyl chloroformate (0.11 mL, 1.13 mmol, 1 eq.) and the thick white precipitate stirred at 0 °C for 30 min. Aqueous ammonia (28%, 0.29 mL) was added to the stirred reaction mixture and stirring continued for a further 30 min. The reaction mixture was diluted with EtOAc (20 mL) washed with H₂O (x 1) and concentrated *in vacuo* to ca. 10 mL. The thick white precipitate was filtered and dried under high vacuum to yield the desired primary amide **180** (115.9 mg, 46 %) as a white solid, mp 158-162 °C; δ_H (400 MHz, DMSO-d₆) 7.34 (6H, bs, Ph and N*H*), 7.22 (1H, bs, N*H*), 6.81 (1H, bs, N*H*), 5.00 (2H, s, C*H*₂Ph), 3.20-3.15 (2H, m, C*H*₂NH), 2.23 (2H, bt, *J* 6.2, C*H*₂CH₂NH). Data in agreement with literature values.[298]

N-(2-carbamoylethyl)acrylamide **182**
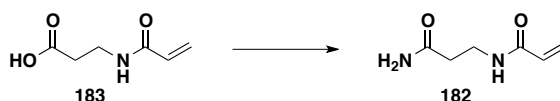
To a stirred solution of β-alanine N-acrylamide **183** (250 mg, 1.75 mmol, 1.0 eq.) in dry THF (2.5 mL) at 0 °C under argon was added Et$_3$N (0.24 mL, 1.75 mmol, 1.0 eq.) and ethyl chloroformate (0.17 mL, 1.75 mmol, 1.0 eq.) and the reaction mixture stirred at 0 °C for 30 min. To the resultant white precipitate was added 28 % aqueous NH$_3$ (0.46 ml) and the mixture stirred for a further 30 min. The thick white precipitate was filtered and the solvent removed from the filtrate. The crude brown residue was purified on silica (MeOH/EtOAc, 1:4) to yield the desired amide **182** (13.8 mg, 6 %) as a white solid, mp = 145-146 °C; R$_f$ = 0.32 (EtOAc/MeOH, 4:1); ν$_{max}$ /cm^{-1} 3353, 3323, 3256, 3179, 2407, 1652, 1626, 1555, 1529, 1432, 1406, 1242, 944; δ$_H$ (400 MHz, MeOD) 6.27-6.18 (2H, m, C*H*$_2$CHCONH *cis* to C=O and CH$_2$C*H*CONH), 5.65 (1H, dd, *J* 7.8, *J* 4.1, C*H*$_2$CHCONH *trans* to C=O), 3.51 (2H, t, *J* 6.9, CH$_2$CHCONHC*H*$_2$), 2.46 (2H, t, *J* 6.9, NH$_2$COC*H*$_2$); δ$_C$ (101 MHz, MeOD) 176.5, 168.4, 132.1, 126.9, 37.0, 36.1; *m/z* (CI) 143 [MH]$^+$; found [MH]$^+$ 143.0842 C$_6$H$_{11}$N$_2$O$_2$ requires 143.0821, Δ 14.7 ppm.

(3-Benzyloxycarbonylamino-propyl)-carbamic acid benzyl ester **184**
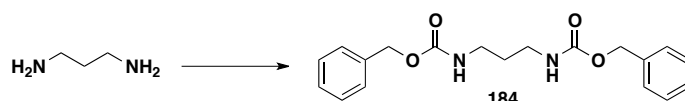
To a solution of propane-1,3-diamine (0.84 mL, 10 mmol, 1.0 eq.) in CH$_2$Cl$_2$ (20 mL) was added triethylamine (2.2 mL, 15 mmol, 1.5 eq.) and benzylchloroformate (1.4 mL, 10 mmol, 1.0 eq.) dropwise yielding immediate formation of a white precipitate and an exotherm, which brings the solution to reflux. The reaction mixture was stirred for 3 h, diluted with CH$_2$Cl$_2$ and extracted with 5 % aq. citric acid. The CH$_2$Cl$_2$ layer was then washed with 1M aq. HCl and the acidic layer back extracted with CH$_2$Cl$_2$. Combined CH$_2$Cl$_2$ layers were dried over MgSO$_4$, filtered and the solvent removed *in vacuo* to yield di-carbamate **184** (1.03 g, 60 %) as a white solid. R$_f$ = 0.68 (100 % EtOAc); δ$_H$ (400 MHz, CDCl$_3$) 7.43-7.32 (10H, m, Ar*H*), 5.24 (2H, bs, N*H*), 5.12 (4H, OC*H*$_2$Ph), 3.29-3.25 (4H, m, 2 x C*H*$_2$), 1.70-1.63 (2H, m, C*H*$_2$).

Carbonic acid benzyl ester phenyl ester **185**
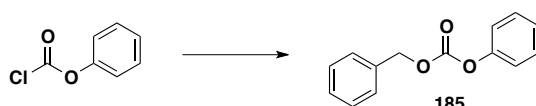
A procedure reported by Pittelkow *et al.* was used with some modifications.[199] To a solution of benzyl alcohol (3.1 mL, 30 mmol, 1.0 eq.) and pyridine (2.9 mL, 36 mmol, 1.2 eq.) in anhydrous CH$_2$Cl$_2$ (30 mL) under argon was added phenyl chloroformate (3.76 mL, 30 mmol, 1.0 eq.) dropwise over ca. 5 min bringing the reaction mixture to reflux. A thick white precipitate was formed from the colourless solution after addition was complete, and the slurry stirred at rt for 4 h. The reaction mixture was diluted with CH$_2$Cl$_2$, washed with H$_2$O (x 1) and 2M H$_2$SO$_4$ (x 2), dried over

MgSO$_4$, filtered and the solvent removed *in vacuo*. The crude oil was purified by vacuum distillation (0.3 mmHg, 170-175 °C) to yield the desired carbonate **185** (4.57 g, 67 %) as a clear oil. R$_f$ = 0.61 (EtOAc/n-hexane, 1:5); ν$_{max}$ /cm^{-1} 1759 (carbonate), 1231, 1206, 694, 687; δ$_H$ (400 MHz, CDCl$_3$) 7.50-7.39 (7H, m, Ar*H*), 7.30-7.26 (1H, m, Ar*H*), 7.23-7.20 (2H, m, Ar*H*), 5.31 (2H, s, C*H*$_2$); δ$_C$ (101 MHz, CDCl$_3$) 153.8, 151.3, 134.9, 129.6, 128.9, 128.8, 128.7, 126.2, 121.2, 70.5; m/z (CI) 246 [MNH$_4$]$^+$; found [MNH$_4$]$^+$ 246.1125 C$_{14}$H$_{16}$O$_3$N requires 246.1130, Δ 2.0 ppm. Data in agreement with literature values.[199]

N-tosyl-DL-phenylalanine **187**
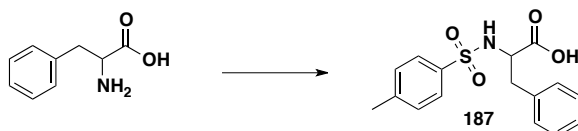
A procedure reported by Hersh *et al*. was used with some modifications.[299] To a solution of DL-phenylalanine (8.33 g, 50 mmol, 1.0 eq.) and sodium carbonate (12.83 g, 121 mmol, 2.4 eq.) in H$_2$O (100 mL) was added tosyl chloride (11.54 g, 61 mmol, 1.2 eq.) in 3 portions (0 h, 18 h, 26 h) and the thick white precipitate stirred at rt for 6 days. The reaction mixture was washed with Et$_2$O and the resulting aqueous layer acidified with conc. HCl and washed with EtOAc (x 2). The EtOAc layers were combined, dried over MgSO$_4$ and the solvent removed *in vacuo* to yield the desired tosylate **187** (2.3 g, 14 %) as a white powder. A small portion (1.8 g) was recrystallised from toluene to yield the desired tosylate **187** (1.42 g) as a white powder, mp = 115-120 °C; R$_f$ = 0.35 (100 % EtOAc); ν$_{max}$ /cm^{-1} 1712, 1695, 1342, 1329, 1169, 1156, 1089, 931, 817, 698, 686; δ$_H$ (400 MHz, CDCl$_3$) 7.59 (2H, d, *J* 8.3, tolyl *H3'*), 7.24-7.20 (5H, m, Ar*H*), 7.08-7.06 (2H, m, Ar*H*), 5.07 (1H, d, *J* 8.7, N*H*), 4.23-4.18 (1H, m, C*H*COOH), 3.10 (1H, dd, *J* 13.9, *J* 5.4, PhC*H*$_2$), 3.00 (1H, dd, *J* 13.9, *J* 6.4, PhC*H*$_2$), 2.40 (3H, s, PhC*H*$_3$); δ$_C$ (101 MHz, DMSO-d$_6$) 172.3, 142.3, 138.2, 136.7, 129.3, 129.2, 128.2, 126.5, 126.3, 57.4, 37.8, 21.0; m/z (CI) 320 [MH]$^+$; found [MH]$^+$ 320.0951 C$_{16}$H$_{18}$O$_4$NS requires 320.0957, Δ 1.7 ppm. Data in agreement with literature values.[299]

(±)-3-[3-Phenyl-2-(toluene-4-sulfonylamino)propionylamino]propylammonium HCl salt **188**
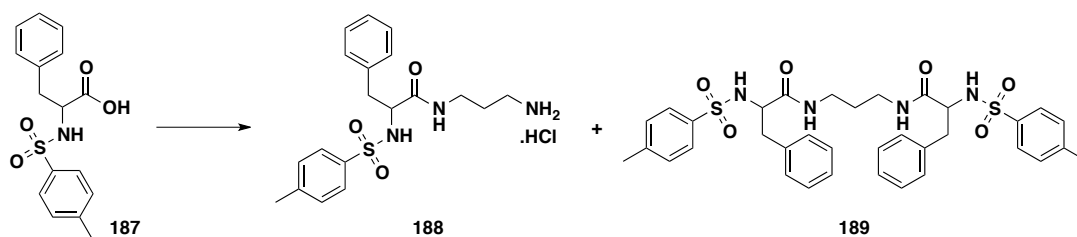
To N-tosyl phenylalanine **187** (319 mg, 1 mmol, 1 eq.) and zirconocene dichloride (15 mg, 5 mol %) was added anhydrous toluene (30 mL) and 1,3-diaminopropane (0.83 mL, 10 mmol, 10 eq.) and the thick precipitate heated to reflux. The resulting colourless solution was heated at reflux with stirring for 3 h, allowed to cool to rt and the toluene removed *in vacuo*. To the resulting residue was added HCl (1 M) (3 mL) and EtOAc (5 mL) and the resulting precipitate filtered to yield the desired amine **188** (97.2 mg, 24 %) as a white solid, mp = 174-180 °C (decomposition). The filtrate was washed with EtOAc to obtain diacylated diamine **189** (175.8 mg, 52 %) as a clear oil.

(±)-3-[3-Phenyl-2-(toluene-4-sulfonylamino)propionylamino]propylammonium HCl salt **188**

188
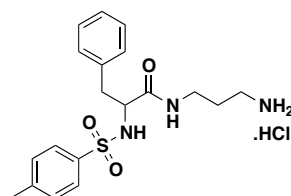
ν_{max} /cm^{-1} 1638, 1570, 1494, 1373, 1285, 1153, 1095, 972, 947, 901, 857, 806, 694; δ_H (400 MHz, DMSO-d$_6$) 7.58 (2H, d, *J* 8.1, tol-*H3'*), 7.31 (2H, d, *J* 8.1, tol-*H2'*), 7.20-7.13 (5H, m, Ph), 3.37 (1H, t, *J* 5.0, TsNHC*H*), 2.96 (1H, dd, *J* 13.4, *J* 4.7, TsNHCHC*H*$_2$Ph), 2.88 (1H, dd, *J* 13.4, *J* 5.4, TsNHCHC*H*$_2$Ph), 2.76 (4H, t, *J* 7.1, CONHC*H*$_2$CH$_2$C*H*$_2$NH$_2$), 2.35 (3H, s, ArC*H*$_3$), 1.71 (2H, p, *J* 7.1, CONHCH$_2$C*H*$_2$CH$_2$NH$_2$); δ_C (101 MHz, DMSO-d$_6$) 171.7, 142.4, 138.4, 137.4, 129.9, 129.4, 127.6, 126.7, 125.7, 58.1, 38.3, 36.8, 27.4, 20.9; *m/z* (ESI) 376 [MH]$^+$; found [MH]$^+$ 376.1704 C$_{19}$H$_{26}$N$_3$O$_3$S requires 376.1695, Δ 2.4 ppm.

3-Phenyl-N-{3-[3-phenyl-2-(toluene-4-sulfonylamino)-propionylamino]-propyl}-2-(toluene-4-sulfonylamino)-propionamide **189**

189
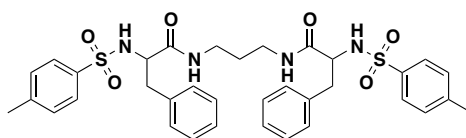
δ_H (400 MHz, CDCl$_3$) 7.96 (1H, bs, N*H*), 7.48 (2H, d, *J* 8.1, tosyl-*H*), 7.37 (2H, d, *J* 8.1, tosyl-*H*), 7.08-6.92 (14H, m, Ar*H*), 3.96-3.88 (2H, m), 3.29-3.25 (2H, bm), 3.17-3.12 (1H, m), 3.05-3.01 (1H, m), 2.97-2.86 (3H, m), 2.73-2.67 (1H, m), 2.31 (6H, s, 2 x C*H*$_3$), 1.82 (2H, bs).

9.7. Alkyne-tagged chemical probe

3-(4-Ethynylbenzenesulfonyl)acrylonitrile **192**
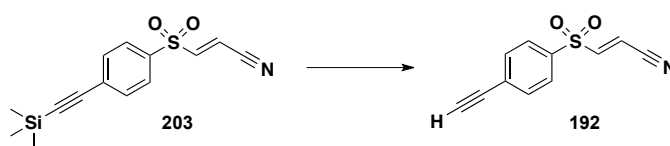
To a solution of TMS-acetylene **203** (5.7 mg, 0.020 mmol, 1.0 eq.) in THF (1 mL) at 0 °C was added TBAF (1.0 M in THF):AcOH, 1:1 (40 µL, 0.020 mmol (TBAF), 1 eq.) and the colourless solution stirred at 0 °C for 5 min and at rt for a further 90 min. The reaction mixture was partitioned between EtOAc and H$_2$O and the layers separated. The aqueous layer was further washed with EtOAc (x 1) and the combined organics were dried over Na$_2$SO$_4$, filtered and the solvent removed *in vacuo*. The crude white solid was purified on silica (EtOAc/n-hex, 1:4) and the isolated product re-purified on silica (EtOAc/n-hex, 1:9). The solvent was partially removed from fractions and left for 16 h to allow the desired product to crystallise. The remaining solvent was removed *via* pipette and the crystals dried under high vacuum to yield the desired terminal acetylene **192** (2.1 mg, 48 %) as a white crystalline solid, mp = 182-185 °C; R$_f$ =

0.63 (n-hex/EtOAc, 7:3); ν_{max} /cm^{-1} 3254, 1330, 1151, 828; δ_H (400 MHz, CDCl$_3$) 7.86 (2H, d, J 8.5, Ar$H2'$), 7.71 (2H, d, J 8.5, Ar$H3'$), 7.21 (1H, d, J 15.7, SO$_2$CH), 6.57 (1H, d, J 15.7, HCCN), 3.36 (1H, s, acetylene-H); δ_C (101 MHz, CDCl$_3$) 148.8, 137.1, 133.6, 129.6, 128.6, 113.3, 111.3, 82.7, 81.6; m/z (EI) 217 [MH]$^+$; found [MH]$^+$ 217.0184 C$_{11}$H$_7$NO$_2$S requires 217.0198 , Δ 6.5 ppm.

4,4'-dibromo-diphenyl sulfone **195**
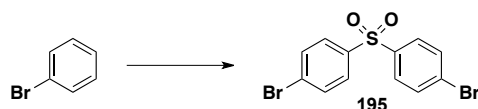
To a solution of bromobenzene (1.00 mL, 9.4 mmol, 1.0 eq.) in anhydrous CHCl$_3$ (10 mL) at 0 °C was added chlorosulfonic acid (0.94 mL, 14.1 mmol, 1.5 eq.) and the reaction mixture stirred at 0 °C for 30 min and at rt for 30 min. The reaction mixture was then added dropwise to ice and extracted with CH$_2$Cl$_2$ (x 1). The organic layer was dried over MgSO$_4$, filtered and the solvent removed *in vacuo*. The crude white solid was purified on silica (EtOAc/n-hex, 1:9) to yield biaryl sulfone **195** (167.1 mg, 9 %) as a white solid, mp = 169-171 °C. R$_f$ = 0.54 (EtOAc/n-hex, 3:7); ν_{max} /cm^{-1} 1573, 1467, 1388, 1327, 1279, 1157, 1100, 1064, 1006, 819, 754, 728; δ_H (400 MHz, CDCl$_3$) 7.79-7.76 (4H, m), 7.65-7.61 (4H, m); δ_C (101 MHz, CDCl$_3$) 140.2, 132.8, 129.2, 128.9; m/z (EI) 376 [M]$^+$. Data in agreement with literature values.[300, 301]

p-Bromophenylsulfonyl hydrazide **197**
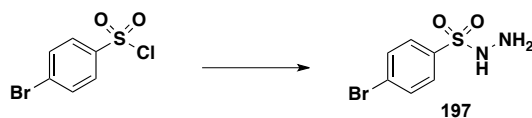
To hydrazine hydrate (4.0 mL, 62.4 mmol, 3.2 eq.) at 0 °C was added *p*-bromobenzenesulfonyl chloride (5.0 g, 19.6 mmol, 1.0 eq.) with vigorous stirring. The solution was stirred at 0 °C for 30 min, diluted with saturated NaCl and extracted with ether (x 1). The solvent was removed from the organic layer *in vacuo* to yield the desired sulfonyl hydrazide **197** (4.4 g, 91 %) as a white powder, mp = 119-122 °C; ν_{max} /cm^{-1} 3284 (NH), 1324, 1155 (SO$_2$); δ_H (400 MHz, DMSO-d$_6$) 8.49 (1H, s, NH), 7.82 (2H, d, J 8.5, ArH), 7.72 (2H, J 8.5, ArH), 4.21 (2H, bs, NH_2); δ_C (101 MHz, MeOD) 138.3, 133.5, 131.0, 128.9. Data in agreement with literature values.[302]

Phenylselenenyl p-bromobenzenesulfonate **198**
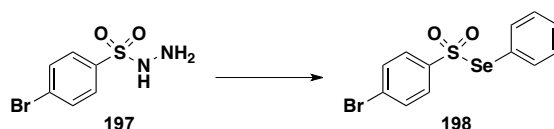
To a solution of benzene seleninic acid (1.62 g, 8.56 mmol, 1.0 eq.) in anhydrous CH$_2$Cl$_2$ (20 mL) at 0 °C was added sulfonylhydrazine **197** (2.14 g, 8.56 mmol, 1.0 eq.) in anhydrous CH$_2$Cl$_2$ (20 mL) dropwise, and the resulting yellow solution stirred at 0 °C for 1 hour. The solvent was removed *in vacuo* and the resulting crude orange residue

recrystallised from methanol to yield the desired selenylsulfonate **198** (2.38g, 74 %) as a light yellow crystalline solid, mp = 84-87 °C; v_{max} /cm^{-1} 1568, 1475, 1465, 1439, 1386, 1318 (SO$_2$), 1274, 1130 (SO$_2$), 1067, 1009, 837, 815, 743, 733, 697, 685; δ_H (400 MHz, CDCl$_3$) 7.53-7.45 (5H, m, C$_6$H$_5$Se), 7.37-7.31 (4H, m, SO$_2$Ar*H*); δ_C (101 MHz, CDCl$_3$) 144.4, 137.4, 132.2, 131.4, 130.0, 128.9, 128.6, 127.9; *m/z* (CI) 394 [MNH$_4$]$^+$; found: [MNH$_4$]$^+$, 393.9017 C$_{12}$H$_{13}$NO$_2$SBrSe requires 393.9016, Δ 0.3 ppm.

3-(4-Bromo-benzenesulfonyl)-acrylonitrile **200**
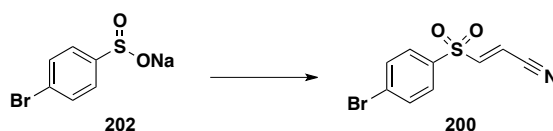
Sodium aryl sulfinate (64 %) **202** (1.22 g, 5.56 mmol, 3.0 eq.) and 2,3-dibromopropanenitrile (0.18 mL, 1.85 mmol, 1.0 eq.) in DMF (2.6 mL) were heated at 80 °C for 1 h. After cooling to rt the reaction mixture was treated with H$_2$O and extracted with EtOAc (x 2). The EtOAc layers were combined and washed with brine (x 6), dried over Na$_2$SO$_4$, filtered and concentrated *in vacuo*. The crude solid was purified on silica (EtOAc/n-hex, 1:5) to yield the desired vinyl sulfone **200** (195.7 mg, 44 %) as a white solid, mp = 177-178 °C ; R$_f$ = 0.56 (n-hex/EtOAc, 2:1); v_{max} /cm^{-1} 3077, 1577, 1390, 1327, 1274, 1147, 1084, 1068, 1009, 945, 820, 809, 746, 623, 562; δ_H (400 MHz, CDCl$_3$) 7.72-7.77 (4H, m, Ar*H*), 7.19 (1H, d, *J* 15.8, ArSO$_2$C*H*), 6.54 (1H, d, *J* 15.8, ArSO$_2$CHC*H*CN); δ_C (101 MHz, CDCl$_3$) 148.7, 136.4, 133.6, 131.1, 130.2, 113.4, 111.4; *m/z* (ESI) 219/220 [BrPhSO$_2$]$^-$, 271/272 [M]$^-$; found [M]$^-$ 270.9298 C$_9$H$_6$NO$_2$SBr requires: 270.9303, Δ 1.8 ppm.

Sodium 4-bromo-benzenesulfinate **202**
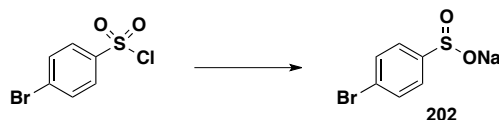
A mixture of anhydrous sodium sulfite (1.98 g, 15.7 mmol, 2.0 eq.), sodium bicarbonate (1.32 g, 15.7 mmol, 2.0 eq.) and H$_2$O (8 mL) was heated at 60-70 °C. To this mixture, *p*-bromobenzenesulfonyl chloride (2.00 g, 7.8 mmol, 1.0 eq.) was added gradually over a 10 minute interval. After 2 h the reaction was allowed to cool and the thick white precipitate was collected by filtration under reduced pressure. The resulting white solid was dried under a high vacuum to yield the desired sulfinate **202** as a mixture with inorganic salts (2.05 g, 70 % sulfinate using 1,3,5-trimethoxybenzene as an internal NMR standard), mp > 235 °C; R$_f$ = 0 (EtOAc/n-hex, 1:1); v_{max} /cm^{-1} 3500 (b), 3250 (b), 1125 (b), 1063, 999, 971, 825, 725, 607, 575; δ_H (400 MHz, D$_2$O) 7.59-7.56 (2H, m, Ar*H*), 7.43-7.40 (2H, m, Ar*H*); δ_C (101 MHz, D$_2$O) 152.6, 131.9, 125.3, 124.1; *m/z* (ESI) 219 [M(^{79}Br)]$^-$, 221 [M(^{80}Br)]$^-$; found [M]$^-$, 218.9107 C$_6$H$_4$O$_2$S^{79}Br requires 218.9115, Δ 3.7 ppm.

3-(4-Trimethylsilanylethynylbenzenesulfonyl)acrylonitrile **203**

Method One: *Oxidation and elimination of α-selenide* **218**
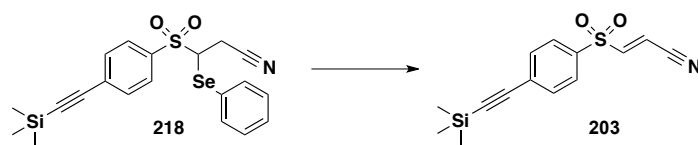
Meta-chloroperoxybenzoic acid (76 mg, 0.35 mmol, 1 eq.) was added portionwise to a solution of selenide **218** (157.8 mg, 0.35 mmol, 1 eq.) in CH_2Cl_2 (5 mL) at 0 °C. After 1 h the reaction was allowed to warm to rt and stirred for a further 3 h before dilution with CH_2Cl_2 and addition of Na_2SO_3 (sat. aq.). The layers were separated and the organic layer washed with H_2O, dried over Na_2SO_4, filtered and the solvent removed *in vacuo*. The crude residue was purified on silica (9:1, n-hex/EtOAc) to yield the desired acrylonitrile **203** (36.8 mg, 36 %) as a white solid, mp = 92-93 °C. R_f = 0.56 (4:1, n-hex/EtOAc); ν_{max} /cm^{-1} 3057, 2161, 1588, 1330, 1249, 1147, 1082, 837, 809, 760; δ_H (400 MHz, CDCl$_3$) 7.82 (2H, d, *J* 8.6, Ar*H2'*), 7.65 (2H, d, *J* 8.6, Ar*H3'*), 7.21 (1H, d, *J* 15.7, SO$_2$C*H*), 6.55 (1H, d, *J* 15.6, *H*CCN), 0.26 (9H, s, TMS); δ_C (101 MHz, CDCl$_3$) 148.8, 136.4, 133.2, 130.6, 128.5, 113.4, 111.1, 102.5, 101.0, -0.2; *m/z* (CI) 307 [MNH$_4$]$^+$; found [MNH$_4$]$^+$ 307.0945 C$_{14}$H$_{19}$N$_2$O$_2$SSi requires 307.0937, Δ 2.6 ppm.

Method Two: *Addition of lithium sulfinate salt* **212** *to 2-chloropropenenitrile*
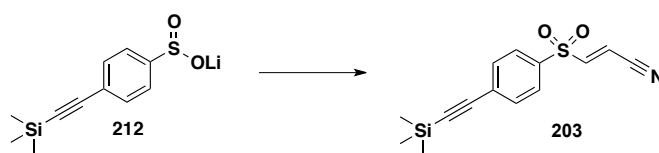
To a solution of sulfinate salt **212** (213.0 mg, 0.51 mmol, 1.0 eq.) in H_2O (0.75 mL) and acetic acid (0.75 mL) was added 2-chloropropenenitrile (41.1 μL, 0.51 mmol, 1.0 eq.) and MeOH (0.75 mL) and the yellow solution stirred at rt for 15 min, warmed to 100 °C for 15 min and allowed to cool to rt. The resulting precipitate was collected by filtration to yield the 3-sulfonyl acrylonitrile **203** (17.6 mg, 16 %) as an off-white powder. Data in agreement with that reported above.

2-Fluoro-4-[(trimethylsilyl)ethynyl]benzonitrile **205**
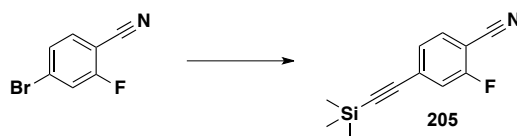
An adaption of a literature procedure was used.[260] A flame dried 2-neck flask was charged with 4-bromo-2-fluorobenzonitrile (110.0 mg, 0.55 mmol, 1.0 eq.), PdCl$_2$(PPh$_3$)$_2$ (20 mg, 0.03 mmol, 5 mol %) and CuI (13 mg, 0.07 mmol, 12.5 mol %) and subjected to 10 successive vacuum-argon cycles. Anhydrous THF (2 mL), sparged with argon was added to the mixture under argon, followed by TMS acetylene (0.16 mL, 1.10 mmol, 2.0 eq.) and anhydrous, sparged Et$_3$N (2.5 mL). Upon addition of the Et$_3$N, the reaction mixture turned rapidly from orange to black to

indicate the generation of Pd(0). The black reaction mixture was stirred at rt for 24 h and filtered through celite to remove the catalyst. The solvent was removed *in vacuo* and the black residue diluted with EtOAc and washed with brine (x 1), 10 % NH$_4$Cl (x 1), brine (x 1), dried over MgSO$_4$, filtered and the solvent removed *in vacuo*. The crude residue was purified on silica (EtOAc/n-hex, 1:19) and the resulting mixture of product and TMS-acetylene dimer separated on silica (gradient elution 100 % n-hex to 100 % EtOAc) to yield the desired TMS-acetylene **205** (85.5 mg, 72 %) as a brown solid, mp = 110-112 °C; R$_f$ = 0.57 (EtOAc/n-hex, 1:19); ν$_{max}$ /cm^{-1} 2242, 1615, 1557, 1493, 1411, 1247, 1159, 1113, 959, 840, 764, 726, 707; δ$_H$ (400 MHz, CDCl$_3$) 7.56-7.52 (1H, m, Ar*H*), 7.32-7.25 (2H, m, Ar*H*), 0.25 (9H, s, Si*Me$_3$*); δ$_C$ (101 MHz, CDCl$_3$) 164.0, 161.5, 133.3, 130.5, 130.4, 128.4, 128.4, 119.7, 119.5, 113.7, 101.8, 101.8, 101.4, 101.3, 101.3, 0.27; *m/z* (CI) 235 [MNH$_4$]$^+$; found [MNH$_4$]$^+$ 235.1075 C$_{12}$H$_{16}$N$_2$SiF requires 235.1067, Δ 3.4 ppm. Data in agreement with literature values.[260]

Racemic trans-N,N'-dimethyl-1,2-cyclohexanediamine **207**
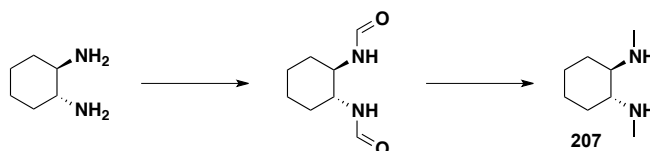
The method of Klapars *et al*. was used with small modifications.[261] Racemic *trans*-1,2-cyclohexanediamine (5 mL, 41.6 mmol, 1.0 equiv.) in ethyl formate (20 mL, 250 mmol) was heated at 50 °C for 6 h. The resulting thick white suspension was allowed to warm to rt and filtered. The filter cake was washed with EtOAc (30 mL) and the solid was dried under high vacuum to yield the *trans-N,N'*-diformyl-1,2-cyclohexanediamine (4.91 g, 70 %) as a white powder which was carried directly on to the next step.

A flame dried 2-neck flask was charged with t*rans-N,N'*-diformyl-1,2-cyclohexanediamine (3.02 g, 17.7 mmol, 1.0 equiv.), fitted with a reflux condenser and purged with argon. Anhydrous THF (20 mL) was added and the resulting suspension cooled to 0 °C. A 1.0 M solution of LiAlH$_4$ in THF (Aldrich Sure/Seal, freshly purchased, 60 mL, 60 mmol) was added dropwise and the slightly cloudy reaction mixture heated at 65 °C for 24 h under argon. The resulting thick white suspension was cooled to 0 °C and carefully quenched by dropwise addition of H$_2$O (2 mL) followed by 20 % aqueous NaOH solution (20 mL). The resulting suspension was stirred at rt for 1 h and filtered through celite eluting with THF (100 mL). The solvent was removed from the filtrate and the residue acidifed with 10 % HCl (30 mL) in water (50 mL) and extracted with CH$_2$Cl$_2$ (3 x 100 mL). The aqueous phase was then basified with 20 % aqueous NaOH (30 mL) and extracted with CH$_2$Cl$_2$ (3 x 50 mL). The organics from the basic extraction were combined, dried over Na$_2$SO$_4$, filtered and concentrated *in vacuo* to give the desired 1,2-*trans* diamine **207** (1.92 g, 76 %) as a clear oil. δ$_H$ (400 MHz, CDCl$_3$) 2.35 (6H, s, C*H$_3$*), 2.08-2.04 (2H, m, C*H*(NHMe)), 2.00-1.93 (2H, m, C*H$_2$*), 1.72-1.63 (2H, m, C*H$_2$*), 1.55 (2H, bs, N*H*), 1.24-1.12 (2H, m, C*H$_2$*), 0.95-0.86 (2H, m, C*H$_2$*); δ$_C$ (101 MHz, CDCl$_3$) 63.5, 33.9, 31.1, 25.2; *m/z* (ESI) 143 [MH]$^+$; found [MH]$^+$ 143.1539 C$_8$H$_{19}$N$_2$ requires 143.1548, Δ 6.3 ppm.

(4-Bromophenylethynyl)trimethylsilane **211**
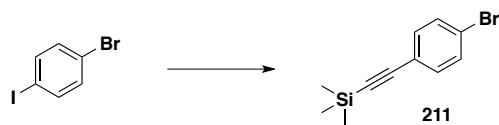
A flame-dried 2-neck flask was charged with 1-bromo-4-iodobenzene (283 mg, 1 mmol, 1 eq.), Pd(PPh$_3$)$_2$Cl$_2$ (35.1 mg, 0.05 mmol, 5 mol %) and CuI (23.8 mg, 0.125 mmol, 12.5 mol%) and subjected to 10 x successive vacuum-argon cycles. Sparged anhydrous THF (4 mL), trimethylsilyl acetylene (0.16 mL, 1.1 eq., 1.1 mmol) and sparged anhydrous Et$_3$N (5 mL) were added *via* syringe to the flask under argon, and the reaction mixture stirred for 18 h under argon. The black slurry was filtered through celite and the solvent removed from the filtrate *in vacuo*. The brown residue was dissolved in EtOAc, washed with brine (x 1), 10 % NH$_4$Cl (x 2), brine (x 1), dried over MgSO$_4$, filtered and the solvent removed *in vacuo*. The crude brown solid was purified on silica (100 % n-hexane) to yield the desired acetylene **211** (243.8 mg, 96 %) as a white solid, mp = 58-59 °C. R$_f$ = 0.6 (100 % n-hexane); ν_{max} /cm^{-1} 2956, 2157, 1483, 1469, 1246, 1009, 840, 816, 755, 663; δ_H (400 MHz, CDCl$_3$) 7.43 (2H, d, *J* 8.5, Ar*H*), 7.32 (2H, d, *J* 8.5, Ar*H*), 0.25 (9H, s, Si(C*H$_3$*)$_3$); δ_C (101 MHz, CDCl$_3$) 133.5, 131.6, 122.9, 122.2, 104.0, 95.7, 0.03; *m/z* (CI) 253 [MH]$^+$; found [MH]$^+$ 253.0034 C$_{11}$H$_{14}$BrSi requires 253.0048, Δ 5.5 ppm. Data in agreement with literature values.[303]

4-Trimethylsilanylethynylbenzenesulfinic acid lithium salt **212**
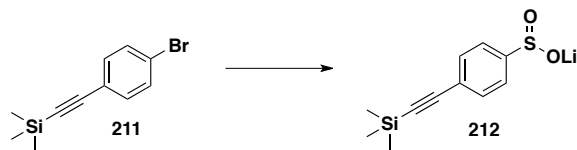
To a colourless solution of 4-bromoarene **211** (1.00 g, 3.9 mmol, 1.0 eq.) in anhydrous THF (50 mL) under argon at -80 °C was added nBuLi (2.5 M in hexanes) (1.7 mL, 4.3 mmol, 1.1 eq.) dropwise and the light yellow solution stirred at -80 °C for 15 min. Gaseous SO$_2$ was bubbled through the reaction mixture for 20 min using the reaction setup indicated in Figure 118, generating a black solution which lightened to yellow after 5 min. The light yellow solution was allowed to warm to rt and the solvent removed *in vacuo*. To the bright yellow residue was added n-hexane and the precipitate collected by filtration. The filter cake was washed thoroughly with n-hexane to generate the desired lithium sulfinate salt **212** (573.2 mg, 59 % sulfinate using 1,3,5-trimethoxybenzene as an internal ^{1}H NMR standard, 35 % yield), as a bright yellow powder, mp > 245 °C. ν_{max} /cm^{-1} 3351 (b), 2158, 1643, 1248, 967, 946, 834, 757; δ_H (400 MHz, DMSO-d$_6$) 7.45 (2H, d, *J* 8.1, Ar*H*), 7.39 (2H, d, *J* 8.1, Ar*H*), 0.22 (9H, s, TMS); δ_C (101 MHz, DMSO-d$_6$) 160.9, 131.0, 124.7, 121.1, 105.7, 93.7, 0.0; *m/z* (EI) 237 [M]$^-$; found [M]$^-$ 237.0389 C$_{11}$H$_{13}$O$_2$SSi requires 237.0406, Δ 7.2 ppm.
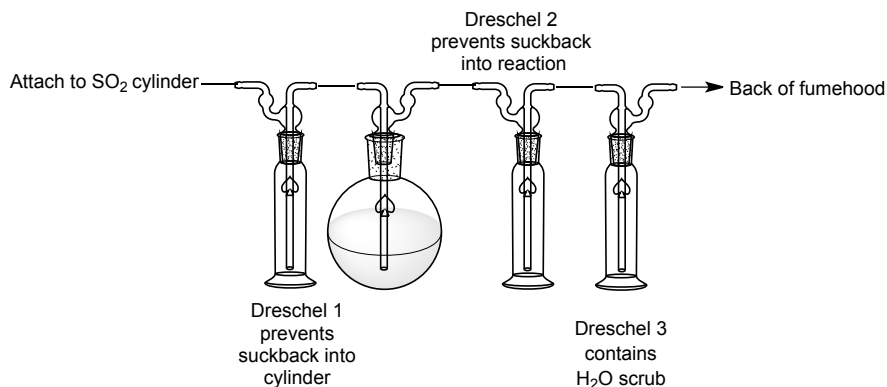
Figure 118

3-(4-Bromobenzenesulfonyl)propionitrile **213**

To a suspension of 4-bromophenylsulfinate salt **202** (1.83 g, 5.3 mmol, 1.0 eq.) in H_2O (6 mL) was added acrylonitrile (0.73 mL, 10.6 mmol, 2 eq.) and acetic acid (0.6 mL, 10.6 mmol, 2 eq.). The reaction was stirred rapidly for 1.5 h at 100 °C and subsequently cooled to rt. The resultant precipitate was filtered, washed thoroughly with H_2O and dried under high vacuum to yield the desired nitrile **213** (1.29 g, 87 %) as a white solid, mp = 113-114 °C; R_f = 0.29 (EtOAc/n-hex, 2:3); ν_{max} /cm^{-1} 2248 (CN), 1576, 1466, 1408, 1386, 1317, 1260, 1137, 1080, 1067, 1007, 821, 744, 743; δ_H (400 MHz, CDCl$_3$) 7.79 (2H, d, *J* 8.8, Ph), 7.76 (2H, d, *J* 8.8, Ph), 3.38 (2H, t, *J* 7.5, SO$_2$C*H$_2$*), 2.82 (2H, t, *J* 7.5, C*H$_2$*CN); δ_C (101 MHz, CDCl$_3$) 136.7, 133.3, 130.4, 129.9, 116.0, 51.2, 12.0; *m/z* (CI) 291 [MNH$_4$(^{79}Br)]$^+$, 293 [MNH$_4$(^{81}Br)]$^+$; found [MNH$_4$(^{79}Br)]$^+$, 290.9802 C$_9$H$_{12}$N$_2$O$_2$S^{79}Br requires 290.9803, Δ 0.3 ppm.

3-(4-Trimethylsilanylethynyl benzenesulfonyl)propionitrile **214**
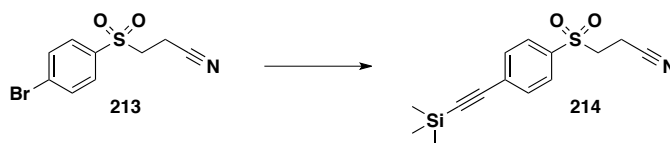
A flame-dried, 2-neck flask was charged with sulfonyl-nitrile **213** (200 mg, 0.73 mmol, 1 eq.), Pd(PPh$_3$)$_2$Cl$_2$ (26 mg, 0.04 mmol, 5 mol%) and CuI (17 mg, 0.09 mmol, 12.5 mol%) and subjected to 10 x vacuum-argon cycles. Argon-sparged THF (2.6 mL), TMS-acetylene (0.11 mL, 0.80 mmol, 1.1 eq.) and Et$_3$N (3.3 mL) were added and the mixture heated to 40 °C for 24 h. The reaction mixture was allowed to cool to rt, filtered through celite and the solvent removed from the filtrate *in vacuo*. The crude brown residue was purified on silica (n-hex/EtOAc, 7:3) to yield the desired acetylene **214** (140.2 mg, 66 %) as an off-white solid, mp = 99-102 °C; R_f = 0.48 (EtOAc/n-hex, 2:3); ν_{max} /cm^{-1} 2259, 2158, 1592, 1315, 1298, 1282, 1249, 1168, 1134, 1087, 842, 759, 742; δ_H (400 MHz, CDCl$_3$) 7.85 (2H, d, *J* 8.4, Ar*H*2'), 7.66 (2H, d, *J* 8.4, Ar*H*3'), 3.38 (2H, t, *J* 7.6, SO$_2$C*H$_2$*), 2.81 (2H, t, *J* 7.6, C*H$_2$*CN), 0.26 (9H, s,

Si(CH_3)$_3$); δ_C (101 MHz, CDCl$_3$) 136.8, 133.1, 130.2, 128.3, 116.0, 102.6, 100.5, 51.2, 12.0, -0.2; *m/z* (CI) 291 [MH]$^+$, 309 [MNH$_4$]$^+$; found [MNH$_4$]$^+$ 309.1095 C$_{14}$H$_{21}$N$_2$O$_2$SiS requires 309.1093, Δ 0.6 ppm.

2-iodoxybenzoic acid 215 and *1-hydroxy-1,2-benziodoxol-3(1H)-one 216*

215 - IBX   **216 - IBA**
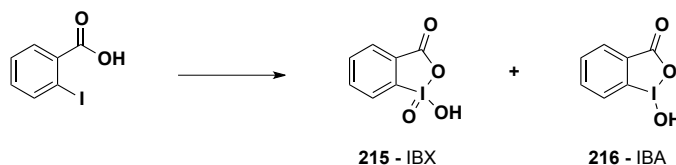
A procedure reported by Santagostino *et al*. was used.[268] 2-iodobenzoic acid (5.0 g, 20 mmol, 1 eq.) was added to a solution of oxone (37.2 g, 61 mmol, 3 eq.) in distilled H$_2$O (200 mL) and the mixture heated to 70 °C for 3 h. The cloudy suspension was cooled to 0 °C for 30 min and the fine precipitate filtered. The filter cake washed with water (x 6) and acetone (x 2) and the solid dried under high vacuum to yield 2-iodoxybenzoic acid **215** (4.24 g, 76 %) as a fine white powder. The filtrate was left at rt for 12 h to allow the crystallisation of a solid which was filtered, washed with H$_2$O (x 6) and acetone (x 2) and dried under high vacuum to yield 1-hydroxy-1,2-benziodoxol-3(1H)-one **216** (434.4 mg, 8 %) as long fine white needles.

2-iodoxybenzoic acid 215

ν_{max} /cm^{-1} 1633, 1331, 1295, 774, 749; δ_H (400 MHz, DMSO-d$_6$) 8.14 (1H, d, *J* 7.9, Ar*H*), 8.04-7.98 (2H, m, Ar*H*), 7.84 (1H, t, *J* 7.3, Ar*H*), 3.43 (1H, bs, O*H*); δ_C (101 MHz, DMSO-d$_6$) 167.5, 146.6, 133.4, 133.0, 131.5, 130.1, 125.0. Data in agreement with literature values.[304]

1-hydroxy-1,2-benziodoxol-3(1H)-one 216

ν_{max} /cm^{-1} 1585, 1556, 1439, 1337, 1300, 1148, 819, 737, 693; δ_H (400 MHz, DMSO-d$_6$) 8.04 (1H, bs, O*H*), 8.01 (1H, dd, *J* 7.5, *J* 1.2, Ar*H*), 7.96 (1H, td, *J* 7.6, *J* 1.4, Ar*H*), 7.84 (1H, d, *J* 7.9, Ar*H*), 7.7 (1H, td, *J* 7.3, *J* 0.6, Ar*H*); *m/z* (CI) 264 [MH]$^+$; found [MH]$^+$ 264.9341 C$_7$H$_6$O$_3$I requires 264.9362, Δ 7.9 ppm. Data in agreement with literature values.[305]

Trimethyl-(4-phenylselanylphenylethynyl)silane 217
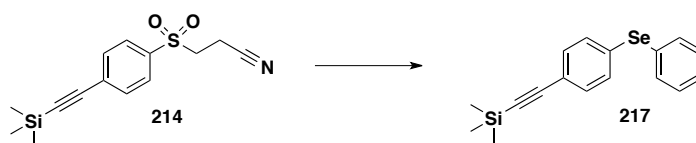
nBuLi (2.5 M in hexane, 0.13 mL, 0.33 mmol, 0.95 eq.) was added dropwise to a stirred solution of diisopropylamine (47.7 µL, 0.34 mmol, 1.0 eq.) in dry THF (3 mL) at -78 °C and the colourless solution stirred at -78 °C for 45 min. A solution of sulfonylnitrile **214** (100 mg, 0.34 mmol, 1.0 eq.) in THF (1 mL) was added dropwise and the brown solution stirred at -78 °C for 1 hour. A solution of PhSeCl (52.1 mg, 0.27 mmol, 0.8 eq.) in THF (1 mL) was added rapidly in one portion, leading to evolution of a white gas. The resulting yellow solution was stirred at -78 °C for 1.5 h

and the mixture quenched with 1 M HCl (0.23 mL), warmed to rt and stirred for 15 min. Water (5.7 mL) was added and the reaction extracted with EtOAc (x 3). The organics were combined, dried over MgSO$_4$, filtered and the solvent removed *in vacuo*. The crude residue was purified on silica (1:9, EtOAc/n-hex) to yield selenide **218** (14.7 mg, 17 %) as an off-white solid. R$_f$ = 0.65 (7:3 n-hex/EtOAc); δ$_H$ (400 MHz, CDCl$_3$) 7.51-7.33 (9H, m, Ar*H*), 0.26 (9H, s, Si(C*H$_3$*)$_3$); δ$_C$ (101 MHz, CDCl$_3$) 144.5, 137.4, 132.2, 131.2, 129.8, 128.7, 127.9, 127.0, 103.1, 99.5, -0.12; *m/z* (EI) 330 [M(^{80}Se)]$^+$, 328 [M(^{78}Se)]$^+$, 314 [M-CH$_4$(^{80}Se)]$^+$, 312 [M-(^{78}Se)]$^+$, 157 [SePh(^{80}Se)]$^+$, 155 [SePh(^{78}Se)]$^+$.

(±)-3-Phenylselanyl-3-(4-trimethylsilanylethynylbenzenesulfonyl)propionitrile **218**
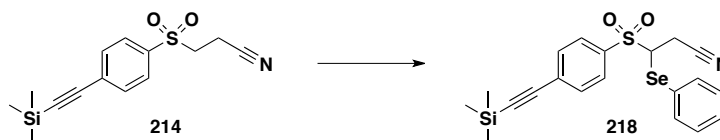
To a solution of N-(phenylseleno)phthalimide (443 mg, 1.47 mmol, 1 eq.) in anhydrous CH$_2$Cl$_2$ (6 mL) under argon at – 78 °C was added LiHMDS (1.0 M in THF, SigmaAldrich SureSeal) (1.47 mL, 1.47 mmol, 1 eq.) and sulfone **214** (427 mg, 1.47 mmol, 1 eq.) as a solution in anhydrous CH$_2$Cl$_2$ (6 mL) and the thick yellow precipitate stirred at -78 °C for 30 min and then removed from the cold bath and allowed to warm to rt. Stirrring was continued at rt for 15 min before addition of H$_2$O and extraction with CH$_2$Cl$_2$ (x 2). Combined organics were dried over Na$_2$SO$_4$, filtered and the solvent removed *in vacuo*. The crude residue was purified on silica (gradient elution, 9:1 to 4:1, n-hex/EtOAc) to yield the desired selenide **218** (143.9 mg, 22 %) as a yellow oil. R$_f$ = 0.36 (4:1, n-hex/EtOAc); ν$_{max}$ /cm^{-1} 2960, 2165, 1590, 1317, 1148, 862, 844; δ$_H$ (400 MHz, CDCl$_3$) 7.88 (2H, d, *J* 8.6, SO$_2$Ar*H2'*), 7.65 (2H, d, *J* 8.6, SO$_2$Ar*H3'*), 7.54 (2H, dd, *J* 8.1, *J* 1.1, SePh*H2'*), 7.41 (1H, tt, *J* 7.5, *J* 1.1, SePh*H4'*), 7.32-7.28 (2H, m, SePh*H3'*), 4.21 (1H, dd, *J* 10.9, *J* 4.0, C*H$_2$*CN), 3.36 (1H, dd, *J* 17.2, *J* 4.0, C*H$_2$*CN), 2.90 (1H, dd, *J* 17.2, *J* 10.9, SO$_2$C*H*(SePh)), 0.30 (9H, s, TMS); δ$_C$ (101 MHz, CDCl$_3$) 136.6, 135.1, 132.7, 130.2, 130.1, 129.8, 129.7, 125.6, 115.7, 102.7, 100.6, 60.9, 20.0, -0.15; *m/z* (EI) 447 [M(^{80}Se)]$^+$, 445 [M(^{78}Se)]$^+$, 432 [M(^{80}Se)-CH$_3$]$^+$, 430 [M(^{78}Se)-CH$_3$]$^+$, 378 [M(^{80}Se)-(2(CH$_3$)+CH$_2$CN)], 376 [M(^{78}Se)-(2(CH$_3$)+CH$_2$CN)], 210 [M(^{80}Se)-(SO$_2$Ar)]$^+$, 208 [M(^{78}Se)-(SO$_2$Ar)]$^+$; found [M(^{80}Se)]$^+$ 447.0236 C$_{20}$H$_{21}$NO$_2$SSi^{80}Se requires 447.0227, Δ 2.0 ppm.

Cis-3-phenylselanyl acrylonitrile **219** and *Trans-3-phenylselanyl acrylonitrile* **220**
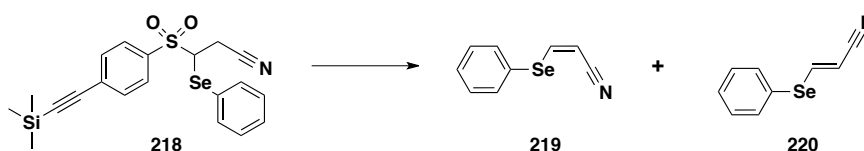
Selenide **218** (18.0 mg, 0.04 mmol, 1 eq.) was stirred at rt with K$_2$CO$_3$ (5.6 mg, 0.04 mmol, 1 eq.) in MeOH (1 mL) for 1 h. The solvent was removed *in vacuo* and the yellow residue redissolved in CH$_2$Cl$_2$, washed with brine (x 2), dried over Na$_2$SO$_4$, filtered and the solvent removed *in vacuo*. The crude residue (9.3 mg) was purified on silica (n-hex/EtOAc, 9:1) to yield the *cis* olefin **219** (1.2 mg, 14 %) as a clear oil and the *trans* olefin **220** (0.9 mg, 11 %) as a clear oil.

Cis-3-phenylselanyl acrylonitrile **219**
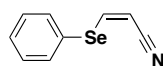
219

R_f = 0.20 (n-hex/EtOAc, 9:1); ν_{max} /cm^{-1} 2923, 2212, 1553, 1477, 1439, 1316, 1022, 741, 688; δ_H (400 MHz, CDCl$_3$) 7.70 (1H, d, *J* 10.4, PhSeC*H*), 7.59-7.57 (2H, m, Ph), 7.40-7.35 (3H, m, Ph), 5.82 (1H, d, *J* 10.4, *H*CCN); *m/z* (EI) 209 [M(^{80}Se)]$^+$, 207 [M(^{78}Se)]$^+$, 182 [M(^{80}Se)-HCN]$^+$, 180 [M(^{78}Se)-HCN]$^+$, 157 [Ph^{80}Se]$^+$, 155 [Ph^{78}Se]$^+$, 77 [Ph]$^+$; found [M(^{80}Se)]$^+$ 208.9754 C$_9$H$_7$NSe requires 208.9744, Δ 4.8 ppm.

Trans-3-phenylselanyl acrylonitrile **220**
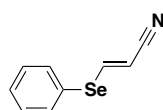
220

R_f = 0.29 (n-hex:EtOAc, 9:1); ν_{max} /cm^{-1} 2214, 1565, 738; δ_H (400 MHz, CDCl$_3$) 7.89 (1H, d, *J* 16.1, PhSeC*H*), 7.58-7.56 (2H, m, Ph), 7.46-7.7.40 (3H, m, Ph), 5.22 (1H, d, *J* 16.1, *H*CCN); *m/z* (EI) 209 [M(^{80}Se)]$^+$, 207 [M(^{78}Se)]$^+$, 182 [M(^{80}Se)-HCN]$^+$, 180 [M(^{78}Se)-HCN]$^+$, 157 [Ph^{80}Se]$^+$, 155 [Ph^{78}Se]$^+$, 77 [Ph]$^+$; found [M(^{80}Se)]$^+$ 208.9757 C$_9$H$_7$NSe requires 208.9744, Δ 6.2 ppm.

3-(4-Ethynylbenzenesulfonyl)propionitrile **221**

To a solution of sulfone **214** (23.1 mg, 0.08 mmol, 1 eq.) in THF (1 mL) at 0 °C was added TBAF (1.0 M solution in THF, 0.08 mL, 0.08 mmol, 1 eq.) dropwise and the reaction stirred at 0 °C for 5 min. The reaction mixture was diluted with EtOAc and washed with H$_2$O (x 1). The aqueous layer was further extracted with EtOAc (x 1) and the combined organics dried over MgSO$_4$, filtered and the solvent removed *in vacuo*. The crude residue was purified on silica (100 % EtOAc) to yield the desired terminal acetylene **221** (9.7 mg, 55 %) as an off-white solid, mp = 121-124 °C. R_f = 0.28 (n-hexane/EtOAc, 7:3); ν_{max} /cm^{-1} 3257, 2932, 2113, 1593, 1313, 1290, 1278, 1135, 1081, 954, 839, 730, 701; δ_H (400 MHz, CDCl$_3$) 7.89 (2H, d, *J* 8.4, Ar*H2'*), 7.71 (2H, d, *J* 8.4, Ar*H3'*), 3.39 (2H, t, *J* 7.7, SO$_2$C*H*$_2$), 3.34 (1H, s, acetylene-*H*), 2.83 (2H, t, *J* 7.7, C*H*$_2$CN); δ_C (101 MHz, CDCl$_3$) 137.4, 133.4, 129.2, 128.4, 115.9, 82.3, 81.6, 51.3, 12.1; *m/z* (EI) 219 [M]$^+$; found [M]$^+$ 219.0344 C$_{11}$H$_9$NO$_2$S requires 219.0354, Δ 4.6 ppm.

10. Appendices

Appendix I HPLC irreversibility results

Separation of mercaptosuccinic acid adducts from the reacting acrylamides
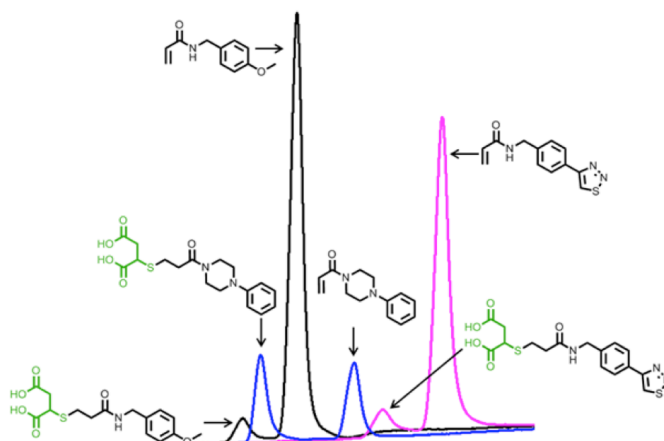
Figure 119 Conjugate addition of mercaptosuccinic acid to acrylamides gave products which were easily separable by HPLC.

Acrylamide irreversibility at pH 8
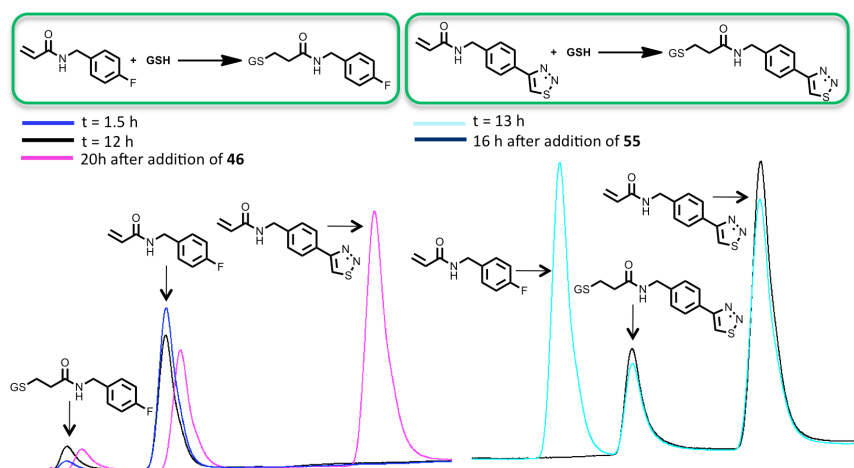
Figure 120 (Left hand side) Black and blue traces show formation of a conjugate addition product over 12 h by addition of GSH to acrylamide **55**. 20 h after addition of a second acrylamide **46**, no formation of a second conjugate addition product was observed, pink trace. **(Right hand side)** Black trace shows the formation of a conjugate addition product by addition of GSH to acrylamide **46** after 13 h. 16h after addition of a second acrylamide **55** no formation of a second conjugate addition product was onbserved, cyan coloured trace.
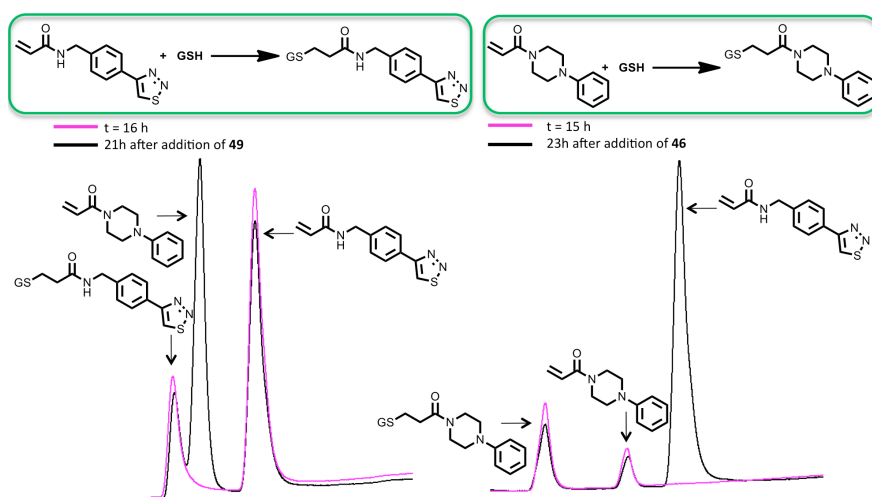
Figure 121 (Left hand side) Pink traces show formation of a conjugate addition product over 16 h by addition of GSH to acrylamide **46**. 21 h after addition of a second acrylamide **49**, there was no observed formation of a second conjugate addition product, black trace. **(Right hand side)** Pink trace shows the formation of a conjugate addition product by addition of GSH to acrylamide **49** after 15 h. 16 h after addition of a second acrylamide **46**, there was still no formation of a second conjugate addition product, black trace.

Acrylamide irreversibility pH 11
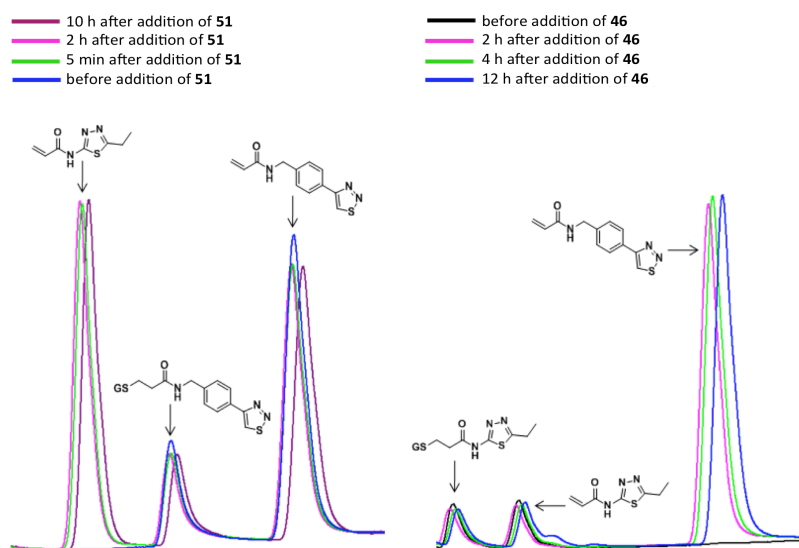
Figure 122 (Left hand side) Blue trace shows the formation of a conjugate addition product on addition of GSH to acrylamide **46**. On addition of a second acrylamide **51**, to this mixture no second conjugate addition product is formed as measured over a 10 h time course. **(Right hand side)** The same experiment was carried out in the reverse manner. Again, no second conjugate addition product was formed over a 12 h period.
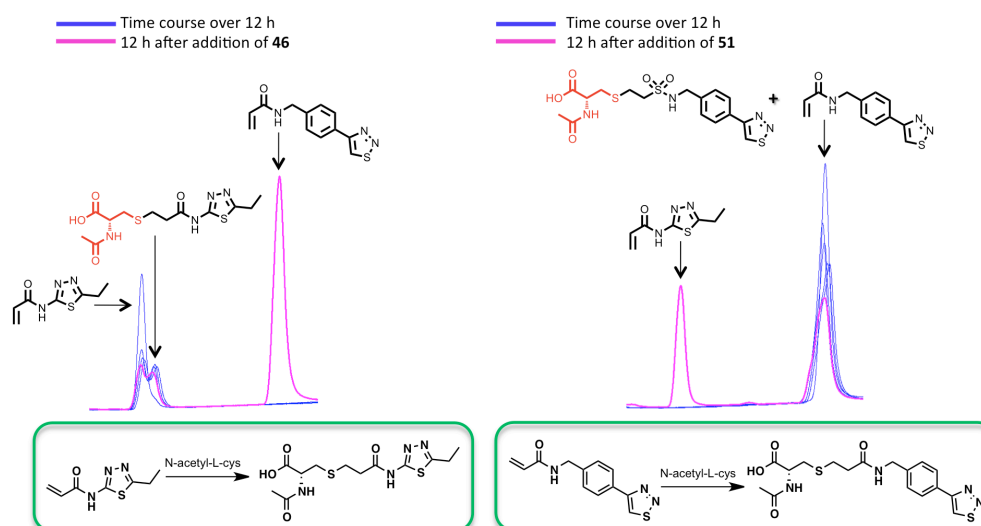
Figure 123 (Left hand side) The blue traces show a time course over 12 h for the addition of *N*-acetyl L-cysteine to acrylamide **51**. 12 h after the addition of a second acrylamide **46**, no formation of a second conjugate addition product was observed, pink trace. **(Right hand side)** Blue traces show a time course over 12 h for the addition of *N*-acetyl L-cysteine to acrylamide **46**. 12 h after the addition of the second conjugate addition product **51**, no formation of a second conjugate addition product was observed, pink trace.

Vinyl sulfonamide irreversibility at pH 11
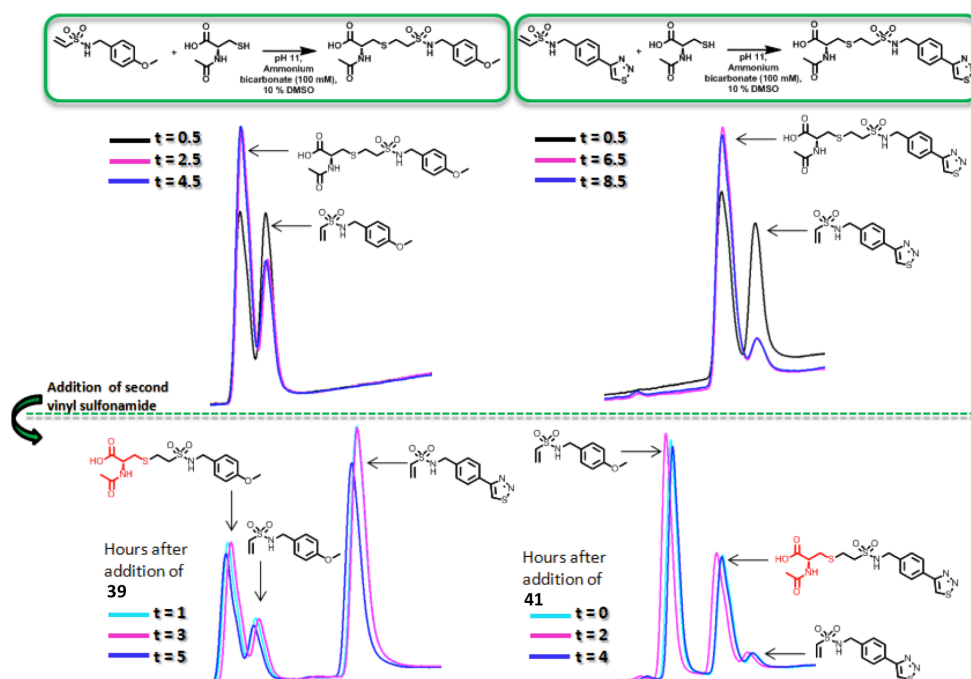
Figure 124 (Top left) Overlay of HPLC traces for addition of **41** to *N*-acetyl L-cysteine. **(Top right)** Overlay of HPLC traces for addition of vinyl sulfonamide **39** to *N*-acetyl L-cysteine. **(Bottom left)** Overlay of HPLC traces after addition of sulfonamide **39** to the mixture of sulfonamide **41** and the **41**-cys conjugate addition product. Irreversibility confirmed by the absence of a further peak due to conjugate addition to sulfonamide **39**. **(Bottom right)** Overlay of HPLC traces after addition of sulfonamide **41** to the mixture of sulfonamide **39** and the **39**-cys conjugate addition product. Irreversibility confirmed by the absence of a further peak due to conjugate addition to sulfonamide **41**.
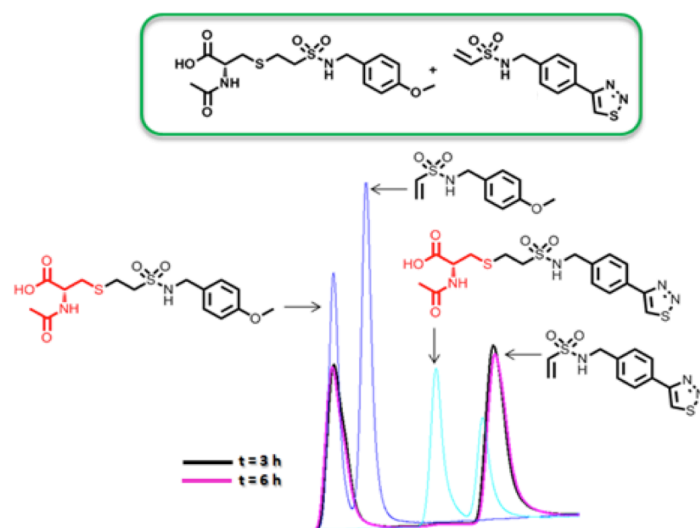
Figure 125 Overlay of 4 different HPLC traces. Dark and light blue traces are to assign the peaks to the different compounds. Black and pink traces show a time course for addition of vinyl sulfonamide **39** to conjugate addition product **59** (pH 11) at 3 and 6 hours respectively.

Appendix II cdc25 MALDI

Mass	Peptide	
700.85	EFFMK	
704.87	FANLIK	
819.91	LGNEYPK	
923.03	GSLIGDFSK	
954.13	KPIVPTDGK	
994.17	EFVIIDCR	● (blue)
1092.26	GYLFHTVAGK	● (yellow)
1254.46	MASMTGGQQMGR	
1274.53	LHYPELYVLK	● (black)
1295.43	CPYEYEGGHIK	● (green)
1521.79	YISPEIMASVLNGK	● (red)
1535.72	VIVVFHSEFSSER	● (purple)
1973.23	GAVNLHMEEEVEDFLLK	● (cyan)
2338.55	SQSYCEPPSYRPMHHEDFK	● (orange)
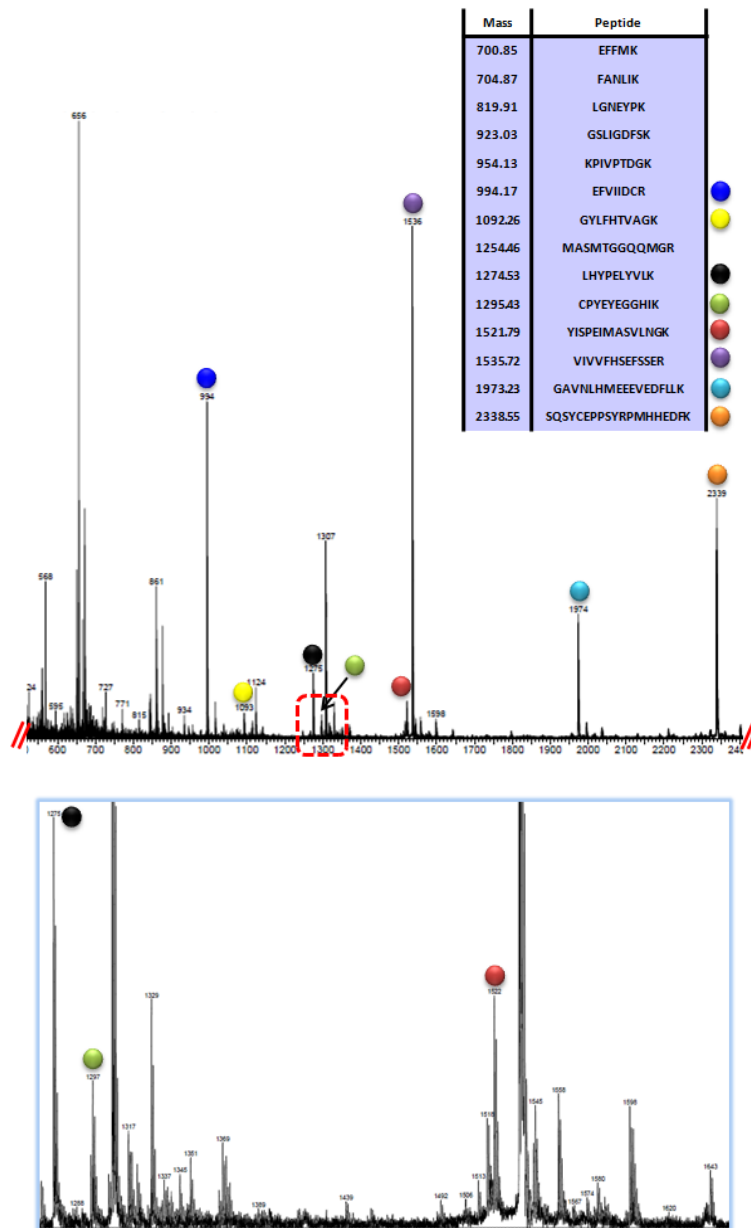
 Figure 126 MALDI MS analysis of the crude peptide mixture resulting from cdc25A trypsin digestion. **(Top)** Spectrum from 500-2400 Da. (Bottom) Zoom of region highlighted within the red dotted line on the top spectrum. Coloured spheres represent the presence of the indicated peptide.

Appendix III Mass spectrometry results

TS with positive control 67 and acrylamide 47 at equimolar concentrations (400 μM)

Sample recipe: 24 μL thymidylate synthase (10 μM) in ammonium bicarbonate (10 mM) and DTT (1 mM) at pH 8, 1 μL ligand stock solution (positive control acrylamide **67** and acrylamide **47**, each at 10 mM) in methanol. Sample was allowed to react for 30 minutes at rt before addition of 0.5 % aq. formic acid (50 μL) and methanol (50 μL) and analysis by ESI mass spectrometry.
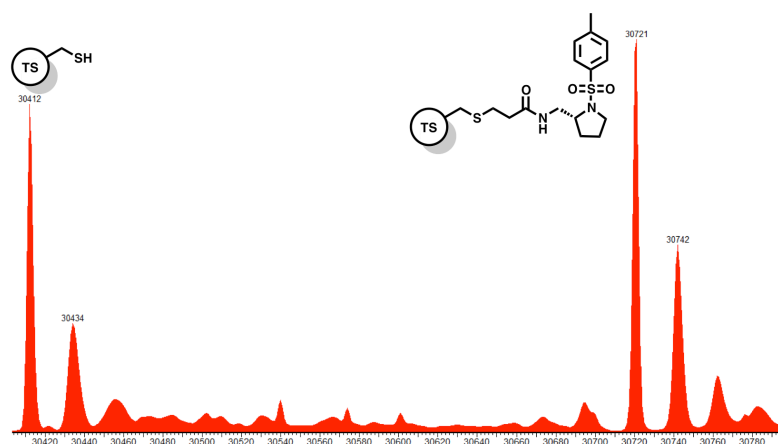
Figure 127 Deconvoluted mass spectrum for TS incubated with acrylamides **47** and **67** (both at 400 μM). An adduct to acrylamide **67** is observed to form as labelled on the spectrum. However, no peak is seen due to the formation of an adduct with acrylamide **47**.

TS with acrylamide 47 under more forcing conditions

Sample recipe: 24 μL thymidylate synthase (10 μM) in ammonium bicarbonate (10 mM), DTT (1 mM) at pH 8, 1 μL acrylamide **47** from 60 mM stock solution in methanol to give a final concentration of 2.4 mM. The sample was allowed to react for 4 hours at rt before addition of 0.5 % aq. formic acid (50 μL) and methanol (50 μL) and analysis by ESI mass spectrometry.
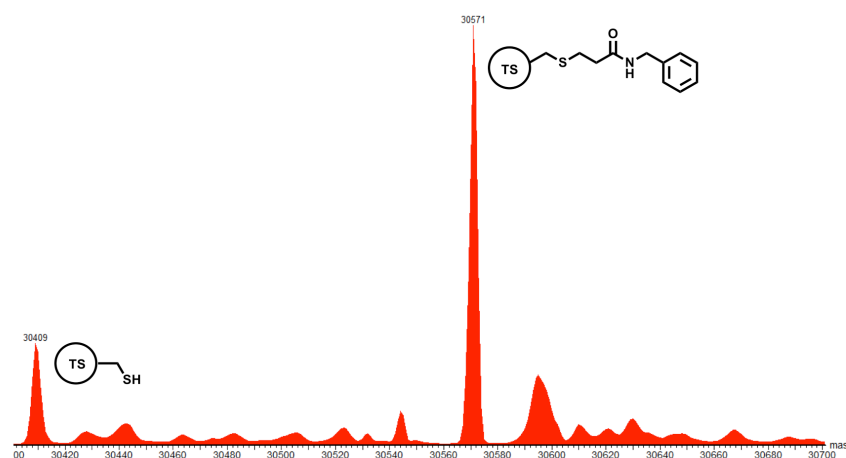
Figure 128 Formation of a TS-**47** adduct under more forcing conditions.

TS with bound sulfate ions

If TS is subjected to only a 6 h dialysis into ammonium bicarbonate from the TRIS-HCl/ammonium sulfate pellet, the sulfate ions are not removed, as observed by ESI-MS (see spectra below).
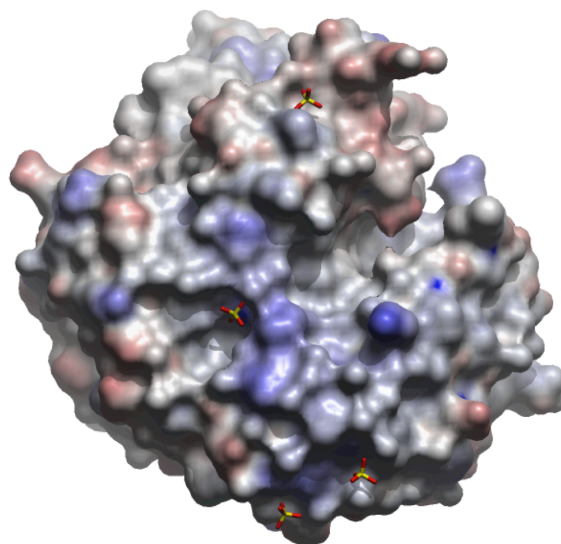
Figure 129 Crystal structure of TS (PDB code 1F4B) with bound sufate ions highlighted as sticks.

LCT21043 30 (0.495) M1 [Ev-528526,It54] (Gs,0.750,800:3000,1.00,L33,R33); Cm (2:115)   TOF MS ES+
1.06e5
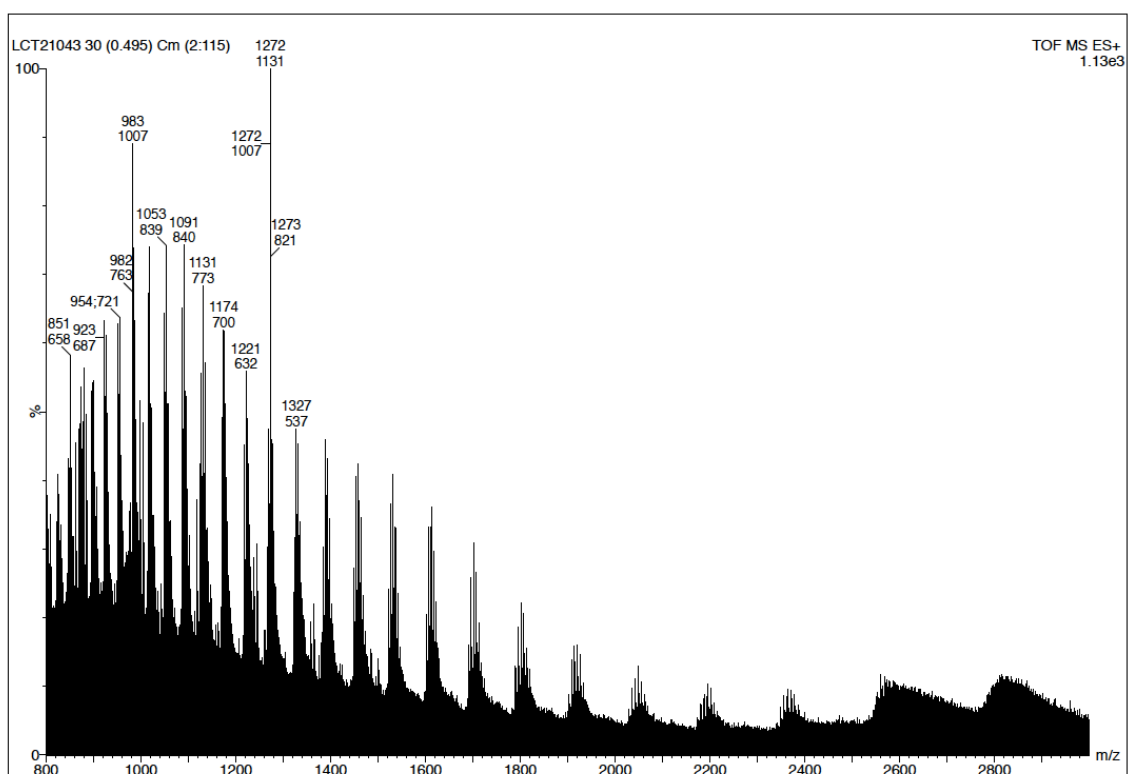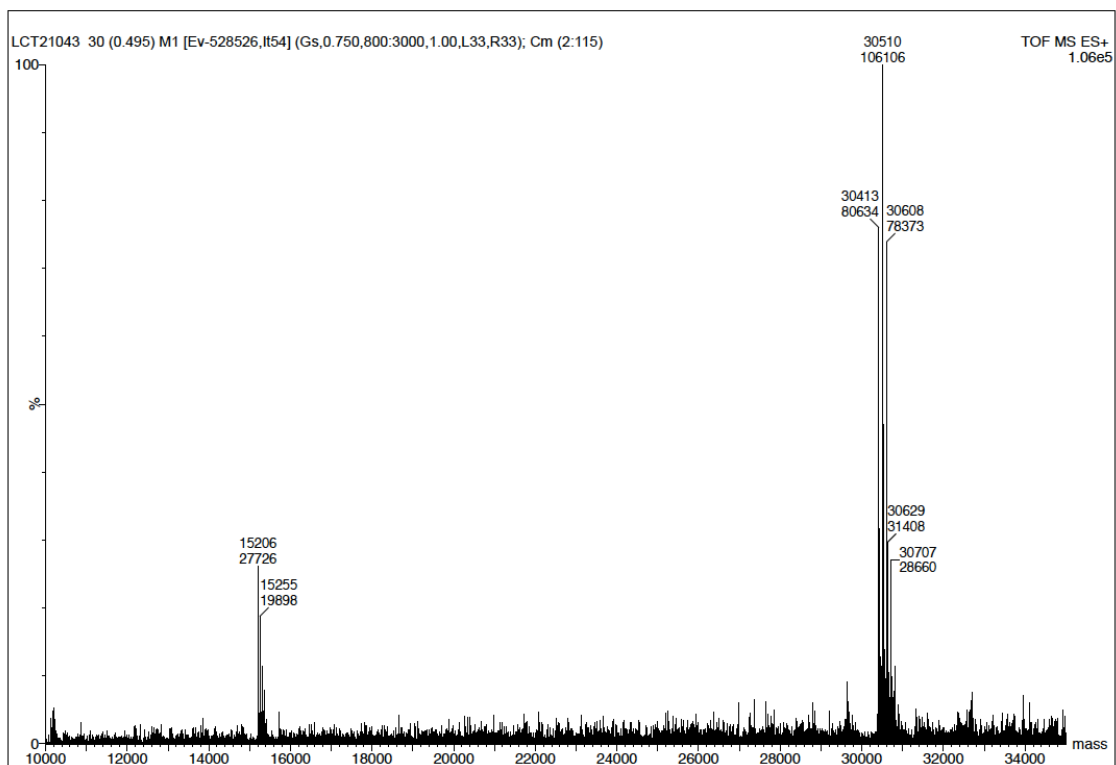
DTT concentration

Initial preparations of TS utilised DTT (5 mM) as a reducing agent to prevent oxidation of the active site cysteine thiol over time. However, it was unexpectedly found that over a one month period at 4 °C, TS formed an adduct with DTT as identified by ESI MS. Spectrophotometric analysis of the same sample of enzyme immediately after purification and after a one month period at 4 °C indicated that less of the enzyme was active, Figure 130. Li *et al*. reported the formation of a DTT adduct with a cysteine residue of adenylate kinase upon aging of the enzyme.[306] To prevent the significant formation of a DTT adduct, the concentration of DTT in the buffer was reduced to 1 mM. Under these conditions, purified TS was stable at 4 °C for 2 weeks, as observed by the spectrophotometric assay and ESI mass spectrometry.
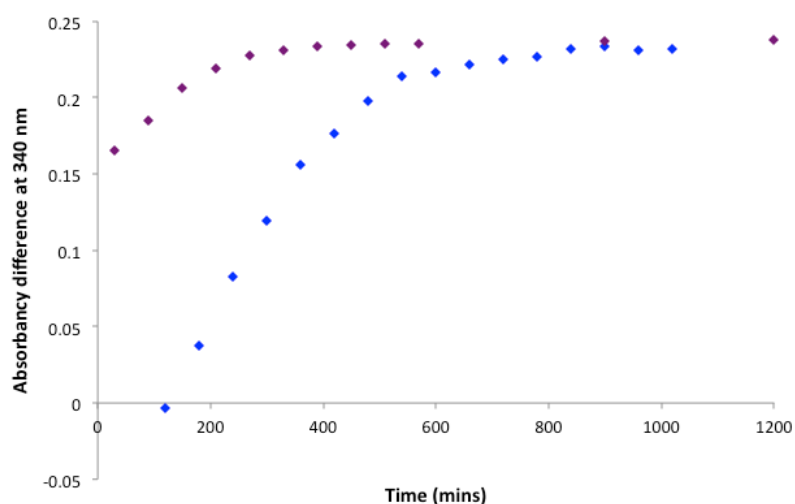
Figure 130 Spectrophotometric assay using the same enzyme sample immediately after purification (purple diamonds) and after 1 month at 4 °C (blue diamonds). Conditions for the assay: dUMP (48 μM), THF (167 μM), TS (8.0 nM), TRIS-HCl (40 mM), $MgCl_2$ (20 mM), βME (100 mM), formaldehyde (12 mM), EDTA (750 μM).

Appendix IV Plasmid sequences

1. pGEM-TS

…gacctgcaggcggccgcactagtgatt**catATG**AAACAGTATTTAGAACTGATGCAAAAAGTGCTCGACGAAGGCACA
CAGAAAAACGACCGTACCGGAACCGGAACGCTTTCCATTTTTGGTCATCAGATGCGTTTTAACCTGCAG
GATGGATTCCCGCTGGTGACAACTAAACGTTGCCACCTGCGTTCCATCATCCACGAACTGCTGTGGTTCC
TGCAGGGCGACACTAACATTGCTTATCTACACGAAAACAATGTCACCATCTGGGACGAATGGGCCGATG
AAAACGGCGACCTCGGGCCAGTGTATGGTAAACAGT**GGCGCGCC**TGGCCAACGCCAGATGGTCGTCAT
ATTGACCAGATCACTACGGTACTGAACCAGCTGAAAAACGACCCGGATTCGCGCCGCATTATTGTTTCA
GCGTGGAACGTAGGCGAACTGGATAAAATGGCGCTGGCACCGTGCCATGCATTCTTCCAGTTCTATGTG
GCAGACGGCAAACTCTCTTGCCAGCTTTATCAGCGCTCCTGTGACGTCTTCCTCGGCCTGCCGTTCAACA
TTGCCAGCTACGCGTTACTGGTG**CATATG**ATGGCGCAGCAGTGCGATCTGGAAGTGGGTGATTTTGTCT
GGACCGGTGGCGATACGCACCTGTACAGCAAT**CATATG**GATCAAACTCATCTGCAATTAAGCCGCGAA
CCGCGTCCGCTGCCGAAGTTGATTATCAAACGTAAACCCGAATCCATCTTCGACTACAGTTTCGAAGAC
TTTGAGATTGAAGGCTACGATCCGCATCCGGGCATTAAAGCGCCGGTGGCTATCT<u>TGA</u>attcaatcccgcggccatg
gcggccgggagcatgcgacgtcgggcccaattcgccc…

Figure 131 Text in capitals is coding, text in lower case is vector sequence. Underlined <u>ATG</u> and <u>TGA</u> represent the start and stop codons respectively. NdeI, AscI and EcoRI sites shown in red, blue and purple respectively.

2. pET21a-TS$_{NdeI}$

…aattcccctctagaaataattttgtttaactttaagaaggagatata**catATG**AAACAGTATTTAGAACTGATGCAAAAAGTGCTCGA
CGAAGGCACACAGAAAAACGACCGTACCGGAACCGGAACGCTTTCCATTTTTGGTCATCAGATGCGTTTT
TAACCTGCAGGATGGATTCCCGCTGGTGACAACTAAACGTTGCCACCTGCGTTCCATCATCCACGAACT
GCTGTGGTTCCTGCAGGGCGACACTAACATTGCTTATCTACACGAAAACAATGTCACCATCTGGGACGA
ATGGGCCGATGAAAACGGCGACCTCGGGCCAGTGTATGGTAAACAGT**GGCGCGCC**TGGCCAACGCCA
GATGGTCGTCATATTGACCAGATCACTACGGTACTGAACCAGCTGAAAAACGACCCGGATTCGCGCCGC
ATTATTGTTTCAGCGTGGAACGTAGGCGAACTGGATAAAATGGCGCTGGCACCGTGCCATGCATTCTTC
CAGTTCTATGTGGCAGACGGCAAACTCTCTTGCCAGCTTTATCAGCGCTCCTGTGACGTCTTCCTCGGCC
TGCCGTTCAACATTGCCAGCTACGCGTTACTGGTG**CATatg**gctagcatgactggtggacagcaaatgggtcgcggatcc**gaattc**g
agctccgtcgacaagcttgcggccgcactcgagcaccaccac…

Figure 132 Text in capitals is coding, text in lower case is vector sequence. Underlined <u>ATG</u> represents the start codon. NdeI, AscI and EcoRI sites shown in red, blue and purple respectively.

3. Plasmid pET21a-TS

…tctagaaataattttgtttaactttaagaaggagatata**cat**<u>**ATG**</u>AAACAGTATTTAGAACTGATGCAAAAAGTGCTCGACGAAG
GCACACAGAAAAACGACCGTACCGGAACCGGAACGCTTTCCATTTTTGGTCATCAGATGCGTTTTAACC
TGCAGGATGGATTCCCGCTGGTGACAACTAAACGTTGCCACCTGCGTTCCATCATCCACGAACTGCTGT
GGTTCCTGCAGGGCGACACTAACATTGCTTATCTACACGAAAACAATGTCACCATCTGGGACGAATGGG
CCGATGAAAACGGCGACCTCGGGCCAGTGTATGGTAAACAGT**GGCGCGCC**TGGCCAACGCCAGATGGT
CGTCATATTGACCAGATCACTACGGTACTGAACCAGCTGAAAAACGACCCGGATTCGCGCCGCATTATT
GTTTCAGCGTGGAACGTAGGCGAACTGGATAAAATGGCGCTGGCACCGTGCCATGCATTCTTCCAGTTC
TATGTGGCAGACGGCAAACTCTCTTGCCAGCTTTATCAGCGCTCCTGTGACGTCTTCCTCGGCCTGCCGT
TCAACATTGCCAGCTACGCGTTACTGGTG**CATATG**ATGGCGCAGCAGTGCGATCTGGAAGTGGGTGATT
TTGTCTGGACCGGTGGCGATACGCACCTGTACAGCAAT**CATATG**GATCAAACTCATCTGCAATTAAGCC
GCGAACCGCGTCCGCTGCCGAAGTTGATTATCAAACGTAAACCCGAATCCATCTTCGACTACAGTTTCG
AAGACTTTGAGATTGAAGGCTACGATCCGCATCCGGGCATTAAAGCGCCGGTGGCTATC<u>**TGA**</u>**attc**gagctcc
gtcgacaagcttgcggccgcactcgagcaccacca…

Figure 133 Text in capitals is coding, text in lower case is vector sequence. Underlined <u>ATG</u> and <u>TGA</u> represent the start and stop codons respectively. NdeI, AscI and EcoRI sites shown in red, blue and purple respectively.

Appendix V Vector maps

1. pGEM-T

T7 ↓	1 start
ApaI	14
AatII	20
SphI	26
BstZI	31
NcoI	37
SacII	46
SpeI	55
NotI	62
BstZI	62
PstI	73
SalI	75
NdeI	82
SacI	94
BstXI	103
NsiI	112
	126
↑ SP6	
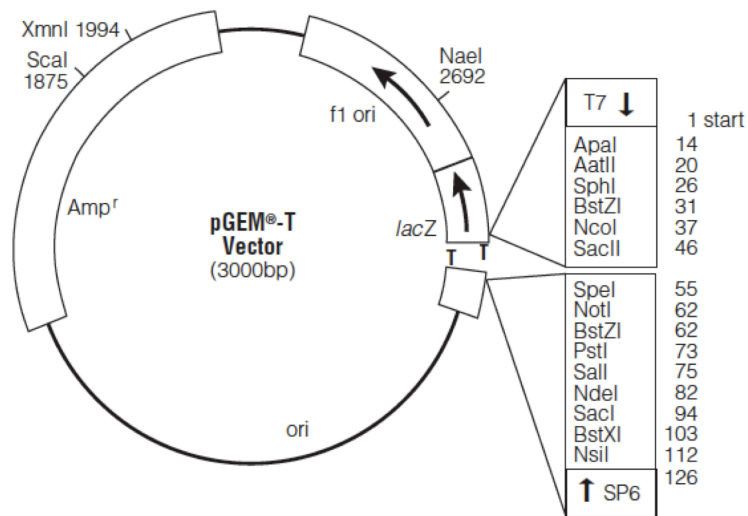
2. pET21a
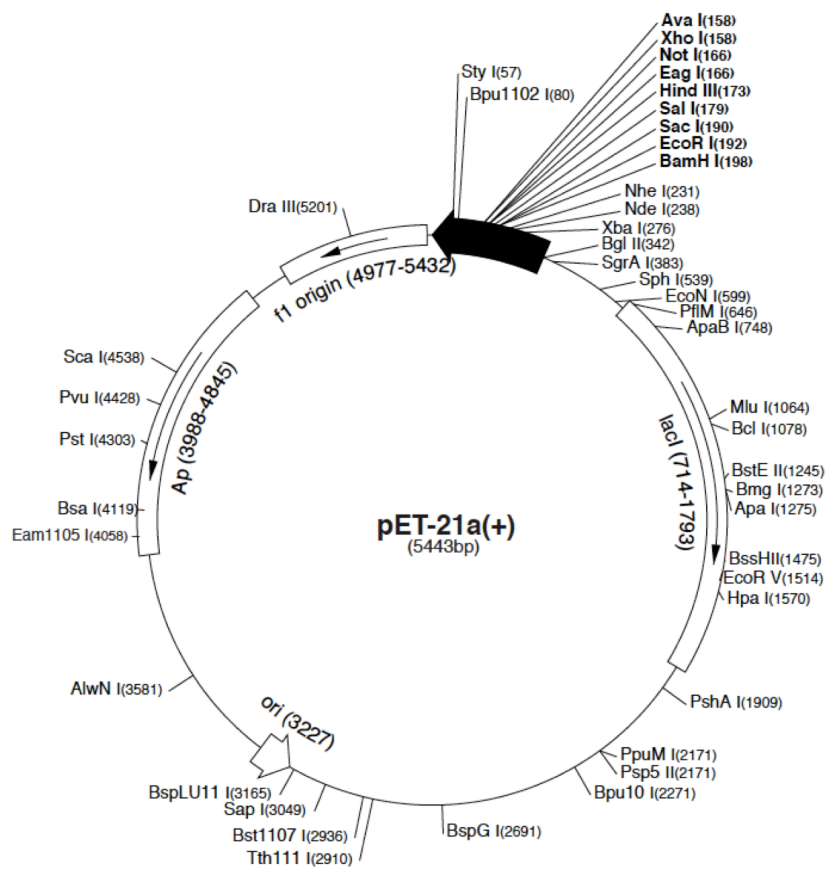
Appendix VI Raw Mass Spectrometry Data I

Figure number	File reference
Figure 60	LCT26206
Figure 62	LCT26355 (back trace)
Figure 63	LCT21186 (100 μM), LCT21187 (200 μM), LCT21188 (400 μM)
Figure 65	LCT26209 (30 min), LCT26212 (60 min), LCT26215 (90 min)
Figure 66	MMX11313 (TS), MMX11315 (TS + positive control acrylamide **67**)
Figure 67	LCT26356 (30 min), LCT26358 (45 min), LCT26360 (60 min), LCT26362 (90 min)
Figure 68	LCT27638 (pH 8.1), LCT27639 (pH 7.9), LCT27640 (pH 7.6), LCT27641 (pH 7.4), LCT27642 (pH 7.3), LCT27643 (pH 7.2)
Figure 69	LCT27675 (pH 8.1), LCT27676 (pH 7.9), LCT27677 (pH 7.6), LCT27678 (pH 7.4), LCT27679 (pH 7.3), LCT27680 (pH 7.2).
Figure 70	LCT27645 (2 min), LCT27647 (30 min), LCT27649 (60 min), LCT27651 (120 min)
Figure 75	LCT27793
Figure 76	LCT27984 (270 min)
Figure 87	LCT26577, LCT26578, LCT26581, LCT26582
Figure 88	LCT26503 (2 min), LCT26504 (10 min), LCT26505 (30 min), LCT26514 (120 min)
Figure 98	LCT27373 (1 h), LCT27377 (2 h), LCT27387 (5 h), LCT27403 (9 h)
Figure 99	LCT27431
Figure 106	LCT28408 (10 min), LCT28415 (1020 min)
Figure 127	LCT21191
Figure 128	LCT26176

Raw data for Figure 60
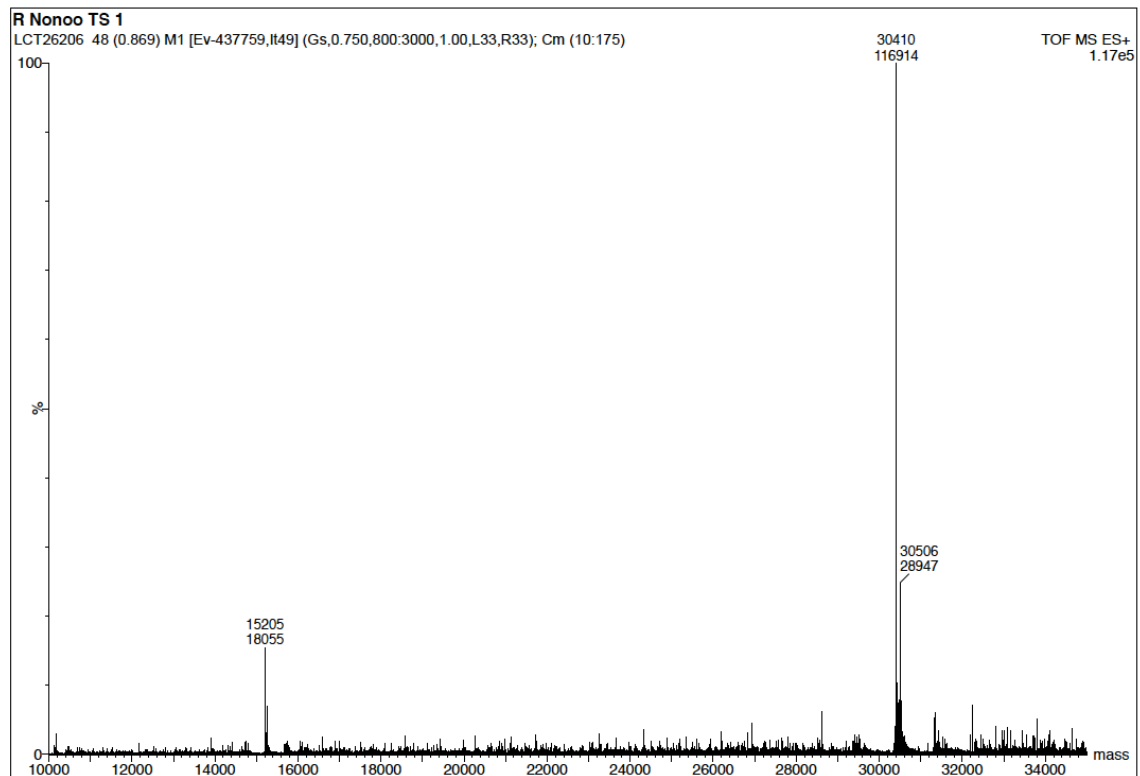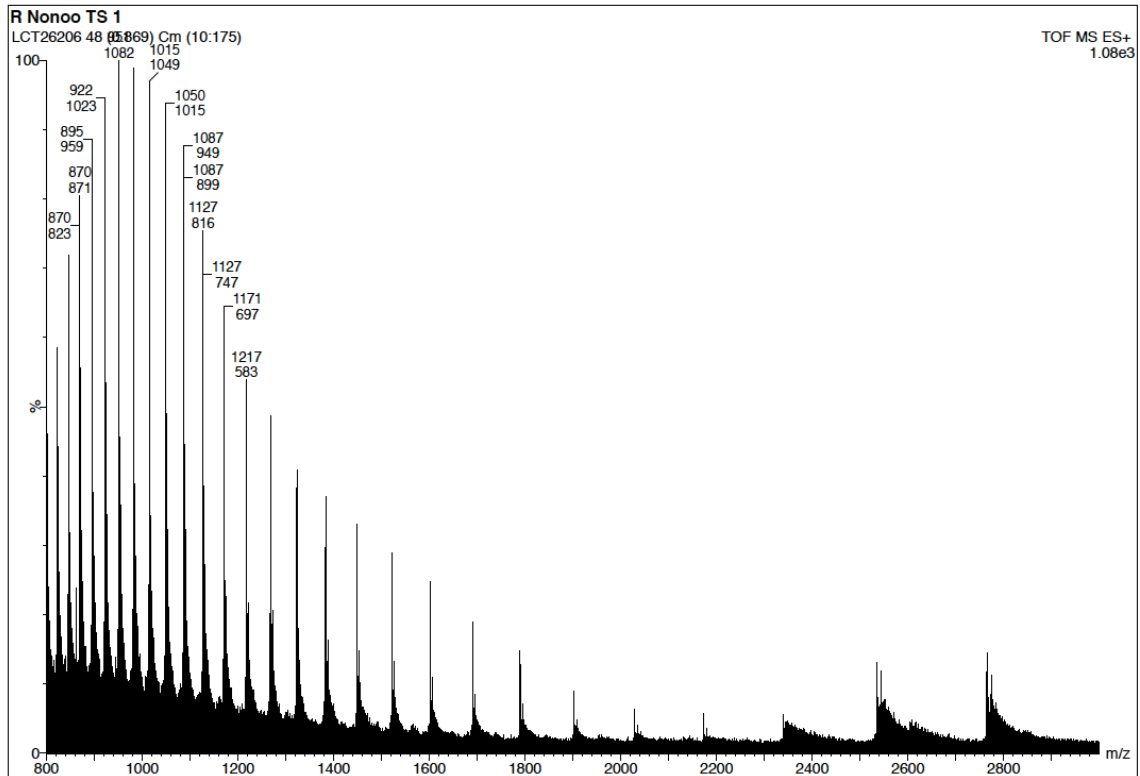
Raw data for Figure 62
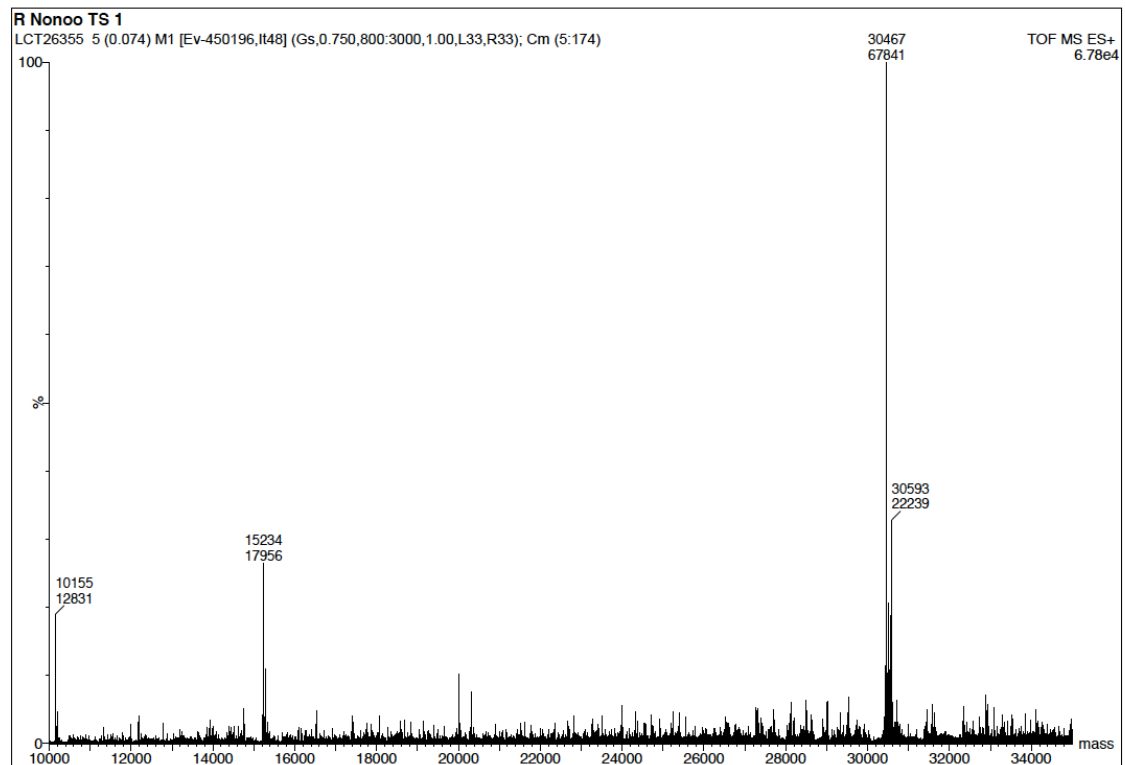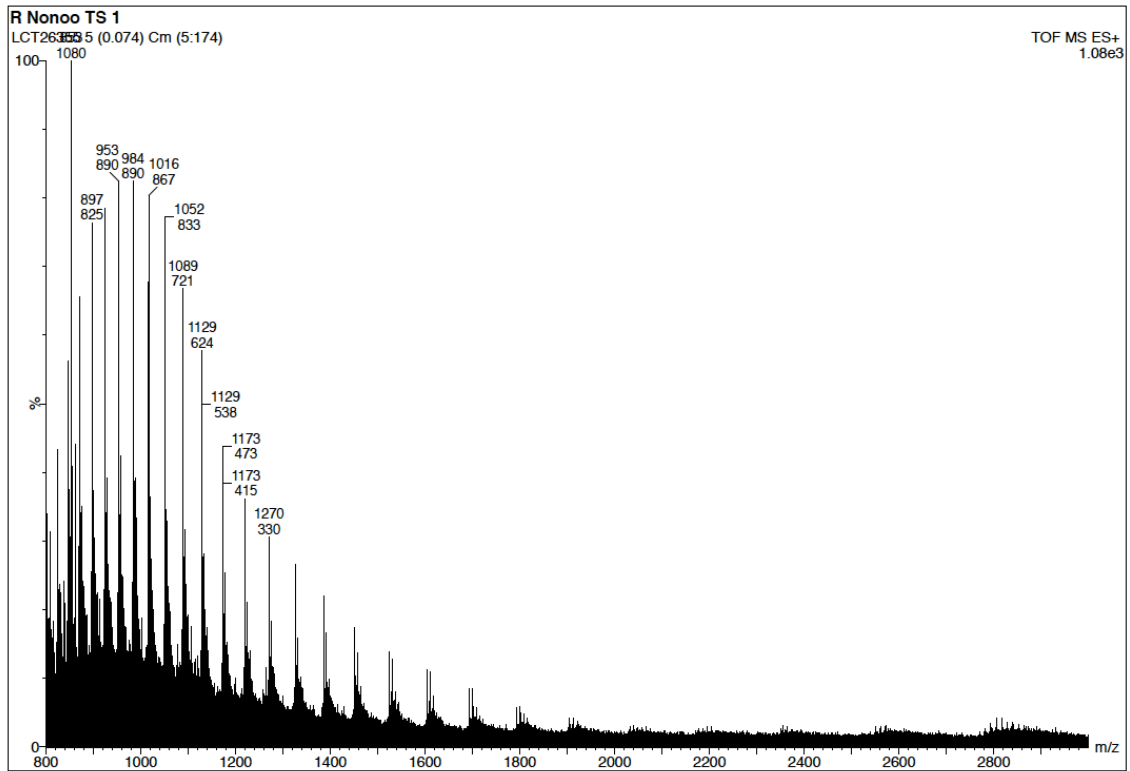
Raw data for Figure 63**: 100 μM**
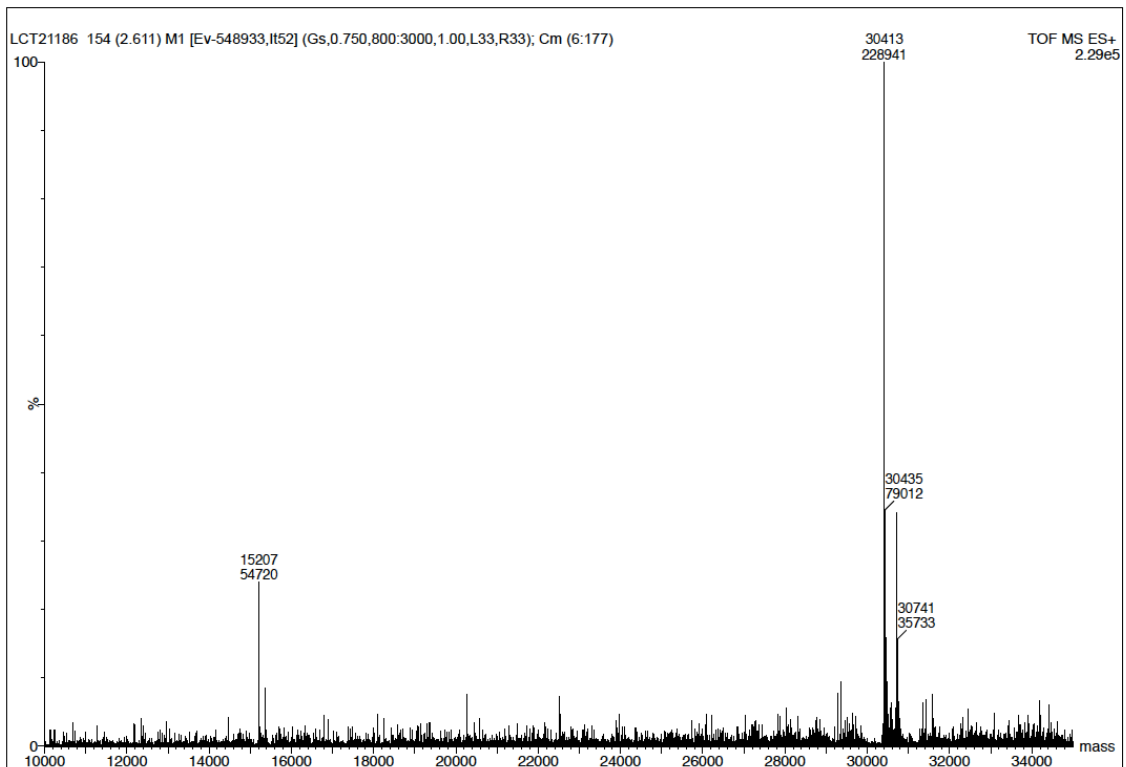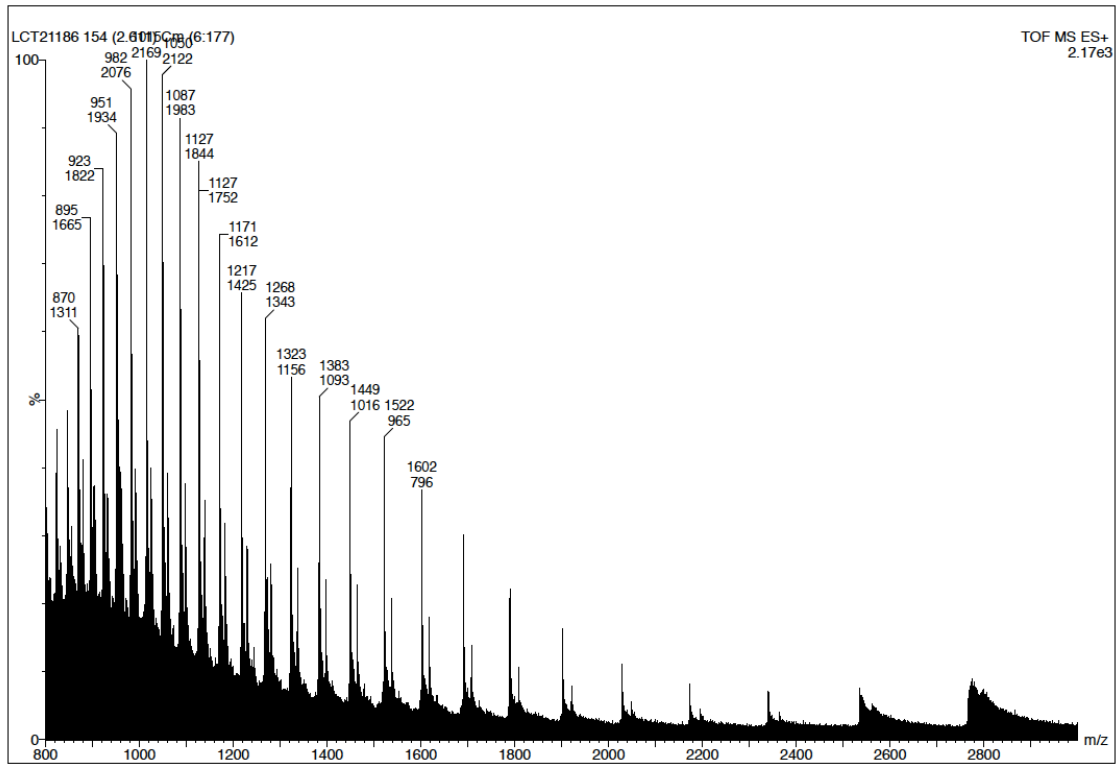
Raw data for Figure 63**: 200 μM**
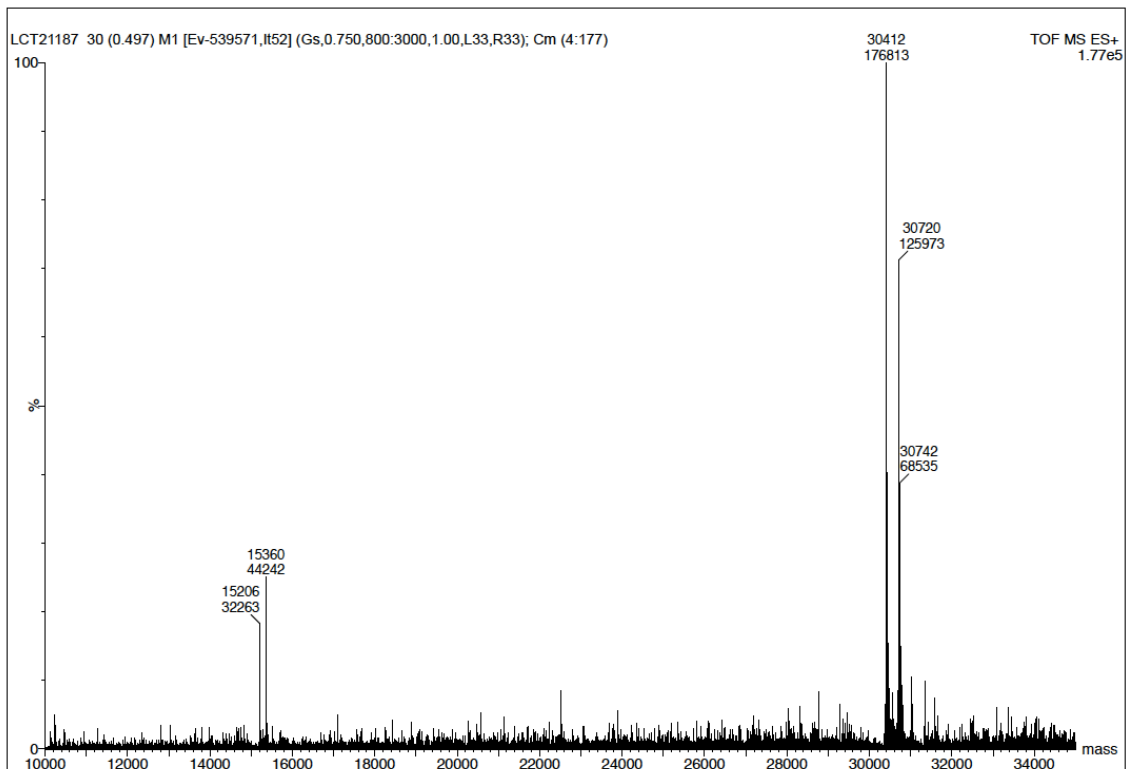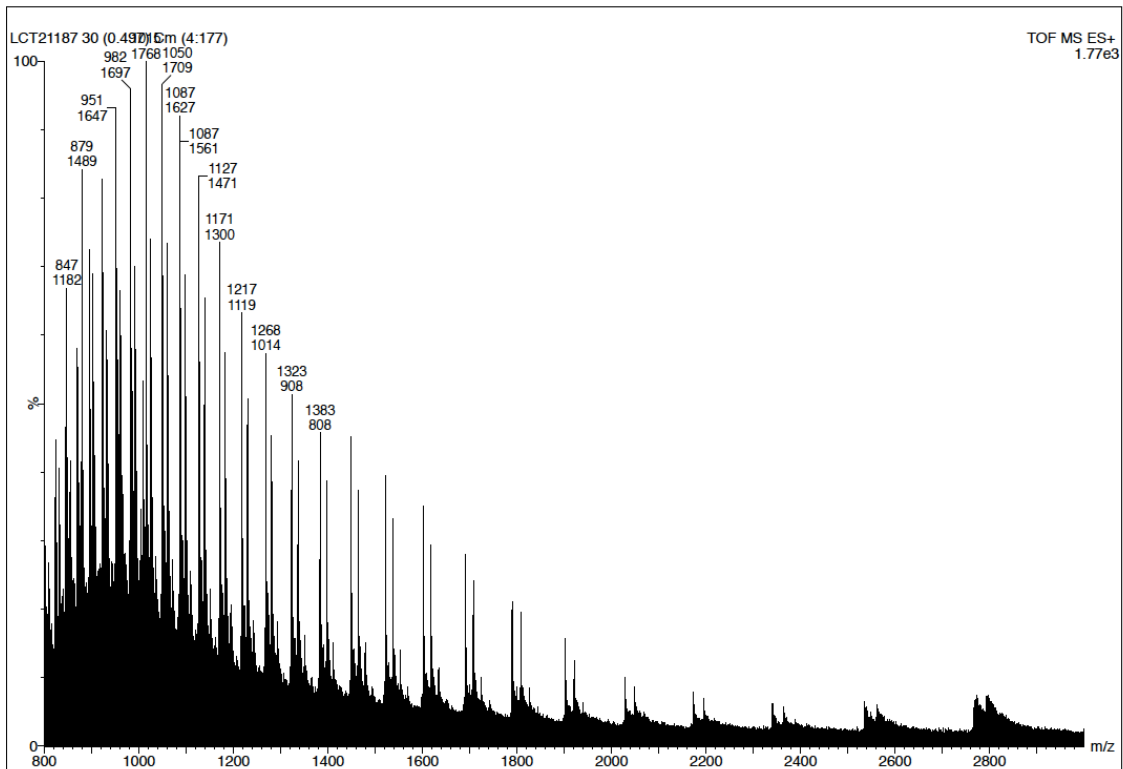
Raw data for Figure 63**: 400 μM**
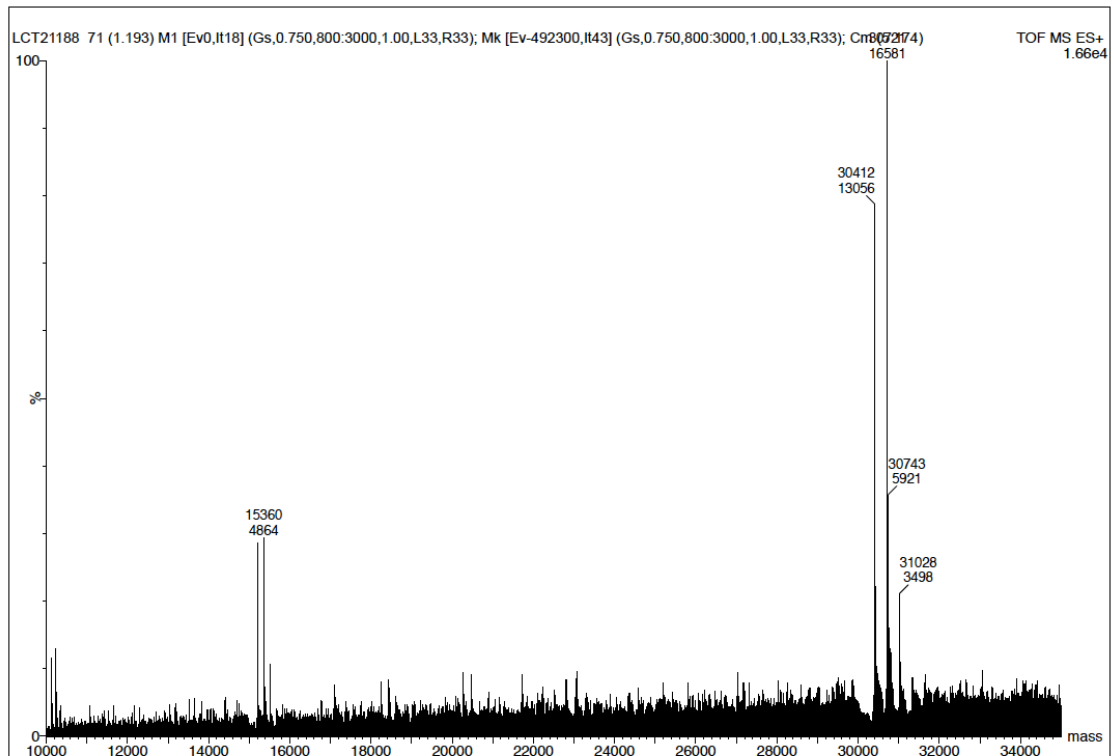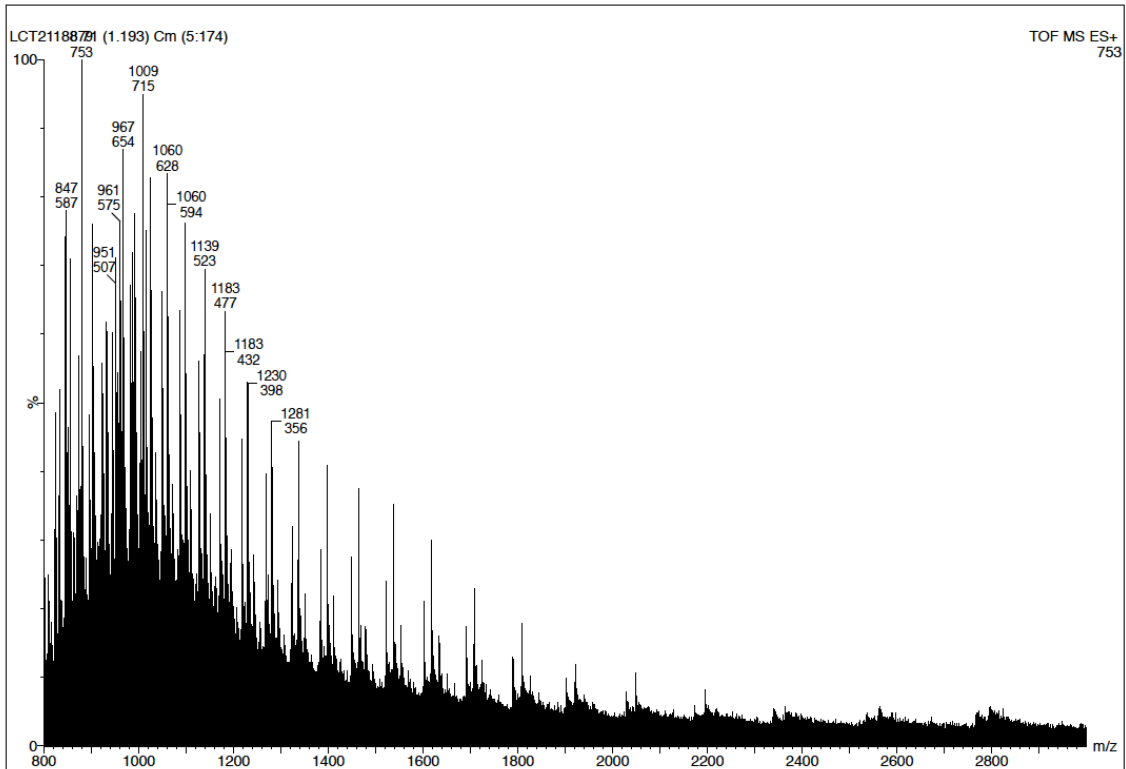
Raw data for Figure 65**: 30 min**
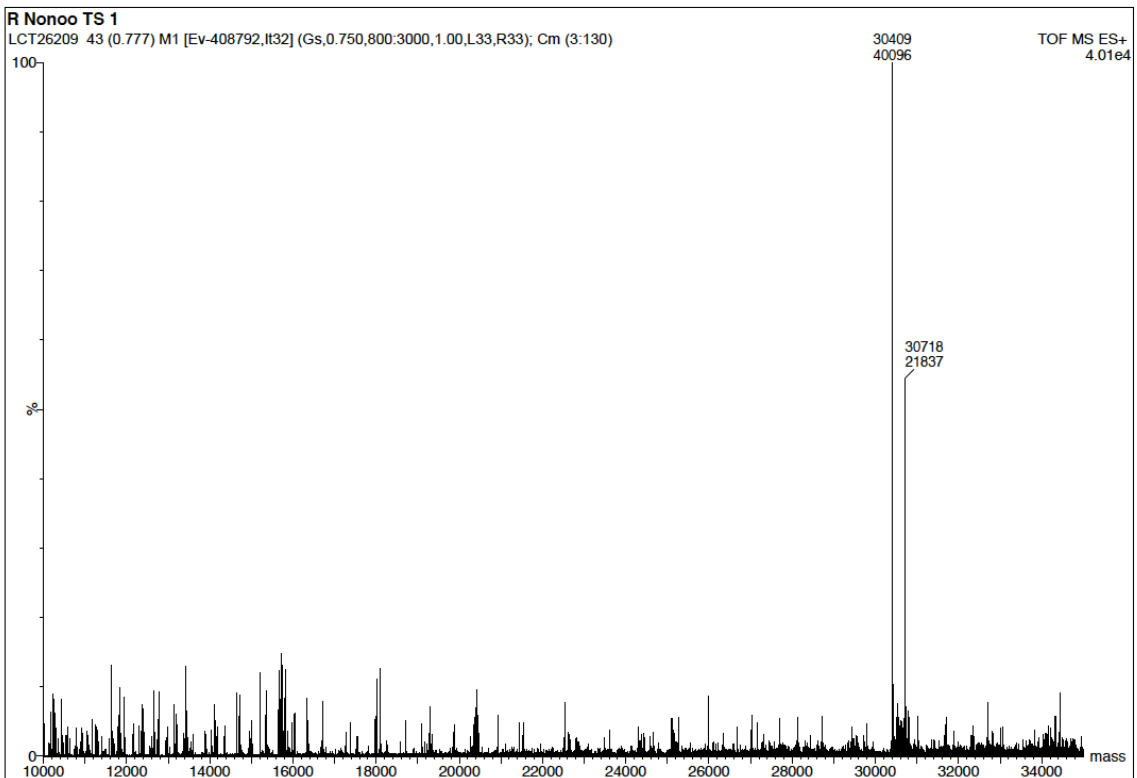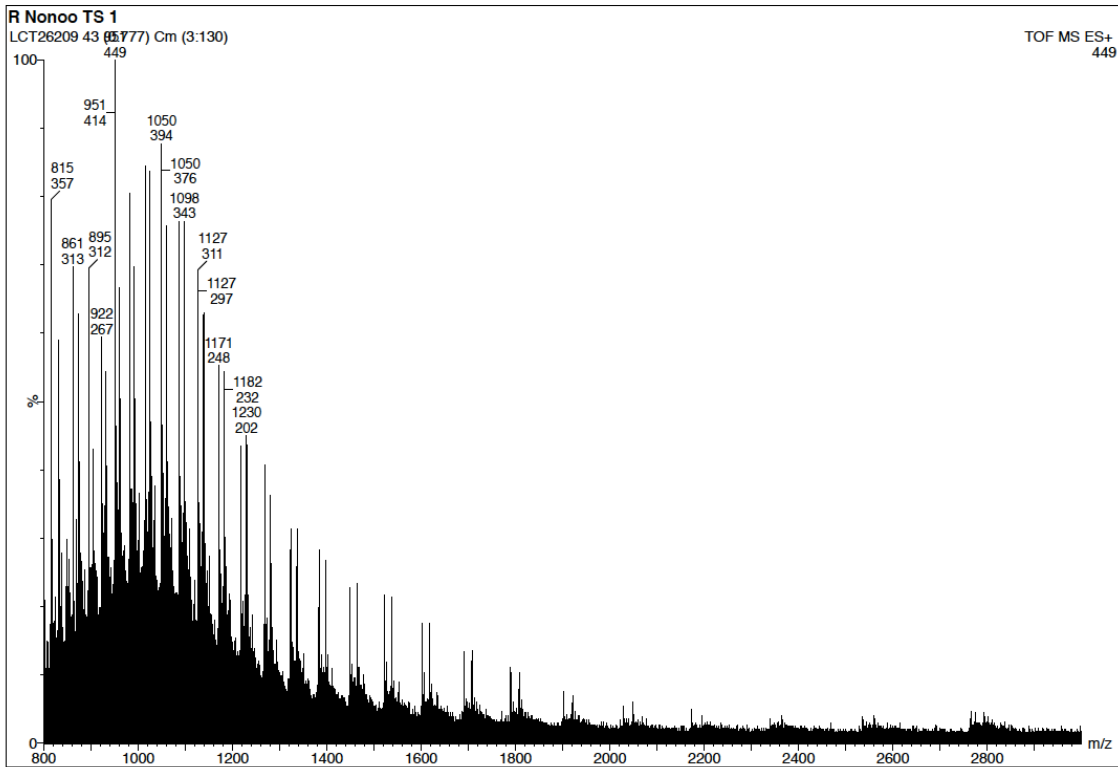
Raw data for Figure 65**: 60 min**
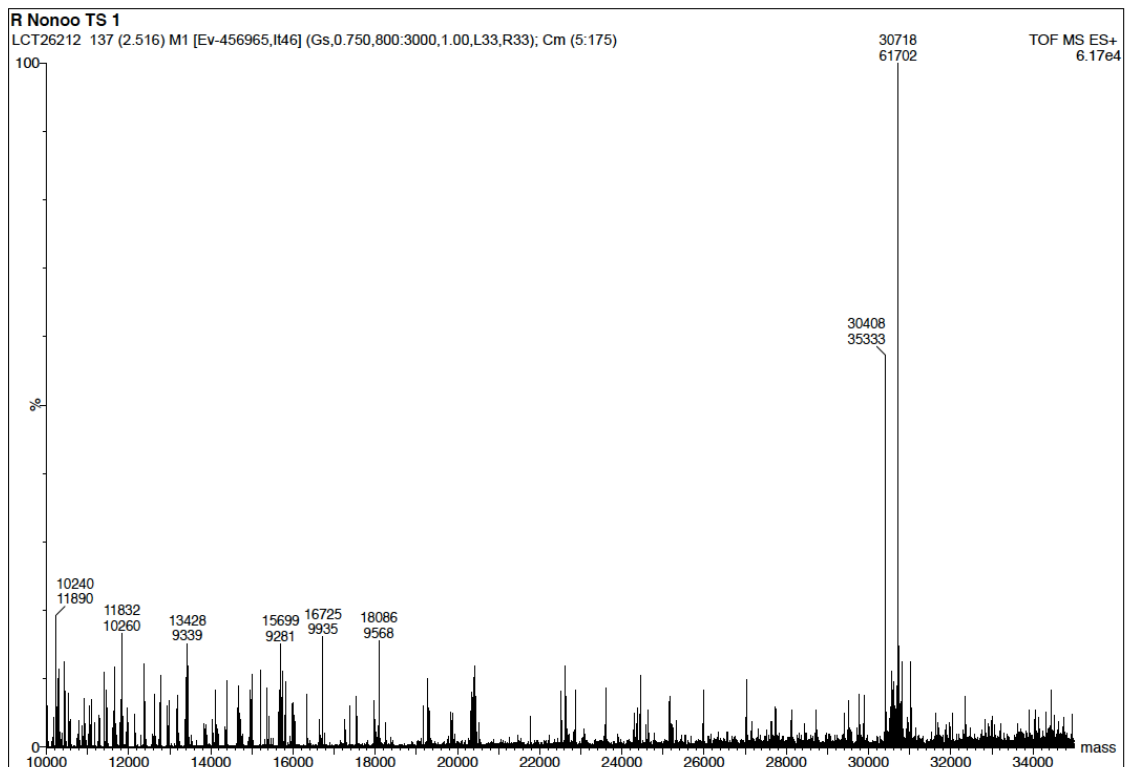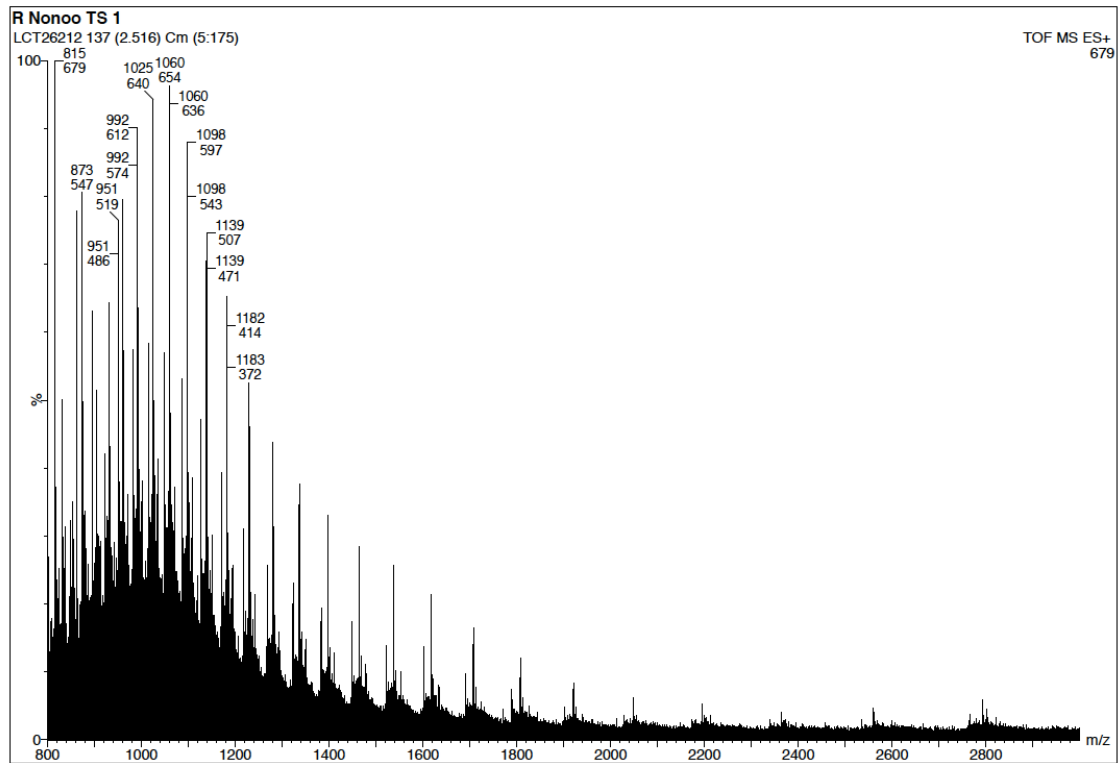
Raw data for Figure 65**: 90 min**

Raw data for Figure 66:

MMX11315 54 (1.801) Cm (3:76)

TOF LD+
2.65e3
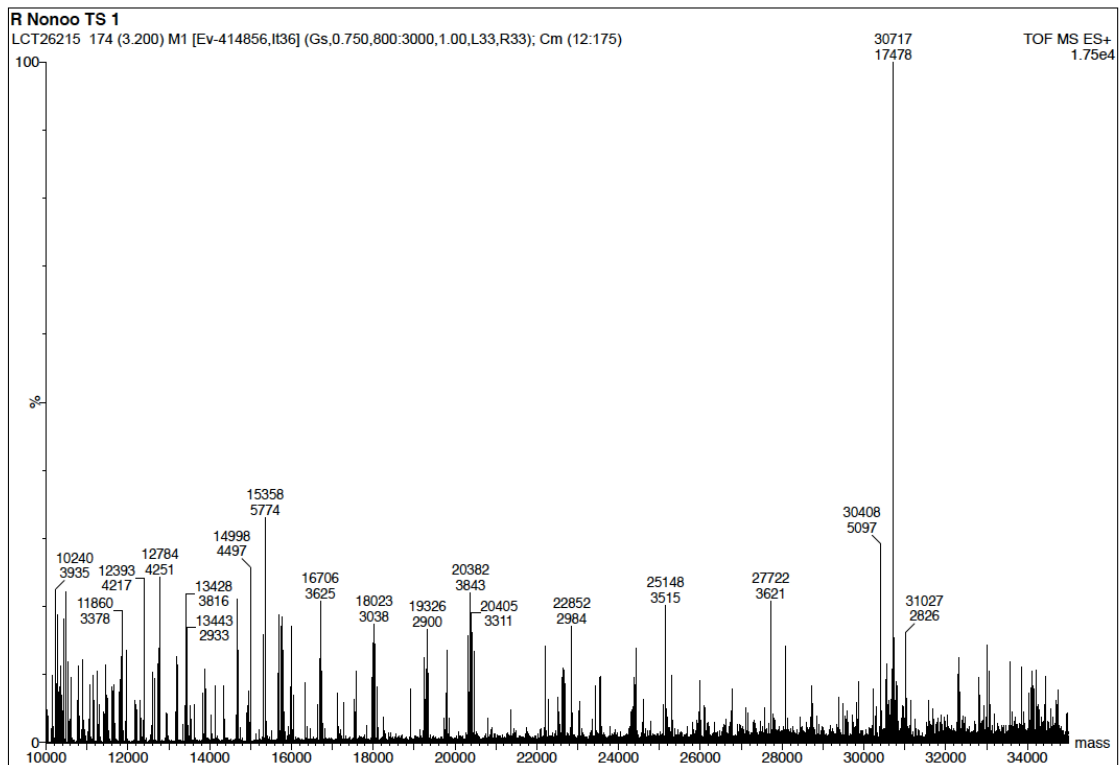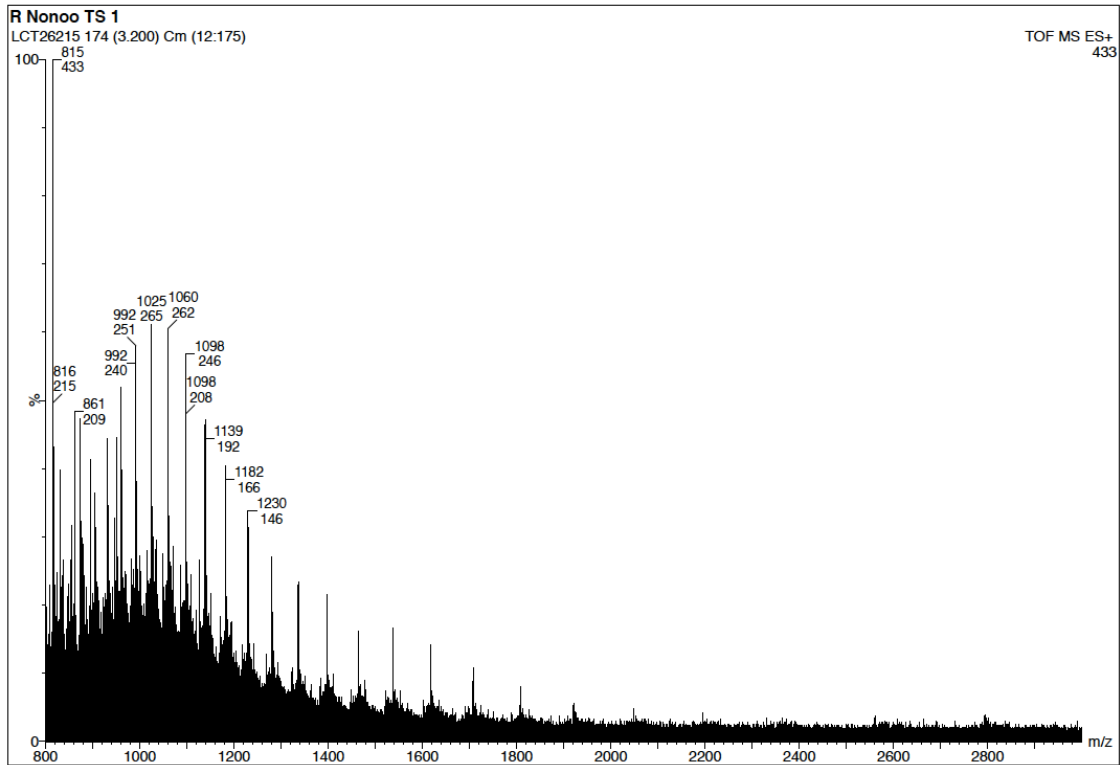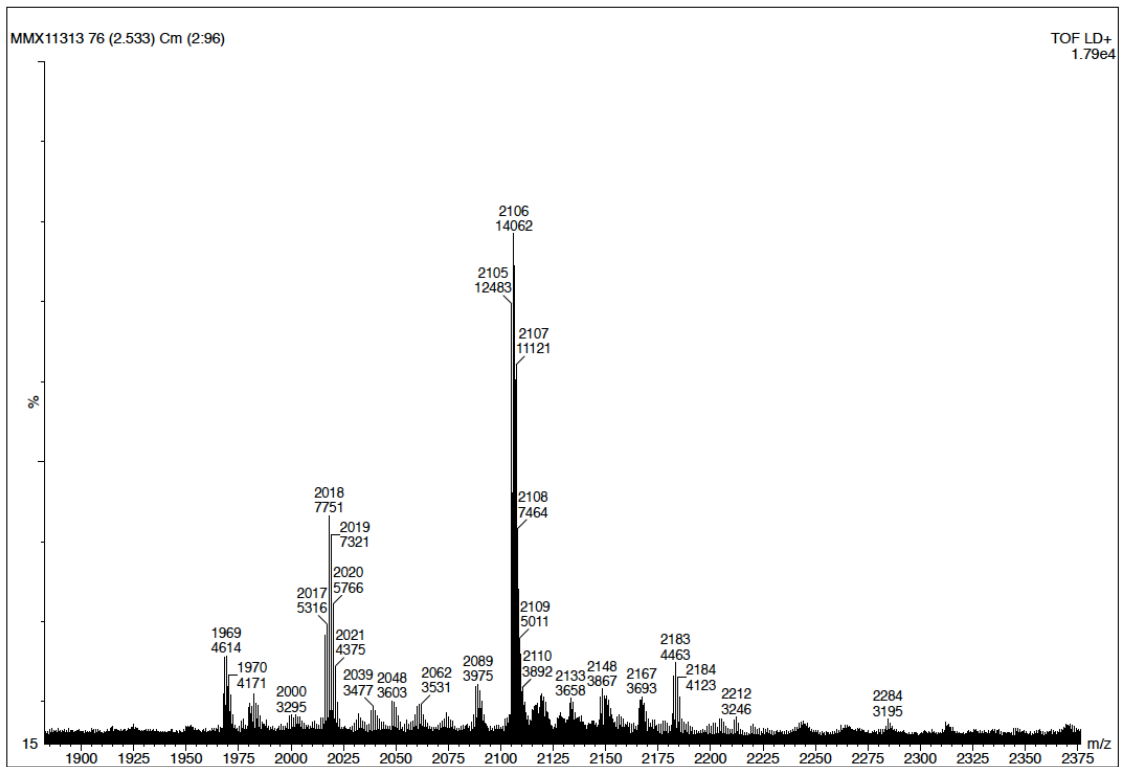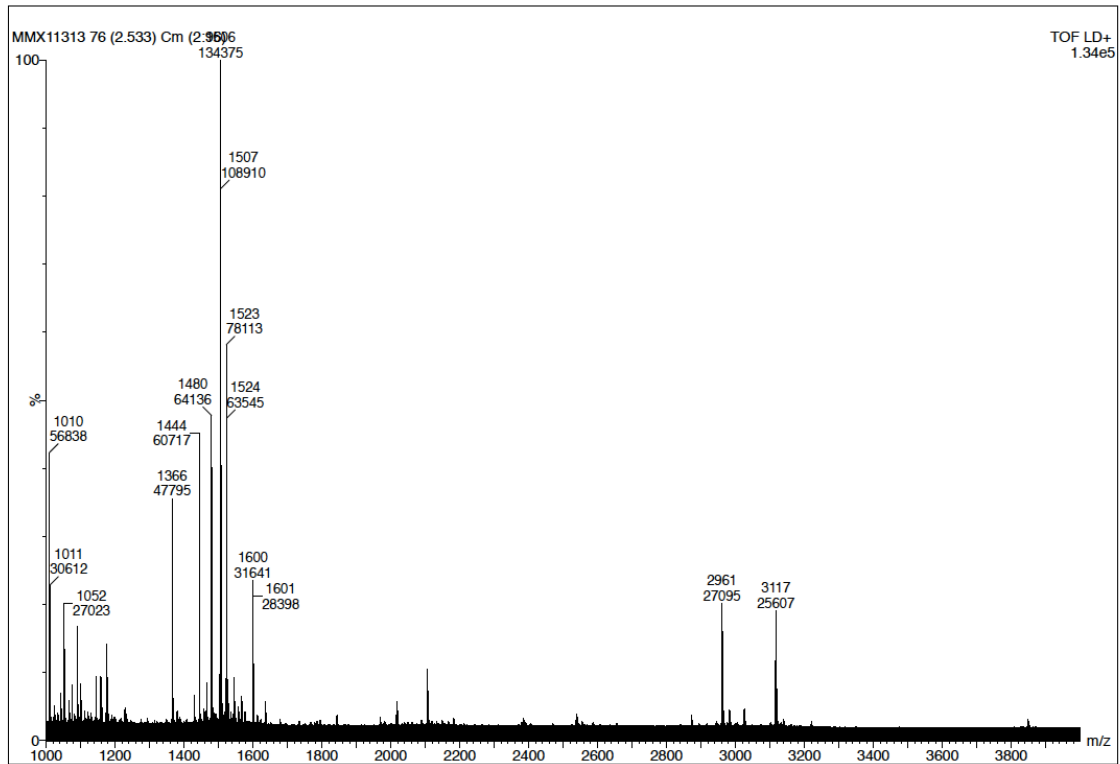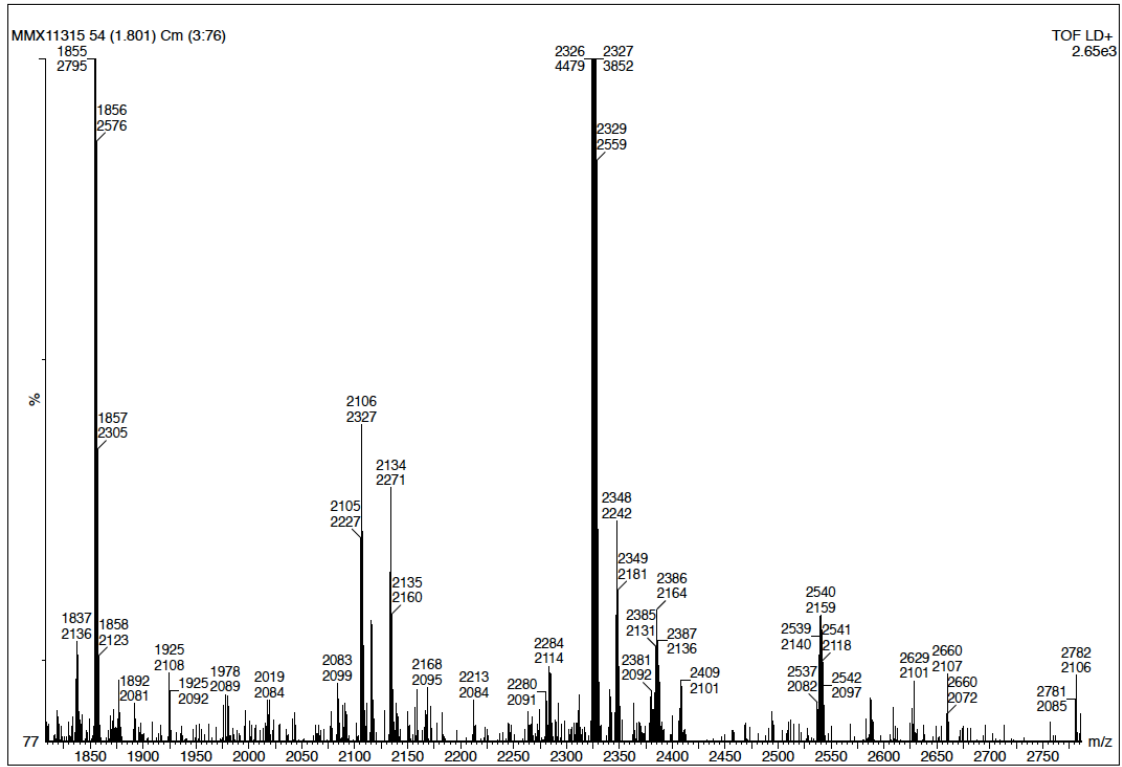
Raw data for Figure 67**: 30 min**
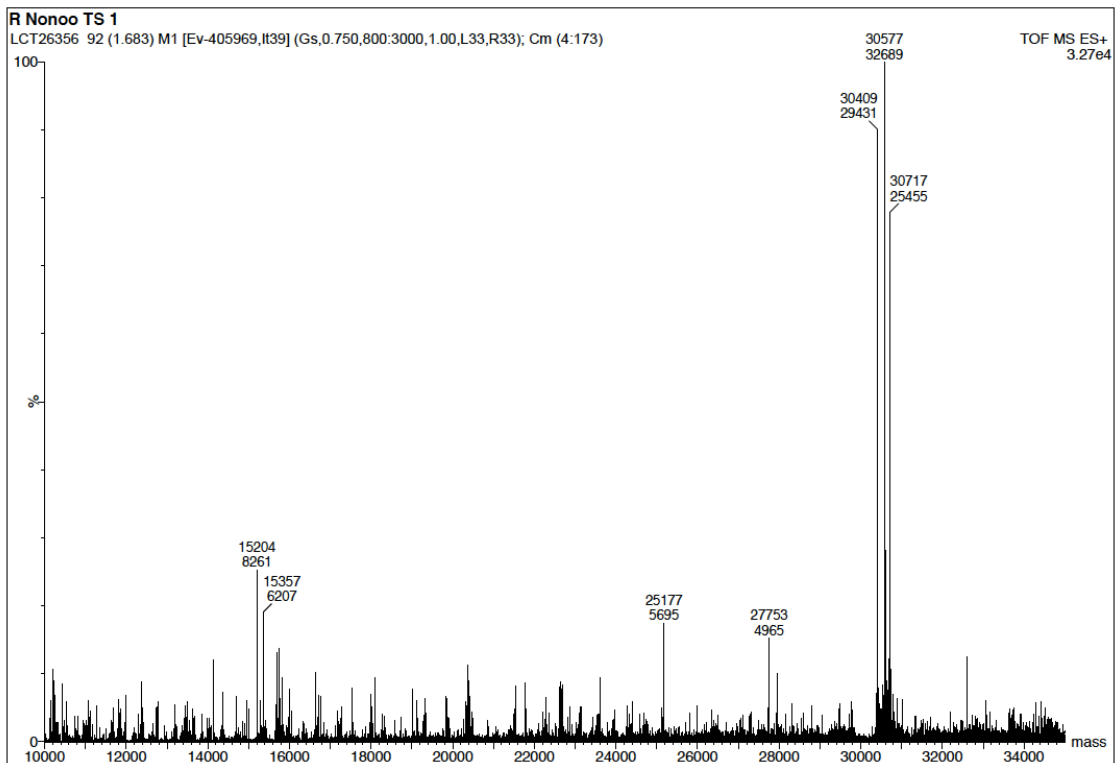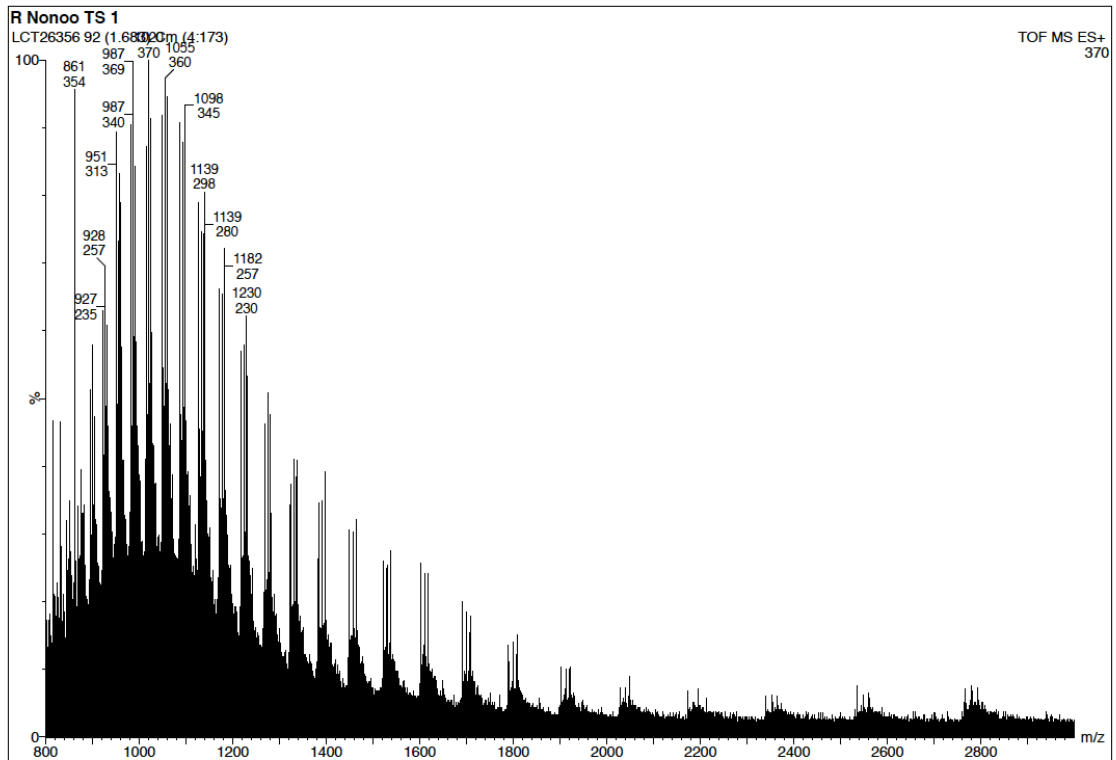
Raw data for Figure 67**: 45 min**
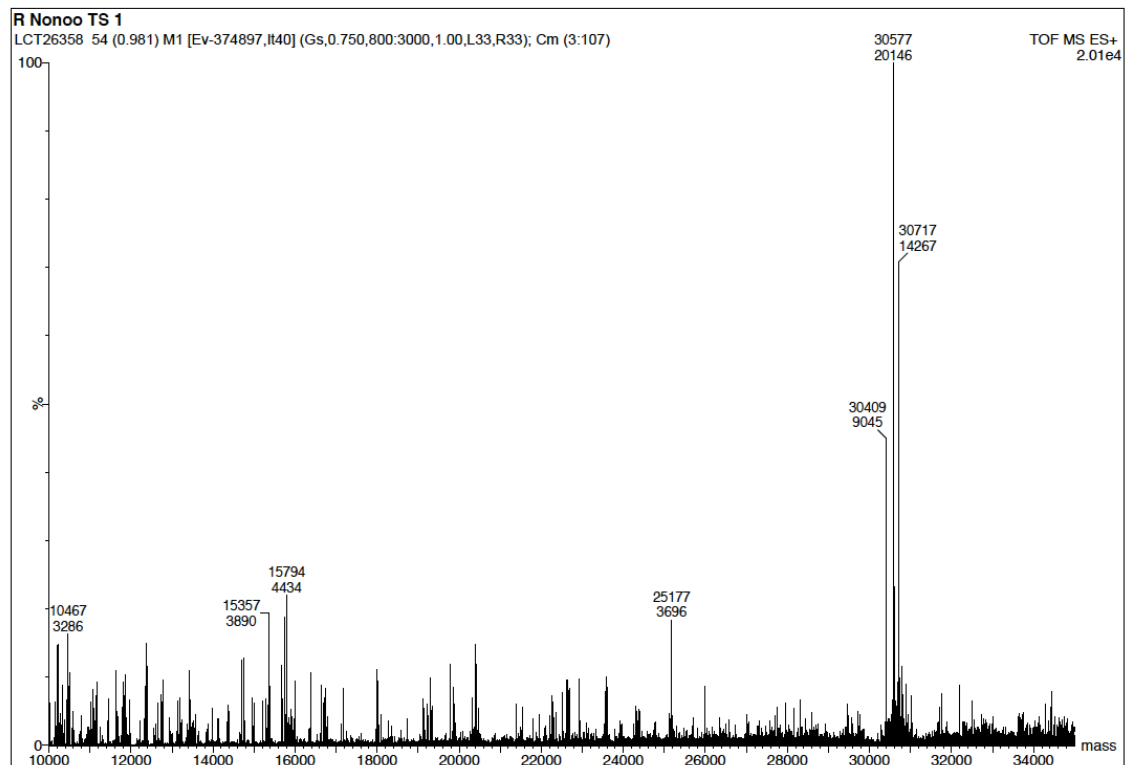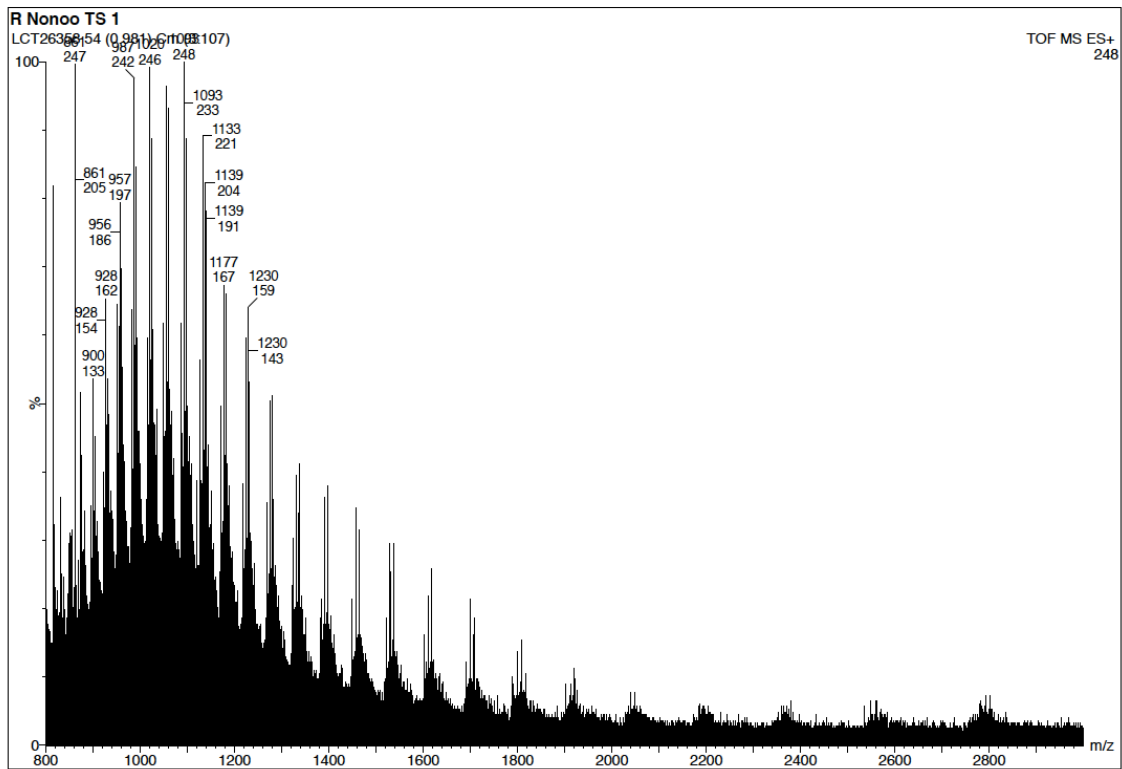
Raw data for Figure 67**: 60 min**
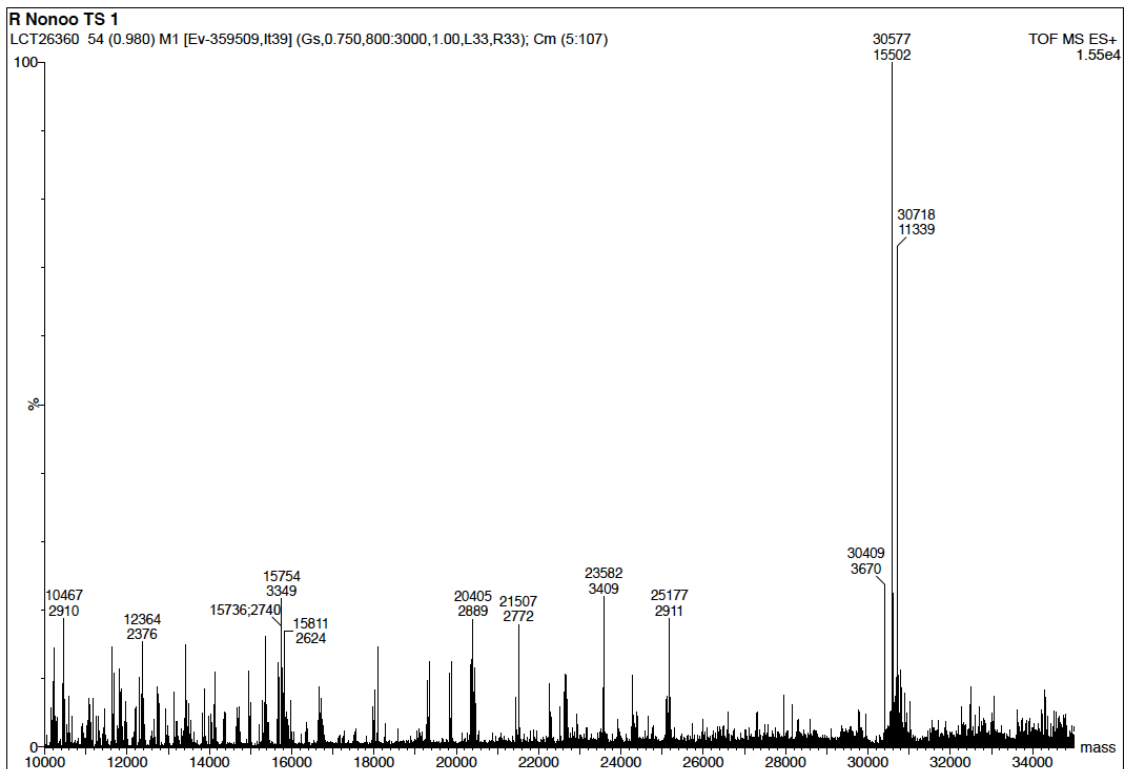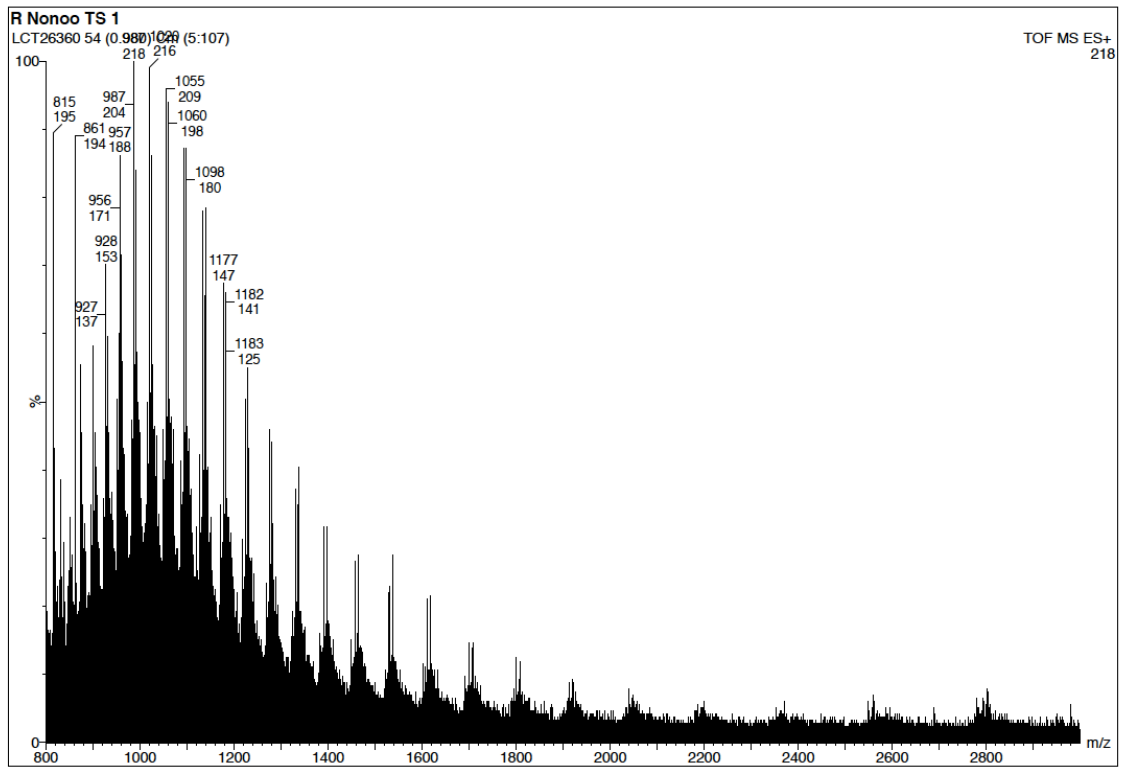
Raw data for Figure 67**: 90 min**
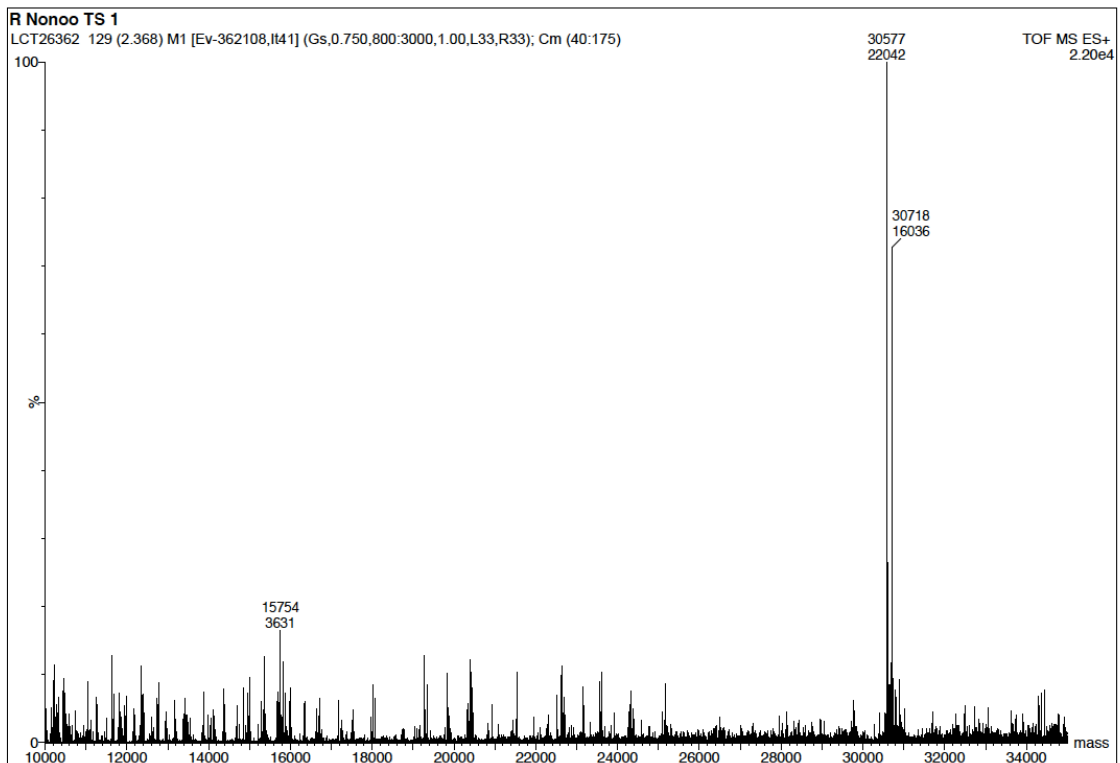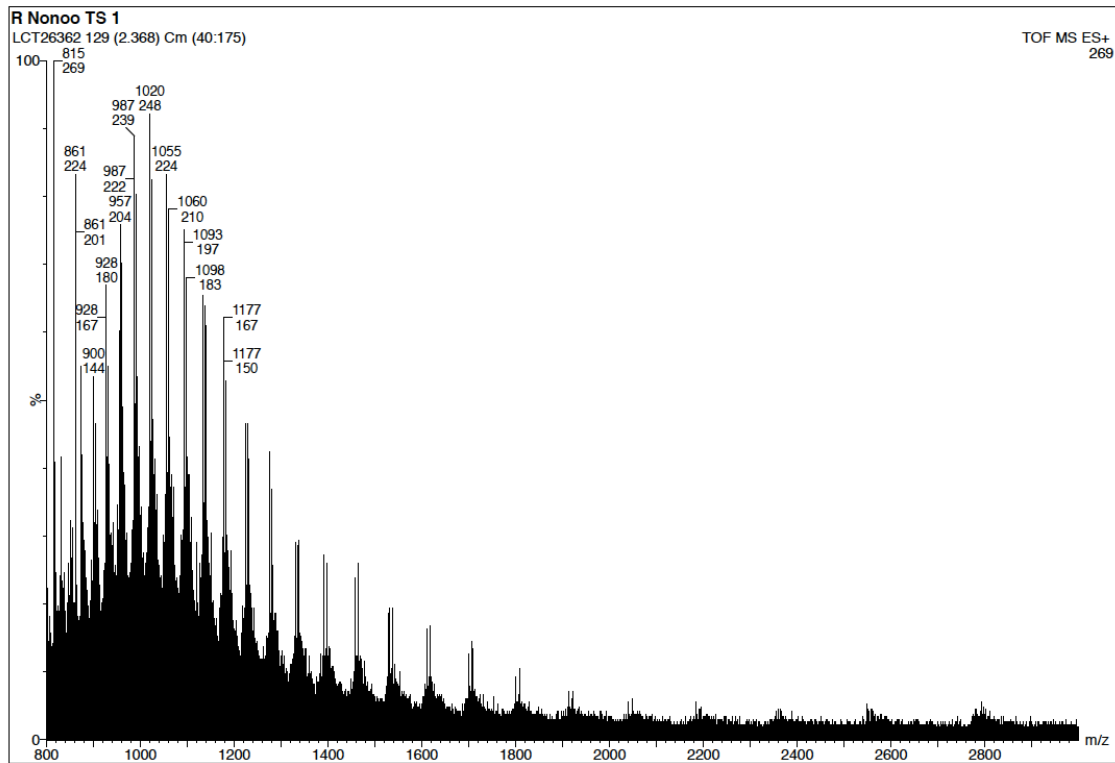
Raw data for Figure 68**: pH 8.1**
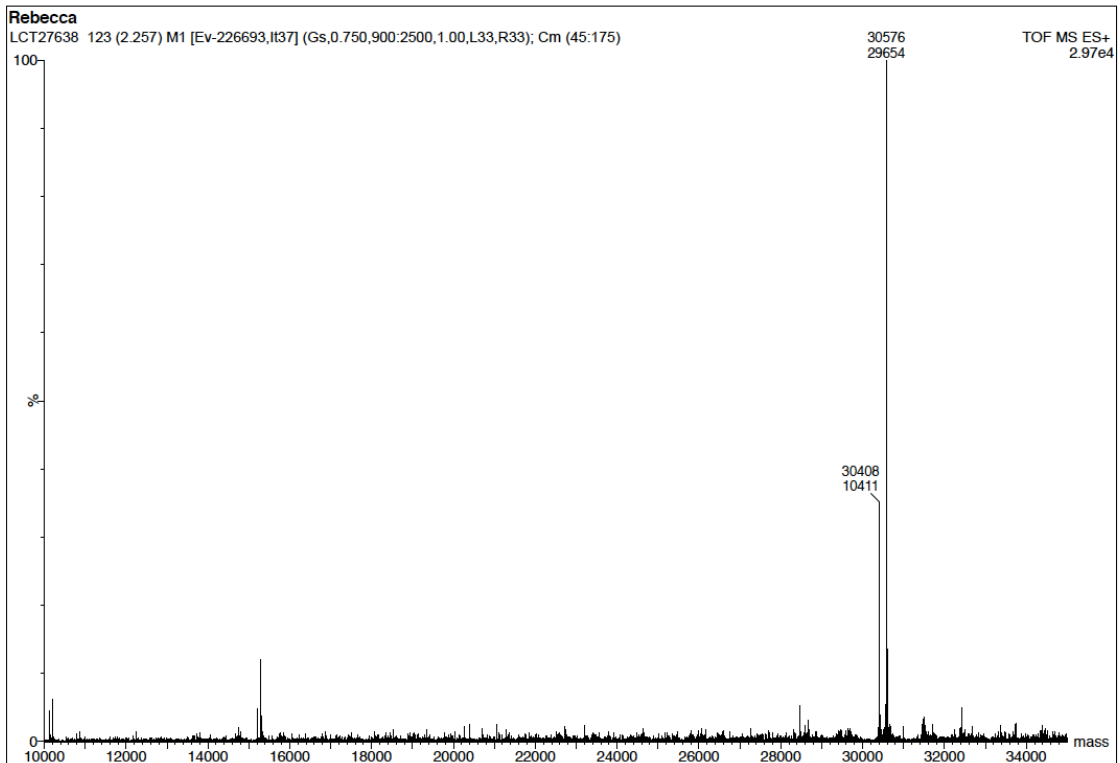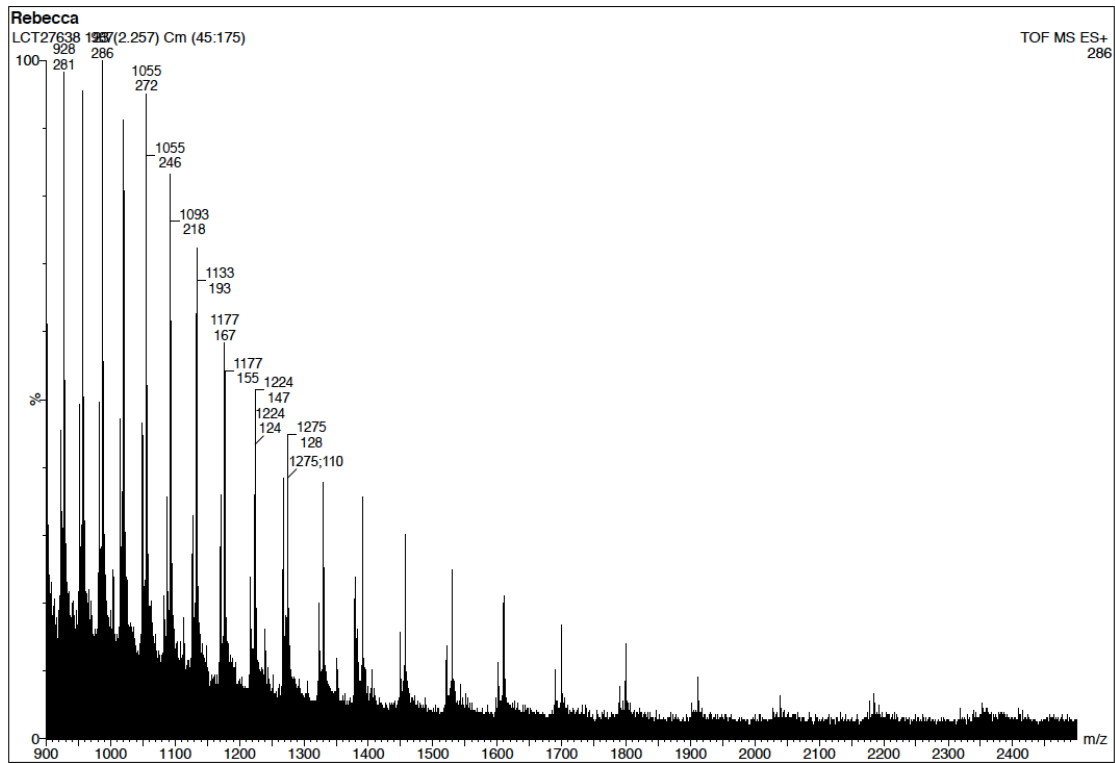
Raw data for Figure 68**: pH 7.9**
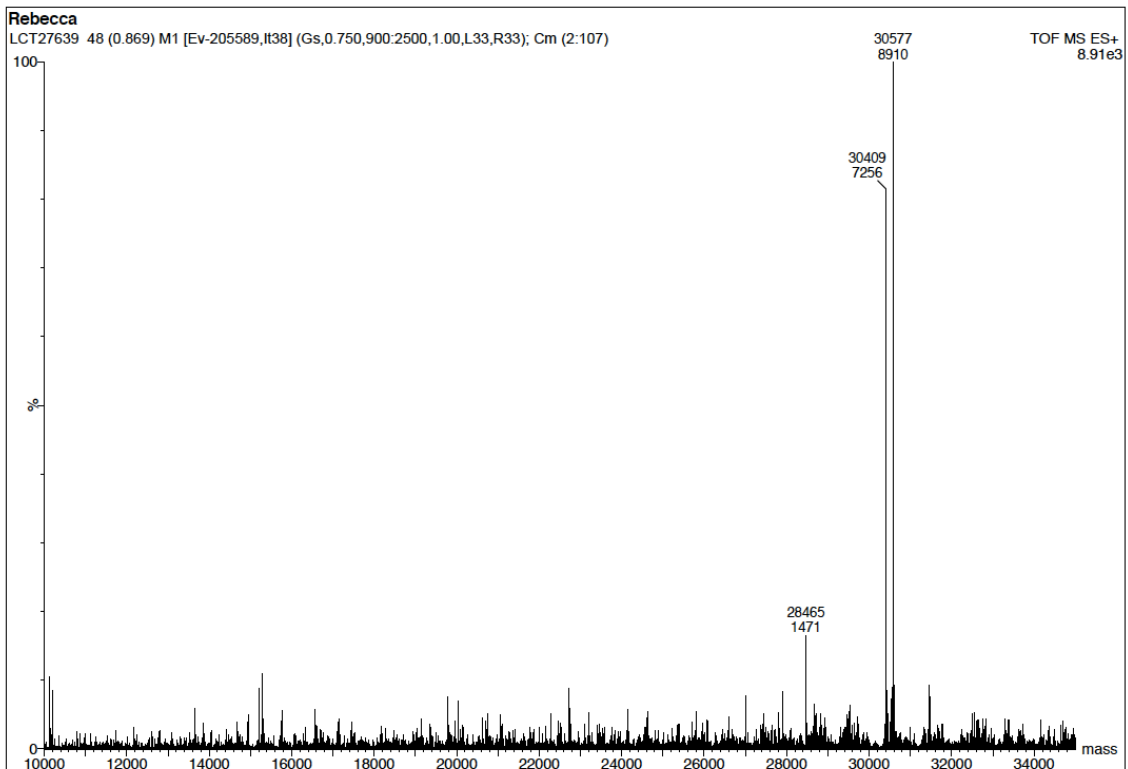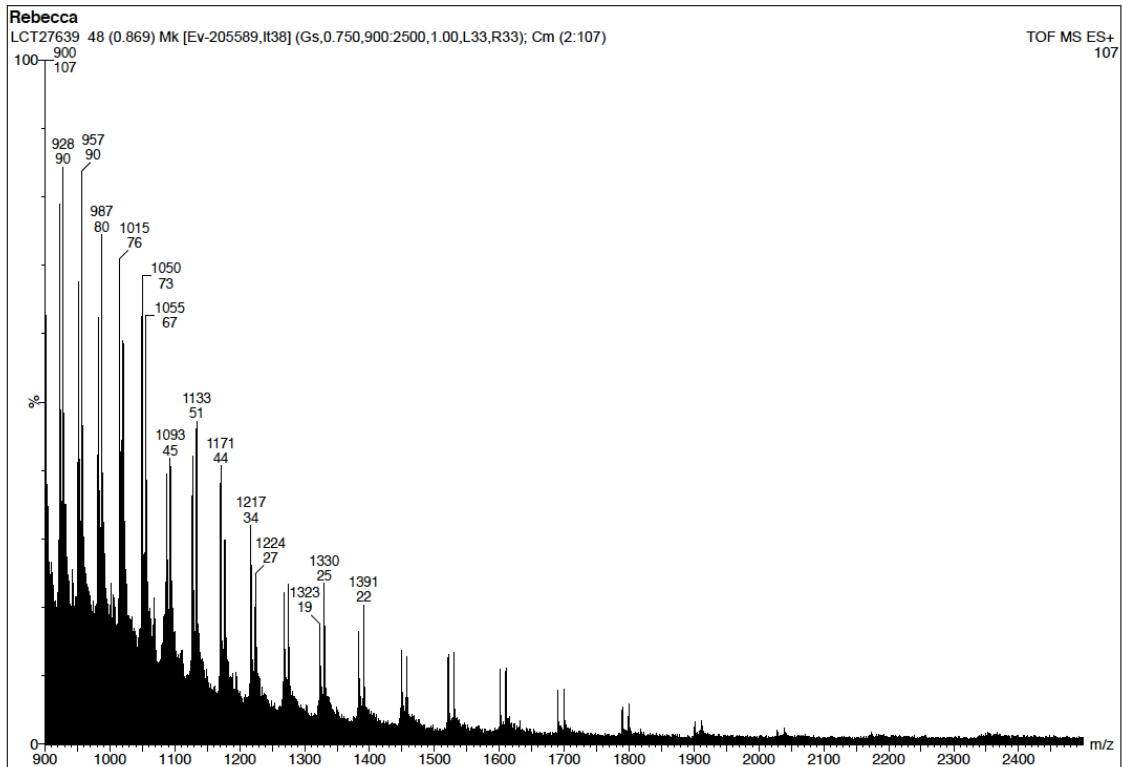
Raw data for Figure 68**: pH 7.6**
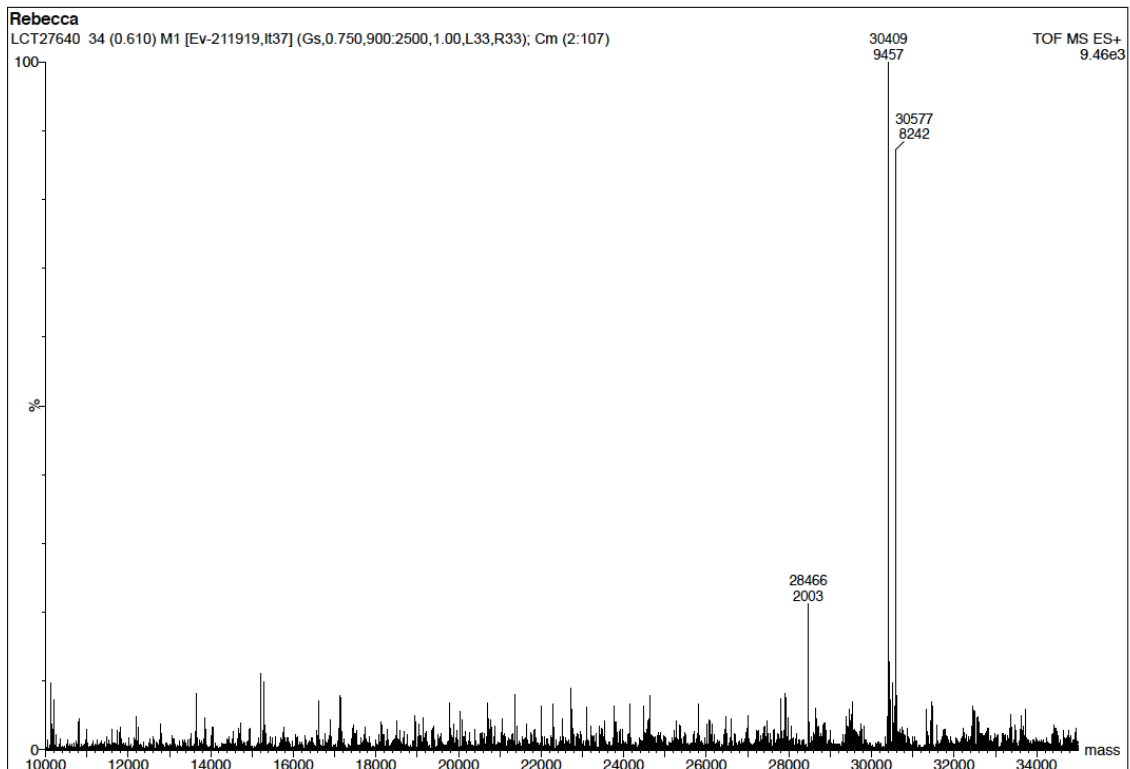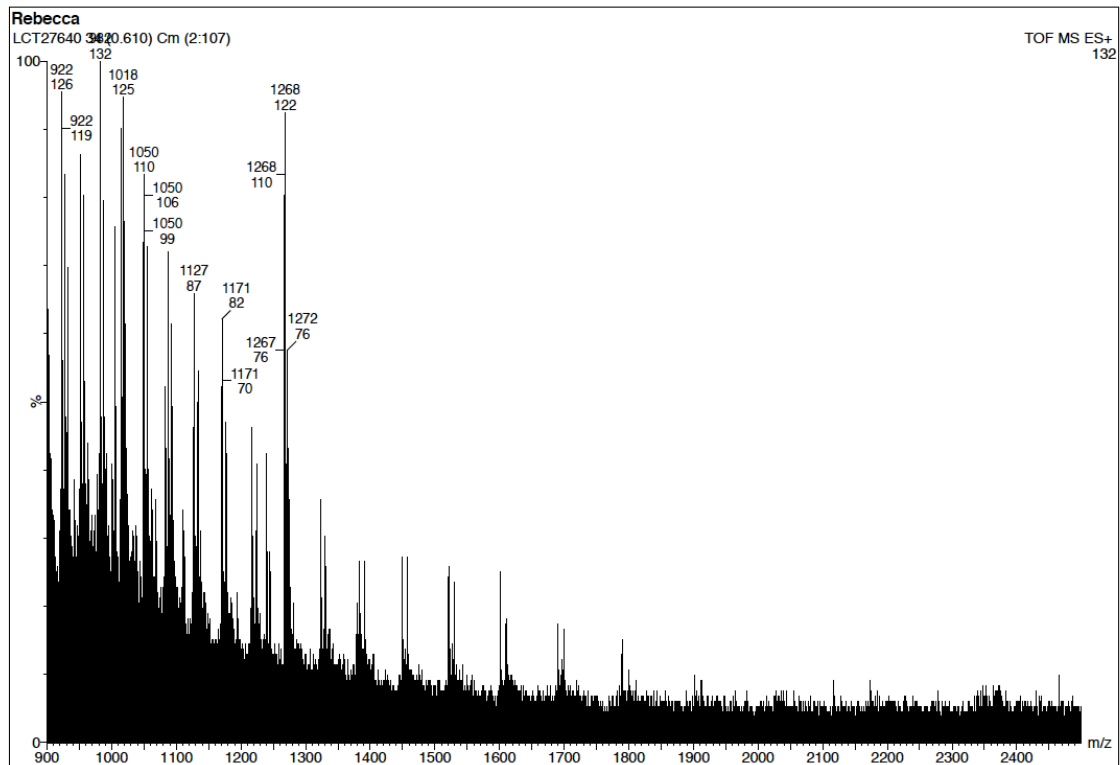
Raw data for Figure 68**: pH 7.4**
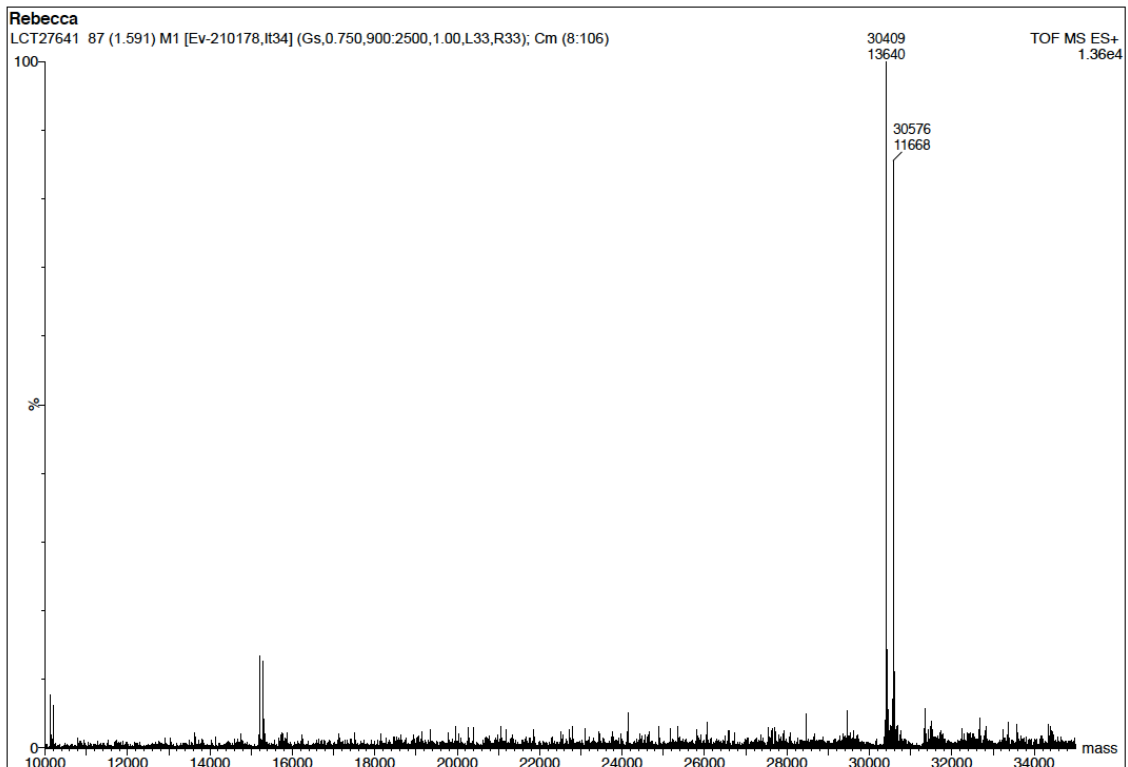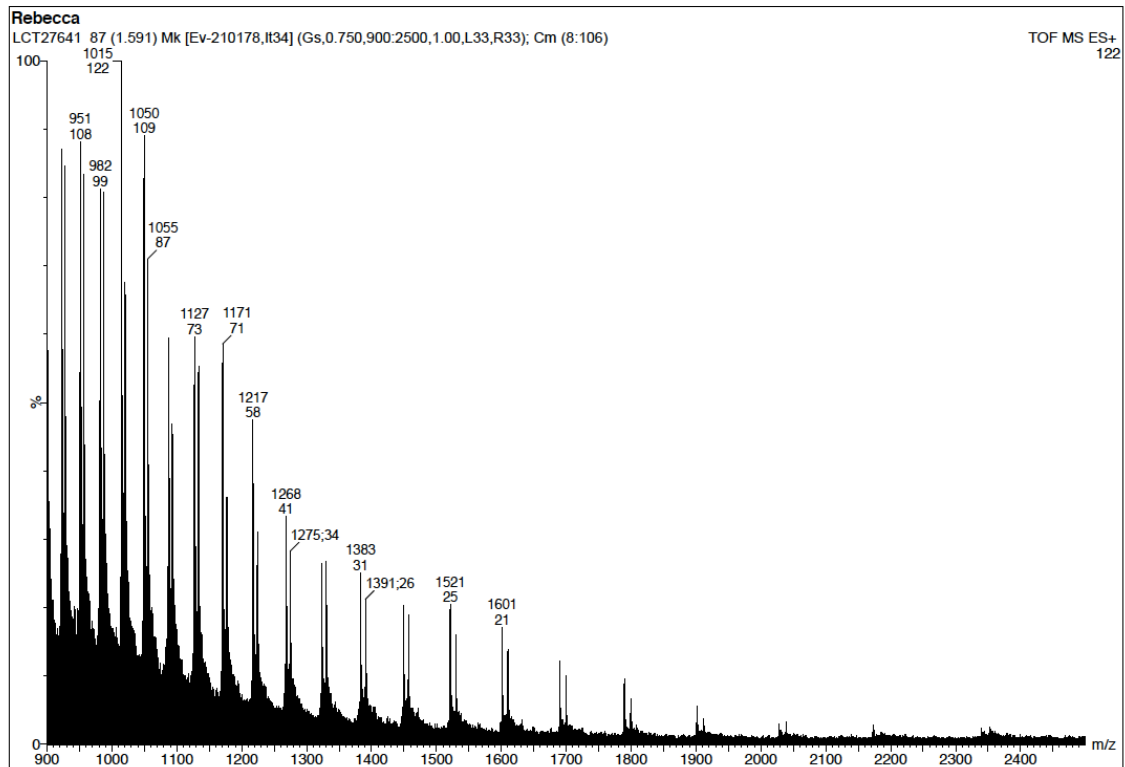
Raw data for Figure 68**: pH 7.3**
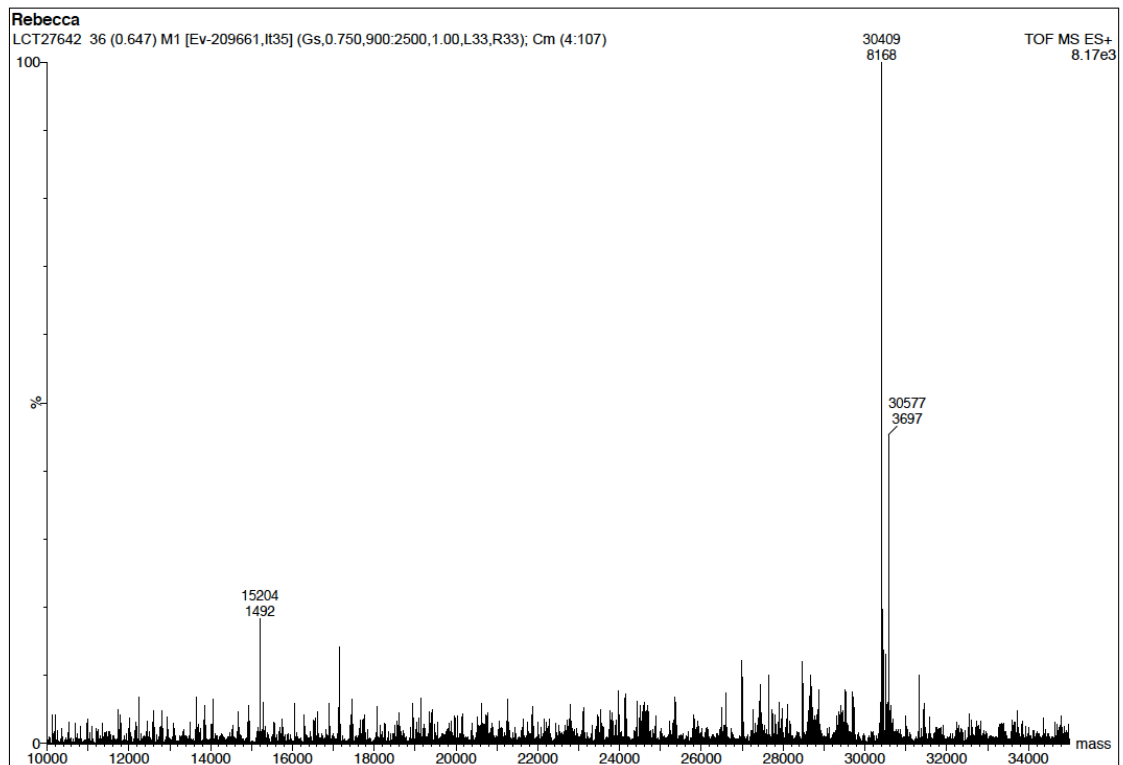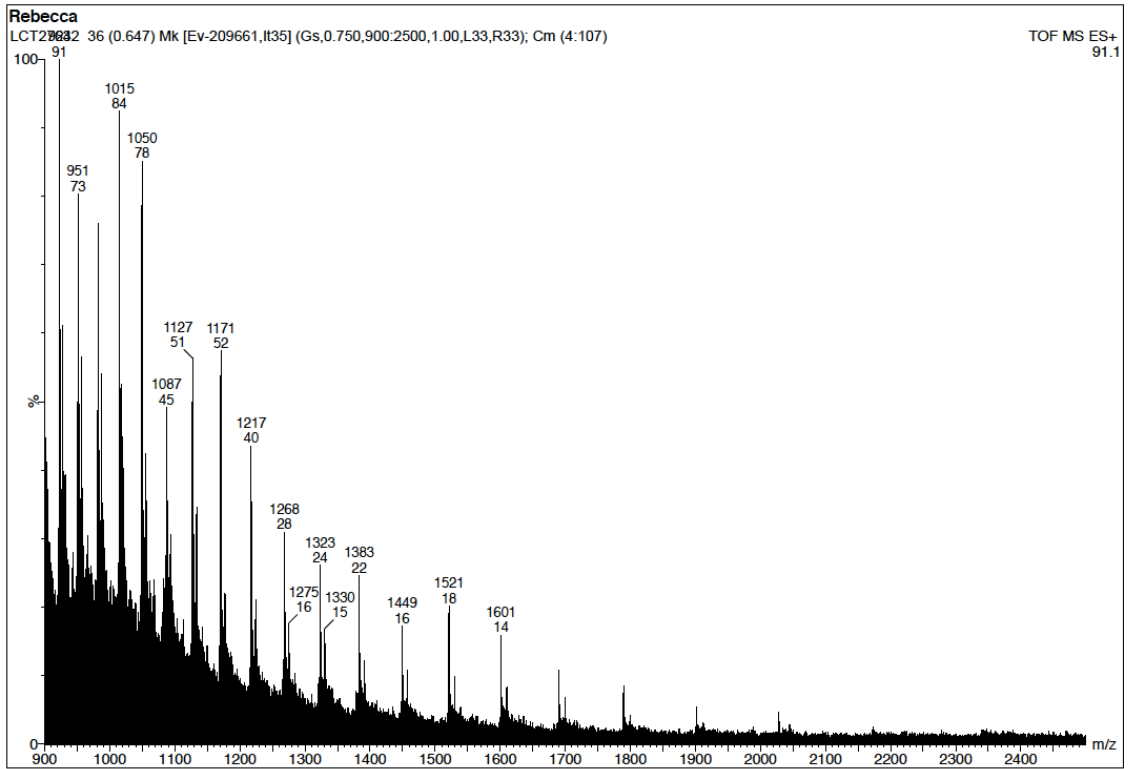
Raw data for Figure 68**: pH 7.2**
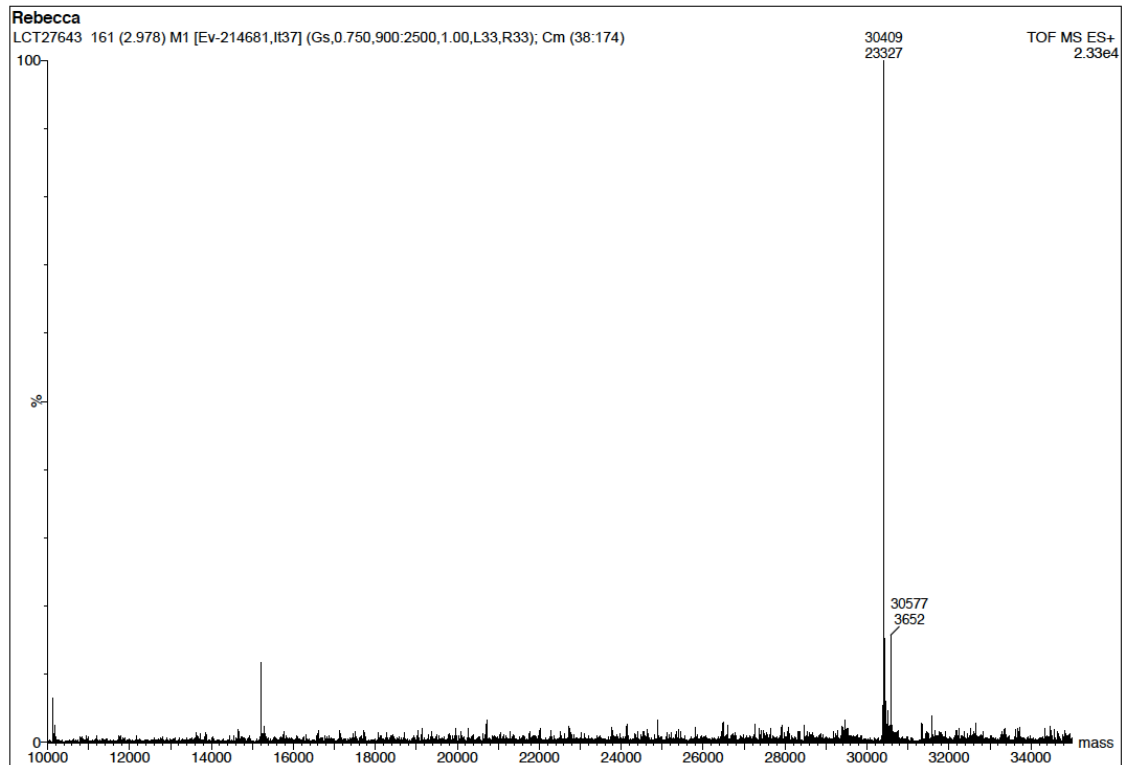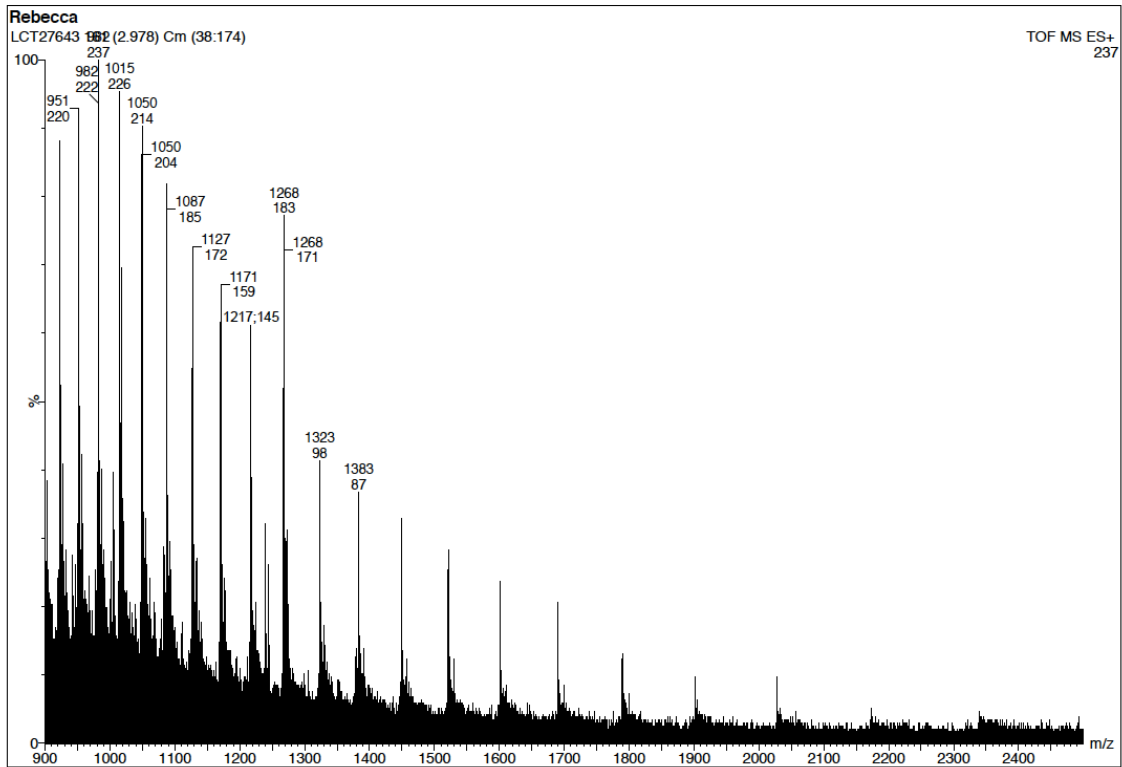
Raw data for Figure 69**: pH 8.1**
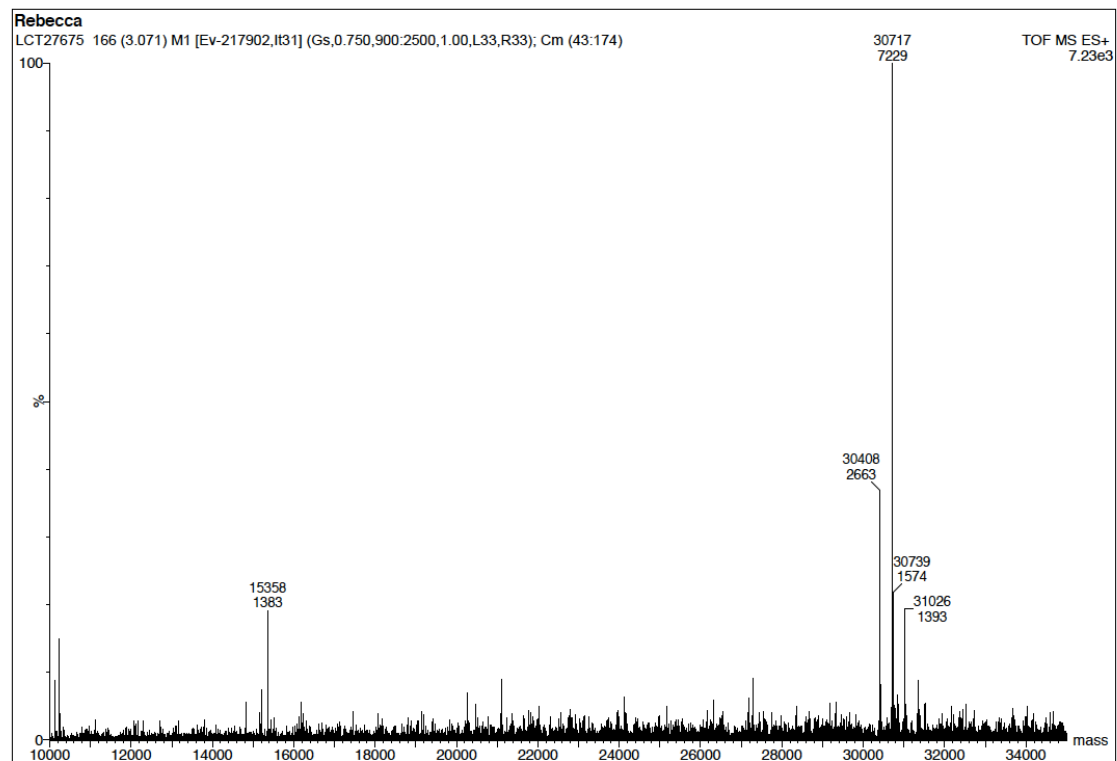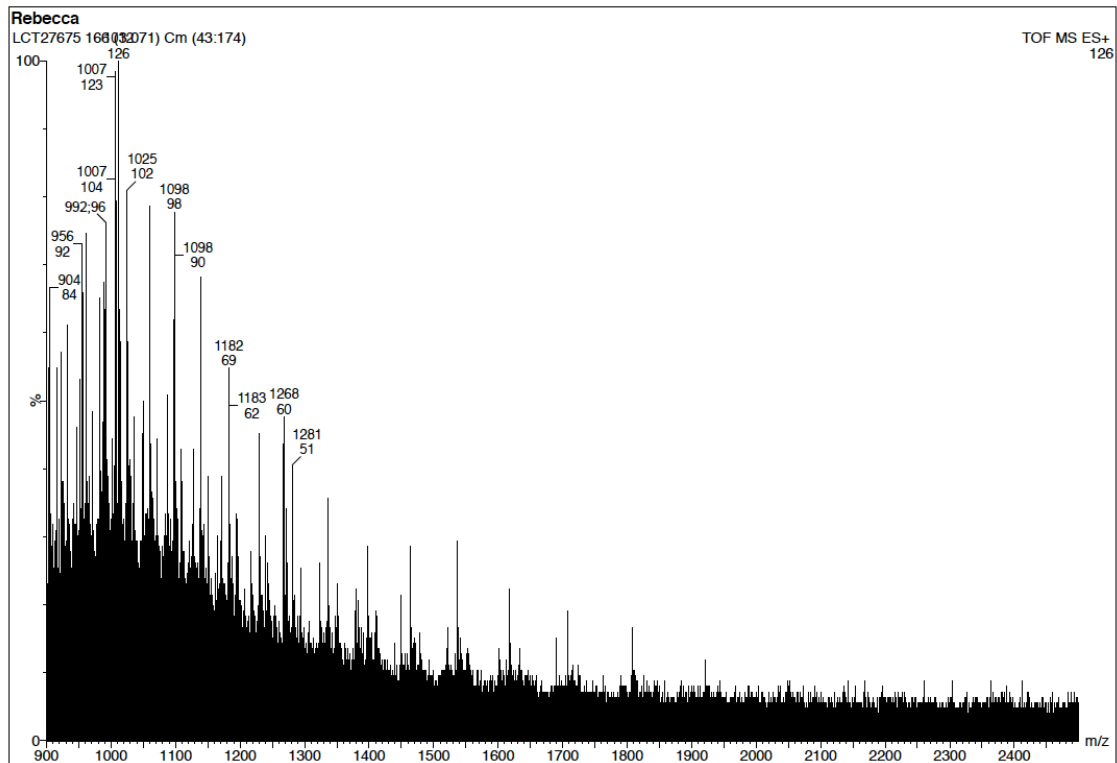
Raw data for Figure 69**: pH 7.9**
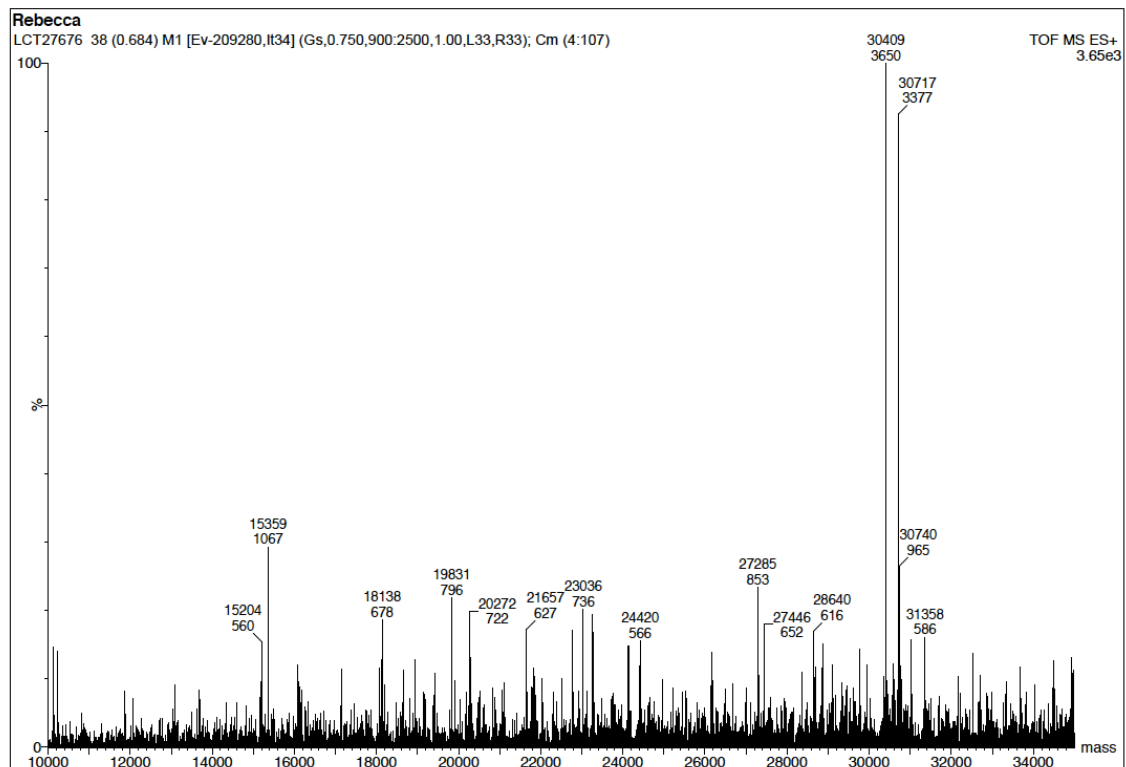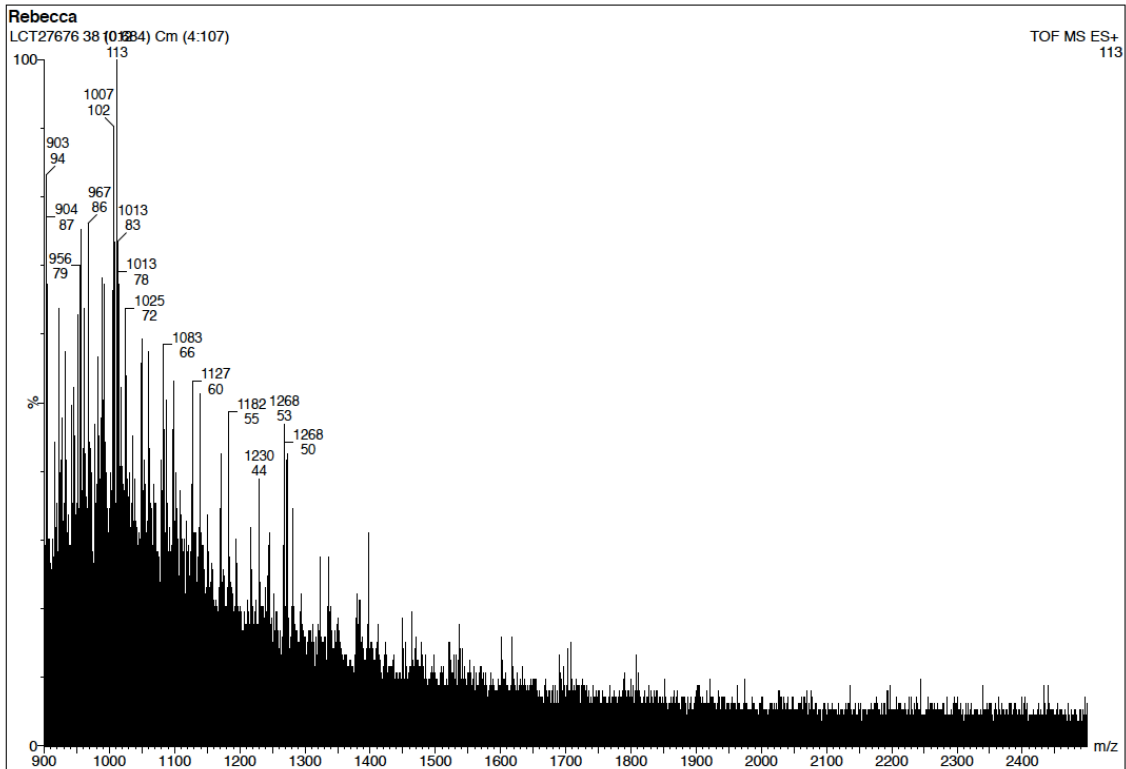
Raw data for Figure 69**: pH 7.6**
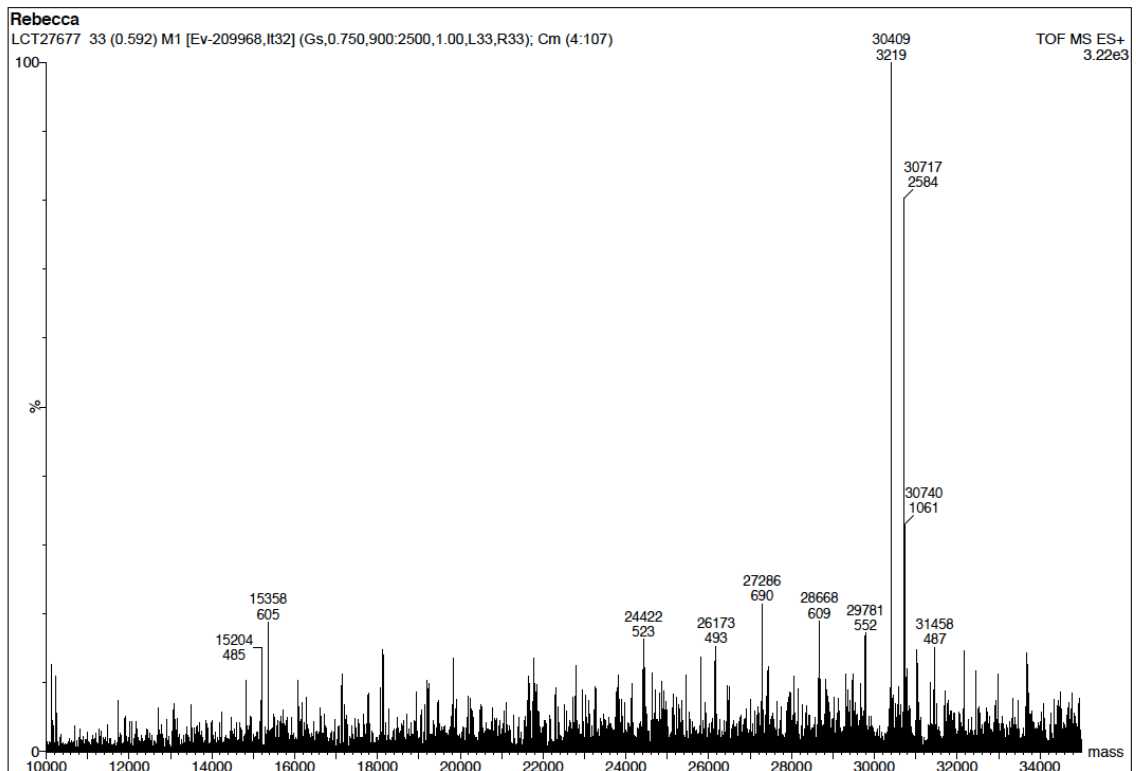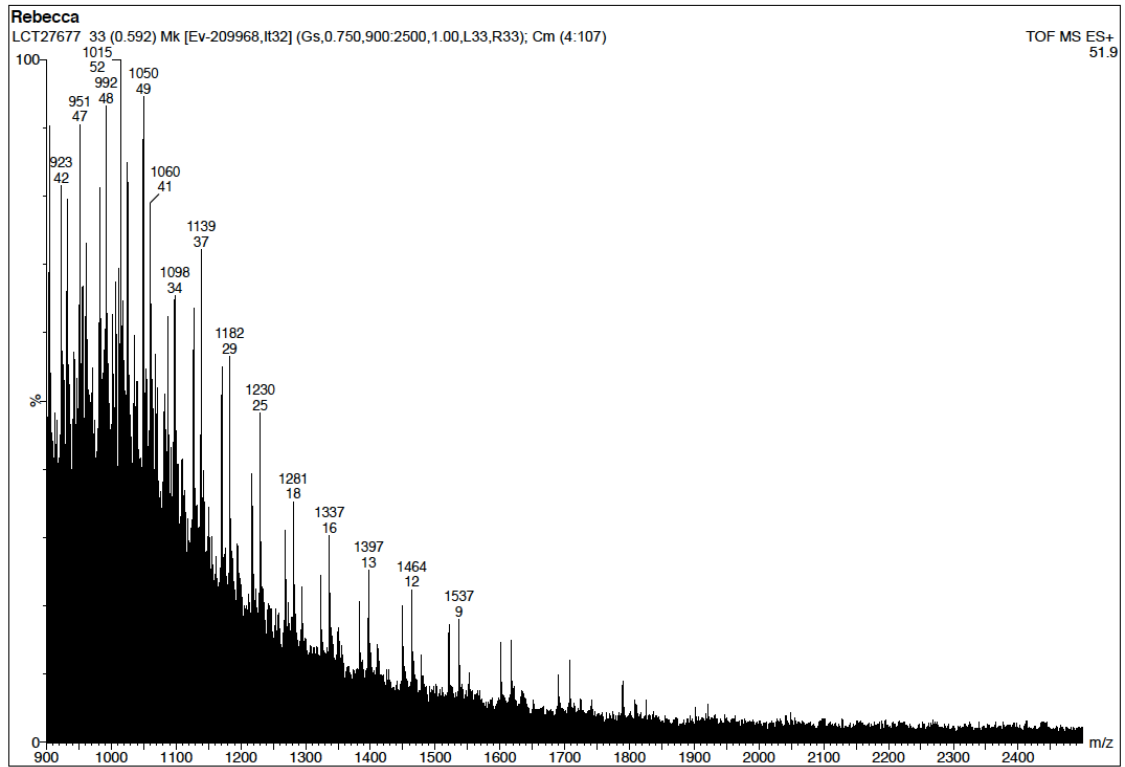
Raw data for Figure 69**: pH 7.4**
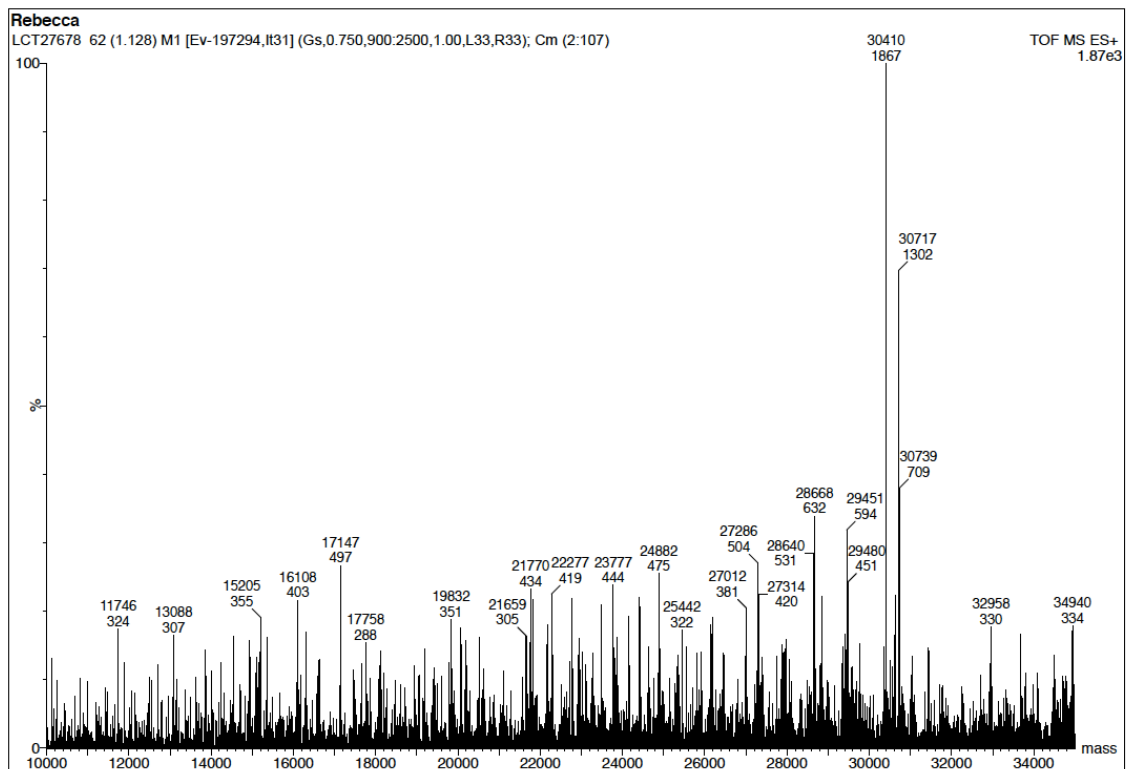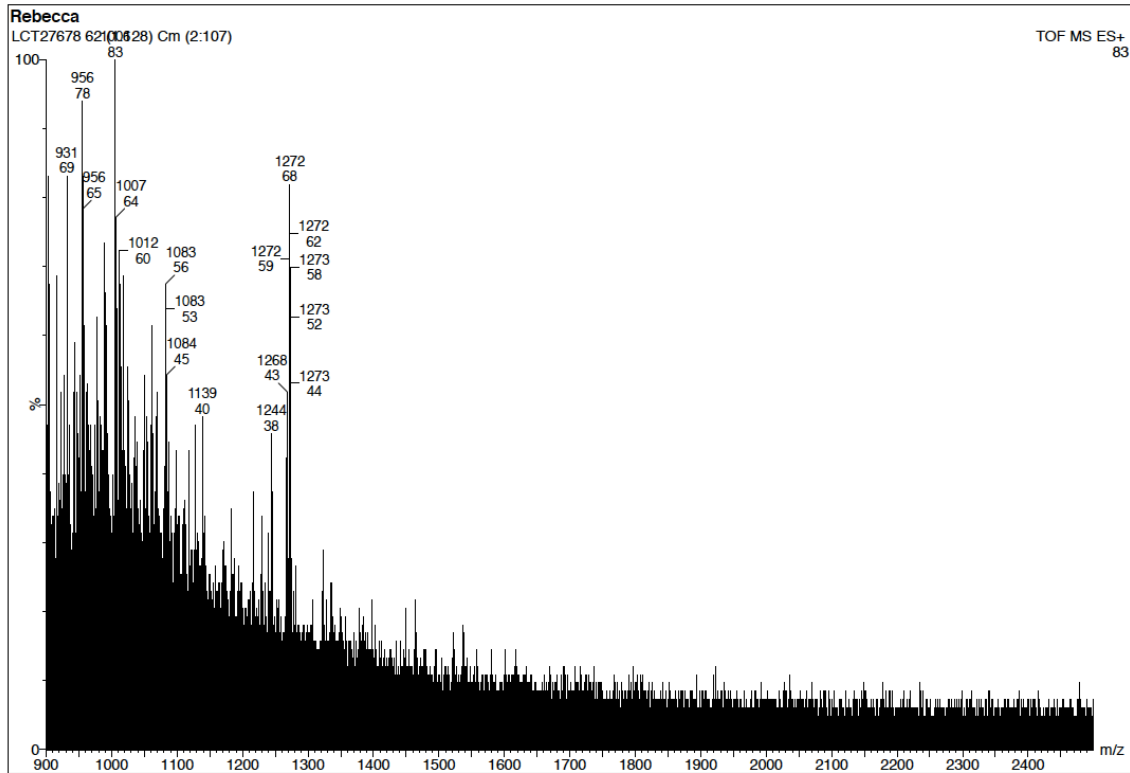
Raw data for Figure 69**: pH 7.3**
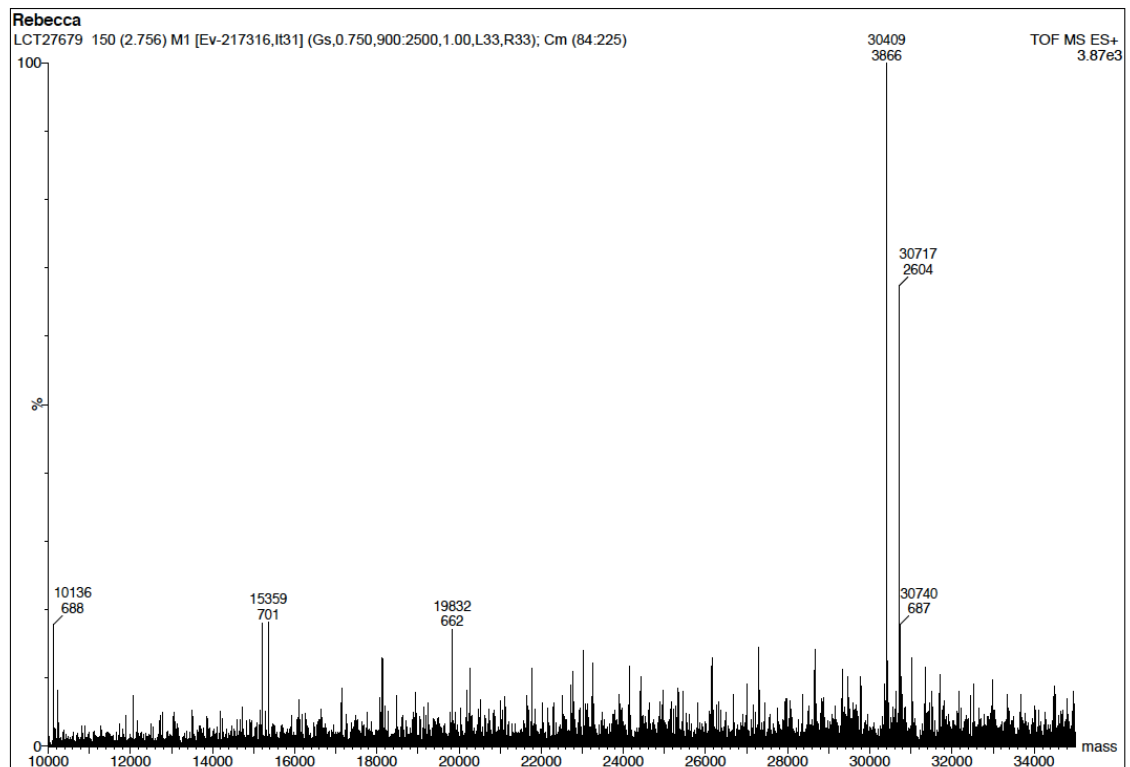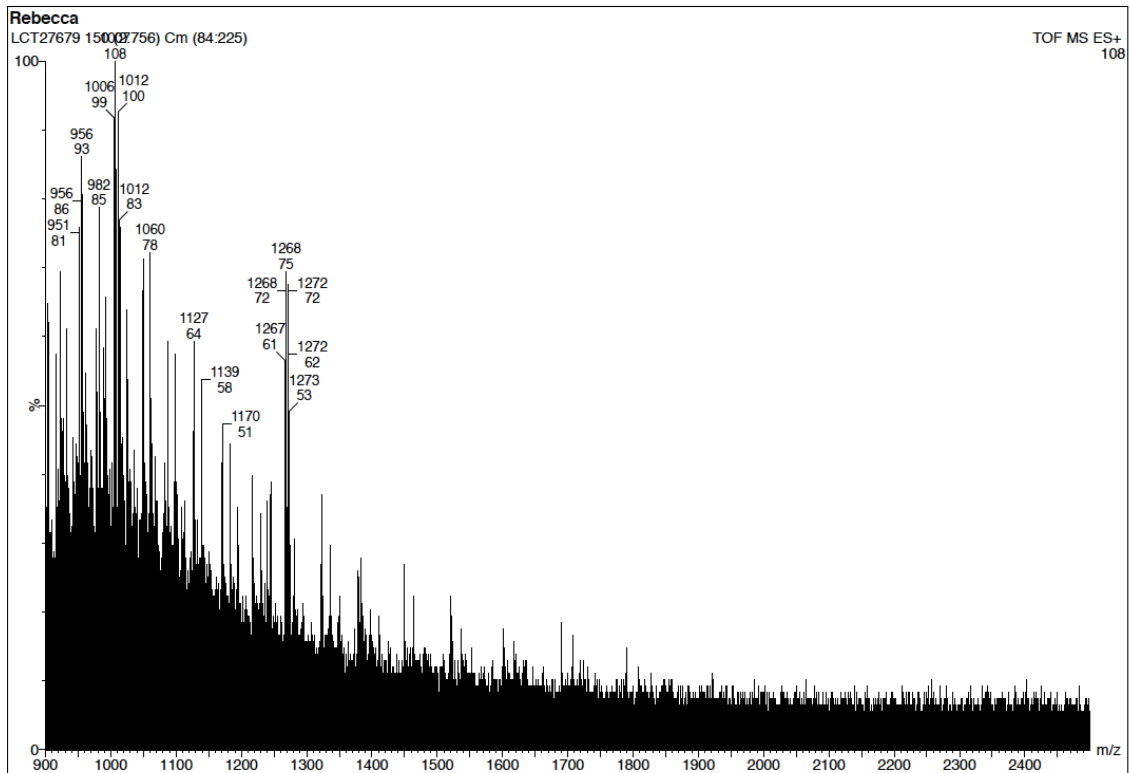
Raw data for Figure 69**: pH 7.2**
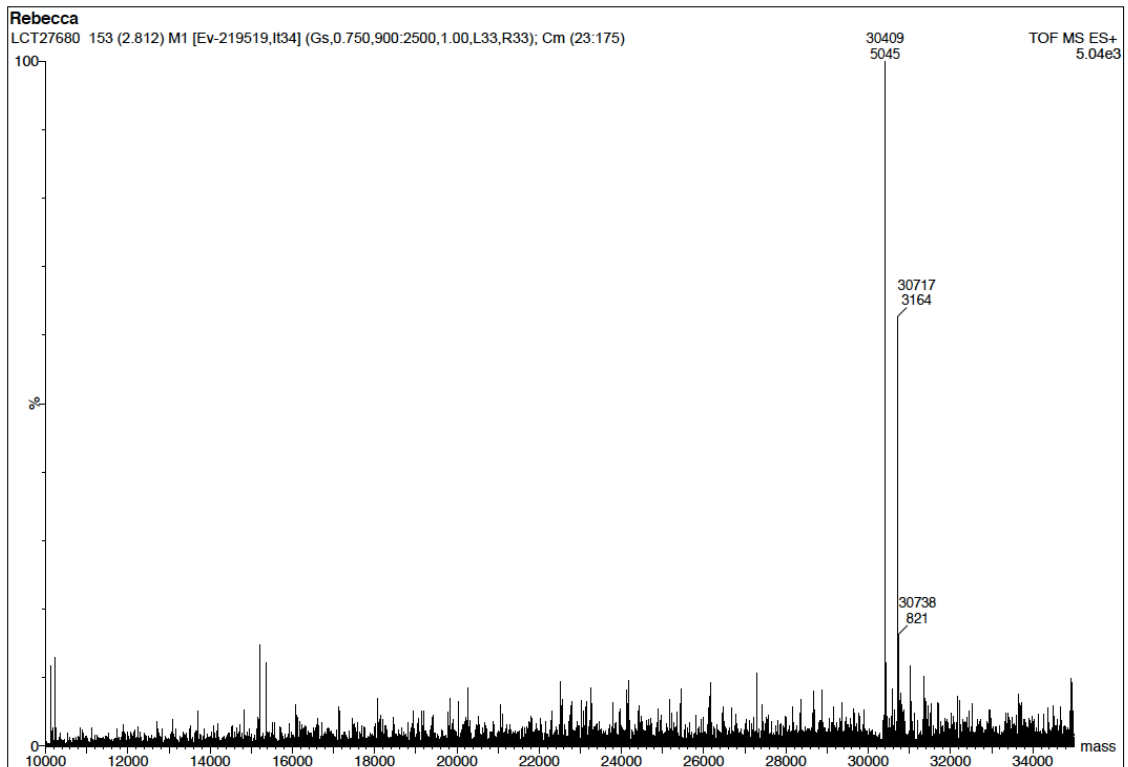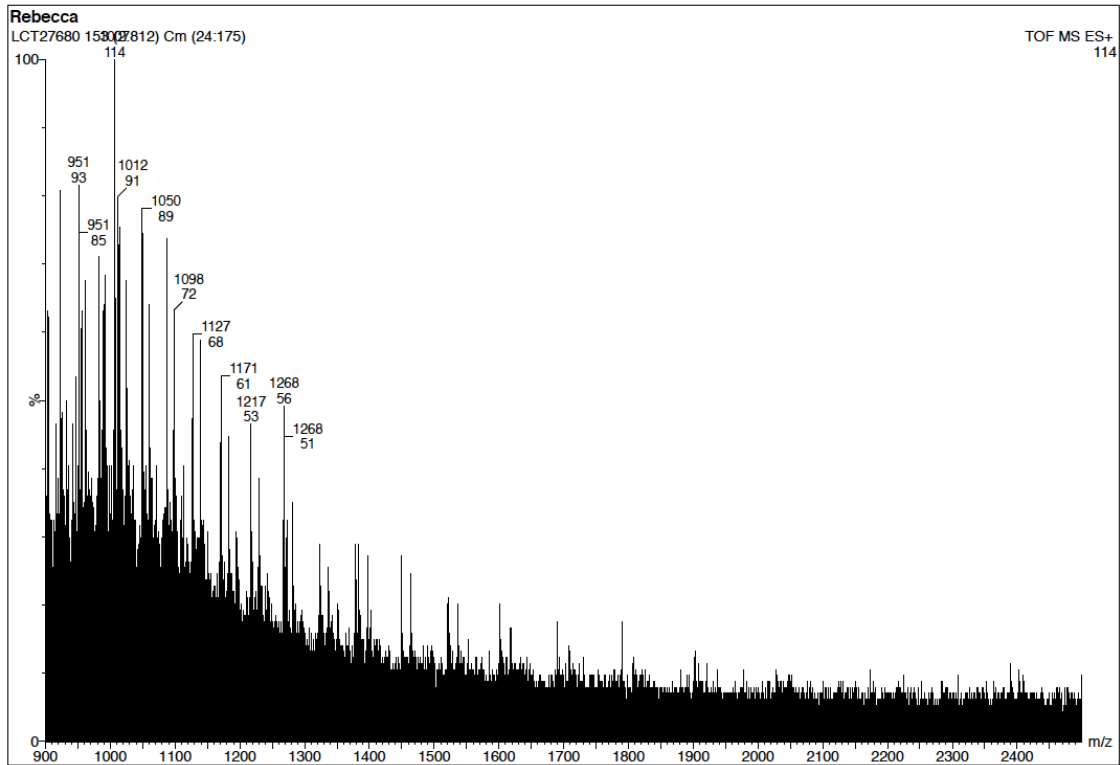
Raw data for Figure 70**: 2 min**
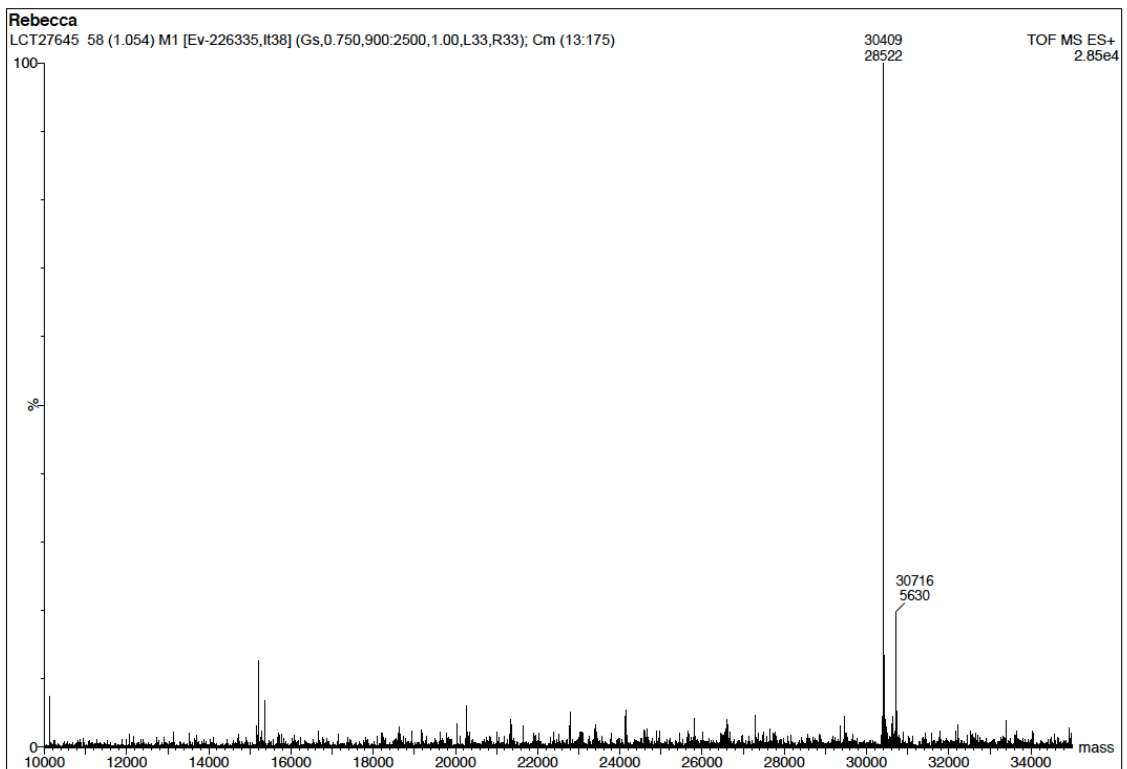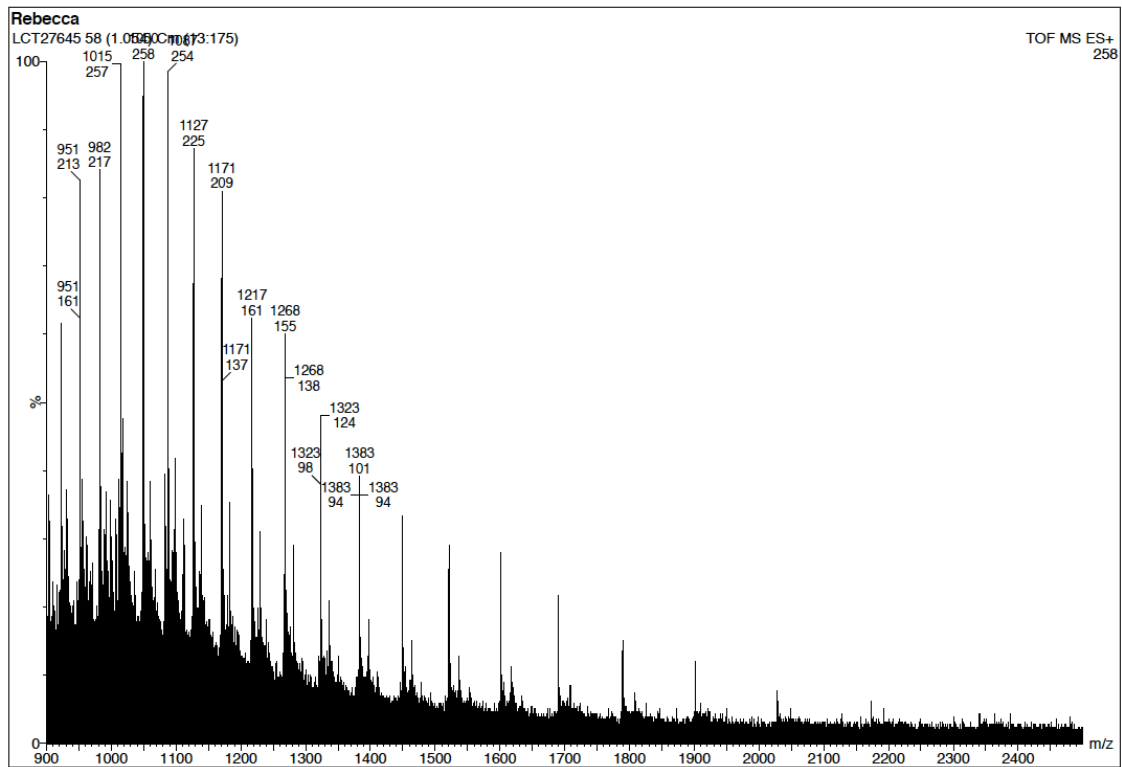
Raw data for Figure 70**: 30 min**
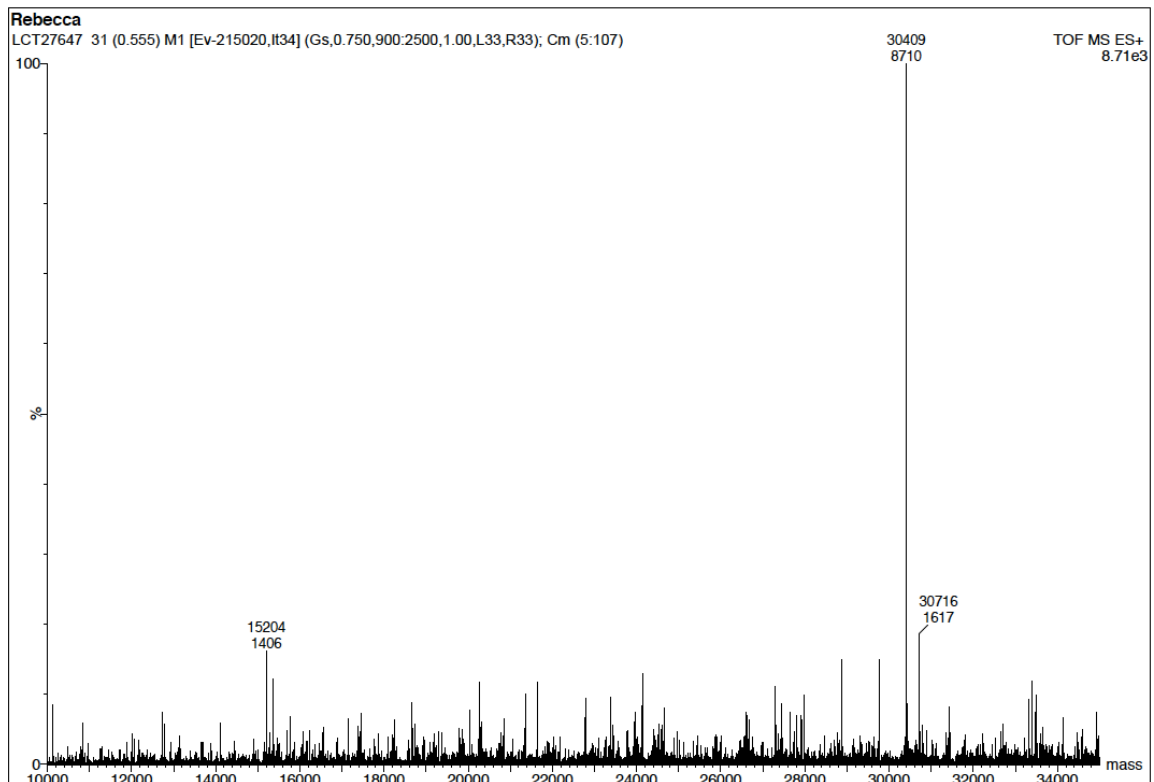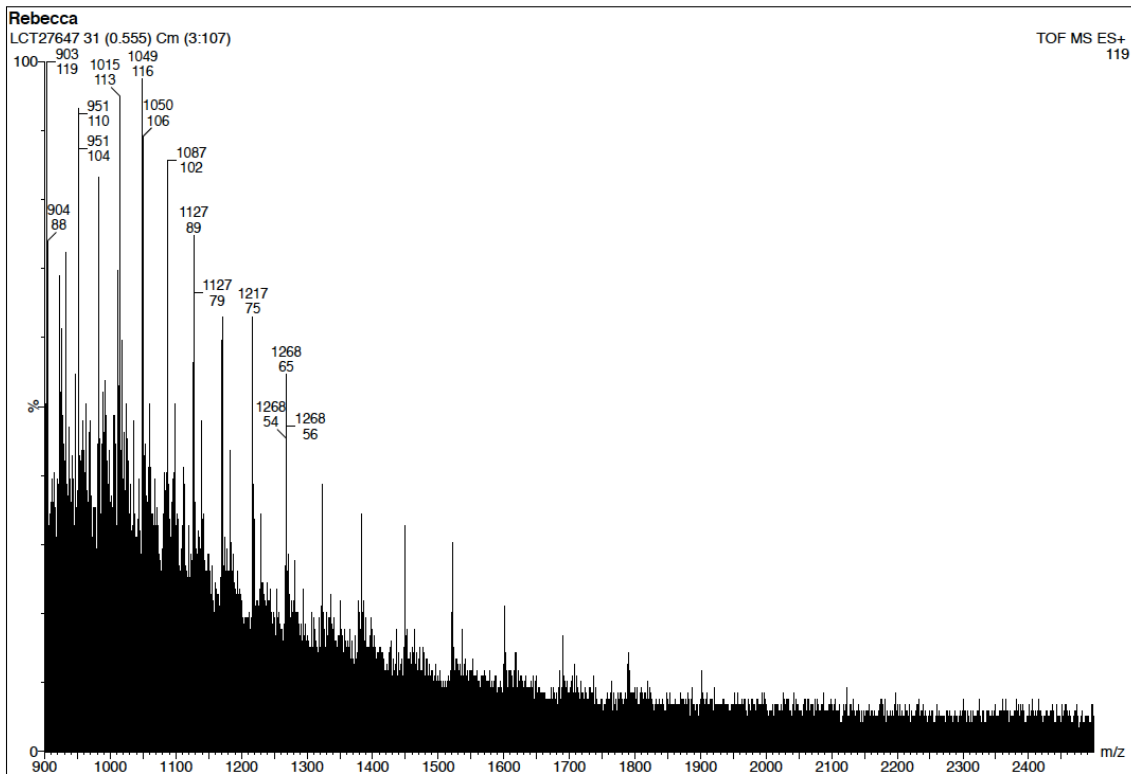
Raw data for Figure 70**: 60 min**
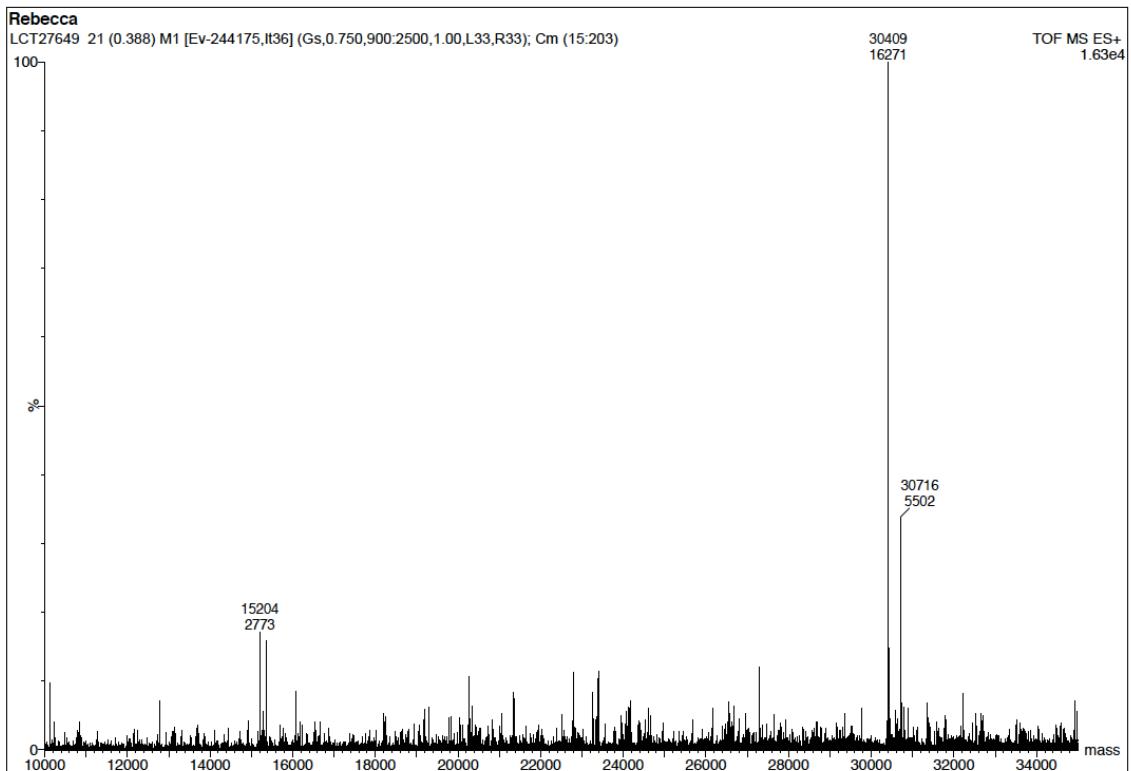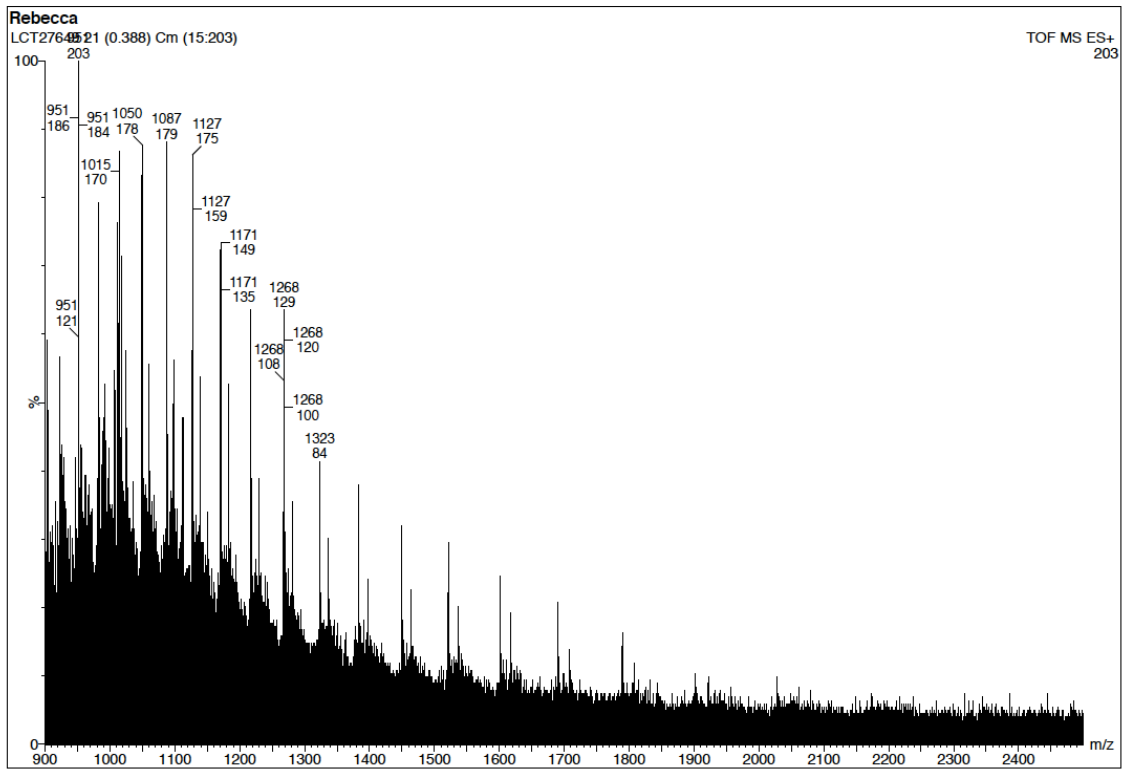
Raw data for Figure 70**: 120 min**
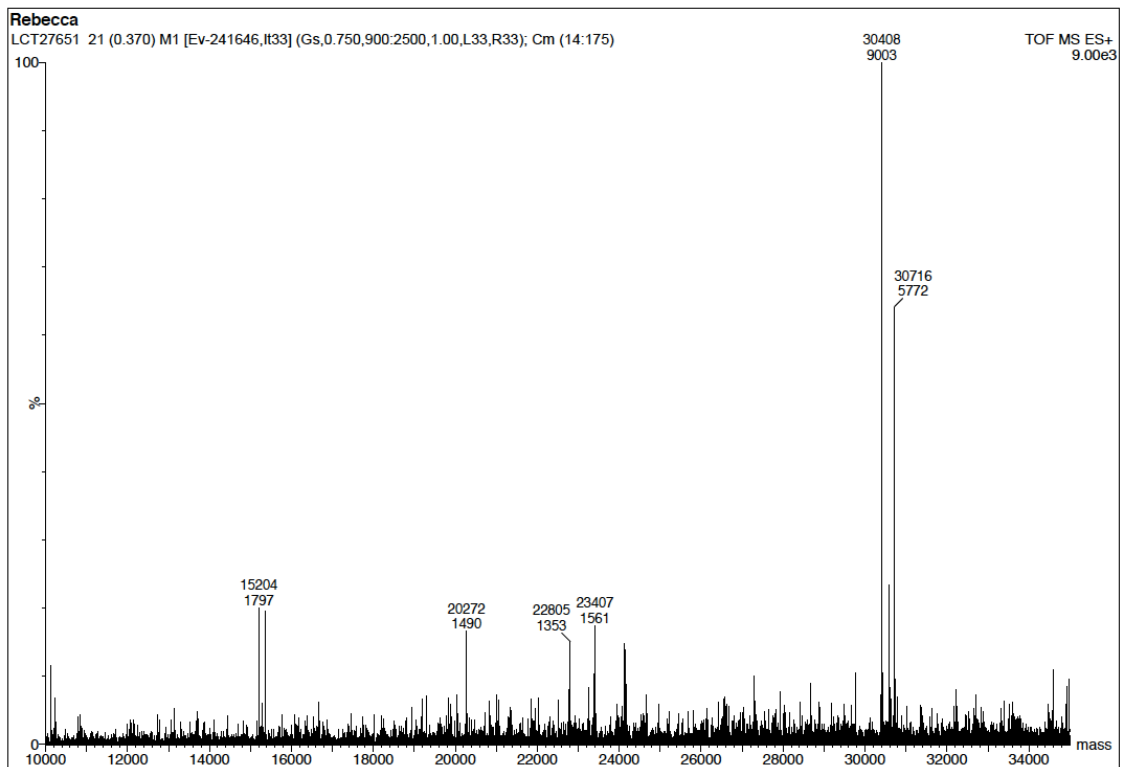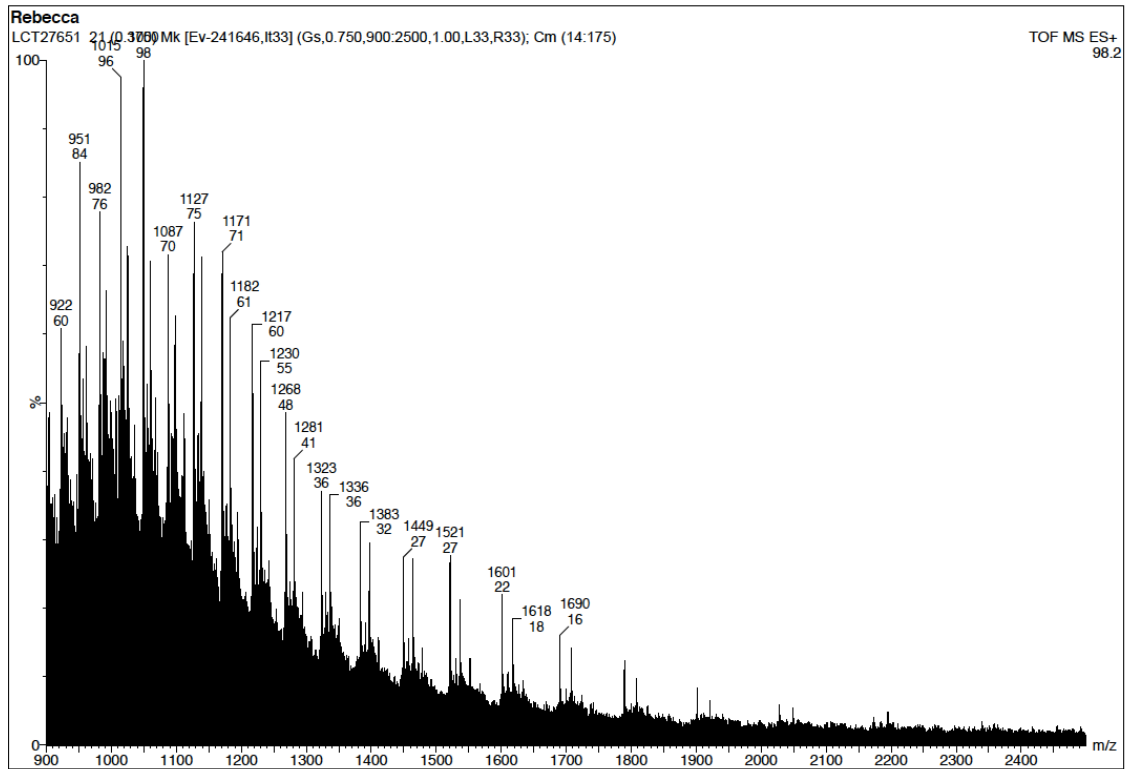
Raw data for Figure 75
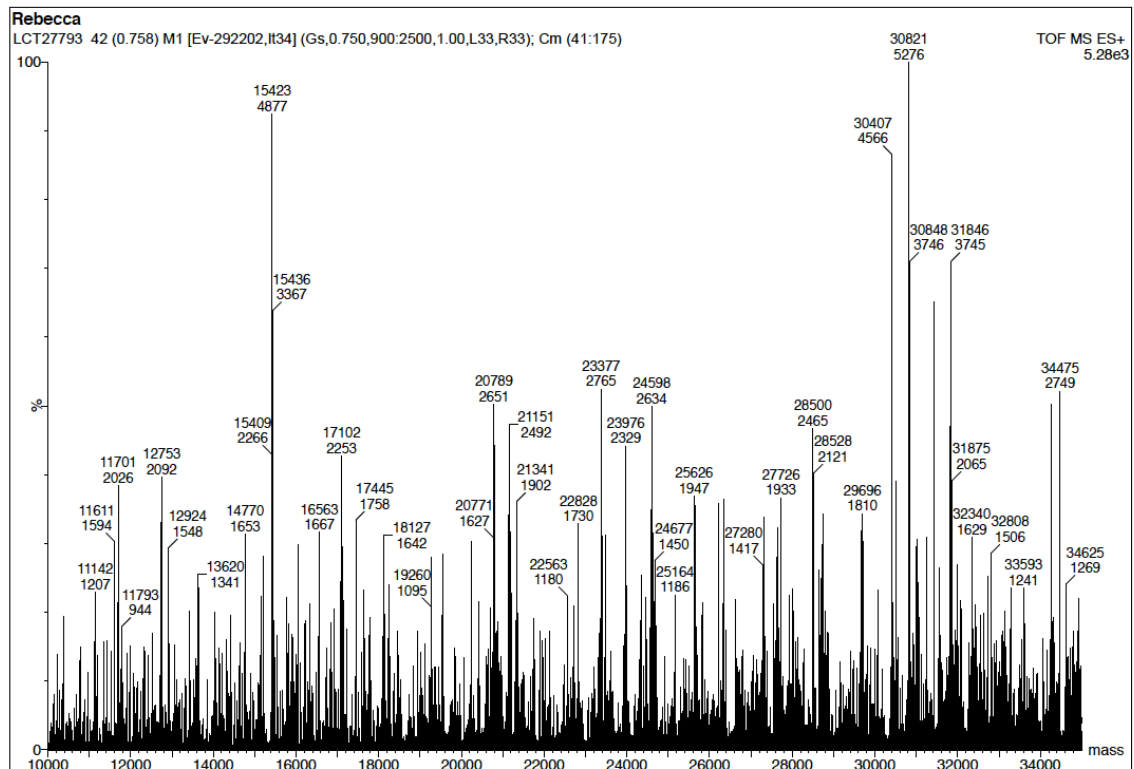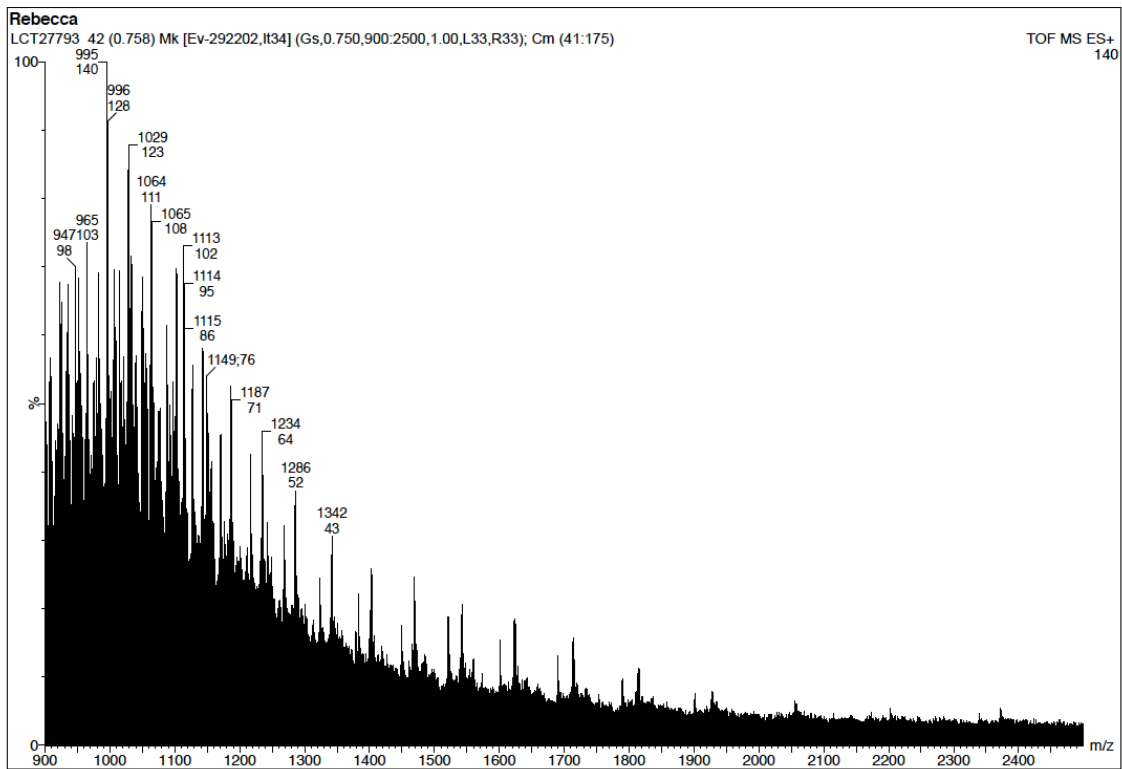
Raw data for Figure 76**: 270 min**
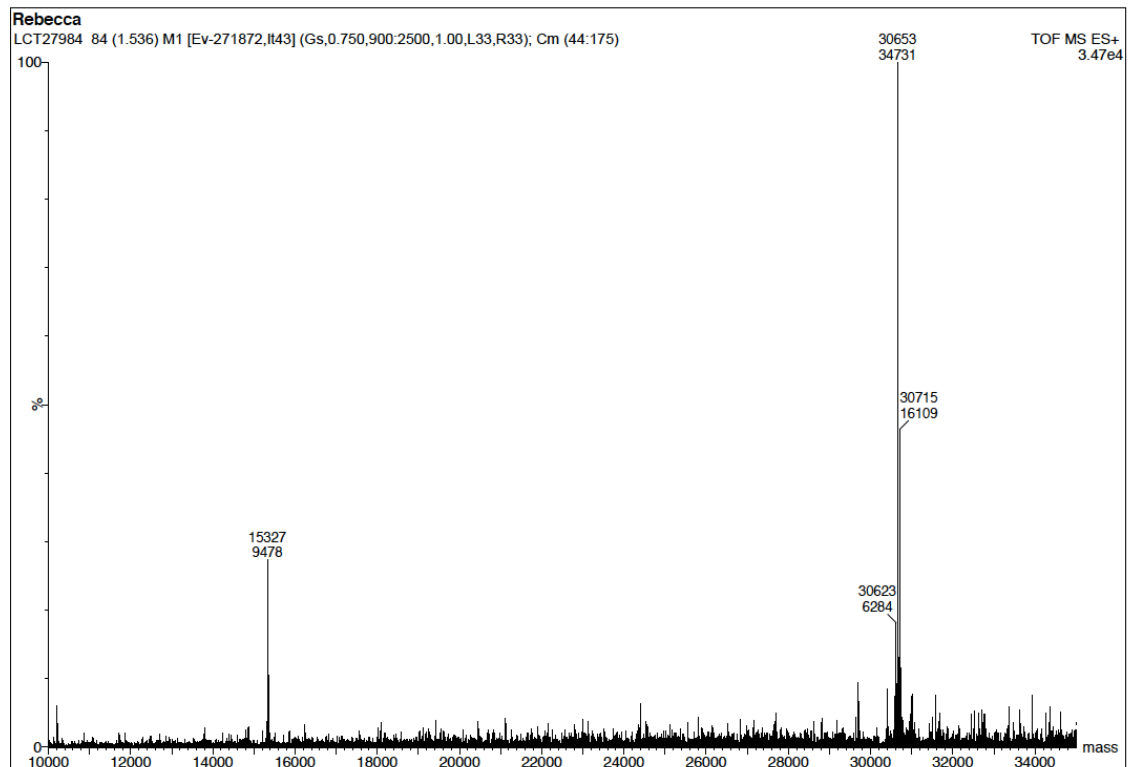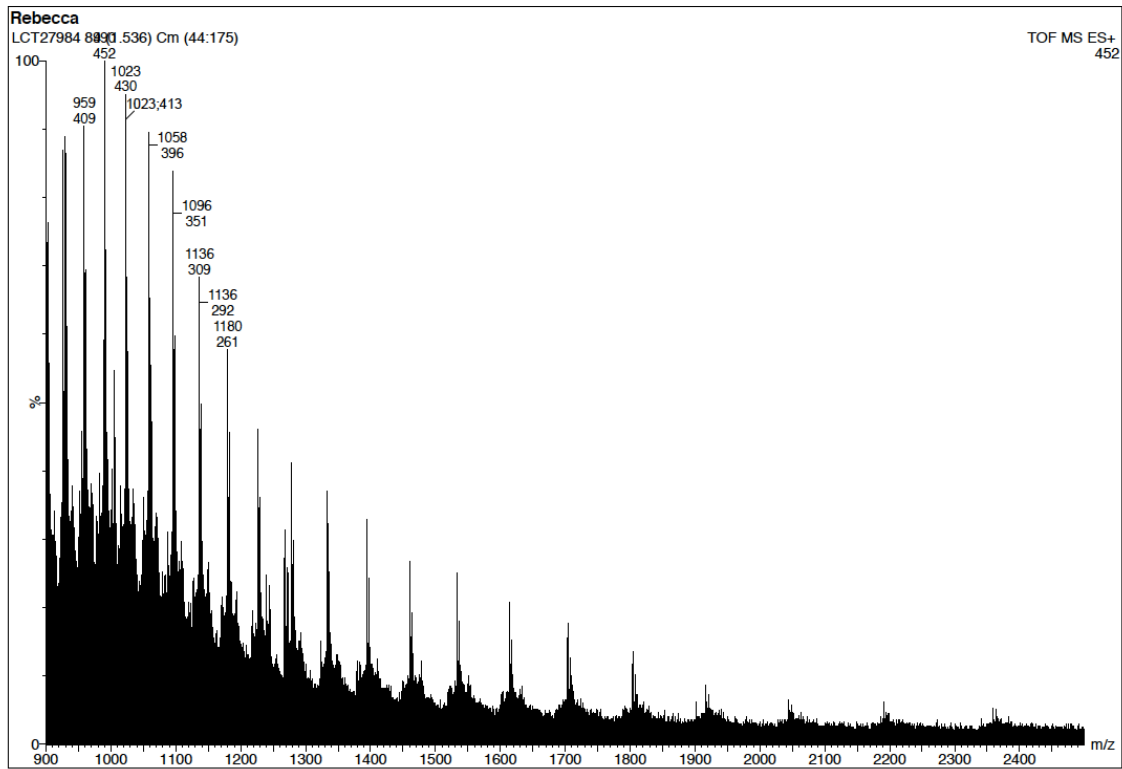
Irreversibility test for acrylamide reaction with TS

Method

Sample 'A': 192 μL TS (10 μM in ammonium bicarbonate (10 mM), DTT (1 mM)) + 8 μL acrylamide **54** (from 250 μM stock in MeOH).

Sample 'B': 192 μL TS (10 μM in ammonium bicarbonate (10 mM), DTT (1 mM)) + 8 μL acrylamide **67** (from 250 μM stock in MeOH).

Both samples A and B were left to equilibrate at room temperature for 3.5 h. A 25 μL aliquot was then taken from both A and B and analysed by ESI MS (Sample A: LCT26577, Sample B: LCT26578).

A 100 μL aliquot was then taken from Sample A and from Sample B, and to each was added 4 μL of the 250 μM stock solution for acrylamides **67** or **54** respectively. Both were subsequently analysed after 60 min (Sample A + **67**: LCT26581, Sample B + **54**: LCT26582).

Raw data for Figure 87**: LCT26577**

R Nonoo TS 1
LCT26577 26 (0.462) M1 [Ev0,It17] (Gs,0.750,900:3000,1.00,L33,R33); Cm (25:175)
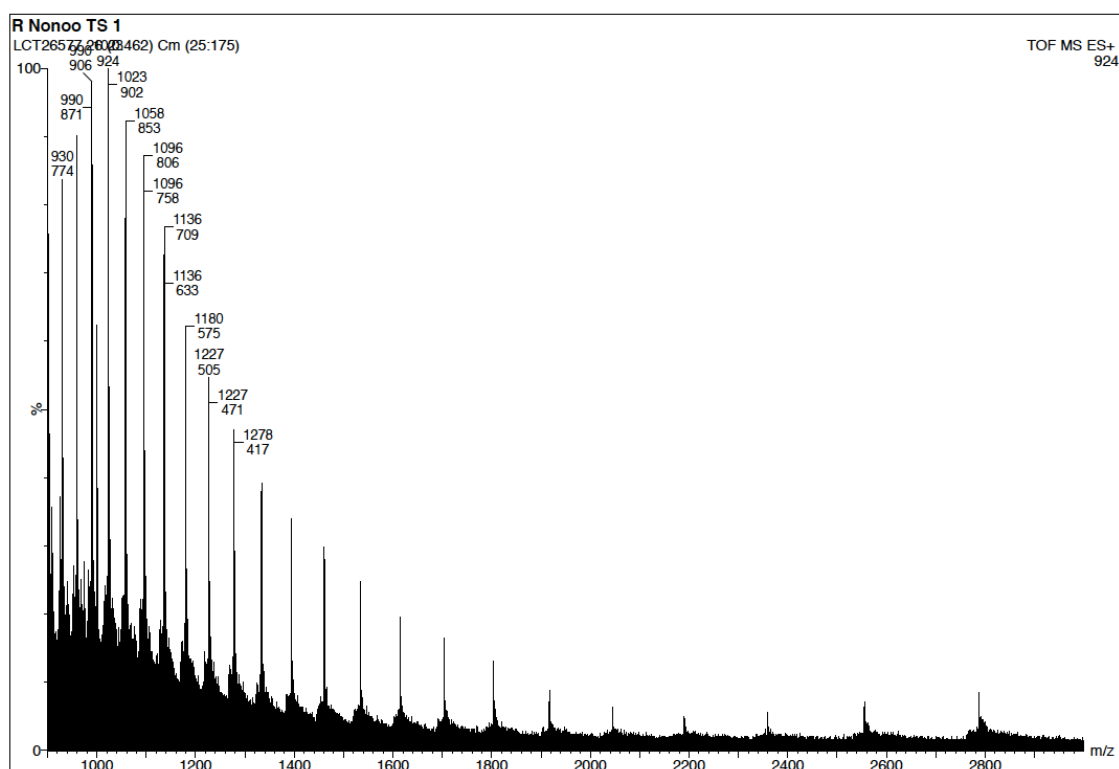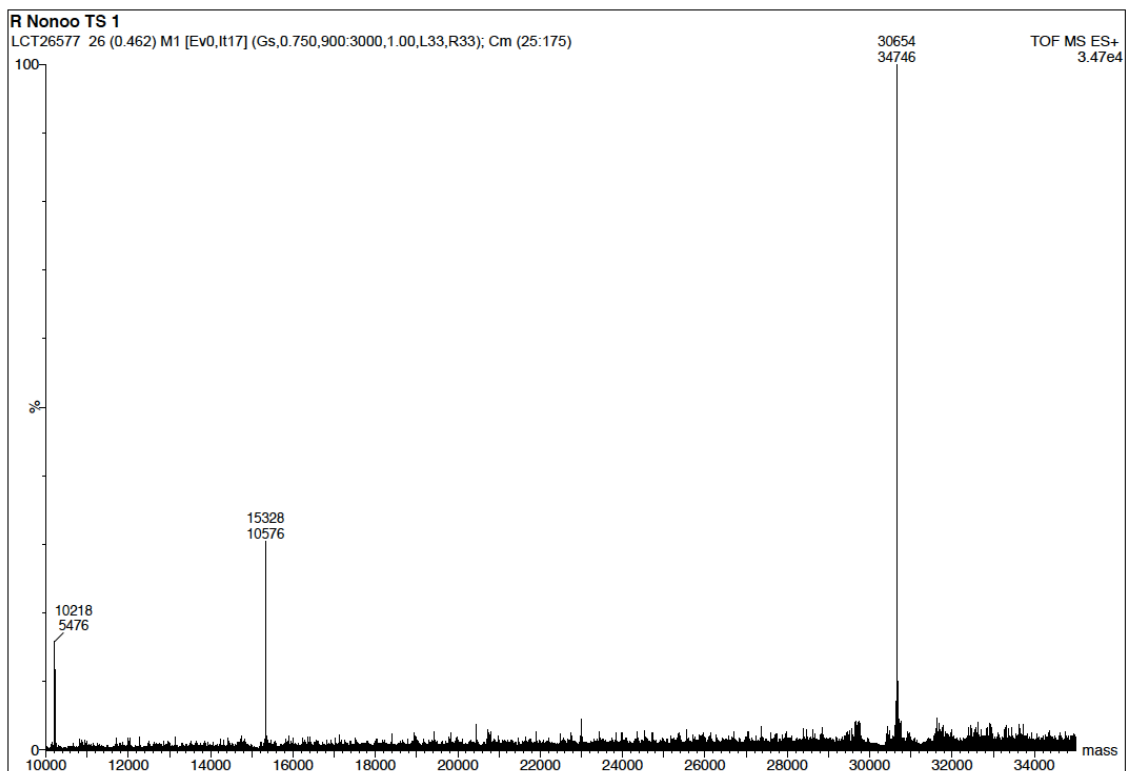
Raw data for Figure 87**: LCT26578**
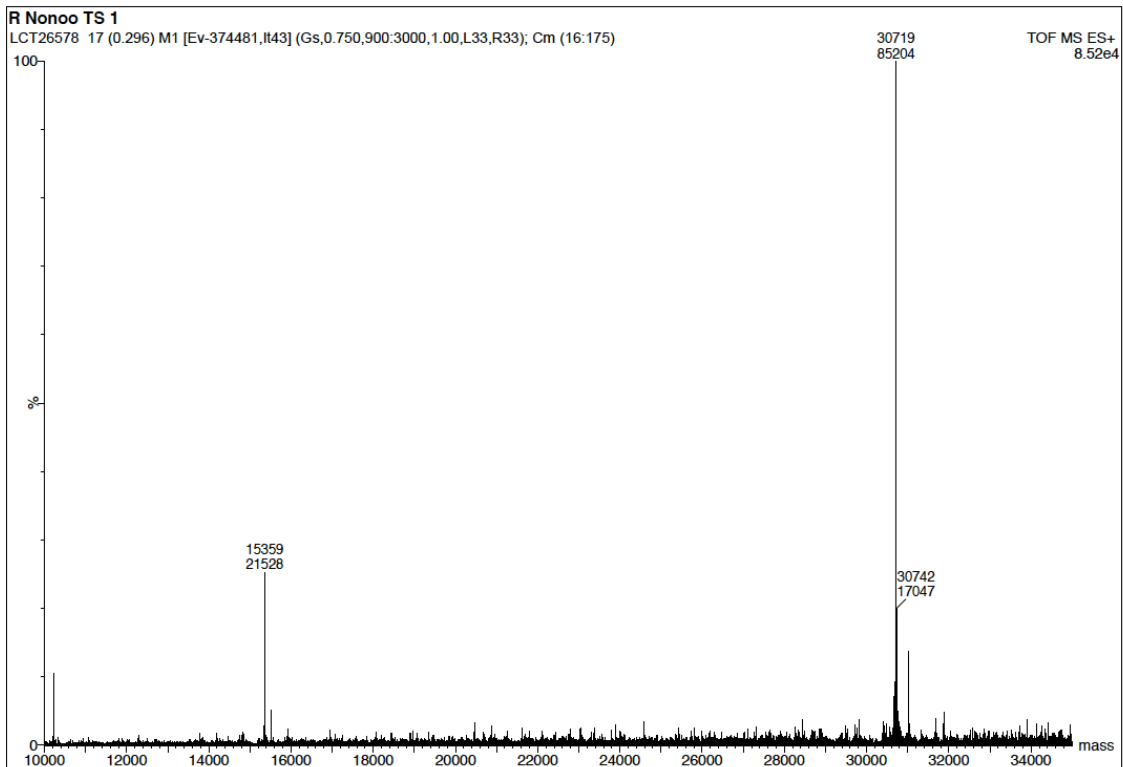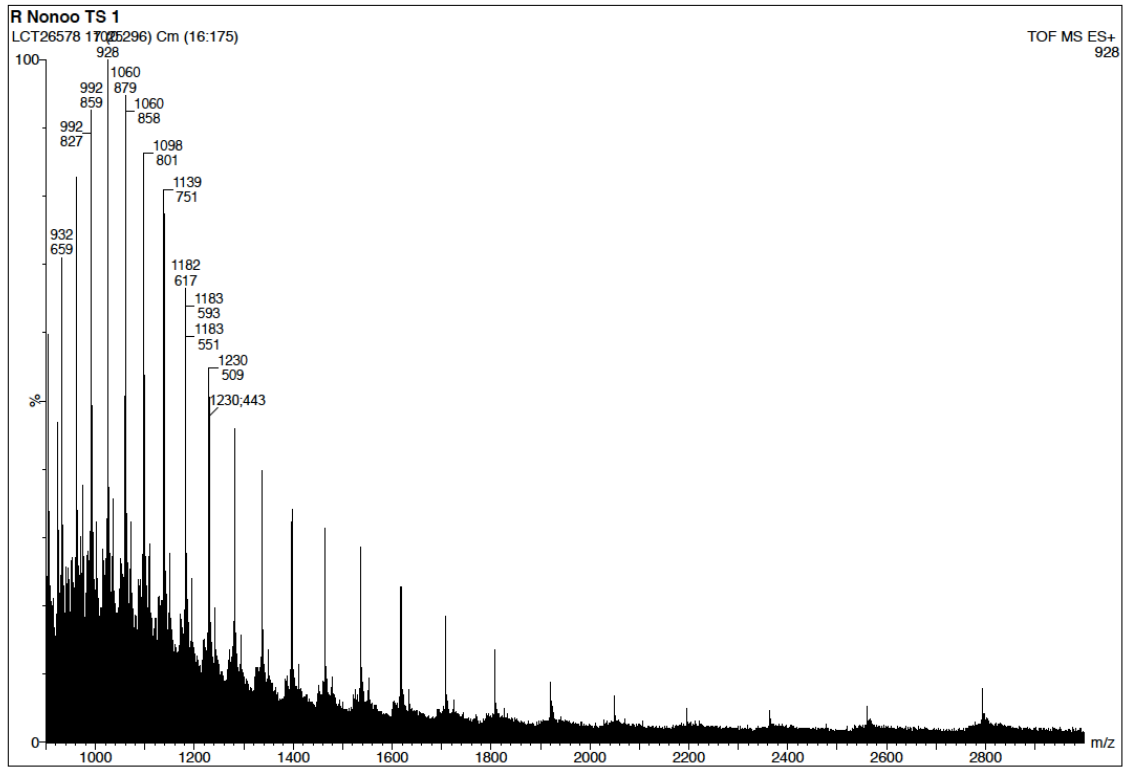
Raw data for Figure 87**: LCT27581**
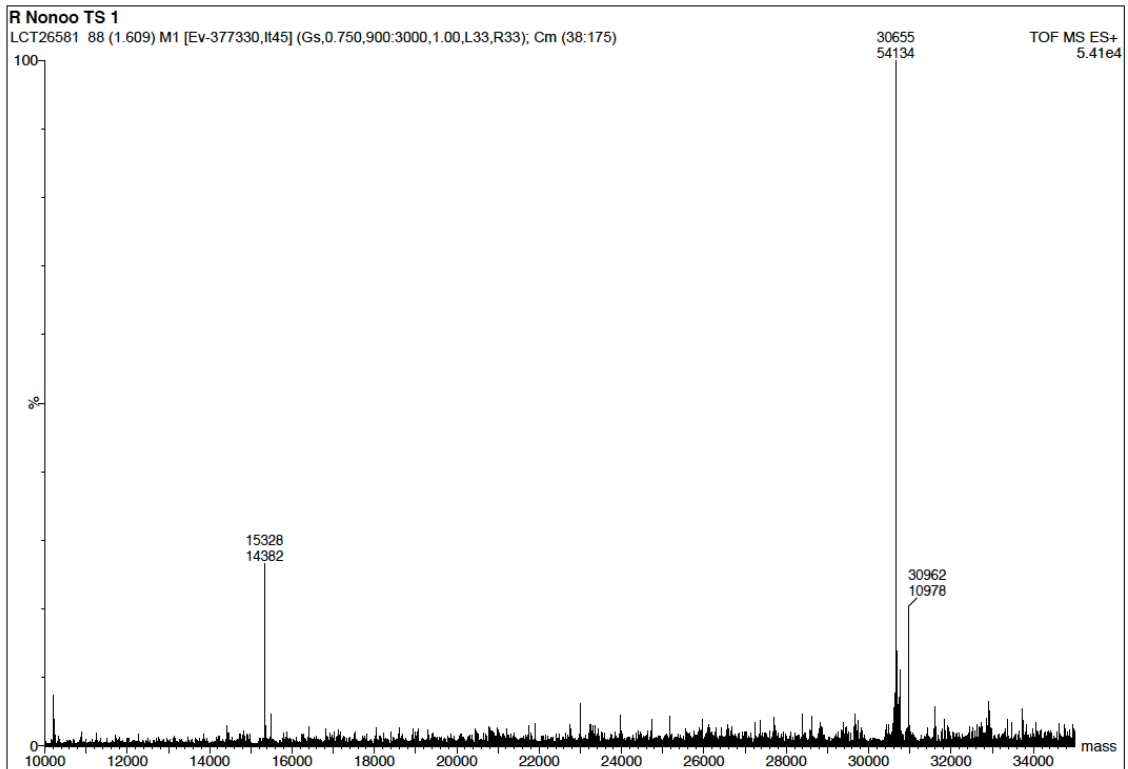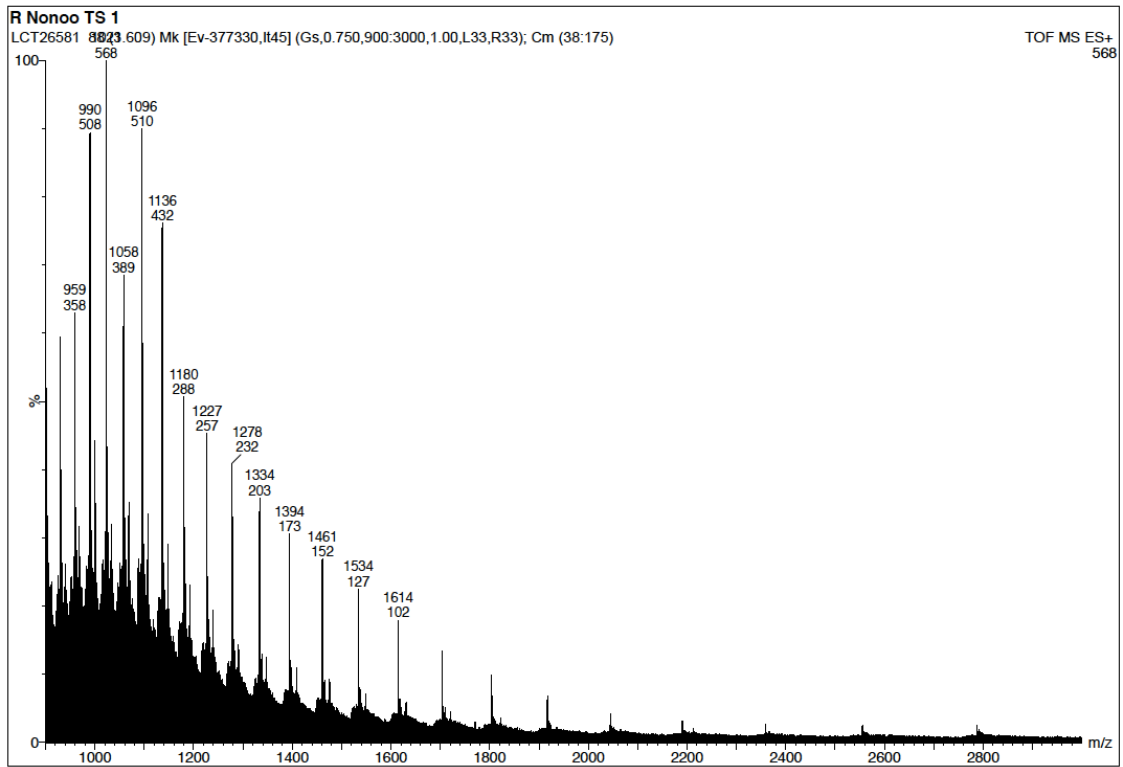
Raw data for Figure 87**: LCT26582**
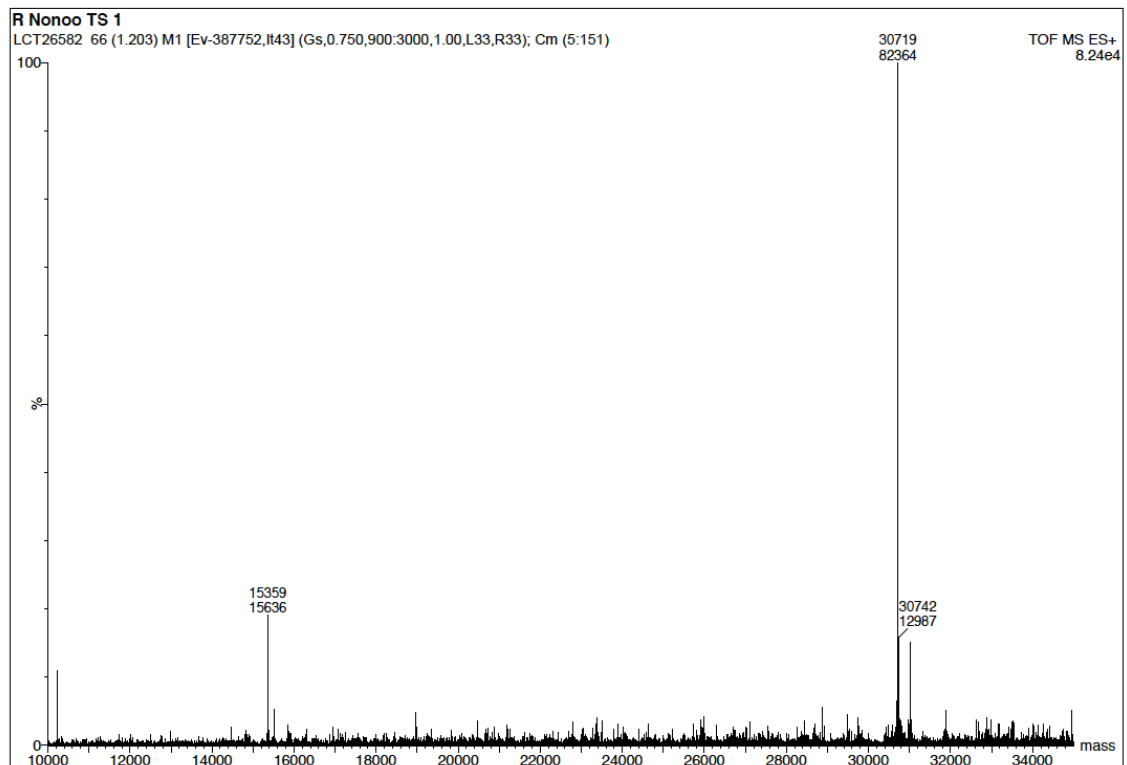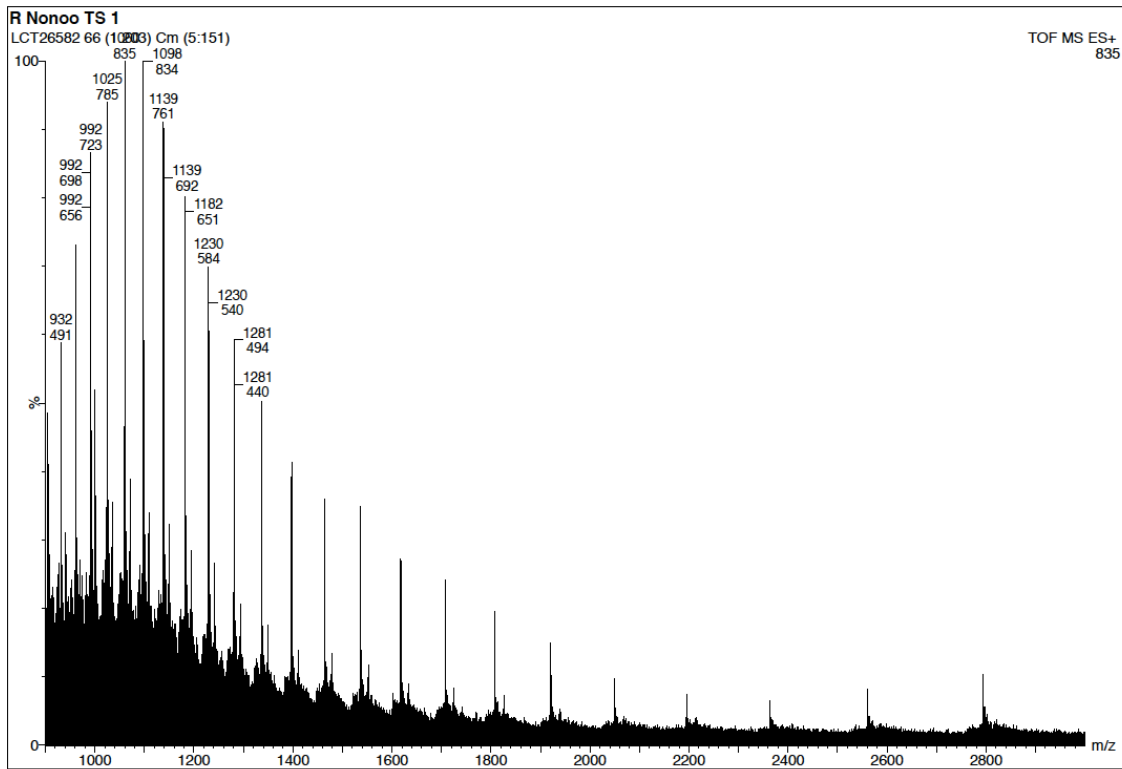
Raw data for Figure 88**: 2 min**
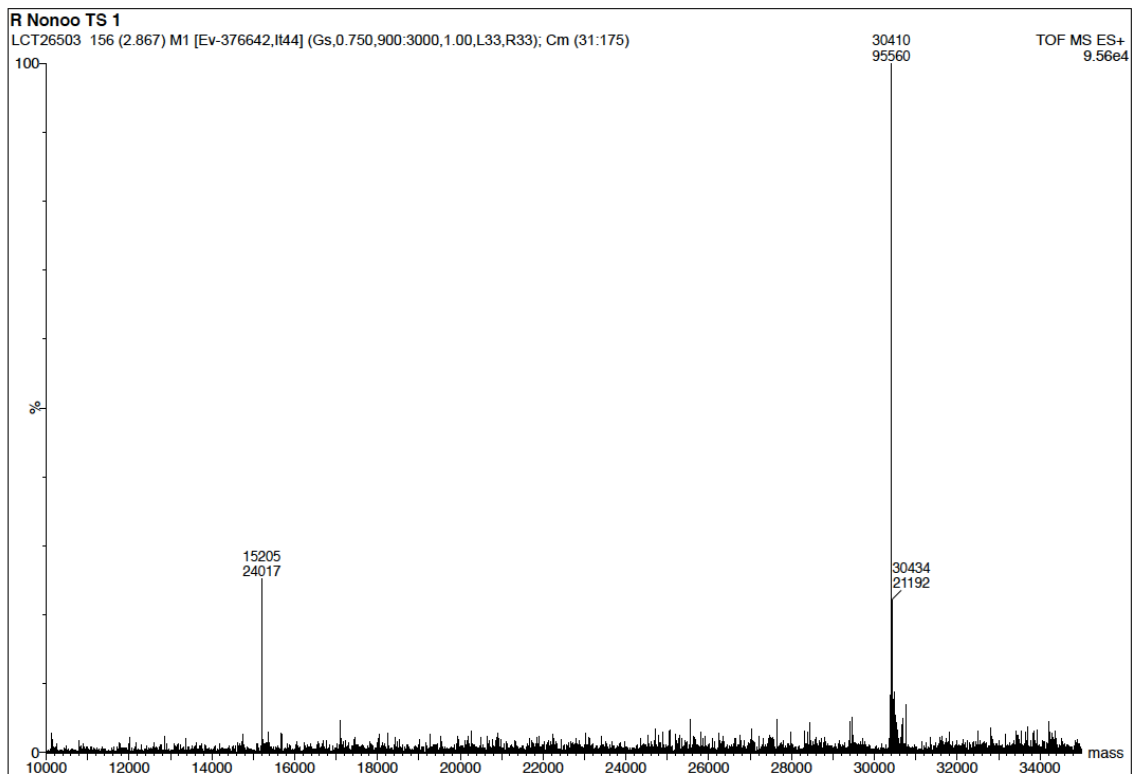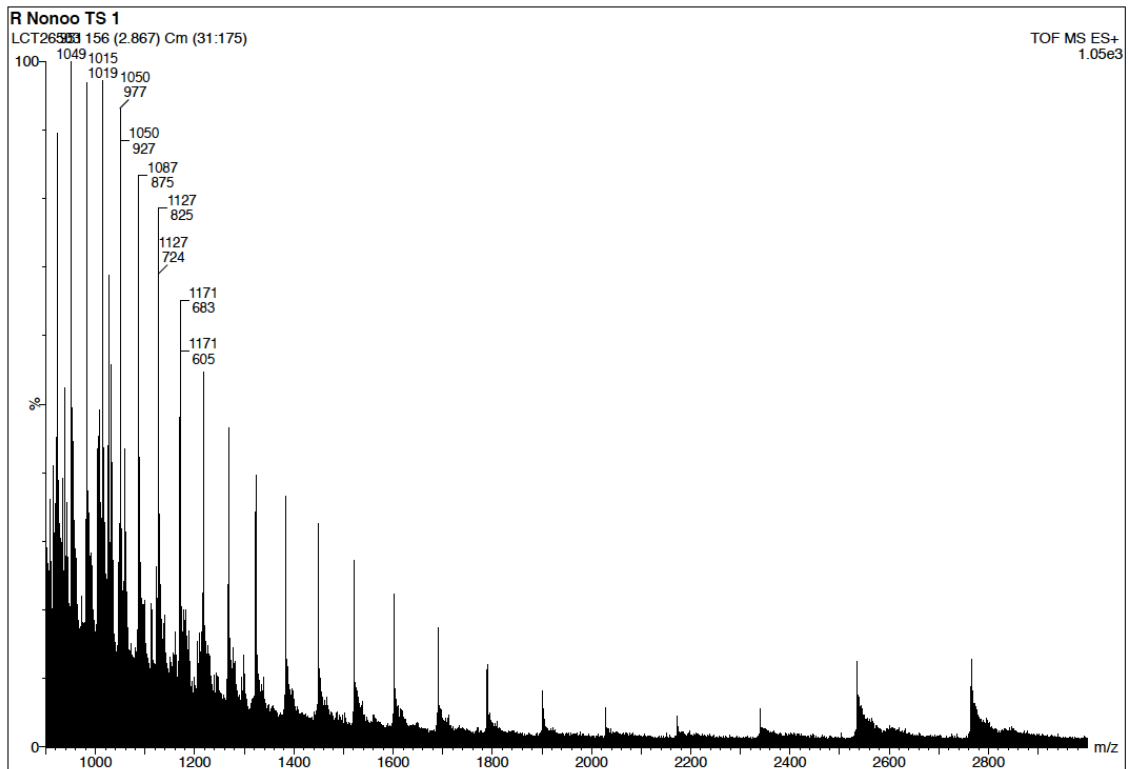
Raw data for Figure 88**: 10 min**
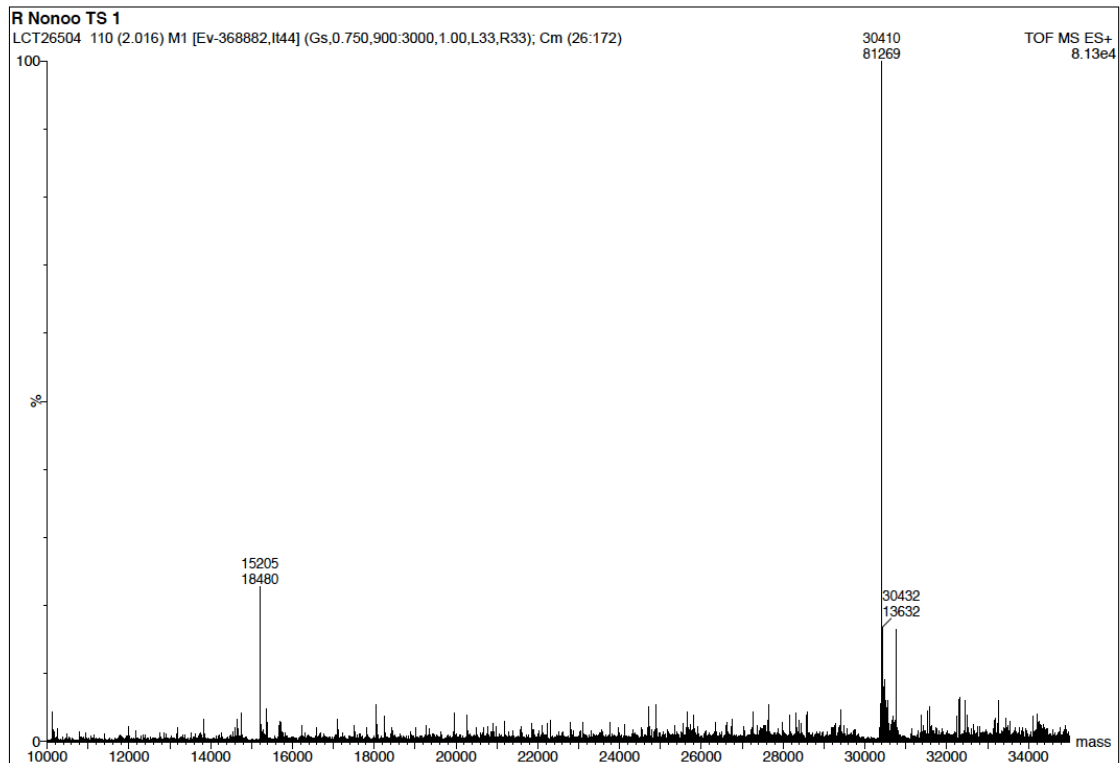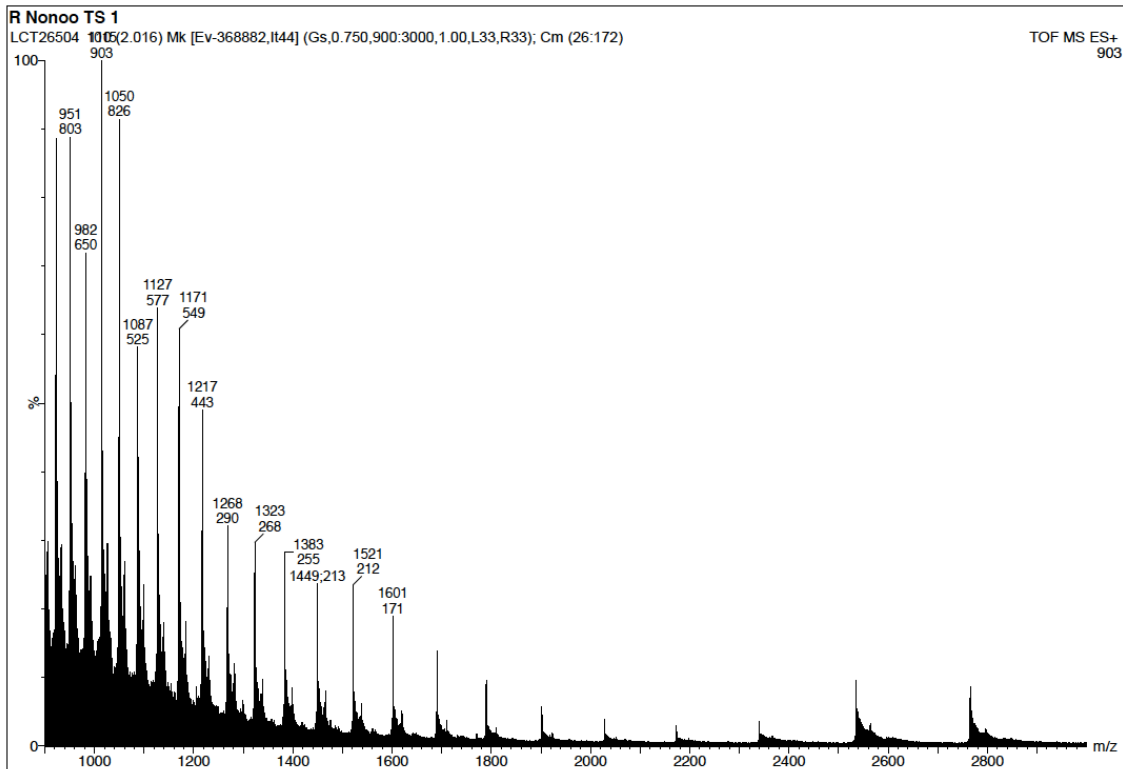
Raw data for Figure 88**: 30 min**
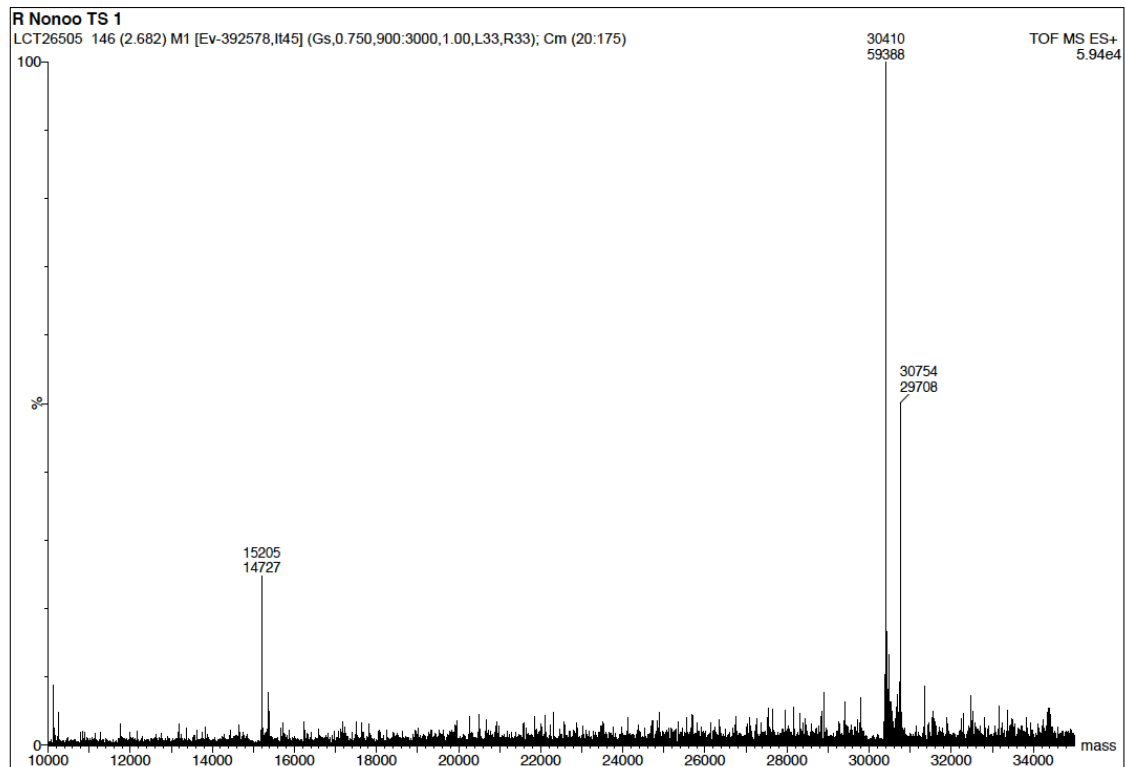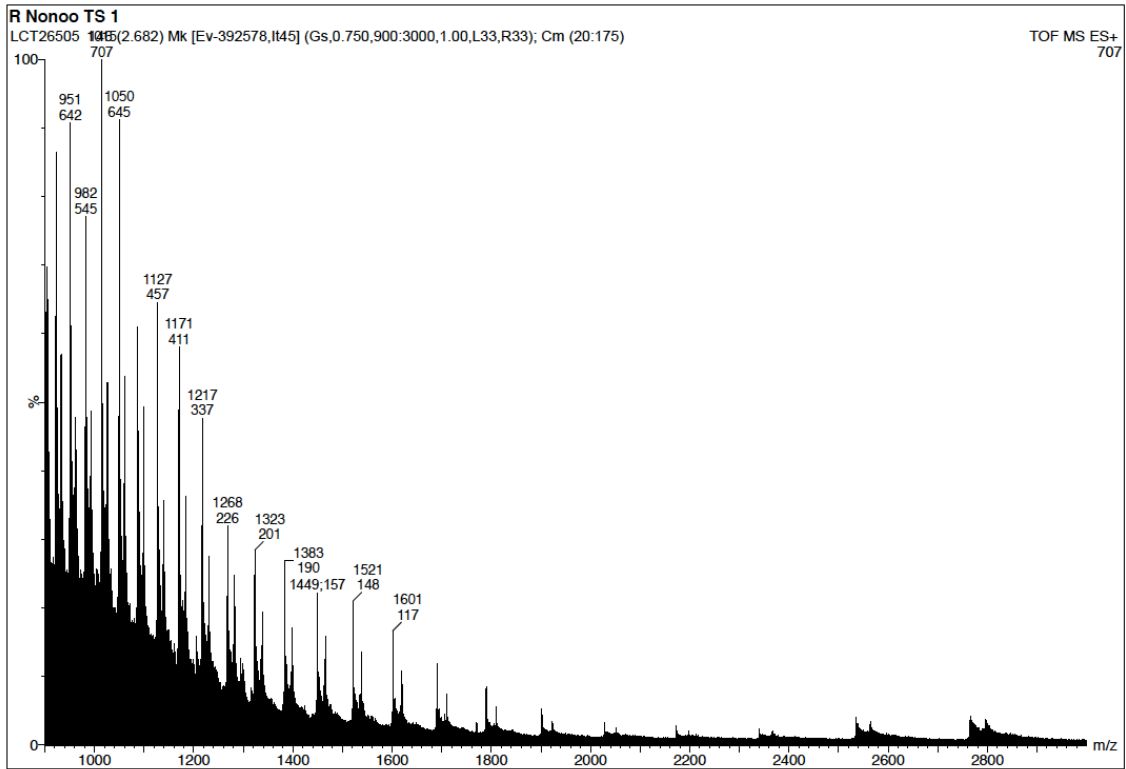
Raw data for Figure 88**: 120 min**
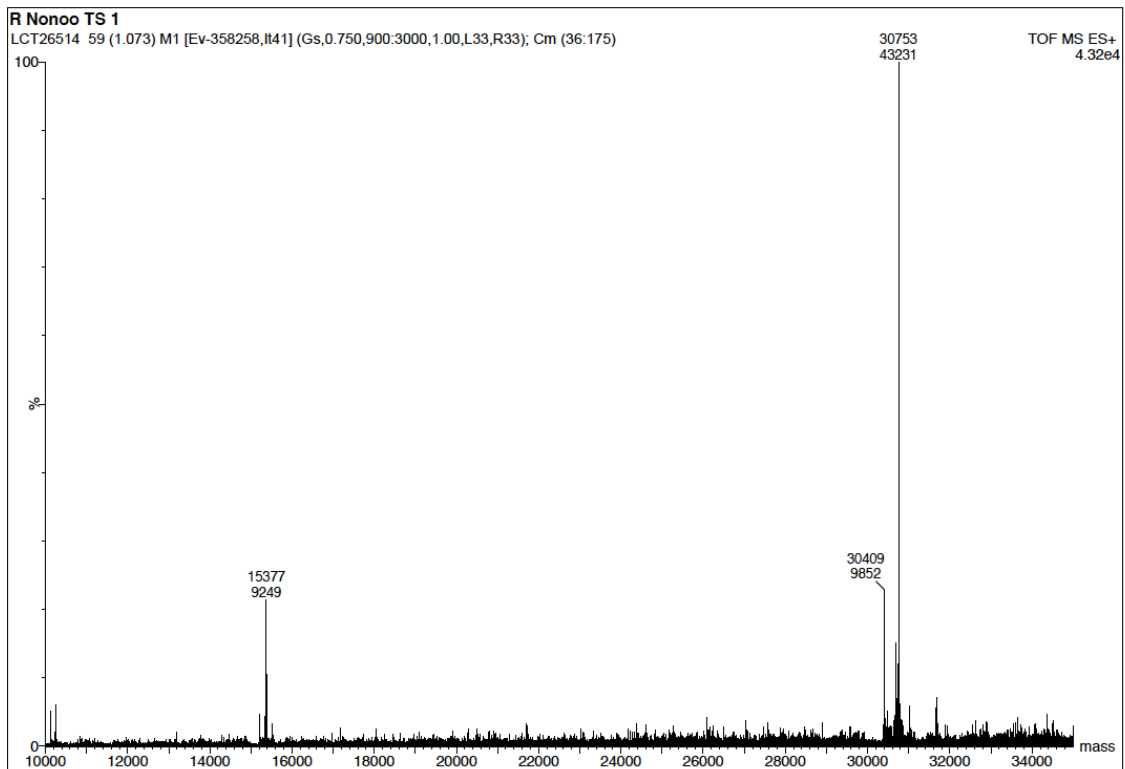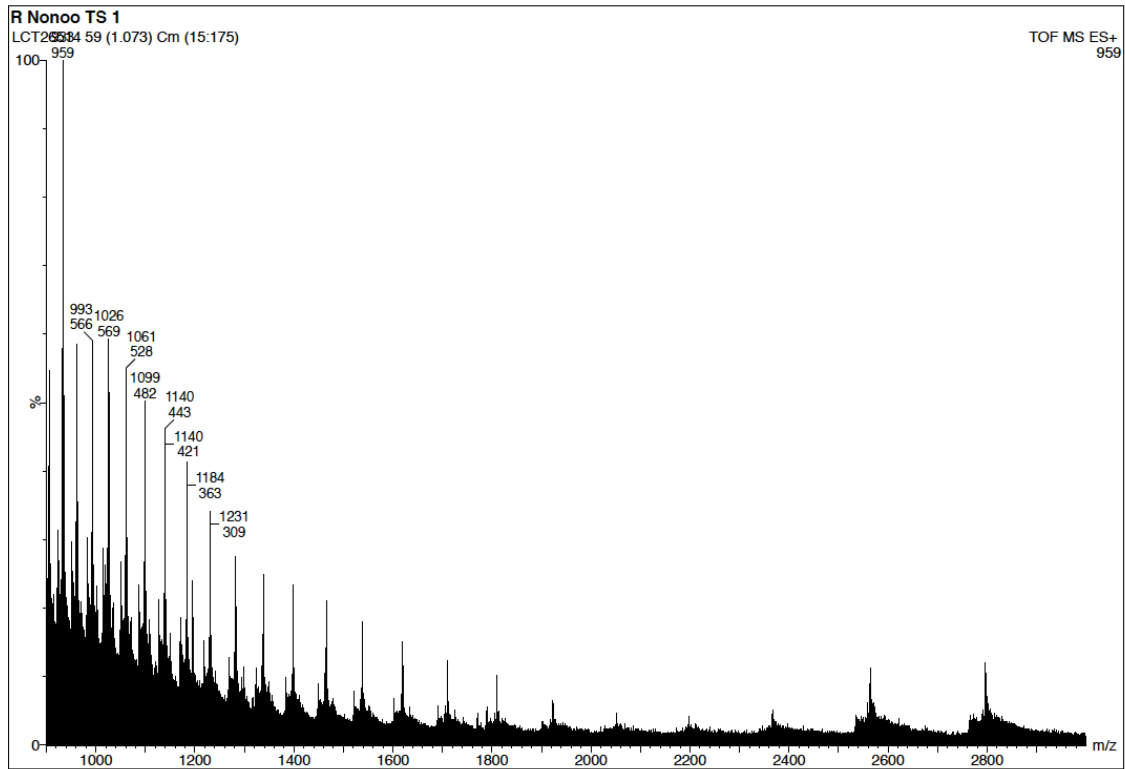
Raw data for Figure 98**: 1 h**
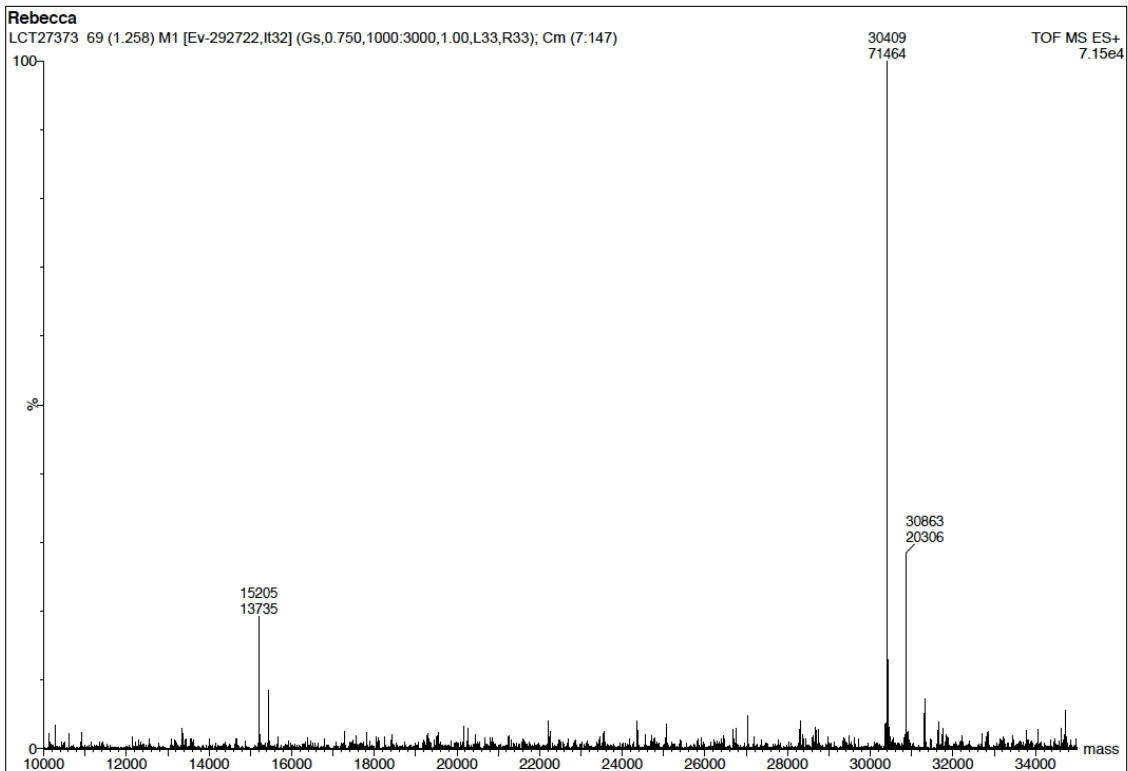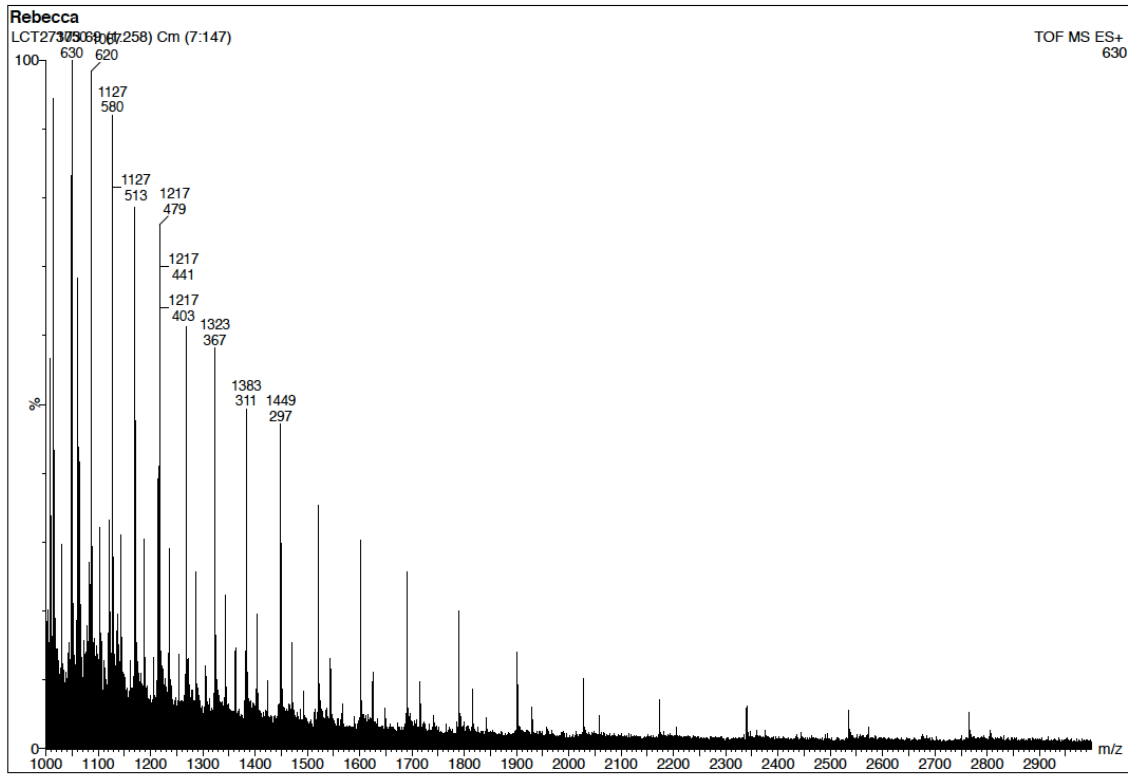
Raw data for Figure 98**: 2 h**
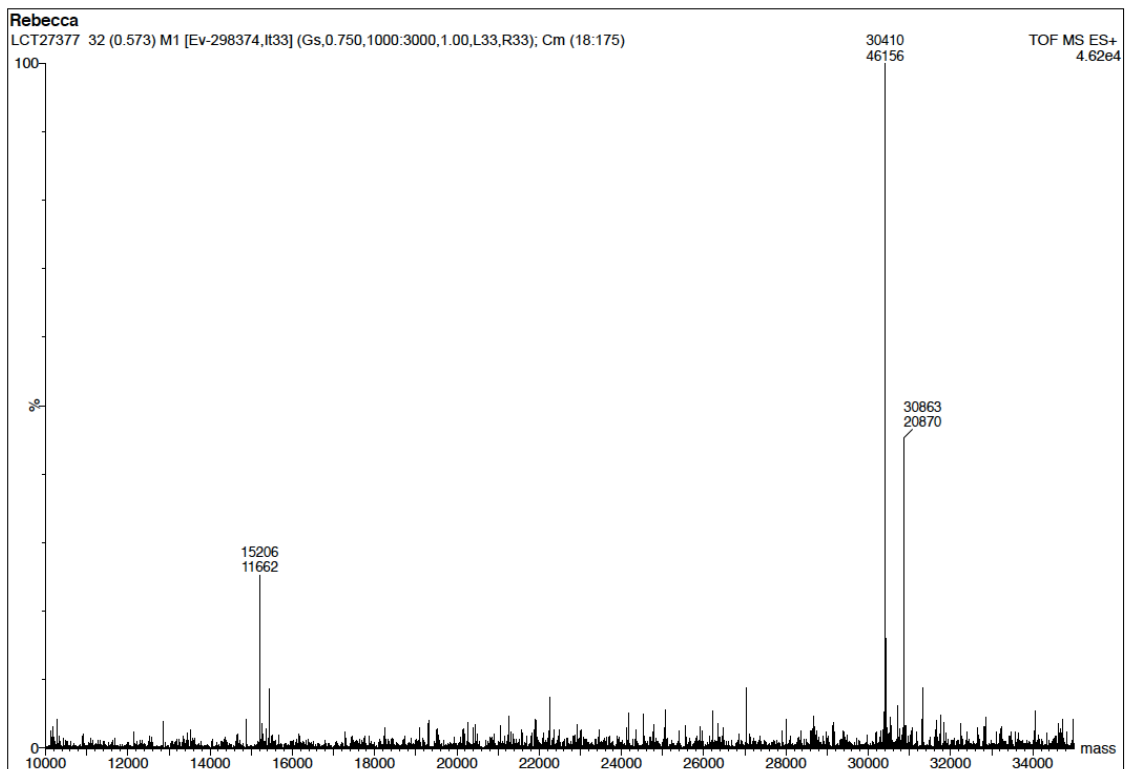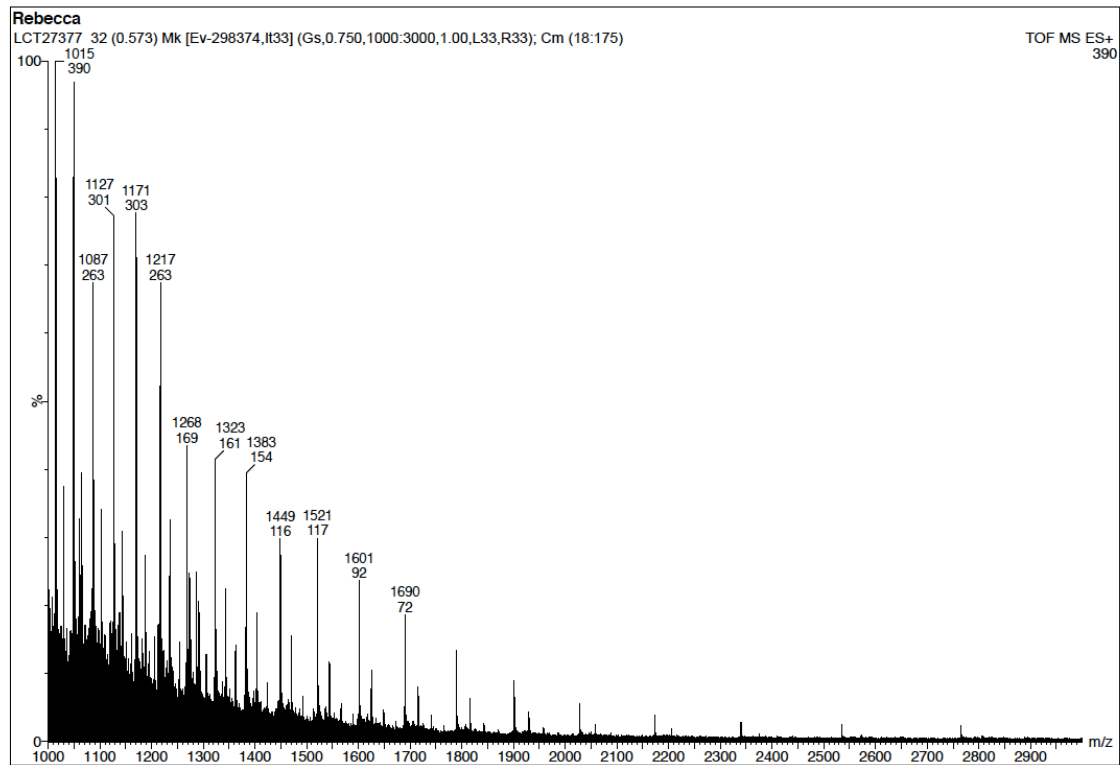
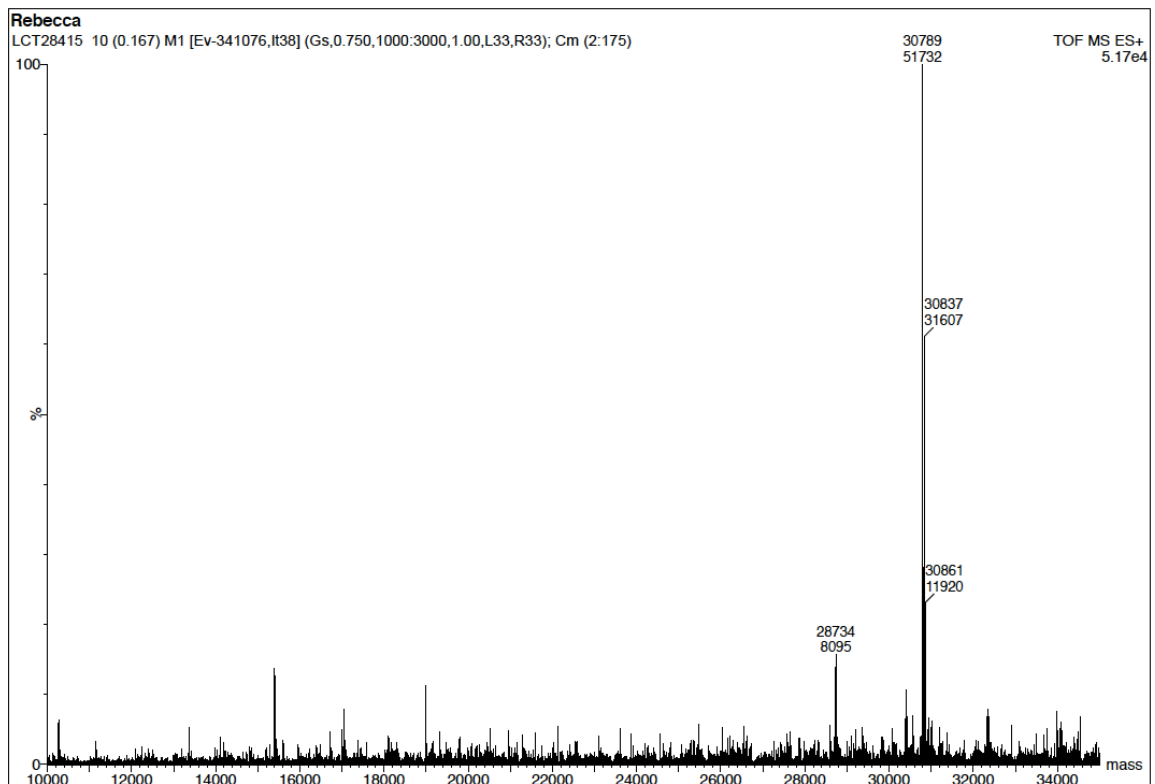**Raw data for** Figure 98**: 5 h**
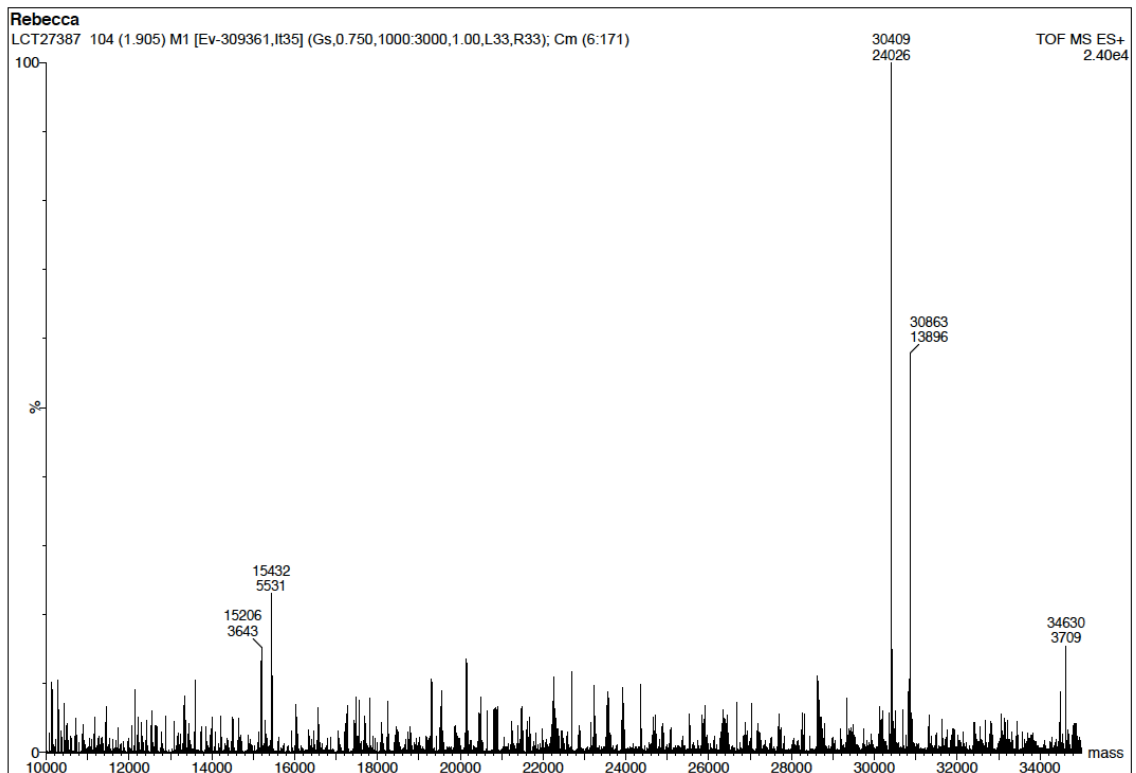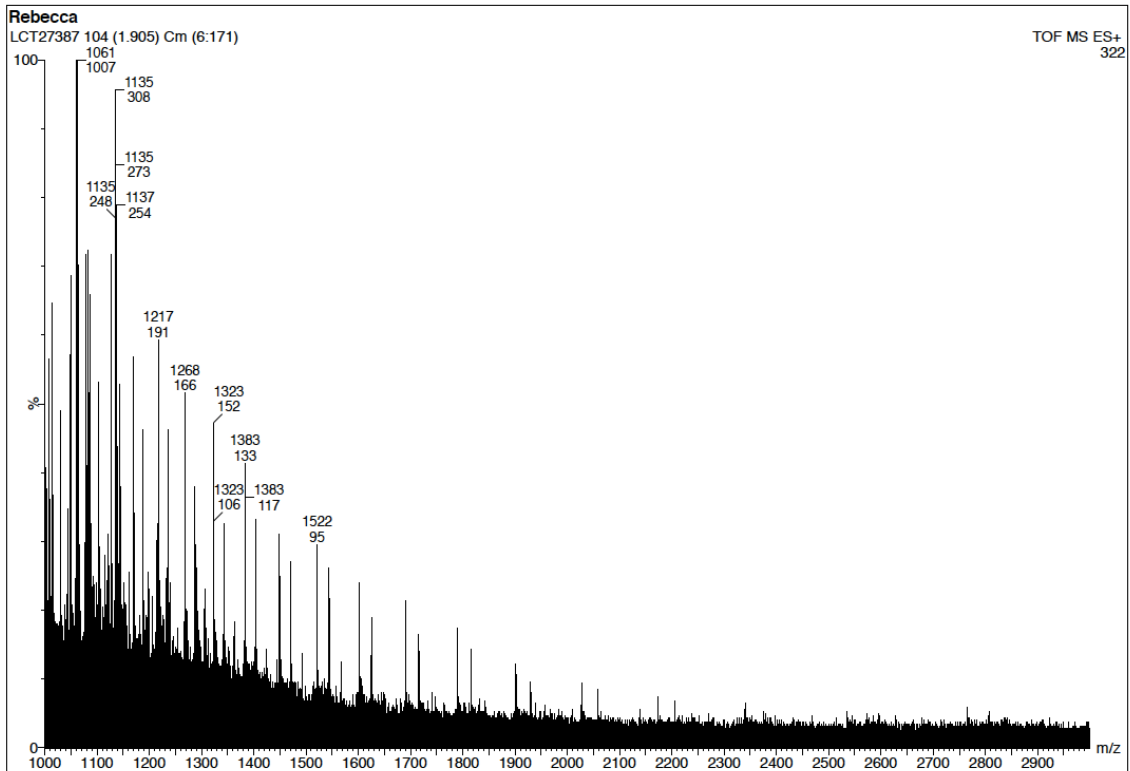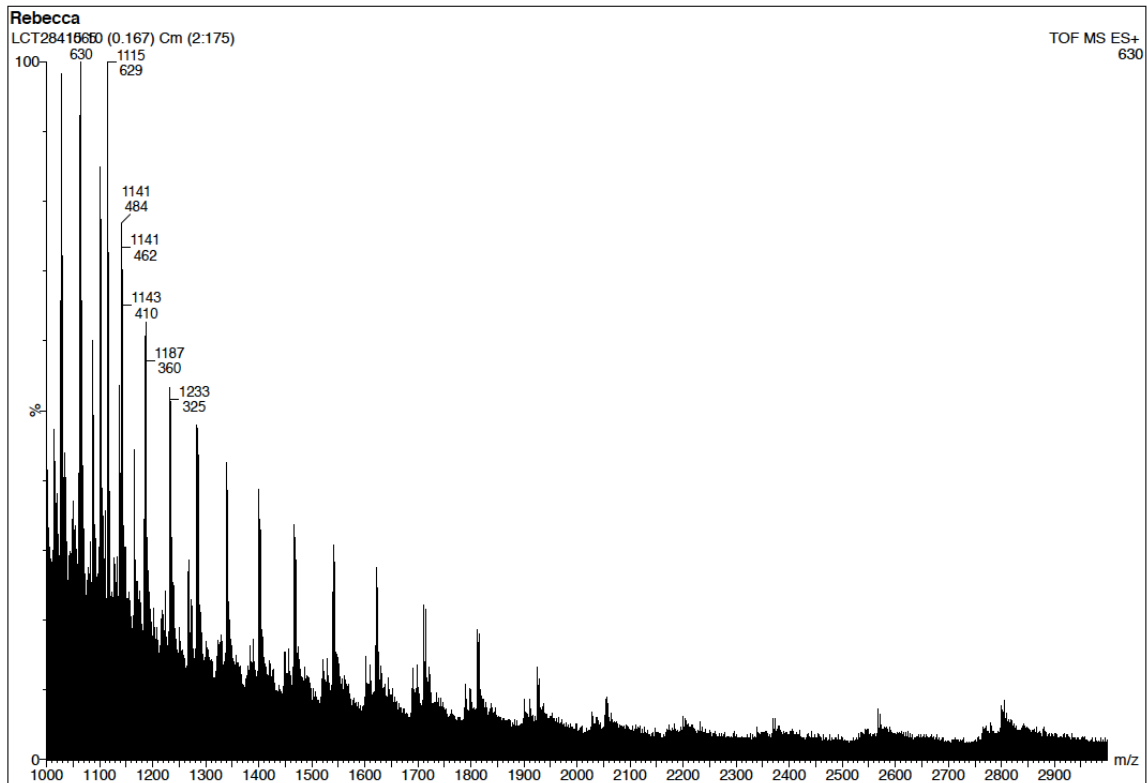
Raw data for Figure 98**: 9 h**
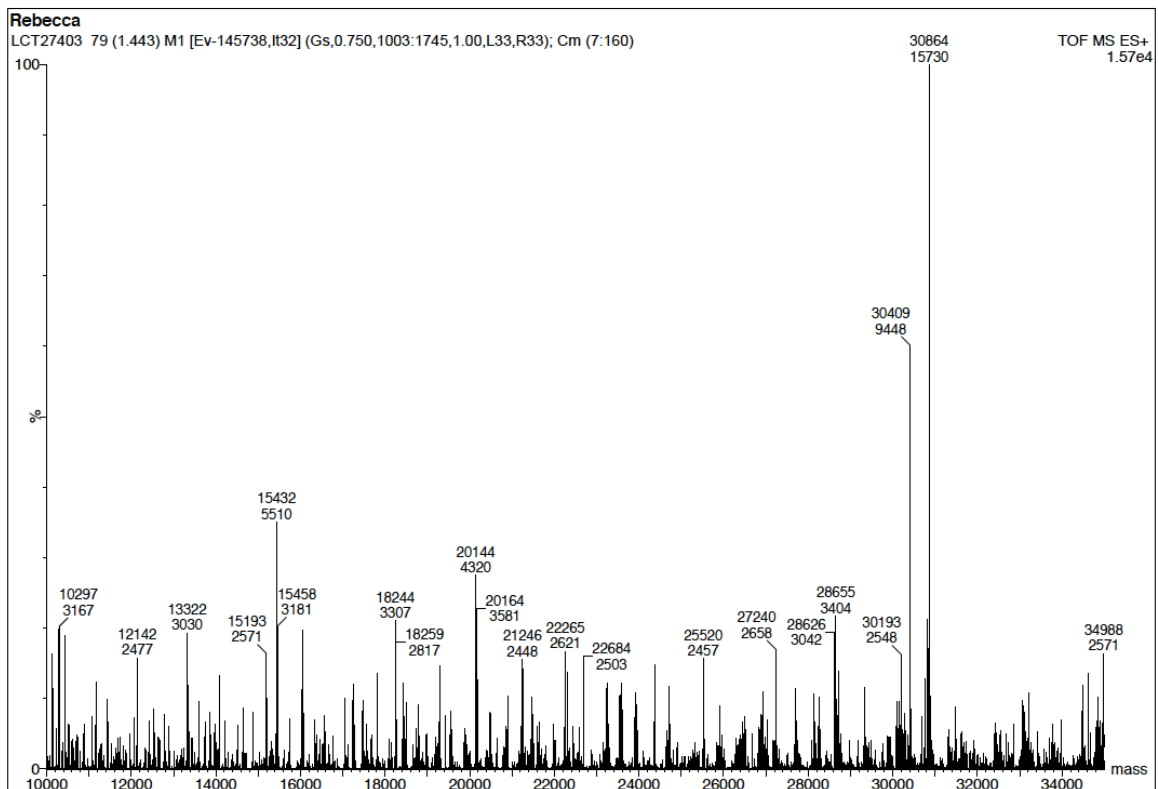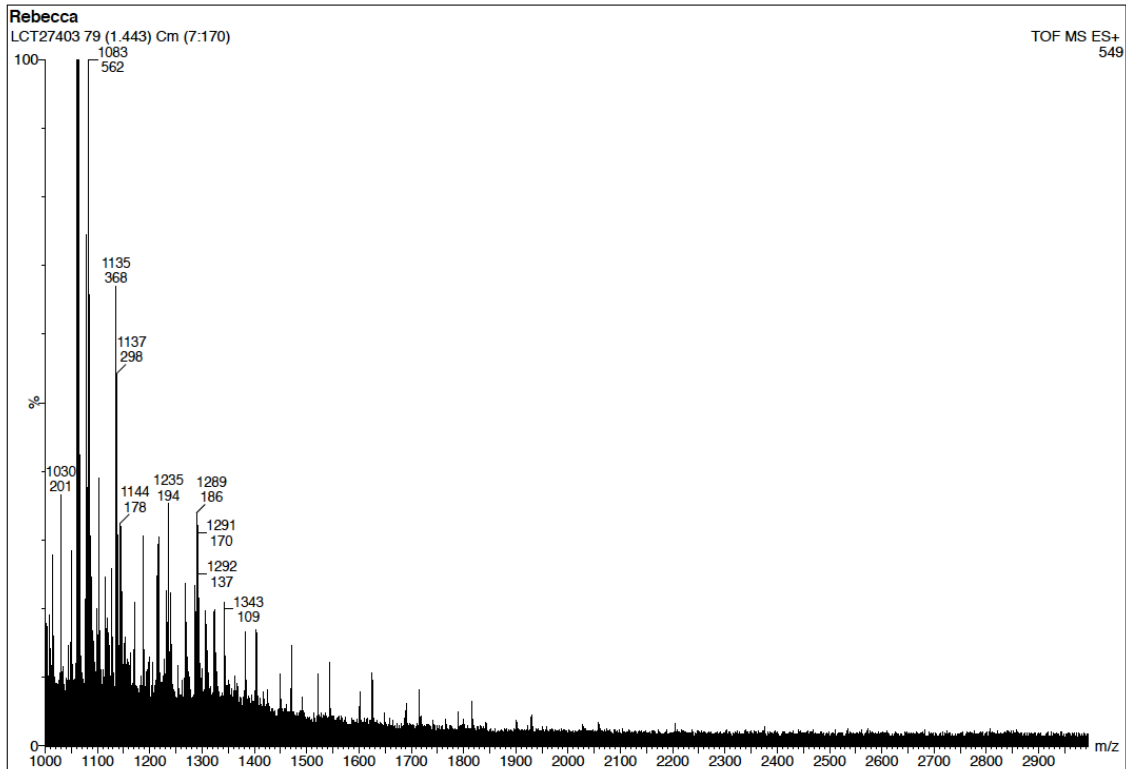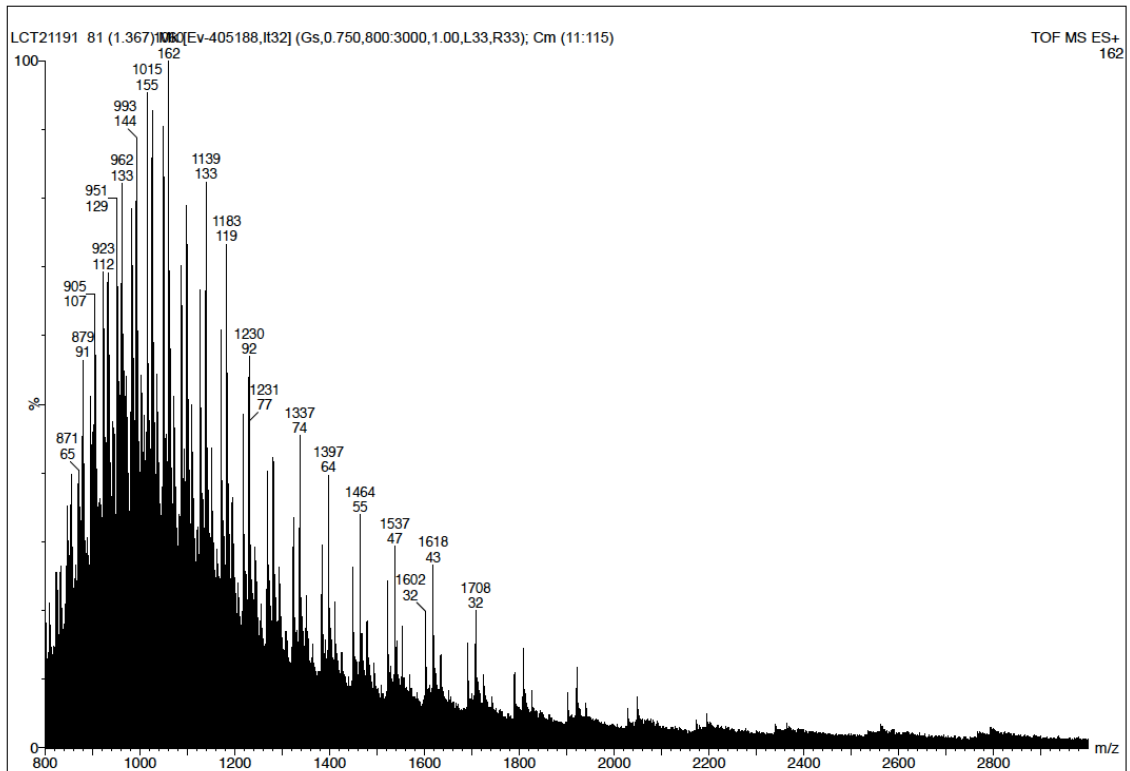
Raw data for Figure 99
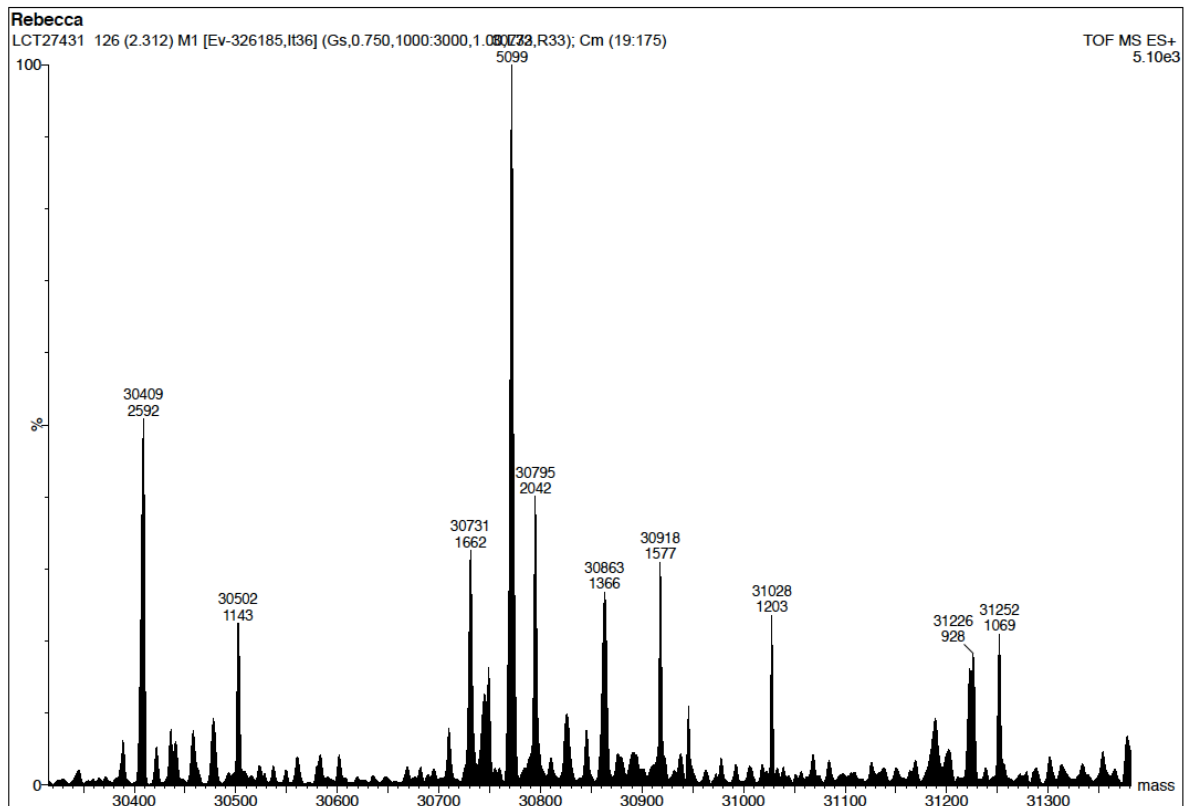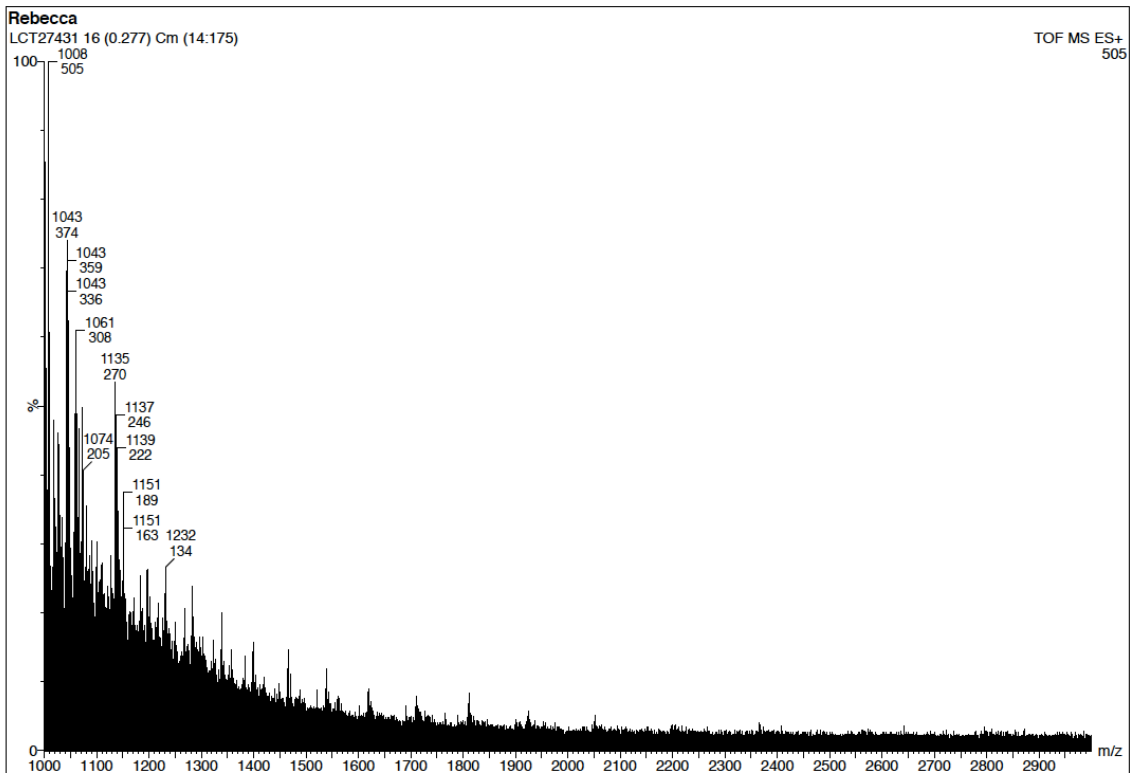
Raw data for Figure 106**: 10 min**
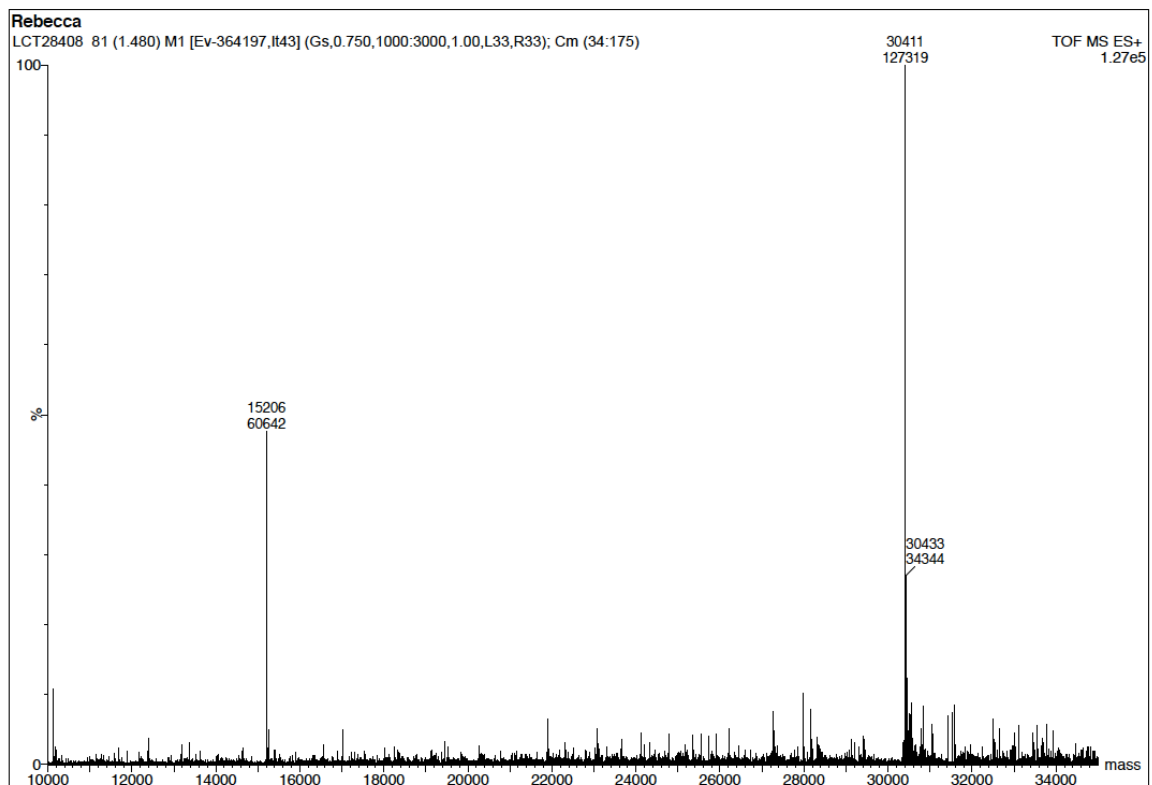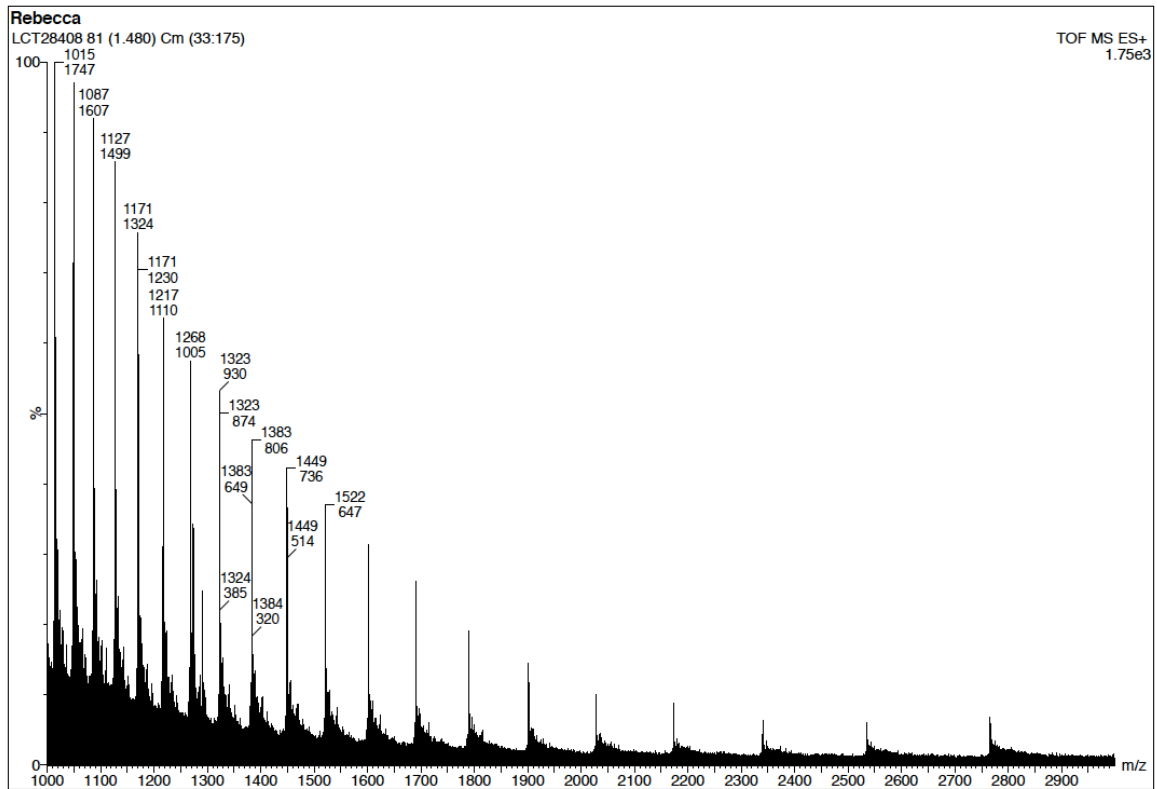
Raw data for Figure 106**: 1020 min**

Raw data for Figure 127
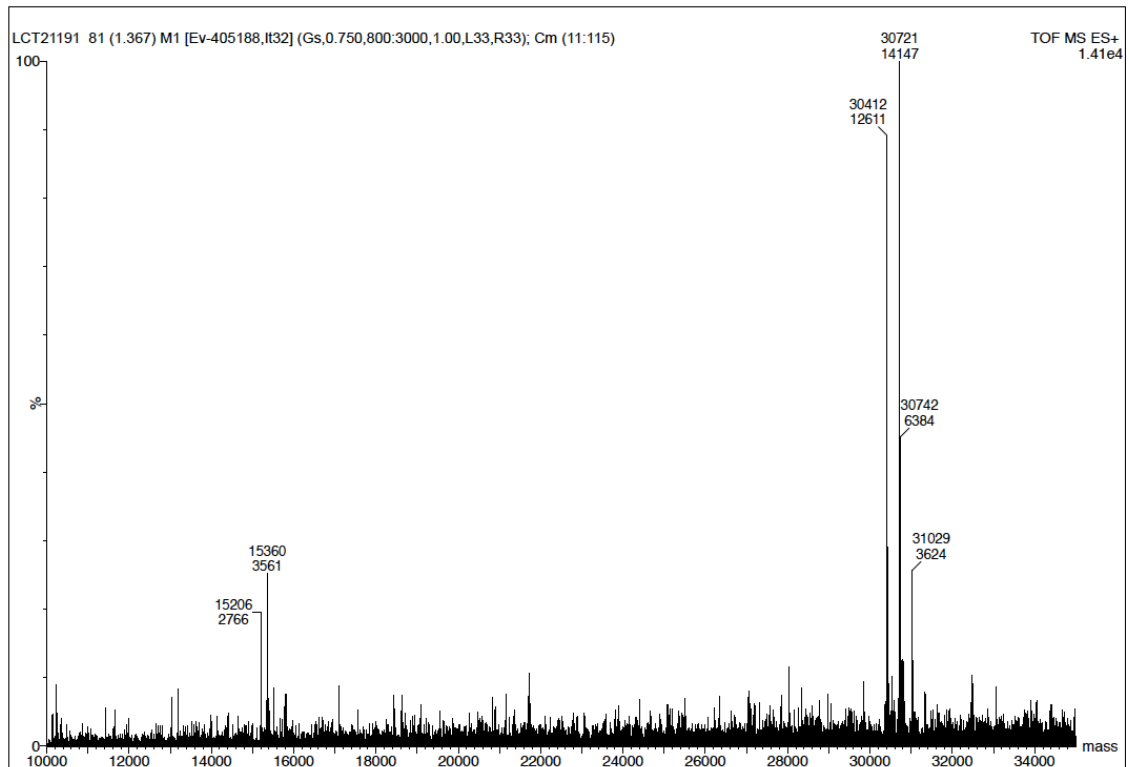
Raw data for Figure 128
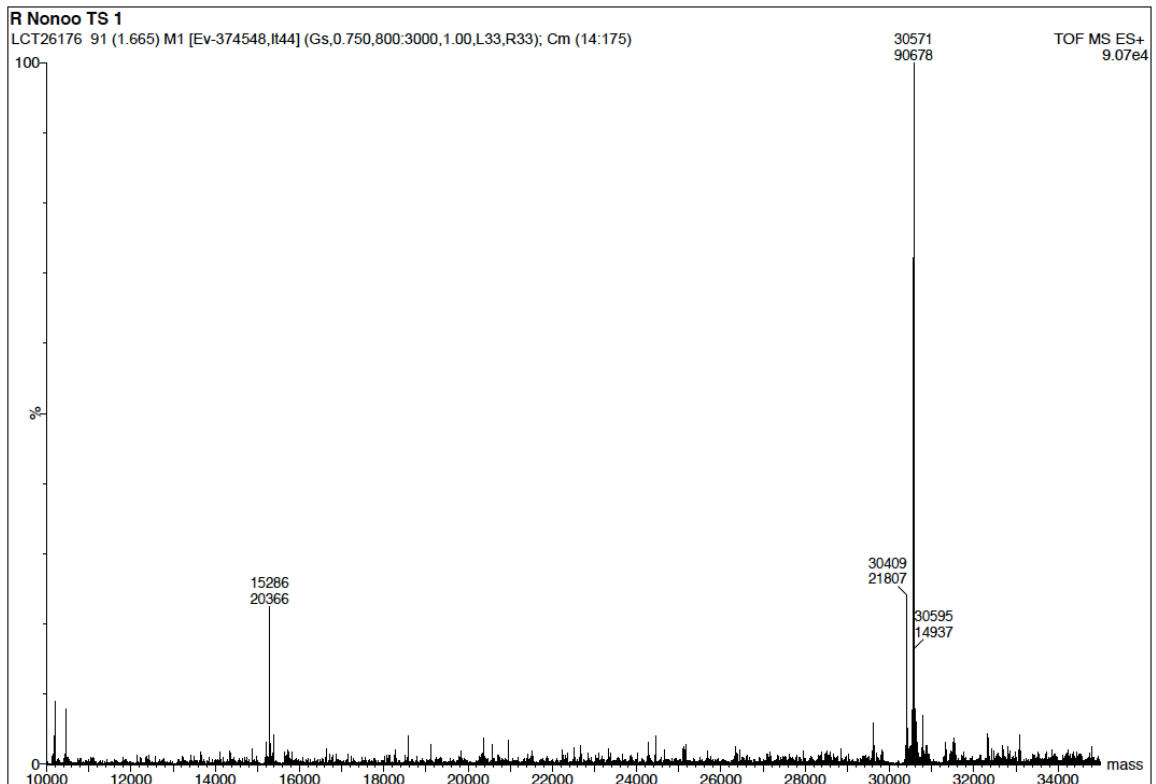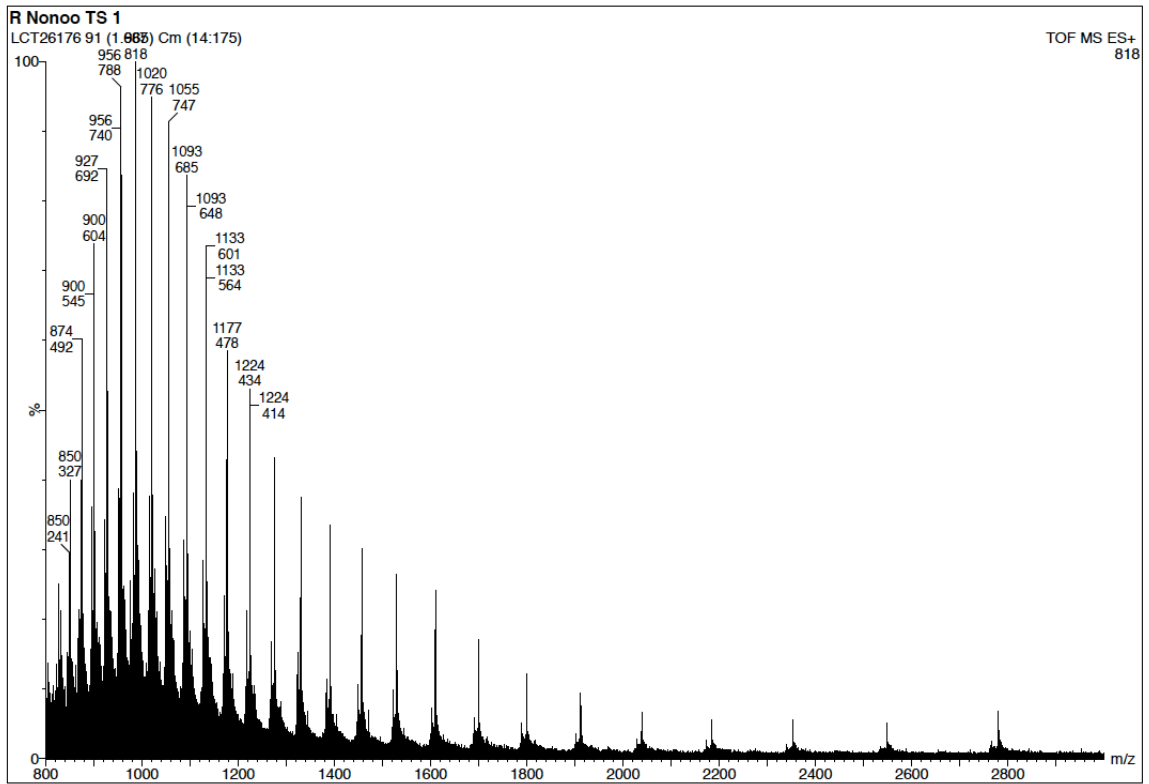
Appendix VII Raw Mass Spectrometry Data II

Experiment	File numbers
Papain	LCT26205
Papain and acrylamides (120 min)	LCT27920
Papain and iodoacetamide (10 min)	LCT26353
P97	LCT26352
P97 and acrylamides (45 and 90 min)	LCT26366 (45 min), LCT26368 (90 min)
Cdc25	LCT28287
Cdc25 and acrylamides (180 min)	LCT287290
Cdc25 and iodoacetamide (10 and 60 min)	LCT287292 (10 min), LCT287293 (60 min)
TS and benzyl piperidine acrylamide **54** over pH range	LCT27681 (pH 8.1), LCT27682 (pH 7.9), LCT27683 (pH 7.6), LCT27684 (pH 7.4), LCT27684 (pH 7.3), LCT27685 (pH 7.2)
Vinyl sulfonamide irreversibility using vinyl sulfonamides **44** and **70**	LCT26571, LCT26572, LCT26579, LCT26580

Appendix VII Raw Mass Spectrometry Data II

Papain

Papain (10 μM) and DTT (1 mM) in ammonium bicarbonate (10 mM) at pH 8.
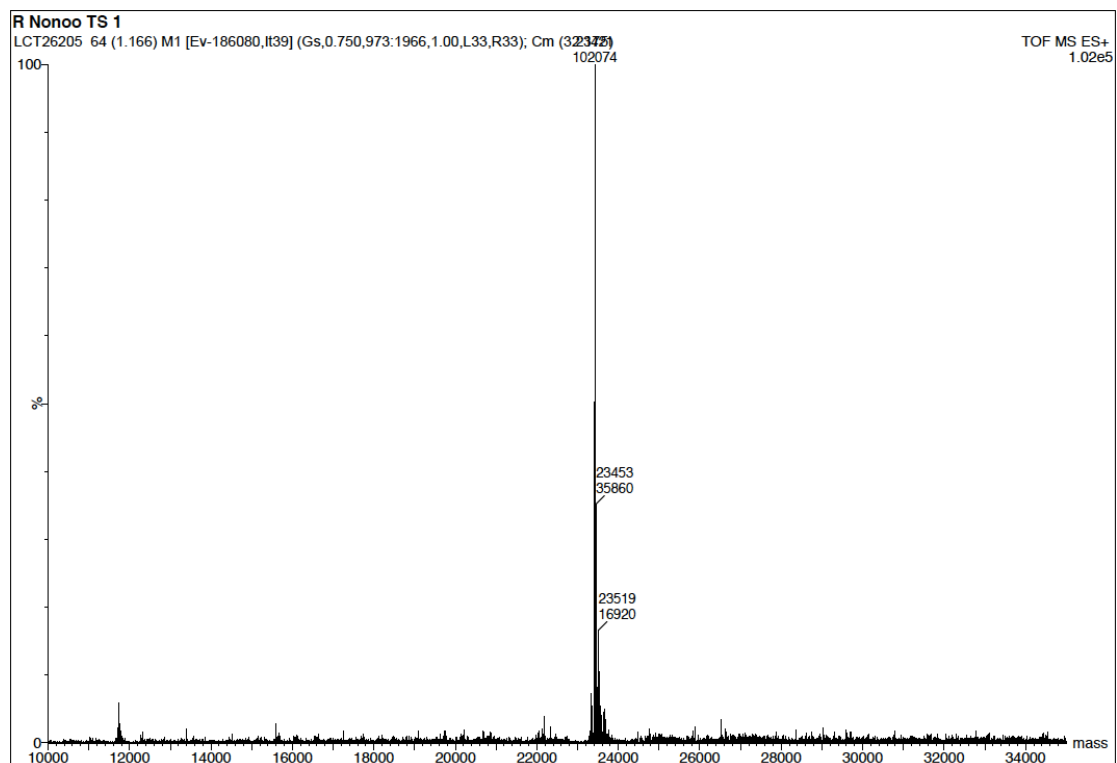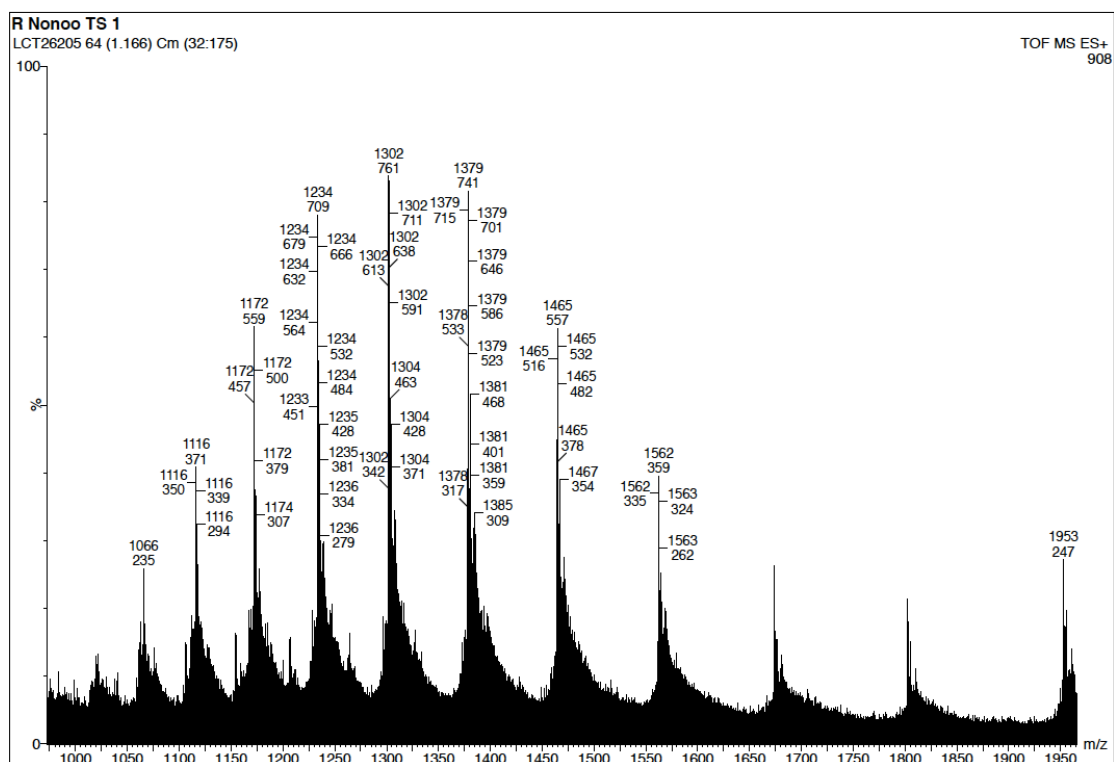
Papain and Acrylamides at 120 min

Papain (10 μM) and DTT (1 mM) with acrylamides **55**, **48**, **47**, **50**, **49**, **54**, **67**, **68**, **119** each at 96 μM in ammonium bicarbonate (10 mM), pH 8, after a 120 min incubation time.
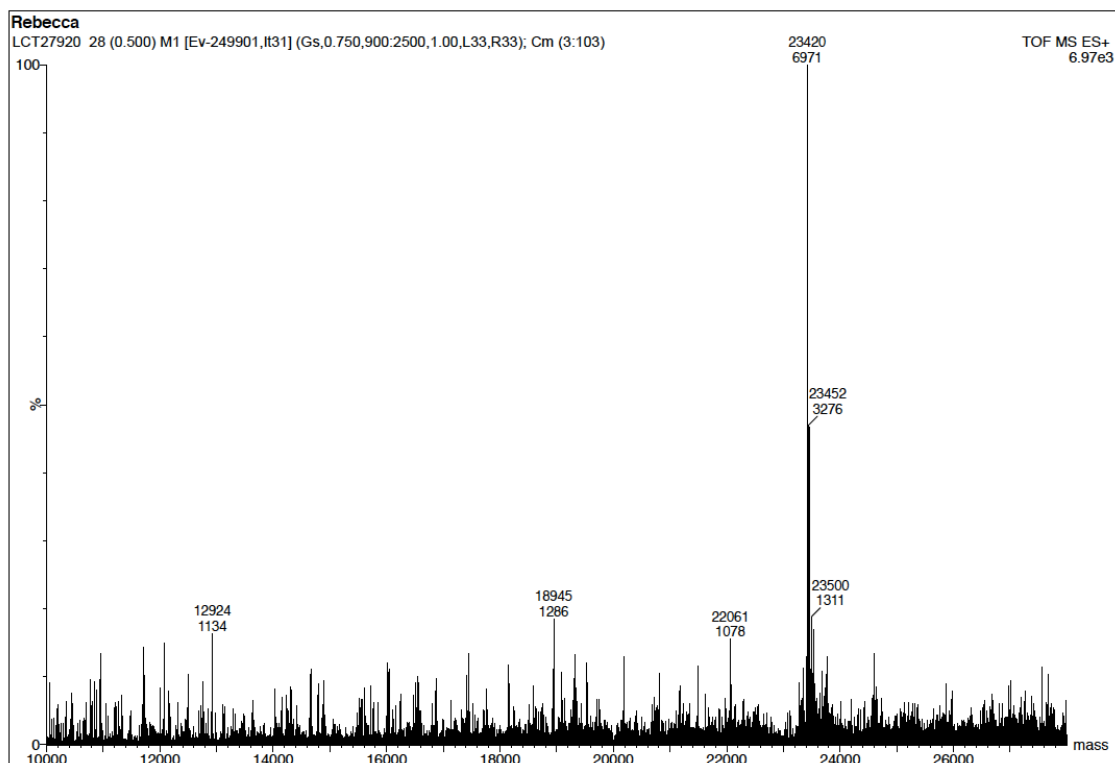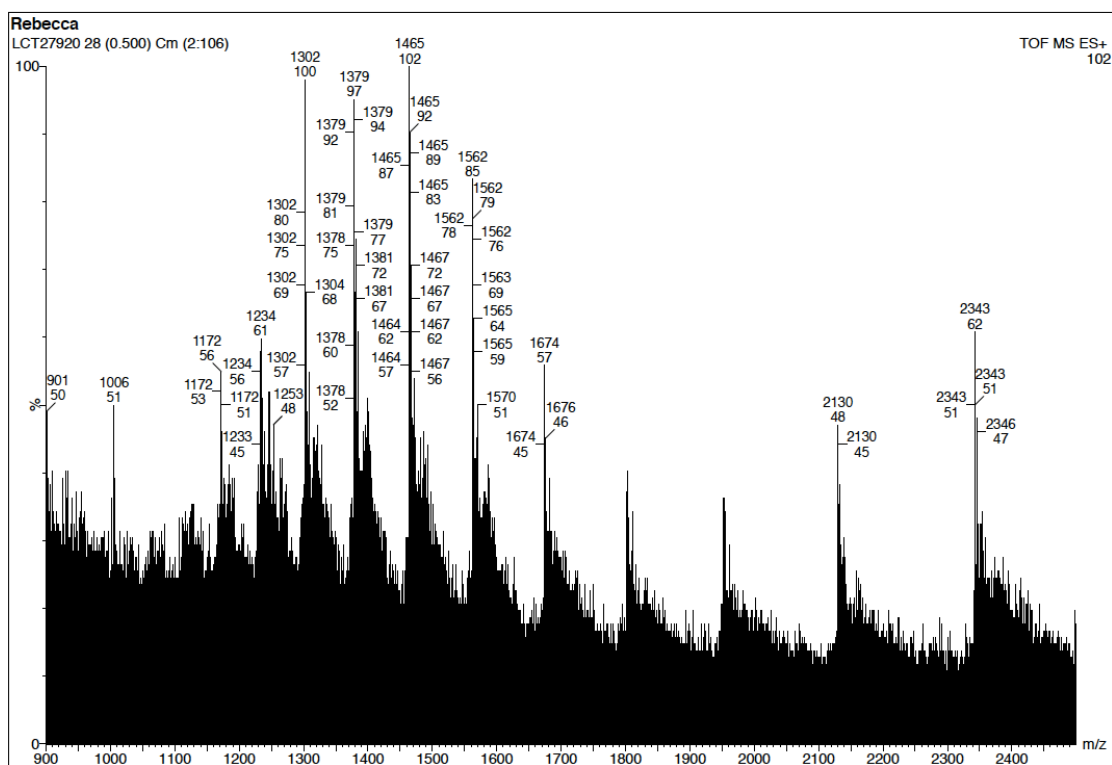
Papain and Iodoacetamide at 10 min

Papain (10 μM), DTT (1mM) and iodoacetamide (4 mM) in ammonium bicarbonate (10 mM), pH 8 after a 10 minute incubation period.

P97
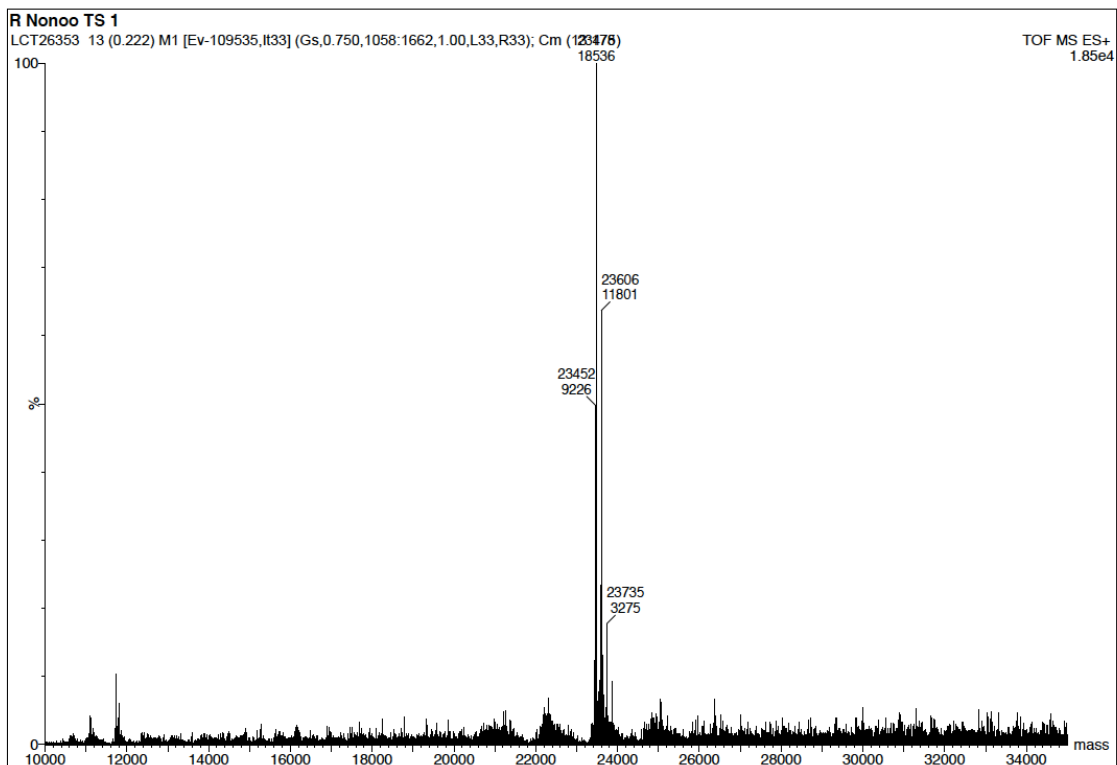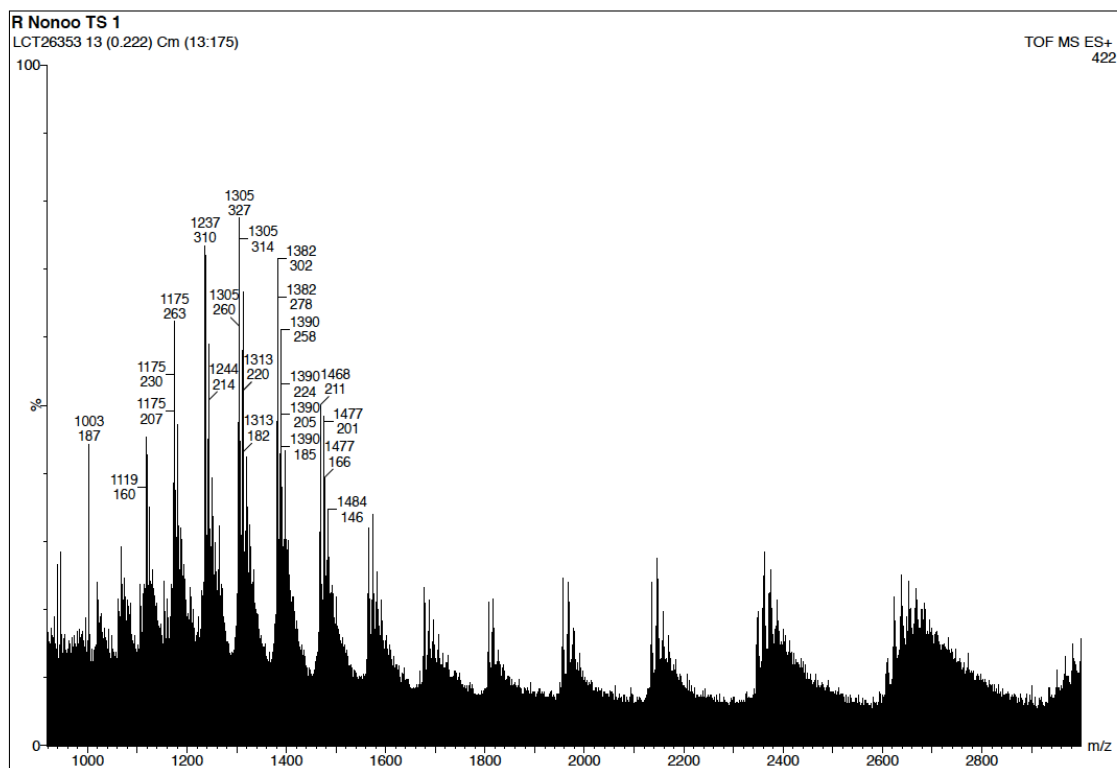
P97 (10 µM) and DTT (1 mM) in ammonium bicarbonate (10 mM), pH 8.
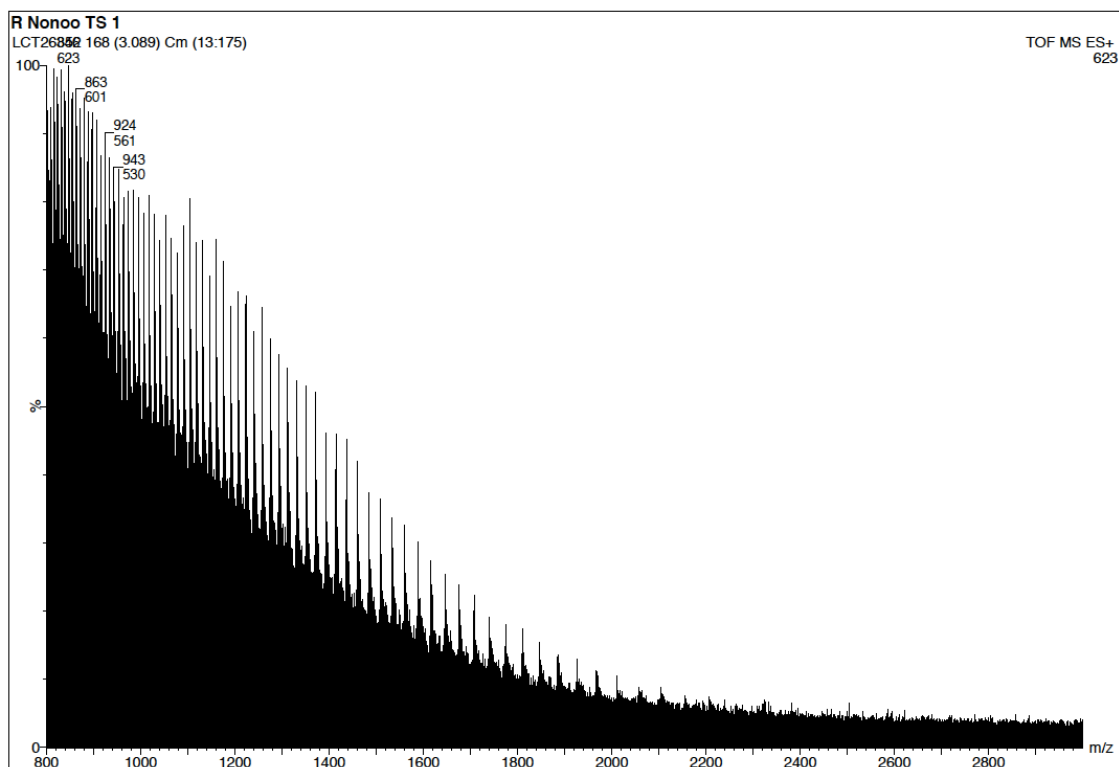
P97 + Acrylamides at 45 min

P97 (10 mM), DTT (1 mM) and acrylamides **55**, **48**, **47**, **50**, **49**, **67**, **68** each at 343 μM in ammonium bicarbonate (10 mM), pH 8, after a 45 min incubation period.
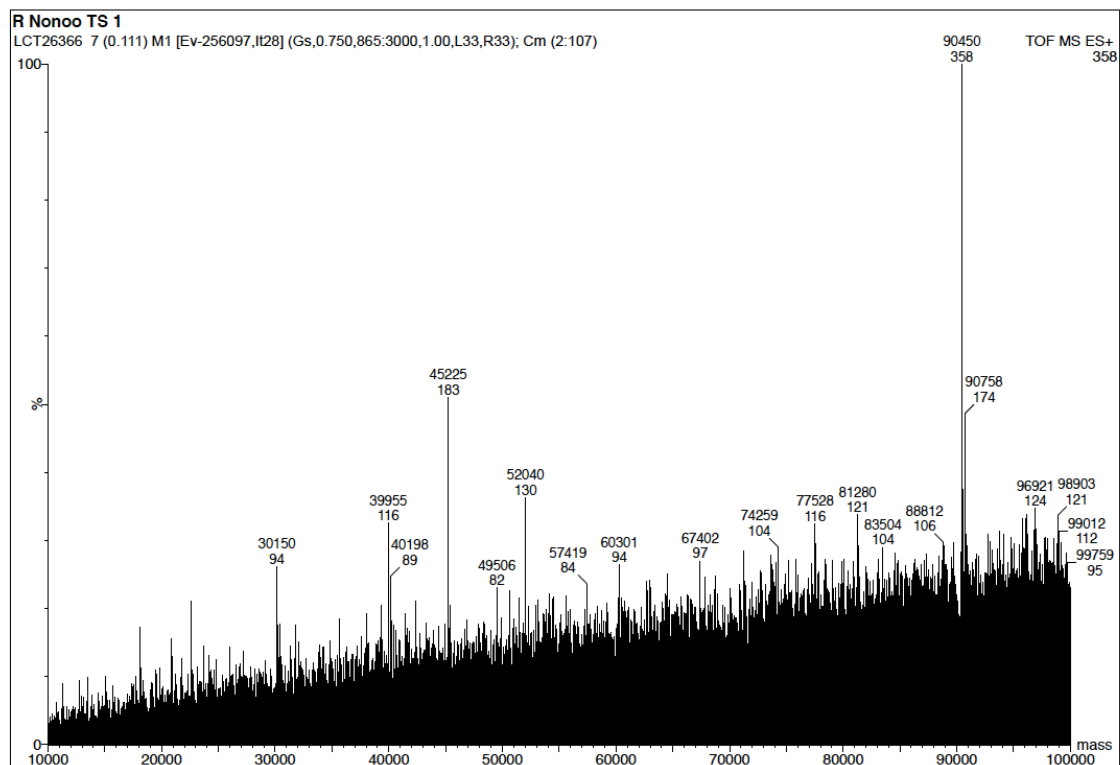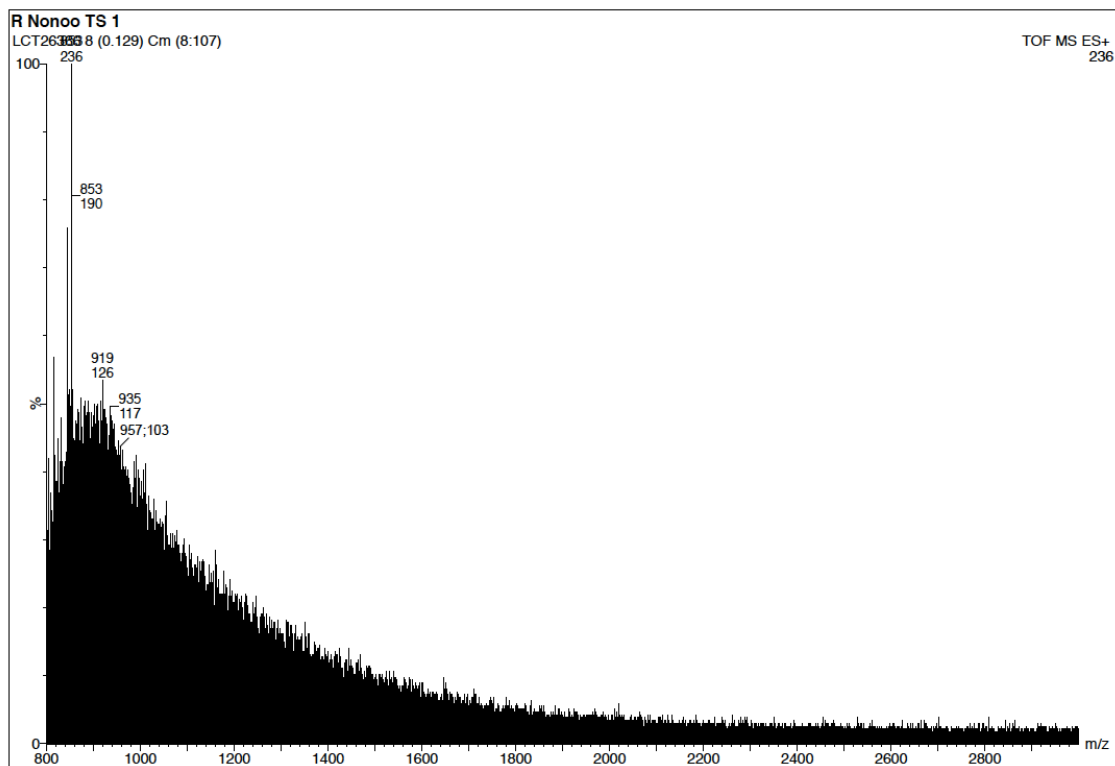
P97 and Acrylamides at 90 min

P97 (10 mM), DTT (1 mM) and acrylamides **55**, **48**, **47**, **50**, **49**, **67**, **68** each at 343 µM in ammonium bicarbonate (10 mM), pH 8, after a 90 min incubation period.
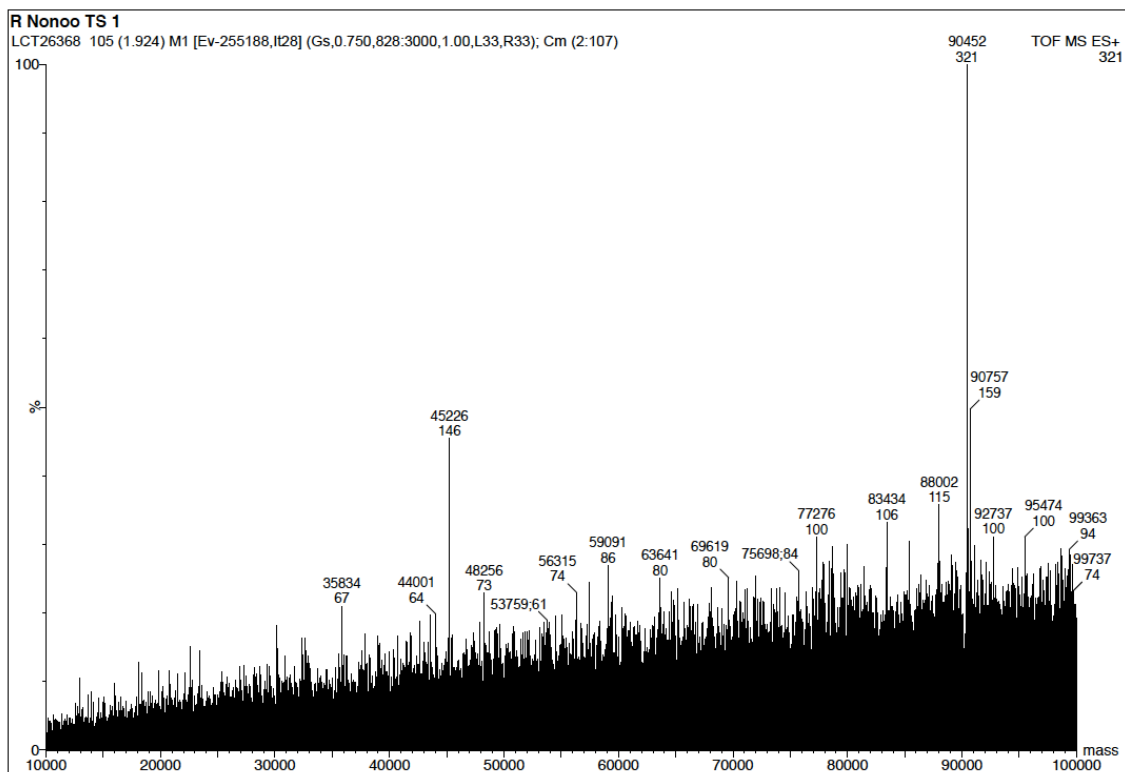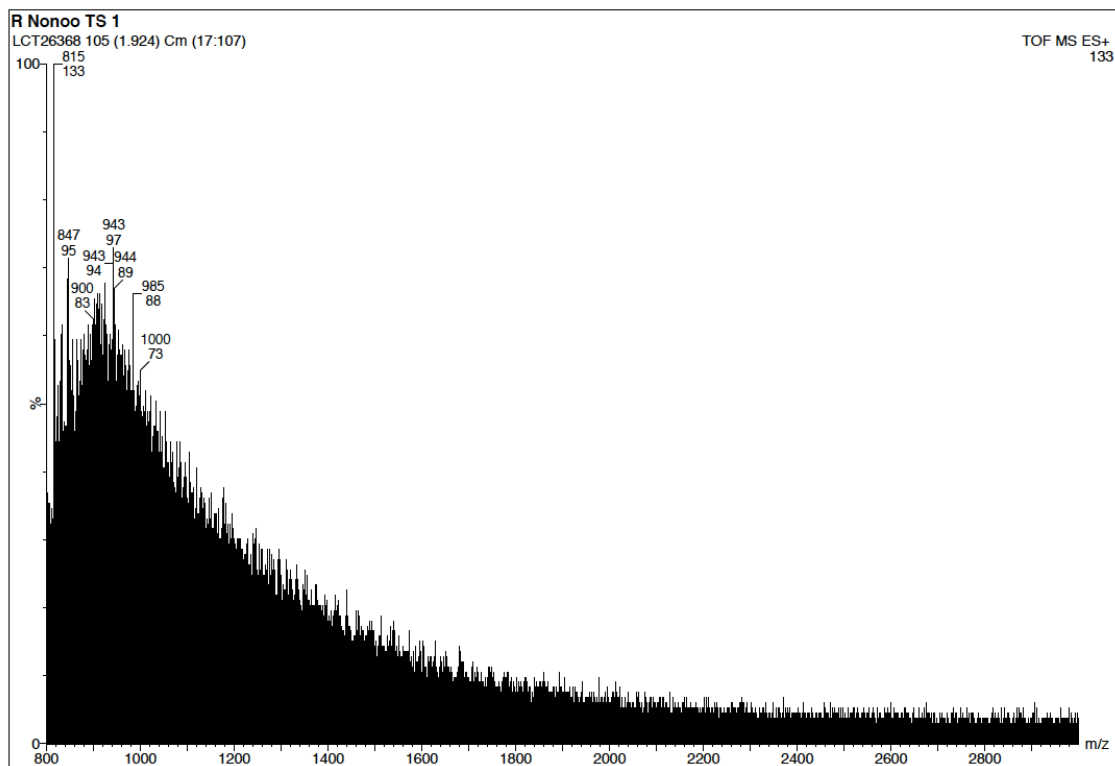
Cdc25A

Cdc25A (10 µM) and DTT (1 mM) in ammonium bicarbonate (10 mM), pH 8.

Cdc25A and Acrylamides at 180 min

Cdc25A (10 μM), DTT (1 mM) and acrylamides **47**, **48**, **49**, **50**, **54**, **55**, **67**, **119** each at 100 μM in ammonium bicarbonate (10 mM), pH 8, after 180 min incubation time.
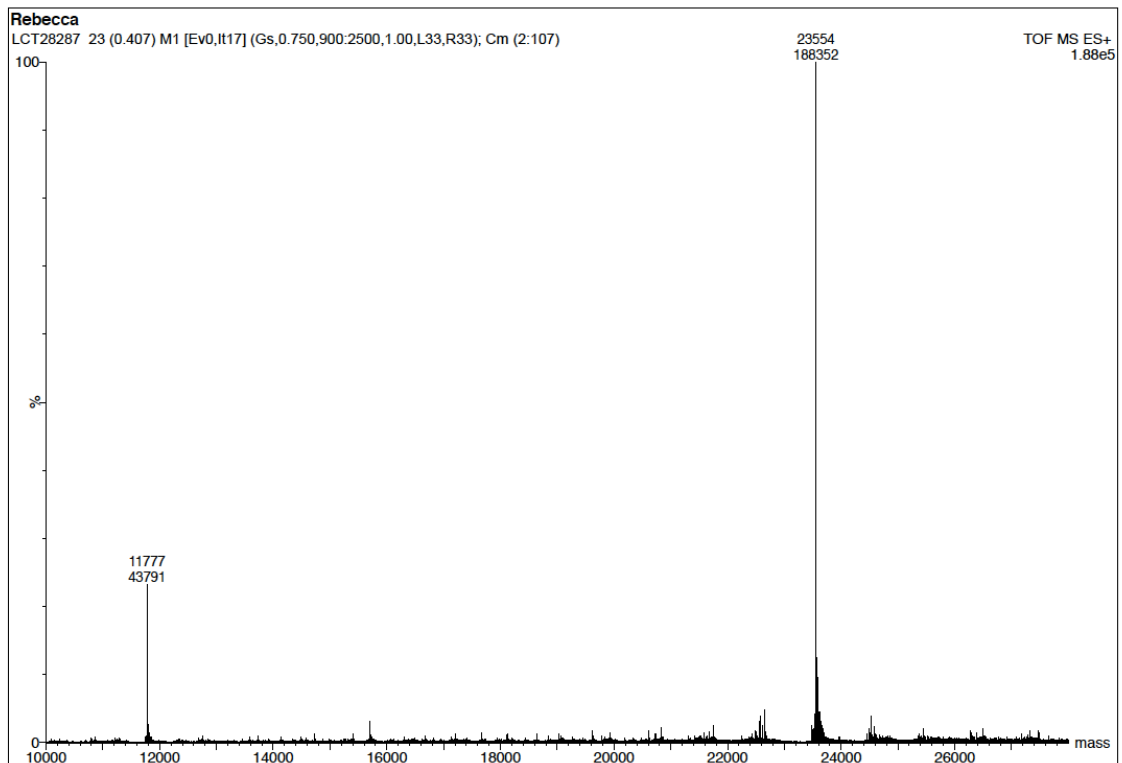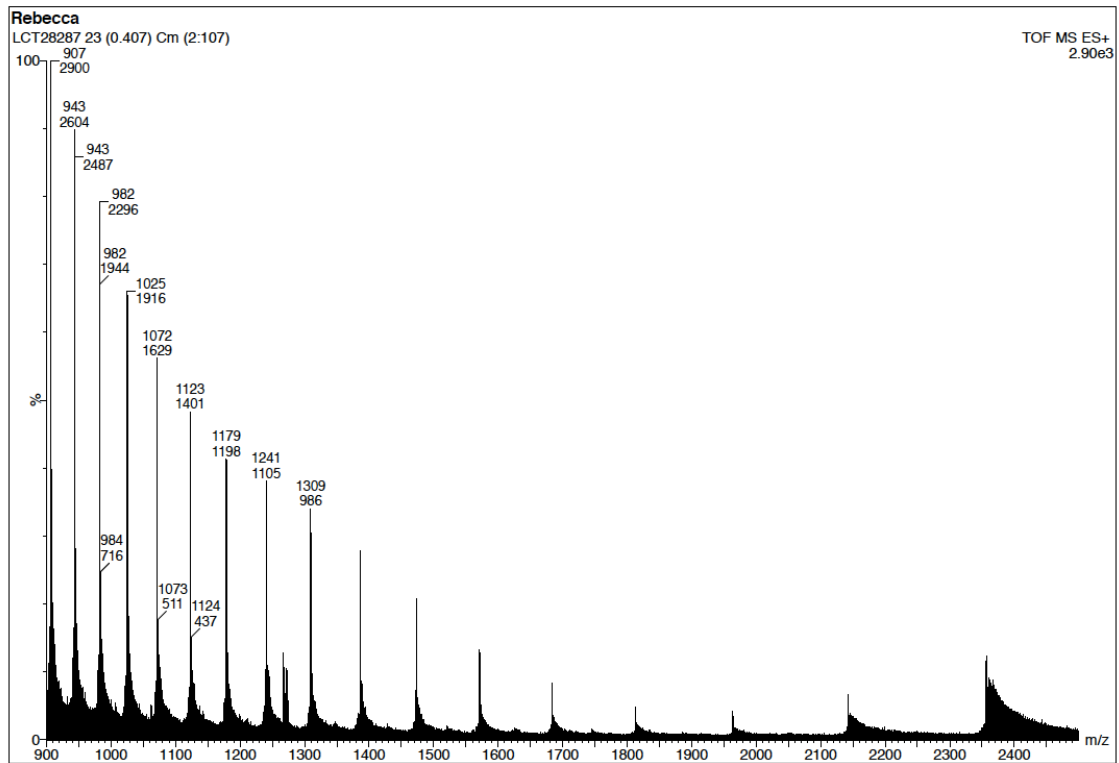
Cdc25A and Iodoacetamide at 10 min

Cdc25A (10 μM), DTT (1 mM) and iodoacetamide (4 mM) in ammonium bicarbonate (10 mM), pH 8 after a 10 min incubation period.

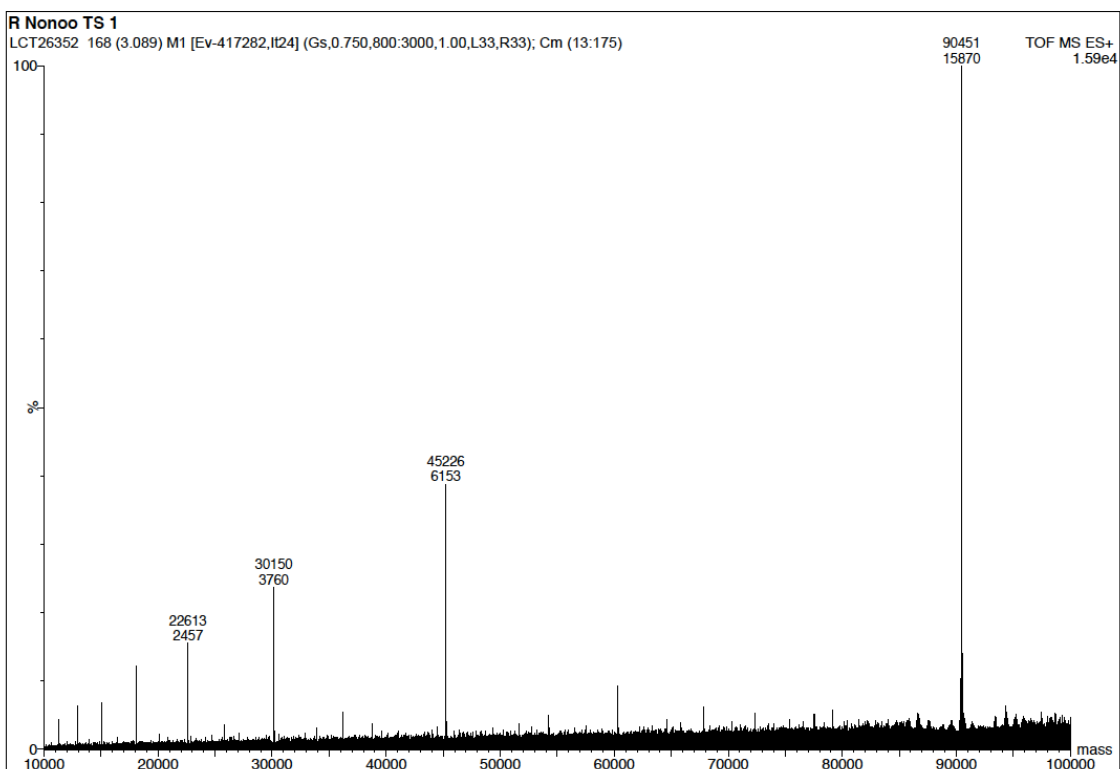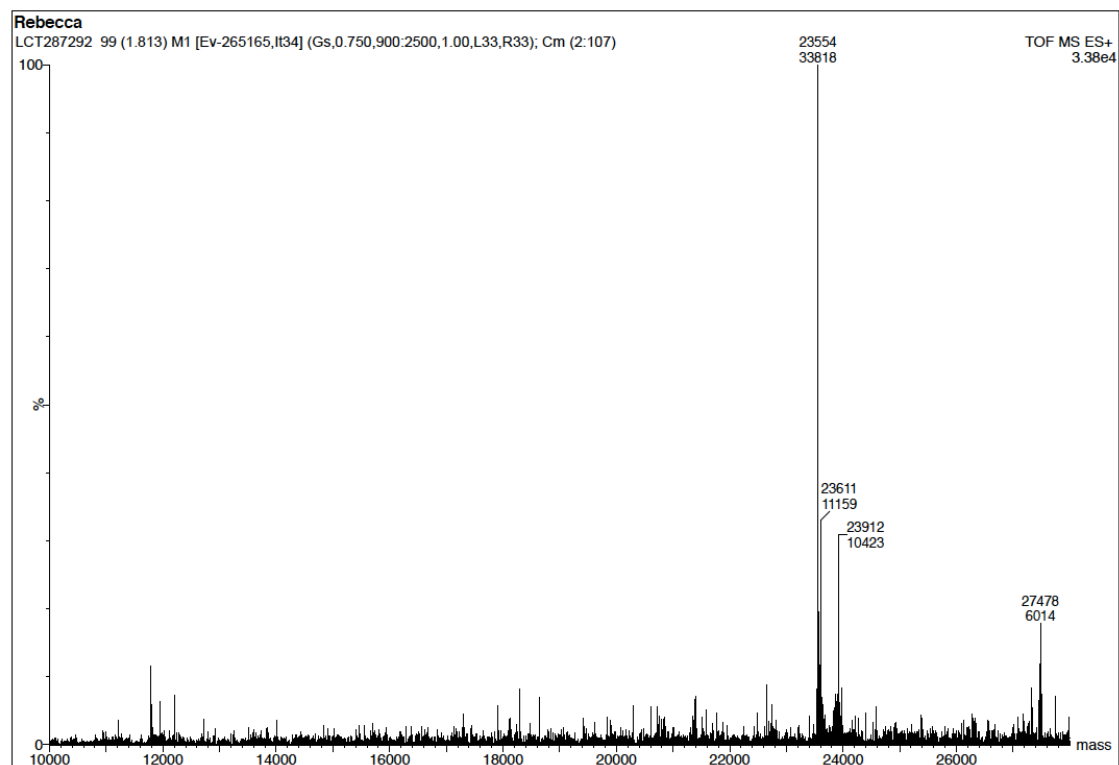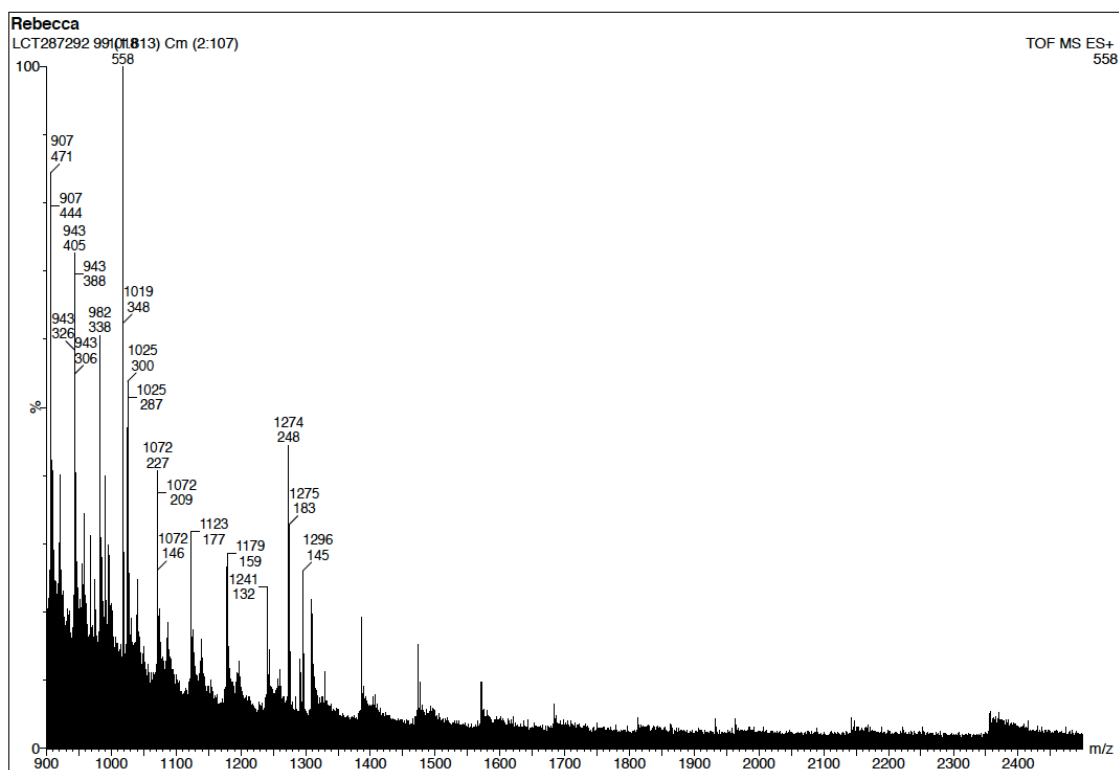## Cdc25A and Iodoacetamide at 60 min

Cdc25A (10 μM), DTT (1 mM) and iodoacetamide (4 mM) in ammonium bicarbonate (10 mM), pH 8 after a 60 min incubation period.
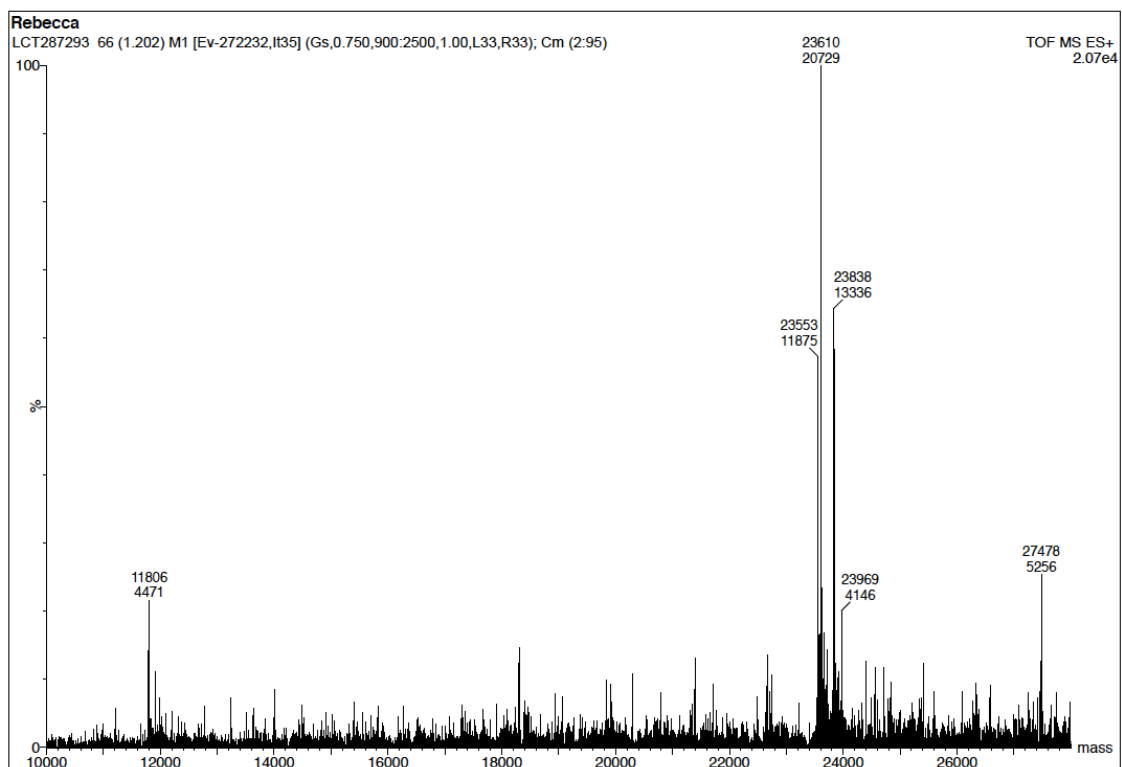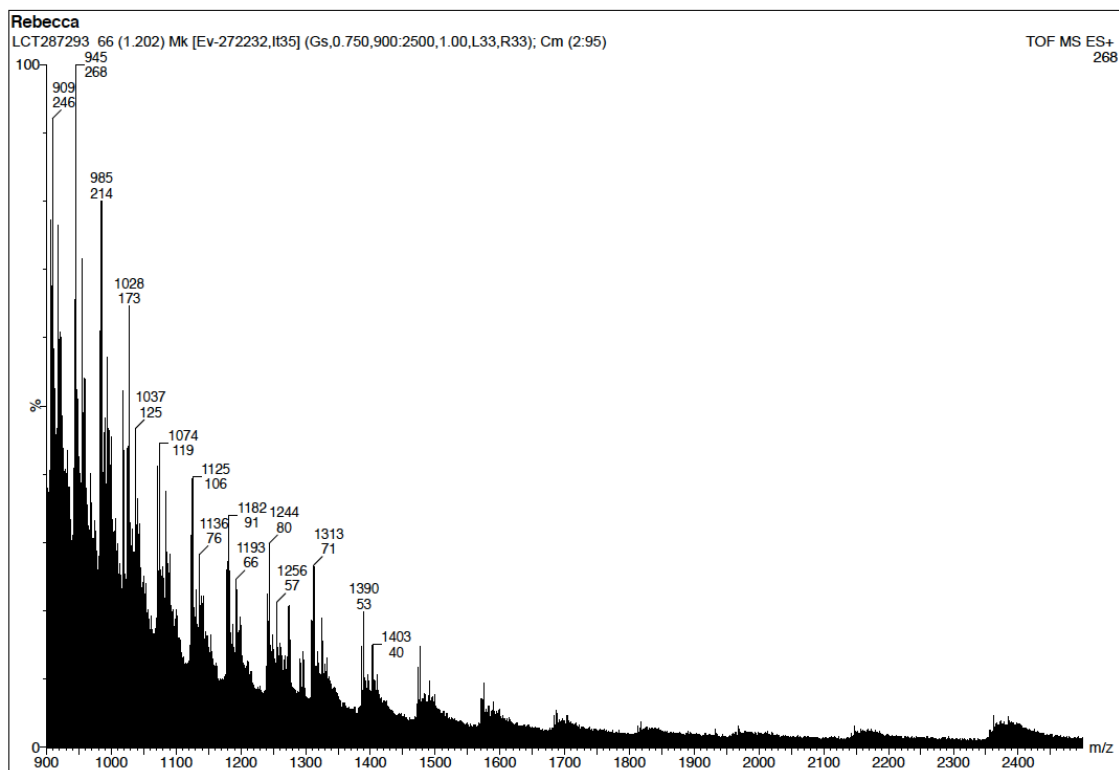
TS and N-benzyl piperidine acrylamide 54 at different pH values

TS (10 μM), DTT (1 mM) and N-benzyl piperidine acrylamide **54** (400 μM) in ammonium bicarbonate (10 mM). Addition of 0.5 % formic acid to adjust the pH to the indicated value.

pH 8.1
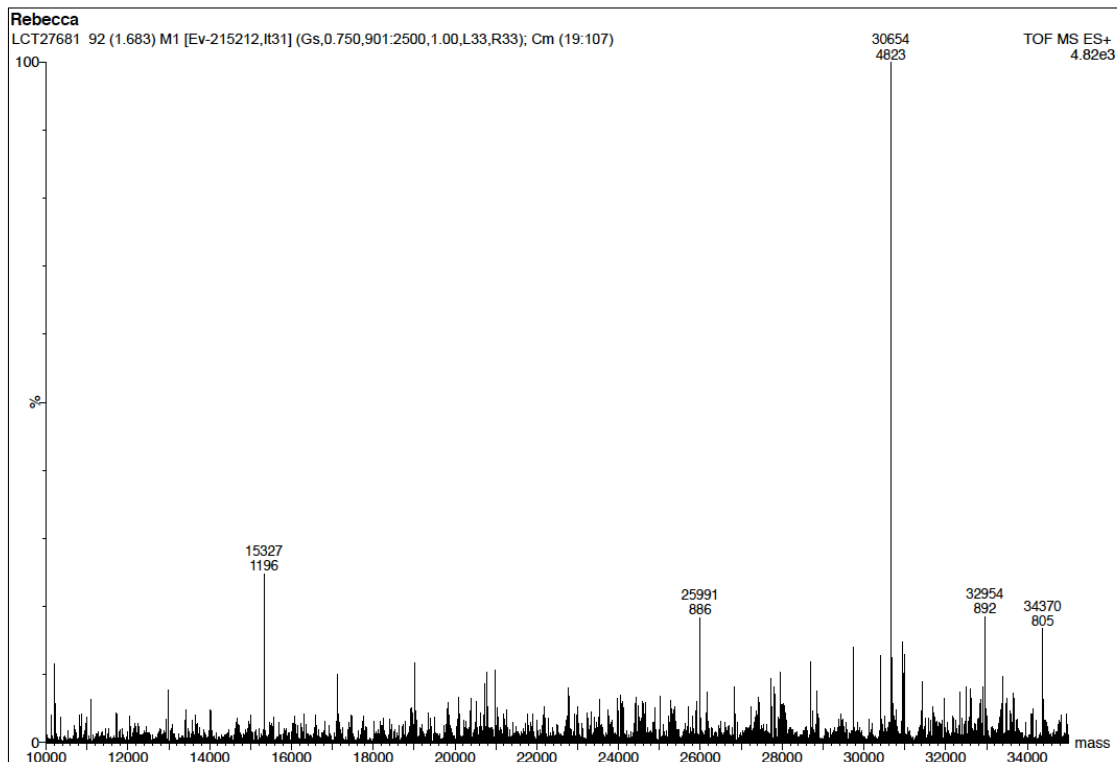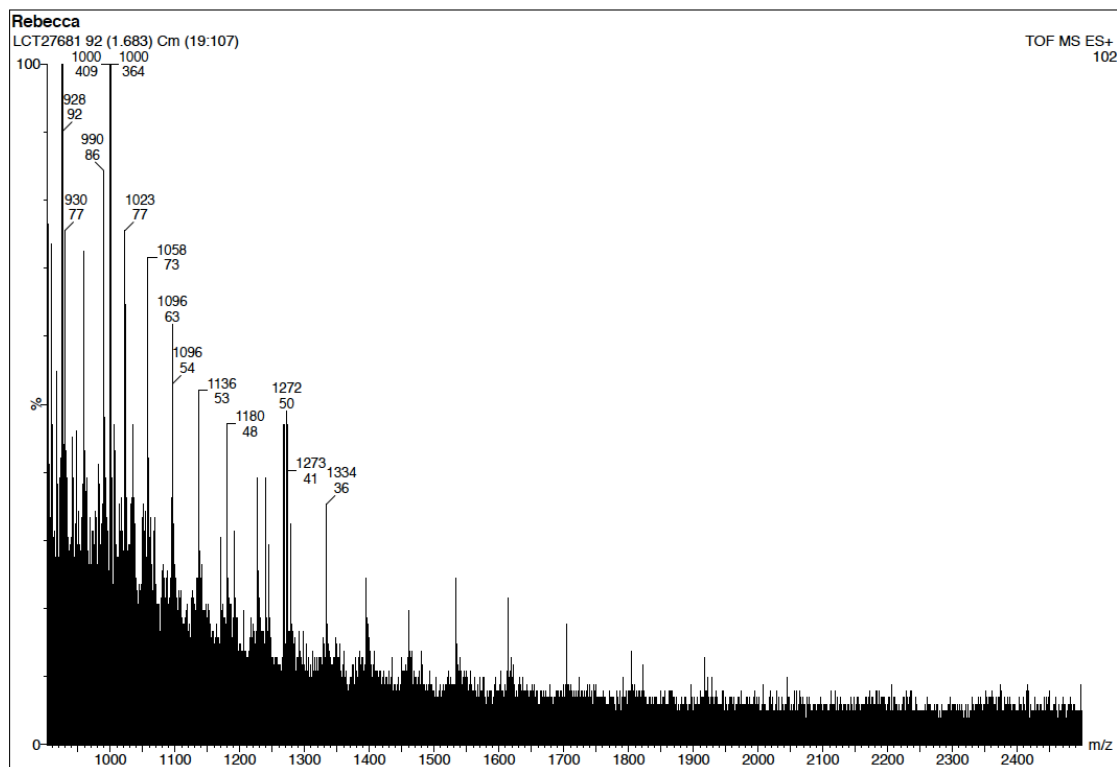
pH 7.9

pH 7.6

pH 7.4

pH 7.3

pH 7.2
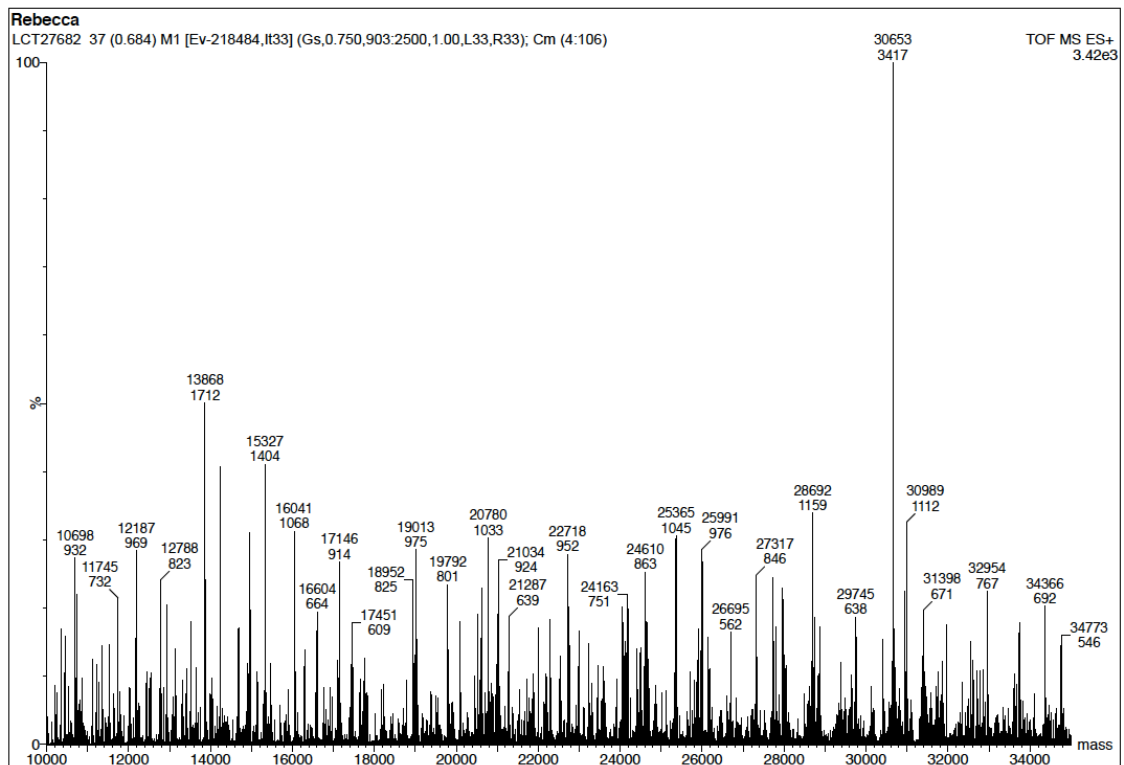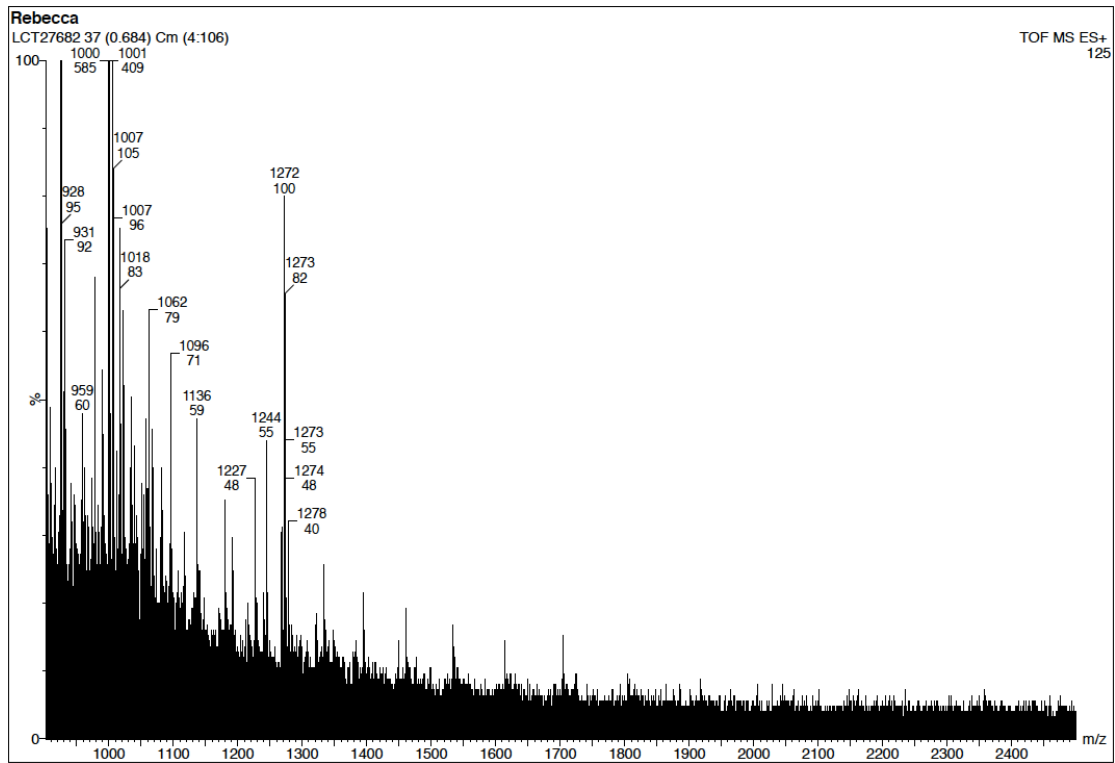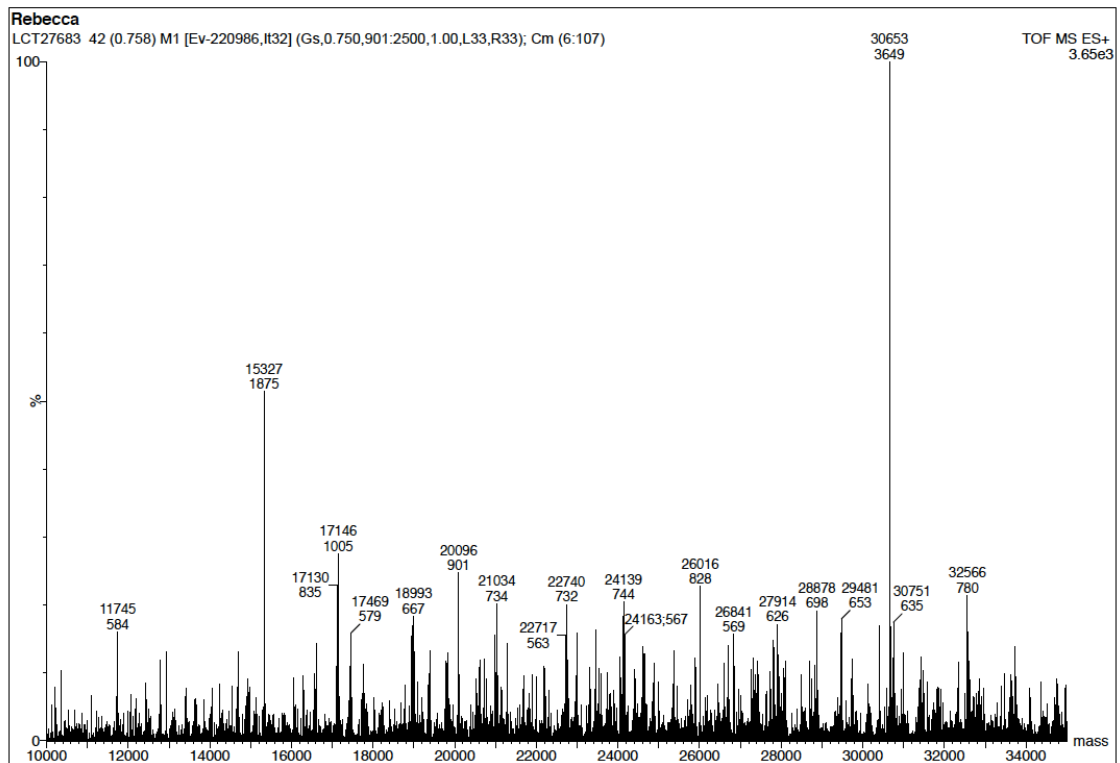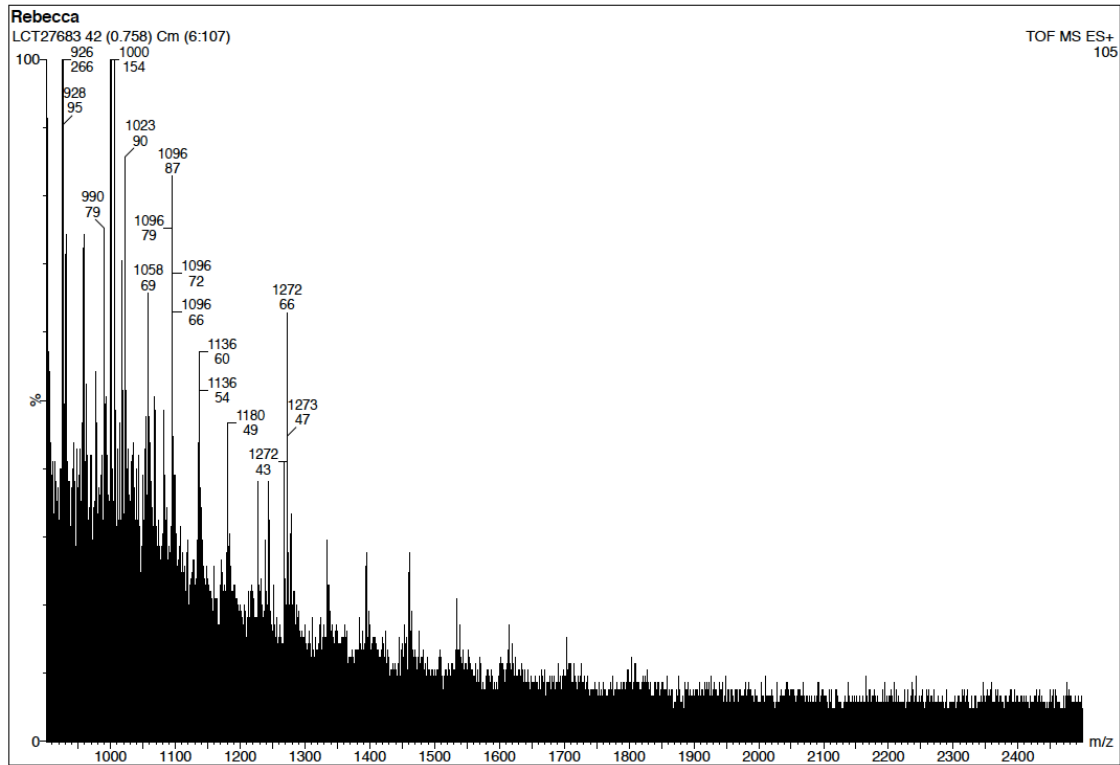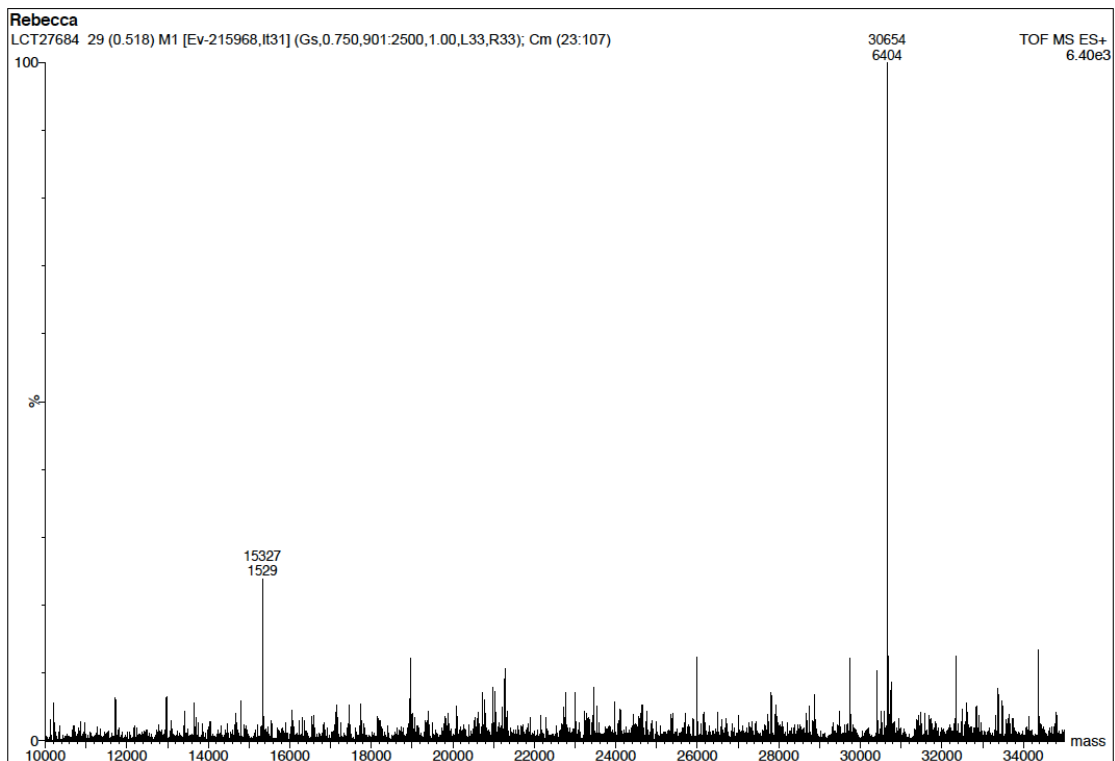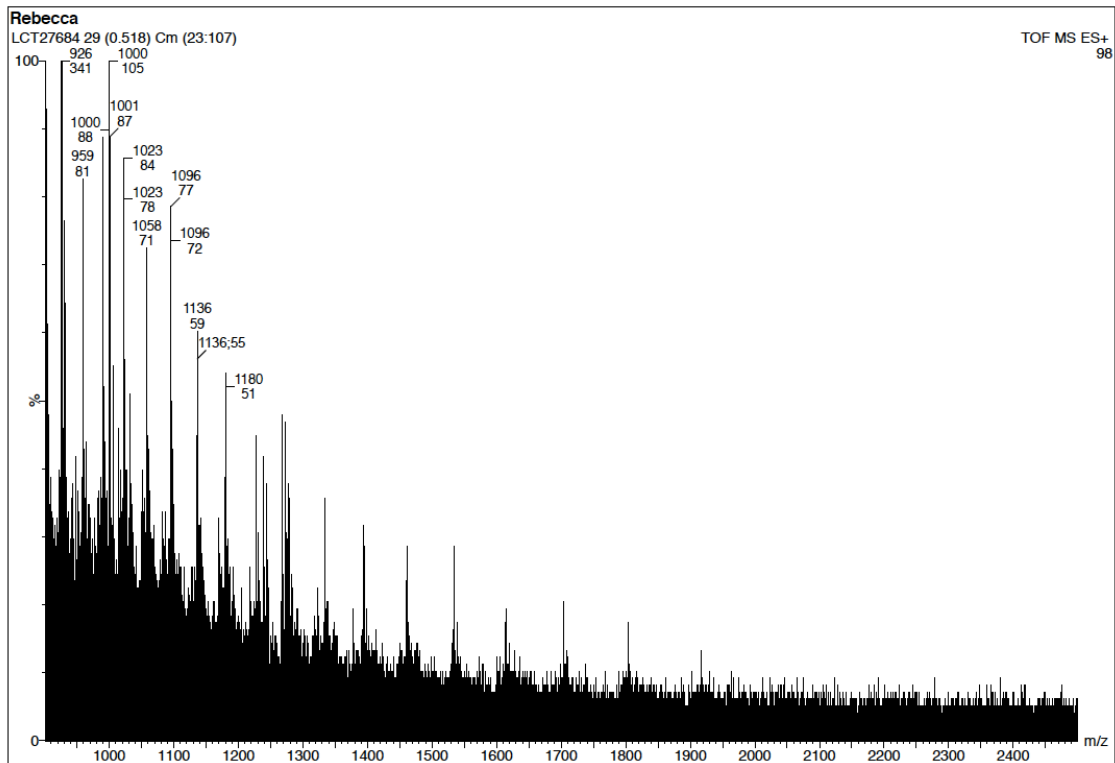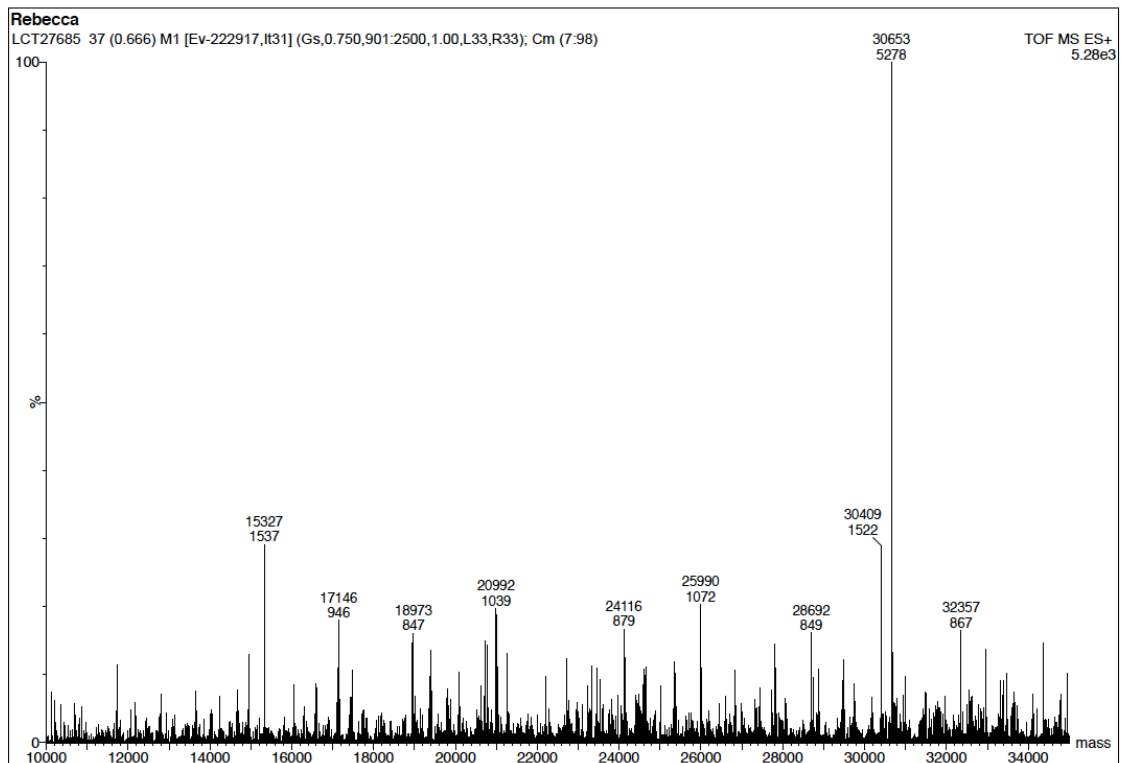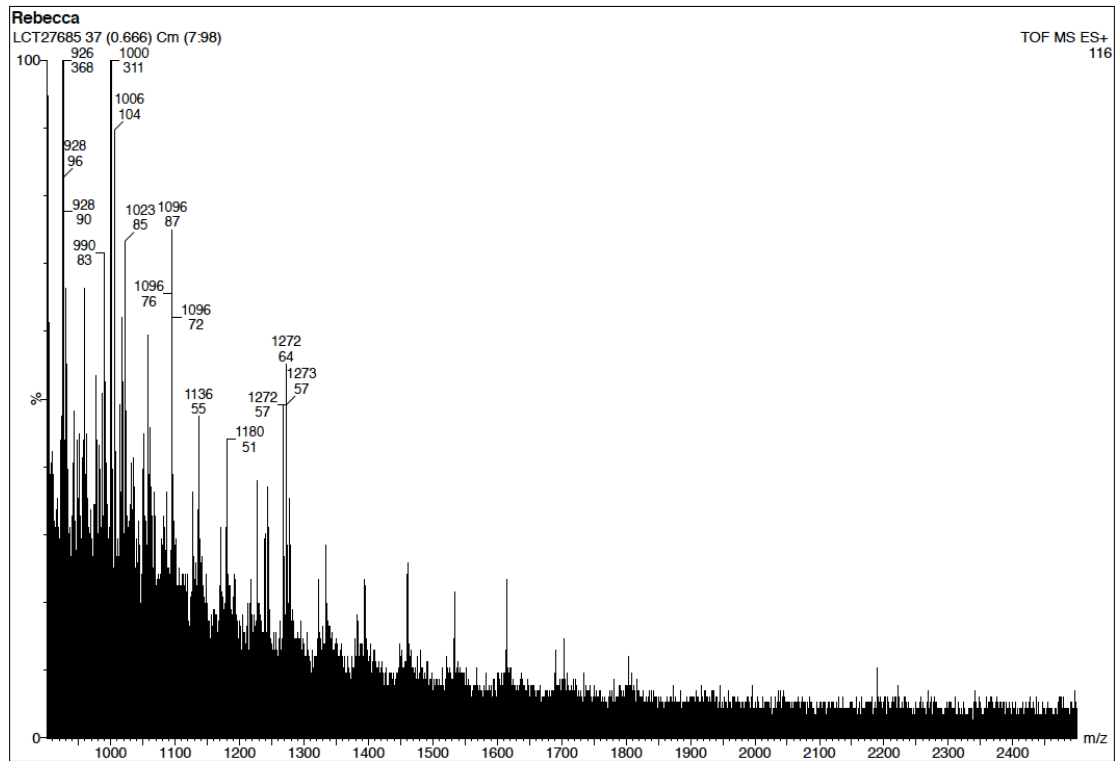
Irreversibility test for vinyl sulfonamide reaction with TS

Method

Sample 'A': 192 μL TS (10 μM in ammonium bicarbonate (10 mM), DTT (1 mM)) + 8 μL vinyl sulfonamide **44** (from 250 μM stock in MeOH).

Sample 'B': 192 μL TS (10 μM in ammonium bicarbonate (10 mM), DTT (1 mM)) + 8 μL vinyl sulfonamide **70** (from 250 μM stock in MeOH).

Both samples A and B were left to equilibrate at room temperature for 2 h. A 25 μL aliquot was then taken from both A and B and analysed by ESI MS (Sample A: LCT26571, Sample B: LCT26572).

A 100 μL aliquot was then taken from Sample A and from Sample B, and to each was added 4 μL of the 250 μM stock solution for vinyl sulfonamides **70** or **44** respectively. Both were subsequently analysed after 120 min (Sample A + **70**: LCT26579, Sample B + **44**: LCT26580).

LCT26571
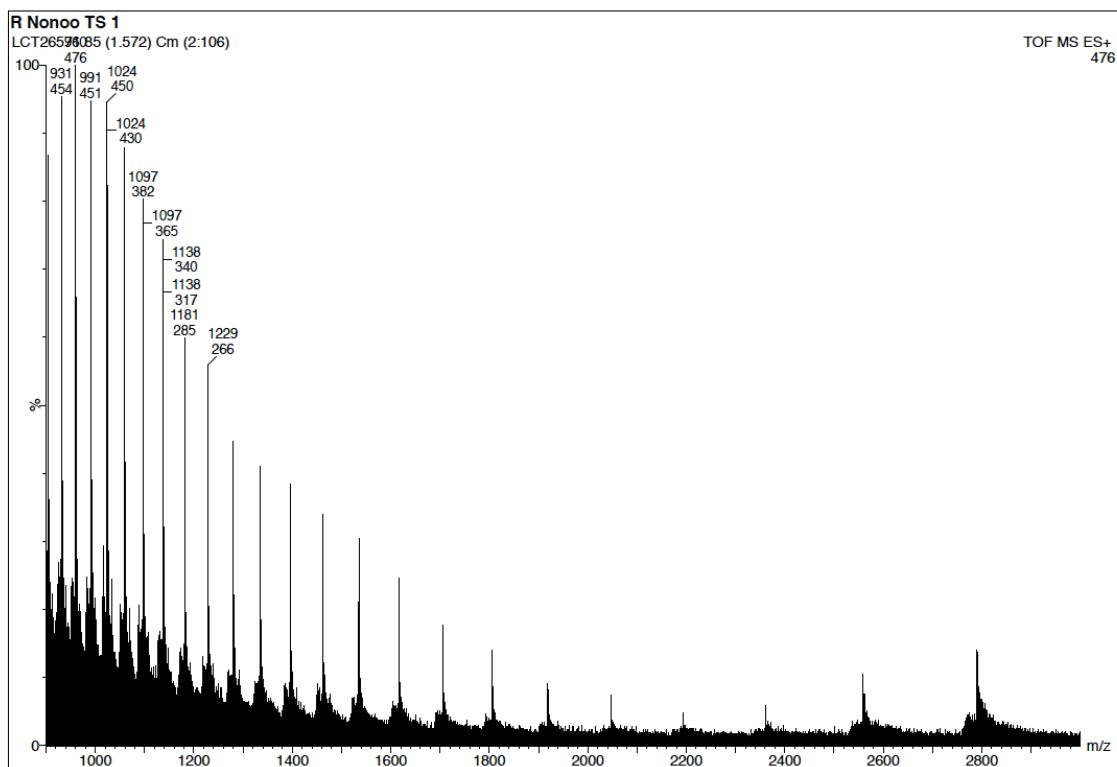
LCT26571 after deconvolution

R Nonoo TS 1
LCT26571 85 (1.572) M1 [Ev-323132,It38] (Gs,0.750,900:3000,1.00,L33,R33); Cm (2:106)   30691   TOF MS ES+
37893   3.79e4

LCT26572

R Nonoo TS 1
LCT26572 89 (1.628) Cm (5:107)   TOF MS ES+
1.33e3
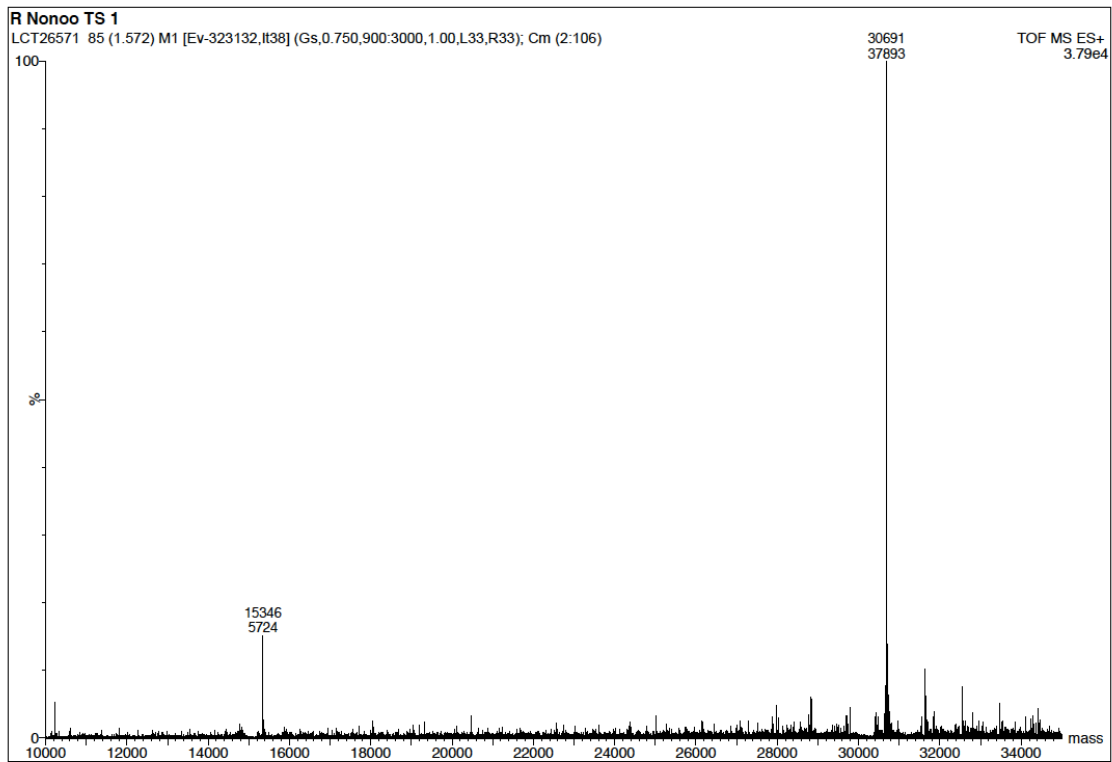
LCT26572 after deconvolution

R Nonoo TS 1
LCT26572 89 (1.628) M1 [Ev-373752,It43] (Gs,0.750,900:3000,1.00,L33,R33); Cm (5:107)   30754   TOF MS ES+
    46455   4.65e4

15377
10502

LCT26579

R Nonoo TS 1
LCT26579 94 (1.720) Cm (4:107)   TOF MS ES+
    1.55e3

1548
934
720
1059
673
991
556
1097
460
1138
375
1181
317
1229
262
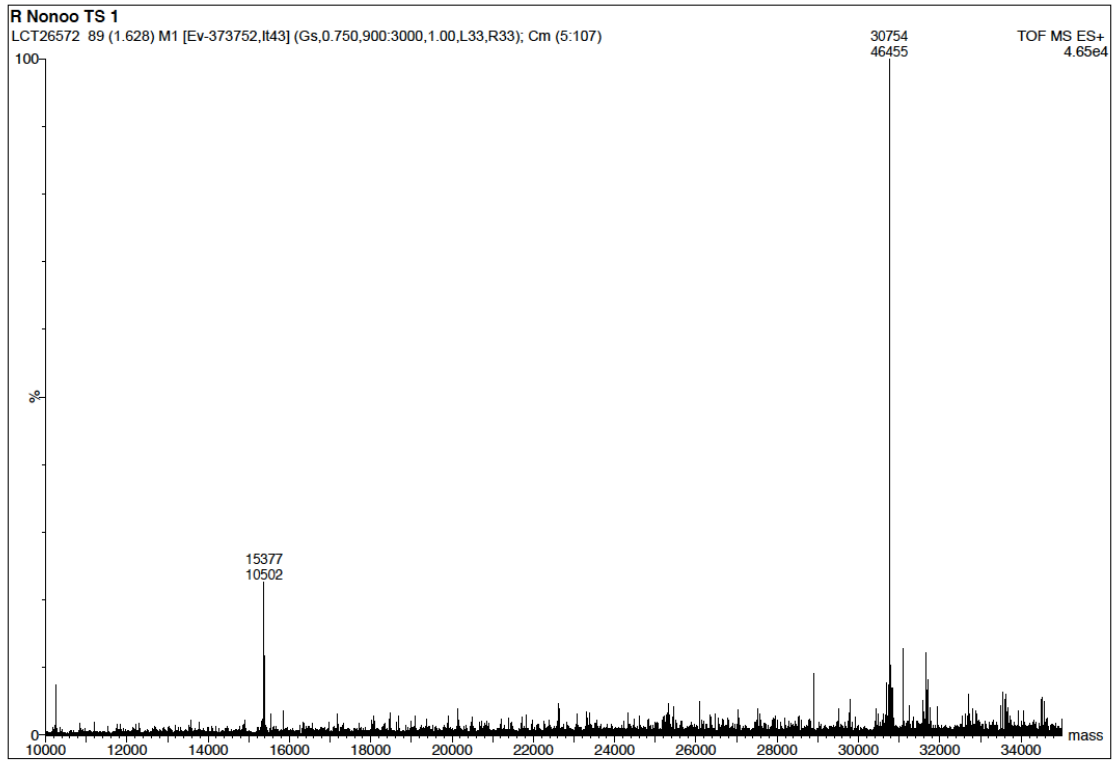
LCT26579 after deconvolution
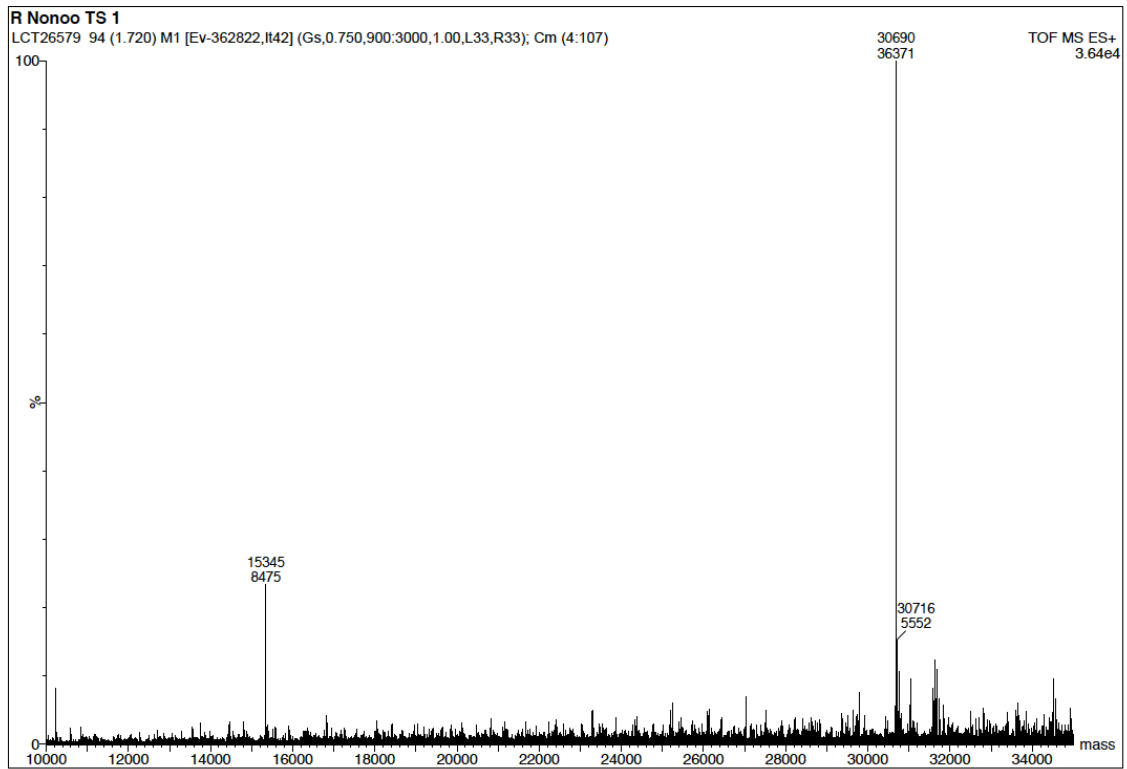
LCT26580
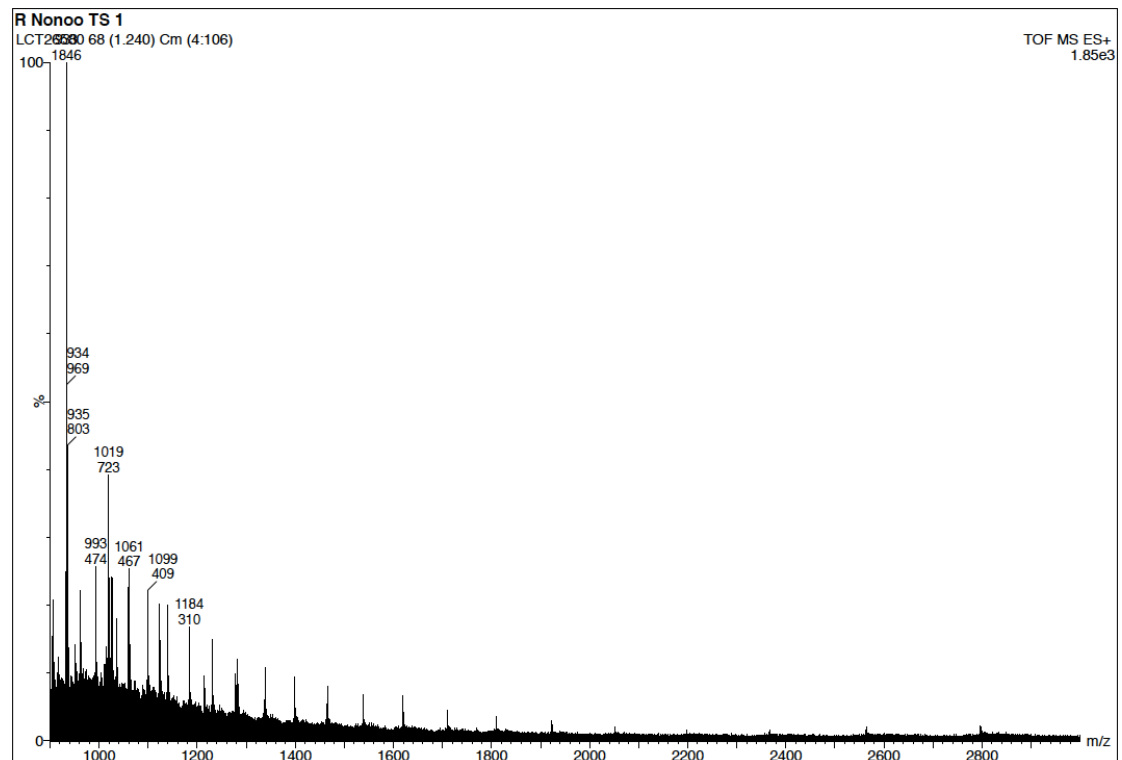
LCT26580 after deconvolution

R Nonoo TS 1
LCT26580 68 (1.240) M1 [Ev-371547,It42] (Gs,0.750,900:3000,1.00,L33,R33); Cm (4:106)
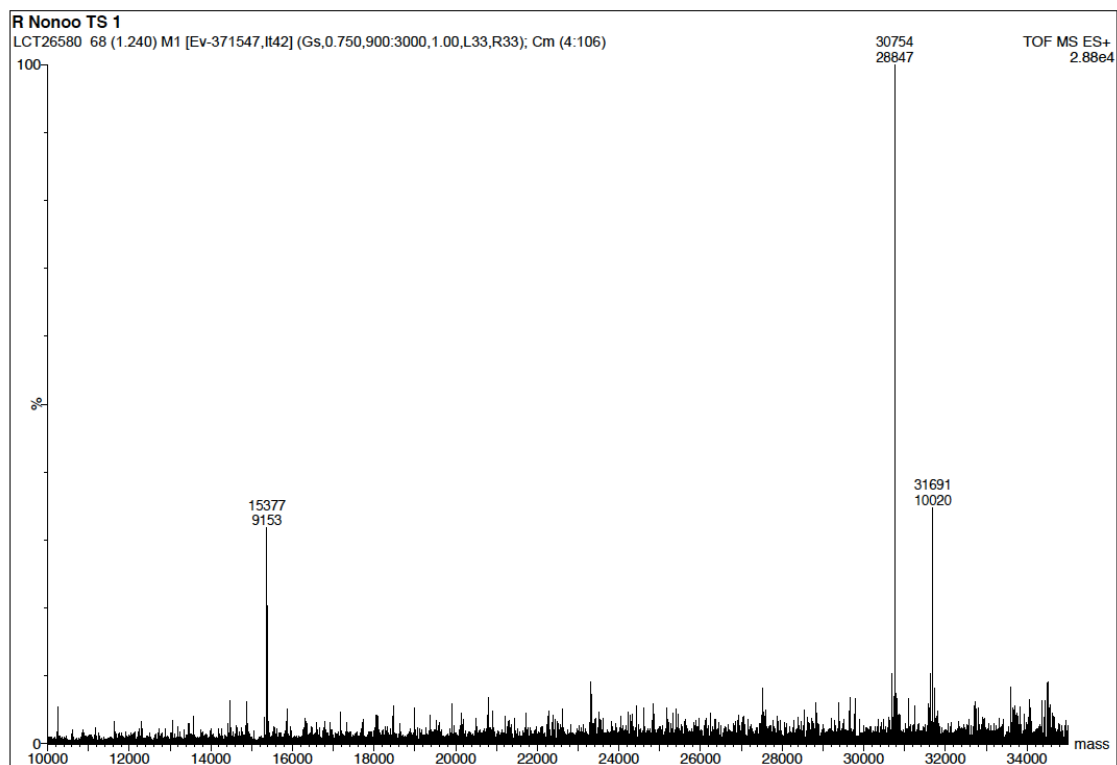
Appendix VIII Original SDS PAGE images

The MW Marker for all SDS PAGE images is composed of proteins with molecular weights as indicated:
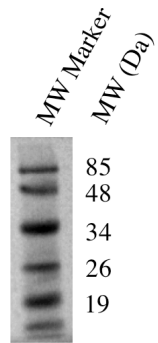
Images from Figure 32
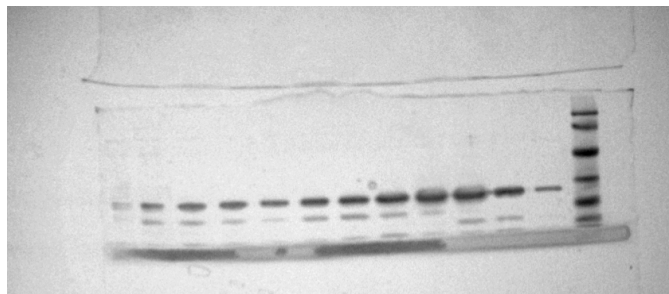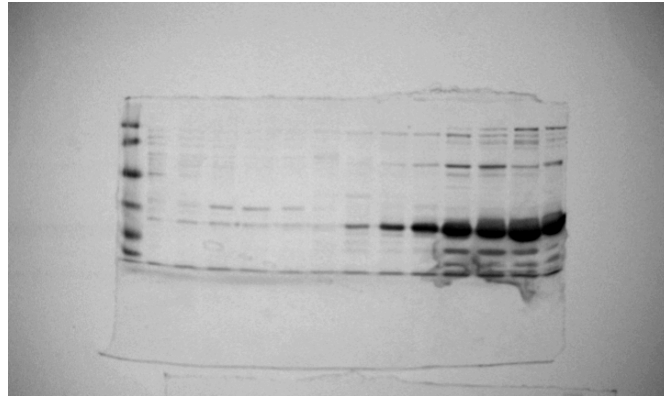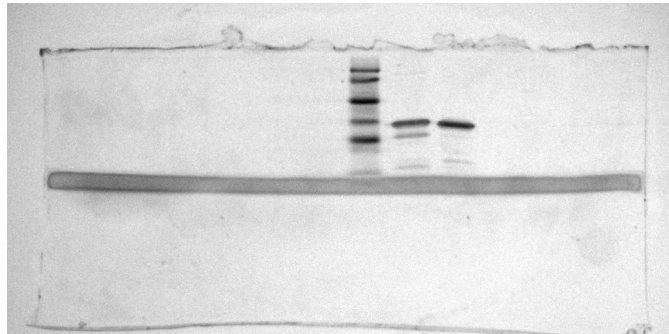
Images from Figure 50
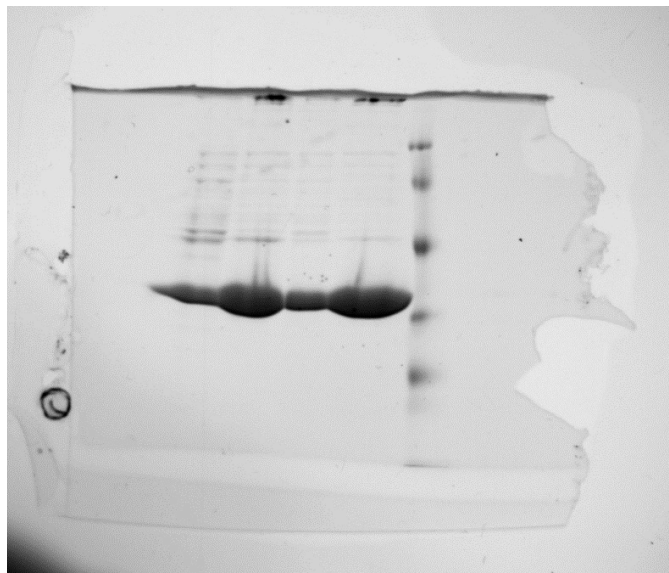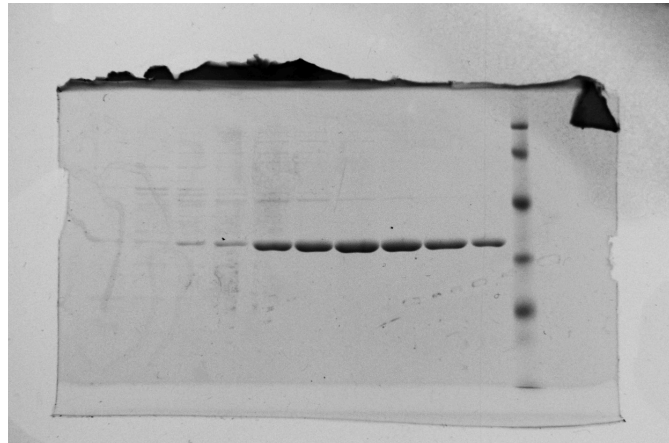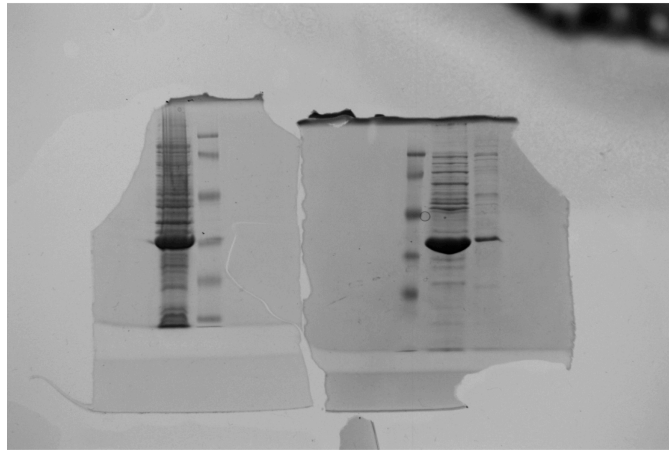
Images from Figure 51
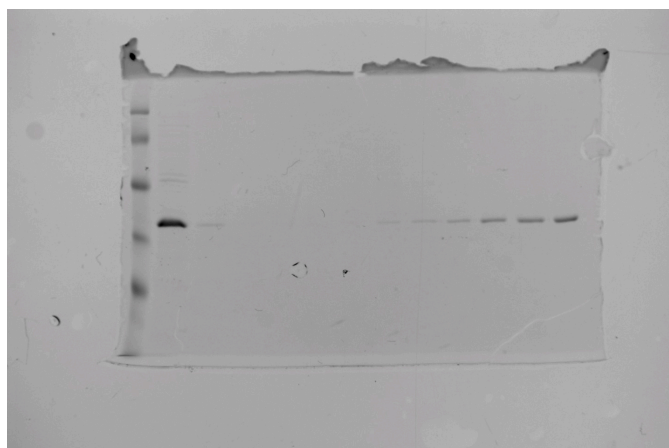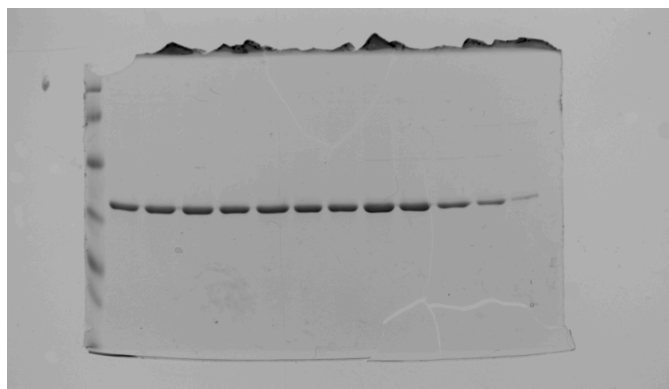
Images from Figure 59
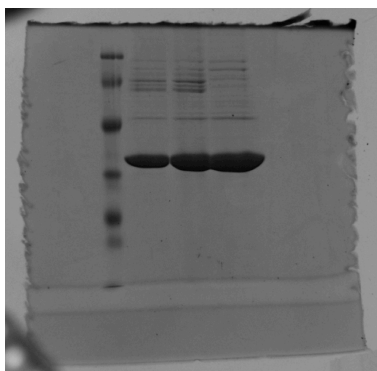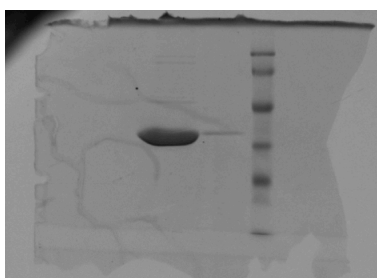
Appendix IX Correlation between olefinic acrylamide ^{1}H NMR shifts and acrylamide reactivity towards 1,4-conjugate addition

^{1}H NMR shifts and J values for the olefinic protons from a selection of acrylamides are shown in the table below.
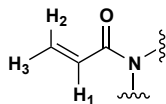
Compound No.	Proton 1	Proton 2	Proton 3	*J* (*trans*)	*J* (*cis*)	*J* (*gem*)
47	6.15	6.35	5.69	17.0	10.3	1.3
48	6.09	6.32	5.66	17.1	10.3	1.3
49	6.64	6.36	5.76	16.7	10.8	1.7
51	6.91	6.68	6.01	17.2	10.0	1.4
52	6.32	6.48	5.82	16.0	10.0	1.0
53	6.10	6.25	5.61	17.0	10.2	1.5
54	6.10	6.30	5.65	17.0	10.2	1.4
55	6.12	6.27	5.63	17.1	10.3	1.7
67	6.21	6.33	5.69	17.3	9.7	1.6
85	6.15	6.27	5.63	16.7	10.0	1.7
86	6.27	6.09	5.59	17.5	10.0	-
91	6.15	6.26	5.62	17.1	9.5	1.9
119	6.03	6.26	5.56	17.0	10.3	1.2
132	6.07	6.16	5.49	17.1	10.0	2.4
134	6.15	6.26	5.57	17.3	10.0	1.8
160	6.05	6.26	5.62	17.0	10.3	1.6
161	6.07	6.26	5.50	16.5	9.9	1.1
162	6.04	6.19	5.54	16.9	10.3	1.7
163	6.03	6.23	5.58	16.9	10.3	1.5
164	6.15	6.24	5.54	17.0	9.8	2.1
165	6.29	6.10	5.62	15.9	9.4	2.4
173	6.11	6.20	5.58	17.0	9.8	2.1

It is interesting to note that the sum of the shifts for the three olefinic protons may give an indication of acrylamide reactivity towards conjugate addition. This may be expected as proton shift by ^{1}H NMR gives an indication of electron shielding, and an electron deficient centre is more susceptible to nucleophilic attack. As shown in the chart below, acrylamide **51** is seen to have the highest olefinic proton shift sum, and this acrylamide was indeed the most reactive acrylamide encountered during HPLC studies. Acrylamide **51** was excluded from tethering studies with protein on the basis of its very high intrinsic reactivity as seen by HPLC. Acrylamide **49** is seen in the chart below to have the second highest olefinic proton shift sum, and this acrylamide was observed by HPLC studies to be the most reactive of those used for tethering studies. If ^{1}H NMR shifts can indeed be used to predict acrylamide reactivity, this would provide a highly useful and quick measure of the suitability of an acrylamide for tethering, overcoming the need for time consuming HPLC studies with a model thiol.
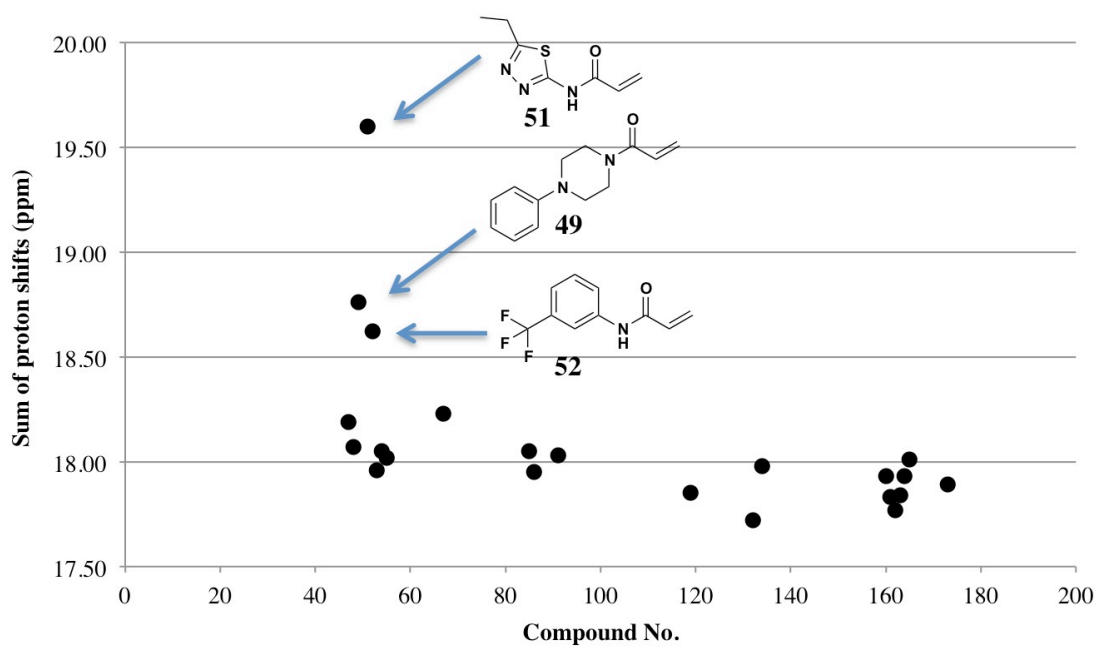
11. Bibliography

[1]   R. S. Bohacek, C. McMartin, W. C. Guida, *Med. Res. Rev.* **1996**, *16*, 3-50.

[2]   M. M. Hann, A. R. Leach, G. Harper, *J. Chem. Inf. Comp. Sci.* **2001**, *41*, 856-864.

[3]   C. A. Lipinski, F. Lombardo, B. W. Dominy, P. J. Feeney, *Adv. Drug. Deliver. Rev.* **1997**, *23*, 3-25.

[4]   P. D. Leeson, B. Springthorpe, *Nat. Rev. Drug Discovery* **2007**, *6*, 881-890.

[5]   M. C. Wenlock, R. P. Austin, P. Barton, A. M. Davis, P. D. Leeson, *J. Med. Chem.* **2003**, *46*, 1250-1256.

[6]   S. J. Teague, A. M. Davis, P. D. Leeson, T. Oprea, *Angew. Chem. Int. Edit.* **1999**, *38*, 3743-3748.

[7]   M. Vieth, M. G. Siegel, R. E. Higgs, I. A. Watson, D. H. Robertson, K. A. Savin, G. L. Durst, P. A. Hipskind, *J. Med. Chem.* **2004**, *47*, 224-232.

[8]   M. Congreve, R. Carr, C. Murray, H. Jhoti, *Drug Discovery Today* **2003**, *8*, 876-877.

[9]   A. L. Hopkins, C. R. Groom, A. Alex, *Drug Discovery Today* **2004**, *9*, 430-431.

[10]   I. D. Kuntz, K. Chen, K. A. Sharp, P. A. Kollman, *P. Natl. Acad. Sci. USA* **1999**, *96*, 9997-10002.

[11]   M. I. Page, W. P. Jencks, *Proc. Natl. Acad. Sci. USA* **1971**, *68*, 1678-1683.

[12]   L. C. Blum, J. L. Reymond, *J. Am. Chem. Soc.* **2009**, *131*, 8732-8733.

[13]   C. W. Murray, M. L. Verdonk, D. C. Rees, *Trends Pharmacol. Sci.* **2012**, *33*, 224-232.

[14]   P. J. Hajduk, G. Sheppard, D. G. Nettesheim, E. T. Olejniczak, S. B. Shuker, R. P. Meadows, D. H. Steinman, G. M. Carrera, P. A. Marcotte, J. Severin, K. Walter, H. Smith, E. Gubbins, R. Simmer, T. F. Holzman, D. W. Morgan, S. K. Davidsen, J. B. Summers, S. W. Fesik, *J. Am. Chem. Soc.* **1997**, *119*, 5818-5827.

[15]   S. B. Shuker, P. J. Hajduk, R. P. Meadows, S. W. Fesik, *Science* **1996**, *274*, 1531-1534.

[16]   N. Howard, C. Abell, W. Blakemore, G. Chessari, M. Congreve, S. Howard, H. Jhoti, C. W. Murray, L. C. Seavers, R. L. van Montfort, *J. Med. Chem.* **2006**, *49*, 1346-1355.

[17]   J. R. Huth, C. Park, A. M. Petros, A. R. Kunzer, M. D. Wendt, X. L. Wang, C. L. Lynch, J. C. Mack, K. M. Swift, R. A. Judge, J. Chen, P. L. Richardson, S. Jin, S. K. Tahir, E. D. Matayoshi, S. A. Dorwin, U. S. Ladror, J. M. Severin, K. A. Walter, D. M. Bartley, S. W. Fesik, S. W. Elmore, P. J. Hajduk, *Chem. Biol. Drug Des.* **2007**, *70*, 1-12.

[18]   C. H. Rohrig, C. Loch, J. Y. Guan, G. Siegal, M. Overhand, *ChemMedChem* **2007**, *2*, 1054-1070.

[19]   P. J. Hajduk, *J. Med. Chem.* **2006**, *49*, 6972-6976.

[20]   M. Congreve, G. Chessari, D. Tisi, A. J. Woodhead, *J. Med. Chem.* **2008**, *51*, 3661-3680.

[21]   P. J. Hajduk, J. Greer, *Nat. Rev. Drug Discovery* **2007**, *6*, 211-219.

[22]   D. E. Scott, A. G. Coyne, S. A. Hudson, C. Abell, *Biochemistry* **2012**, *51*, 4990-5003.

[23]   W. Jahnke, D. A. Erlanson, *Fragment-based approaches in drug discovery*, Wiley, **2006**.

[24]   G. E. De Kloe, D. Bailey, R. Leurs, I. J. P. de Esch, *Drug Discovery Today* **2009**, *14*, 630-646.

[25]   J. Tsai, J. T. Lee, W. Wang, J. Zhang, H. Cho, S. Mamo, R. Bremer, S. Gillette, J. Kong, N. K. Haass, K. Sproesser, L. Li, K. S. M. Smalley, D. Fong, Y. L. Zhu, A. Marimuthu, H. Nguyen, B. Lam, J. Liu, I. Cheung, J. Rice, Y. Suzuki, C. Luu, C. Settachatgul, R. Shellooe, J. Cantwell, S. H. Kim, J. Schlessinger, K. Y. J. Zhang, B. L. West, B. Powell, G. Habets, C. Zhang, P. N. Ibrahim, P. Hirth, D. R. Artis, M. Herlyn, G. Bollag, *Proc. Natl. Acad. Sci. USA* **2008**, *105*, 3041-3046.

[26]   C. W. Murray, D. C. Rees, *Nat. Chem.* **2009**, *1*, 187-192.

[27]   R. Campos-Olivas, *Curr. Top. Med. Chem.* **2011**, *11*, 43-67.

[28]   H. Jhoti, A. Cleasby, M. Verdonk, G. Williams, *Curr. Opin. Chem. Biol.* **2007**, *11*, 485-493.

[29]   I. Navratilova, A. L. Hopkins, *Med. Chem. Lett.* **2010**, *1*, 44-48.

[30]   J. E. Ladbury, G. Klebe, E. Freire, *Nat. Rev. Drug Discovery* **2010**, *9*, 23-27.

[31]   A. Ciulli, C. Abell, *Curr. Opin. Biotechnol.* **2007**, *18*, 489-496.

[32]   A. Jadhav, R. S. Ferreira, C. Klumpp, B. T. Mott, C. P. Austin, J. Inglese, C. J. Thomas, D. J. Maloney, B. K. Shoichet, A. Simeonov, *J. Med. Chem.* **2010**, *53*, 37-51.

[33]   B. A. Tounge, M. H. Parker, *Method. Enzymol.* **2011**, *493*, 3-20.

[34]   M. Mayer, B. Meyer, *Angew. Chem. Int. Edit.* **1999**, *38*, 1784-1788.

[35]   D. A. Erlanson, R. S. McDowell, T. O'Brien, *J. Med. Chem.* **2004**, *47*, 3463-3482.

[36]   M. Pellecchia, B. Becattini, K. J. Crowell, R. Fattorusso, M. Forino, M. Fragai, D. Jung, T. Mustelin, L. Tautz, *Expert Opin. Ther. Tar.* **2004**, *8*, 597-611.

[37]   C. A. Lepre, J. M. Moore, J. W. Peng, *Chem. Rev.* **2004**, *104*, 3641-3675.

[38]   Y. S. Wang, C. Strickland, J. H. Voigt, M. E. Kennedy, B. M. Beyer, M. M. Senior, E. M. Smith, T. L. Nechuta, V. S. Madison, M. Czarniecki, B. A. McKittrick, A. W. Stamford, E. M. Parker, J. C. Hunter, W. J. Greenlee, D. F. Wyss, *J. Med. Chem.* **2010**, *53*, 942-950.

[39]   D. P. Ryan, J. M. Matthews, *Curr. Opin. Struc. Biol.* **2005**, *15*, 441-446.

[40]   B. Schuster-Bockler, A. Bateman, *Genome Biol.* **2008**, *9*, 1, R9.

[41]   T. Clackson, J. A. Wells, *Science* **1995**, *267*, 383-386.

[42]   C. D. Thanos, W. L. DeLano, J. A. Wells, *Proc. Natl. Acad. Sci. USA* **2006**, *103*, 15422-15427.

[43]   Y. A. Muller, B. Li, H. W. Christinger, J. A. Wells, B. C. Cunningham, A. M. DeVos, *Proc. Natl. Acad. Sci. USA* **1997**, *94*, 7192-7197.

[44]   J. A. Wells, C. L. McClendon, *Nature* **2007**, *450*, 1001-1009.

[45]   M. F. Schmidt, J. Rademann, *Trends Biotechnol.* **2009**, *27*, 512-521.

[46]   I. Huc, J. M. Lehn, *Proc. Natl. Acad. Sci. USA* **1997**, *94*, 2106-2110.

[47]   M. Hochgurtel, H. Kroth, D. Piecha, M. W. Hofmann, C. Nicolau, S. Krause, O. Schaaf, G. Sonnenmoser, A. V. Eliseev, *Proc. Natl. Acad. Sci. USA* **2002**, *99*, 3382-3387.

[48]   M. Hochgurtel, R. Biesinger, H. Kroth, D. Piecha, M. W. Hofmann, S. Krause, O. Schaaf, C. Nicolau, A. V. Eliseev, *J. Med. Chem.* **2003**, *46*, 356-358.

[49]   D. E. Scott, G. J. Dawes, M. Ando, C. Abell, A. Ciulli, *ChemBioChem* **2009**, *10*, 2772-2779.

[50]   M. S. Congreve, D. J. Davis, L. Devine, C. Granata, M. O'Reilly, P. G. Wyatt, H. Jhoti, *Angew. Chem. Int. Edit.* **2003**, *42*, 4479-4482.

[51]   D. A. Erlanson, A. C. Braisted, D. R. Raphael, M. Randal, R. M. Stroud, E. M. Gordon, J. A. Wells, *Proc. Natl. Acad. Sci. USA* **2000**, *97*, 9367-9372.

[52]   N. A. Thornberry, *Chem. Biol.* **1998**, *5*, R97-R103.

[53]   I. C. Choong, W. Lew, D. Lee, P. Pham, M. T. Burdett, J. W. Lam, C. Wiesmann, T. N. Luong, B. Fahr, W. L. DeLano, R. S. McDowell, D. A. Allen, D. A. Erlanson, E. M. Gordon, T. O'Brien, *J. Med. Chem.* **2002**, *45*, 5005-5022.

[54]   T. O'brien, B. T. Fahr, M. M. Sopko, J. W. Lam, N. D. Waal, B. C. Raimundo, H. E. Purkey, P. Pham, M. J. Romanowski, *Acta Crystallogr. F.* **2005**, *61*, 451-458.

[55]   J. A. Hardy, J. Lam, J. T. Nguyen, T. O'Brien, J. A. Wells, *Proc. Natl. Acad. Sci. USA* **2004**, *101*, 12461-12466.

[56]   T. R. Matek, *Annu. Rev. Immunol.* **2008**, *26*, 453-479.

[57]   J. W. Tilley, L. Chen, D. C. Fry, S. D. Emerson, G. D. Powers, D. Biondi, T. Varnell, R. Trilles, R. Guthrie, F. Mennona, G. Kaplan, R. A. LeMahieu, M. Carson, R. J. Han, C. M. Liu, R. Palermo, G. Ju, *J. Am. Chem. Soc.* **1997**, *119*, 7589-7590.

[58]   M. R. Arkin, M. Randal, W. L. DeLano, J. Hyde, T. N. Luong, J. D. Oslob, D. R. Raphael, L. Taylor, J. Wang, R. S. McDowell, J. A. Wells, A. C. Braisted, *Proc. Natl. Acad. Sci. USA* **2003**, *100*, 1603-1608.

[59]   D. A. Erlanson, J. A. Wells, A. C. Braisted, *Annu. Rev. Biophys. Biomol. Struct.* **2004**, *33*, 199-223.

[60]   T. O. Johnson, J. Ermolieff, M. R. Jirousek, *Nat. Rev. Drug Discovery* **2002**, *1*, 696-709.

[61]   D. A. Erlanson, R. S. McDowell, M. M. He, M. Randal, R. L. Simmons, J. Kung, A. Waight, S. K. Hansen, *J. Am. Chem. Soc.* **2003**, *125*, 5602-5603.

[62]   M. T. Cancilla, M. M. He, N. Viswanathan, R. L. Simmons, M. Taylor, A. D. Fung, K. Cao, D. A. Erlanson, *Bioorg. Med. Chem. Lett.* **2008**, *18*, 3978-3981.

[63]   N. Keen, S. Taylor, *Nat. Rev. Cancer* **2004**, *4*, 927-936.

[64]   A. Whitty, *Nat. Chem. Biol.* **2008**, *4*, 435-439.

[65]   J. L. Kice, G. E. Ekman, *J. Org. Chem.* **1975**, *40*, 711-716.

[66]   R. Boutros, V. Lobjois, B. Ducommun, *Nat. Rev. Cancer* **2007**, *7*, 495-507.

[67]   B. Aressy, B. Ducommun, *Anti-Cancer Agents Med. Chem.* **2008**, *8*, 818-824.

[68]   K. Kristjansdottir, J. Rudolph, *Chem. Biol.* **2004**, *11*, 1043-1051.

[69]   A. Lavecchia, C. Di Giovanni, E. Novellino, *Expert Opin. Ther. Pat.* **2010**, *20*, 405-425.

[70]   E. B. Fauman, J. P. Cogswell, B. Lovejoy, W. J. Rocque, W. Holmes, V. G. Montana, H. Piwnica-Worms, M. J. Rink, M. A. Saper, *Cell* **1998**, *93*, 617-625.

[71]   R. A. Reynolds, A. W. Yem, C. L. Wolfe, M. R. Deibel, C. G. Chidester, K. D. Watenpaugh, *J. Mol. Biol.* **1999**, *293*, 559-568.

[72]   J. Sohn, J. Rudolph, *J. Mol. Biol.* **2006**, *362*, 1060-1071.

[73]   J. Sohn, K. Kristjansdottir, A. Safi, B. Parker, B. Kiburz, J. Rudolph, *Proc. Natl. Acad. Sci. USA* **2004**, *101*, 16437-16441.

[74]   R. Sohn, J. M. Parks, G. Buhrman, P. Brown, K. Kristjansdottir, A. Safi, H. Edelsbrunner, W. T. Yang, J. Rudolph, *Biochemistry* **2005**, *44*, 16563-16573.

[75]   G. J. L. Bernardes, E. J. Grayson, S. Thompson, J. M. Chalker, J. C. Errey, F. El Oualid, T. D. W. Claridge, B. G. Davis, *Angew. Chem. Int. Edit.* **2008**, *47*, 2244-2247.

[76]   M. H. Potashman, M. E. Duggan, *J. Med. Chem.* **2009**, *52*, 1231-1246.

[77]   J. Singh, R. C. Petter, T. A. Baillie, A. Whitty, *Nat. Rev. Drug discovery* **2011**, *10*, 307-317.

[78]   Q. Liu, Y. Sabnis, Z. Zhao, T. Zhang, S. J. Buhrlage, L. H. Jones, N. S. Gray, *Chem. Biol.* **2013**, *20*, 146-159.

[79]   W. Li, J. L. Blankman, B. F. Cravatt, *J. Am. Chem. Soc.* **2007**, *129*, 9594-9595.

[80]   E. Zartler, M. Shapiro, *Fragment-based drug discovery: a practical approach*, Wiley, Oxford, **2008**.

[81]   G. Chen, A. Heim, D. Riether, D. Yee, Y. Milgrom, M. A. Gawinowicz, D. Sames, *J. Am. Chem. Soc.* **2003**, *125*, 8130-8133.

[82]   A. D. Moorhouse, J. E. Moses, *ChemMedChem* **2008**, *3*, 715-723.

[83]   A. J. Kirby, *Adv. Phys. Org. Chem.* **1981**, *17*, 183-278.

[84]   W. P. Jencks, *Proc. Natl. Acad. Sci. USA* **1981**, *78*, 4046-4050.

[85]   X. Hu, R. Manetsch, *Chem. Soc. Rev.* **2010**, *39*, 1316-1324.

[86]   J. F. Chase, P. K. Tubbs, *Biochem. J.* **1969**, *111*, 225-235.

[87]   J. Inglese, S. J. Benkovic, *Tetrahedron* **1991**, *47*, 2351-2364.

[88]   S. E. Greasley, T. H. Marsilje, H. Cai, S. Baker, S. J. Benkovic, D. L. Boger, I. A. Wilson, *Biochemistry* **2001**, *40*, 13538-13547.

[89]   D. L. Boger, N. E. Haynes, M. S. Warren, J. Ramcharan, P. A. Kitos, S. J. Benkovic, *Bioorg. Med. Chem.* **1997**, *5*, 1839-1846.

[90]   R. Nguyen, I. Huc, *Angew. Chem. Int. Ed.* **2001**, *40*, 1774-1776.

[91]   V. P. Mocharla, B. Colasson, L. V. Lee, S. Roper, K. B. Sharpless, C. H. Wong, H. C. Kolb, *Angew. Chem. Int. Edit.* **2005**, *44*, 116-120.

[92]   J. D. Cheeseman, A. D. Corbett, J. L. Gleason, R. J. Kazlauskas, *Chemistry* **2005**, *11*, 1708-1716.

[93]   Y. H. Yu, L. Ye, K. Haupt, K. Mosbach, *Angew. Chem. Int. Edit.* **2002**, *41*, 4459-4463.

[94]   T. Asaba, T. Suzuki, R. Ueda, H. Tsumoto, H. Nakagawa, N. Miyata, *J. Am. Chem. Soc.* **2009**, *131*, 6989-6996.

[95]   B. Heltweg, F. Dequiedt, B. L. Marshall, C. Branch, M. Yoshida, N. Nishino, E. Verdin, M. Jung, *J. Med. Chem.* **2004**, *47*, 5235-5243.

[96]   X. Hu, J. Sun, H. G. Wang, R. Manetsch, *J. Am. Chem. Soc.* **2008**, *130*, 13820-13821.

[97]   N. Shangguan, S. Katukojvala, R. Greenburg, L. J. Williams, *J. Am. Chem. Soc.* **2003**, *125*, 7754-7755.

[98]   R. V. Kolakowski, N. Shangguan, R. R. Sauers, L. J. Williams, *J. Am. Chem. Soc.* **2006**, *128*, 5695-5702.

[99]   M. D. Wendt, W. Shen, A. Kunzer, W. J. McClellan, M. Bruncko, T. K. Oost, H. Ding, M. K. Joseph, H. C. Zhang, P. M. Nimmer, S. C. Ng, A. R. Shoemaker, A. M. Petros, A. Oleksijew, K. Marsh, J. Bauch, T. Oltersdorf, B. A. Belli, D. Martineau, S. W. Fesik, S. H. Rosenberg, S. W. Elmore, *J. Med. Chem.* **2006**, *49*, 1165-1181.

[100]   A. M. Petros, J. Dinges, D. J. Augeri, S. A. Baumeister, D. A. Betebenner, M. G. Bures, S. W. Elmore, P. J. Hajduk, M. K. Joseph, S. K. Landis, D. G. Nettesheim, S. H. Rosenberg, W. Shen, S. Thomas, X. Wang, I. Zanze, H. Zhang, S. W. Fesik, *J. Med. Chem.* **2006**, *49*, 656-663.

[101]   S. S. Kulkarni, X. Hu, K. Doi, H. G. Wang, R. Manetsch, *Chem. Biol.* **2011**, *6*, 724-732.

[102]   H. C. Kolb, M. G. Finn, K. B. Sharpless, *Angew. Chem. Int. Ed.* **2001**, *40*, 2004-2021.

[103]   D. T. S. Rijkers, R. Merkx, C. B. Yim, A. J. Brouwer, R. M. J. Liskamp, *J. Pept. Sci.* **2010**, *16*, 1-5.

[104] K. B. Sharpless, R. Manetsch, *Expert Opin. Drug. Dis.* **2006**, *1*, 525-538.

[105] W. L. Mock, T. A. Irra, J. P. Wepsiec, M. Adhya, *J. Org. Chem.* **1989**, *54*, 5302-5308.

[106] E. Saxon, C. R. Bertozzi, *Science* **2000**, *287*, 2007-2010.

[107] E. Saxon, J. I. Armstrong, C. R. Bertozzi, *Org. Lett.* **2000**, *2*, 2141-2143.

[108] W. G. Lewis, L. G. Green, F. Grynszpan, Z. Radic, P. R. Carlier, P. Taylor, M. G. Finn, K. B. Sharpless, *Angew. Chem. Int. Edit.* **2002**, *41*, 1053-1057.

[109] R. Manetsch, A. Krasinski, Z. Radic, J. Raushel, P. Taylor, K. B. Sharpless, H. C. Kolb, *J. Am. Chem. Soc.* **2004**, *126*, 12809-12818.

[110] A. Krasinski, Z. Radic, R. Manetsch, J. Raushel, P. Taylor, K. B. Sharpless, H. C. Kolb, *J. Am. Chem. Soc.* **2005**, *127*, 6686-6692.

[111] M. Whiting, J. Muldoon, Y. C. Lin, S. M. Silverman, W. Lindstrom, A. J. Olson, H. C. Kolb, M. G. Finn, K. B. Sharpless, J. H. Elder, V. V. Fokin, *Angew. Chem. Int. Edit.* **2006**, *45*, 1435-1439.

[112] J. Singh, R. C. Petter, A. F. Kluge, *Curr. Opin. Chem. Biol.* **2010**, *14*, 475-480.

[113] D. W. Fry, A. J. Bridges, W. A. Denny, A. Doherty, K. D. Greis, J. L. Hicks, K. E. Hook, P. R. Keller, W. R. Leopold, J. A. Loo, D. J. McNamara, J. M. Nelson, V. Sherwood, J. B. Smaill, S. Trumpp-Kallmeyer, E. M. Dobrusin, *Proc. Natl. Acad. Sci. USA* **1998**, *95*, 12022-12027.

[114] A. J. Chmura, M. S. Orton, C. F. Meares, *Proc. Natl. Acad. Sci. USA* **2001**, *98*, 8480-8484.

[115] K. Levitsky, C. J. Ciolli, P. J. Belshaw, *Org. Lett.* **2003**, *5*, 693-696.

[116] M. Hagel, D. Q. Niu, T. St Martin, M. P. Sheets, L. X. Qiao, H. Bernard, R. M. Karp, Z. D. Zhu, M. T. Labenski, P. Chaturvedi, M. Nacht, W. F. Westlin, R. C. Petter, J. Singh, *Nat. Chem. Biol.* **2011**, *7*, 22-24.

[117] G. W. Rewcastle, D. K. Murray, W. L. Elliott, D. W. Fry, C. T. Howard, J. M. Nelson, B. J. Roberts, P. W. Vincent, H. D. H. Showalter, R. T. Winters, W. A. Denny, *J. Med. Chem.* **1998**, *41*, 742-751.

[118] J. J. Reddick, J. M. Cheng, W. R. Roush, *Org. Lett.* **2003**, *5*, 1967-1970.

[119] M. Li, R. S. Wu, J. S. C. Tsai, S. J. Salamone, *Bioorg. Med. Chem. Lett.* **2003**, *13*, 383-386.

[120] C. H. Qiao, D. J. Wilson, E. M. Bennett, C. C. Aldrich, *J. Am. Chem. Soc.* **2007**, *129*, 6350-6351.

[121] L. S. Brinen, E. Hansell, J. M. Cheng, W. R. Roush, J. H. McKerrow, R. J. Fletterick, *Structure* **2000**, *8*, 831-840.

[122] W. R. Roush, J. M. Cheng, B. Knapp-Reed, A. Alvarez-Hernandez, J. H. McKerrow, E. Hansell, J. C. Engel, *Bioorg. Med. Chem. Lett.* **2001**, *11*, 2759-2762.

[123] C. E. Lough, D. J. Currie, H. L. Holmes, *Can. J. Chem.* **1968**, *46*, 775-781.

[124] I. M. Serafimova, M. A. Pufall, S. Krishnan, K. Duda, M. S. Cohen, R. L. Maglathlin, J. M. McFarland, R. M. Miller, M. Frodin, J. Taunton, *Nat. Chem. Biol.* **2012**, *8*, 471-476.

[125] B. L. Shi, R. Stevenson, D. J. Campopiano, M. F. Greaney, *J. Am. Chem. Soc.* **2006**, *128*, 8459-8467.

[126] B. L. Shi, M. F. Greaney, *Chem. Commun.* **2005**, 886-888.

[127] J. Singh, R. C. Petter, A. F. Kluge, *Curr. Opin. Chem. Biol.* **2010**, *14*, 475-480.

[128] M. R. Barnes, I. C. Gray, *Bioinformatics for geneticists*, Wiley, Chichester, **2003**.

[129] R. H. Nonoo, *Fragment Tethering To Discover Novel Inhibitors Of Cdc25 Phosphatases*, MRes Thesis, Imperial College London **2009**.

[130] H. J. Sterling, J. D. Batchelor, D. E. Wemmer, E. R. Williams, *J. Am. Soc. Mass. Spectrom.* **2010**, *21*, 1045-1049.

[131] L. W. Hardy, J. S. Finermoore, W. R. Montfort, M. O. Jones, D. V. Santi, R. M. Stroud, *Science* **1987**, *235*, 448-455.

[132] M. Belfort, G. Maley, J. Pedersenlane, F. Maley, *Proc. Natl. Acad. Sci. USA* **1983**, *80*, 4914-4918.

[133] C. W. Carreras, D. V. Santi, *Annu. Rev. Biochem.* **1995**, *64*, 721-762.

[134] D. A. Matthews, J. E. Villafranca, C. A. Janson, W. W. Smith, K. Welsh, S. Freer, *J. Mol. Biol.* **1990**, *214*, 937-948.

[135] P. V. Danenberg, R. J. Langenbach, C. Heidelberger, *Biochemistry* **1974**, *13*, 926-933.

[136] D. V. Santi, C. S. McHenry, H. Sommer, *Biochemistry* **1974**, *13*, 471-481.

[137] D. A. Matthews, K. Appelt, S. J. Oatley, N. H. Xuong, *J. Mol. Biol.* **1990**, *214*, 923-936.

[138] W. D. Huang, D. V. Santi, *J. Biol. Chem.* **1994**, *269*, 31327-31329.

[139] J. E. Barrett, D. A. Maltby, D. V. Santi, P. G. Schultz, *J. Am. Chem. Soc.* **1998**, *120*, 449-450.

[140] J. S. Finer-Moore, D. V. Santi, R. M. Stroud, *Biochemistry* **2003**, *42*, 248-256.

[141] W. A. Munroe, C. A. Lewis, R. B. Dunlap, *Biochem. Biophys. Res. Commun.* **1978**, *80*, 355-360.

[142] N. Nagahara, *J. Amino Acids* **2011**, *2011*, 709404.

[143] J. Phan, E. Mahdavian, M. C. Nivens, W. Minor, S. Berger, H. T. Spencer, R. B. Dunlap, L. Lebioda, *Biochemistry* **2000**, *39*, 6969-6978.

[144] A. W. Williams, R. B. Dunlap, S. H. Berger, *Biochemistry* **1998**, *37*, 7096-7102.

[145] S. Kawase, S. W. Cho, J. Rozelle, R. M. Stroud, J. Finer-Moore, D. V. Santi, *Protein Eng.* **2000**, *13*, 557-563.

[146] N. Touroutoglou, R. Pazdur, *Clin. Cancer Res.* **1996**, *2*, 227-243.

[147] E. Chu, M. A. Callender, M. P. Farrell, J. C. Schmitz, *Cancer Chemoth. Pharm.* **2003**, *52*, S80-S89.

[148] B. K. Shoichet, R. M. Stroud, D. V. Santi, I. D. Kuntz, K. M. Perry, *Science* **1993**, *259*, 1445-1450.

[149] S. E. Webber, T. M. Bleckman, J. Attard, J. G. Deal, V. Kathardekar, K. M. Welsh, S. Webber, C. A. Janson, D. A. Matthews, W. W. Smith, S. T. Freer, S. R. Jordan, R. J. Bacquet, E. F. Howland, C. L. J. Booth, R. W. Ward, S. M. Hermann, J. White, C. A. Morse, J. A. Hilliard, C. A. Bartlett, *J. Med. Chem.* **1993**, *36*, 733-746.

[150] T. J. Stout, C. R. Sage, R. M. Stroud, *Structure* **1998**, *6*, 839-848.

[151] T. J. Stout, D. Tondi, M. Rinaldi, D. Barlocco, P. Pecorari, D. V. Santi, I. D. Kuntz, R. M. Stroud, B. K. Shoichet, M. P. Costi, *Biochemistry* **1999**, *38*, 1607-1617.

[152] J. L. Aull, H. H. Daron, *Biochim. Biophys. Acta* **1980**, *614*, 31-39.

[153] F. W. Studier, B. A. Moffatt, *J. Mol. Biol.* **1986**, *189*, 113-130.

[154] L. M. Changchien, A. Garibian, V. Frasca, A. Lobo, G. F. Maley, F. Maley, *Protein Expression Purif.* **2000**, *19*, 265-270.

[155] A. J. Wahba, M. Friedkin, *J. Biol. Chem.* **1961**, *236*, PC11-12.

[156] D. Niculescu-Duvaz, I. Scanlon, I. Niculescu-Duvaz, C. J. Springer, *Tetrahedron Lett.* **2005**, *46*, 6919-6922.

[157] B. R. Lahue, Z. K. Wan, J. K. Snyder, *J. Org. Chem.* **2003**, *68*, 4345-4354.

[158] H. Pan, *Rapid Commun. Mass Spectrom.* **2008**, *22*, 3555-3560.

[159]   A. R. Katritzky, O. Meth-Cohn, C. W. Rees, *Comprehensive organic functional group transformations*, Pergamon, Oxford, **1995**.

[160]   I. Paterson, *Tetrahedron* **1988**, *44*, 4207-4219.

[161]   D. Lizos, R. Tripoli, J. A. Murphy, *Chem. Commun.* **2001**, 2732-2733.

[162]   D. E. Lizos, J. A. Murphy, *Org. Biomol. Chem.* **2003**, *1*, 117-122.

[163]   A. P. Bruins, *J. Chromatogr. A* **1998**, *794*, 345-357.

[164]   A. El-Aneed, A. Cohen, J. Banoub, *Appl. Spectrosc. Rev.* **2009**, *44*, 210-230.

[165]   M. A. Kelly, M. M. Vestling, C. C. Fenselau, P. B. Smith, *Org. Mass Spectrom.* **1992**, *27*, 1143-1147.

[166]   J. D. Carbeck, J. C. Severs, J. M. Gao, Q. Y. Wu, R. D. Smith, G. M. Whitesides, *J. Phys. Chem. B* **1998**, *102*, 10596-10601.

[167]   L. Konermann, D. J. Douglas, *Biochemistry* **1997**, *36*, 12296-12302.

[168]   J. C. Y. Leblanc, D. Beuchemin, K. W. M. Siu, R. Guevremont, S. S. Berman, *Org. Mass Spectrom.* **1991**, *26*, 831-839.

[169]   J. A. Loo, R. R. O. Loo, H. R. Udseth, C. G. Edmonds, R. D. Smith, *Rapid Commun. Mass Spectrom.* **1991**, *5*, 101-105.

[170]   T. R. Covey, R. F. Bonner, B. I. Shushan, J. Henion, *Rapid Commun. Mass Spectrom.* **1988**, *2*, 249-256.

[171]   P. D. Schnier, D. S. Gross, E. R. Williams, *J. Am. Soc. Mass. Spectrom.* **1995**, *6*, 1086-1097.

[172]   A. T. Iavarone, J. C. Jurchen, E. R. Williams, *J. Am. Soc. Mass. Spectrom.* **2000**, *11*, 976-985.

[173]   S. Searles, M. Tamres, F. Block, L. A. Quarterman, *J. Am. Chem. Soc.* **1956**, *78*, 4917-4920.

[174]   H. K. Hall, *J. Am. Chem. Soc.* **1957**, *79*, 5441-5444.

[175]   G. W. Stevenson, D. Williamson, *J. Am. Chem. Soc.* **1958**, *80*, 5943-5947.

[176]   A. Wissner, E. Overbeek, M. F. Reich, M. B. Floyd, B. D. Johnson, N. Mamuya, E. C. Rosfjord, C. Discafani, R. Davis, X. Q. Shi, S. K. Rabindran, B. C. Gruber, F. Ye, W. A. Hallett, R. Nilakantan, R. Shen, Y. F. Wang, L. M. Greenberger, H. R. Tsou, *J. Med. Chem.* **2003**, *46*, 49-63.

[177]   J. U. Jeong, B. Tao, I. Sagasser, H. Henniges, K. B. Sharpless, *J. Am. Chem. Soc.* **1998**, *120*, 6844-6845.

[178]   A. H. Lewin, G. B. Sun, L. Fudala, H. Navarro, L. M. Zhou, P. Popik, A. Faynsteyn, P. Skolnick, *J. Med. Chem.* **1998**, *41*, 988-995.

[179]   R. E. Martin, P. Mohr, H. P. Maerki, W. Guba, C. Kuratli, O. Gavelle, A. Binggeli, S. Bendels, R. Alvarez-Sanchez, A. Alker, L. Polonchuk, A. D. Christ, *Bioorg. Med. Chem. Lett.* **2009**, *19*, 6106-6113.

[180]   M. D. Varney, G. P. Marzoni, C. L. Palmer, J. G. Deal, S. Webber, K. M. Welsh, R. J. Bacquet, C. A. Bartlett, C. A. Morse, C. L. J. Booth, S. M. Herrmann, E. F. Howland, R. W. Ward, J. White, *J. Med. Chem.* **1992**, *35*, 663-676.

[181]   H. T. Spencer, J. E. Villafranca, J. R. Appleman, *Biochemistry* **1997**, *36*, 4212-4222.

[182]   A. Ciulli, C. Abell, *Curr. Opin. Biotechnol.* **2007**, *18*, 489-496.

[183]   R. H. Nonoo, A. Armstrong, D. J. Mann, *ChemMedChem* **2012**, *7*, 2082-2086.

[184]   V. M. Krishnamurthy, V. Semetey, P. J. Bracher, N. Shen, G. M. Whitesides, *J. Am. Chem. Soc.* **2007**, *129*, 1312-1320.

[185]   M. Mammen, S. K. Choi, G. M. Whitesides, *Angew. Chem. Int. Edit.* **1998**, *37*, 2755-2794.

[186]   R. S. Kane, *Langmuir* **2010**, *26*, 8636-8640.

[187]   R. O. Blaustein, P. A. Cole, C. Williams, C. Miller, *Nat. Struct. Biol.* **2000**, *7*, 309-311.

[188]   R. O. Blaustein, *J. Gen. Physiol.* **2002**, *120*, 203-216.

[189]   K. L. Prime, G. M. Whitesides, *J. Am. Chem. Soc.* **1993**, *115*, 10714-10721.

[190]   C. Visintin, A. E. Aliev, D. Riddall, D. Baker, M. Okuyama, P. M. Hoi, R. Hiley, D. L. Selwood, *Org. Lett.* **2005**, *7*, 1699-1702.

[191]   G. V. Smith, F. Notheisz, *Heterogeneous catalysis in organic chemistry*, Academic Press, **1999**.

[192]   N. J. Westwood, N. S. J. Isambert, WO2005121096, **2005**.

[193]   C. L. Allen, A. R. Chhatwal, J. M. Williams, *Chem. Commun.* **2012**, *48*, 666-668.

[194]   A. Bisai, G. Pandey, M. K. Pandey, V. K. Singh, *Tetrahedron Lett.* **2003**, *44*, 5839-5841.

[195]   J. Wu, X. L. Hou, L. X. Dai, *J. Org. Chem.* **2000**, *65*, 1344-1348.

[196]   S. Minakata, Y. Okada, Y. Oderaotoshi, M. Komatsu, *Org. Lett.* **2005**, *7*, 3509-3512.

[197]   S. Matsukawa, K. Tsukamoto, *Org. Biomol. Chem.* **2009**, *7*, 3792-3796.

[198]   A. R. Jacobson, A. N. Makris, L. M. Sayre, *J. Org. Chem.* **1987**, *52*, 2592-2594.

[199]   M. Pittelkow, R. Lewinsky, J. B. Christensen, *Synthesis* **2002**, 2195-2202.

[200]   C. Norbury, P. Nurse, *Annu. Rev. Biochem.* **1992**, *61*, 441-470.

[201]   D. O. Morgan, *Nature,* **1995**, *374*, 131-134.

[202]   S. V. Ekholm, S. I. Reed, *Curr. Opin. Cell Biol.* **2000**, *12*, 676-684.

[203]   A. B. Pardee, *Science* **1989**, *246*, 603-608.

[204]   C. J. Sherr, *Trends Biochem. Sci.* **1995**, *20*, 187-190.

[205]   M. E. Ewen, H. K. Sluss, C. J. Sherr, H. Matsushime, J. Kato, D. M. Livingston, *Cell* **1993**, *73*, 487-497.

[206]   J. Kato, H. Matsushime, S. W. Hiebert, M. E. Ewen, C. J. Sherr, *Genes Dev.* **1993**, *7*, 331-342.

[207]   L. Connell-Crowley, J. W. Harper, D. W. Goodrich, *Mol. Biol. Cell* **1997**, *8*, 287-301.

[208]   E. K. Flemington, S. H. Speck, W. G. Kaelin, Jr., *Proc. Natl. Acad. Sci. USA* **1993**, *90*, 6914-6918.

[209]   A. R. Black, J. Azizkhan-Clifford, *Gene* **1999**, *237*, 281-302.

[210]   A. S. Lundberg, R. A. Weinberg, *Mol. Cell. Biol.* **1998**, *18*, 753-761.

[211]   J. W. Harbour, R. X. Luo, A. Dei Santi, A. A. Postigo, D. C. Dean, *Cell* **1999**, *98*, 859-869.

[212]   F. Girard, U. Strausfeld, A. Fernandez, N. J. Lamb, *Cell* **1991**, *67*, 1169-1179.

[213]   M. Pagano, R. Pepperkok, F. Verde, W. Ansorge, G. Draetta, *EMBO J.* **1992**, *11*, 961-971.

[214]   A. Koff, A. Giordano, D. Desai, K. Yamashita, J. W. Harper, S. Elledge, T. Nishimoto, D. O. Morgan, B. R. Franza, J. M. Roberts, *Science* **1992**, *257*, 1689-1694.

[215]   M. Malumbres, M. Barbacid, *Nat. Rev. Cancer* **2009**, *9*, 153-166.

[216]   G. Draetta, F. Luca, J. Westendorf, L. Brizuela, J. Ruderman, D. Beach, *Cell* **1989**, *56*, 829-838.

[217]   K. Riabowol, G. Draetta, L. Brizuela, D. Vandre, D. Beach, *Cell* **1989**, *57*, 393-401.

[218]   M. Glotzer, A. W. Murray, M. W. Kirschner, *Nature* **1991**, *349*, 132-138.

[219]   J. H. Hoeijmakers, *Nature* **2001**, *411*, 366-374.

[220]   A. Sancar, L. A. Lindsey-Boltz, K. Unsal-Kacmaz, S. Linn, *Annu. Rev. Biochem.* **2004**, *73*, 39-85.

[221]   R. Agami, R. Bernards, *Cell* **2000**, *102*, 55-66.

[222]   L. L. Pontano, P. Aggarwal, O. Barbash, E. J. Brown, C. H. Bassing, J. A. Diehl, *Mol. Cell. Biol.* **2008**, *28*, 7245-7258.

[223]   M. K. Santra, N. Wajapeyee, M. R. Green, *Nature* **2009**, *459*, 722-725.

[224]   J. P. Alao, *Mol. Cancer* **2007**, *6*, 24.

[225]   Y. T. Kwak, R. Li, C. R. Becerra, D. Tripathy, E. P. Frenkel, U. N. Verma, *J. Biol. Chem.* **2005**, *280*, 33945-33952.

[226]   D. C. Guttridge, C. Albanese, J. Y. Reuther, R. G. Pestell, A. S. Baldwin, Jr., *Mol. Cell. Biol.* **1999**, *19*, 5785-5799.

[227]   J. A. DiDonato, M. Hayakawa, D. M. Rothwarf, E. Zandi, M. Karin, *Nature* **1997**, *388*, 548-554.

[228]   N. D. Perkins, *Nat. Rev. Mol. Cell Biol.* **2007**, *8*, 49-62.

[229]   M. A. Brach, R. Hass, M. L. Sherman, H. Gunji, R. Weichselbaum, D. Kufe, *J. Clin. Invest.* **1991**, *88*, 691-695.

[230]   J. W. Pierce, R. Schoenleber, G. Jesmok, J. Best, S. A. Moore, T. Collins, M. E. Gerritsen, *J. Biol. Chem.* **1997**, *272*, 21096-21103.

[231]   A. Duarte, *The interplay between MYCN and the DNA damage response: modulation of MYCN expression, its interactions with components of the DNA damage response and cellular responses to N-myc following genotoxic stress,* PhD Thesis, Imperial College London, **2012**.

[232]   D. A. Jeffery, M. Bogyo, *Curr. Opin. Biotechnol.* **2003**, *14*, 87-95.

[233]   U. Rix, G. Superti-Furga, *Nature Chem. Biol.* **2009**, *5*, 616-624.

[234]   M. Tyers, M. Mann, *Nature* **2003**, *422*, 193-197.

[235]   H. Overkleeft, *Bioorg. Med. Chem.* **2012**, *20*, 552-553.

[236]   E. M. Sletten, C. R. Bertozzi, *Angew. Chem. Int. Ed.* **2009**, *48*, 6974-6998.

[237]   A. E. Speers, G. C. Adam, B. F. Cravatt, *J. Am. Chem. Soc.* **2003**, *125*, 4686-4687.

[238]   H. Ovaa, P. F. van Swieten, B. M. Kessler, M. A. Leeuwenburgh, E. Fiebiger, A. M. van den Nieuwendijk, P. J. Galardy, G. A. van der Marel, H. L. Ploegh, H. S. Overkleeft, *Angew. Chem. Int. Ed.* **2003**, *42*, 3626-3629.

[239]   V. V. Rostovtsev, L. G. Green, V. V. Fokin, K. B. Sharpless, *Angew. Chem. Int. Ed.* **2002**, *41*, 2596-2599.

[240]   C. W. Tornoe, C. Christensen, M. Meldal, *J. Org. Chem.* **2002**, *67*, 3057-3064.

[241]   Q. Wang, T. R. Chan, R. Hilgraf, V. V. Fokin, K. B. Sharpless, M. G. Finn, *J. Am. Chem. Soc.* **2003**, *125*, 3192-3193.

[242]   A. E. Speers, B. F. Cravatt, *Chem. Biol.* **2004**, *11*, 535-546.

[243]   A. T. Wright, B. F. Cravatt, *Chem. Biol.* **2007**, *14*, 1043-1051.

[244]   R. J. W. Cremlyn, *Chlorosulfonic acid: a versatile reagent*, Royal Society of Chemistry, Cambridge, **2002**.

[245]   T. G. Back, S. Collins, M. V. Krishna, *Can. J. Chem.* **1987**, *65*, 38-42.

[246]   T. G. Back, S. Collins, *J. Org. Chem.* **1981**, *46*, 3249-3256.

[247]   R. A. Gancarz, J. L. Kice, *J. Org. Chem.* **1981**, *46*, 4899-4906.

[248]   R. A. Gancarz, J. L. Kice, *Tetrahedron Lett.* **1980**, *21*, 4155-4158.

[249]   Y. H. Kang, J. L. Kice, *J. Org. Chem.* **1984**, *49*, 1507-1511.

[250]   T. G. Back, S. Collins, *Tetrahedron Lett.* **1980**, *21*, 2215-2218.

[251]   Y. L. Shi, M. Shi, *Org. Biomol. Chem.* **2005**, *3*, 1620-1621.

[252]   S. R. Dubbaka, P. Vogel, *Chemistry* **2005**, *11*, 2633-2641.

[253]   S. R. Dubbaka, P. Vogel, *J. Am. Chem. Soc.* **2003**, *125*, 15292-15293.

[254]   S. R. Dubbaka, P. Vogel, *Org. Lett.* **2004**, *6*, 95-98.

[255]   Z. H. Guan, W. Zuo, L. B. Zhao, Z. H. Ren, Y. M. Liang, *Synthesis* **2007**, 1465-1470.

[256]   S. P. McIlroy, E. Clo, L. Nikolajsen, P. K. Frederiksen, C. B. Nielsen, K. V. Mikkelsen, K. V. Gothelf, P. R. Ogilby, *J. Org. Chem.* **2005**, *70*, 1134-1146.

[257]   A. Elangovan, Y. H. Wang, T. I. Ho, *Org. Lett.* **2003**, *5*, 1841-1844.

[258]   S. Thorand, N. Krause, *J. Org. Chem.* **1998**, *63*, 8551-8553.

[259]   F. Firooznia, T. Lin, S. So, B. Wang, H. Yun, EP2358677 A1, **2011**.

[260]   A. A. Farahat, A. Kumar, M. Say, D. Barghash Ael, F. E. Goda, H. M. Eisa, T. Wenzler, R. Brun, Y. Liu, L. Mickelson, W. D. Wilson, D. W. Boykin, *Bioorg. Med. Chem.* **2010**, *18*, 557-566.

[261]   A. Klapars, S. L. Buchwald, *J. Am. Chem. Soc.* **2002**, *124*, 14844-14845.

[262]   M. Gilligan, A. C. Humphries, T. Ladduwahetty, K. J. Merchant, EP1858852 A1, **2006**.

[263]   A. K. Banerjee, C. A. Penamatheud, M. C. Decarrasco, *J. Chem. Soc. Perkin Trans. 1* **1988**, 2485-2490.

[264]   J. R. Hwu, J. M. Wetzel, *J. Org. Chem.* **1992**, *57*, 922-928.

[265]   A. B. Turner, H. J. Ringold, *J. Chem. Soc.* **1967**, 1720-1730.

[266]   K. C. Nicolaou, T. Montagnon, P. S. Baran, Y. L. Zhong, *J. Am. Chem. Soc.* **2002**, *124*, 2245-2258.

[267]   D. A. Evans, D. J. Adams, E. E. Kwan, *J. Am. Chem. Soc.* **2012**, *134*, 8162-8170.

[268]   M. Frigerio, M. Santagostino, S. Sputore, *J. Org. Chem.* **1999**, *64*, 4537-4538.

[269]   D. B. Dess, J. C. Martin, *J. Am. Chem. Soc.* **1991**, *113*, 7277-7287.

[270]   S. V. Ley, N. J. Anthony, A. Armstrong, M. G. Brasca, T. Clarke, D. Culshaw, C. Greck, P. Grice, A. B. Jones, B. Lygo, A. Madin, R. N. Sheppard, A. M. Z. Slawin, D. J. Williams, *Tetrahedron* **1989**, *45*, 7161-7194.

[271]   A. Armstrong, S. V. Ley, *Synlett* **1990**, 323-325.

[272]   S. V. Ley, A. Armstrong, D. Diezmartin, M. J. Ford, P. Grice, J. G. Knight, H. C. Kolb, A. Madin, C. A. Marby, S. Mukherjee, A. N. Shaw, A. M. Z. Slawin, S. Vile, A. D. White, D. J. Williams, M. Woods, *J. Chem. Soc. Perkin Trans. 1* **1991**, 667-692.

[273]   S. Yamazaki, Y. Yanase, E. Tanigawa, S. Yamabe, H. Tamura, *J. Org. Chem.* **1999**, *64*, 9521-9528.

[274]   N. A. Porter, V. H. T. Chang, D. R. Magnin, B. T. Wright, *J. Am. Chem. Soc.* **1988**, *110*, 3554-3560.

[275]   J. Blumbach, D. A. Hammond, D. A. Whiting, *J. Chem. Soc. Perkin Trans. 1* **1986**, 261-268.

[276]   F. G. Bordwell, M. Vanderpuy, N. R. Vanier, *J. Org. Chem.* **1976**, *41*, 1885-1886.

[277]   Z. Rappoport, I. Marek, *The chemistry of organolithium compounds*, Wiley, Chichester, **2006**.

[278]   F. Gao, X. X. Yan, O. Zahr, A. Larsen, K. Vong, K. Auclair, *Bioorg. Med. Chem. Lett.* **2008**, *18*, 5518-5522.

[279]   M. Li, R. S. Wu, J. S. Tsai, S. J. Salamone, *Bioorg. Med. Chem. Lett.* **2003**, *13*, 383-386.

[280]   J. Zhang, T. P. Loh, *Chem. Commun.* **2012**, *48*, 11232-11234.

[281]   T. A. Barf, P. deBoer, H. Wikstrom, S. J. Peroutka, K. Svensson, M. D. Ennis, N. B. Ghazal, J. C. McGuire, M. W. Smith, *J. Med. Chem.* **1996**, *39*, 4717-4726.

[282]   K. A. Winans, C. R. Bertozzi, *Chem. Biol.* **2002**, *9*, 113-129.

[283]   L. B. Zhu, L. Cheng, Y. X. Zhang, R. G. Xie, J. S. You, *J. Org. Chem.* **2007**, *72*, 2737-2743.

[284]   X. C. Cambeiro, M. A. Pericas, *Adv. Synth. Catal.* **2011**, *353*, 113-124.

[285]   F. R. Bisogno, A. Cuetos, A. A. Orden, M. Kurina-Sanz, I. Lavandera, V. Gotor, *Adv. Synth. Catal.* **2010**, *352*, 1657-1661.

[286]   V. Sandanayaka, B. Mamat, R. K. Mishra, J. Winger, M. Krohn, L. M. Zhou, M. Keyvan, L. Enache, D. Sullins, E. Onua, J. Zhang, G. Halldorsdottir, H. Sigthorsdottir, A. Thorlaksdottir, G. Sigthorsson, M. Thorsteinnsdottir, D. R. Davies, L. J. Stewart, D. E. Zembower, T. Andresson, A. S. Kiselyov, J. Singh, M. E. Gurney, *J. Med. Chem.* **2010**, *53*, 573-585.

[287]   A. Slaitas, E. Yeheskiely, *Eur. J. Org. Chem.* **2002**, 2391-2399.

[288]   J. H. Huang, P. O'brien, *Synthesis* **2006**, 425-434.

[289]   AstraZeneca, WO2004/000294, **2003**.

[290]   Y. Yamamoto, H. Hasegawa, H. Yamataka, *J. Org. Chem.* **2011**, *76*, 4652-4660.

[291]   O. Itsenko, T. Kihlberg, B. Langstrom, *J. Org. Chem.* **2004**, *69*, 4356-4360.

[292]   D. L. Romero, R. A. Olmsted, T. J. Poel, R. A. Morge, C. Biles, B. J. Keiser, L. A. Kopta, J. M. Friis, J. D. Hosley, K. J. Stefanski, D. G. Wishka, D. B. Evans, J. Morris, R. G. Stehle, S. K. Sharma, Y. Yagi, R. L. Voorman, W. J. Adams, W. G. Tarpley, R. C. Thomas, *J. Med. Chem.* **1996**, *39*, 3769-3789.

[293]   C. L. Allen, S. Davulcu, J. M. J. Williams, *Org. Lett.* **2010**, *12*, 5096-5099.

[294]   S. R. Walker, W. T. Jiao, E. J. Parker, *Bioorg. Med. Chem. Lett.* **2011**, *21*, 5092-5097.

[295]   Y. A. Lin, J. M. Chalker, N. Floyd, G. J. L. Bernardes, B. G. Davis, *J. Am. Chem. Soc.* **2008**, *130*, 9642-9643.

[296]   A. Bentolila, I. Vlodavsky, R. Ishai-Michaeli, O. Kovalchuk, C. Haloun, A. J. Domb, *J. Med. Chem.* **2000**, *43*, 2591-2600.

[297]   C. Schmuck, T. Rehm, L. Geiger, M. Schafer, *J. Org. Chem.* **2007**, *72*, 6162-6170.

[298]   M. Nahrwold, A. Stoncius, A. Penner, B. Neumann, H. G. Stammler, N. Sewald, *Beilstein J. Org. Chem.* **2009**, *5*.

[299]   W. H. Hersh, P. Xu, C. K. Simpson, J. Grob, B. Bickford, M. S. Hamdani, T. Wood, A. L. Rheingold, *J. Org. Chem.* **2004**, *69*, 2153-2163.

[300]   H. Rheinboldt, E. Giesbrecht, *J. Am. Chem. Soc.* **1946**, *68*, 973-978.

[301]   A. R. Suarez, M. C. Brinon, M. M. Debertorello, M. Gonzalezsierra, P. Josephnathan, *J. Chem. Soc. Perkin Trans. 2* **1990**, 2071-2074.

[302]   H. O. House, P. C. Gaa, D. Vanderveer, *J. Org. Chem.* **1983**, *48*, 1661-1670.

[303]   O. Plietzsch, A. Schade, A. Hafner, J. Huuskonen, K. Rissanen, M. Nieger, T. Muller, S. Bräse, *Eur. J. Org. Chem.* **2013**, 283-299.

[304]   M. Frigerio, M. Santagostino, *Tetrahedron Lett.* **1994**, *35*, 8019-8022.

[305]   S. Nicolai, S. Erard, D. F. Gonzalez, J. Waser, *Org. Lett.* **2010**, *12*, 384-387.

[306]   X. Li, Y. Han, X. M. Pan, *FEBS Lett.* **2001**, *507*, 169-173.